Vadim P. Nikolaenko
Yury S. Astakhov
Editors

Orbital Fractures

A Physician's Manual

Springer

Orbital Fractures

Vadim P. Nikolaenko • Yury S. Astakhov
Editors

Orbital Fractures

A Physician's Manual

Springer

Editors
Vadim P. Nikolaenko, MD, PhD, DSc
Ophthalmology
Saint-Petersburg State Hospital No. 2
Saint-Petersburg
Russia

Yury S. Astakhov, MD, PhD, DSc
Ophthalmology
I.P. Pavlov First Saint Petersburg State
Medical University
Saint-Petersburg
Russia

Authorized translation of the 1st Russian language edition
Orbital Fractures – A Physician's Manual by Vadim P. Nikolaenko and Yury S. Astakhov
© LLC Eco-Vektor, Saint-Petersburg, Russia, 2012, www.eco-vector.com
All Rights Reserved

ISBN 978-3-662-46207-2 ISBN 978-3-662-46208-9 (eBook)
DOI 10.1007/978-3-662-46208-9

Library of Congress Control Number: 2015934822

Springer Heidelberg New York Dordrecht London
© Springer-Verlag Berlin Heidelberg 2015
This work is subject to copyright. All rights are reserved by the Publisher, whether the whole or part of the material is concerned, specifically the rights of translation, reprinting, reuse of illustrations, recitation, broadcasting, reproduction on microfilms or in any other physical way, and transmission or information storage and retrieval, electronic adaptation, computer software, or by similar or dissimilar methodology now known or hereafter developed.
The use of general descriptive names, registered names, trademarks, service marks, etc. in this publication does not imply, even in the absence of a specific statement, that such names are exempt from the relevant protective laws and regulations and therefore free for general use.
The publisher, the authors and the editors are safe to assume that the advice and information in this book are believed to be true and accurate at the date of publication. Neither the publisher nor the authors or the editors give a warranty, express or implied, with respect to the material contained herein or for any errors or omissions that may have been made.

Printed on acid-free paper

Springer is part of Springer Science+Business Media (www.springer.com)

Preface

Craniofacial injury has drawn particular attention in the last years due to increasing rates of motor vehicle accidents, deteriorating crime rates, domestic violence, and terrorist threat.

Over the last 15–20 years, the research effort provided a large amount of data, new diagnostic and treatment strategies of midface injuries appeared. Still, there is pressing need especially among resident and young specialists in comprehensive textbooks and manuals to critically review this large body of knowledge and provide evidence-based information on natural history, clinical presentation, diagnosis, and treatment of orbital fractures.

The authors attempted to summarize all relevant clinical topics on signs and symptoms, diagnosis, and treatment of orbital fractures through the prism of years of clinical practice and research data.

This manual consists of eight chapters. The first chapter is a discussion of bony and soft tissue anatomy of the orbit as well as its vascular and nerve supply. The second chapter deals with the imaging of the orbit. The third chapter focuses on the clinical presentation, diagnosis, and treatment of the most common orbital fractures—fractures of the orbital floor. The fourth chapter highlights isolated medial wall fractures, while in the fifth chapter, medial wall fractures are discussed in the context of naso-orbito-ethmoid injuries. The sixth and seventh chapters review the injury to the orbit associated with zygomatic and maxillary fractures. Finally, the eighth chapter covers the essentials of frontobasilar fractures.

This manual would be impossible without the support and expertise of our colleagues—experienced specialists in anatomy, imaging, otolaryngology, maxillofacial surgery, and neurosurgery. We would like to acknowledge the invaluable help of professor I. Gaivoronovsky, MD, PhD, Head of Department of Anatomy, Military Medical Academy (Chap. 1). Professor S. Karpischenko, MD, PhD, Head of Department of Otolaryngology, St. Petersburg State Medical University, shared his expertise in multiple orbital injuries and trauma to sinuses (Chaps. 4 and 5). Professor G. Khatskevich, MD, PhD, Head of Department of Pediatric Dentistry, and assistant professors M. Soloviev and I. Trofimov, MD, PhD, Department of Pediatric Dentistry from St. Petersburg State Medical University, were coauthors of Chaps. 6 and 7. Professor Yu. Shulev, MD, PhD, Department of Neurosurgery, North-Western State Medical University, shared his extensive knowledge in Chap. 8.

CT and MRI anatomy of the orbit (Chap. 2) was discussed in collaboration with G. Trufanov, MD, PhD (Head of Department of Radiology), E. Burlachenko (Department of Radiology), V. Lugina (Department of Ophthalmology) from Military Medical Academy, St. Petersburg, Russia, and V. Zakharov, MD, PhD, Head of Department of Radiology, State Clinical Hospital #2, St. Petersburg, Russia.

The purpose of *Orbital Fractures: Physician's Manual* is to serve as a textbook for a wide range of medical specialists including ophthalmologists, maxillofacial surgeons, neurosurgeons, neurologists, otolaryngologists, radiologists, and emergency doctors. This book is an excellent resource for all medical students, residents in ophthalmology, and fellows who desire to broaden their spectrum of knowledge in orbital pathology.

This manual is our first experience in describing a multidisciplinary approach to orbital injuries. The authors would be very grateful for comments and feedback from the readers.

Saint-Petersburg, Russia — Vadim P. Nikolaenko, MD, PhD, DSc
Saint-Petersburg, Russia — Yury S. Astakhov, MD, PhD, DSc

Acknowledgment

Authors would like to thank Edward Cherney, MD, PhD, who thorougly reviewed the book and whose patientce and expertise made the English editions of this book possible.

Contents

1 Clinical Anatomy of the Orbit and Periorbital Area 1
Vadim P. Nikolaenko, Yury S. Astakhov, and Ivan V. Gaivoronsky

2 Radiological Examination of the Orbit 69
Vadim P. Nikolaenko, Yury S. Astakhov, Gennadiy E. Trufanov, Evgeniy P. Burlachenko, Valery V. Zakharov, and Valentina D. Lugina

3 Orbital Floor Fractures 121
Vadim P. Nikolaenko and Yury S. Astakhov

4 Medial Wall Fractures 231
Vadim P. Nikolaenko, Yury S. Astakhov, and Sergei A. Karpischenko

5 Naso-Orbito-Ethmoid Fractures 251
Vadim P. Nikolaenko, Yury S. Astakhov, and Sergei A. Karpischenko

6 Zygomaticoorbital Fractures 271
Vadim P. Nikolaenko, Yury S. Astakhov, Mikhail M. Soloviev, G. Khatskevich, and Igor G. Trofimov

7 Maxillary Fractures 303
Vadim P. Nikolaenko, Yury S. Astakhov, Mikhail M. Soloviev, G. Khatskevich, and Igor G. Trofimov

8 Frontobasilar Fractures 325
Vadim P. Nikolaenko, Yury S. Astakhov, Yury A. Shulev, and Sergei A. Karpischenko

Clinical Anatomy of the Orbit and Periorbital Area

1

Vadim P. Nikolaenko, Yury S. Astakhov, and Ivan V. Gaivoronsky

Contents

1.1 Bones Forming the Orbit 3
1.2 Soft Tissues of the Orbit 16
1.3 Blood Supply to the Orbit 37
1.4 Characteristics of the Cranial Nerves Involved in Innervation of the Orbital Complex 42
1.5 Anatomy of Paranasal Sinuses 57
1.6 Anatomy of the Temporal, Infratemporal, and Pterygopalatine Fossae 61
References 64
Further Reading 67

The orbit is a paired bony socket in the facial portion of the skull located on both sides of the nasal root. The three-dimensional reconstruction of the orbit is more likely to be shaped like a pear than like a quadrilateral pyramid losing one of its facets in the orbital apex area (as it is conventionally described in the textbooks) (Fig. 1.1a).

V.P. Nikolaenko, MD, PhD (✉)
Department of Ophthalmology, Saint Petersburg State Hospital No. 2, Saint-Petersburg, Russia

Department of Otolaryngology and Ophthalmology, Medical Faculty, Saint-Petersburg State University, Saint-Petersburg, Russia
e-mail: dr.nikolaenko@mail.ru

Y.S. Astakhov
Department of Ophthalmology, I.P. Pavlov First Saint Petersburg State Medical University, Saint-Petersburg, Russia

City Ophthalmologic Center at Saint Petersburg State Hospital No. 2, Saint-Petersburg, Russia

I.V. Gaivoronsky
Department of Normal Anatomy, Kirov Military Medical Academy, Saint-Petersburg, Russia

Department of Morphology, Saint-Petersburg State University, Saint-Petersburg, Russia

© Springer-Verlag Berlin Heidelberg 2015

V.P. Nikolaenko, Y.S. Astakhov (eds.), *Orbital Fractures: A Physician's Manual*,
DOI 10.1007/978-3-662-46208-9_1

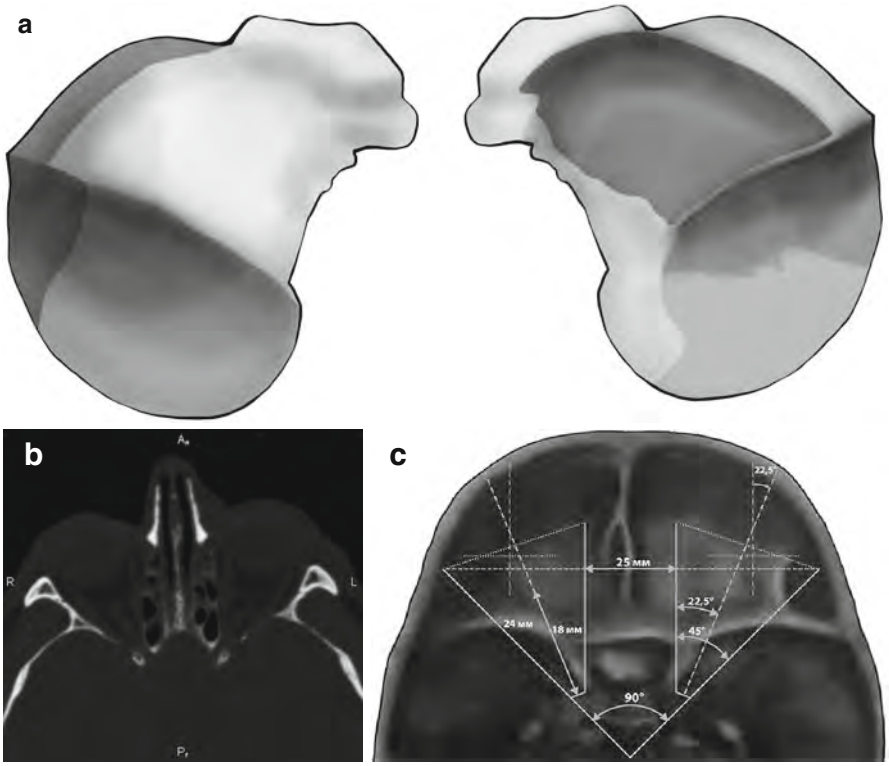

Fig. 1.1 Orbit anatomy: (**a**) pear-shaped 3D model of the orbit; (**b**, **c**) axial cross-sectional images of the orbits and the main parameters of the interorbital topographic and anatomic relationships: the medial orbital walls are almost parallel; the lateral orbital walls make a right angle. The interorbital distance is 25 mm; the angle between the optic nerves is 45°; the angle between the optic nerve and the optic axis is 22.5°

The axes of the orbital pyramids converge backward and diverge forward; the medial orbital walls are almost parallel, while the lateral ones make a right angle [1]. If the optic nerves are taken as the reference points, the normal divergence angle of the optical axes does not exceed 45°, which can be clearly seen in the computed axial tomography scans (Fig. 1.1b, c). The permanent adduction stimulus induced by divergence of the orbits (to maintain orthophoria) is responsible for the fact that the medial rectus is the strongest extraocular rectus muscle. Elimination of the convergence stimulus in individuals with a blind eye causes a noticeable temporal deviation of the blind eye (exotropia).

The divergence angle of the optical axes determines the *interorbital distance* (the distance between the anterior lacrimal crests). It is the crucial element of facial harmony. The normal interorbital distance in adults varies from 18.5 mm to 30.7 mm; the ideal value is 25 mm. Both decreased (*stenopia*) and increased (*euryopia*) interorbital distances are indicative of a severe craniofacial anomaly.

The average length of the anteroposterior axis ("depth") of the orbit in adults is 45 mm. Hence, all orbital manipulations (retrobulbar injections, subperiosteal blunt dissection, and sizing of the grafts placed to repair bone defects) should not be performed more than 35 mm posterior from the bony orbital margin and 1 cm away from the optic canal (*canalis opticus*).

One should bear in mind that *the orbital depth can vary in a rather broad range,* the "deep and narrow" and "shallow and wide" orbits being the extreme variants. Attempts have been made to calculate the distance between the orbital margin and the apex that could serve as a reference to help plan for a safe surgical intervention. The results were so variable that they proved to be unreliable for surgical planning. Hence, interventions on the orbit must be preceded by obligatory axial and sagittal computed tomography followed by a thorough analysis of the images.

The volume of the orbital cavity (*cavitas orbitalis*) is somewhat smaller than it is generally believed to be (23–26 cm^3), and the eyeball occupies only 6.5–7 cm^3 [2]. The orbital volume in females is 10 % smaller than that in males. Ethnicity has a significant effect on orbital parameters.

The horizontal dimension (width) of the orbital opening (*aditus orbitalis*) is approximately 4 cm in adults; the vertical dimension (height) of the orbital opening does not exceed 3.5 cm.

1.1 Bones Forming the Orbit

The orbit is formed by seven bones: the maxilla, frontal, zygomatic, ethmoid, sphenoid, lacrimal, and palatine bones.

Each orbital wall is formed by several bones. If one uses the medial orbital wall as a reference point and follows a counterclockwise direction, the number of bones forming the orbital walls is represented by the *mnemonic rule* "*4–3–2–2*" (Table 1.1).

Table 1.1 Bones forming the orbit

Orbital walls	Bones forming the orbital walls	Adjacent structures
Medial	Frontal process of the maxilla Lacrimal bone Orbital plate of the ethmoid bone Body of the sphenoid bone (*The components of the medial wall are listed in the front–back direction*)	Ethmoidal labyrinth Sphenoid sinus Nasal cavity Cribriform plate of the ethmoid bone at the level of the frontoethmoidal suture
Inferior	Orbital surface of the body of the maxilla	Infraorbital canal
	Orbital surface of the zygomatic bone	Maxillary sinus
	Orbital process of the palatine bone	
	(The internal, external, and posterior portions, respectively)	
Lateral	Orbital surface of the zygomatic bone; orbital surface of the greater wing of the sphenoid bone	Temporal fossa Pterygopalatine fossa Middle cranial fossa
Superior	Orbital portion of the frontal bone; lesser wing of the sphenoid bone	Anterior cranial fossa Frontal sinus

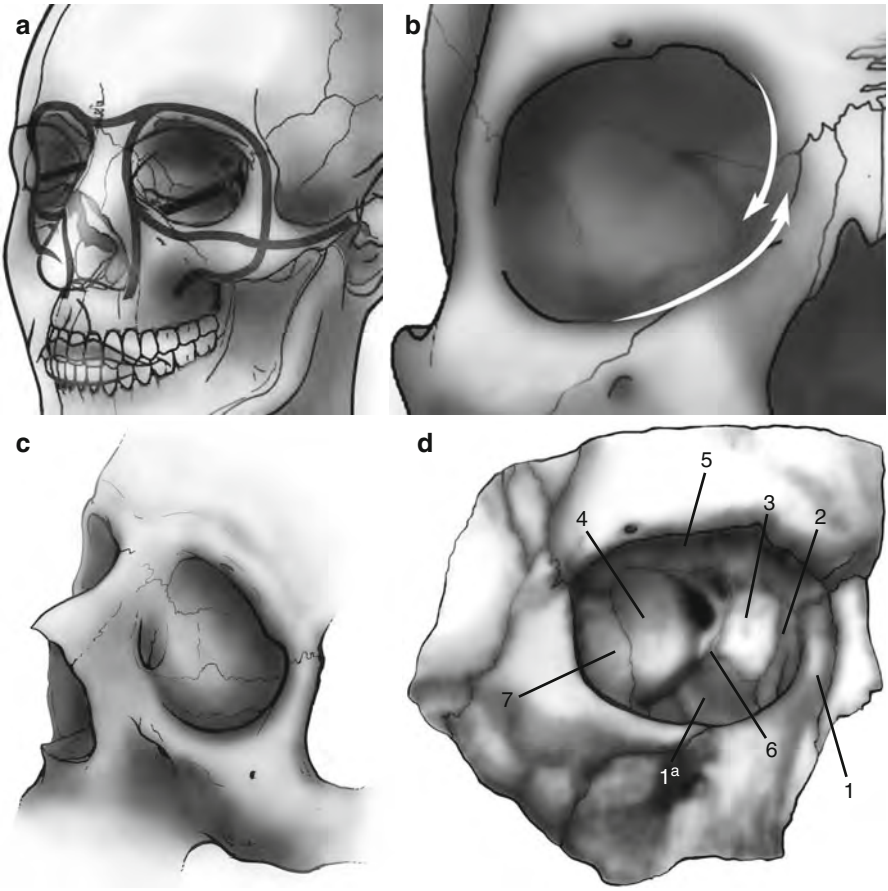

Fig. 1.2 Anatomy of the orbital margins and walls. (**a**) Involvement of the orbital opening in the system of midfacial pillars; (**b**) a spiral structure of the orbital opening [2]; (**c**) structure of the medial orbital margin and the lacrimal sac fossa; (**d**) bones forming the orbit: (*1*) frontal process of the maxilla (*processus frontalis maxillae*), (*1a*) orbital surface of the maxilla (*facies orbitalis maxillae*), (*2*) lacrimal bone (*os lacrimale*), (*3*) orbital plate of the ethmoid bone (*lamina orbitalis ossis ethmoidalis*), (*4*) orbital surface of the greater wing of the sphenoid bone (*facies orbitalis alae majoris ossis sphenoidalis*), (*5*) orbital surface of the orbital portion of the frontal bone (*facies orbitalis ossis frontalis*), (*6*) orbital process of the perpendicular plate of the palatine bone (*processus orbitalis laminae perpendicularis ossis palatini*), (*7*) orbital surface of the zygomatic bone (*facies orbitalis ossis zygomatici*) (Fig. 1.2a was taken from the website www.aofoundation.org)

Orbital Margins The orbital margins (supraorbital, *margo supraorbitalis*; infraorbital, *margo infraorbitalis*; lateral, *margo lateralis*; and medial, *margo medialis*) form the so-called external orbital framework that ensures mechanical strength of the entire orbital complex and is a part of the complex system of facial counterforces or "stiffener plates" that reduce facial skeleton deformation during chewing and when one acquires a traumatic brain injury (Fig. 1.2a). Furthermore, the profile

of the orbital margin plays the key role in formation of the contour of the upper and middle thirds of the face.

The orbital margins lie in different planes: the lateral margin is posteriorly displaced as compared to the medial one, while the inferior margin is posteriorly displaced as compared to the superior one. Thus, a spiral structure with *90° angles is formed*. This structure ensures a wide field of vision and downward/outward gaze but leaves the anterior half of the eyeball unprotected against an injuring agent moving from the same direction. The spiral structure of the orbital opening is broken near the medial margin where it forms the lacrimal sac fossa (*fossa sacci lacrimalis*) (Fig. 1.2b, c) [2].

The position of the orbital opening with respect to the frontal, horizontal, and sagittal planes is referred to as "the spatial architecture of the orbital opening" with its main parameters, *inclination of the orbital opening* and *orbital openness*. The average inclination of the orbital opening is 8–13° and is determined by the degree to which the supraorbital margin protrudes compared to the infraorbital one.

Orbital openness characterizes the position of the orbital opening with respect to the sagittal plane drawn through the medial margin. The average openness values are 104–108°.

The *lateral and supraorbital margins* (*margo lateralis et supraorbitalis*) formed by the thickened edges of the zygomatic and frontal bones are the strongest ones. As for the supraorbital margin, the well-developed frontal sinus is a very important factor of its mechanical strength as it dampens hits to this region.

The continuity of the supraorbital margin at the boundary between its middle and internal one-thirds is interrupted by the supraorbital notch (*incisura supraorbitalis*). The supraorbital artery, vein, and nerve (*a.*, *v.*, *et n. supraorbitalis*) pass through it. The shape of the notch can vary; it is approximately 4.6 mm wide and 1.8 mm high.

In 25 % of the population (and up to 40 % in the female population), there is a foramen (*foramen supraorbitale*), or a small bony canal, instead of the bony notch, through which the aforementioned neurovascular bundle passes. The foramen is usually smaller than the notch (3.0×0.6 mm).

The *infraorbital margin* (*margo infraorbitalis*) formed by the maxilla and the zygomatic bone is characterized by lower strength; hence, the orbit exposed to blunt trauma undergoes transient wavelike deformation that spreads to the inferior wall and causes an isolated ("blowout") fracture with displacement of the muscles and adipose tissue inferior to the globe, into the maxillary sinus. The infraorbital margin typically remains intact.

The upper portion of the *medial orbital margin* (*margo medialis*) is formed by the nasal part of the frontal bone (*pars nasalis ossis frontalis*). The lower portion of the medial margin consists of the posterior lacrimal crest of the lacrimal bone and the anterior lacrimal crest of the maxilla (Fig. 1.2c).

Bony Orbital Walls The *lateral wall of the orbit* (*paries lateralis*) is the thickest and strongest of the four walls. Its anterior portion is formed by the zygomatic bone, while the posterior portion is formed by the orbital surface of the greater wing of the sphenoid bone. The length of the lateral wall, measuring from the orbital margin to the superior orbital fissure, is 40 mm (Fig. 1.2d).

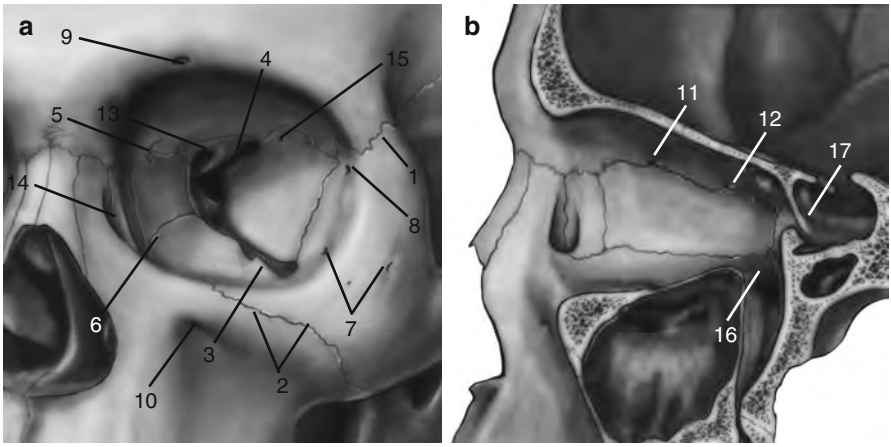

Fig. 1.3 Borders of the orbital walls. Oblique frontal (**a**) and parasagittal (**b**) views. The lateral wall is bordered anteriorly by the frontozygomatic (*1*) and zygomaticomaxillary (*2*) sutures and posteriorly by the inferior (*3*) and superior (*4*) orbital fissures. The medial wall is bordered superiorly by a line running along the frontoethmoidal suture (*5*) and inferiorly by the ethmoidomaxillary suture (*6*). The outer border of the upper wall is the superior orbital fissure (*4*); the inner border is the line continuing the frontoethmoidal suture (*5*) anteriad and posteriad. The inferior wall of the orbit (orbital floor) is bordered on its lateral side by the inferior orbital fissure (*3*) and, on its medial side, by the ethmoidomaxillary suture (*6*) continued anteriad and posteriad. The figure also shows the foramina: (*7*) zygomaticofacial foramen; (*8*) zygomaticotemporal foramen; (*9*) supraorbital foramen; (*10*) infraorbital foramen; (*11* and *12*) anterior and posterior ethmoidal foramina; (*13*) optic foramen; (*14*) lacrimal sac fossa connecting with the nasolacrimal duct (not shown); and (*15*) meningo-orbital foramen of the greater wing of the sphenoid bone. The oblique parasagittal slice of the orbit illustrates its topographic relationships with the pterygopalatine fossa (*16*) and cavernous sinus (*17*)

The frontozygomatic (sutura frontozygomatica) and zygomaticomaxillary (sutura zygomaticomaxillaris) sutures are the anterior borders of the lateral wall; the superior and inferior orbital fissures are the posterior borders (Fig. 1.3).

The orbital surface of the greater wing of the sphenoid bone (*facies orbitalis alae majoris ossis sphenoidalis*) has heterogeneous thickness. Its anterolateral one-third, which is connected to the orbital surface of the zygomatic bone by the sphenozygomatic suture (*sutura sphenozygomatica*), and the posteromedial one-third, which forms the lower border of the superior orbital fissure, are relatively thin. Therefore, the sphenozygomatic suture area is a convenient landmark for performing external orbitotomy.

The central one-third, *trigone* (or the sphenosquamous suture, *sutura sphenosquamosa*), is characterized by high strength. This triangular region separates the orbit from the middle cranial fossa, thus simultaneously forming both the lateral wall of the orbit and the skull base (Fig. 1.1b). This should be taken into account when performing external orbitotomy: one should bear in mind that the average distance between the lateral orbital margin and the middle cranial fossa is 31 mm [3].

The sphenofrontal foramen lies contiguously with the sphenofrontal suture (*sutura sphenofrontalis*) in the greater wing of the sphenoid bone, near the anterior margin of the superior orbital fissure. The sphenofrontal foramen contains a branch of the lacrimal artery, the *recurrent meningeal artery* (anastomosis between *a. meningea media* from the basin of the external carotid artery and the ophthalmic artery from the basin of the internal carotid artery).

The frontozygomatic suture (*sutura frontozygomatica*) provides rigid fixation of the zygomatic bone to the frontal bone. Due to its length and architecture, the sphenozygomatic suture plays a crucial role in zygomatic bone repositioning in patients with zygomatic fractures.

The zygomaticofacial (*canalis zygomaticofacialis*) and zygomaticotemporal (*canalis zygomaticotemporalis*) canals contain the corresponding homonymous arteries and nerves exiting the orbital cavity through its lateral wall and terminating in the zygomatic and temporal areas (Fig. 1.3a). Care should be taken when dissecting the temporal muscle during external orbitotomy so that the artery and nerve are not accidentally injured.

Whitnall's orbital tubercle (*tuberculum orbitale Whitnall*), a small elevation on the orbital margin of the zygomatic bone that is found in 95 % of people, localizes 11 mm below the frontozygomatic suture and 4–5 mm behind the orbital margin [4]. This important anatomical landmark is connected to:

1. Ligament attaching the lateral rectus muscle (*lacertus musculi recti lateralis*, "sentinel ligament")
2. Suspensory ligament of the lower eyelid (Lockwood's inferior transverse ligament)
3. Lateral palpebral ligament
4. Lateral horn of the levator aponeurosis
5. Orbital septum (tarso-orbital fascia)
6. Lacrimal gland fascia

The lateral orbital wall separates the orbital contents from the temporal and the pterygopalatine fossae (and from the middle cranial fossa near the orbital apex).

The *superior orbital wall* (*orbital roof, paries superior*) is formed primarily by the frontal bone, its smooth and concave orbital surface, and in its posterior portion by the 1.5 cm long flat lesser wing of the sphenoid bone (*ala minor ossis sphenoidalis*). It is triangular in shape, just as the inferior and lateral walls.

The lacrimal fossa (*fossa glandulae lacrimalis*), a small impression where the homonymous gland resides, is found near the base of the zygomatic process of the frontal bone, immediately behind the supraorbital margin.

The trochlear fossa (*fossa trochlearis*) lies 4 mm medially to the supraorbital margin. It is usually adjacent to the trochlear spine (*spina trochlearis*), a small bony protrusion near the junction between the orbital roof and the medial wall. The tendinous portion of the superior oblique muscle passes through and abruptly changes direction as it passes through a tendinous (or cartilaginous) loop connected to the trochlear spine (Fig. 1.4) [5, 6].

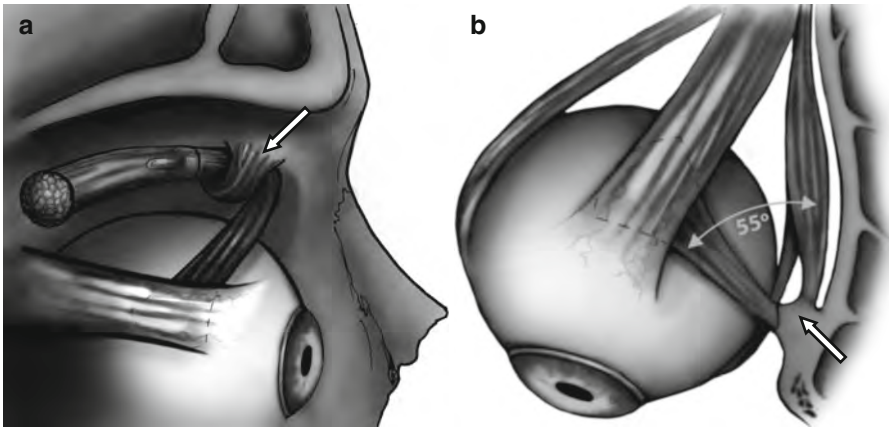

Fig. 1.4 The anatomy of the trochlea

Damaged trochlea resulting from injuries or surgical intervention (in particular, frontal sinus surgeries) causes dysfunction of the superior oblique and persistent bothersome diplopia.

The aforementioned frontal sinus is located inside the superior orbital wall (orbital roof). The sinus occupies its anterointernal portion and spreads backward for up to a half or two-thirds of the depth of the orbit. In some cases, it may reach the posterior portions (i.e., the lesser wing of the sphenoid bone). In the posterior two-thirds of the orbit, the superior wall is much thinner compared to the anterior one-third. Nevertheless, it is rather deformity resistant due to the thickness of the frontal bone, the arc-shaped profile of the orbital surface, and the dampening effect of the frontal sinus.

As a result, fractures of the superior orbital wall are rare. However, the presence of these fractures is always indicative of a high-energy injury and suggests a high probability of open head injury and deserves the closest attention.

The longest (45 mm) orbital wall—the *medial orbital wall* (*paries medialis*)—is formed in its anteroposterior direction by the frontal process of the maxilla, the lacrimal, and the ethmoid bones and the body and the lesser wing of the sphenoid bone. *It is bordered superiorly by the frontoethmoidal suture and inferiorly by the ethmoidomaxillary suture* (Fig. 1.3). Unlike the other walls, it is rectangular in shape.

The medial wall is based on the orbital plate of the ethmoid bone, 3.5–5.0 × 1.5–2.5 cm in size and only 0.25 mm thick; it is also known as lamina papyracea ("paper-like sheet"). It is the largest but the weakest component of the medial wall. The orbital plate of the ethmoid has a slightly concave shape; hence, the maximum orbital width corresponds to a point 1.5 cm deeper from the plane of orbital opening. As a result, the transcutaneous and transconjunctival approaches to the medial wall of the orbit do not provide an adequate view of its entire area.

The orbital plate consists of approximately 10 honeycomb-shaped cells separated by septa into the anterior and posterior portions. The large and numerous small septa between the ethmoidal cells (*cellulae ethmoidales*) reinforce the medial wall from the direction of the nose. Hence, the medial wall is stronger than the inferior one, especially in case of a branched network of ethmoidal septa and a relatively small size of the orbital plate [7, 8].

In 50 % of orbits, the ethmoidal labyrinth reaches the posterior lacrimal crest; in other 40 % of cases, it reaches the frontal process of the maxilla [9].

The anterior portion of the orbital plate of the ethmoid bone is adjacent to the lacrimal bone and the frontal process of the maxilla. These form the medial orbital margin that is a part of the facial reinforcing structures and considerably strengthens the medial orbital wall. The body and lesser wing of the sphenoid bone, which is adjacent to the posterior surface of the ethmoid bone, forms the orbital apex near the optic canal.

The frontoethmoidal suture is an important landmark indicating the upper boundary of the ethmoidal labyrinth. Therefore, osteotomy above the frontoethmoidal suture is fraught with the danger of damaging the dura mater in the frontal lobe area.

At the level of the frontoethmoidal suture, 24 and 36 mm behind the anterior lacrimal crest, the medial orbital wall contains the *anterior and posterior ethmoidal foramina* (*foramina ethmoidalia anterior et posterior*). These foramina lead to the homonymous canals where the homonymous branches of the ophthalmic artery and the nasociliary nerve run from the orbit to the ethmoidal cells and the nasal cavity. It should be emphasized that the posterior ethmoidal foramen lies at the boundary between the superior and the medial orbital walls deep in the frontal bone only 6 mm away from the optic foramen (*mnemonic rule*: *24–12–6*, where 24 is the distance (mm) between the anterior lacrimal crest and the anterior ethmoidal foramen, 12 is the distance between the anterior and posterior ethmoidal foramina, and 6 is the distance between the posterior ethmoidal foramen and the optic canal). The exposure of the posterior ethmoidal foramen during subperiosteal dissection of the orbital tissues absolutely indicates that any further interventions in this area should be terminated to avoid optic nerve damage.

The lacrimal sac fossa is the most important structure in the medial orbital wall. It is 13 × 7 mm in size and is formed by the anterior lacrimal crest of the frontal process of the maxilla and the lacrimal bone with its posterior lacrimal crest (Fig. 1.2b, c).

The lower portion of the fossa reaches the 10–12 mm long bony nasolacrimal canal (*canalis nasolacrimalis*) that runs deep in the maxilla and opens into the inferior nasal meatus 30–35 mm away from the external nasal opening.

The medial orbital wall separates the orbit from the nasal cavity, the ethmoidal labyrinth, and the sphenoid sinus. This fact is of great clinical significance as these sinuses are likely to be a source of acute or chronic inflammation which can spread to the contiguous orbital soft tissues. Both the insignificant thickness of the medial

wall and the natural (*anterior and posterior ethmoidal*) foramina contribute to this possibility. Furthermore, congenital dehiscence occurs in the lacrimal bone and the orbital lamina of the ethmoid bone rather frequently. It is a variant of the norm but, when present, can act as an additional portal of infection.

The *inferior orbital wall* (*orbital floor, paries inferior*), the roof of the maxillary sinus, is primarily formed by the *orbital surface of the body of maxilla*, by the *zygomatic bone* in the antero-exterior portion, and by the *small orbital process of the perpendicular plate of the palatine bone* in the posterior portion. The inferior wall is the only orbital wall that is not partially formed by the sphenoid bone.

The inferior orbital wall is shaped like an equilateral triangle. It is the shortest (~20 mm long) wall. It does not reach the orbital apex and is adjacent to the inferior orbital fissure and the pterygopalatine fossa. *The line running along the inferior orbital fissure forms the outer border of the orbital floor. The inner border is the continuation of the ethmoidomaxillary suture anteriad and posteriad* (Fig. 1.3).

The area of the inferior orbital wall is ~6 cm^2 [10] and is less than 0.5 mm thick. Thus, the inferior and medial walls are the thinnest of all the orbital walls; this anatomy explains well why the predominance of orbital fractures involves these two walls.

The infraorbital groove is the thinnest portion of the orbital floor. It divides the orbital floor into approximately equal parts and becomes a canal anteriorly. The posterior part of the internal half of the inferior wall is slightly stronger. The remaining portions of the inferior wall are rather resistant to mechanical impact. The junction between the medial and inferior orbital walls, which is supported by the medial wall of the maxillary sinus, is the thickest area.

The inferior wall has a characteristic S-shaped profile, which must be taken into account when shaping titanium implants used to repair orbital floor defects. If the reconstructed orbital wall has a flat profile, the orbital volume will increase, and enophthalmos will persist in the postoperative period (Fig. 1.5).

A 15° elevation of the inferior orbital wall toward the orbital apex and its complex profile prevent a surgeon from accidentally damaging the deeper orbital areas with a blunt instrument and make direct optic nerve damage during orbital floor reconstruction unlikely.

As mentioned above, the posteromedial portion of the inferior orbital wall is formed by the *orbital process of the perpendicular plate of the palatine bone*. It rests in a medial direction slightly above the crossing point between the infraorbital nerve and the inferior orbital fissure. Unlike the surrounding maxilla, the orbital process of the perpendicular plate of the palatine bone is inherently strong. Hence, it is rarely affected in individuals with orbital fractures and can be used as a landmark of the orbital apex. Furthermore, it plays a crucial role in repairing fractures involving the entire floor, and the orbital process of the perpendicular plate of the palatine bone is the only site where the posterior implant edge can be placed.

Another significant clinical aspect is the proximity of the maxillary sinus. This proximity allows for contiguous spread of inflammation in acute and chronic sinusitis.

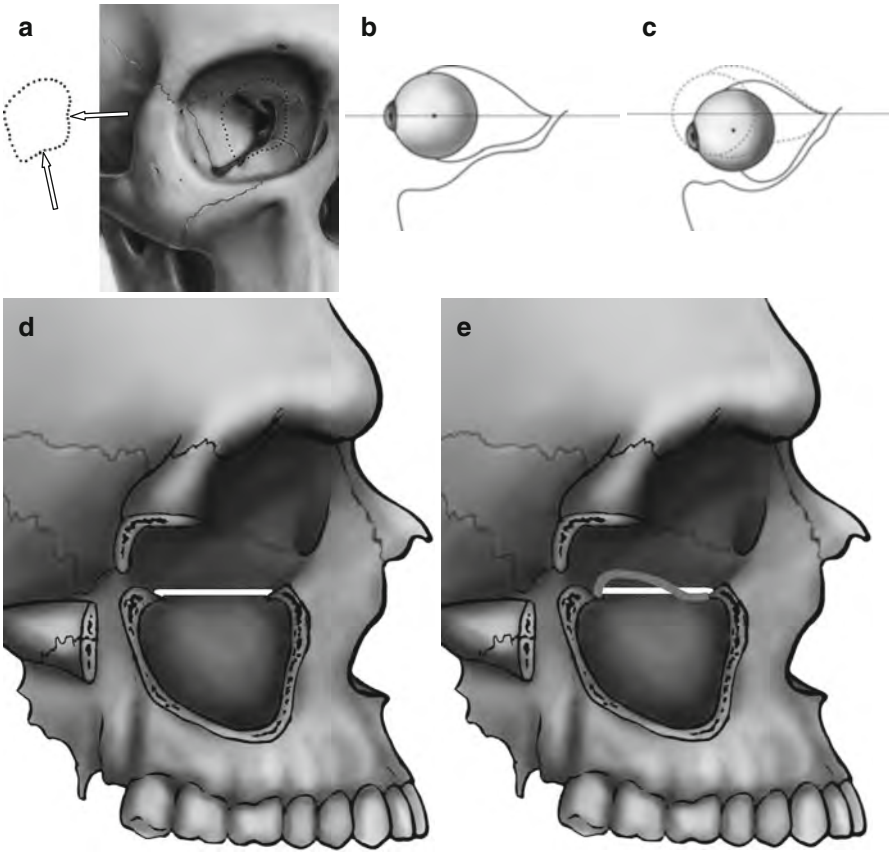

Fig. 1.5 Complex profile of the orbital walls. (**a**, **b**) Position of some areas of the inferior and medial walls of the so-called internal orbit (*arrows*) ensuring the proper position of the eyeball in the orbit; (**c**) disappearance of the S-shaped profile of the inferior orbital wall (orbital floor) after its fracture; (**d**) incorrect and (**e**) the optimal contour of the implant used to repair the missing orbital wall

Clinical Anatomy of the Orbital Apex In terms of craniofacial surgery, the orbit is conventionally subdivided into three areas: the *external orbit* (consisting of the zygomatic bone and the nasoethmoidal complex, i.e., the frontal process of the maxilla, the nasal portion of the frontal bone, and nasal, lacrimal, and ethmoid bones), the *internal orbit*, and the *deep orbit* (*its apex*), which starts from the anterior edge of the inferior orbital fissure, is formed by the sphenoidal bone, and occupies 20 % of the orbital volume (Fig. 1.6) [11]. *The landmarks (borders) of the orbital apex* include the infraorbital nerve, the inferior orbital fissure, the orbital process of the perpendicular plate of the palatine bone, and the greater wing of the sphenoid bone. The area where the four anatomical landmarks listed above merge is known as the *orbital confluence* (*confluens orbitae*).

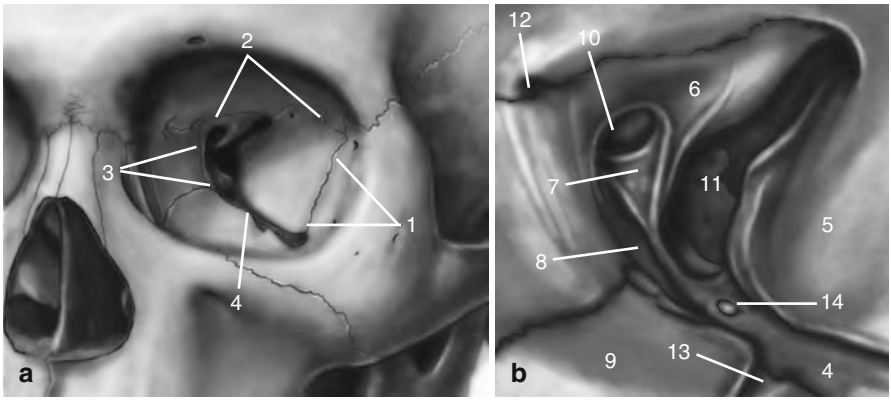

Fig. 1.6 Anatomy of the orbital apex. (**a**) Borders of the orbital apex follow the sphenozygomatic (*1 sutura sphenozygomatica*), sphenofrontal (*2 sutura sphenofrontalis*), and sphenoethmoidal (*3 sutura sphenoethmoidalis*) sutures, as well as the inferior orbital fissure (*4*). Thus, the bony structures of the orbital apex are formed by the sphenoid bone. (**b**) Topographic anatomy of the optic foramen and orbital fissures: (*5*) the greater wing of the sphenoid bone; (*6*) the lesser wing of the sphenoid bone; (*7*) the body of the sphenoid bone; (*8*) palatine bone; (*9*) maxilla; (*10*) optic foramen; (*11*) superior orbital fissure; (*12*) posterior ethmoidal foramen; (*13*) infraorbital groove; and (*14*) round foramen (According to [27, 60] with amendments)

Inferior Orbital Fissure (Fissura Orbitalis Inferior) This fissure is the downward continuation of the superior orbital fissure. It separates the lateral and inferior walls. The anterior portions of the inferior orbital fissure open into the infratemporal fossa, while the posterior portions open into the pterygopalatine fossa localized behind the maxillary sinus. The fissure is bound superiorly by the orbital surface of the greater wing of the sphenoid bone and inferiorly by the orbital surface of the maxilla, zygomatic bone, and orbital process of the perpendicular plate of the palatine bone. The inferior orbital fissure is approximately 2 cm long; its width varies from 1 to 5 mm. The anterior edge of the fissure is 20 (sometimes even 6–15) mm away from the infraorbital margin and is the border of the inferior orbital wall. The lumen of the inferior orbital fissure is covered by a connective tissue septum with smooth muscle fibers interwoven: the so-called orbital muscle of Müller (m. orbitalis) which has sympathetic innervation. *The possible proximity of the inferior orbital fissure to the orbital margin should be taken into account when reconstructing blowout fractures of the orbital floor. The appreciably dense periosteum adherent to the fissure edges can be mistaken for incarcerated soft tissues in the fracture area, while the club-shaped expansion of the anterior orbital edge observed in 42 % of individuals can be mistaken for the fracture area. Attempts to dissect the periosteum away from the edges of the inferior orbital fissure can cause severe hemorrhage from the infraorbital artery:*

- The maxillary nerve (*n. maxillaris*, V_2)
- The zygomatic nerve (*n. zygomaticus*) and its branches: the zygomaticofacial branch (*r. zygomaticofacialis*) and the zygomaticotemporal branch (*r. zygomaticotemporalis*) supplying the secretory fibers for the lacrimal gland through the anastomosis with the lacrimal nerve

- Infraorbital nerve (*n. infraorbitalis*) and infraorbital artery (*a. infraorbitalis*)
- Small orbital branches of the pterygopalatine ganglion (*ganglion pterygopalatinum*)
- Branch or branches of the inferior orbital vein anastomosing with the pterygoid venous plexus and the deep facial vein. Thus, the venous network of the face, the pterygopalatine fossa, paranasal sinuses, and the cavernous sinus are all interconnected. It should be mentioned that in individuals with infectious cellulitis of the deep facial tissues, paranasal sinuses, and facial bones, infection may spread to the cavernous sinus through the inferior ophthalmic vein and cause its thrombosis.

An aperture with a regular circular shape, the *foramen rotundum*, is located behind the junction between the superior and inferior orbital fissures, on the external surface of the skull base. It connects the middle cranial fossa with the pterygopalatine fossa (near the orbit) and hosts the second branch of trigeminal nerve, the maxillary nerve (*n. maxillaris*).

The orbital apex contains two apertures: the optic foramen and the superior orbital fissure.

The *optic foramen* is found in the superomedial portion of the orbital apex along an imaginary horizontal line passing through the anterior and posterior ethmoidal foramina, approximately 6 mm behind the latter [12, 13]. The optic foramen is surrounded by the common tendinous ring (*annulus tendineus communis Zinn*) from where all the rectus extraocular muscles originate.

The optic canal (*canalis opticus*) is 6.5 mm in diameter and 8–10 mm long. It is oriented inward at an angle of 45° and upward at an angle of 15°. The lateral wall of the channel is formed by two roots of the lesser wing of the sphenoid bone and forms the internal wall of the superior orbital fissure. The medial wall of the optic canal is formed by the body of the sphenoid bone and is less than 1 mm thick. The 2–3 mm thick upper wall of the canal serves as a floor of the anterior cranial fossa. The orbital foramen in the canal is vertically oval shaped; the middle portion is round; the intracranial foramen is horizontally oval shaped. This gives the ophthalmic artery an arcuate path [14–20]. In addition to the optic nerve and the ophthalmic artery, the canal contains the sympathetic fibers of the carotid plexus.

The superior orbital fissure (*fissura orbitalis superior*) is a border between the superior and lateral orbital walls (Fig. 1.7). It is formed by the body and wings of the sphenoid bone, connects the orbital cavity and the middle cranial fossa, and is closed with a connective tissue membrane. Two portions can be distinguished: the *inner* or *lower* one (so-called intraconal; it is wider and has an oblique vertical orientation, i.e., opens into the muscular cone) and the *outer* one (upper; it is narrower, oriented obliquely horizontally, forward and upward *extraconal*). A border between these portions is the bony protrusion in the middle of the lower edge of the orbital fissure (*spina recti lateralis*) which is the origin of the lateral crus of the lateral rectus.

The average length of the superior orbital fissure is 22 mm. Its width varies significantly, which is an anatomical factor for the development of superior orbital fissure syndrome [21].

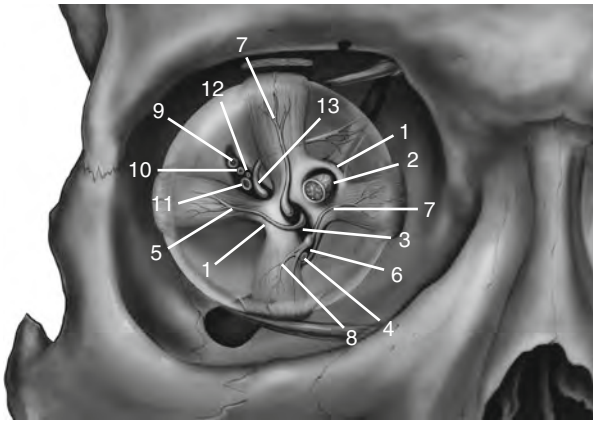

Fig. 1.7 Contents of the superior orbital fissure. (*1*) The common tendinous ring (*annulus tendineus communis Zinn*) surrounding the so-called oculomotor foramen, which is comprised of the optic foramen (*2*) and the lower (intraconal) compartment of the superior orbital fissure (*3*). The contents of the lower portion of the superior orbital fissure: (*4*) nasociliary nerve (*n. nasociliaris*), (N); (*5*) abducens nerve (*n. abducens*, n. VI) (A); (*6*) sympathetic and parasympathetic fibers (S); (*7, 8*) the superior and inferior branches of the oculomotor nerve (n. III) (O^2). A mnemonic rule $NASO^2$ (naso-squared) was proposed by Jordan and Anderson [29] to help memorize the topographic anatomy of the intraconal compartment of the superior orbital fissure. The content of the upper portion of the fissure in the lateral-to-medial direction: (*9*) lacrimal nerve (L); (*10*) recurrent branch of the middle meningeal artery (M); (*11*) superior ophthalmic vein (S); (*12*) frontal nerve (F); and (*13*) trochlear nerve (T). A mnemonic rule LMSFT (look: Michigan state football team) [29] (Cited by Zide and Jelks [60] with amendments) helps memorize the topographic anatomy of the extraconal compartment of the superior orbital fissure

The lumen of the superior orbital fissure contains a number of critical anatomical structures (Table 1.2):

1. The ophthalmic nerve (*n. ophthalmicus*), the first branch of the trigeminal nerve, ensures sensory innervation of all the structures in the orbital complex. Usually within the superior orbital fissure, the ophthalmic nerve divides into three main branches: the lacrimal (*n. lacrimalis*), frontal (*n. frontalis*), and nasociliary (*n. nasociliaris*) nerves.
2. All the oculomotor nerves of the orbit: oculomotor (*n. oculomotorius*), trochlear (*n. trochlearis*), and abducent (*n. abducens*) nerves.
3. The superior ophthalmic vein (*v. ophthalmica superior*) or the ophthalmic venous sinus formed by connection of the superior and the inconstant inferior ophthalmic veins.
4. The fissure sometimes contains the aforementioned recurrent meningeal artery (*a. meningea recurrens*), which frequently has the most lateral position. Even more rarely, the central retinal vein passes through the fissure (in cases when it anastomoses directly with the cavernous sinus instead of the superior ophthalmic vein).

Table 1.2 Orbital foramina and fissures

Anatomical structure	Topographic anatomy	Contents
Supraorbital notch (foramen)	Separates the medial and middle thirds of the supraorbital margin	Supraorbital nerve (the branch of the frontal nerve from the ophthalmic nerve, V_1)
Anterior ethmoidal foramen	24 mm away from the medial orbital margin at the level of the frontoethmoidal suture	Homonymous neurovascular bundle
Posterior ethmoidal foramen	12 mm behind the anterior ethmoidal foramen, 6 mm away from the optic foramen	Homonymous neurovascular bundle
Foramina on the zygomatic bone		Zygomaticofacial and zygomaticotemporal neurovascular bundles
Nasolacrimal canal	Starts in the lacrimal sac fossa and opens into the inferior nasal meatus under the inferior nasal concha	Nasolacrimal duct
Infraorbital foramen	Localizes 4–10 mm below the infraorbital margin	Infraorbital neurovascular bundle (from V_2)
Optic canal	6.5 mm in diameter, 10 mm long	Optic nerve, ophthalmic artery, sympathetic fibers
Superior orbital fissure	22 mm long. The superior orbital fissure is confined to the greater and lesser wings of the sphenoid bone.	External portion: superior ophthalmic vein; lacrimal, frontal, and trochlear nerves
	Localizes below and laterally from the optic foramen and is separated into two (external and internal) portions by the crus of the lateral rectus muscle	Internal portion: superior and inferior branches of the oculomotor nerve, nasociliary nerve, abducens nerve; sympathetic and parasympathetic fibers
Inferior orbital fissure	Formed by the sphenoid, zygomatic, and palatine bones and the maxilla	Infraorbital and zygomatic nerves (V_2), inferior ophthalmic vein
Sphenofrontal foramen	Sphenofrontal suture	Recurrent meningeal artery anastomosing with the lacrimal artery

The structures in the superior orbital fissure are found in the aforementioned extra- and intraconal compartments.

The *upper (extraconal) compartment of the superior orbital fissure* contains (in the lateral-to-medial direction) the following structures:

- Lacrimal nerve (*n. lacrimalis*) from the first branch (*n. ophthalmicus*) of the trigeminal nerve.
- A branch of the middle meningeal artery.
- Superior ophthalmic vein.
- Frontal nerve (*n. frontalis*) from the first branch (*n. ophthalmicus*) of the trigeminal nerve.
- Trochlear nerve (*n. trochlearis*); the extraconal localization of the trochlear nerve explains why certain mobility of the eye is retained even after a perfectly performed retrobulbar block.

The lower (intraconal) compartment of the superior orbital fissure contains the following structures:

- Nasociliary nerve (*n. nasociliaris* from n. ophthalmicus)
- Abducent nerve (*n. abducens*, n. VI)
- Sympathetic and parasympathetic fibers
- Upper and lower branches of the oculomotor nerve (*n. oculomotorius*, n. III)

1.2 Soft Tissues of the Orbit

According to the International Anatomical Nomenclature, the soft tissues of the orbit include the structures localized inside bony walls and bounded anteriorly by the *orbital septum* (*septum orbitale*):

- Orbital periosteum (*periorbita*)
- Muscle fasciae (*fasciae musculares*)
- Orbital fat body (*corpus adiposum orbitae*)
- Levator palpebrae superioris (*m. levator palpebrae superioris*)
- Orbital muscle and Müller's tarsal muscles (*m. orbitalis, m. tarsalis superior, m. tarsalis inferior*)
- Lacrimal gland
- Extraocular muscles
- Optic nerve and its sheaths
- Eyeball
- Nerves, arteries, veins, and lymphatic channels

The bony orbital walls are lined with thin but strong periosteum (*periorbita*). It is tightly adherent to the walls in the area of the orbital opening (the place where the orbital septum is attached to the bone, *arcus marginalis*, 6–10 mm wide), bone sutures, orbital foramina and fissures, and the posterior lacrimal crest. The periosteum spreads over the large openings (the superior and inferior orbital fissures), to interconnect with the connective tissue membranes and the dura mater in their lumen (Fig. 1.8). In other areas, the periosteum can be easily separated to form a *subperiosteal space* both by a blunt instrument used during a surgical intervention or by blood or an exudate in certain pathological conditions.

Posteriorly, near the orbital apex, the periosteum is interwoven with the perineural optic nerve sheath at the site where it enters the bony canal. Anteriorly, the periosteum spreads to the orbital septum and the frontal, buccal, and zygomatic areas. It spreads to the temporal and pterygopalatine fossae through the inferior orbital fissure. The periosteum lines the lacrimal sac fossa; its continuation, fascia of the lacrimal sac (*diaphragma lacrimalis*), surrounds the lacrimal sac.

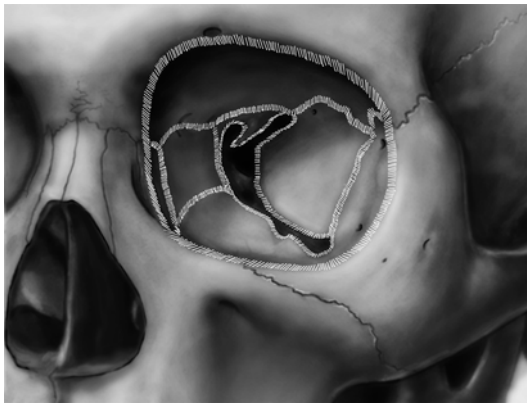

Fig. 1.8 Regions where the periosteum is tightly attached to the bone (hatched areas)

The periosteum consists of two layers (the dense outer and loose inner layers) and mechanically hinders infection or tumor spreading from paranasal sinuses to the orbit.

The orbital periosteum receives abundant blood supply both from the bones and from the orbit. Two vascular systems anastomose with one another; thus, the periosteum cannot be considered a serious barrier for hematogenous dissemination of pathological agents [22]. Sensory innervation is ensured by small branches of the ophthalmic nerve (n. V_1).

The periosteum on the side of the orbital cavity is lined with a thin loose fascia merging with muscle sheaths.

The *orbital fasciae* comprise a complex well-organized 3D structure, which includes the following [23–26]:

1. Fascial sheath of eyeball (Tenon's capsule, *vagina bulbi*).
2. Sheaths of the extraocular muscles (and the intermuscular fascia connecting them).
3. Trabeculae separating the adipose lobules of the orbit.
4. Fibers that spread from the sheaths of extraocular muscles to orbital walls and eyelids (*supporting ligaments and the tendinous expansion of the lateral rectus*, *lacertus musculi recti lateralis*) and are components of a more sophisticated orbital suspensory system [27] (Figs. 1.9, 1.10, 1.11, 1.12, and 1.13). In turn, it is subdivided into the anterior and posterior suspensory systems:
   A. *The anterior suspensory system* of the orbit maintains the proper position of the eyeball and eyelids, suspends to the lacrimal gland (*Sommering's ligament*), and ensures proper movements of the superior oblique tendon in the trochlear region. The system consists of three parts:
      I. *Suspensory apparatus of the eyeball*:
         - Lateral and medial supporting ligaments (tendinous expansions of the medial and lateral rectus muscles)
         - Lateral and medial palpebral ligaments

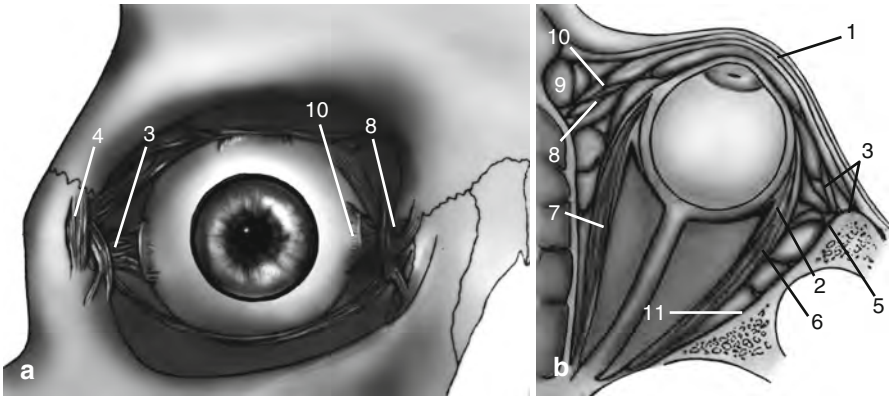

Fig. 1.9 Schematic view of the anterior suspensory system of the orbit. (**a**) Anterior view, (**b**) dorsal view. (*1*) Orbicularis oculi muscle; (*2*) bulbar sheath (Tenon's capsule); (*3*) lateral palpebral ligament; (*4*) retinaculum laterale; (*5*) supporting ligament system of the lateral rectus muscle; (*6*) lateral rectus muscle; (*7*) medial rectus muscle; (*8*) retinaculum mediale; (*9*) lacrimal sac fossa; (*10*) medial palpebral ligament; and (*11*) periosteum

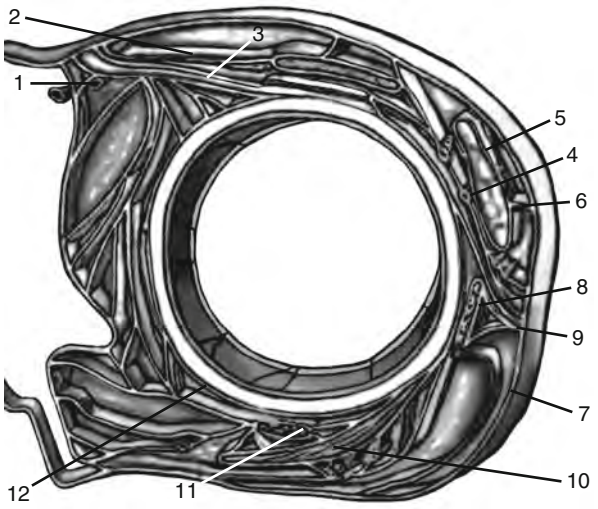

Fig. 1.10 Anatomy of the fascial system of the orbit at the level of the eyeball equator. The oblique coronal view. The extensive adhesion of the lateral rectus muscle sheath (*8*) to retinaculum laterale (*9*) (supporting ligament of the lateral rectus muscle) is worth mentioning. Another feature is the dense adhesion of the inferior oblique muscle to the adjacent inferior rectus muscle, forming the inferior (*10*) muscle complex. (*1*) Supraorbital nerve; (*2*) Whitnall's ligament; (*3*) ligament of the superior oblique muscle; (*4*) lacrimal vein; (*5*) lacrimal gland; (*6*) Sommering's ligament attaching the lacrimal gland to the periosteum (*7*); (*11*) inferior branch of the oculomotor nerve; (*12*) Tenon's capsule (According to Dutton [27] with amendments)

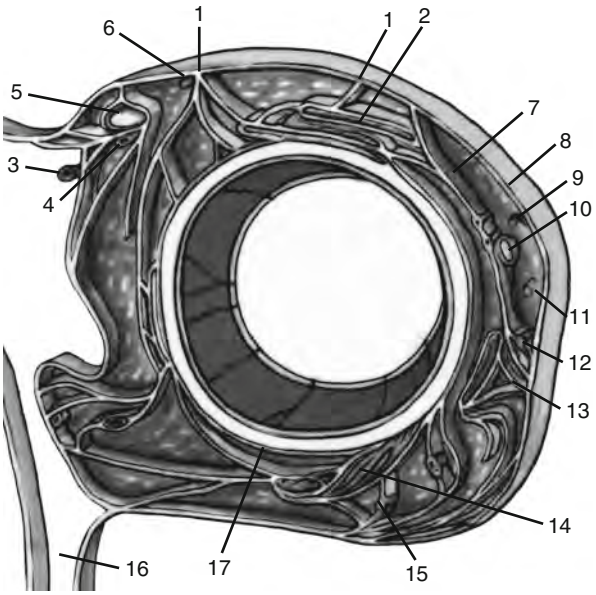

Fig. 1.11 Anatomy of the fascial system of the orbit at the level of the posterior pole of the eye. Oblique coronal view. Ligaments (*1*) attaching the superior muscle complex (*2*) to the orbital roof; (*3*) ophthalmic artery; (*4*) superior ophthalmic vein; (*5*) tendon of the superior oblique muscle; (*6*) supraorbital nerve; (*7*) superolateral area of the intermuscular fascia; (*8*) periosteum; (*9*) lacrimal nerve; (*10*) lacrimal gland; (*11*) zygomatic nerve; (*12*) zygomaticotemporal nerve; (*13*) retinaculum laterale; (*14*) inferior oblique muscle; (*15*) small branch of the oculomotor nerve innervating the inferior oblique muscle; (*16*) nasolacrimal canal; and (*17*) Tenon's capsule (According to Dutton [27] with amendments)

II. *Upper portion of the anterior suspensory system*:
- Whitnall's superior transverse ligament
- Adhesion of the fasciae of the levator palpebrae superioris and the superior rectus, forming in the so-called superior muscle complex
- Sommering's ligament attaching the lacrimal gland to the periosteum
- Upper portion of Tenon's capsule

III. *Lower portion of the anterior suspensory system*:
- Densified fascia around the inferior rectus (capsulopalpebral fascia)
- Lockwood's inferior transverse ligament
- Lower portion of Tenon's capsule (Fig. 1.9)

B. *Posterior suspensory system of the orbit* consists of smaller anatomical structures, including:
- Common tendinous ring of Zinn
- Fascial adhesions between the superior orbital wall (orbital roof), the levator palpebrae superioris, and the superior rectus
- Ligament suspending the superior ophthalmic vein
- Orbital muscle of Müller

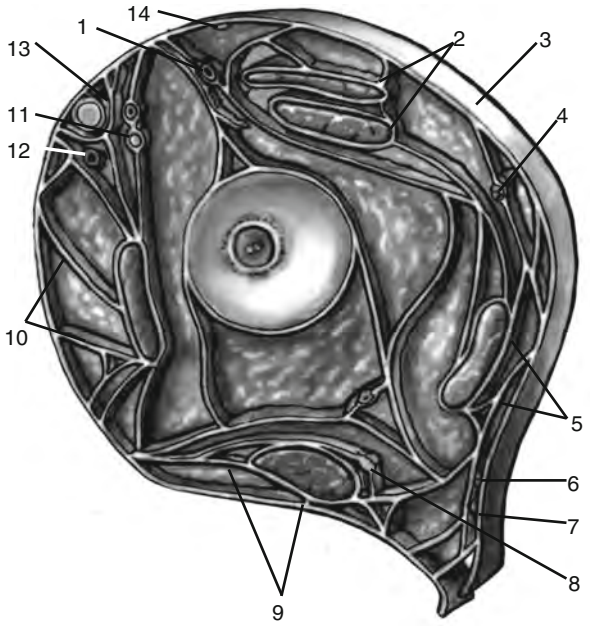

Fig. 1.12 Anatomy of the fascial system of the orbit at the level of the posterior pole of the eye. Oblique coronal view. (*1*) Superior ophthalmic vein attached to the orbital roof by a ligament; (*2*) common fascial system of the superior rectus muscle and the levator palpebrae superioris muscle; (*3*) periosteum; (*4*) lacrimal vein; (*5*) supporting ligament of the lateral rectus muscle; (*6*) zygomatic nerve; (*7*) zygomaticofacial nerve; (*8*) small branch of the oculomotor nerve innervating the inferior oblique muscle; (*9*) supporting ligament of the inferior rectus muscle; (*10*) supporting ligament of the medial rectus muscle; (*11*) nasociliary nerve; (*12*) ophthalmic artery; (*13*) fascial system of the superior oblique muscle; and (*14*) frontal nerve. The adipose tissue is separated by connective tissue septa into appreciably large globules. The orbital veins lying between the septal sheets, which makes their spatial arrangement relatively constant. The arteries pass directly through the adipose globules, thus making their arrangement rather variable (According to Dutton [27] with amendments)

Tenon's fascia of the eyeball (*vagina bulbi*) separates the retrobulbar adipose tissue from the eyeball. Anteriorly, it is tightly attached by the episclera directly behind the limbus. Posteriorly, Tenon's fascia is attached to the sclera around the optic nerve by interweaving with its sheath. Along its remaining length, Tenon's capsule is separated from the sclera by a slit-like episcleral space (*spatium episclerale*) intergrown with thin connective tissue septa. Tenon's fascia of the eyeball is the thinnest in the area where the optic nerve passes and the thickest in the intermuscular space between the "tunnels" for extraocular muscles. Tenon's capsule is interwoven with extrinsic (external) muscle sheaths (which, in turn, are connected with the (inter)muscular fascia) and layers separating the orbital adipose tissue into individual lobules (Fig. 1.14) [24–26, 28]. Thus, the eyeball, Tenon's capsule, and the orbital fat are connected by elastic adhesions whose presumable function is to dampen the eye movements.

Muscle Fascia (Fig. 1.14) The muscle fascia interweaves with the anterior thirds of the sheaths of the rectus muscles (mostly at points where their ligaments are attached to the fibrous tunic of the eyeball) into an integral system and becomes

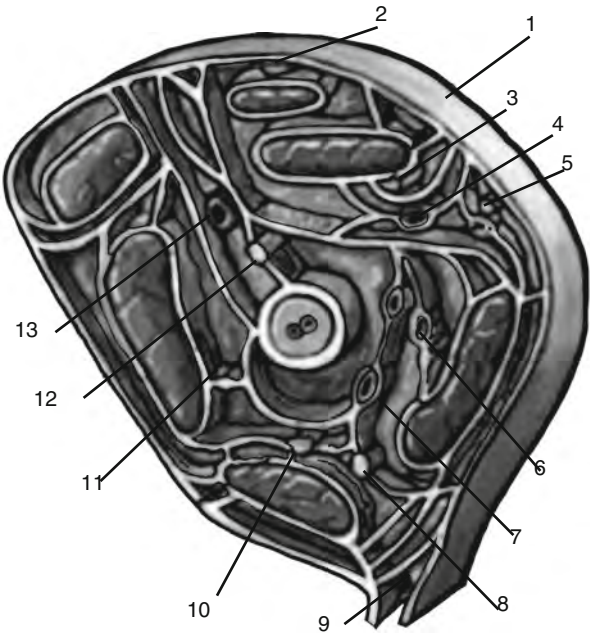

Fig. 1.13 Anatomy of the fascial system of the orbit behind the eyeball. Oblique coronal view. (*1*) Periosteum; (*2*) frontal nerve; (*3*) superior branch of the oculomotor nerve innervating the superior rectus muscle; (*4*) superior ophthalmic vein and the ligament fixing it; (*5*) lacrimal nerve; (*6*) abducens nerve; (*7*) inferior ophthalmic vein; (*8*) small branch of the oculomotor nerve connecting with the inferior oblique muscle; (*9*) zygomatic nerve; (*10*) small branch of the oculomotor nerve connecting with the inferior rectus muscle; (*11*) branch of the oculomotor nerve connecting with the medial rectus muscle; (*12*) nasociliary nerve; and (*13*) ophthalmic artery. It comes under notice that the structure of the ligament system of the orbit becomes simpler and results in elimination of the intraconal space (According to Dutton [27] with amendments)

noticeably thinner in its posterior portion near the common tendinous ring. As a result, the border between the central (intraconal) and peripheral (extraconal) surgical spaces is eliminated near the orbital apex. Thus, the conventional concept suggesting that there is a muscular funnel as a continuous cone formed by muscle fascia is not consistent with the reality [29].

A thinner inner wall of muscle sheaths is adherent to the septa separating the lobules of the intraconal (i.e., lying within the muscular cone) compartment of adipose tissue. The outer, considerably thicker portion of the sheaths is attached to the orbital walls with connective tissue cords. The thickest cords can be found in the anterior segments of the orbit, where they form *supporting ligaments* or *tendinous expansions of muscles* that control the amplitude of eye movements [30].

The supporting ligament of the medial rectus is attached to the bone at several points behind the posterior lacrimal crest and to the tarso-orbital fascia, the lacrimal caruncle, and the plica semilunaris (Fig. 1.15).

The thickest ligament (the ligament of the lateral rectus) is attached to the posterior edge of Whitnall's orbital tubercle, the lateral conjunctival fornix, the

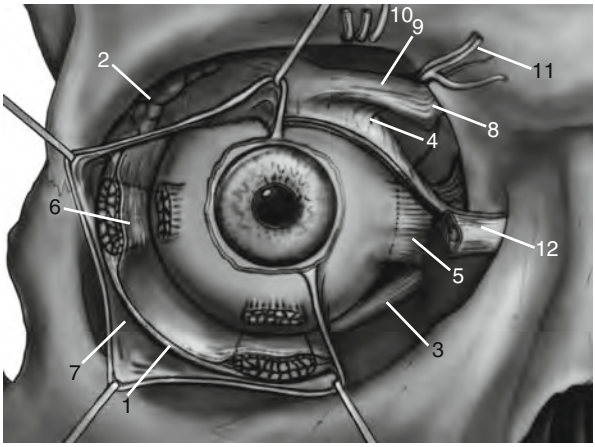

Fig. 1.14 Tenon's fascia of the eyeball. Anterior view. (*1*) (inter)muscular fascia residing under Tenon's capsule and connecting the sheaths of extraocular muscles into an integral system; (*2*) orbital portion of the lacrimal gland; (*3*) Lockwood's ligament; (*4*) levator aponeurosis; (*5*) ligament supporting the medial rectus muscle; (*6*) muscle sheath; (*7*) Tenon's fascia; (*8*) trochlea; (*9*) Whitnall's ligament; (*10*) supraorbital neurovascular bundle; (*11*) supratrochlear nerve; and (*12*) medial palpebral ligament

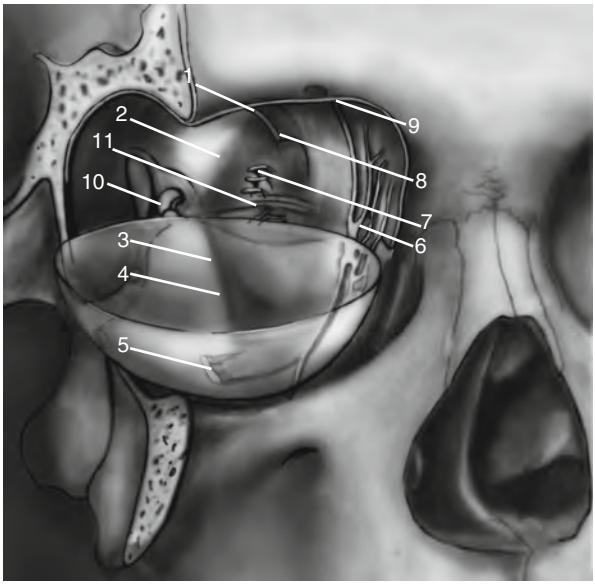

Fig. 1.15 Anatomy of the most well-developed supporting system of the medial rectus muscle that reaches the inferior wall, the inferior rectus muscle, and the superior muscle complex. (*1*) Ligament suspending the superior ophthalmic vein; (*2*) attachment of the muscle sheath to the orbital roof; (*3, 4*) fibers attaching the muscle to the orbital floor; (*5*) region of adhesion between the fascial sheaths of the inferior rectus and inferior oblique muscles; (*6*) supporting ligament of the medial rectus muscle; (*7*) points of fixation to the posterior pole of the eyeball; (*8*) medial horn of the levator aponeurosis; (*9*) its attachment to the orbit; (*10*) optic nerve; and (*11*) medial rectus muscle

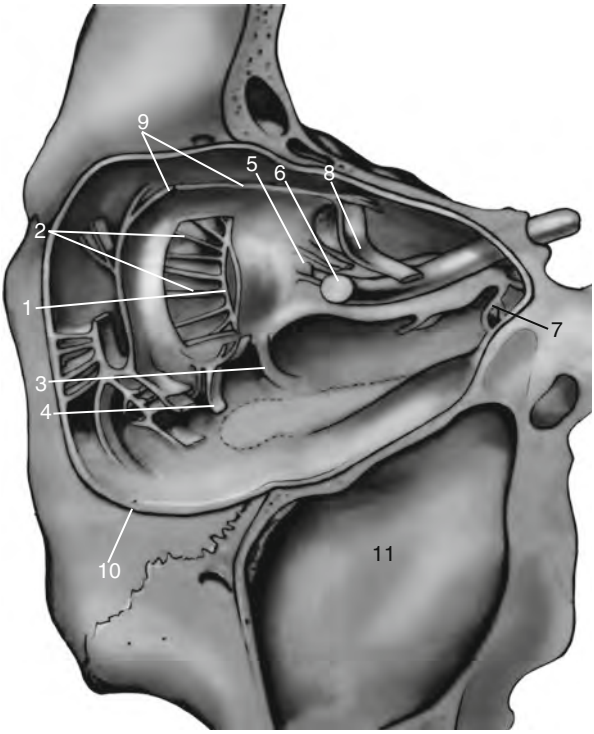

Fig. 1.16 Anatomy of the attaching system of the lateral rectus muscle. (*1*) Lateral rectus muscle; (*2*) numerous adhesions between its sheath and the lateral orbital wall; (*3, 4*) attachments to the sheaths of the inferior rectus and inferior oblique muscles; (*5*) delicate adhesions to the dura mater of the optic nerve (*6*); (*7*) point where the lateral rectus muscle is attached to the orbital floor; (*8*) ligament suspending the superior ophthalmic vein; (*9*) lateral horn of the levator aponeurosis; (*10*) periosteum; and (*11*) maxillary sinus

tarso-orbital fascia, and further the lateral orbital wall along the entire length of the ligament up to the common tendinous ring (Fig. 1.16). Efficient contraction of the belly of the lateral rectus passing round the sclera would probably be impossible if attachment of its sheath was not so extensive [27].

The medial palpebral ligament (*lig. palpebrale mediale*) consists of the anterior and posterior crura. The anterior crus is a wide fibrous structure attaching the eyelids to the anterior lacrimal crest of the frontal process of the maxilla. It gives rise to the superficial heads of the pretarsal and preseptal portions of the palpebral part of the orbicularis oculi muscle that is responsible for voluntary (winking) and involuntary (blinking) movements of the eyelids (Fig. 1.17a).

The posterior crus of the medial palpebral ligament attached to the posterior lacrimal crest and the lacrimal sac fossa pulls the internal portions of the eyelid backward, thus providing their tight contact with the ocular surface. In addition, the deep heads of the pretarsal (*m. tensor m. tarsalis Horner*) and preseptal (*L. Jones muscle*) portions of the orbicularis oculi muscle, which originate from the posterior lacrimal crest and the surrounding fascia, merge with the posterior crus. Thus, the medial palpebral ligament plays a crucial role in lacrimal pump function by shortening the lacrimal canaliculi and displacing the lacrimal puncta inward (Fig. 1.17b).

Furthermore, the medial palpebral ligament is attached by the so-called superior supporting crus to the frontal bone and provides the medial angle profile of the palpebral fissure.

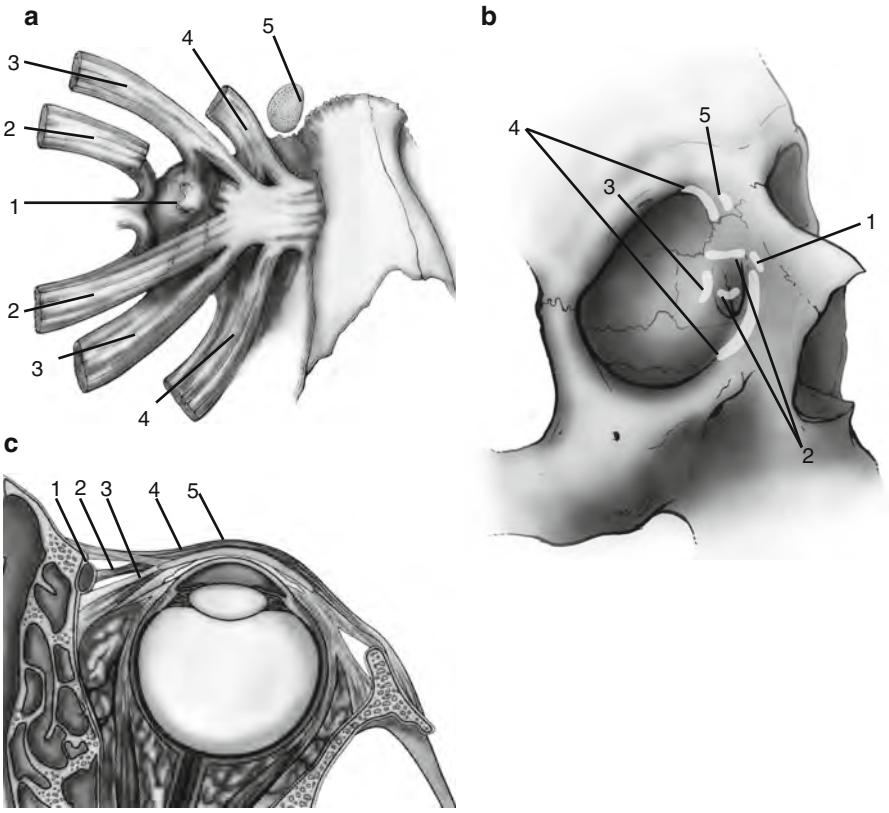

Fig. 1.17 Anatomy of the medial palpebral ligament. (**a**) Superficial and deep heads of the pretarsal (*2*) and preseptal (*3*) portions of the palpebral part of the orbicularis oculi muscle, which form the lacrimal pump together with the lacrimal sac fascia (*1*); (*4*) orbital portion of the orbicularis oculi muscle; (*5*) origination of the corrugator supercilii muscle (*m. corrugator supercilii*) (Adapted from Jones and Wobig [62]). (**b**) Sites where the portions of the palpebral part of the orbicularis oculi muscle are attached: (*1*) medial palpebral ligament; (*2*) deep head of the preseptal portion; (*3*) deep head of the pretarsal portion; (*4*) orbital portion of the orbicularis oculi muscle; (*5*) corrugator supercilii muscle (m. corrugator supercilii). (**c**) Axial section of retinaculum mediale: (*1*) lacrimal sac; (*2*) Jones' muscle; (*3*) Horner's muscle; (*4*) pretarsal portion of the palpebral part of the orbicularis oculi muscle; and (*5*) tarsus

The combination of soft tissue structures attached to the periosteum of the posterior lacrimal crest forms the medial retinaculum (*retinaculum mediale*). These structures include the inferior and superior transverse (Lockwood's and Whitnall's) ligaments, the supporting ligament of the medial rectus, Horner's muscle, the medial horn of the levator aponeurosis, and the tarso-orbital fascia.

Lateral palpebral ligament (*lig. palpebrale laterale*) is 10.5 mm long, 1 mm thick, and 3 mm wide. It continues in the tarsal plates and fibers of the orbicularis oculi muscle, ensuring attachment of the lateral canthal angle and tarsi to Whitnall's

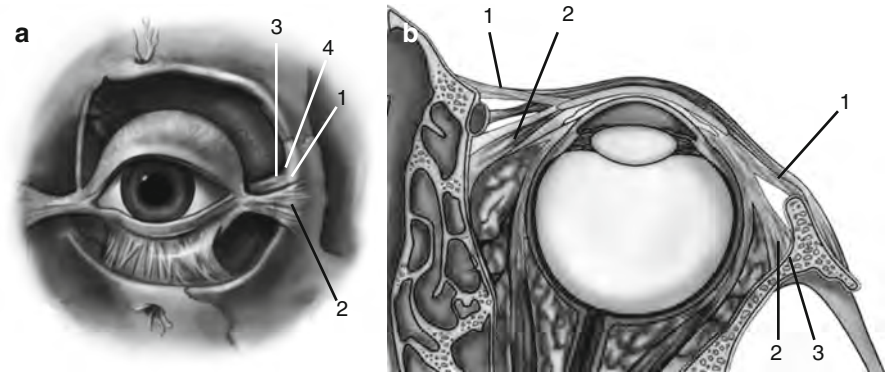

Fig. 1.18 Anatomy of the lateral palpebral ligament. (**a**) Anterior view: (*1*) Eisler's space filled with adipose tissue; (*2*) anterior crus of the lateral palpebral ligament or the superficial lateral canthal tendon; (*3*) posterior crus of the lateral palpebral ligament attached to Whitnall's tubercle (*4*). (**b**) Axial section of the medial and lateral palpebral ligaments: (*1*) anterior crus; (*2*) posterior crus; and (*3*) Whitnall's tubercle

orbital tubercle. Some fibers of the lateral palpebral ligament [31] are attached directly to the lateral orbital margin (Fig. 1.18).

The middle point of the lateral palpebral ligament is 10 mm inferior to the frontozygomatic suture and 2–3 mm superior to the middle point of the medial ligament.

As the lateral ligament approaches the tubercle, it becomes wider, up to 6–7 mm, due to its merging with the lateral horn of the levator aponeurosis, deep fibers of the pretarsal portion of the orbicularis oculi muscle, supporting ligament of the lateral rectus, as well as Lockwood's and Whitnall's ligaments. The combination of connective tissue structures attached to Whitnall's tubercle forms the so-called lateral retinaculum (retinaculum laterale).

Adhesion of the supporting ligament of the lateral rectus to the palpebral ligament makes lateral displacement of the external canthal angle by 2 mm when maintaining an extreme sideward gaze possible in order to expand the peripheral field of view.

Flowers et al. [32] distinguish the so-called external tarsal strip, an independent anatomical structure connecting the inferior tarsus with the inferolateral orbital margin and being attached 3 mm below and 1 mm deeper the lateral ligament (i.e., ~4–5 mm posteriorly the orbital margin).

The anterior portions of the sheaths of the superior rectus and the levator palpebrae superioris muscle are connected by intermuscular fascia [33], forming the so-called superior muscle complex (Fig. 1.19). *Whitnall's superior transverse ligament* acts as a supporting ligament that limits palpebral retraction during supraduction and enhances the efficiency of levator contraction [34, 35]. This horizontal whitish structure made of collagen and elastin lies in the upper eyelid 10 mm above the superior tarsus and is the compacted anterior sheet of the connective tissue tunic of

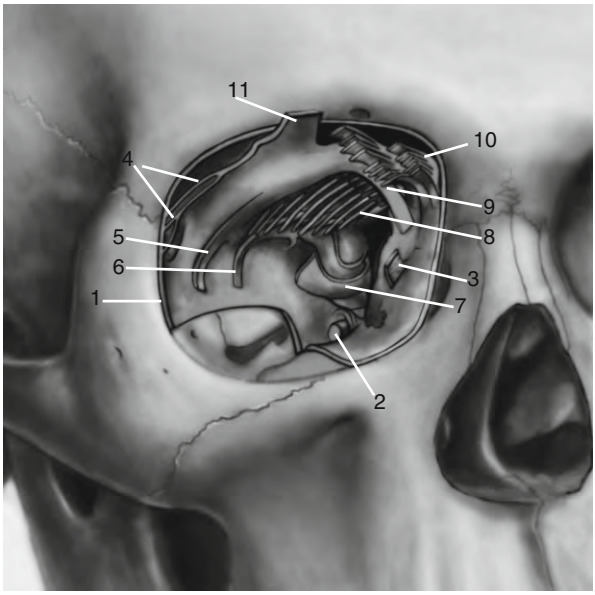

Fig. 1.19 Anatomy of the system supporting the superior rectus muscle, the levator palpebrae superioris muscle, and the superior oblique muscle. (*1*) Periosteum; (*2*) optic nerve; (*3*) superior oblique muscle; (*4*) lateral horn of the levator aponeurosis; (*5, 6*) its attachment to the ligaments of the lateral rectus muscle; (*7*) ligament suspending the superior ophthalmic vein; (*8*) connective tissue septa between the sheath of the superior oblique muscle and the posterior surface of the eyeball; (*9*) medial horn of the levator aponeurosis; (*10*) trochlear ligament system; (*11*) point where the levator palpebrae superioris muscle is attached to the tarsal plate and palpebral skin

the levator palpebrae superioris muscle. The medial edge of the ligament is attached to the trochlear fascia and the tendon of the superior rectus muscle, sharing its fibers with *retinaculum mediale*. The lateral edge of the ligament is attached to the fascia of the orbital portion of the lacrimal gland and the frontozygomatic suture by intertwining with *retinaculum laterale* (Fig. 1.20).

Behind Whitnall's ligament, the posterior surface of the levator aponeurosis and the superior surface of the superior rectus are also connected by dense intermuscular fascia with the *suspensory ligament of the superior conjunctival fornix* originating from its anterior surface (Fig. 1.21). Furthermore, the medial edges of these muscles are bound by connective tissue septa [36].

The *horns of the levator aponeurosis* are wide fibrous structures at aponeurotic edges that have nothing to do with Whitnall's ligament and are situated below it (Fig. 1.20). The *lateral horn* is thicker than the medial one; it separates the lacrimal gland into the palpebral and orbital lobes; then it reaches the retinaculum laterale and is attached to Whitnall's tubercle. The *medial horn* passes superiorly to the tendon of the superior oblique muscle, forming a weak adhesion to Whitnall's ligament. Then it reaches the *retinaculum mediale* and is attached to the medial palpebral ligament and the posterior lacrimal crest. *The lateral and posterior medial*

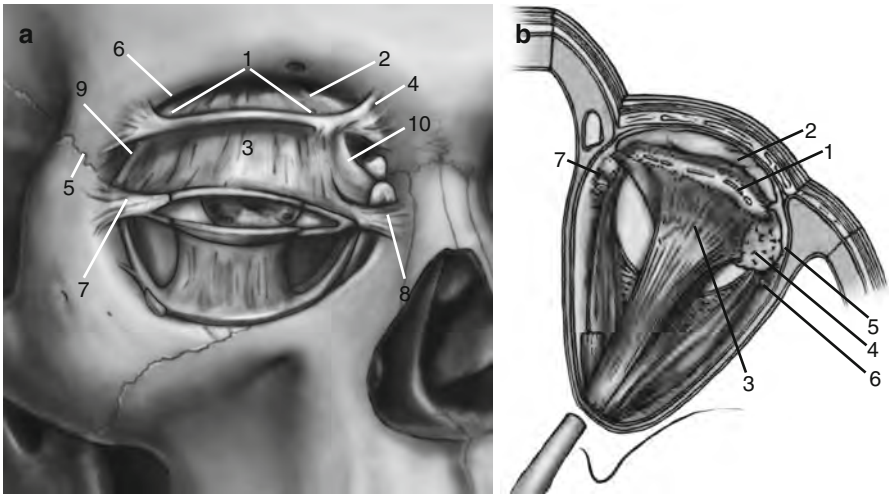

Fig. 1.20 Whitnall's superior transverse ligament. (**a**) Anterior view: (*1*) Whitnall's ligament; (*2*) levator palpebrae superioris muscle; (*3*) levator aponeurosis; (*4*) trochlea; (*5*) frontozygomatic suture; (*6*) lacrimal gland; (*7*) lateral palpebral ligament; (*8*) medial palpebral ligament; (*9*) lateral horn of the levator aponeurosis; and (*10*) medial horn of the levator aponeurosis. (**b**) Dorsal view: (*1*) Whitnall's ligament; (*2*) preaponeurotic fat pad of the upper eyelid; (*3*) levator palpebrae superioris muscle; (*4*) orbital portion of the lacrimal gland; (*5*) Whitnall's tubercle; (*6*) supporting ligament of the lateral rectus muscle; and (*7*) supporting ligament of the medial rectus muscle

adhesions of the horns of levator aponeurosis play a crucial role in maintaining proper position of the eyelids and the eyeball.

Levator aponeurosis is interwoven with subcutaneous tissues (but not with the palpebral skin). It is connected to the preseptal portion of the orbicularis oculi muscle and the tarso-orbital fascia 2–3 mm superior to the tarsus edge, forming an upper eyelid fold 8–10 mm away from the eyelid edge. Furthermore, one-third of fibers from the levator aponeurosis are tightly interwoven with the lower one-third of the anterior surface of the superior tarsus [37, 38].

The *superior tarsal muscle* (*m. tarsalis superior Müller*) originates from the inferior levator surface 20–22 mm away from the upper edge of the tarsus. The tight contact with the levator palpebrae superioris muscle is maintained only at its origin; then the muscles can be easily separated, forming *Jones' postaponeurotic space*. The muscle is attached to the upper edge of the tarsus where there lies the *peripheral arterial arc* between the tarsal muscle and the levator (Fig. 1.21).

The merged sheaths of the inferior rectus and inferior oblique muscles form the *inferior muscle complex* (Fig. 1.22) attached by thin supporting ligaments to the orbital floor. The thick branch of the sheath of the inferior rectus, known as the *capsulopalpebral head*, passes superiorly and inferiorly around the inferior oblique muscle, goes anterior, and merges with Lockwood's ligament in front of the inferior oblique muscle to form the *capsulopalpebral fascia*, an analogue of the levator

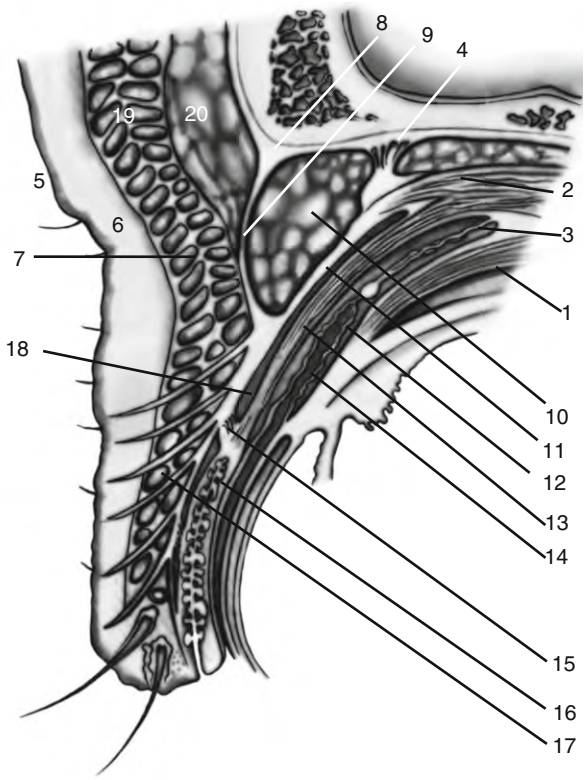

Fig. 1.21 Anatomy of the upper eyelid. (*1*) Superior rectus muscle; (*2*) levator palpebrae superioris muscle; (*3*) ligament suspending the superior conjunctival fornix; (*4*) Whitnall's ligament; (*5*) skin; (*6*) subcutaneous tissue; (*7*) preseptal portion of the orbicularis oculi muscle; (*8*) arcus marginalis; (*9*) orbital septum (tarso-orbital fascia); (*10*) preaponeurotic fat pad; (*11*) levator aponeurosis; (*12*) superior conjunctival fornix; (*13*) Müller's muscle; (*14*) conjunctiva; (*15*) adhesions between the levator aponeurosis and Müller's muscle; (*16*) superior tarsus; (*17*) pretarsal portion of the orbicularis oculi muscle; (*18*) Jones' postaponeurotic space; (*19*) frontal muscle forming the anterior border of the eyebrow fat pad (*20*) together with the orbicularis oculi muscle. It continues inferiorly as adipose tissue localizing behind the orbital and preseptal portion of the orbicularis oculi muscle (retro-orbicularis oculi fat, ROOF) and being a component of the superficial musculoaponeurotic system (SMAS)

aponeurosis (Fig. 1.23) [39]. The capsulopalpebral fascia does not have its own motor innervation but imitates contractions of the inferior rectus muscle, thus ensuring 3–5 mm retraction of the lower eyelid during infraduction of the eyeball.

Adrenergic smooth muscle fibers of the inferior tarsal muscle (*m. tarsalis inferior*) lie between the capsulopalpebral fascia and the conjunctiva of the lower eyelid. The inferior tarsal muscle is similar to Müller's muscle but is less compact and is not directly attached to the tarsus (Fig. 1.23). The fibers of the capsulopalpebral fascia and the inferior tarsal muscle are interwoven with the tarso-orbital fascia 4–5 mm inferiorly to the lower edge of the inferior tarsus and are attached to it as a single layer (they are the two *lower eyelid retractors*).

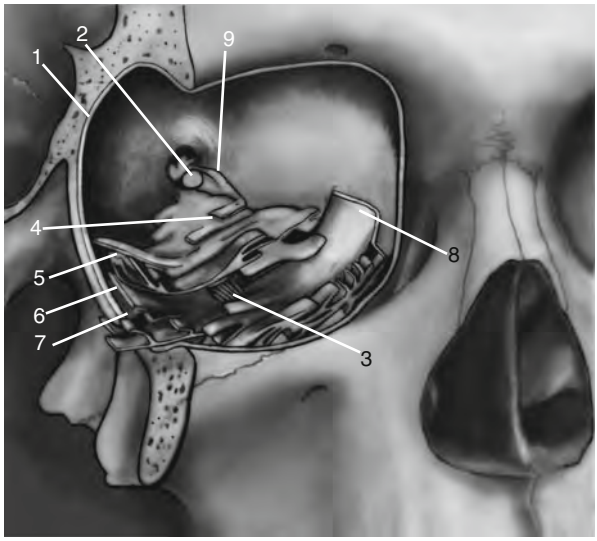

Fig. 1.22 Ligamentary apparatus of the inferior rectus and inferior oblique muscles. (*1*) Periosteum; (*2*) optic nerve; (*3*) inferior oblique muscle; (*4*) ligament supporting the inferior rectus muscle; (*5, 6*) adhesions with the sheath of the lateral rectus muscle; (*7*) points where the muscles are attached to the lateral orbital wall; (*8*) contact points with the sheath of the medial rectus muscle; (*9*) ligament suspending the superior ophthalmic vein

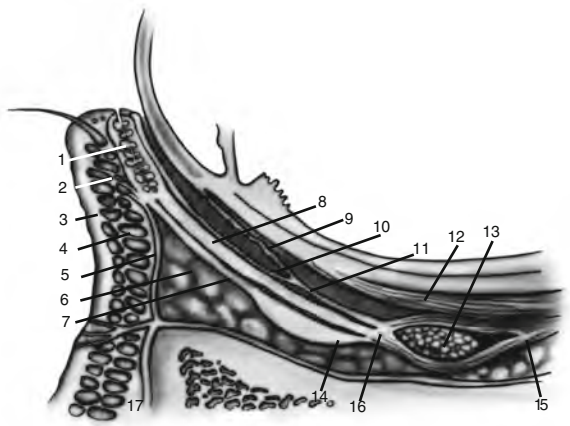

Fig. 1.23 Anatomy of the lower eyelid. (*1*) Inferior tarsus (*tarsus inf.*); (*2*) pretarsal portion of the orbicularis oculi; (*3*) skin; (*4*) preseptal portion of the orbicularis oculi; (*5*) orbital septum; (*6*) adipose tissue of the orbit; (*7*) capsulopalpebral fascia; (*8*) inferior tarsal muscle; (*9*) conjunctiva; (*10*) inferior conjunctival fornix; (*11*) ligament supporting the inferior conjunctival fornix; (*12*) inferior rectus muscle; (*13*) inferior oblique muscle; (*14*) Lockwood's inferior transversal ligament; (*15*) capsulopalpebral head; (*16*) capsulopalpebral fascia; (*17*) suborbital fat pad

Lockwood's inferior transverse ligament consists of the interwoven fasciae of the inferior muscle complex, the supporting muscular ligaments, the thickening of Tenon's capsule, the sheath of the inferior rectus muscle, and the lower eyelid retractors [40]. This "hammock," 40–45 mm long, 5–8 mm wide, and 1 mm thick, is suspended between Whitnall's tubercle and the periosteum behind the posterior

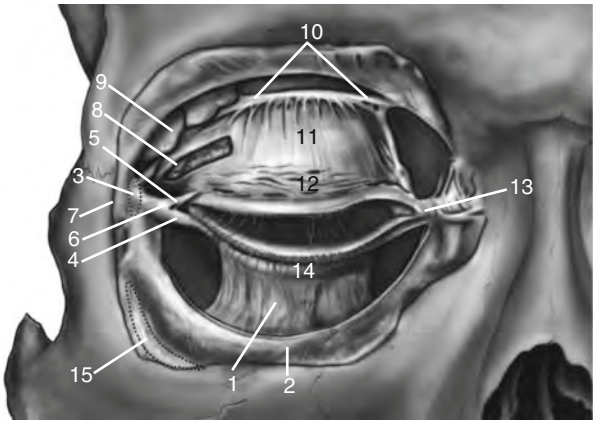

Fig. 1.24 Anatomy of the capsulopalpebral fascia. (*1*) Capsulopalpebral fascia; (*2*) partially excised orbital septum; (*3*) fat-filled recess of Eisler's fat pad; (*4*) inferior crus of the lateral palpebral ligament; (*5*) superior crus of the lateral palpebral ligament; (*6*) lateral palpebral ligament; (*7*) Whitnall's tubercle; (*8*) palpebral portion of the lacrimal gland; (*9*) orbital portion of the lacrimal gland; (*10*) Whitnall's ligament; (*11*) levator aponeurosis; (*12*) superior tarsus (tarsus sup.); (*13*) medial palpebral ligament; (*14*) inferior tarsus (*tarsus inf.*); (*15*) premarginal fat-filled recess

lacrimal crest. It is best defined in the projection of the inferior oblique muscle (Figs. 1.23 and 1.24). The anterior portions of Lockwood's ligament are interwoven with the inferior conjunctival fornix as a suspensory ligament. In addition, Lockwood's fascia is connected to the lower edge of the inferior tarsus, Tenon's capsule, the preseptal portion of the orbicularis oculi muscle, and the palpebral skin at the level of the subtarsal fold through the palpebral fascia.

The *common tendinous ring* (annulus tendineus communis Zinn) is a connective tissue structure formed by the dura mater that penetrates into the orbit through the optic canal. Near the optic foramen, the dura mater is split into two sheets: one of those is interwoven with the periosteum, while the second one forms the optic nerve sheath. The base of the common tendinous ring lies in the slit-like space between these sheets.

Tightly merged with the periosteum of the orbital apex around the optic foramen and the superior orbital fissure, the ring surrounds the *oculomotor foramen* (Fig. 1.7). Furthermore, fibers of the common tendinous ring are interwoven with the superomedial portion of the perineural sheath of the optic nerve, causing pain sensations accompanying the eye movements in patients with retrobulbar neuritis. Tight adhesion of the common tendinous ring to the optic nerve sheaths also explains the emergence of traumatic optic neuropathy caused by a frontal shock. This type of shock causes the inertial anteriad displacement of the eyeball, resulting in abrupt tension of the intraocular and canal portions of the optic nerve and therefore in a rupture of the feeding pial vessels [41–44].

In the lumen of the superior orbital fissure, the posterior surface of the ring is merged with the dura mater. Finally, the lower fibers of the common tendinous ring are interwoven with the orbital muscle of Müller closing the lumen of the inferior orbital fissure.

The common tendinous ring consists of the superior arc-shaped ligament (*Lockwood's superior orbital tendon*) and the thicker inferior arc-shaped ligament (*Zinn's inferior orbital tendon*). The superior, lateral, and medial rectus muscles originate from the superior ligament; the inferior ligament gives rise to the inferior rectus. Although the levator palpebrae superioris and the superior oblique muscles are situated in immediate proximity to the ring, they originate from the periosteum of the lesser wing and the body of the sphenoid bone, respectively, and lie above the superior rectus.

Proper spatial position of the levator palpebrae superioris and the superior rectus muscles as they pass anteriad is maintained by the *suspensory system of diffusely arranged ligaments attached to the orbital roof*. The fascial adhesions between the levator palpebrae superioris and the superior rectus muscles further ensure fine-tuning of the degree of upper eyelid retraction during upward gaze. Finally, the *suspensory ligament of the superior ophthalmic vein* originates from the inferior surface of the superior rectus muscle.

The orbital muscle of Müller (m. orbitalis Müller, m. sphenomaxillaris) bridges the inferior orbital fissure and separates the orbit from the pterygopalatine fossa lying below it. The function of this smooth muscle structure in humans remains unknown. The muscle may affect blood outflow due to its proximity to the inferior ophthalmic vein. It is most likely that Müller's muscle is a rudimentary structure that has lost its original function during the evolution of the orbital walls [27].

The orbital cavity is filled with orbital fat (*corpus adiposum orbitae*), which forms an elastic cushion for the eyeball. The fat is encapsulated in a thin connective tissue capsule and permeated with connective tissue trabeculae (the septa that divide it into small segments in the anterior portion and larger sections, in the posterior portion). The multiple septa of the orbital fat are an integral part of the ligamentary system of the eyeball and the orbit (Fig. 1.25a). As a result, even entrapment of the adipose tissue only in the fracture area may cause severe oculomotor disorders (Fig. 1.25b).

Orbital adipose tissue is not a homogenous medium that can migrate from one orbital section to another one. It occupies three compartments: (1) anterior to the extraocular muscles, (2) inward from the muscular cone (extraconally), and (3) in the muscular cone (intraconally). These compartments form the corresponding surgical spaces.

In the depth of the upper eyelid, the orbital septum (anteriorly) and the levator aponeurosis (posteriorly) bound the *central preaponeurotic fat pad* and the smaller *medial fat pad*, which are separated by the trochlea (Fig. 1.25c). The lacrimal gland occupies the position of the lateral fat pad.

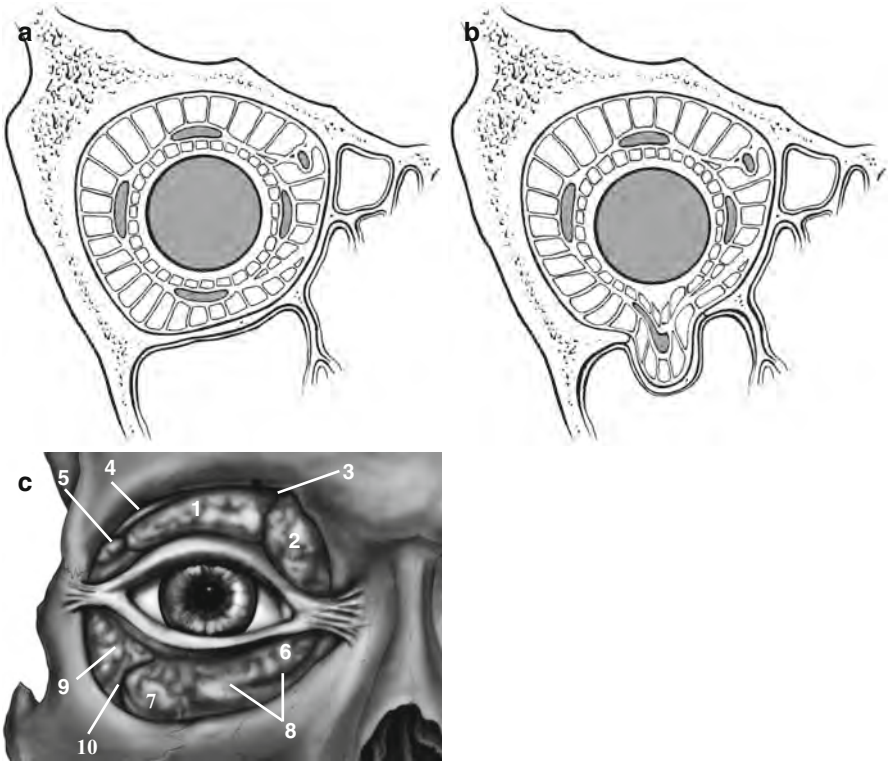

Fig. 1.25 Connective tissue system of the orbital fat body (According to Koornneef [61]). (**a**) Normal condition, (**b**) blowout fracture of the orbital floor. (**b**) Shows that the connective tissue septa and adipose tissue are the primary structures to be entrapped in the bone defect. The muscle typically is adjacent to the fracture area. Nevertheless, the disrupted architectonics is enough to cause muscular imbalance; (**c**) Fat pads of the eyelids: (*1*) central preaponeurotic fat pad of the upper eyelid; (*2*) medial fat pad of the upper eyelid; (*3*) trochlea; (*4*) lacrimal gland; (*5*) Eisler's fat pad; (*6*) medial fat pad of the lower eyelid; (*7*) central fat pad of the lower eyelid; (*8*) the inferior oblique muscle separating them; (*9*) lateral fat pad of the lower eyelid; (*10*) arc-shaped ligament coming off the capsulopalpebral fascia and attached to the inferolateral orbital edge; it separates the central and lateral fat pads of the lower eyelid

The central preaponeurotic fat pad is a loose yellow structure. The medial fat pad of the upper eyelid is denser and lighter (pale yellow or white). The infratrochlear nerve (*n. infratrochlearis*, the terminal branch of the nasociliary nerve) and the medial palpebral artery (*a. palpebralis medialis*) from the ophthalmic artery system pass through it.

The lower eyelid contains three retroseptal fat pads. The *medial* and *central fat pads* are separated by the inferior oblique muscle. The central and the *lateral fat pads* are separated by the arc-shaped ligament coming off the capsulopalpebral fascia and attached to the inferolateral margin of the orbit [45].

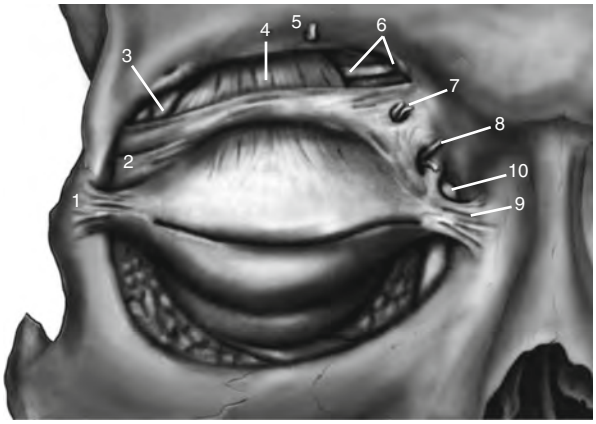

Fig. 1.26 Anatomy of the orbital septum (*septum orbitale*). (*1*) Lateral palpebral ligament; (*2*) the lateral portion of the septum attached behind the lateral palpebral ligament, forming Eisler's space; (*3*) palpebral portion of the lacrimal gland; (*4*) the levator palpebrae superioris muscle; (*5*) supraorbital nerve; (*6*) tendon of the superior oblique muscle and the trochlea residing behind the orbital septum; (*7, 8*) runout areas of the supra- and infratrochlear nerves; (*9*) anterior crus of the medial palpebral ligament; (*10*) lacrimal sac with its fornix localized extraorbitally (preseptally) and its lower half localized in the orbit (retroseptally)

Displacement or loss of the pre-equatorial fat after injury has no effect on the position of the eye in the orbit but may deepen the upper eyelid sulcus. Post-equatorial fractures of the orbital walls cause enophthalmos due to displacement of the posterior portions of the orbital fat outside the orbit.

The *orbital septum* (tarso-orbital fascia, *septum orbitale*) is a well-defined thin multilayered fascial structure in the frontal plane and is the anterior soft tissue border of the sophisticated suspensory orbital system. Due to its mechanical strength, the orbital septum acts as a barrier preventing the spread of infection inside the orbit.

The orbital septum originates from the maxillary periosteum and the orbital floor periosteum at the orbital margin (known as *arcus marginalis*) and goes deep into the eyelids where it interweaves with eyelid retractors. The loose tissue known as suborbicular fascia (*fascia suborbicularis*) lies directly in front of the fascia. It is separated into small sections and is in the same plane as the *zygomatic fat pad* and the *fat pad* lying under the orbicularis oculi muscle (Fig. 1.26) [46]. The suborbicular fascia is covered with a thin layer of the preseptal portion of the orbicularis oculi muscle and skin [47].

Temporally, the tarso-orbital fascia is interwoven with the lateral horn of the levator aponeurosis and is attached to the lateral orbital margin 1.5 mm anteriad from Whitnall's tubercle and the lateral palpebral ligament, thus forming the slit-like space known as the fat-filled recess of Eisler.

In the superomedial portion of the orbital opening, the orbital septum goes above the supraorbital notch and lies in front of the trochlea.

Medially, the orbital septum is attached to the posterior lacrimal crest of the lacrimal bone, thus being located posteriorly to the fornix of the lacrimal sac and Horner's muscle and anteriorly to the ligament attaching the medial rectus. The attachment point of the orbital septum then is displaced in a downward–forward direction, crosses the lacrimal sac fossa, reaches the anterior lacrimal crest at the level of the lacrimal tubercle (the attachment point of the anterior crus of the medial palpebral ligament), and further descends to the infraorbital margin. Thus, the fornix of the lacrimal sac is located extraorbitally (preseptally), while its inferior half lies inside the orbit (retroseptally).

Several millimeters outward from the zygomaticomaxillary suture, the tarso-orbital fascia goes to the facial surface of the zygomatic bone and spreads up to the frontozygomatic suture, forming the premarginal recess, up to 3–4 mm deep (which actually is the inferior continuation of the recess of Eisler).

Deep in the upper eyelid, the tarso-orbital fascia is not interwoven with the upper tarsal margin. To be more exact, it is interwoven with the epimysium of the levator palpebrae superioris muscle at the point where it merges with the levator aponeurosis 10 mm away from the eyelid margin or 2–5 mm away from the upper tarsal margin. The thin continuation of the tarso-orbital fascia further covers the anterior tarsal surface, acting as an additional portion of the levator aponeurosis [48].

Deep in the lower eyelid, the fascia is interwoven with the inferior tarsal margin (sometimes it can be preliminarily merged to the lower eyelid retractor 4–5 mm away from the inferior tarsal plate).

Table 1.3 lists the important reference data on the anatomy of extraocular muscles.

Table 1.3 Some anatomical aspects of the extraocular muscles

Muscle	Properties
Levator palpebrae superioris muscle (m. levator palpebrae superioris)	*Point of origin*: a thin narrow tendon attached to the lesser wing of the sphenoid bone posteriorly to the common tendinous ring and infero-exteriorly to the optic foramen
	Insertion point: the orbital septum 2–3 mm superiorly to the tarsal margin (8–10 mm away from the eyelid margin), preseptal portion of the palpebral part of the orbicularis oculi muscle and the adjacent subcutaneous tissues, the lower one-third of the anterior surface of the superior tarsus
	Function: elevates the upper eyelid
	Blood supply: superior (lateral) muscular artery (a branch of the ophthalmic artery), supraorbital artery, posterior ethmoidal artery, peripheral arterial arcade of the upper eyelid
	Innervation: bilateral via the superior branch of the oculomotor nerve (n. III). The superior branch of n. III enters the levator inferiorly, on the border between its posterior and middle thirds, 12–13 mm away from the orbital apex
	Anatomical details: the muscle belly length is 40 mm, and the aponeurosis length is 20–40 mm. The lateral horn of the levator aponeurosis divides the lacrimal gland into the orbital and palpebral portions connected by a small isthmus

Table 1.3 (continued)

Muscle	Properties
Superior tarsal muscle (m. tarsalis superior)	*Point of origin*: the inferior surface of the levator palpebrae superioris muscle, 20–22 mm away from the superior tarsal margin
	Insertion point: the superior margin of the superior tarsus, where the peripheral arterial arcade localizes between the superior tarsal muscle and the levator palpebrae superioris muscle
	Function: elevates the upper eyelid by up to 2 mm
	Blood supply: the superior (lateral) muscular artery (a branch of the ophthalmic artery), supraorbital artery, posterior ethmoidal artery, peripheral arterial arcade of the upper eyelid
	Innervation: sympathetic innervation of the internal carotid plexus
	Anatomical details: tight contact between the superior tarsal muscle with the levator palpebrae superioris muscle remains only in the muscle portion near its point of origin. Then the muscles can be easily separated, forming Jones' postaponeurotic space
Superior rectus muscle (m. rectus superior)	*Point of origin*: Lockwood's superior orbital tendon (a fragment of the common tendinous ring), in direct proximity from the perineural sheath of the optic nerve
	Insertion point: in the sclera, 6.7 mm away from the limbus (at a certain tilt angle) and slightly medially to the vertical axis of eyeball rotation, which explains the variety of its functions
	Function: the primary function, supraduction (75 % of muscular effort); the secondary function, incycloduction (16 % of muscular effort); the tertiary function, adduction (9 % of muscular effort)
	Blood supply: superior (lateral) muscular branch of the ophthalmic artery; the lacrimal, supraorbital, and posterior ethmoidal arteries
	Innervation: the superior branch of the ipsilateral oculomotor nerve (n. III). Motor fibers typically penetrate into this one and almost all other muscles on the border between its posterior and middle thirds
	Anatomical details: the muscle is attached to the sclera posteriorly to the ora serrata. As a result, scleral perforation caused by a bridle suture pass posterior to the muscle insertion results in a retinal defect. Together with the levator palpebrae superioris muscle, the superior rectus muscle forms the superior muscle complex
Inferior rectus muscle (m. rectus inferior)	*Point of origin*: the inferior tendon of Zinn (a fragment of the common tendinous ring)
	Insertion point: to the sclera 5.9 mm away from the limbus (at a certain tilt angle) and slightly medially to the vertical axis of eyeball rotation, which explains the variety of its functions
	Function: the primary function, infraduction (73 %); the secondary function, excycloduction (17 %); and the tertiary function, adduction (10 %)
	Blood supply: the inferior (medial) muscular branch of the ophthalmic artery, the supraorbital artery
	Innervation: the inferior branch of the ipsilateral oculomotor nerve (n. III)
	Anatomical details: together with the inferior oblique muscle forms the inferior muscle complex

(continued)

Table 1.3 (continued)

Muscle	Properties
Lateral rectus muscle (m. rectus lateralis)	*Point of origin*: the medial crus originates from Lockwood's superior tendon (a fragment of the common tendinous ring); the inconstant (lateral) crus originates from the bony spur (*spina recti lateralis*) in the middle of the inferior margin of the superior orbital fissure
	Insertion point: to sclera 6.3 mm away from the limbus
	Function: the primary function—abduction (99.9 % of muscular effort)
	Blood supply: the superior (lateral) muscular branch from the ophthalmic artery, the lacrimal artery, sometimes the infraorbital artery and the inferior (medial) muscular branch of the ophthalmic artery
	Innervation: the ipsilateral abducens nerve (n. VI)
	Anatomical details: has the thickest attaching ligament
Medial rectus muscle (m. rectus medialis)	*Point of origin*: Lockwood's superior orbital ligament (a fragment of the common tendinous ring) in direct proximity to the perineural sheath of the optic nerve
	Insertion point: to the sclera 5 mm away from the limbus
	Function: the primary function—abduction (99.9 % of muscular effort)
	Blood supply: the inferior (medial) muscular branch of the ophthalmic artery; the posterior ethmoidal artery
	Innervation: the inferior branch of the ipsilateral oculomotor nerve (n. III)
	Anatomical details: the strongest extraocular muscle
Inferior oblique muscle (m. obliquus inferior)	*Point of origin*: periosteum of the flat area of the orbital surface of the maxilla anteriorly to the lacrimal crest near the opening of the nasolacrimal duct
	Insertion point: the postero-exterior surface of the eyeball slightly posteriorly to the vertical axis of eyeball rotation
	Function: the primary function, excycloduction (59 %); the secondary function, supraduction (40 %); and the tertiary function, abduction (1 %)
	Blood supply: the inferior (medial) muscular branch of the ophthalmic artery; supraorbital artery; rarely, the lacrimal artery
	Innervation: the inferior branch of the contralateral oculomotor nerve (n. III) passing along the outer margin of the inferior rectus muscle and penetrating into the inferior oblique muscle at the level of the eyeball equator rather than at the border between the posterior and medial thirds of the muscle as it occurs for the rest of extraocular muscles. This 1–1.5 mm thick branch (containing parasympathetic fibers innervating the pupillary sphincter) is often affected during reconstruction of a fracture of the orbital floor, causing postoperative Adie's syndrome
	Anatomical details: hemorrhage caused by resection of the muscle from the sclera is attributable to the absence of tendon
Superior oblique muscle (m. obliquus superior)	*Point of origin*: periosteum of the body of sphenoid bone posteriorly to the superior rectus muscle
	Insertion point: sclera of the posterosuperior quadrant of the eyeball
	Function: the primary function, incycloduction (65 %); the secondary function, infraduction (32 %); and the tertiary function, abduction (3 %)
	Blood supply: the superior (lateral) muscular branch from the ophthalmic artery, the lacrimal artery, and the anterior and posterior ethmoidal arteries
	Innervation: contralateral trochlear nerve (n. IV)
	Anatomical details: the longest tendon (26 mm); the trochlea is the functional origin of the muscle

Table 1.4 Anastomoses of the internal and external carotid arteries

Internal carotid artery	External carotid artery
A. lacrimalis (branch of a. ophthalmica)	Ramus orbitalis a. meningea media (seu a. meningea recurrens), branch of a. maxillaris
A. zygomaticotemporalis (branch of a. lacrimalis)	Aa. temporales profundae (branches of a. maxillaris)
A. zygomaticofacialis (branch of a. lacrimalis)	A. transversa faciei (branch of a. temporalis superficialis)
A. supraorbitalis (branch of a. ophthalmica)	A. frontalis (branch of a. temporalis superficialis)
A. palpebralis medialis superior (branch of a. ophthalmica)	A. zygomaticoorbitalis (branch of a. temporalis superficialis)
A. palpebralis medialis inferior (branch of a. ophthalmica)	A. transversa faciei (branch of a. temporalis superficialis)
A. palpebralis medialis inferior (branch of a. ophthalmica)	A. angularis (the terminal branch of a. facialis)
A. dorsalis nasi (branch of a. ophthalmica)	A. angularis (the terminal branch of a. facialis)
Inferior (medial) muscular branch of a. ophthalmica	Communicant branch of a. infraorbitalis
Marginal vascular arcade of the lower eyelid	A. infraorbitalis (branch of a. maxillaris)

1.3 Blood Supply to the Orbit

Blood is supplied to the orbit and the periorbital area mostly via branches of the internal carotid artery (ICA) anastomosing with the external carotid artery (ECA) (Table 1.4).

The ICA enters the cranial cavity through the *internal aperture of carotid canal* (*apertura interna canalis carotici*) in the temporal bone, which opens within the *foramen lacerum*; passes near the *posterior clinoid process* (*processus clinoideus posterior*) of the sphenoid bone; and turns abruptly to enter the cavernous sinus along with the abducent nerve. In the sinus, the ICA takes an S-shaped turn (*carotid siphon*). After leaving the cavernous sinus, the ICA gives off the first large intracranial *branch*, the *ophthalmic artery* (*a. ophthalmica*). Before the ophthalmic artery, the ICA gives off several small branches (*r. sinus cavernosi*) going to the dura mater of the outer wall of the cavernous sinus. A blunt force trauma in young individuals and atherosclerotic changes in elderly patients may cause the formation of a carotid-cavernous (rupture of the ICA siphon deep in the sinus) or dural-cavernous (rupture of small arteries feeding the wall of the cavernous sinus) fistula, respectively. The former condition is accompanied by obvious clinical signs and usually requires surgical intervention. Most dural fistulas connecting the small arteries of the external wall of the cavernous sinus to its venous plexus are accompanied by less evident clinical signs or imaging findings[1] and can be watched conservatively because of the high probability of spontaneous closure.

[1] Conjunctival injection, ocular hypertension, in some cases a deficit of abduction. CT-confirmed expansion of the superior ophthalmic vein and swelling of the extraocular muscles.

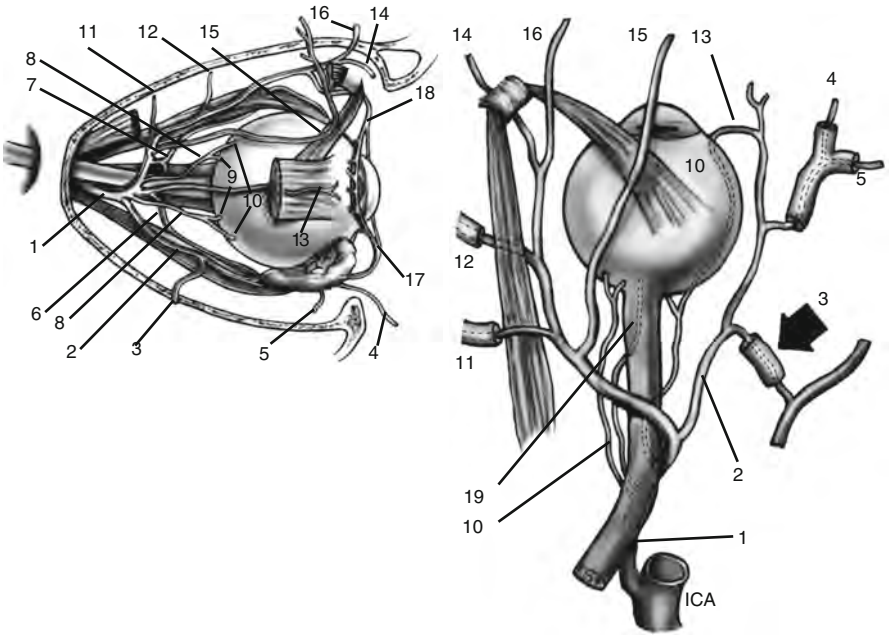

Fig. 1.27 Orbital arteries (dorsal view). (*1*) Ophthalmic artery (*a. ophthalmica*); (*2*) lacrimal artery (*a. lacrimalis*); (*3*) recurrent branch of the middle meningeal artery (*r. recurrens seu r. anastomoticus cum a. meningea media*); (*4*) zygomaticofacial artery (*a. zygomaticofacialis*); (*5*) zygomaticotemporal artery (*a. zygomaticotemporalis*); (*6*) lateral muscular artery (*a. muscularis lateralis*); (*7*) medial muscular artery (*a. muscularis medialis*); (*8*) posterior ciliary arteries (*aa. ciliares posteriores*) occurring in 50 % of cases; (*9*) short posterior ciliary arteries (*aa. ciliares posteriores breves*); (*10*) long posterior ciliary arteries (*aa. ciliares posteriores longae*); (*11*) posterior ethmoidal artery (*a. ethmoidalis posterior*); (*12*) anterior ethmoidal artery (*a. ethmoidalis anterior*); (*13*) anterior ciliary artery (*a. ciliaris anterior*); (*14*) dorsal nasal artery (*a. dorsalis nasi*); (*15*) supraorbital artery (*a. supraorbitalis*); (*16*) supratrochlear artery (*a. supratrochlearis*); (*17*) lateral palpebral artery (*a. palpebralis lateralis*); (*18*) medial palpebral artery (*a. palpebralis medialis*); (*19*) central retinal artery (*a. centralis retinae*)

Inside the orbit, the ophthalmic artery gives off three groups of branches, which were comprehensively described by Hayreh (1962) [49–53]:

- *Ophthalmic* (*posterior branches supplying blood to the eyeball*): the central retinal artery (*the first branch of the ophthalmic artery*), 15–20 short posterior ciliary arteries, and 2 long posterior ciliary arteries
- *Orbital* (*median branches supplying the extraocular muscles*): lateral and medial muscular arteries giving off six branches to the rectus muscles and the lacrimal artery giving off the seventh muscular artery to the lateral rectus muscle
- *Extraorbital* (*anterior branches supplying the facial tissues*): the anterior and posterior ethmoidal arteries (in addition to their primary function, they attach the ophthalmic artery to the medial orbital wall), the supraorbital artery, and the terminal branches of the ophthalmic artery (supra- and infratrochlear arteries, the dorsal nasal artery) (Fig. 1.27) [2, 49–53]

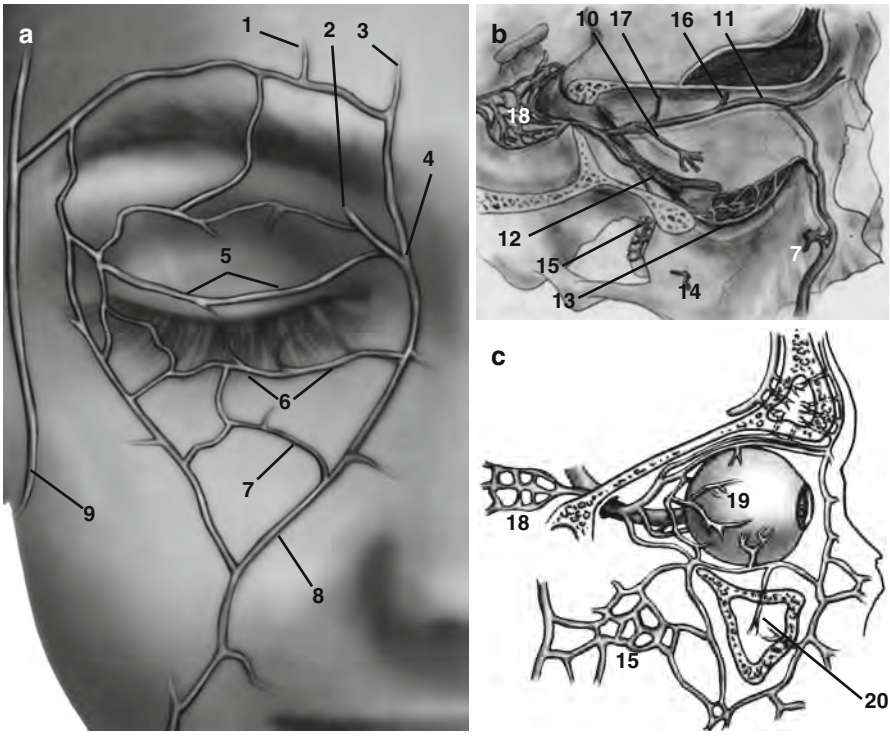

Fig. 1.28 Venous network of the face and orbit. (**a**) Venous network of the eyelids and periorbital area: (*1*) supraorbital vein (*v. supraorbitalis*); (*2*) supratrochlear veins (*vv. supratrochleares*); frontal vein (*v. frontalis*); (*4*) angular vein (*v. angularis*); (*5*) superior palpebral veins (*vv. palpebrales superiores*); (*6*) inferior palpebral veins (*vv. palpebrales inferiores*); (*7*) infraorbital vein (*v. infraorbitalis*); (*8*) facial vein (*v. facialis*); (*9*) superficial temporal veins (*vv. temporales superficiales*); (**b**, **c**) orbital veins: (*10*) lacrimal vein tributaries (descending); (*11*) superior ophthalmic vein; (*12*) inferior ophthalmic vein; (*13*) venous plexus of the orbital floor; (*14*) zygomaticofacial vein; (*15*) pterygoid plexus; (*16*) anterior ethmoidal vein; (*17*) posterior ethmoidal vein; (*18*) cavernous sinus; (*19*) vorticose veins; (*20*) veins of the maxillary sinus flowing into the venous plexus of the orbital floor

The central retinal artery, the pial perforant branches, and the short posterior ciliary arteries are involved in the *blood supply to the optic nerve*.

As opposed to other body parts and organs, the *orbital veins* (as well as cerebral veins) typically do not run parallel to the arteries. Only the central retinal vein and the anterior ciliary veins accompany the homonymous arteries. Another feature of the anatomy of orbital veins is that they have no valves. In this case, the direction of blood flow is determined by pressure gradient only, which makes infection spread from the anterior orbit to the posterior orbit (the orbital apex) (Fig. 1.28).

Most of the blood is drained from the globe through the vorticose veins (*vv. vorticosae*). It is then evacuated from the dense plexus of orbital veins via three routes. The main drainage is maintained through the superior ophthalmic vein that usually

unites with the inferior ophthalmic vein to form a single trunk near the orbital apex, which further flows into the cavernous sinus (route 1). In the case of a carotid-cavernous fistula, a crucial role is played by the inferior ophthalmic vein due to its numerous anastomoses with the facial veins (route 2) and the branches flowing into the pterygoid plexus of the pterygopalatine fossa (route 3).

The superior ophthalmic vein is the main venous collector in the orbit. It is 1.5 mm in diameter. The vein is formed by coalescence of two branches: the upper one, which is the continuation of the supraorbital vein, and the lower one, which anastomoses with the angular vein. As the superior ophthalmic vein passes to the superior orbital fissure, it collects blood from multiple tributaries (ciliary, superior vorticose, lacrimal, and ethmoidal veins).

Originating from the plexus of the inferior orbital wall, the inconstant inferior ophthalmic vein collects blood from the lateral rectus muscle, the inferior muscle complex and the adjacent conjunctiva, the inferior vorticose veins, and the lacrimal sac. The vein then forms two branches: one of those coalesces with the superior ophthalmic vein, while the second one coalesces with the pterygoid plexus.

The central retinal vein usually passes by the superior ophthalmic vein and flows directly into the cavernous sinus.

The paired cavernous sinuses are lateral to the body of the sphenoid bone, i.e., is adjacent to the lateral wall of the sphenoidal sinus. It starts anteriorly behind the internal (the widest) portion of the superior orbital fissure and stretches up to the apex of the petrous portion of the temporal bone (Fig. 1.29). The cavernous sinus acts as a venous collector in the orbit. Furthermore, it communicates with the superior and inferior petrous sinuses and with the pterygoid plexus.

The cavernous sinus contains the abovementioned carotid siphon (the S-shaped cavernous portion of ICA) and sympathetic fibers of III, IV, V_1, and VI cranial nerve pairs. The carotid siphon is a venous plexus communicating with the contralateral sinus via anterior and posterior intercavernous sinuses. The presence of the intercavernous sinuses can explain a bilateral ocular paralysis that is sometimes observed in patients with an unilateral thrombosed sinus. The parasympathetic fibers from the Edinger–Westphal nucleus enter the orbit via the cavernous sinus along with the oculomotor nerve. One should bear in mind that it is not the only source of parasympathetic innervation of orbital structures; branches of the pterygopalatine ganglion are another source. In most cases, the maxillary nerve (V_2) lies adjacent to the posteroinferior surface of the cavernous sinus but does not reside deep in its wall, as opposed to an existing opinion.

It is believed that the orbit contains no lymphatic vessels [54]. The only exceptions are the arachnoid sheath of the optic nerve and the lacrimal gland [55, 56]. The lymphatic system in the eyelids is subdivided into deep (for the posterior, conjunctival–tarsal lamina) and superficial (for the anterior, musculocutaneous lamina). The inner half of the eyelids (mostly the lower eyelid) drain to submandibular lymph nodes, while the outer half of the lower eyelid and the greatest portion of the upper eyelid drain to the preauricular lymph nodes [54, 57, 58] (Fig. 1.30).

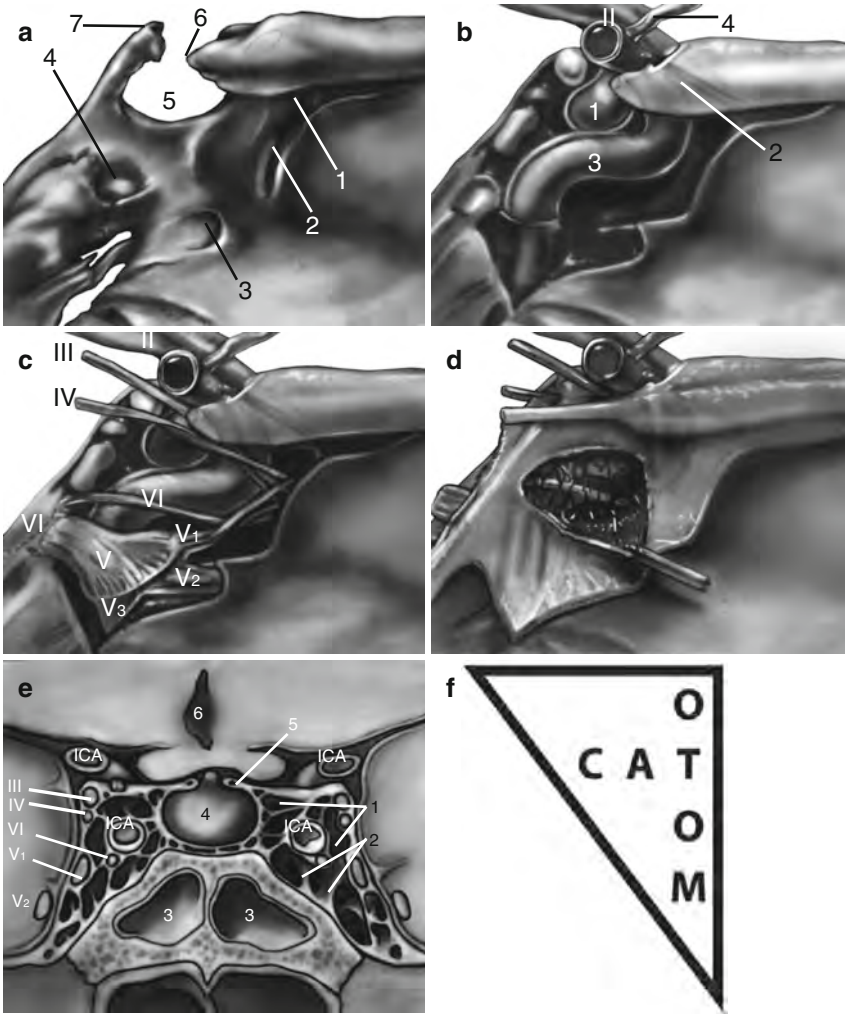

Fig. 1.29 Parasagittal section of the cavernous sinus. (**a**) Bony landmarks: (*1*) optic foramen; (*2*) superior orbital fissure; (*3*) round foramen; (*4*) carotid canal; (*5*) sella turcica; (*6*) anterior clinoid process localized laterally from the optic canal; (*7*) posterior clinoid process. (**b**) Carotid siphon; II optic nerve; (*1*) pituitary gland; (*2*) ophthalmic artery separating from the ICA (*3*) immediately after it passes through the superior wall of the cavernous sinus; (*4*) the anterior communicating artery. (**c**) Arrangement of cranial nerves in the cavernous sinus. All the nerves (except for the abducens nerve) are tightly attached to the outer sinus wall. N. VI passes directly in the sinus lumen, being partially attached to the ICA siphon. Although the maxillary nerve tightly contacts the wall, it still does not lie between its laminae. II optic nerve; III oculomotor nerve containing motor and parasympathetic fibers; IV trochlear nerve; V_1 ophthalmic nerve; V_2 the maxillary nerve; V_3 the mandibular nerve; VI abducens nerve. (**d**) Outer sinus wall. (**e**) Frontal section of the cavernous sinus: (*1*) cavernous sinus; (*2*) Willis' cords; ICA internal carotid artery; III oculomotor nerve; IV trochlear nerve; VI abducens nerve; V_1 ophthalmic nerve; V_2 maxillary nerve; (*3*) sphenoidal sinus; (*4*) the pituitary gland; (*5*) diaphragm of sella turcica; (*6*) the third ventricle. (**f**) The mnemonic rule "O, cat Tom" mentioning the cartoon character can be used to memorize the topographic anatomy of the cavernous sinus, where O (*n. oculomotorius*), c (*a. carotis interna*), a (*n. abducens*), t (*n. trochlearis*), o (*n. ophthalmicus*, n. V_1), m (*n. maxillaris*, n. V_2) (According to Zide and Jelks [60] with amendments)

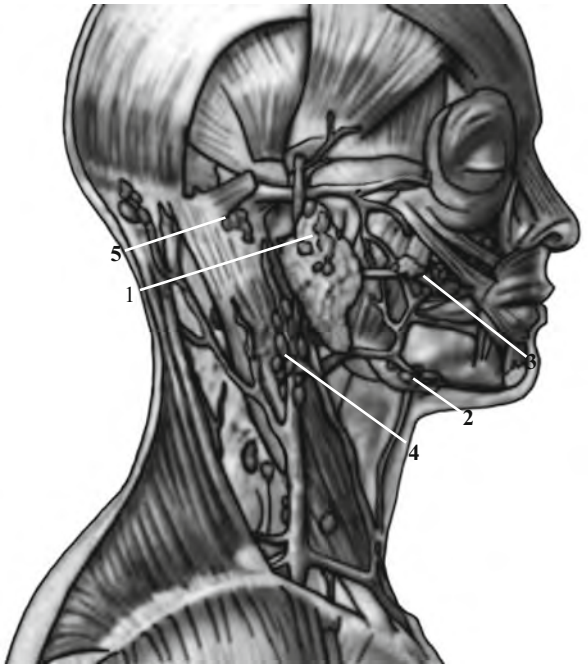

Fig. 1.30 The lymphatic system of the eyelids. (*1*) Preauricular nodes collecting lymph from the lateral half of the lower eyelid and the greater portion of the upper eyelid; (*2*) submandibular nodes collecting lymph from the medial half of eyelids (mostly the lower one); (*3*) buccal lymph nodes; (*4*) superficial cervical lymph nodes; (*5*) mastoid lymph node

1.4 Characteristics of the Cranial Nerves Involved in Innervation of the Orbital Complex

The *optic nerve* (*n. opticus, n. II*) is subdivided into four portions: the 0.8 mm long *intraocular* portion (pars intraocularis), the 24–25 mm long *orbital* portion (pars orbitalis), the *canal* portion (pars canalis) that is no longer than 8–10 mm, and the 10–16 mm long *intracranial* portion (pars intracranialis). The optic nerve contains ~1.5 million axons. The nerve diameter near the optic disk is 1.5 mm; the nerve becomes twice as thick (up to 3.0 mm) immediately behind the optic disk due to myelination of nerve fibers. In the orbital portion, the diameter of the nerve reaches 4.5 mm, which is caused by the presence of perineural sheaths.

The difference between the length of the orbital portion of the optic nerve (25 mm) and the distance between the posterior pole of the eye and canalis opticus (18 mm) is of great clinical significance. The S-shaped curve of the optic nerve formed due to the extra 7 mm ensures free movements of the eyeball and has a dampening function in traumas.

The oculomotor nerve (*n. oculomotorius, n. III*) consists of three components with clearly defined functions. The *somatic efferent* (*motor*) *component* innervates 4 of 6 extraocular muscles and the levator palpebrae superioris muscle, thus playing a key role in providing involuntary and voluntary eye movements. The *visceral efferent* (*motor*) *component* ensures parasympathetic innervation of the sphincter

pupillae and the ciliary muscle (the accommodative function). Furthermore, it contains *somatic afferent fibers* providing proprioceptive sensitivity of the innervated muscles. The oculomotor nerve contains 24,000 axons.

The *somatic efferent* (*motor*) *component* originates from a nuclear complex (two major lateral large-cell nuclei, two accessory Edinger–Westphal small-cell nuclei, and an accessory small-cell unpaired Perlia's nucleus) residing in the central gray matter of the mesencephalic tegmentum under the floor of the Sylvian aqueduct at the level of the superior colliculi of the corpora quadrigemina (Figs. 1.31 and 1.32). On the coronal section of the brainstem, the nuclear complex of the oculomotor nerve forms a V letter bound medially by the Edinger–Westphal nucleus and inferolaterally by the medial longitudinal fasciculus.

The motor and visceral efferent fibers originating from the nuclear complex run forward, in the ventral direction, partially cross, and pass through the red nucleus.

After leaving the cerebral peduncles in the interpeduncular fossa, the oculomotor nerve passes near the interpeduncular cistern and the cerebellar tentorium and between the posterior cerebral and the superior cerebellar arteries (Fig. 1.33). The intracranial portion of n. III is 25 mm long. The nerve pierces the dura mater and penetrates into the lateral wall of the cavernous sinus, where it passes superior to the trochlear nerve. The oculomotor nerve enters the orbit via the intraconal portion of

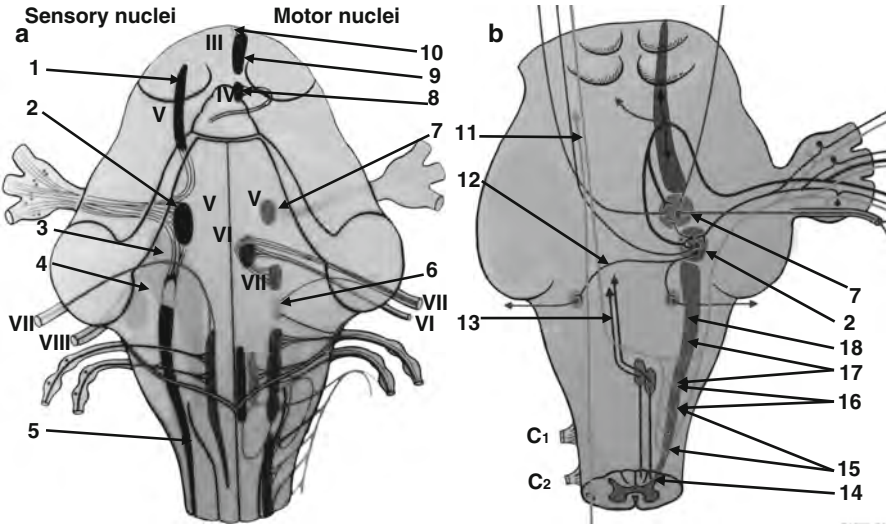

Fig. 1.31 Topographic anatomy of the nuclei of certain cranial nerves (III–VIII). (**a**) (*1*) mesencephalic nucleus and the mesencephalic tract of the trigeminal nerve; (*2*) pontine (the main sensory) nucleus of the trigeminal nerve; (*3*) vestibular nuclei; (*4*) cochlear nucleus; (*5*) spinal nucleus and tract of the trigeminal nerve; (*6*) superior and inferior salivary nuclei; (*7*) motor nucleus of the trigeminal nerve; (*8*) trochlear nucleus; (*9*) oculomotor nucleus; (*10*) Edinger–Westphal vegetative (parasympathetic) nucleus; (**b**) (*11*) spinal and trigeminal lemniscus; (*12*) reflex arc of the blink and corneal reflexes; (*13*) medial lemniscus; (*14*) substantia gelatinosa; (*15*) ophthalmic nerve; (*16*) maxillary nerve; (*17*) mandibular nerve; (*15–17*) the spinal tract; (*18*) nucleus of the spinal tract

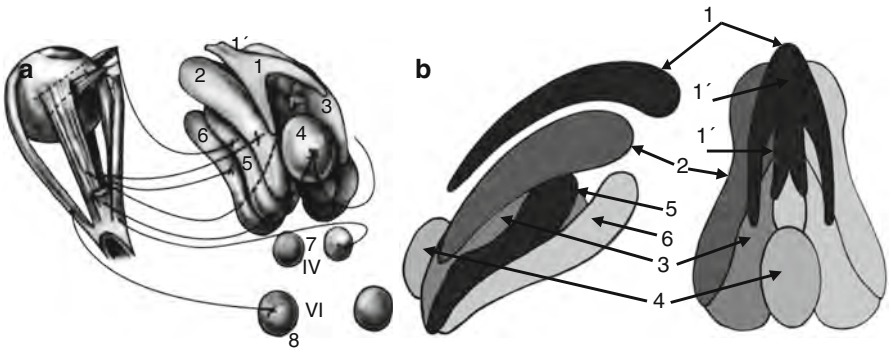

Fig. 1.32 Topographic anatomy of the group of nuclei of the oculomotor nerve. (**a**) posterodorsal view, (**b**) laterodorsal view: (*1*) Edinger–Westphal parasympathetic nuclei (*1'* Perlia's nucleus); (*2*) the nucleus innervating the ipsilateral inferior rectus muscle; (*3*) the nucleus innervating the ipsilateral superior rectus muscle; (*4*) centrally localized unpaired caudate nucleus innervating both levator palpebrae superioris muscles; (*5*) nucleus of the contralateral inferior oblique muscle; (*6*) nucleus of the ipsilateral medial rectus muscle; (*7*) trochlear nucleus innervating the contralateral superior oblique muscle; (*8*) abducens nucleus innervating the ipsilateral lateral rectus muscle

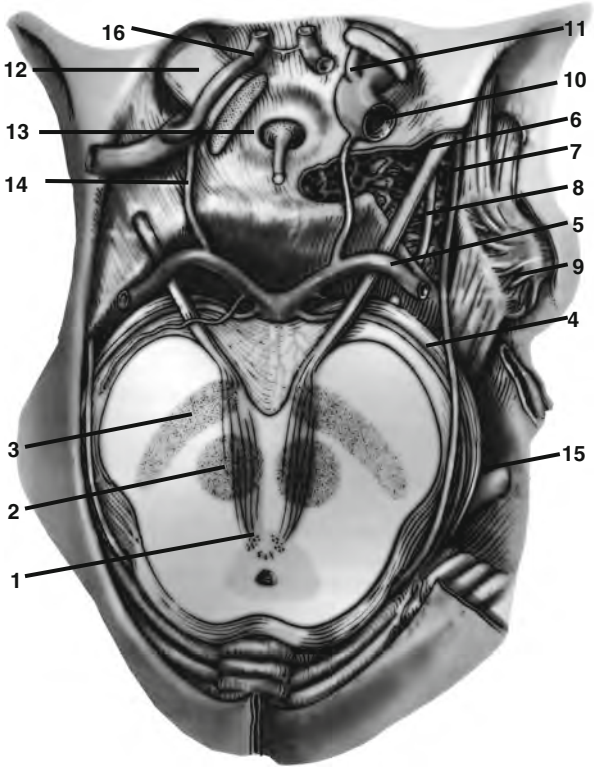

Fig. 1.33 Topographic anatomy of pairs of cranial nerves III–VI and the internal carotid artery on the skull base. (*1*) Oculomotor nuclei; (*2*) red nucleus; (*3*) substantia nigra; (*4*) superior cerebellar artery; (*5*) posterior cerebral artery; (*6*) oculomotor nerve; (*7*) trochlear nerve; (*8*) abducens nerve; (*9*) trigeminal nerve; (*10*) internal carotid artery; (*11*) ophthalmic artery; (*12*) optic nerve; (*13*) sella turcica; (*14*) posterior communicating artery; (*15*) vestibular nerve; and (*16*) anterior cerebral artery

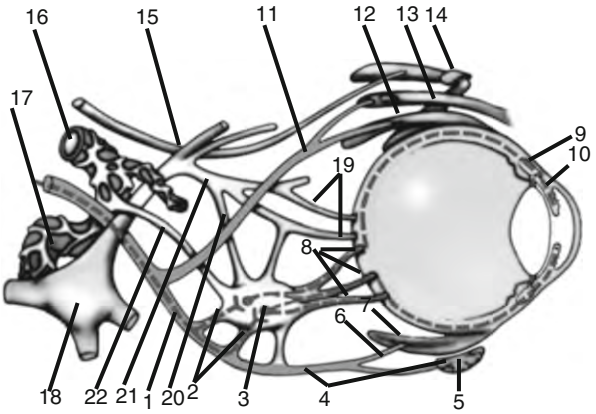

Fig. 1.34 Terminal branches of the oculomotor nerve (n. III). (*1*) *The inferior branchlet*; (*2*) the outer branch of the inferior branch supplying parasympathetic fibers (shown as a *dashed line*) to the ciliary ganglion (*3*) and motor fibers (*4*) (shown as a *solid line*) to the inferior oblique muscle (*5*); (*6*) middle branchlet of the inferior branch, which innervates the inferior rectus muscle (*7*); (*8*) short ciliary nerves; (*9*) ciliary muscle; (*10*) iris; (*11*) *the superior branch* innervating the superior rectus muscle (*12*) and the levator palpebrae superioris muscle (*13*); (*14*) superior oblique muscle; (*15*) trochlear nerve; (*16*) internal carotid artery; (*17*) its sympathetic plexus; (*18*) trigeminal ganglion; (*19*) long posterior ciliary nerves; (*20*) sensory root of the ciliary ganglion connecting it to the nasociliary nerve (*21*); (*22*) sympathetic root of the ciliary ganglion formed by the fibers of the sympathetic plexus of the internal carotid and the ophthalmic arteries

the superior orbital fissure. The nerve is usually divided into the upper and lower branches at the level of the cavernous sinus wall.

The *superior branch* ascends outward from the optic nerve and innervates the levator palpebrae superioris and the superior rectus muscles. The larger *inferior branch* is divided into three small branches: the outer (a parasympathetic root of the ciliary ganglion and fibers for the inferior oblique), the middle (inferior rectus), and the internal (medial rectus muscle) (Fig. 1.34).

Thus, the oculomotor nerve innervates the following muscles:

1. Ipsilateral superior rectus muscle
2. Levator palpebrae superioris muscle, bilaterally
3. Ipsilateral medial rectus muscle
4. Contralateral inferior oblique muscle
5. Ipsilateral inferior rectus muscle

The *visceral efferent* (*motor*) *component* originates from the accessory Edinger–Westphal small-cell lateral nuclei. Preganglionic parasympathetic fibers, along with somatic motor fibers, run ventrally through the mesencephalon, interpeduncular fossa, cavernous sinus, and superior orbital fissure.

When the oculomotor nerve passes through the cavernous sinus wall, the parasympathetic fibers are distributed diffusely. After it leaves the superior orbital fissure, the parasympathetic fibers concentrate in its inferior branch (passing laterally

from the inferior rectus muscle and being inserted in the inferior oblique muscle postero-inferiorly). Then, the fibers move from the inferior branch through the parasympathetic root of the ciliary ganglion containing the second-order neurons (Fig. 1.34). Postganglionic fibers leave the ciliary ganglion as 5 or 6 short ciliary nerves that are inserted in the posterior pole of the eye not far away from the optic nerve, mainly on the temporal side. The fibers run forward in the perichoroidal space to end in the ciliary muscle and in the sphincter pupillae as 70–80 sectorally innervated individual bundles.

The somatic afferent fibers originate from proprioceptors of the extraocular muscles and run as a component of the branches of the oculomotor nerve up to the cavernous sinus. In the sinus wall, they enter the ophthalmic nerve (V_1) via the communicating branches and reach the trigeminal ganglion housing the first-order neurons. The second-order neurons, which are responsible for proprioceptive sensation, originate in the mesencephalic nucleus of the V pair (in the mesencephalic tegmentum).

The nucleus of the trochlear nerve (n. IV) lies in the mesencephalic tegmentum at the level of the inferior colliculi of the corpora quadrigemina, anteriorly to the central gray matter and ventrally from the Sylvian aqueduct. Superior to the trochlear nucleus, there is a complex of oculomotor nuclei. Another neighboring structure is the myelinated medial longitudinal fasciculus (Figs. 1.31, 1.32, and 1.33).

Fibers leaving the nucleus run dorsally, going around the Sylvian aqueduct, decussate in the superior medullary velum, and exit from the dorsal surface of the brainstem surface posteriorly to the contralateral inferior colliculus of the midbrain tectum (quadrigeminal plate). Thus, the trochlear nerve is the only nerve whose fibers decussate completely and exit from the dorsal cerebral surface.

After leaving the brainstem and reaching the cisterna cruralis (or the quadrigeminal cistern), the trochlear nerve runs laterally around the cerebral peduncle and turns to the anterior surface of the brainstem to lie between the posterior cerebral and the superior cerebellar arteries, together with the oculomotor nerve. Then it enters the lateral wall of the cavernous sinus where it runs near n. III, V_1, and VI.

Since it has the longest (~75 mm) intracranial portion, the trochlear nerve is affected in blunt force trauma more often compared to other cranial nerves.

The trochlear nerve enters the orbit via the extraconal portion of the superior orbital fissure, lateral to the common tendinous ring (because of this fact, abduction and infraduction of the eyeball may be observed after retrobulbar block).

In the orbit, the trochlear nerve runs medially between the superior muscle complex and the orbital roof and enters the proximal one-third of the superior oblique muscle. In addition to somatic efferent fibers, it also contains afferent fibers that ensure proprioceptive sensation of the innervated muscles. The course of these fibers is similar to that of the fibers in n. III. The number of fibers in the trochlear nerve is the smallest (1,500).

The *abducens nucleus* (n. VI) lies in the caudal section of the tegmentum of the pons, almost at the midline above the floor of the fourth ventricle (rhomboid fossa) at the level of the facial colliculus, inferiorly and dorsally to the facial nucleus. The root filaments of the nerve run forward through the entire pons and exit from the

inferior (ventral) cerebral surface in the notch between the pons Varolii and the pyramid of medulla oblongata. Lateral to the basilar artery, the abducent nerve ascends along the anterior surface of the pons up to the petrous portion of the temporal bone. Finally, the abducens nerve and the inferior petrosal sinus lie inferior to the *petrosphenoid* (*or Gruber's*) *ligament* (*ligamentum petrosphenoidale*), which forms the *Dorello canal* together with the apex of the pyramid of the temporal bone. Then the nerve takes an abrupt turn forward, pierces the dura mater, and enters the cavernous sinus (it lies lateral to the internal carotid artery). The abducens nerve is the only nerve that coalesces with the carotid siphon rather than with the cavernous sinus wall. After it leaves the sinus, the nerve enters the orbit via the intraconal portion of the superior orbital fissure (it lies inferiorly to the oculomotor nerve) and approaches the lateral rectus muscle.

Due to the fact that the abducens nerve has a long intracranial portion and lies in the narrow Dorello canal, it is frequently affected in blunt force trauma.

Innervation of Conjugate Eye Movements *The horizontal gaze center* (*pontine gaze center*) lies in the paramedian pontine reticular formation near the abducens nucleus. It sends commands to the ipsilateral abducens nucleus and the contralateral oculomotor nucleus via the *medial longitudinal fasciculus*. As a result, the ipsilateral lateral rectus muscle receives the command for abduction, while the contralateral medial rectus muscle receives the command for adduction. In addition to the extraocular muscles, the medial longitudinal fasciculus unites the anterior and posterior groups of cervical muscles, fibers of basal and vestibular nuclei, and those of the cerebral cortex to form a single functional unit. Other potential centers of reflectory horizontal conjugate eye movements are Brodmann areas 18 and 19 of the occipital lobe. Brodmann area 8 is the potential center of voluntary eye movements.

The *vertical gaze center* is presumably located in the reticular formation of the periaqueductal gray matter of the mesencephalon at the level of the superior colliculi of the corpora quadrigemina and consists of several specialized nuclei. The posterior wall of the third ventricle contains the *prestitial nucleus* maintaining upward gaze. The *nucleus of posterior commissure* (*Darkshevich's nucleus*) is responsible for downward gaze. The *interstitial nucleus of Cajal* and *Darkshevich's nucleus* provide conjugate rotatory eye movements. The conjugate rotatory eye movements might also be ensured by neuronal aggregation on the anterior border of the superior colliculus.

Darkshevich's nucleus and the interstitial nucleus of Cajal are the integrating subcortical gaze centers. They give rise to the medial longitudinal fasciculus containing fibers from cranial nerve pairs III, IV, VI, VIII, and XI and the cervical plexus.

The *trigeminal nerve* (*n. trigeminus, n. V*) is the largest cranial nerve. It consists of the sensory (radix sensoria) and motor (radix motoria) components. The *sensory component* provides tactile, temperature, and pain innervation for the frontoparietal area of the scalp, eyelids, facial skin, mucous membranes of the nasal and oral cavities, teeth, eyeball, lacrimal gland, extraocular muscles, etc.

The *motor component* provides innervation of the muscles of mastication. The motor fibers are contained only in the mandibular nerve, which is considered to be

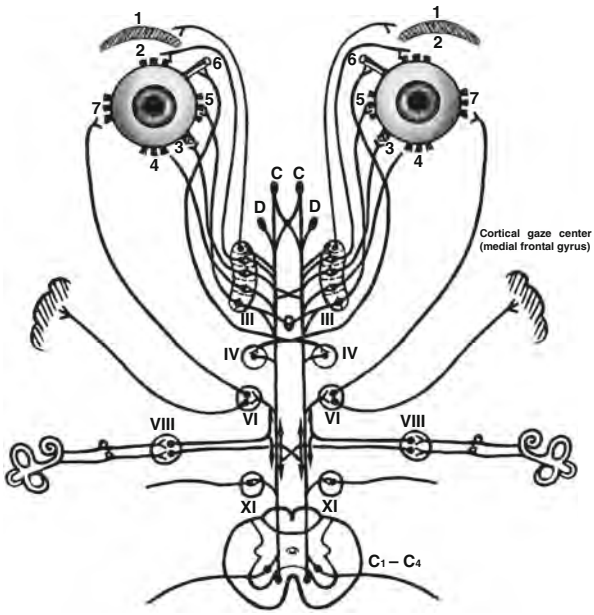

Fig. 1.35 Connections of the medial longitudinal fasciculus with the motor nuclei of cranial nerves innervating the extraocular and cervical muscles. *C* nucleus of Cajal; *D* Darkshevich's nucleus; (*1*) levator palpebrae superioris muscle; (*2*) superior rectus muscle; (*3*) inferior oblique muscle; (*4*) inferior rectus muscle; (*5*) medial rectus muscle; (*6*) superior oblique muscle; (*7*) lateral rectus muscle; (*III*) oculomotor nucleus; (*IV*) trochlear nucleus; (*VI*) abducens nucleus; (*VIII*) vestibular nuclei; (*XI*) nucleus of the accessory nerve

a mixed nerve, because it also provides the proprioceptive sensitivity of the muscles of mastication.

The *trigeminal ganglion and the trigeminal nucleus complex. The trigeminal* (*semilunar or Gasserian*) *ganglion* (*gangl. trigeminale*) ensures sensory innervation of the face. It lies in the trigeminal cavity (*cavum trigeminale, s. Meckel*) formed by layers of the cranial dura mater on the trigeminal impression (*impressio trigeminalis*) of the apex of the petrous bone. The relatively large (15–18 mm) trigeminal ganglion has its concave side oriented posteriad and its convex side oriented anteriad. Three major branches of the trigeminal nerve originate from its anterior convex margin: the ophthalmic (V_1), maxillary (V_2), and mandibular (V_3) nerves, which leave the cranial cavity through the superior orbital fissure, the foramen rotundum, and the foramen ovale, respectively (Figs. 1.31 and 1.35). The motor root passes around the trigeminal ganglion on its inner side and runs to the foramen ovale, where it coalesces with the third branch of the trigeminal nerve to make it a mixed nerve.

The trigeminal ganglion contains pseudounipolar cells whose peripheral processes end in receptors providing the sensations of touch and pressure, as well as discriminative, temperature, and pain sensations. The central processes of the trigeminal cells enter the pons Varolii at the point where the middle cerebellar peduncle is separated from the pons and ends in the *pontine* (*principal sensory*) *nucleus of the trigeminal nerve* (tactile and discriminative sensation), *the spinal nucleus of the trigeminal nerve* (pain and temperature sensation), and *the mesencephalic nucleus of the trigeminal nerve* (proprioceptive sensation) (Fig. 1.31b).

The *pontine* (*nucl. pontinus n. trigemini*), or the principal sensory nucleus, lies in the dorsolateral portion of the upper part of the pons, lateral to *the motor nucleus of*

the trigeminal nerve. The axons of the second-order neurons that form this nucleus migrate to the opposite side and ascend to the ventrolateral nucleus of the thalamus as a component of the contralateral medial lemniscus.

Tactile fibers are involved in the formation of the corneal reflex arc. Impulses from the ocular mucous membrane travel along the ophthalmic nerve to reach the pontine nucleus of the trigeminal nerve (the afferent portion of the arc). Then the impulses switch to the facial nerve via the reticular formation cells and reach the orbicularis oculi muscle, thus providing the eye closure reflex for both eyes when only one eye is touched (the efferent portion of the arc).

The *spinal trigeminal nucleus* (*nucl. spinalis n. trigemini*) is the inferior continuation of the principal sensory nucleus along the entire medulla oblongata up to the *substantia gelatinosa* of the posterior horns of the cervical spine (C_4). The spinal trigeminal nucleus provides pain and temperature sensations. The afferent fibers are supplied to this nucleus along the *spinal tract of the trigeminal nerve*.

When fibers reach the *caudal portion* (*pars caudalis*) *of the spinal trigeminal nucleus,* they follow a strict somatotopic order and are oriented as an upside-down projection of the face and head. The pain sensation fibers within the ophthalmic nerve (V_1) end in the most caudal point; they are followed by fibers of the maxillary nerve (V_2). Finally, fibers in the mandibular nerve (V_3) have the most rostral (cranial) arrangement (Fig. 1.31b). Nociceptive fibers from cranial nerves VII, IX, and X (external ear, posterior one-third of the tongue, larynx, and pharynx) are attached to the spinal cord tract of the trigeminal nerve.

The *middle subnucleus* (*pars interpolaris*) receives pain afferents from the dental pulp. The *middle and rostral* (*pars rostralis*) *portions* may also be responsible for pressure and touch perception.

The second-order neurons originating from the spinal nucleus travel to the opposite side to form a wide fan-shaped bundle, which runs through the pons and the midbrain to the thalamus to end in its ventral lateral nucleus. The axons of third (thalamic)-order neurons are encapsulated in the posterior limb of internal capsule and run toward the caudal portion of the postcentral gyrus, where the center of projection of overall sensitivity for the head is located.

The *mesencephalic nucleus of the trigeminal nerve* (*nucl. mesencephalicus n. trigemini*) is the superior continuation of the pontine nucleus. It lies lateral to the aqueduct and is responsible for proprioceptive sensation originating from *baroreceptors and muscle spindle sensory receptors* of the muscles of mastication and mimic and oculomotor (extraocular) muscles.

The *motor, or masticatory, nucleus* (*nucl. motorius n. trigemini s. nucl. masticatorius*) lies in the lateral pontine tegmentum, medially to the sensory nucleus. It receives impulses from both hemispheres, the reticular formation, red nuclei, midbrain tectum, medial longitudinal fasciculus, and mesencephalic nucleus (with which the motor nucleus is bridged by the monosynaptic reflex arc). The axons of the motor nucleus form the motor root running to the muscles of mastication (the lateral and medial pterygoid muscles, the masseter and temporal muscle), the tensor tympani muscle, the tensor veli palatini muscle, the mylohyoid muscle, and the anterior belly of the digastric muscle.

The *ophthalmic nerve* (V_1) lies in the cavernous sinus wall, lateral to the internal carotid artery, between the oculomotor and trochlear nerves. The ophthalmic nerve enters the orbit through the superior orbital fissure and divides into three branches (frontal, lacrimal, and nasociliary) that maintain sensory innervation of the orbit and the upper one-third of the face (Fig. 1.36).

The *frontal nerve* is the largest branch; it runs in the orbit between the levator palpebrae superioris muscle and periosteum of the orbital roof and innervates the medial half of the upper eyelid and the corresponding conjunctival portions, the forehead, the scalp, the frontal sinuses, and a half of the nasal cavity. As the frontal nerve leaves the orbit, it is divided into two terminal branches (the supraorbital and the supratrochlear nerves).

The *lacrimal nerve* is the thinnest branch; it lies along the superior margin of the lateral rectus muscle and ensures sensory innervation of the conjunctiva and skin near the lacrimal gland. In addition, it contains postganglionic parasympathetic fibers involved in the lacrimation reflex.

The *nasociliary nerve* is the only branch of the ophthalmic nerve that enters the orbit through the intraconal portion of the superior orbital fissure. It gives off a small branch forming the sensory root of the ciliary ganglion. Because these fibers are peripheral processes of pseudounipolar cells of the trigeminal ganglion, they pass through the ciliary ganglion without being involved in synaptic transmission. They leave the ciliary ganglion as 5–12 short ciliary nerves that are involved in sensory innervation of the cornea, iris, and ciliary body. These nerves also contain sympathetic vasomotor nerve fibers from the superior cervical ganglion. The nasociliary nerve gives off a number of branches: two long ciliary nerves, the anterior and posterior (nerve of Luschka) ethmoidal nerves (innervation of the nasal mucous membrane, sphenoidal sinus, and posterior ethmoidal cells), and the infratrochlear nerve (innervation of the lacrimal canaliculi, the medial palpebral ligament, and the nasal tip, which is attributable for the emergence of Hutchinson's sign (1866): vesicular skin lesions at the tip and sides of the nose in patients with herpes zoster).

As mentioned above, although the maxillary nerve (V2) is in tight contact with the cavernous sinus wall, it does not lie between the layers of the dura mater that forms its outer wall.

When leaving the foramen rotundum, the maxillary nerve gives off a large (up to 4.5 mm thick) branch, the infraorbital nerve (*n. infraorbitalis*).

Together with the infraorbital artery (*a. infraorbitalis*, a branch of *a. maxillaris*), it enters the orbit through the center of the inferior orbital fissure and lies below the periosteum. Then, the nerve and the artery run in the infraorbital groove (*sulcus infraorbitalis*) of the orbital floor. The infraorbital groove anteriorly becomes a 7–15 mm long canal running deep in the orbital surface of the body of the maxilla almost parallel to the medial orbital wall. Near the canine fossa, the canal opens to form the round-shaped *infraorbital foramen* (*foramen infraorbitale*), 4.4 mm in diameter. In adults, the infraorbital foramen lies 4–12 mm below the midpoint of the infraorbital margin (9 mm on average).

It should be mentioned that, contrary to common belief, the supra- and infraorbital foramina are not located on a single vertical line known as the *linea facialis*.

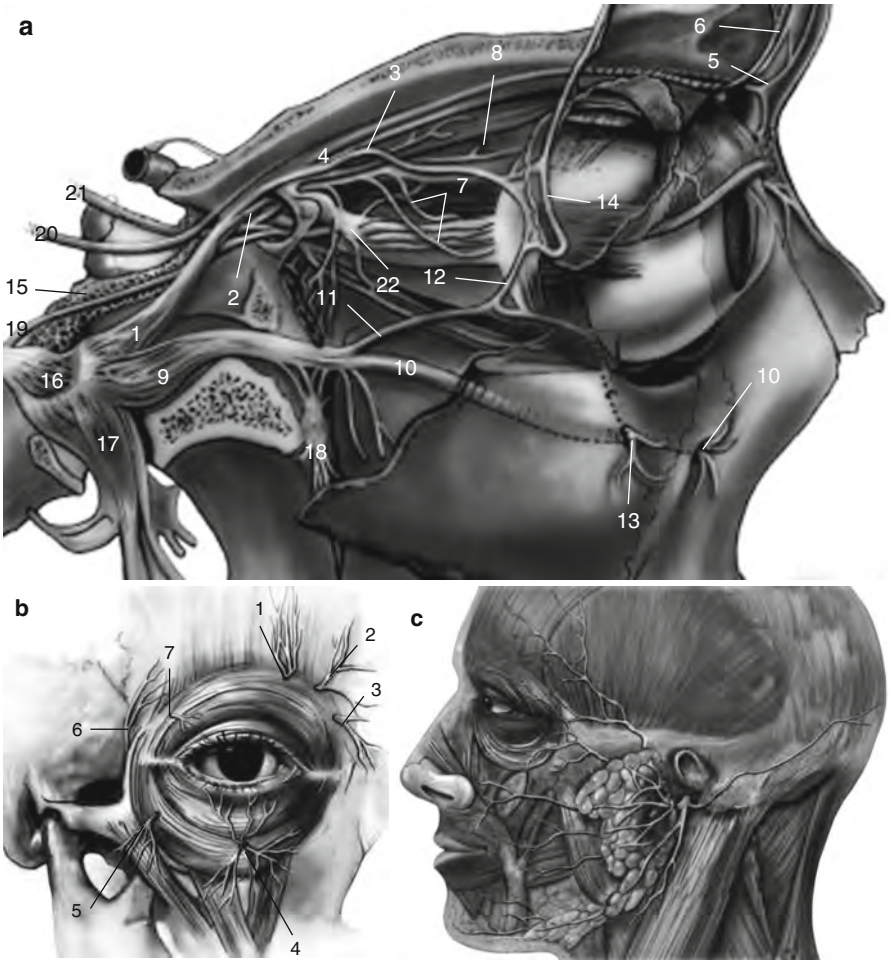

Fig. 1.36 Anatomy of the trigeminal nerve. (**a**) Oblique parasagittal view: (*1*) ophthalmic nerve; (*2*) nasociliary nerve; (*3*) lacrimal nerve; (*4*) frontal nerve; (*5*) supratrochlear nerve; (*6*) supraorbital nerve; (*7*) long ciliary nerves; (*8*) anterior ethmoidal nerve; (*9*) maxillary nerve; (*10*) infraorbital nerve; (*11*) zygomatic nerve; (*12*) its anastomosis with the lacrimal nerve; (*13*) zygomaticofacial nerve; (*14*) zygomaticofrontal nerve; (*15*) the sympathetic plexus around the carotid siphon; (*16*) trigeminal ganglion; (*17*) mandibular nerve; (*18*) pterygopalatine ganglion; (*19*) abducens nerve; (*20*) trochlear nerve; (*21*) oculomotor nerve; (*22*) ciliary ganglion. (**b**) Final branches of the trigeminal nerve: (*1*) supraorbital nerve; (*2*) supratrochlear nerve; (*3*) infratrochlear nerve; (*4*) infraorbital nerve; (*5*) zygomaticofacial branch of the zygomatic nerve; (*6*) zygomaticotemporal branch of the zygomatic nerve; (*7*) lacrimal nerve

In over 70 % of cases, the distance between the infraorbital foramina is 0.5–1 cm greater than that between the supraorbital notches. An opposite situation is typical for the cases when a supraorbital foramen is formed instead of the supraorbital notch. The average vertical distance between the supraorbital notch and the infraorbital foramen is 44 mm.

The zygomatic nerve (*n. zygomaticus*) pierces the orbital periosteum and enters the orbit from the infratemporal fossa through the inferior orbital fissure, where it immediately divided into two branches: the zygomaticofacial (*r. zygomaticofacialis*) and zygomaticotemporal (*r. zygomaticotemporalis*); both nerve trunks enter the *corresponding canals* of the zygomatic bone to reach the skin of the zygomatic and temporal areas. The zygomaticotemporal branch in the orbit gives off the important anastomosis with the lacrimal nerve containing postganglionic parasympathetic fibers originating from the pterygopalatine ganglion.

The facial nerve (n. facialis, n. VII) consists of three components, each of those being responsible for a specific type of innervation:

- *Motor efferent innervation* of the mimic muscles originating from the second pharyngeal arch: the posterior belly of the digastric muscle, stylohyoid and stapedius muscles, and platysma
- *Secretory efferent* (*parasympathetic*) *innervation*: the lacrimal, submandibular, and sublingual glands; glands of the nasopharyngeal mucosa; and the hard and soft palates
- *Gustatory* (*specialized afferent*) *innervation*: gustatory receptors of the anterior two-thirds of the tongue and the hard and soft palates (Fig. 1.37)

Motor fibers are the main component of the facial nerve; the secretory and gustatory fibers are separated from the motor ones by a membrane and form the *intermediate nerve* (nerve of Wrisberg, n. intermedius). According to the International Anatomical Nomenclature, the intermediate nerve is a component of the facial nerve (n. VII).

The motor nucleus of the facial nerve is found in the ventrolateral portion of the pontine tegmentum at the boundary with medulla oblongata. The fibers leaving the nucleus run medially and dorsally and pass around the abducens nucleus (*internal genu of the facial nerve*). They form the *facial colliculus* (*colliculus facialis*) on the floor of the fourth ventricle and then run ventrolaterally to the caudal portion of the pons to exit from the ventral surface of the brain in the cerebellopontine angle. The nerve root is adjacent to the root of the eight pairs of nerves (the vestibulocochlear nerve), superior and lateral to the olivary body, and contains fibers of the intermediate nerve. The facial nerve further enters the internal acoustic meatus and the *facial nerve canal* (or Fallopian canal of the petrous portion of the temporal bone). The *geniculate ganglion* (*gangl. geniculi*) lies at the point of canal curvature.

Two portions of the facial nerve are divided at the level of the geniculate ganglion. The motor fibers pass through the geniculate ganglion, make a right angle turn posterolaterally, and exit the pyramid of the temporal bone through the stylomastoid foramen. After it exits the canal, the facial nerve gives off the branches running to the stylohyoid muscle and the posterior belly of the digastric muscle; then it forms a plexus in the parotid gland (Fig. 1.37b).

Branches of the *parotid plexus* are involved in the innervation of voluntary movements of facial muscles (Fig. 1.37c):

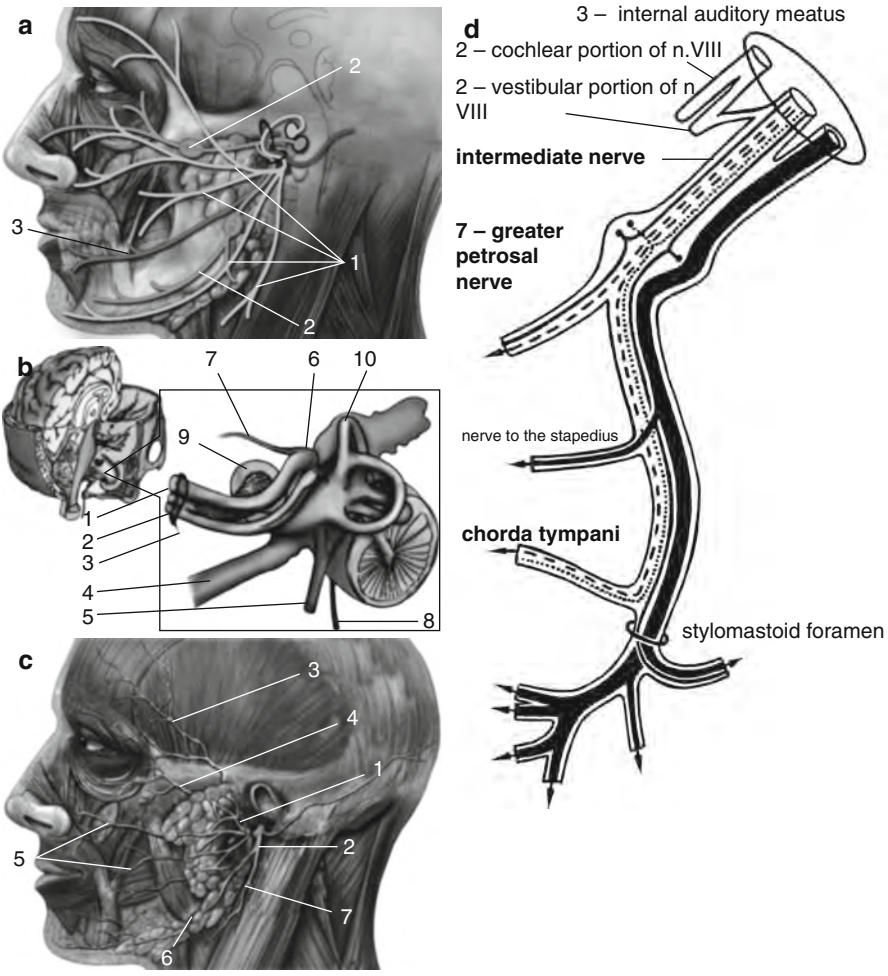

Fig. 1.37 Anatomy of the facial nerve. (**a**) Components of the facial nerve: (*1*) motor efferent fibers; (*2*) secretory parasympathetic efferent fibers; (*3*) afferent gustatory fibers. (**b**) Anatomy of the intracranial portion of the facial nerve: (*1*) facial nerve; (*2*) vestibulocochlear nerve; (*3*) internal acoustic meatus; (*4*) Eustachian tube; (*5*) facial nerve; (*6*) geniculate ganglion; (*7*) greater petrosal nerve; (*8*) chorda tympani; (*9*) cochlea; (*10*) semicircular canal. (**c**) Motor fibers of the facial nerve: (*1*) superior (temporofacial) branch; (*2*) inferior (cervicofacial) branch; (*3*) temporal branches; (*4*) zygomatic branches; (*5*) buccal branches; (*6*) marginal mandibular branch; (*7*) cervical branch. (**d**) Levels of lesions of the facial nerve in patients with peripheral facial palsy (▬ motor fibers, ▬ sensory fibers, - - secretory fibers, and ····· gustatory fibers)

- *Temporal branches* (*rr. temporales*): posterior, medial, and anterior branches. They innervate the superior and anterior auricular muscles, the frontal belly of the supracranial muscle, and the superior half of the *orbicularis oculi muscle* and the *corrugator supercilii* muscle.

- *2–3 zygomatic branches* (*rr. zygomatici*) pass anterosuperiorly and approach the zygomatic muscles and the inferior half of the *orbicularis oris muscle* (which needs to be taken into account when performing Nadbath, O'Brien, van Lindt akinesia).
- 3–4 appreciably thick buccal branches (rr. buccales) are given off from the superior principal branch of the facial nerve and send their branches to the greater zygomatic muscle, the risorius and the buccinator muscles, the levator and depressor anguli oris muscles, the orbicularis oculi muscle, and the nasal muscle.
- The marginal mandibular branch (r. marginalis mandibulae) innervates the depressor anguli oris and the depressor labii inferioris muscles and the mentalis muscle.
- The cervical branch (r. colli) in form of 2 or 3 nerves reaches the platysma muscle.

Thus, *the facial nerve innervates the eyelid protractors* (*m. orbicularis oculi, m. procerus, m. corrugator supercilii*) *and one eyelid retractor muscle* (*m. frontalis*).

Voluntary movements of facial muscles are regulated by the motor cortex (*precentral gyrus, gyrus precentralis*) via the corticonuclear tract running in the posterior limb of the internal capsule and reaching both the ipsi- and contralateral motor nuclei of the facial nerve. *The portion of the nucleus innervating the superior mimic muscles is innervated ipsi- and contralaterally. The portion of the nucleus innervating the inferior mimic muscles receives corticonuclear fibers only from the contralateral motor cortex*. This fact is of great clinical significance, since the central and peripheral facial nerve palsies are accompanied by different clinical signs. *The unilateral interruption of the corticonuclear tract leaves the innervation of the frontal muscle intact (central palsy). The disturbance at the level of the nucleus, root, or peripheral nerve results in paresis of all the mimic muscles in the ipsilateral half of the face* (*Bell's peripheral palsy*) (Fig. 1.38).

Clinical signs of peripheral palsy:

- Pronounced facial asymmetry
- Facial muscle atrophy
- Superciliary ptosis
- Smoothened frontal and nasolabial folds
- Downturning mouth
- Lacrimation
- Lagophthalmos
- Lack of lip seal
- Food falling out from the oral cavity when chewing on the ipsilateral side

The combination of Bell's palsy with abducens nerve palsy indicates that the pathological process is localized in the brainstem; the combination with the vestibulocochlear nerve disorder indicates that the pathological process is localized in the internal acoustic meatus (Table 1.5).

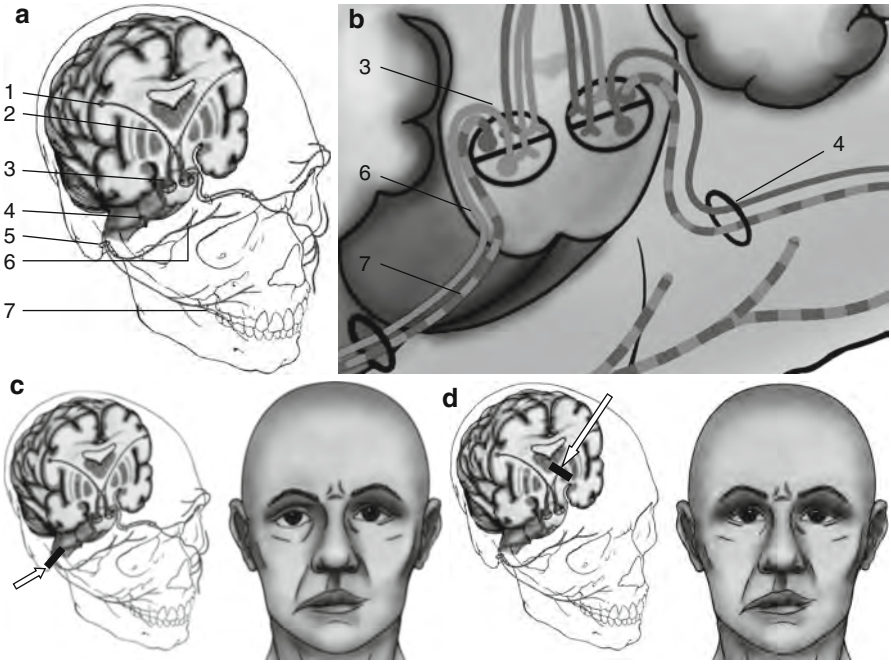

Fig. 1.38 Regulation of voluntary movements of facial muscles in the normal condition (**a**, **b**) and in individuals with facial nerve lesion at different levels (**c**, **d**). (*1*) Precentral gyrus; (*2*) corticonuclear tract; (*3*) motor nucleus of the facial nerve; (*4*) internal acoustic meatus; (*5*) stylomastoid foramen; (*6*) bilateral innervation of the upper mimic muscles (via the temporal and zygomatic branches of the facial nerve); (*7*) contralateral innervation of the lower mimic muscles (via the buccal branches and the marginal mandibular branch). The lesion at the level of the stylomastoid foramen (shown as an *arrow* in **c**) causes paresis of all the mimic muscles on the ipsilateral half of the face, at the level of the corticonuclear tract (shown as an *arrow* in **d**) paresis of the inferior muscles on the contralateral half of the face

Central facial nerve palsy is caused by injury of motor cortical neurons or their axons in the corticonuclear tract in the posterior limb of the internal capsule that end in the motor nucleus of the facial nerve. As a result, the voluntary contractions of the inferior muscles on the contralateral side of the face are affected. Voluntary movements of muscles in the superior half of the face are retained due to bilateral innervations.

Clinical signs of central palsy:

- Facial asymmetry
- Contralateral muscle atrophy in the inferior half of the face (as opposed to peripheral palsy).
- No superciliary ptosis (as opposed to peripheral palsy).
- The frontal folds are not smoothened (as opposed to peripheral palsy).
- Preserved conjunctival reflex (due to the well-retained innervations of the orbicularis oculi muscle).

Table 1.5 Topical diagnosis of peripheral facial palsy (Erb's scheme)

Level of nerve lesion	Symptom complex
Below the point of origin of the chorda tympani in the facial nerve canal	Paresis of the ipsilateral mimic muscles; ipsilateral sweating disorder
Above the point of origin of the chorda tympani and below the stapedius nerve (n. stapedius)	The same + impaired gustatory sensation on the anterior two-thirds of the ipsilateral half of the tongue; decreased salivation by the ipsilateral glands
Above the point of origin of n. stapedius and below the point of origin of the greater petrosal nerve	The same + auditory impairment
Above the point of origin of the greater petrosal nerve, the geniculate ganglion area	The same + decreased reflex lacrimation; dryness of the ipsilateral half of the nasopharynx; vestibular disorders are possible
Above the geniculate ganglion in the internal acoustic meatus	The same + disappearance of reflex and affective lacrimation (crying), hearing impairment (a variant of hyperacusis)
Internal acoustic meatus	Peripheral muscle paralysis, hearing impairment or loss, reduced excitability of the vestibular apparatus; ipsilateral depression of lacrimal and salivary secretion; absence of corneal and McCarthy's supraorbital reflexes; gustatory disturbance in patients with the overall sensitivity of the tongue being intact (V_3)

- Smoothened nasolabial fold (contralaterally).
- Lack of lip seal (contralaterally).
- Food falling out from the oral cavity when chewing on the contralateral side.

The *secretory parasympathetic fibers of the facial nerve* stimulate secretion of the submandibular, sublingual, and lacrimal glands, as well as glands of the nasopharyngeal and palatine mucosa.

The efferent parasympathetic fibers originate from a diffused aggregation of neurons in the caudal portion of the pons, which sits inferiorly to the motor nucleus of the facial nerve. These neuronal aggregations are known as the superior salivary nucleus (*nucl. salivatorius superior*) *and lacrimal nucleus* (*nucl. lacrimalis*). The axons of these neurons are a component of the intermediate nerve.

The intermediate nerve leaves the brainstem lateral to the motor root of the facial nerve. In the facial nerve canal, the vegetative fibers are divided into two bundles: the *greater petrosal nerve* (innervating the lacrimal gland and the nasal and palatine glands) and the *chorda tympani* (innervating the submandibular and sublingual salivary glands). The chorda tympani also contains sensory fibers (gustatory sensitivity) that run to the anterior two-thirds of the tongue.

After it separates from the geniculate ganglion, the greater petrosal nerve runs forward and medial, exits the temporal bone through the hiatus for the greater petrosal nerve, and passes through the homonymous groove toward the foramen lacerum. The nerve enters the base of the skull through the foramen lacerum, where it merges with the deep petrosal nerve (*n. petrosus profundus*) from the

sympathetic plexus of the internal carotid artery. Their merging gives rise to the *nerve of pterygoid canal* (*n. canalis pterygoidei*, or the *Vidian nerve*) running toward the *pterygopalatine ganglion* (gangl. pterygopalatinum) along the *pterygoid canal*. Within the ganglion, the nerve of the pterygoid canal combines with the maxillary nerve (V_2). Postganglionic fibers given off by the pterygopalatine ganglion neurons run through the zygomatic and zygomaticotemporal nerves to reach the lacrimal nerve (n. lacrimalis, V_1) innervating the lacrimal gland. Thus, parasympathetic innervation of the lacrimal gland is independent of the innervation of the eyeball and depends on the innervation of the salivary glands to a greater extent.

The *ciliary ganglion* (*ganglion ciliare*) plays the crucial role in providing the sensory, sympathetic, and parasympathetic innervation of orbital structures. It is a flat rectangular structure (2 mm in size) that is adjacent to the outer surface of the optic nerve; it sits 10 mm away from the optic foramen and 15 mm away from the posterior pole of the eye (Fig. 1.34) [59].

The ciliary ganglion has three roots:

1. The well-developed *sensory root* contains sensory fibers from the cornea, iris, and ciliary body (the components of the nasociliary nerve (V_1)).
2. The *parasympathetic* (*motor*) *root* within the outer branchlet of the lower branch of n. III reaches the ciliary ganglion where it forms the synaptic transmission and leaves the ciliary ganglion as short ciliary nerves innervating the sphincter pupillae and the ciliary muscle.
3. The thin *sympathetic root* of the ciliary ganglion; its structure (as well as that of the entire sympathetic orbital system) is still to be thoroughly studied. Sympathetic innervation of the eye begins in the ciliospinal center of Budge (the lateral horns C_8–T_2). The fibers leaving the center ascend to the superior cervical ganglion where they switch to the next-order neuron whose axons form the *internal carotid plexus* (*plexus caroticus internus*). After leaving the carotid siphon, sympathetic fibers enter the abducens nerve root but soon relocate to the nasociliary nerve and enter the orbit through the superior orbital fissure passing through the ciliary ganglion. Appearing as long ciliary nerves, they innervate the iris dilator muscle and probably the choroidal vessels. The second portion of sympathetic fibers enter the orbit within the ophthalmic artery and innervate the superior and inferior tarsal muscles, Müller's muscle, orbital vessels, perspiratory glands, and probably the lacrimal gland.

1.5 Anatomy of Paranasal Sinuses

The orbit is surrounded by paranasal sinuses (accessory nasal sinuses) on three sides, which are in the facial and cranial bones. These paired structures communicate with the nasal cavity and are lined with mucous membrane covered with ciliated epithelium (Fig. 1.39).

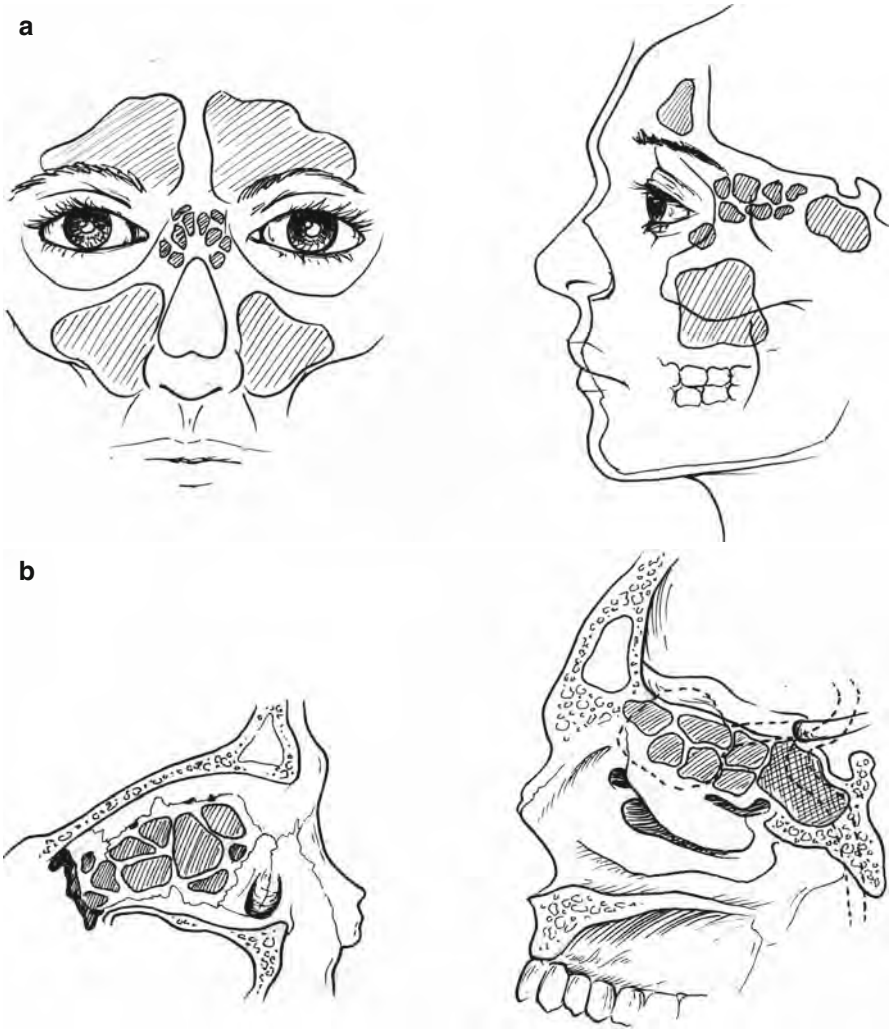

Fig. 1.39 Topographic anatomy of the orbit and paranasal sinuses. (**a**) The neighborhood of accessory sinuses with three orbital walls is attributable for the key role of sinusitis in the emergence of orbital infection. (**b**) Ethmoidal cells (hatched areas) and the adjacent sphenoidal sinus (double hatched area)

Phylogenetically, they are the derivatives of the ethmoidal labyrinth that have lost their original olfactory function.

The maxillary and frontal sinuses, as well as the anterior ethmoidal cells, are the anterior sinuses; the medial and posterior ethmoidal cells and sphenoidal sinuses are the posterior ones.

The ethmoidal labyrinth is the only sinus that starts to develop prenatally and is pneumatized by the time of birth. The ethmoidal labyrinth reaches its final shape

and size by the age of 12–14. The cribriform plate of the ethmoid bone is the upper border of the labyrinth; the base of the superior and medial nasal conchae acts as the medial border. The labyrinth posteriorly reaches the anterior wall of the sphenoid sinus.

The ethmoidal labyrinth consists of 8–13 small cavities (cells) of the ethmoid bone, which are separated by thin bony laminae. There are *anterior* and *medial* cells (that open to the middle nasal meatus) and *posterior* cells that drain into the superior nasal meatus.

The *maxillary sinus* is shaped like a pyramid with round corners that can penetrate in the maxillary processes to an appreciably large depth. The maxillary sinus acquires its final size (10–40 cm^3) at the age of 2–4. The sinus borders superiorly with the orbit, inferiorly with the maxillary alveolar process, and medially with the nasal cavity as it forms its lateral wall. The anterolateral wall faces the facial surface; the posterolateral wall of the maxillary sinus is the anterior wall of the pterygopalatine fossa.

Unlike the ethmoidal labyrinth, the maxillary sinus does not have septa reinforcing its walls. Hence, the inferior orbital wall is most likely to be fractured in blunt force trauma, although it is not the thinnest one.

The *sphenoidal sinus* is adjacent to the orbital apex and is localized superoposterior to the middle nasal conchae. Among all the paranasal sinuses, this sinus is the last one to end its postnatal development. In elderly people, it sometimes extends to the sella turcica wall, anterior clinoid process, and wings of the sphenoid bone and posteriorly reaches the clivus of occipital bone.

The sphenoidal sinus has six walls. The anterior wall facing the nasal cavity and its medial portion continues into a sphenoidal concha. Its lateral portion is adjacent to the posterior ethmoidal cells. The anterior wall contains an aperture of the sphenoid sinus that opens into the posterior portion of the superior nasal meatus. The posterior sinus wall is formed by the body of sphenoid bone. The inferior wall is adjacent anteriorly to the nasal cavity; posteriorly, to the pharyngeal fornix; and infero-exteriorly, to the pterygoid canal. The anterior one-third of the superior wall of the sphenoid sinus is adjacent anteriorly to the prechiasmatic sulcus; the medial and posterior one-thirds are adjacent to the sella turcica. The external portion of the superior wall and the superior portion of the lateral sinus wall are adjacent to the internal carotid artery and cavernous sinus. The septum separating the sphenoidal sinuses is the medial wall.

Proximity to the optic canal and cavernous sinus explains the so-called parasellar syndrome in patients with sphenoiditis.

The *frontal sinus* starts to develop from the middle nasal meatus in children older than 1 year. It is possible to image this by X-ray when the child is eight or older. The sinus acquires its final size (5 cm^3) by the age of 12 (Fig. 1.40).

The shape and size of frontal sinuses vary significantly. The upper border may reach the frontal eminences; the lower one may reach the supraorbital margins; the posterior one can extend to the lesser wings of the sphenoid bone; and the lateral one out to the zygomatic processes. Abnormalities of the frontal sinus are observed in 20 % of people (unilateral (10 %) or bilateral (4 %) absence, hypoplasia).

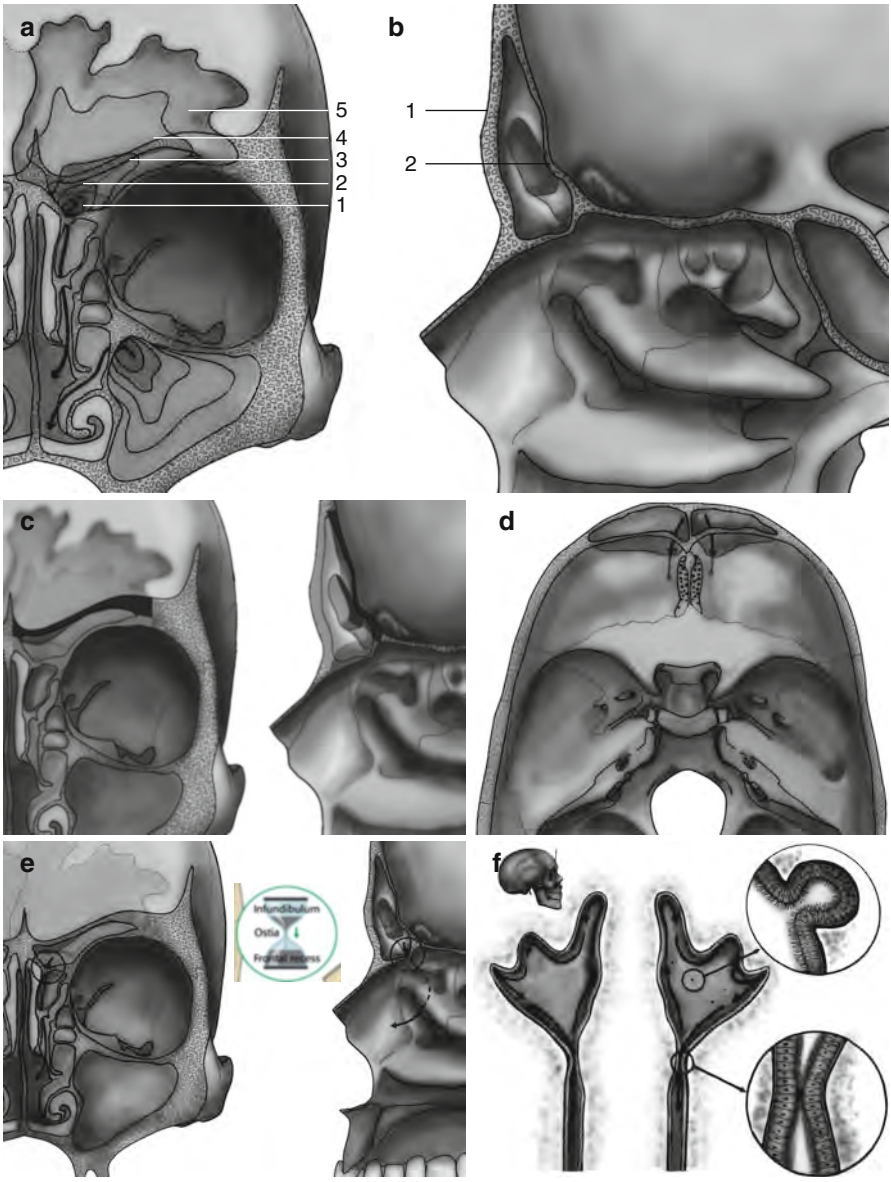

Fig. 1.40 Anatomy of the frontal sinus. (**a**) Evolution of the sinus size with age; (*1*) younger than 1 year; (*2*) 2–4 years; (*3*) 3–7 years; (*4*) 4–12 years; (*5*) sinus size in an adult; (**b**) different thickness (2–12 and 0.1–4 mm, respectively) and mechanical strength of its anterior (*1*) and posterior (*2*) walls; (**c**) topographic anatomy of the frontal sinus (adjacency to the orbit, anterior cranial fossa, and ethmoidal labyrinth); (**d**) the ostium localizes in the posterior–inferior–medial part of the sinus; (**e**) anatomy of the frontonasal duct (*encircled*): ethmoidal infundibulum; ostium, the most narrow (3–4 mm) portion of the frontonasal duct; frontal recess; (**f**) foramina of Breschet (The data were taken from the website www.aofoundation.org)

The anterior wall of the frontal sinus is formed by the anterior lamina of squama frontalis. The posterior, inferior, and medial walls are formed by the posterior lamina of squama frontalis.

The anterior wall of the frontal sinus is much thicker and stronger than its posterior wall that is not involved in the facial suture system (Fig. 1.40b). Hence, injuries destroying the anterior wall may also damage the posterior wall of the sinus. If this is the case, liquorrhea will be the result as the posterior wall is tightly connected to the dura mater at the ethmoidal roof.

Depending on pneumatization sources, the sinus may consist of one or several compartments. The septum of the frontal sinuses (the medial wall) is an inferior continuation of the crista galli.

The exterior half of the inferior wall of the frontal sinus is the roof of the orbit, and the posterointernal half hosts the frontonasal duct (Fig. 1.40c–e). It is the only anatomical structure responsible for sinus drainage and therefore plays the key role in treating its fractures. The craniocaudal course of the frontonasal duct is characterized by significant variability, which makes it difficult to elaborate a strategy for surgical treatment and to prognosticate outcomes. The duct opens in the anterior part of the middle nasal meatus, near the uncinate process. A total of 85 % of people have no frontonasal duct; in these cases, the sinus drains into the middle nasal meatus through the ethmoidal infundibulum.

The frontal sinus walls contain the foramina of Breschet (1917), the veins providing blood drainage from the sinus, which may facilitate spread of infection to the brain, passing through these foramina. In these areas, the mucous membrane is tightly adherent to the floor of special bony grooves (Fig. 1.40e). As a result, when performing sinus obliteration surgery, there is a risk of leaving mucous cells which may lead to subsequent mucocoele development.

1.6 Anatomy of the Temporal, Infratemporal, and Pterygopalatine Fossae

The temporal fossa (*fossa temporalis*) has an anterior, medial, and lateral wall. The anterior wall is formed by zygomatic processes of the frontal bone and the maxilla and by the zygomatic bone. The medial wall is formed by planum temporale. The lateral wall is formed by the zygomatic arc (arcus zygomaticus) (Fig. 1.41).

The temporal fossa hosts:

- The temporal muscle (m. temporalis)
- The superficial temporal artery (a. temporalis superficialis) and some of its branches (rr. auriculares anteriores, a. zygomaticoorbitalis, a. temporalis media)
- The deep temporal artery (a. temporalis profunda), a branch of a. maxillaris
- The superficial temporal vein (v. temporalis superficialis), a tributary of v. retromandibularis

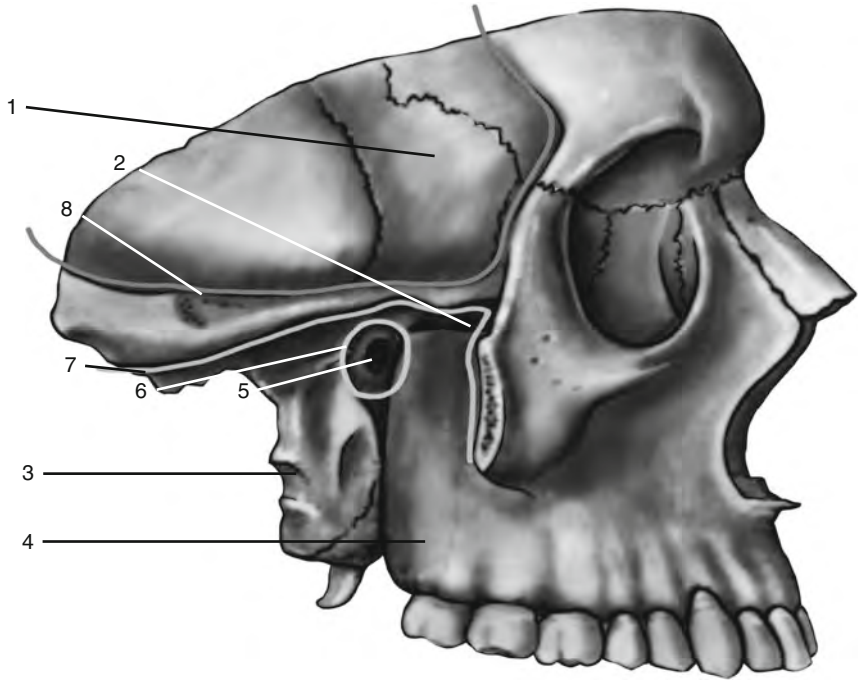

Fig. 1.41 Topographic anatomy of the temporal, infratemporal, and pterygopalatine fossae. (*1*) ala major ossis sphenoidalis; (*2*) fissura orbitalis inferior; (*3*) lamina lateralis processus pterygoidei; (*4*) tuber maxillae; (*5*) for. sphenopalatinum; (*6*) fossa pterygopalatina; (*7*) fossa infratemporalis; (*8*) fossa temporalis

- Superficial, middle, and deep temporal veins (vv. temporales superficiales, mediae et profundae), tributaries of v. retromandibularis
- The auriculotemporal nerve (n. auriculotemporalis)
- Deep temporal nerves (nn. temporales profundi)
- Branches of the parotid plexus of facial nerve (plexus intraparotideus nervi facialis)

Infratemporal fossa (*fossa infratemporalis*) has anterior, superior, and medial walls (Fig. 1.41). The anterior wall is formed by the zygomatic process and the maxillary tuber (*processus zygomaticus* et *tuber maxillae*) and the zygomatic bone (*os zygomaticum*). The superior wall is not continuous; it is formed by the temporal bone (*os temporale*) and the infratemporal surface of the greater wing of the sphenoid bone below the infratemporal crest (*facies infratemporalis alae majoris ossis sphenoidalis*). The medial wall is formed by the lateral lamina of the pterygoid process of the sphenoid bone (*lamina lateralis processus pterygoidei ossis sphenoidalis*).

The *infratemporal crest* (*crista infratemporalis*) is the border between the temporal and infratemporal fossae.

Contents of the infratemporal fossa:

- The medial and lateral pterygoid muscles.
- The maxillary artery (a. maxillaris) and its branches separating within the maxillary and pterygoid sections: a. auricularis profunda, a. tympanica anterior, a. alveolaris inferior, a. meningea media, a. masseterica, rr. pterygoidei, and a. buccalis.
- The pterygoid venous plexus (pl. venosus pterygoideus).
- The retromandibular vein (v. retromandibularis).
- The mandibular nerve (n. mandibularis, the branch of n. trigeminus) and its branches: n. alveolaris inferior, n. auriculotemporalis, n. massetericus, and nn. pterygoidei medialis et lateralis, n. buccalis.
- The following vessels run through the posterior alveolar foramina (foramina alveolaria posteriora): a. alveolaris posterior superior (from a. maxillaris) and rr. alveolares superiores posteriores (branches of n. infraorbitalis from n. maxillaris, the second branch of n. trigeminus).

The *pterygopalatine fossa* (*fossa pterygopalatina*) has three walls: the anterior, posterior, and medial ones. The anterior wall is formed by the maxillary tuber (tuber maxillae). The posterior wall is formed by the pterygoid process of the sphenoid

Table 1.6 Structures communicating with the pterygopalatine fossa and their contents

Communicating structure	Contents		
	Arteries	Veins	Nerves
Foramen rotundum (foramen rotundum)			N. maxillaris (n. V_2)
Inferior orbital fissure (fissura orbitalis inferior)	A. infraorbitalis	V. infraorbitalis	N. zygomaticus et N. infraorbitalis (branches of n. maxillaris, from n. trigeminus)
Pterygoid canal (canalis pterygoideus)	A. canalis pterygoidei (from a. palatina descendens from a. maxillaris)	V. canalis pterygoidei (tributary of pl. venosus pterygoideus)	N. canalis pterygoidei (coalescence of N. petrosus major and N. petrosus profundus)
Sphenopalatine foramen (foramen sphenopalatinum)	A. sphenopalatina (from a. maxillaris)	V. sphenopalatina (tributary of pl. venosus pterygoideus)	Rr. nasales posteriores superiores mediales et laterales (from ganglion pterygopalatinum)
Greater palatine canal (canalis palatinus major)	A. palatina descendens (from a. maxillaris)	Vv. palatinae (tributary of pl. venosus pterygoideus)	N. palatinus major et rr. nasales posteriores inferiores (from ganglion pterygopalatinum)
Pterygomaxillary fissure (fissura pterygomaxillaris)	A. maxillaris; aa. palatinae minores (from a. palatina descendens from a. maxillaris)	Plexus venosus pterygoideus (tributary of v. mandibularis)	Nn. palatini minores (from ganglion pterygopalatinum)

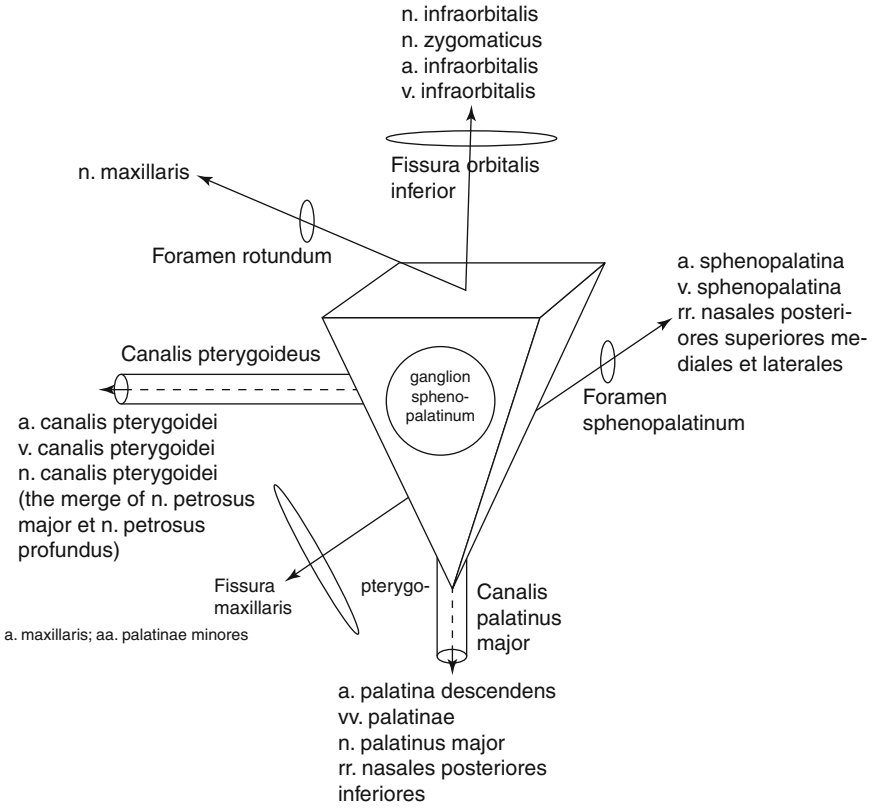

Fig. 1.42 Structures communicating with the pterygopalatine fossa and their contents

bone (processus pterygoideus ossis sphenoidalis). The medial wall is formed by the perpendicular lamina of the ethmoid bone (lamina perpendicularis ossis ethmoidalis).

The pterygopalatine fossa communicates with various topographic cranial structures: through the foramen rotundum with the middle cranial fossa, through the inferior orbital fissure with the orbit, through the pterygoid canal (canalis pterygoideus) with the inferior surface of the skull base, and through the pterygomaxillary fissure with the infratemporal fossa. It should be mentioned that some of these foramina cannot be found on individual bones and are formed only at bone junctions (the sphenopalatine foramen, the greater palatine canal, and the inferior orbital fissure).

These foramina contain numerous vessels and nerves (Table 1.6 and Fig. 1.42).

References

1. Lemke B. N. (1987). Anatomy of ocular adnexa and orbit. In B. C. Smith (Ed.), *Ophthalmic plastic and reconstructive surgery* (Vols. 1 and 2, pp 3–74). St. Louis: C.V. Mosby.

2. Whitnall, S. E. (1932). *Anatomy of the human orbit*. London: Oxford University Press.
3. Simonton, J. T., Garber, P. F., & Ahl, N. (1977). In margins of safety in lateral orbitotomy. *Archives of Ophthalmology, 95*(7), 1229–1231.
4. Whitnall, S. E. (1911). On a tubercle on the malar bone, and on the lateral attachments of the tarsal plates. *Journal of Anatomy and Physiology, 45*(pt 4), 426–432.
5. Fink, W. H. (1948). The surgical anatomy of the superior oblique muscle. *Transactions of the American Ophthalmological Society, 46*, 154–184.
6. Helveston, E. M., Merriam, W. W., Ellis, F. D., et al. (1982). The trochlea: A study of the anatomy and physiology. *Ophthalmology, 89*(2), 124–133.
7. Jo, A., Rizen, V., Nikolic, V., & Banovic, B. (1989). The role of orbital wall morphological properties and their supporting structures in the etiology of "blow-out" fractures. *Surgical and Radiologic Anatomy, 11*(3), 241–248.
8. Song, W. K., Lew, H., Yoon, J. S., et al. (2009). Role of medial orbital wall morphologic properties in orbital blow-out fractures. *Investigative Ophthalmology & Visual Science, 50*(2), 495–499.
9. Blaylock, W. K., Moore, C. A., & Linberg, J. V. (1990). Anterior ethmoid anatomy facilitates dacryocystorhinostomy. *Archives of Ophthalmology, 108*(12), 1774–1777. Philadelphia: Saunders.
10. Ploder, O., Klug, C., Voracek, M., et al. (2002). Evaluation of computer-based area and volume measurement from coronal computed tomography scans in isolated blowout fractures of the orbital floor. *Journal of Oral and Maxillofacial Surgery, 60*(11), 1267–1272.
11. Evans, B. T., & Webb, A. A. (2007). Post-traumatic orbital reconstruction: Anatomical landmarks and the concept of the deep orbit. *The British Journal of Oral & Maxillofacial Surgery, 45*(3), 183–189.
12. Nguyen, P. N., & Sullivan, P. (1992). Advances in the management of orbital fractures. *Clinics in Plastic Surgery, 19*(1), 87–98.
13. Movassaghi, K., & Janecka, I. (2005). Optic nerve decompression via mid-facial translocation approach. *Annals of Plastic Surgery, 54*(3), 331–335.
14. Bergen, M. P. (1981). A literature review of the vascular system in the human orbit. *Acta Morphologica Neerlando-Scandinavica, 19*(4), 273–305.
15. Bergen, M. P. (1982). Relationships between the arteries and veins and the connective tissue system in the human orbit. *Acta Morphologica Neerlando-Scandinavica, 20*(1), 1–15.
16. Bergen, M. P. (1982). Relationships between the arteries and veins and the connective tissue system in the human orbit. *Acta Morphologica Neerlando-Scandinavica, 20*(1), 17–26.
17. Bergen, M. P. (1982). Relationship between the arteries and veins and the connective tissue system in the human orbit. *Acta Morphologica Neerlando-Scandinavica, 20*(1), 27–42.
18. Bergen, M. P. (1982). A spatial reconstruction of the orbital vascular pattern in relation with the connective tissue system. *Acta Morphologica Neerlando-Scandinavica, 20*(2), 117–137.
19. Bergen, M. P. (1982). Microvessels in the human orbit in relation to the connective tissue system. *Acta Morphologica Neerlando-Scandinavica, 20*(2), 139–150.
20. Bergen, M. P. (1982). Some histological aspects of the structure of the connective tissue system and its relationships with the blood vessels in the human orbit. *Acta Morphologica Neerlando-Scandinavica, 20*(4), 293–308.
21. Reymond, J., Kwiatkowski, J., & Wysocki, J. (2008). Clinical anatomy of the superior orbital fissure and the orbital apex. *Journal of Cranio-Maxillo-Facial Surgery, 36*(6), 346–353.
22. Lang, J. (1975). The vascularization of the periorbita. *Gegenbaurs Morphologisches Jahrbuch, 121*(2), 174–191.
23. Manson, P. N., Clifford, C. M., Su, C. T., et al. (1986). Mechanisms of global support and posttraumatic enophthalmos: I. The anatomy of the ligament sling and its relation to intramuscular cone orbital fat. *Plastic and Reconstructive Surgery, 77*(2), 193–202.
24. Koornneef, L. (1977). Details of the orbital connective tissue system in the adult. *Acta Morphologica Neerlando-Scandinavica, 15*(1), 1–34.
25. Koornneef, L. (1977). New insights in the human orbital connective tissue. Result of a new anatomical approach. *Archives of Ophthalmology, 95*(7), 1269–1273.
26. Koornneef, L. (1977). The architecture of the musculo-fibrous apparatus in the human orbit. *Acta Morphologica Neerlando-Scandinavica, 15*(1), 35–64.

27. Dutton, J. J. (1994). *Atlas of clinical and surgical orbital anatomy*. Philadelphia: Saunders.
28. Koornneef, L. (1979). Orbital septa: Anatomy and function. *Ophthalmology, 86*(5), 876–880.
29. Jordan, D. R., & Anderson, R. L. (1996) *Surgical anatomy of the ocular adnexa: A clinical approach* (Ophthalmology monographs: 9) (p. 134). LEO.
30. Hosokawa, H. (1956). A note on the fibrous apparatus surrounding the human eyeball. *Okajimas Folia Anatomica Japonica, 28*(1–6), 165–181.
31. Knize, D. M. (2002). The superficial lateral canthal tendon: Anatomic study and clinical application to lateral canthopexy. *Plastic and Reconstructive Surgery, 109*(3), 1149–1157.
32. Flowers, R. S., Nassif, J. M., Rubin, P. A., et al. (2005). A key to canthopexy: the tarsal strap. A fresh cadaveric study. *Plastic and Reconstructive Surgery, 116*(6), 1752–1758.
33. Fink, W. H. (1957). An anatomical study of the check mechanism of the vertical muscles of the eyes. *American Journal of Ophthalmology, 44*(6), 800–809.
34. Whitnall, S. E. (1911). On a ligament acting as a check to the action of the levator palpebrae superioris muscle. *Journal of Anatomy and Physiology, 45*(pt 2), 131–139.
35. Anderson, R. L., & Dixon, R. S. (1979). The role of Whitnall's ligament in ptosis surgery. *Archives of Ophthalmology, 97*(4), 705–707.
36. Anderson, R. L., & Beard, C. (1977). The levator aponeurosis. Attachments and their clinical significance. *Archives of Ophthalmology, 95*(8), 1437–1441.
37. Collin, J. R., Beard, C., & Wood, I. (1978). Experimental and clinical data on the insertion of the levator palpebrae superioris muscle. *American Journal of Ophthalmology, 85*(6), 792–801.
38. Stasior, G. O., Lemke, B. N., Wallow, I. H., et al. (1993). Levator aponeurosis elastic fiber network. *Ophthalmic Plastic and Reconstructive Surgery, 9*(1), 1–10.
39. Hawes, M. J., & Dortzbach, R. K. (1982). The microscopic anatomy of the lower eyelid retractors. *Archives of Ophthalmology, 100*(8), 1313–1318.
40. Lockwood, C. B. (1886). The anatomy of the muscles, ligaments, and fascia of the orbit, including an account of the capsule of tenon, the check ligaments of recti, and of the suspensory ligament of the eye. *Journal of Anatomy and Physiology, 20*(pt 1), 1–25.
41. Anderson, R. L., Panje, W. R., & Gross, C. E. (1982). Optic nerve blindness following blunt forehead trauma. *Ophthalmology, 89*(5), 445–455.
42. Chang, E. L., & Bernardino, C. R. (2004). Update on orbital trauma. *Current Opinion in Ophthalmology, 15*(5), 411–415.
43. Papageorgiou, K. I., Mathew, R. G., Ghazi-Nouri, S. M., et al. (2007). Optochiasmal avulsion secondary to minor occipital trauma. *Orbit, 26*(1), 71–74.
44. Soparkar, C. N. S., & Patrinely, J. R. (2007). The eye examination in facial trauma for the plastic surgeon. *Plastic and Reconstructive Surgery, 120*(7 Suppl. 2), S49–S56.
45. Castanares, S. (1951). Blepharoplasty for herniated intraorbital fat: Anatomical basis for a new approach. *Plastic and Reconstructive Surgery, 8*(1), 46–58.
46. Putterman, A. M., & Urist, M. J. (1974). Surgical anatomy of the orbital septum. *Annals of Ophthalmology, 6*(3), 290–294.
47. Meyer, D. R., Linberg, J. V., Wobig, J. L., & McCormick, S. A. (1991). Anatomy of the orbital septum and associated eyelid connective tissues. *Ophthalmic Plastic and Reconstructive Surgery, 7*(2), 104–113.
48. Reid, R. R., Said, H. K., Yu, M., et al. (2006). Revisiting upper eyelid anatomy: Introduction of the septal extension. *Plastic and Reconstructive Surgery, 117*(1), 65–66.
49. Hayreh, S. S., & Dass, R. (1962). The ophthalmic artery: I. Origin and intracranial and intracanalicular course. *British Journal of Ophthalmology, 46*(2), 65–98.
50. Hayreh, S. S., & Dass, R. (1962). The ophthalmic artery: II. Intraorbital course. *British Journal of Ophthalmology, 46*(3), 165–185.
51. Hayreh, S. S. (1962). The ophthalmic artery: III. Branches. *British Journal of Ophthalmology, 46*(4), 212–247.
52. Hayreh, S. S. (1963). The central artery of the retina. Its role in the blood supply of the optic nerve. *British Journal of Ophthalmology, 47*(11), 651–663.

53. Hayreh, S. S. (1963). The cilio-retinal arteries. *British Journal of Ophthalmology, 47*(2), 71–89.
54. Duke-Elder, S., & Wybar, K. C. (1961). The anatomy of the visual system. In S. Duke-Elder (Ed.), *System of ophthalmology* (pp. 551–567). New York: Kimpton.
55. Sherman, D. D., Gonnering, R. S., Wallow, I. H., et al. (1993). Identification of orbital lymphatics: Enzyme histochemical light microscopic and electron microscopic studies. *Ophthalmic Plastic and Reconstructive Surgery, 9*(3), 153–169.
56. Gausas, R. E., Gonnering, R. S., Lemke, B. N., et al. (1999). Identification of human orbital lymphatics. *Ophthalmic Plastic and Reconstructive Surgery, 15*(4), 252–259.
57. Cook, B. E., Lucarelli, M. J., Lemke, B. N., et al. (2002). Eyelid lymphatics I: Histochemical comparisons between the monkey and human. *Ophthalmic Plastic and Reconstructive Surgery, 18*(1), 18–23.
58. Cook, B. E., Lucarelli, M. J., Lemke, B. N., et al. (2002). Eyelid lymphatics II: A search for drainage patterns in the monkey and correlations with human lymphatics. *Ophthalmic Plastic and Reconstructive Surgery, 18*(1), 99–106.
59. Doxanas, M. T., & Anderson, R. L. (1984). *Clinical orbital anatomy*. Baltimore: Williams & Wilkins.
60. Zide, B. M., & Jelks, G. W. (1985). *Surgical anatomy of the orbit*. New York: Raven.
61. Koornneef, L. (1988). Eyelid and orbital fascial attachments and their clinical significance. *Eye, 2*(pt 2), 130–134.
62. Jones, L. T., & Wobig, J. L. (1977). The Wendell L. Hughes Lecture. Newer concepts of tear duct and eyelid anatomy and treatment. *Transactions. Section on Ophthalmology. American Academy of Ophthalmology and Otolaryngology*, 83(4 Pt 1), 603–616.

Further Reading

Collin, J. R., Beard, C., & Wood, I. (1979). Terminal course of nerve supply to Müller's muscle in the rhesus monkey and its clinical significance. *American Journal of Ophthalmology, 87*(2), 234–246.
Gioia, V. M., Linberg, J. V., & McCormick, S. A. (1987). The anatomy of the lateral canthal tendon. *Archives of Ophthalmology, 105*(4), 529–532.
Goldberg, R. A., Hannani, K., & Toga, A. W. (1992). Microanatomy of the orbital apex. Computed tomography and microcryoplaning of soft and hard tissue. *Ophthalmology, 99*(9), 1447–1452.
Kakizaki, H., Zako, M., Nakano, T., et al. (2005). The levator aponeurosis consists of two layers that include smooth muscle. *Ophthalmic Plastic and Reconstructive Surgery, 21*(4), 281–284.
Kakizaki, H., Jinsong, Z., Zako, M., et al. (2006). Microscopic anatomy of Asian lower eyelids. *Ophthalmic Plastic and Reconstructive Surgery, 22*(6), 430–433.
Lowe, J. B., Cohen, M., Hunter, D. A., et al. (2005). Analysis of the nerve branches to the orbicularis oculi muscle of the lower eyelid in fresh cadavers. *Plastic and Reconstructive Surgery, 116*(6), 1743–1749.
Lyon, D. B., Lemke, B. N., Wallow, I. H., & Dortzbach, R. K. (1992). Sympathetic nerve anatomy in the cavernous sinus and retrobulbar orbit of the cynomolgus monkey. *Ophthalmic Plastic and Reconstructive Surgery, 8*(1), 1–12.
Sacks, J. G. (1984). The shape of the trochlea. *Archives of Ophthalmology, 102*(6), 932–933.
Stewart, W. B. (Ed.). (1993). *Surgery of the eyelid, orbit, and lacrimal system* (Vol. 3, Ophthalmology monographs: 8). LEO, San Francisco: American Academy of Ophthalmology.
Tucker, S. M., & Linberg, J. V. (1994). Vascular anatomy of the eyelids. *Ophthalmology, 101*(6), 1118–1121.
Warwick, R. (1976). *Eugene Wolff's anatomy of the eye and orbit* (7th ed.). Philadelphia: WB Saunders.

Radiological Examination of the Orbit

2

Vadim P. Nikolaenko, Yury S. Astakhov,
Gennadiy E. Trufanov, Evgeniy P. Burlachenko,
Valery V. Zakharov, and Valentina D. Lugina

Contents

2.1 CT and MRI Anatomy of the Orbit. 81
References 118

V.P. Nikolaenko, MD, PhD, DSc (✉)
Department of Ophthalmology, Saint Petersburg State Hospital No. 2, Saint-Petersburg, Russia

Department of Otolaryngology and Ophthalmology, Medical Faculty, Saint-Petersburg State University, Saint-Petersburg, Russia
e-mail: dr.nikolaenko@mail.ru

Y.S. Astakhov, MD, PhD, DSc
Department of Ophthalmology, I.P. Pavlov First Saint Petersburg State Medical University, Saint-Petersburg, Russia

City Ophthalmologic Center at Saint Petersburg State Hospital No. 2, Saint-Petersburg, Russia
e-mail: astakhov73@mail.ru

G.E. Trufanov, MD, PhD
Scientific Investigational Radiological Unit, V.A.Almazov Federal North-West Medical Research Centre, Saint-Petersburg, Russia
e-mail: burep@yandex.ru

E.P. Burlachenko, MD
CT Department, Kirov Military Medical Academy, Saint-Petersburg, Russia
e-mail: burep@yandex.ru

V.V. Zakharov, MD, PhD
Head of the X-ray Diagnostics department Saint Petersburg State No.2, Saint-Petersburg, Russia

V.D. Lugina, MD
X-ray Department of the Ophthalmology Department, Kirov Military Medical Academy, Saint-Petersburg, Russia
e-mail: irterehova@yandex.ru

© Springer-Verlag Berlin Heidelberg 2015

V.P. Nikolaenko, Y.S. Astakhov (eds.), *Orbital Fractures: A Physician's Manual*,
DOI 10.1007/978-3-662-46208-9_2

Radiological diagnosis is the key instrumental method to examine both normal and pathological conditions of the orbit.

The radiological diagnosis can be further divided into X-ray diagnostic imaging, ultrasonic diagnosis, X-ray computed tomography, radionuclide diagnosis, and magnetic resonance imaging.

The algorithm of emergency radiological examination of an injured person should rely on the following principles:

- The maximum possible extension of indications for emergency radiological diagnosis
- Participation of an experienced trauma team that should include maxillofacial trauma surgeons, radiologists experienced in reading facial and cranial trauma conditions, an anesthesiologist to ensure the safety of the patient's airway, and possibly neurosurgeons
- The principle of reasonable minimal sufficiency (i.e., performing the most informative examination that would allow one to make a diagnosis in a timely manner)
- The possibility of performing emergency intervention at any time

X-ray diagnostic imaging remains the simplest and most widely used method for performing the *initial assessment* of the condition of the orbit. *The indications for radiographic examination include any injuries to soft tissues of the head and suspected craniofacial trauma*.

When positioning the patient's head for radiological diagnosis, one should use the conventional planes to properly orient the central X-ray beam. The main planes are listed below:

1. *The sagittal plane* (the median sagittal plane) runs longitudinally down the head along the sagittal suture and divides the head into the right and left halves.
2. *The transverse (horizontal) plane* is perpendicular to the sagittal and the frontal planes and passes through the external acoustic foramina and infraorbital margins (the infraorbital meatal line), thus dividing the head into the superior and inferior sections.
3. *The frontal plane* (the plane of the auricular vertical line) that is perpendicular to the sagittal and horizontal planes and runs vertically through the external acoustic foramina and divides the head into the anterior and posterior sections.

The first stage of emergency X-ray diagnostic imaging of a patient with craniofacial trauma is to assess the condition of the cranial bones. *The main (standard) examination positions* include anteroposterior and posteroanterior, right and left lateral recumbent, axial, nasofrontal, frontal, nasomental, anterior, and posterior semiaxial.

The examination starts with scanning the skull in two mutually perpendicular views, the anteroposterior and the lateral. If necessary, the X-ray images in the posteroanterior and posterior semiaxial views are obtained simultaneously.

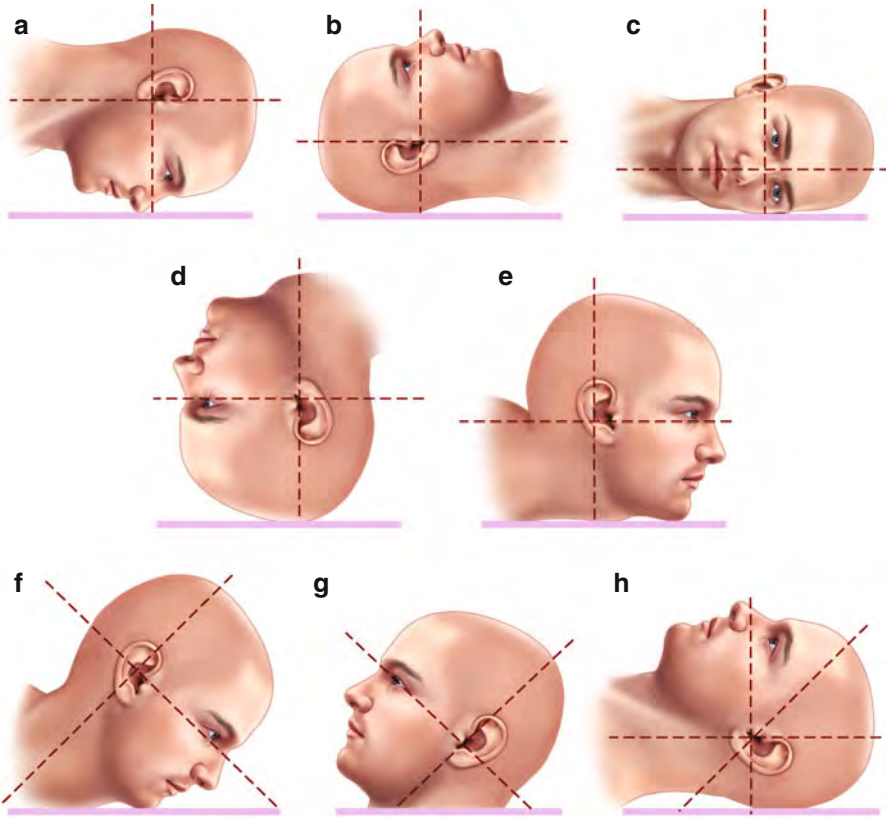

Fig. 2.1 The main views of the skull: (**a**, **b**) the anterior and posterior views. The auricular vertical plane runs parallel to the X-ray film holder, while the median sagittal plane and the horizontal plane run perpendicular to it. (**c**) The lateral view. The median sagittal plane is oriented parallel to the X-ray film holder, while the auricular vertical and horizontal planes are oriented perpendicular to it. (**d, e**) The parietal (**d**) and mental (**e**) axial views, when the horizontal plane is oriented parallel to the X-ray film holder plane, while the sagittal and the auricular vertical planes are oriented perpendicular to it. (**f, g**) Anterior (**f**) and posterior (**g**) semiaxial views, when the horizontal and auricular vertical planes are oriented at an angle of 45° with respect to the X-ray film holder, while the median sagittal plane is strictly perpendicular to it. If position (**g**) is infeasible, position (**h**) is used

In patients with severe head injury, X-ray diagnostic imaging is performed in a supine position using four views: the posteroanterior, posterior semiaxial, and two lateral ones.

Craniofacial trauma requires X-ray imaging in the nasomental and anterior semiaxial (occipitomental) views, which ensures proper imaging in most cases (Fig. 2.1).

X-ray imaging of the skull using the *anteroposterior view* provides a general overview of the condition of the calvarial bones, cranial sutures, and temporal pyramids. It is difficult to interpret the condition of the orbit because the images of the bones of the skull base overlap those of the upper sections of the orbit. However, the orbital opening and the orbital floor are clearly discernible (Fig. 2.2).

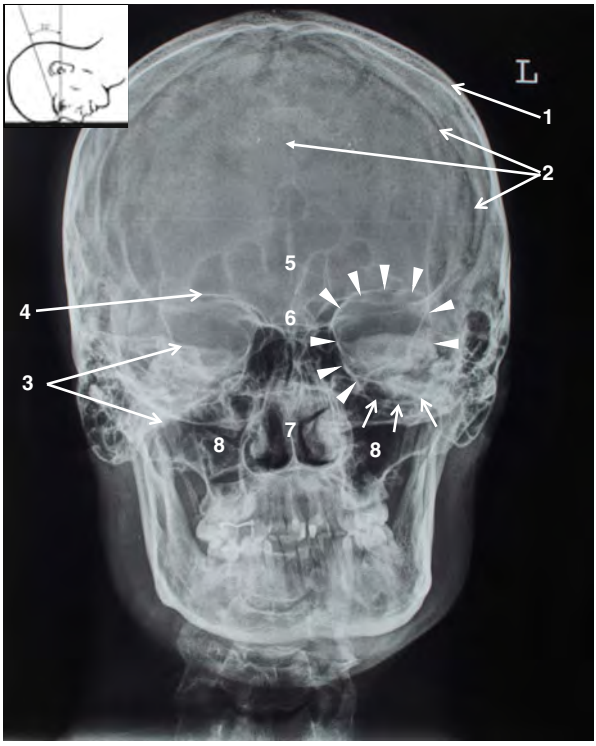

Fig. 2.2 X-ray image of the skull in the anteroposterior view (nasofrontal position): The calvarial bones (*1*) and cranial sutures (*2*) are clearly discernible. The image of the temporal pyramids (*3*) overlaps that of the orbit (*4*), resulting in fragmentary image of the orbital opening (shown with *small triangular arrows*) and the infraorbital margin in particular (*small arrows*). The superior orbital wall is imaged rather clearly. Furthermore, frontal sinuses (*5*), cribriform plate of the ethmoidal labyrinth (*6*), nasal cavity (*7*), and maxillary sinuses (*8*) are seen in the image

X-ray imaging of the skull in the *posteroanterior view* is mainly performed for patients with severe head injury. Such orbital structures as wings of the sphenoid bone and the superior orbital fissures are clearly seen in the images.

X-ray imaging of the skull using the *lateral view* also presents an overview and is rather useful to assess the condition of the calvarial bones and the skull base (but not the facial skeleton). Paranasal sinuses, sella turcica, anterior and posterior clinoid processes, nasopharynx, and lamina cribrosa of the ethmoid bone are clearly discernible in the images. This view presents the best image of the lateral margin and the superior orbital wall. It is difficult to interpret the condition of the orbital floor using the lateral view due to its S-shaped profile and elevation toward the orbital apex. Also, the overlap of the images of both orbits results in several contours of the orbital floor seen on a single image [1] (Fig. 2.3).

A standard X-ray examination of the orbit and periorbital structures includes occipitofrontal (Caldwell's) projection, nasomental projection, Waters anterior semiaxial (occipitomental) projection, and lateral and parietal (submentovertex) projections (Table 2.1).

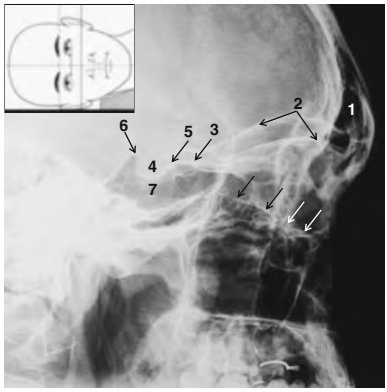

Fig. 2.3 X-ray image of the skull in the lateral view: Frontal sinuses (*1*), jugum sphenoidale (*3*), sella turcica (*4*), anterior (*5*) and posterior (*6*) clinoid processes, and sphenoidal sinus (*7*) are seen in the image. This view provides the best image of the lateral margin and the orbital roof (*2*). It is difficult to interpret the condition of the orbital floor (shown with *arrows*) using the lateral view due to its S-shaped profile, elevation toward the orbital apex, and summation of the images of both orbits, resulting in several contours of the orbital floor seen in an image

Table 2.1 The main X-ray projections used to diagnose orbital fractures

Projection	Anatomical structure being visualized	Pathological changes being visualized
Occipitomental	The anterior two-thirds of the orbital floor, the zygomatic arch Maxillary sinus	Fractures of the superior and inferior orbital walls with vertical displacement of the fragments Sinusitis, hemosinus
Occipitofrontal	Frontal sinus, ethmoidal labyrinth Innominate line Sphenoid bone Posterior one-third of the orbital floor	Hemosinus, mucocele, fracture of sinus walls Fracture of the medial and lateral orbital walls Lateral wall fracture Blow-out fracture
Lateral	Superior orbital wall Sella turcica	Fracture of the superior wall Pituitary disorders
Basal (submentovertex)	Sphenoid sinus and ethmoidal labyrinth Lateral orbital wall Zygomatic arch	Fracture Lateral orbital wall fracture Fracture of the zygomatic arch
Rhese's oblique anterior	Optic canal	Fracture of canal walls

In addition to the aforementioned standard projections, three specialized ones are used: nasal projection, frontal protuberance projection, and Rhese's oblique anterior (posterior) projection (Fig. 2.4).

Caldwell's occipitofrontal projection (1918) allows one to study the contours of the orbital opening, the lacrimal sac fossa, and the medial and lateral orbital walls but not the infraorbital margin. This is because it is difficult to assess the infraorbital

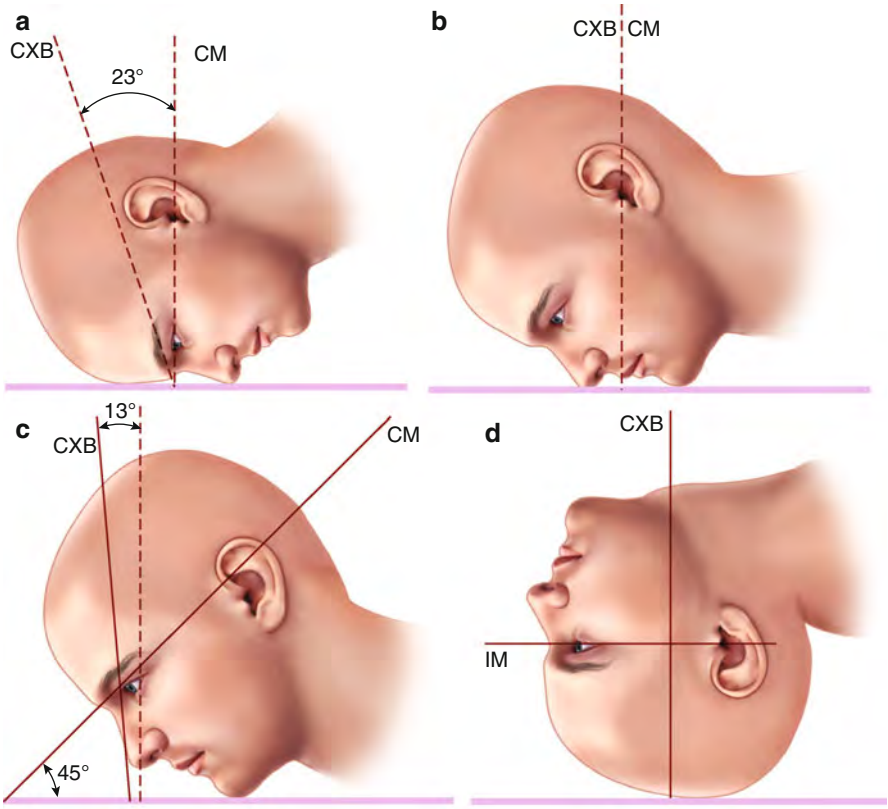

Fig. 2.4 Projections used for X-ray imaging of the orbit: *CM* canthomeatal (or the orbitomeatal) line connecting the lateral canthus and the external acoustic foramen (the physiological horizontal line), *CXB* central X-ray beam. (**a**) Caldwell's occipitofrontal (anterior fronto-occipital) projection. A prone patient touches the X-ray film holder with his/her nose tip and forehead. The angle between the X-ray beam direction and the canthomeatal line (15–23°) moves the shadow from the temporal bone downward from the image of the orbit. (**b**) Nasomental projection. The nose and chin of a prone patient are tightly pressed against the X-ray film holder. (**c**) Waters anterior semi-axial (occipitomental) projection. A prone patient touches the X-ray film holder only with his/her chin; the nose tip lies 0.5–1.5 cm above the X-ray film holder. The angle between the canthomeatal line and the central X-ray beam is 37–45°. (**d**) The basal (axial, submentovertex) projection. A cushion is placed under the shoulders of a patient lying supine so that his/her head tilted back touched the X-ray film holder with the bregma, while the infraorbitomeatal line (IM) is parallel to the X-ray cassette and perpendicular to the central X-ray beam. (**e**) Rhese's oblique anterior projection. The head of a patient lying prone is positioned in such a manner that the superciliary area, the zygomatic bone, and the nose tip were pressed against the X-ray film holder. The beam is centered for the opposite parietal protuberance; the sequential images of both orbits are obtained strictly symmetrically

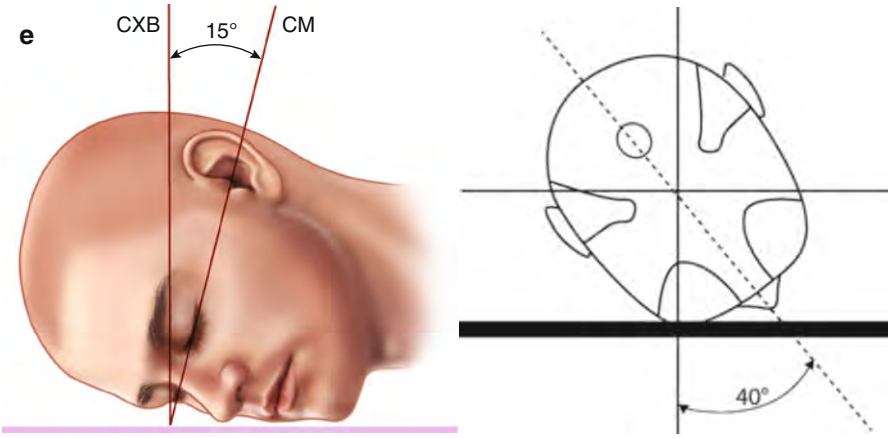

Fig. 2.4 (continued)

margin because the shadow from the inferior orbital wall overlaps the margin with the anterior one-third of the inferior orbital wall imaged below the margin, the middle one-third lies at its level, and the posterior one-third imaged above the margin [2]. In this view, such anatomical structures as the superior and inferior orbital fissures and wings of the sphenoid bone are overlapped by temporal pyramids (Figs. 2.2 and 2.4a).

An image using the nasomental projection with patient's nose being tightly pressed to the X-ray cassette is an overview image of the orbits in the anteroposterior view, which allows one to compare the shape and size of margo orbitalis. Furthermore, this projection is the one to be used when examining the frontal and maxillary sinuses and the ethmoidal labyrinth. Finally, facial bones are clearly visualized in the nasomental projection (Figs. 2.4b and 2.5).

The Waters and Waldron (1915) semiaxial occipitomental projection is indispensable for assessing the condition of the anterior portions of the medial wall, the roof and floor of the orbit, the zygomatic bones, the lesser wing of the sphenoid bone, the infraorbital foramen, as well as the maxillary sinuses and the ethmoidal labyrinth (Figs. 2.4c and 2.6). Due to the clear image of the superior orbital wall, as well as the anterior and middle one-thirds of the inferior orbital walls, the projection is used to visualize the vertically displaced roof and floor fragments, including the diagnosis of blow-out and blow-in fractures of the orbital roof and floor. When interpreting an image, one should bear in mind that the image of the orbital floor is 10 mm below the contour of the infraorbital margin due to specific features of the projection.

Thus, the occipitomental and occipitofrontal projections need to be used to perform a thorough analysis of the condition of the inferior orbital wall.

The Schuller's (1905) and Bowen's (1914) basal (axial, parietal, submentovertex) projection visualizes the lateral wall of the orbit and maxillary sinus along its

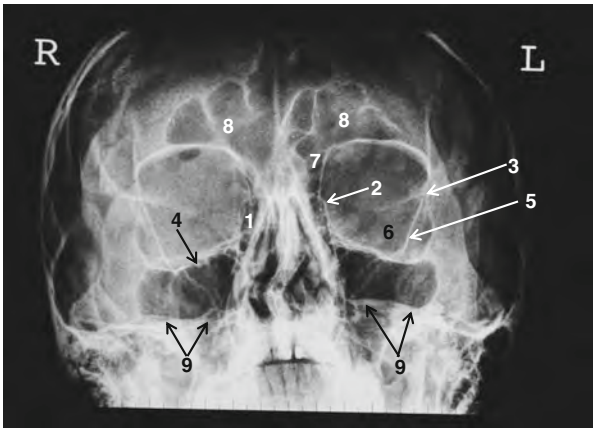

Fig. 2.5 X-ray image of the orbits in anteroposterior projection (Caldwell's occipitofrontal projection) allows one to assess the contours of the orbital opening, the lacrimal sac fossa (*1*), and the medial (*2*) and lateral (*3*) walls of the orbit. It is difficult to assess the infraorbital margin (*4*), since it is overlapped by the shadow of the inferior wall (with the anterior one-third of the inferior wall lying above the margin, the middle one-third lying at its level, and the superior one-third lying above the margin). (*5*) Innominate line, (*6*) the greater wing of the sphenoid bone, (*7*) ethmoidal labyrinth, (*8*) frontal sinus, and (*9*) margin of the pyramid of the temporal bone

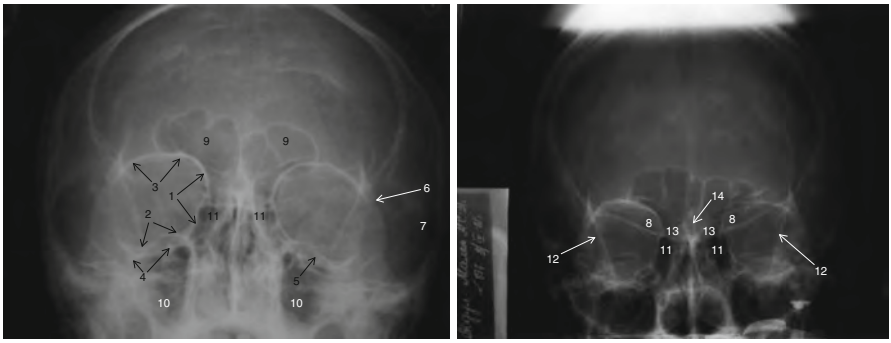

Fig. 2.6 X-ray imaging in the anterior semiaxial (occipitomental) projection according to Waters and Waldron (1915): Since the shadow of the pyramid of the temporal bone is moved downward, the projection clearly visualizes the medial (*1*), inferior (*2*), and superior (*3*) walls of the orbit, the infraorbital margin (*4*) and the infraorbital canal (*5*), the frontozygomatic suture (*6*), the zygomatic arch (*7*), the lesser wing of the sphenoid bone (*8*), as well as the frontal (*9*) and maxillary sinuses (*10*) and ethmoidal labyrinth (*11*). (*12*) Innominate line (linea innominata), (*13*) cribriform plate of the ethmoid bone, and (*14*) crista galli

entire length, the nasopharynx, the pterygoid processes of the sphenoid bone, the pterygopalatine fossa, the sphenoidal sinus, and the ethmoidal labyrinth (Figs. 2.4d and 2.7). Meanwhile, the medial half of the orbits is overlapped by the image of the maxillary tooth row. The position cannot be used in patients with suspected injury of the cervical spine since it involves hyperextension of the neck.

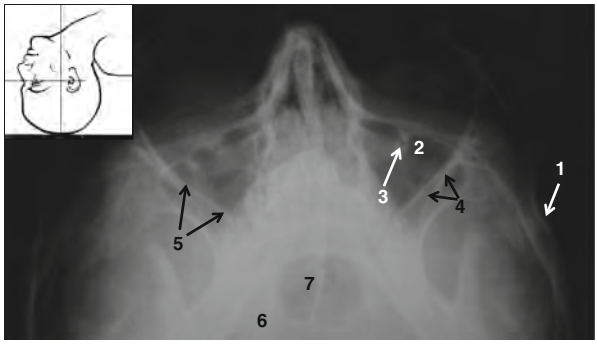

Fig. 2.7 X-ray image of the orbit in the Schuller's (1905) and Bowen's (1914) axial projection: *1* zygomatic arch, *2* orbit, *3* infraorbital canal, *4* lateral wall of the orbit, *5* posterior wall of the maxillary sinus, *6* pterygoid process of the sphenoid bone, *7* sphenoidal sinus

The nasal projection (the anterior sagittal projection) is used to assess the condition of the wings of the sphenoid bone and the superior orbital fissures. Due to variability in structure of the sphenoid bone, it is difficult to analyze the images of the superior orbital fissures recorded using the nasal projection; therefore, special attention should be paid to the symmetry of the shape and size of the superior orbital fissures when assessing the images obtained from this projection. Mild orbital asymmetry is a normal variant, while more pronounced differences (more than 2 mm) are abnormal.

The frontal protuberance projection is obtained with a 3–4 cm-thick bandage placed under the nose tip and the central X-ray beam is directed anteriad from the external acoustic meatus. This projection visualizes the inferior orbital fissures.

Sequential X-ray imaging of the right and left orbits in the *Rhese's oblique anterior (posterior) projections* (1911) is performed to visualize the optic canals (Fig. 2.4). The vertical and horizontal size of the optic foramen in the resulting image is normally 6 and 5 mm, respectively; the interorbital asymmetry of the size of optic foramina in 96% of patients is less than 1 mm. Both the increased vertical diameter (up to 6.5 mm and more) and obvious (more than 1 mm) asymmetry of optic foramina are indicative of a pathological state.

In addition to the optic foramen, the image displays the roots of the lesser wing of the sphenoid bone and the upper sections of the ethmoidal labyrinth. The pneumatized anterior clinoid process can be mistaken for the optic foramen. In order to avoid misinterpretation of the X-ray image, one should bear in mind that the optic foramen is viewed near the lateral margin of the *jugum sphenoidale*.

The Rhese's projection is rarely used at this time because it has been replaced by the routine use of CT studies.

The interpretation of orbital X-rays is more difficult and complex than the interpretation of fractures at other locations because of the complex facial anatomy. The complex X-ray image of the facial skeleton, projection distortions, and the effect of overlapping of different bone structures add to the difficulties of interpretation. Orbital walls are thin flat compact structures; hence, the image formed on the film as a perpendicular X-ray beam passes through them is almost unidentifiable.

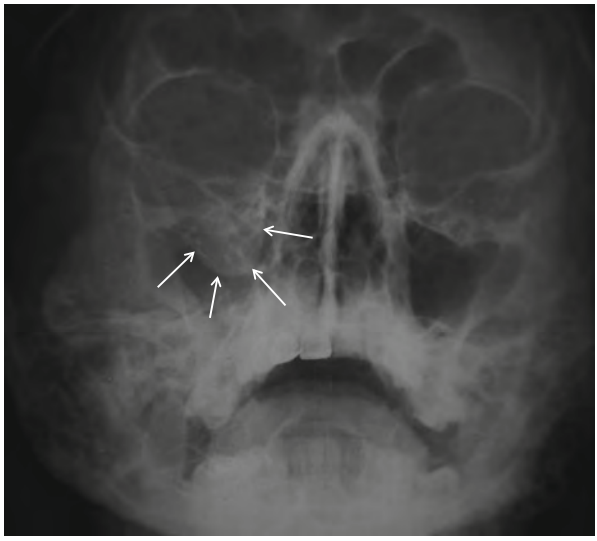

Fig. 2.8 Blow-out fracture of the inferior orbital wall: the *arrows* indicate the orbital soft tissues prolapsed into the maxillary sinus

The tangential orientation of X-rays is the only way to obtain a clear linear shadow with localization and configuration typical of each orbital wall.

Thus, the radiologic diagnosis of fractures of the bones of the middle facial area is often made by the interpretation of *indirect signs* such as the altered smoothness of the contour of the orbit, zygomatic arches, etc. and the deformation of the contour of the orbital and paranasal sinuses or the bone surface. The radiologic interpretation in other locations may use more *direct signs such as* formation of the typical fracture line or the displacement of bone fragments. An analysis of the radiologic lines of interest for a physician includes their discontinuity, fragmentation, or step-like and angular deformities. Other indirect signs of damage to the orbit include thickening and induration of periorbital soft tissues caused by hemorrhage and reactive edema, subcutaneous or orbital emphysema, blood in the sinuses, induration of the soft tissue under the roof of the maxillary sinus, and pneumocephalus (Fig. 2.8) [3, 4].

Unfortunately, often times numerous labor-consuming X-ray examinations of the orbit fail to give useful information [5], thus leading to misinterpretation and increase of time before the proper diagnosis is made [6, 7]. The probability of a fracture not being detected by X-ray imaging and subsequently diagnosed using coronal computed tomography is 10–13 % for the inferior wall fractures and 20–50 % for the medial wall fractures [4, 8]. Hence, diagnostic X-ray imaging *is currently used for examination of the skull and the orbit only as a screening method* [6, 9–11].

The final diagnosis and formation of a treatment plan should be based on the results of computed tomography (CT), which is regarded as the gold standard of radiological diagnosis of orbital fractures [12–14]. Modern equipment is capable of scanning the head structures within several seconds and producing high-resolution images, while the radiation exposure of patients remains minimal.

CT indications include suspected head injury and damage to the facial soft tissues [15].

CT scanning is typically started with examining the head with 2–3 mm table feed for assessing the base of the skull and 8 mm table feed for analyzing the supratentorial structures [16, 17]. The extent of the examination goes from the base of the cerebrum to the bregma. The plane of the slices is parallel to the plane running along the orbitomeatal line, which is conventionally used for brain examination.

Assessment of the maxillofacial region is performed in the scanning area parallel to the plane of the hard palate with a 1–2 mm slice thickness. The examined area includes the zone from the floor of the oral cavity to the end of the frontal sinuses. When the condition of the horizontal bony structures and the ostiomeatal complex needs to be assessed, CT scanning is performed again in the coronal view.

Targeted CT scanning of the orbit is necessary for the detection of periorbital edema or an orbital wall fracture.

Examination in at least two planes, the *axial* (horizontal) and *coronal* (frontal), with slice thickness less than 3 mm is used to ensure the optimal imaging of the orbit.

The *axial slices* are oriented parallel to the physiological horizontal line. This line which connects the infraorbital margin to the external auditory foramen and diverges 10° from the orbitomeatal line and to the optic nerve. This plane can be used to assess the orbit's condition but cannot show the damage to the inferior and superior orbital walls [18]. Coronal CT scanning is required to search for damage to those walls and subsequently assess them [19, 20].

During coronal CT examination, a patient lies prone with his chin resting on the elevated head support so that his head was tilted back as much as possible. If necessary, the maximum extension of the cervical spine is supplemented with the negative tilt angle of a scanning device. The slices are made from the orbital opening toward its apex.

The coronal (frontal) CT scans are most informative when analyzing the condition of all four orbital walls [21, 22]. Supplementation of the coronal projection with oblique sagittal reconstructions makes it simpler to assess the length of the fracture, the volume of tissues displaced to the maxillary sinus or the ethmoidal labyrinth, and the degree of entrapment of extraocular muscles in a bone defect [23–25].

The following conditions can impede obtaining coronal images: a critical condition of a patient, endotracheal intubation (the image of the tube overlaps the contour of the orbit), or a neck injury that impedes its hyperextension. Multispiral computed tomography is used in these cases as it has a high scanning rate and can generate 3D and multiplanar reconstructions [26, 27]. Furthermore, there is no need for neck hyperextension to obtain coronal cross sections of the orbit.

The proven advantages of CT scanning are many. These include its versatility and high accuracy, the possibility of rapid assessment of the condition of several anatomic regions during the same study (such as the head, abdomen, pelvis, and spine), and clear imaging of small-scale and combined fractures which can include several orbital walls. CT scanning is also highly useful when there are many bone fragments and can help identify metal or low-contrast ferromagnetic foreign bodies that may be present in the orbit. Furthermore, CT scanning can be used to diagnose trauma complications, such as retrobulbar or subperiosteal hematoma, hemorrhage to the subsheath space of the optic nerve and the inferior rectus and inferior oblique,

and orbital cellulitis and abscess. CT scanning also has relatively low cost, and allows access for emergency resuscitation if necessary,

A significant drawback of CT scanning is the radiation exposure of the crystalline lens [28, 29] if multiple repeat scans are performed. Moreover, the position of a graft covering a bony defect with respect to extraocular muscles and orbital fat sometimes cannot be properly assessed compared to the preoperative control CT scans.

Magnetic resonance imaging (MRI) of the orbits provides T1-, T2-, and proton density-weighted images in three mutually perpendicular planes using various software programs.

Magnetic resonance imaging plays a secondary role in the evaluation of orbital fractures for many diverse reasons [10–12]. MRI is not good for the imaging of bone fragments and cannot be used if there are ferromagnetic foreign bodies whose displacement and/or heating may cause severe secondary injury[1]. Also, MRI imaging is a long scanning procedure (up to 1 h) during which a patient needs to remain motionless, and it has a high cost (2–3 times as expensive as CT scanning) [30, 31]. There are numerous non-facial contraindications limiting the use of MRI to diagnose orbital traumas: presence of a pacemaker, metal implants, permanent makeup and tattoos (which may create artifacts and impede interpretation of the images), claustrophobia, involuntary motions of a patient during the examination, and the lack of access for emergency resuscitation equipment for life support if the need should arise [30–33].

Meanwhile, the undisputable advantages of MRI include good imaging of soft tissues, the absence of radiation exposure, and the possibility of obtaining images in all possible (axial, coronal, sagittal, and oblique) views without changing the position of the patient's body [34].

Taking into account the aforementioned facts, nuclear magnetic resonance is used to estimate the position of an implant in the orbit and possible residual entrapment of a muscle or adipose tissue in the fracture area [28, 29], to diagnose traumatic carotid–cavernous fistula, to search for nonmetal foreign bodies, to analyze fluid accumulation in the orbit and subperiosteal space and the dynamics of conversion of methemoglobin to hemosiderin (evolution of orbital hematoma), etc. Furthermore, MRI is a useful method for assessing the condition of the orbital apex, the parasellar region, and structures of the posterior cranial fossa and the portion of the optic nerve located inside the canal and the skull [30, 31, 33, 35, 36].

Ultrasonic diagnosis of orbital fractures has recently been put into practice. The main arguments in its favor are economic reasonability, wide use of ultrasonic equipment, and absence of radiation exposure. The use of ultrasonography is most justifiable to diagnose fractures of the infraorbital margin and anterior segments of the orbital floor. Ultrasonography is characterized by poor sensitivity when used to assess fractures without dislocation of bone fragments; the reasonability of using this method to diagnose medial orbital wall fractures needs further research. Currently, ultrasonography does not provide the usefulness or the accuracy of CT scanning, although it can be used instead of radiological examination at the first stage of fracture imaging.

[1] A single case of damaging the posterior segment of the eye ball with an unnoticed metal fragment during MRI has been described in literature [37].

2.1 CT and MRI Anatomy of the Orbit

The bony walls of the orbits are clearly seen in cross-sectional CT images; they form a truncated cone with its vertex facing the skull base. One should take into account that the CT scanner cannot build images of bones thinner than 0.1 mm. Hence, the images of the medial, inferior, and superior orbital walls sometimes are discontinuous, which may mislead a physician. The small size of the bone "defect," absence of angular dislocations of the "fracture" edges, and elimination of contour discontinuity at the next cross sections allow one to distinguish between these artifacts from an actual fracture.

Bony walls of the orbit are characterized by pronounced T1 and T2 hypointense signal due to low proton content and are poorly seen in MRI images.

The *adipose tissue of the orbit* is clearly seen both in CT (density of 100 HU) and MRI images, where it has a hyperintense T2 signal and low T1 signal.

The *optic nerve* in CT images has a density of 42–48 HU. In ultrasonography images, it appears as a hypoechogenic band. MRI allows one to trace the optic nerve over its entire length, up to the optic chiasm. Axial and sagittal MRI with fat suppression is the most effective method for visualizing it. The subarachnoid space surrounding the optic nerve is better imaged in T2-weighted MRI scans with fat suppression in the frontal plane. The thickness of the optic nerve on the axial cross section fluctuates from 4.2 ± 0.6–5.5 ± 0.8 mm due to its S-shaped profile and the *apparent* thickening as it enters the scanning plane and thinning as it leaves the scanning plane.

Bulbar sheaths are seen on ultrasonography and CT images as a whole (density of 50–60 HU). They can be distinguished according to the intensity of the MRI signal. The sclera has a T1 and T2 hypointense signal and looks like a clear dark band; the choroid and retina are hyperintense in T1- and proton density-weighted MR images.

The signal intensity of *extraocular muscles* in MRI scans is considerably different from that of retrobulbar fat tissue; thus, extraocular muscles are clearly seen along their entire length. In CT scans, they are characterized by density of 68–75 HU. The superior rectus is 3.8 ± 0.7 mm thick; the superior oblique, 2.4 ± 0.4 mm; the lateral rectus, 2.9 ± 0.6 mm; the medial rectus, 4.1 ± 0.5 mm; and the inferior rectus, 4.9 ± 0.8 mm.

A number of pathologies are associated with extraocular muscles thickening. Traumatic reasons include contusional edema and intramuscular hematoma. Other pathologies include orbital cellulitis and carotid–cavernous and dural cavernous fistulas, endocrine ophthalmopathy, orbital pseudotumor, lymphoma, amyloidosis, sarcoidosis, and metastatic tumors.

The superior ophthalmic vein in axial and coronal cross sections is 1.8 ± 0.5 and 2.7 ± 1 mm in diameter. Enlargement may be indicative of a number of pathologies, such as impeded venous outflow from the orbit (carotid–cavernous or dural cavernous fistulas), increased inflow (orbital arteriovenous malformations, vascular or metastatic tumors), varix of the superior ophthalmic vein, or endocrine ophthalmopathy.

Blood in paranasal sinuses has a density of 35–80 HU depending on the age of the hemorrhage. Inflammatory processes are more likely to cause limited fluid

accumulation and look as a near-wall or polypoid mucosal thickening with density of 10–25 HU.

Emphysema of the orbit and paraorbital tissues and pneumocephalus are frequent radiological signs of the fractures of orbital walls bordered by paranasal sinuses.

CT and MRI anatomy of the orbit are shown in Figs. 2.9, 2.10, 2.11, 2.12, 2.13, 2.14, 2.15, 2.16, 2.17, 2.18, 2.19, 2.20, 2.21, 2.22, 2.23, 2.24, 2.25, 2.26, 2.27, 2.28, 2.29, 2.30, 2.31, 2.32, 2.33, 2.34, 2.35, 2.36, 2.37, 2.38, 2.39, 2.40, 2.41, 2.42, 2.43, and 2.44

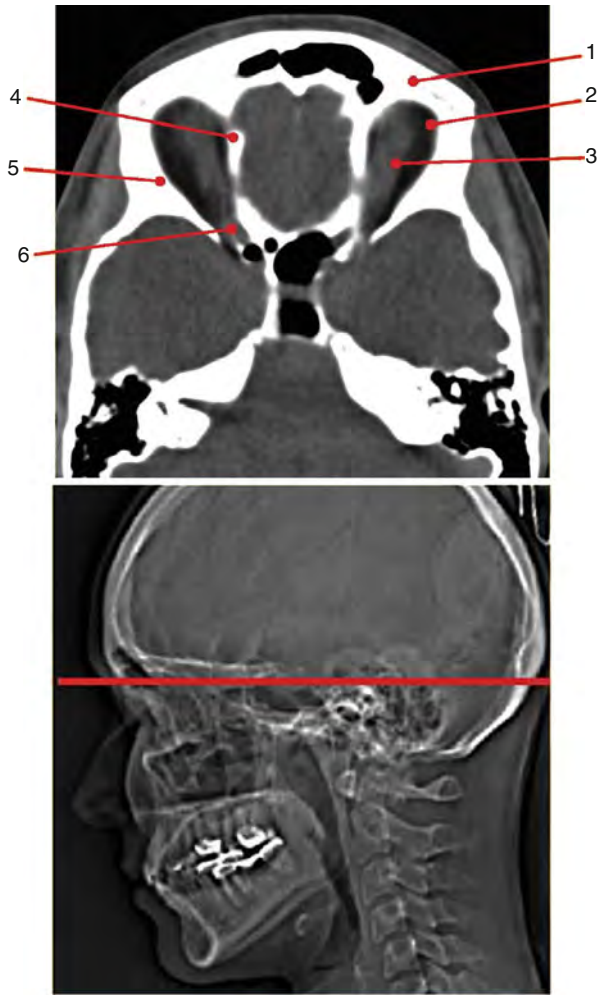

Fig. 2.9 Axial CT scan of the orbit: *1* frontal bone, *2* lacrimal gland, *3* superior rectus, *4* orbital lamina of the ethmoid bone, *5* sphenoid bone, *6* superior orbital fissure

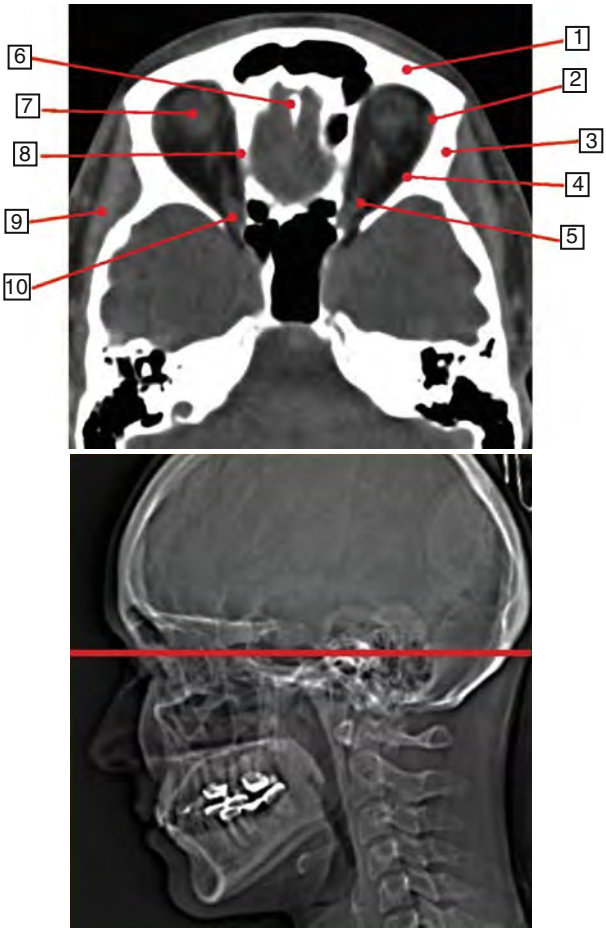

Fig. 2.10 Axial CT scan of the orbit: *1* frontal bone, *2* lacrimal gland, *3* sphenoid bone, *4* retrobulbar fat, *5* superior rectus, *6* crista galli, *7* eye ball, *8* orbital lamina of the ethmoid bone, *9* temporal muscle, *10* superior orbital fissure

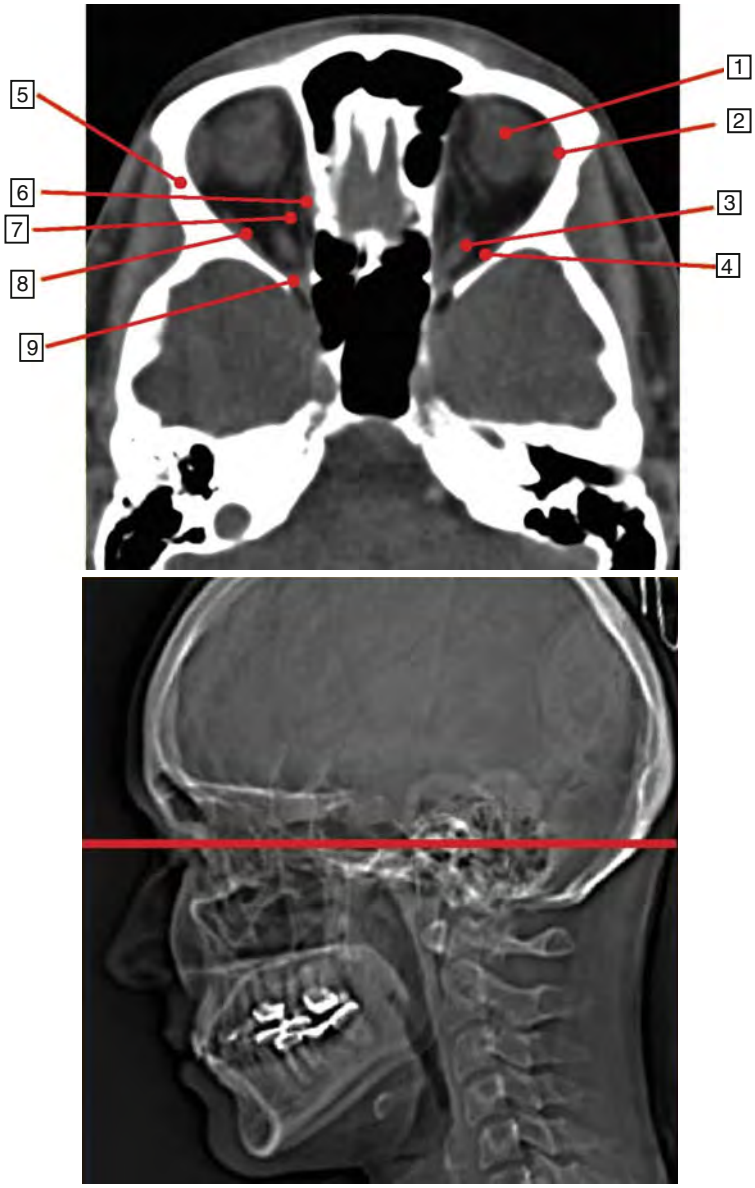

Fig. 2.11 Axial CT scan of the orbit: *1* eye ball, *2* lacrimal gland, *3* optic nerve, *4* retrobulbar fat, *5* sphenoid bone, *6* medial rectus, *7* superior oblique, *8* lateral rectus, *9* superior orbital fissure

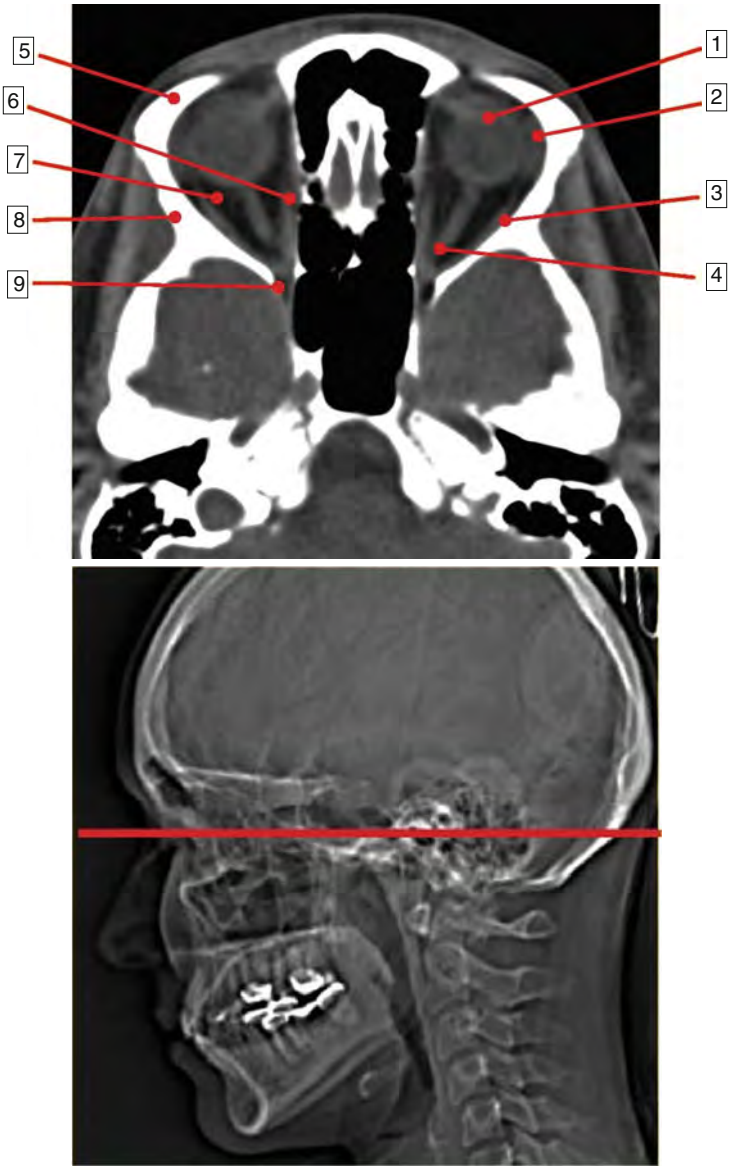

Fig. 2.12 Axial CT scan of the orbit: *1* eye ball, *2* lacrimal gland, *3* lateral rectus, *4* optic nerve, *5* zygomatic process of the frontal bone, *6* medial rectus, *7* retrobulbar fat, *8* sphenoid bone, *9* superior orbital fissure

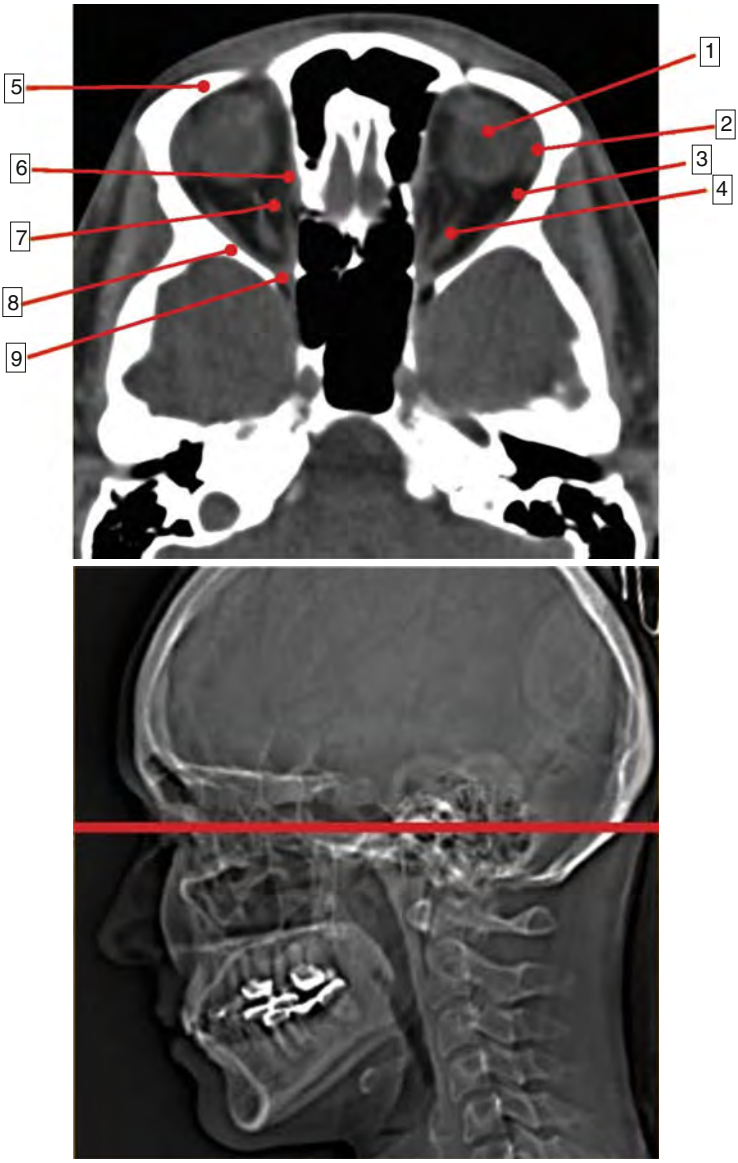

Fig. 2.13 Axial CT scan of the orbit: *1* eye ball, *2* lacrimal gland, *3* lateral rectus, *4* optic nerve, *5* zygomatic process of the frontal bone, *6* medial rectus, *7* retrobulbar fat, *8* sphenoid bone, *9* superior orbital fissure

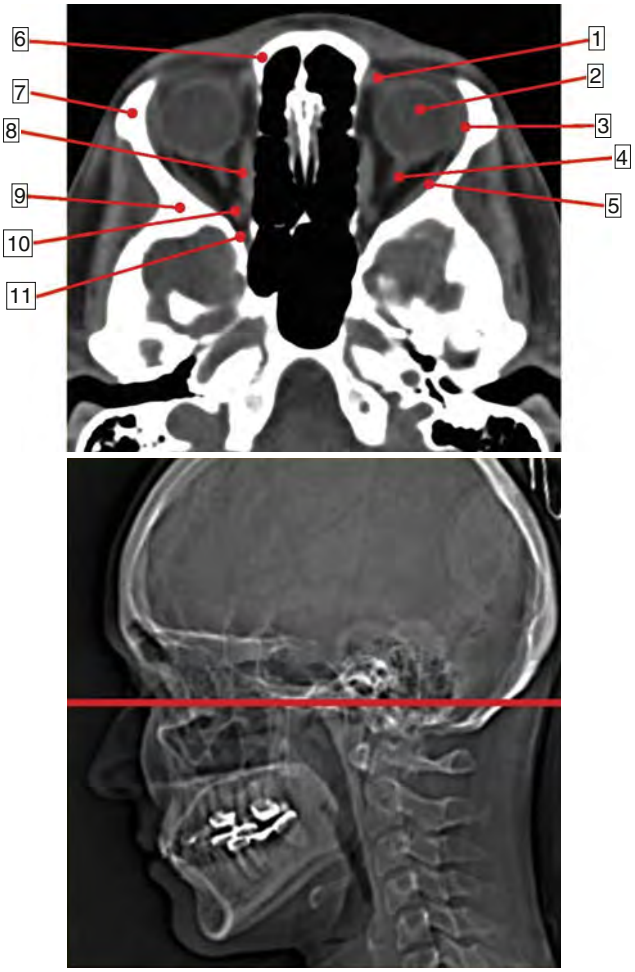

Fig. 2.14 Axial CT scan of the orbit: *1* inferior oblique, *2* eye ball, *3* lacrimal gland, *4* optic nerve, *5* lateral rectus, *6* nasal bone, *7* zygomatic process of the frontal bone, *8* medial rectus, *9* sphenoid bone, *10* inferior rectus, *11* superior orbital fissure

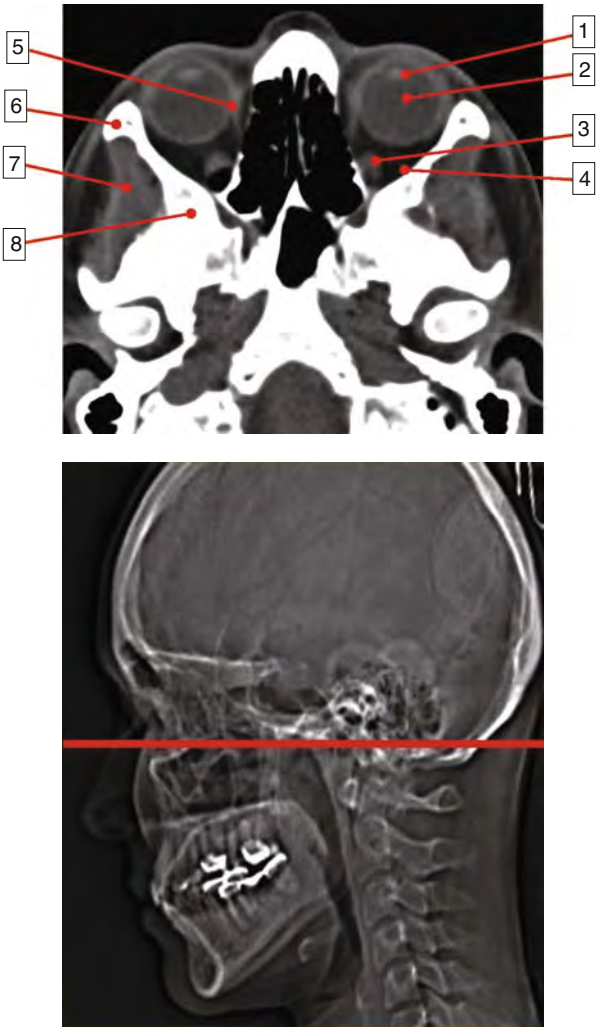

Fig. 2.15 Axial CT scan of the orbit: *1* crystalline lens, *2* vitreous body, *3* inferior rectus, *4* retrobulbar fat, *5* medial rectus, *6* zygomatic bone, *7* temporal muscle, *8* sphenoidal bone

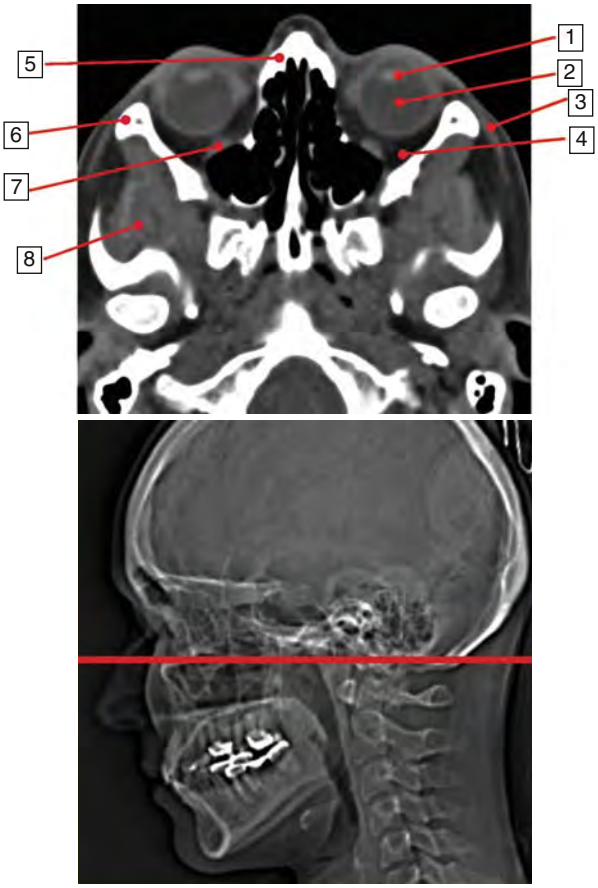

Fig. 2.16 Axial CT scan of the orbit: *1* crystalline lens, *2* vitreous body, *3* platysma muscle, *4* retrobulbar fat, *5* nasal bone, *6* zygomatic bone, *7* inferior rectus, *8* temporal muscle

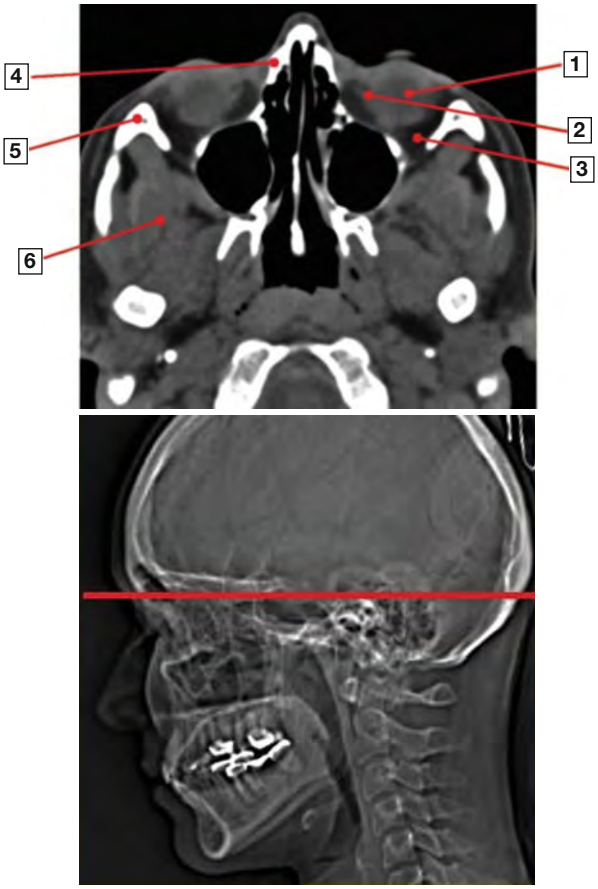

Fig. 2.17 Axial CT scan of the orbit: *1* eye ball, *2* inferior oblique, *3* retrobulbar fat, *4* nasal bone, *5* zygomatic bone, *6* temporal muscle

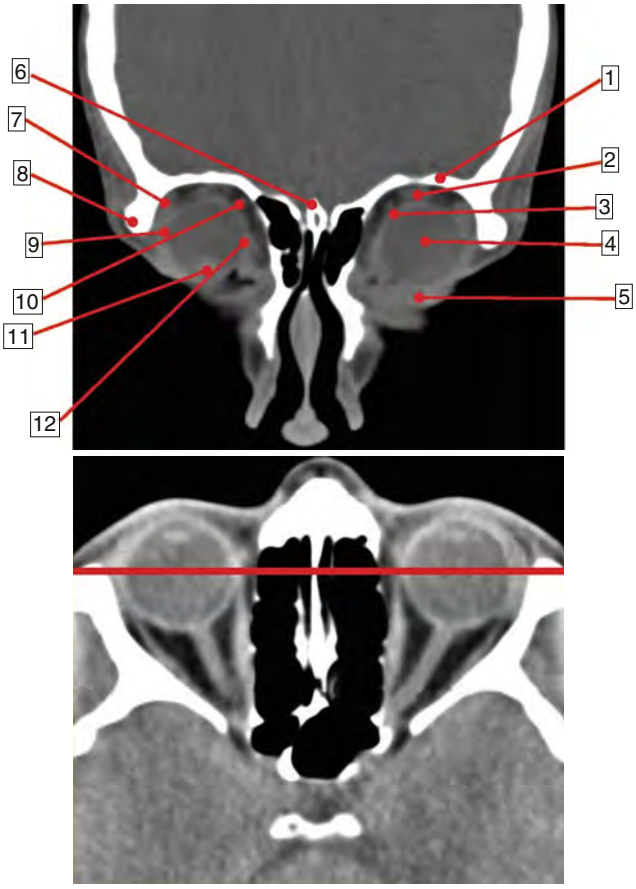

Fig. 2.18 Coronal CT scan of the orbit: *1* frontal bone, *2* levator palpebrae superioris, *3* superior oblique, *4* eye ball, *5* orbicularis oculi, *6* crista galli, *7* lacrimal gland, *8* zygomatic process of the frontal bone, *9* lateral rectus, *10* superior oblique, *11* inferior rectus, *12* medial rectus

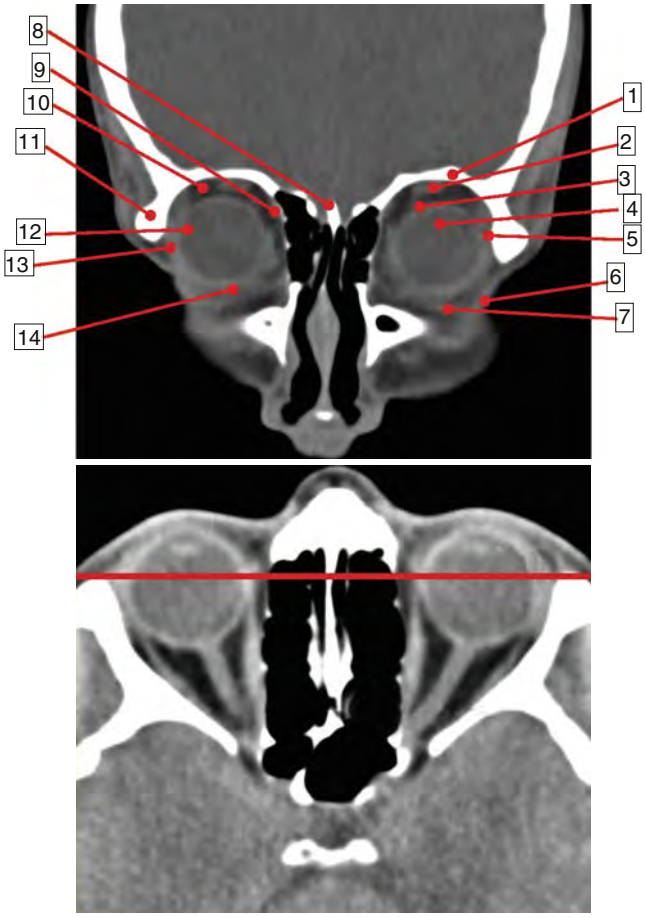

Fig. 2.19 Coronal CT scan of the orbit: *1* frontal bone, *2* levator palpebrae superioris, *3* superior rectus, *4* eye ball, *5* lateral rectus, *6* orbicularis oculi, *7* inferior oblique, *8* crista galli, *9* superior oblique, *10* lacrimal gland, *11* zygomatic process of the frontal bone, *12* eye ball, *13* lateral rectus, *14* inferior rectus

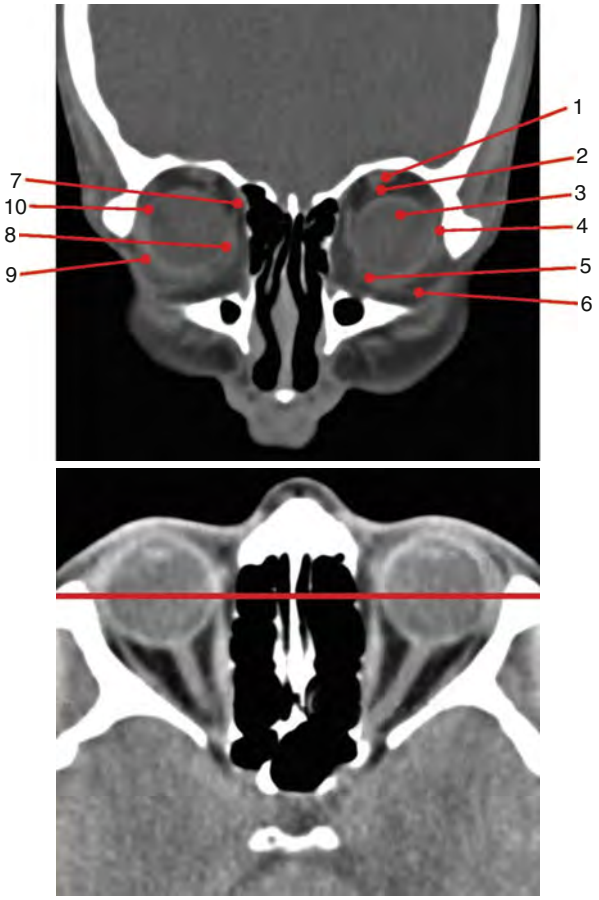

Fig. 2.20 Coronal CT scan of the orbit: *1* levator palpebrae superioris, *2* superior rectus, *3* eye ball, *4* lateral rectus, *5* inferior rectus, *6* inferior oblique, *7* superior oblique, *8* medial rectus, *9* retrobulbar fat, *10* lacrimal gland

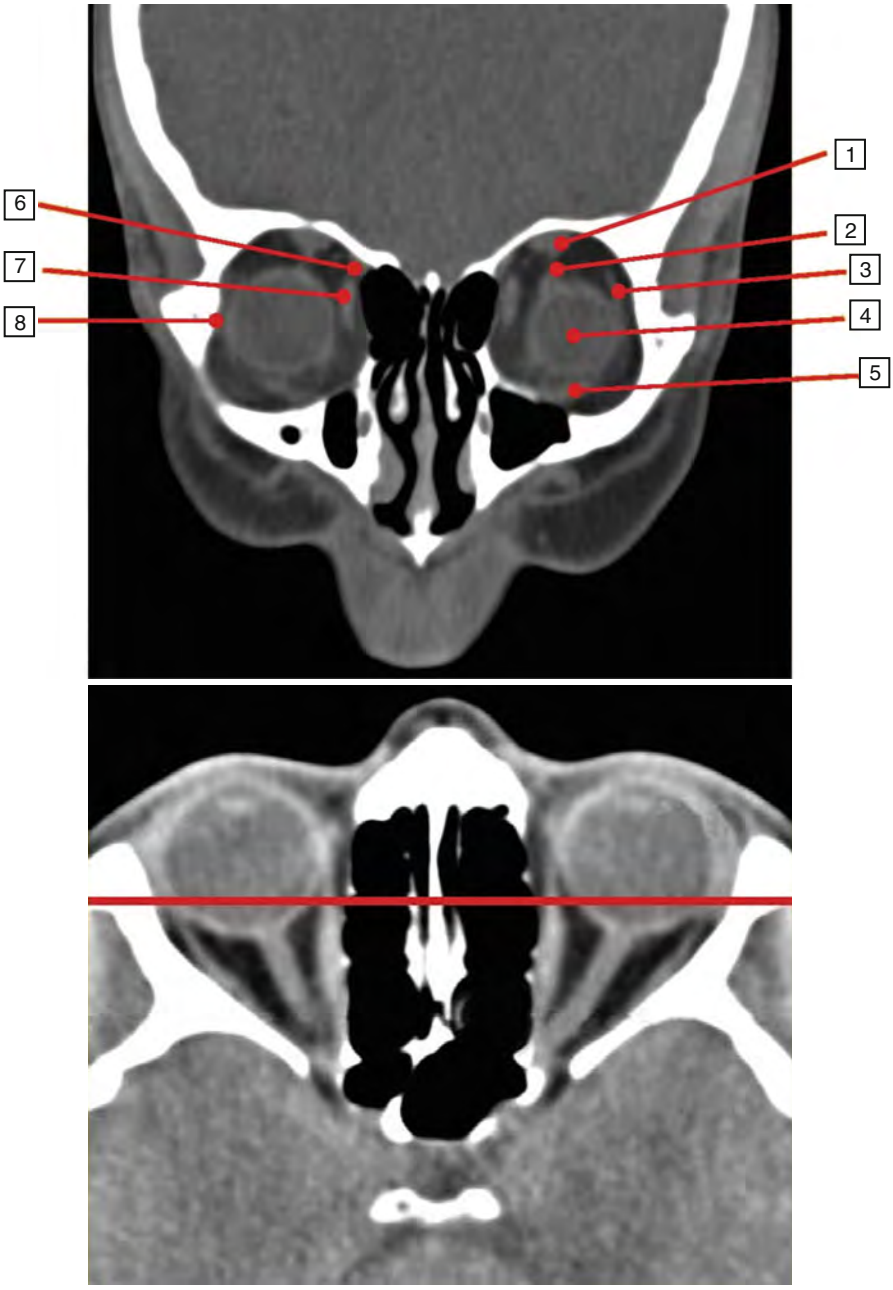

Fig. 2.21 Coronal CT scan of the orbit: *1* levator palpebrae superioris, *2* superior rectus, *3* lacrimal gland, *4* eye ball, *5* inferior rectus, *6* superior oblique, *7* medial rectus, *8* lateral rectus

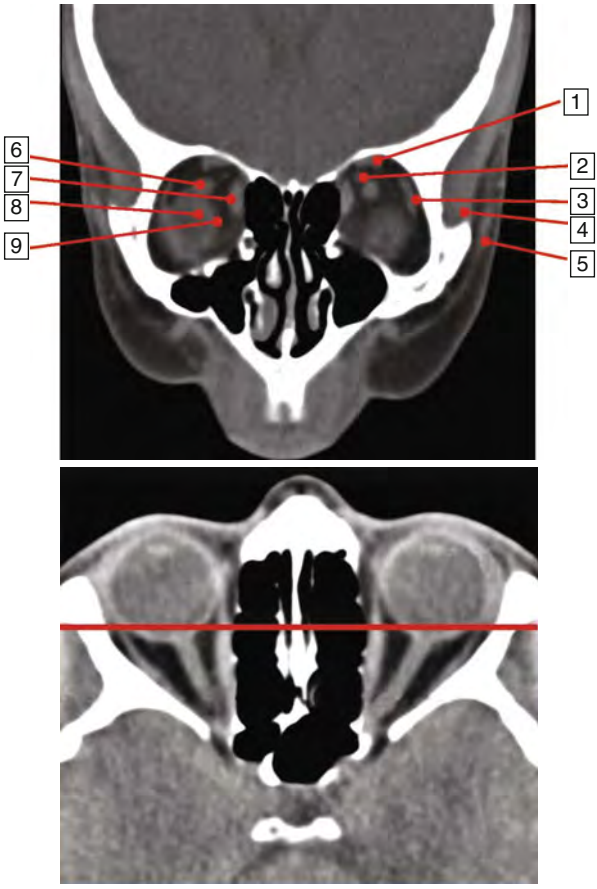

Fig. 2.22 Coronal CT scan of the orbit: *1* levator palpebrae superioris, *2* superior rectus, *3* lateral rectus, *4* temporal muscle, *5* platysma muscle, risorius muscle, *6* optic nerve, *7* medial rectus, *8* eye ball, *9* retrobulbar fat

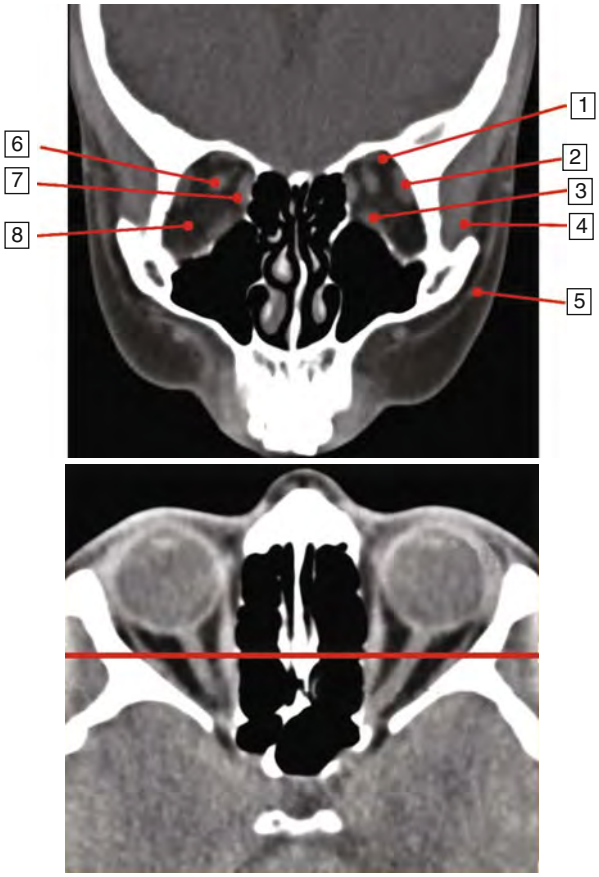

Fig. 2.23 Coronal CT scan of the orbit: *1* levator palpebrae superioris, *2* lateral rectus muscle, *3* inferior rectus, *4* temporal muscle, *5* platysma muscle, risorius muscle, *6* optic nerve, *7* medial rectus, *8* retrobulbar fat

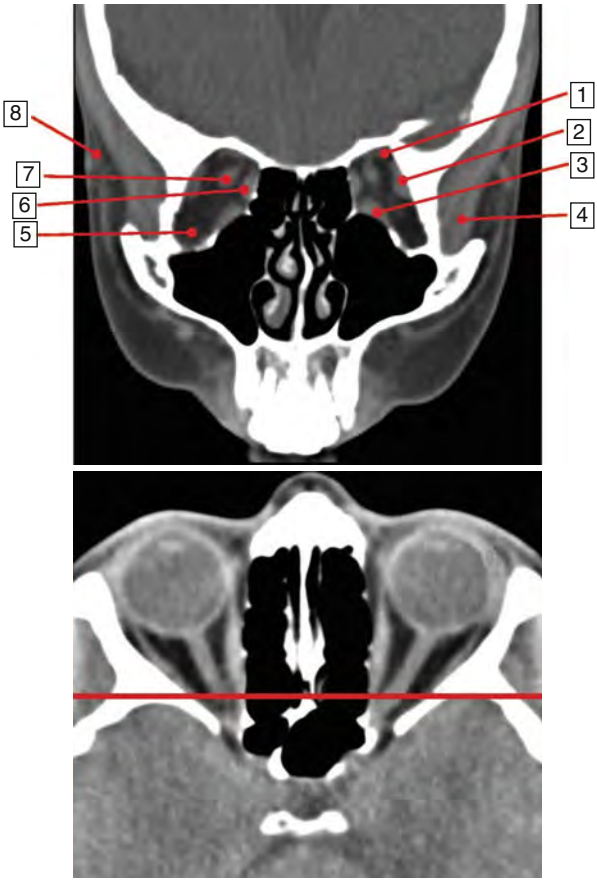

Fig. 2.24 Coronal CT scan of the orbit: *1* levator palpebrae superioris, *2* lateral rectus, *3* inferior rectus, *4* temporal muscle, *5* orbital fat, *6* medial rectus, *7* optic nerve, *8* platysma muscle

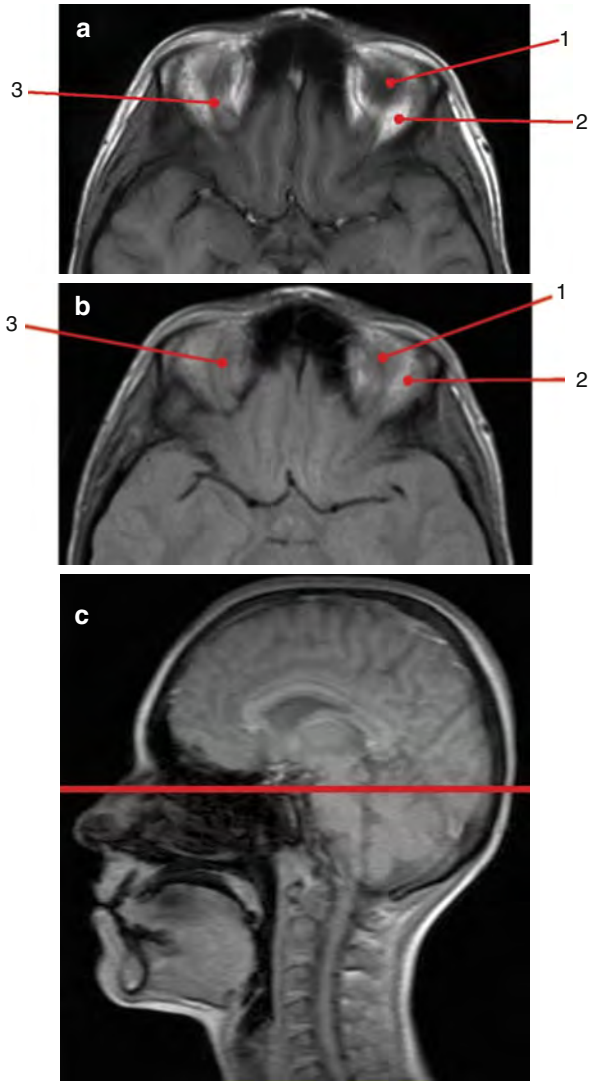

Fig. 2.25 Axial MRI scan of the orbit: *1* eye ball, *2* retrobulbar fat, *3* superior rectus. (**a**) T1-MRI, (**b**) T2-MRI, (**c**) Image plane

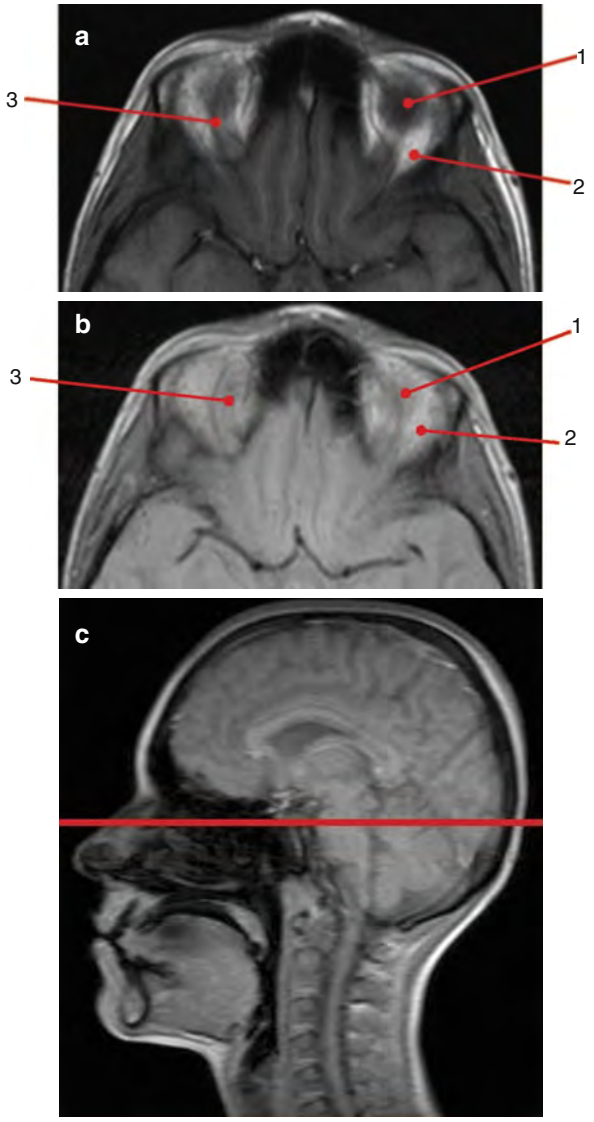

Fig. 2.26 Axial MRI scan of the orbit: *1* eye ball, *2* retrobulbar fat, *3* superior rectus. (**a**) T1-MRI, (**b**) T2-MRI, (**c**) Image plane

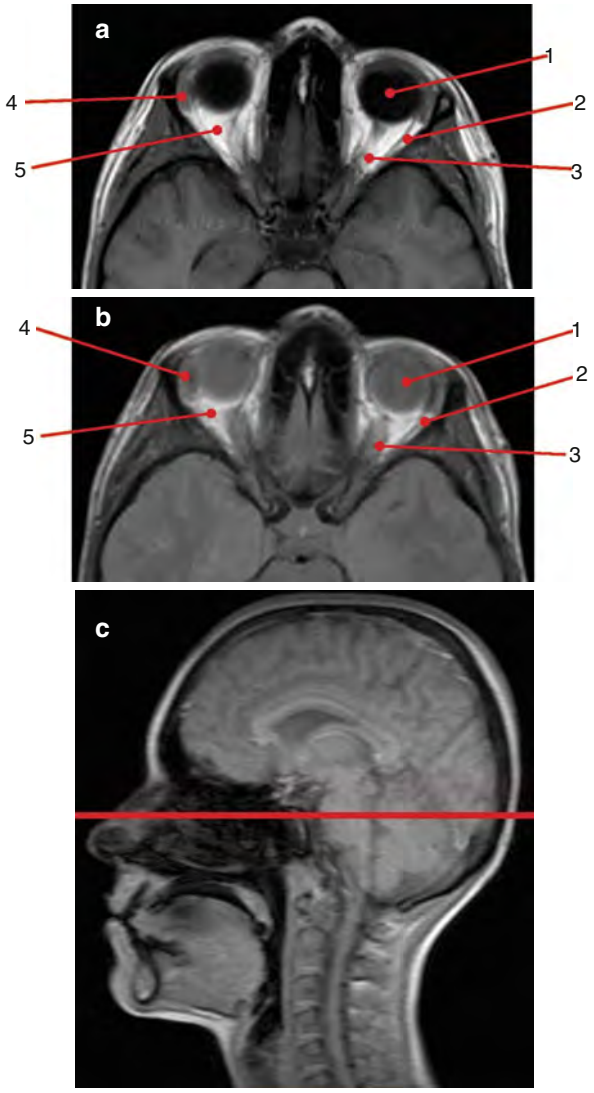

Fig. 2.27 Axial MRI scan of the orbit: *1* eye ball, *2* lateral rectus, *3* superior rectus, *4* lacrimal gland, *5* retrobulbar fat. (**a**) T1-MRI, (**b**) T2-MRI, (**c**) Image plane

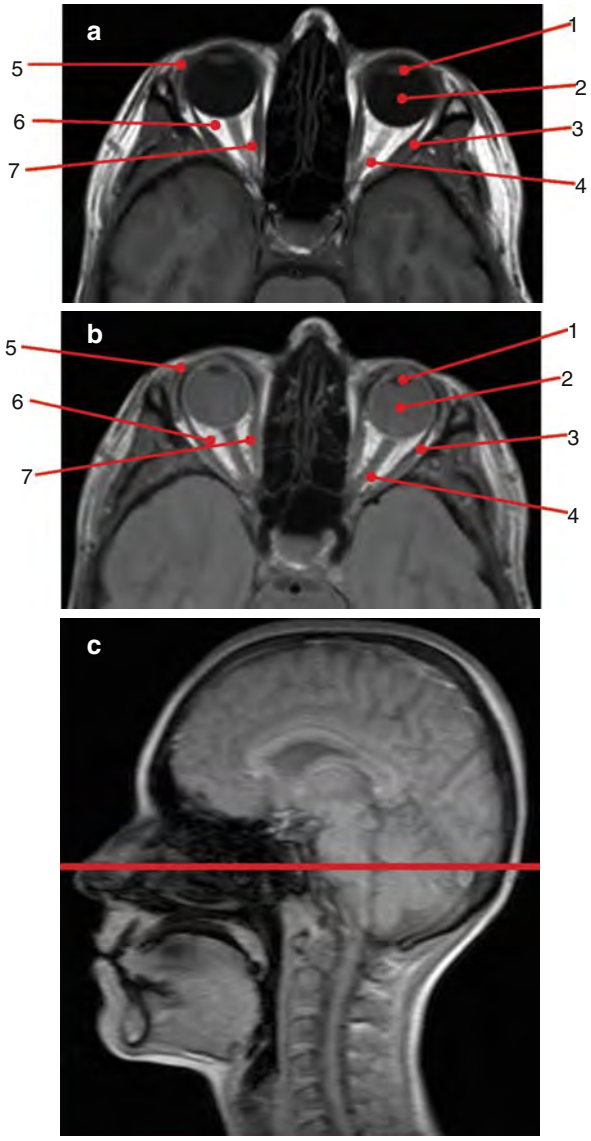

Fig. 2.28 Axial MRI scan of the orbit: *1* crystalline lens, *2* vitreous, *3* lateral rectus, *4* optic nerve, *5* lacrimal gland, *6* retrobulbar tissue, *7* medial rectus. (**a**) T1-MRI, (**b**) T2-MRI, (**c**) Image plane

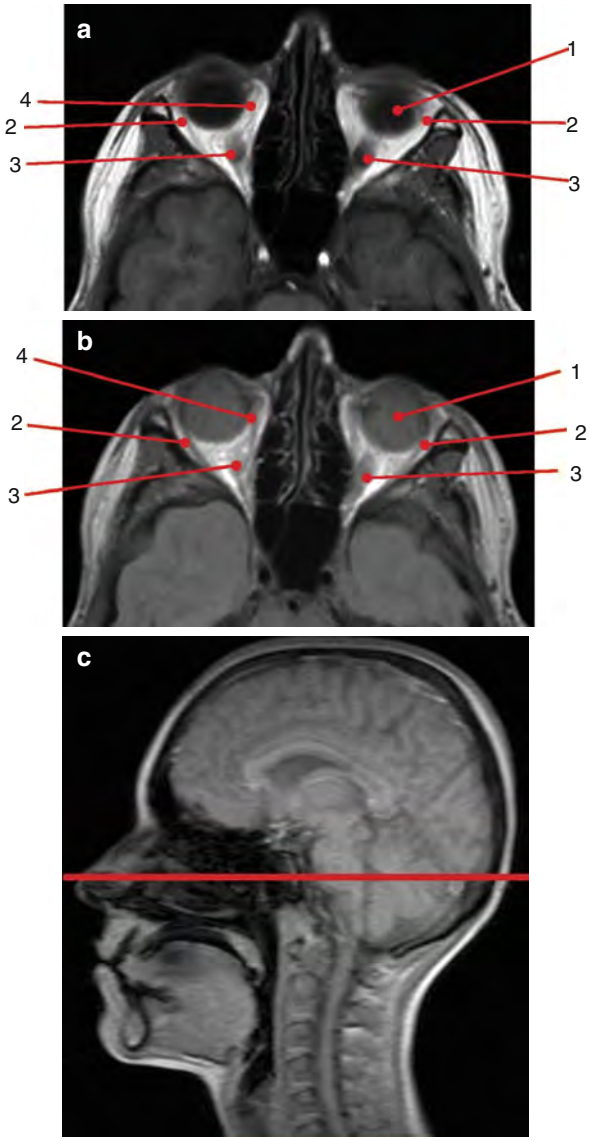

Fig. 2.29 Axial MRI scan of the orbit: *1* eye ball, *2* lateral rectus, *3* inferior rectus, *4* medial rectus. (**a**) T1-MRI, (**b**) T2-MRI, (**c**) Image plane

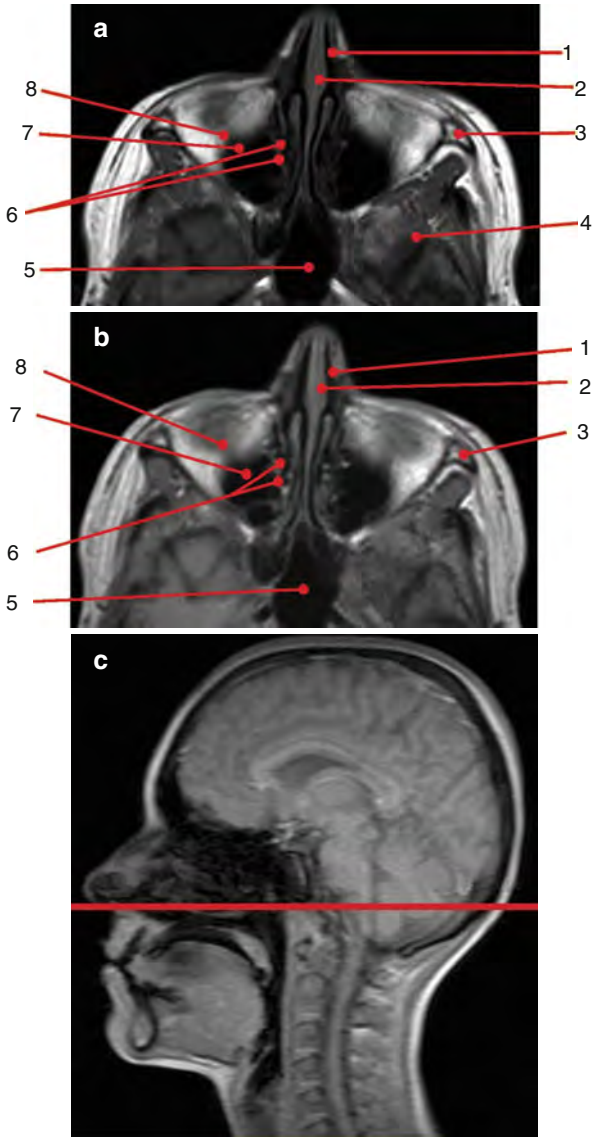

Fig. 2.30 Axial MRI scan of the orbit: *1* nasal cavity, *2* nasal septum, *3* zygomatic bone, *4* temporal lobe of the cerebrum, *5* sphenoidal sinus, *6* ethmoidal air cells, *7* right maxillary sinus, *8* inferior rectus. (**a**) T1-MRI, (**b**) T2-MRI, (**c**) Image plane

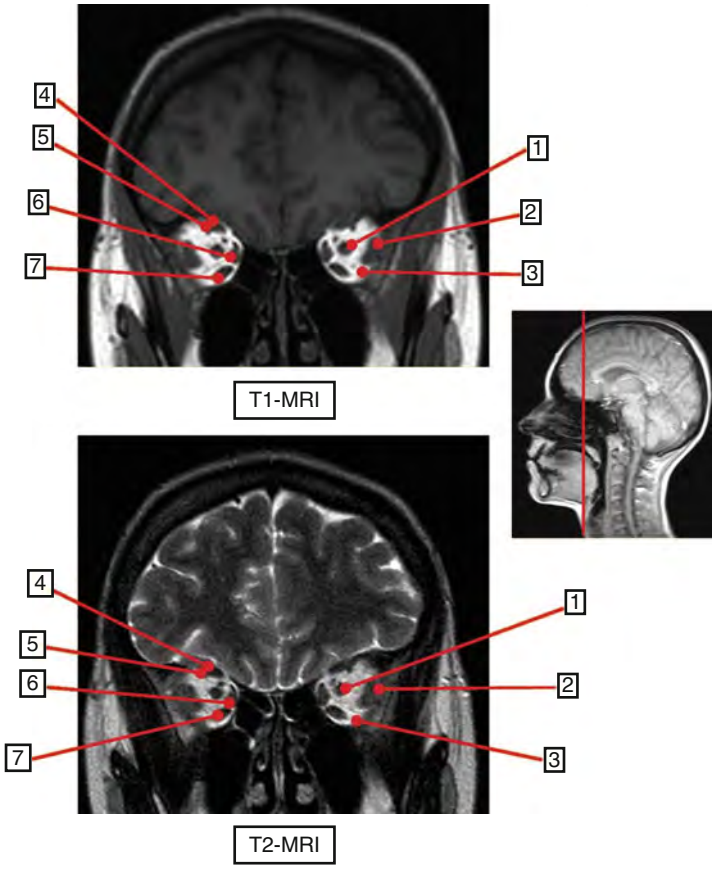

Fig. 2.31 Coronal MRI scan of the orbit: *1* optic nerve, *2* lateral rectus, *3* orbital fat, *4* levator palpebrae superioris, *5* superior rectus, *6* medial rectus, *7* inferior rectus

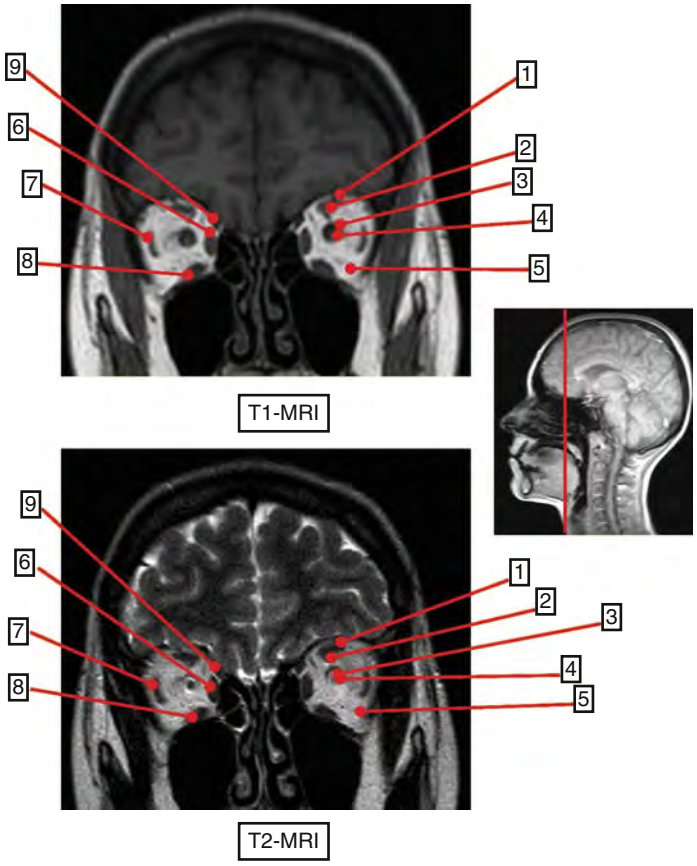

Fig. 2.32 Coronal MRI scan of the orbit: *1* levator palpebrae superioris, *2* superior rectus, *3* optic canal, *4* optic nerve, *5* retrobulbar fat, *6* medial rectus, *7* lateral rectus, *8* inferior rectus, *9* superior oblique

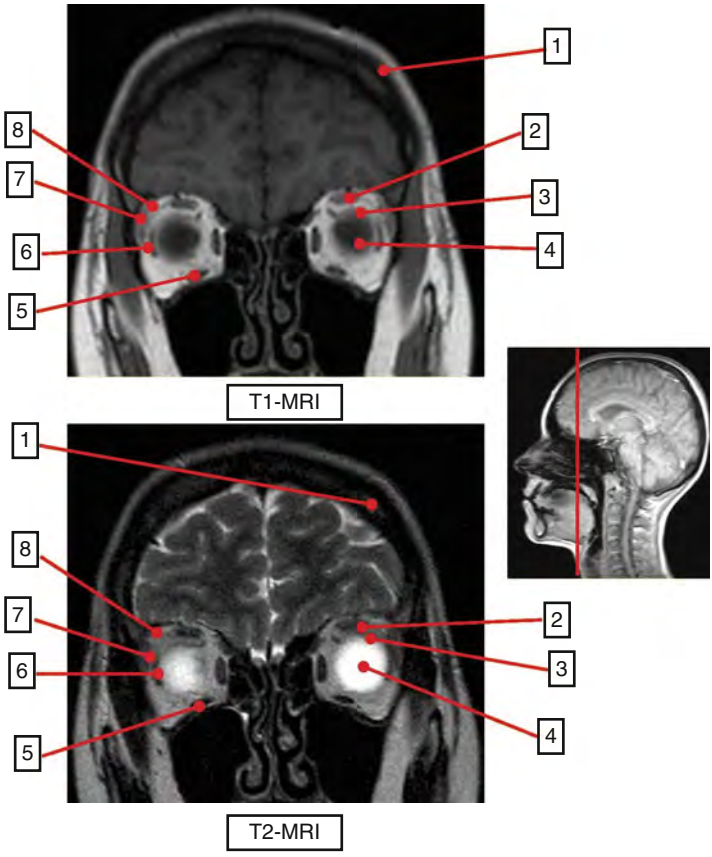

Fig. 2.33 Coronal MRI scan of the orbit: *1* frontal bone, *2* levator palpebrae superioris, *3* superior rectus, *4* eye ball, *5* inferior rectus, *6* lateral rectus, *7* lacrimal gland, *8* parabulbar tissue

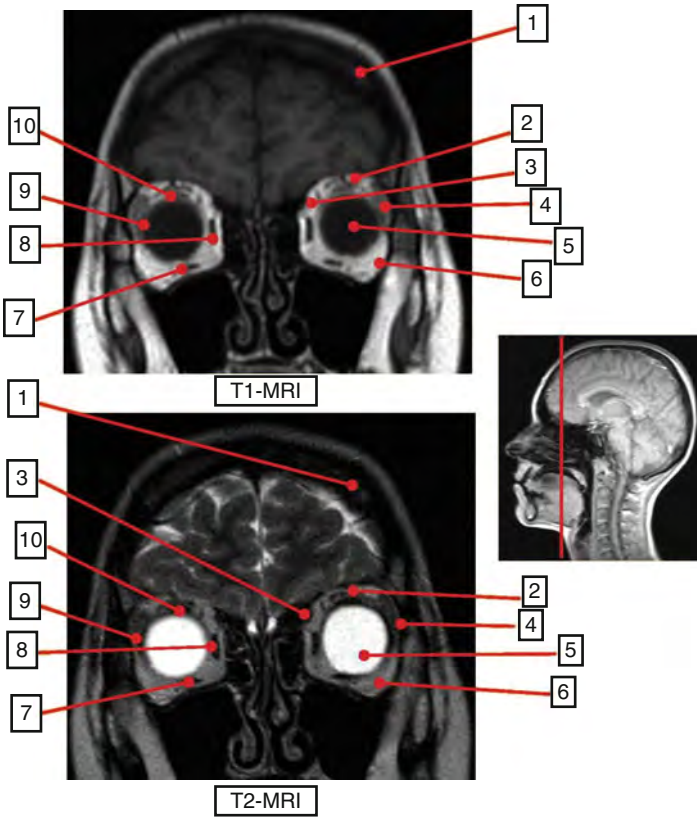

Fig. 2.34 Coronal MRI scan of the orbit: *1* frontal bone, *2* levator palpebrae superioris, *3* superior oblique, *4* lacrimal gland, *5* eye ball, *6* orbital fat, *7* inferior rectus, *8* medial rectus, *9* lateral rectus, *10* superior rectus

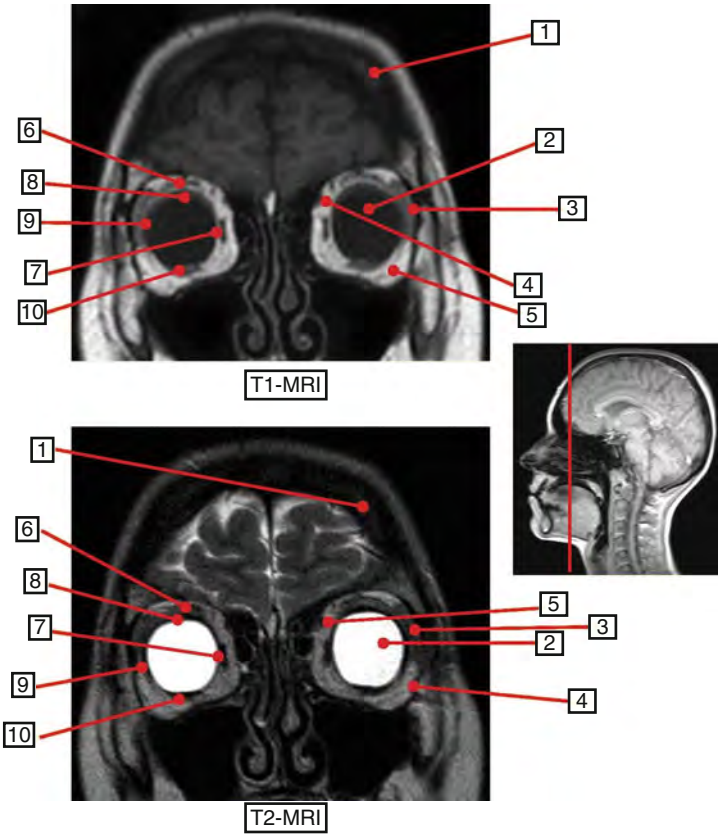

Fig. 2.35 Coronal MRI scan of the orbit: *1* frontal bone, *2* eye ball, *3* lacrimal gland, *4* superior oblique, *5* orbital fat, *6* levator palpebrae superioris, *7* medial rectus, *8* superior rectus, *9* lateral rectus, *10* inferior rectus

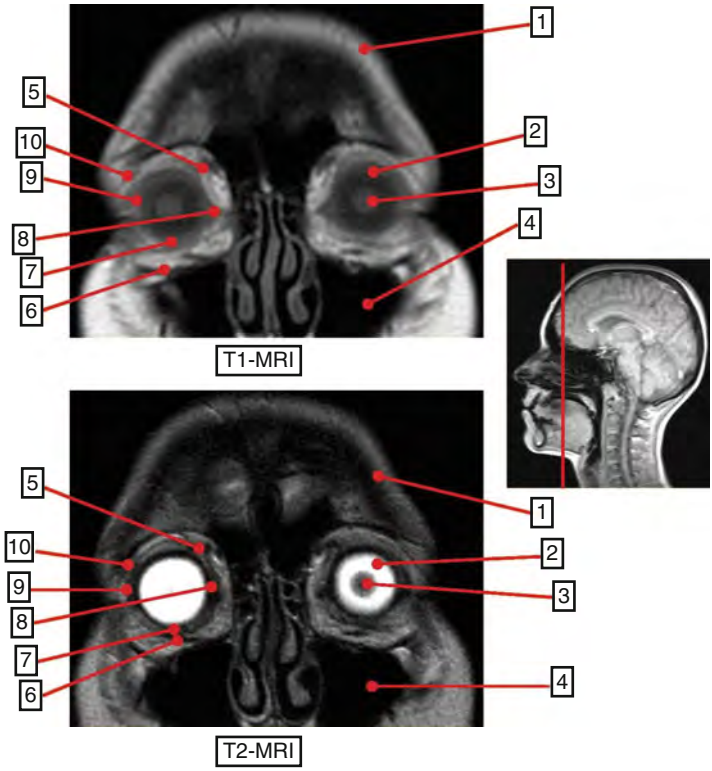

Fig. 2.36 Coronal MRI scan of the orbit: *1* frontal bone, *2* eye ball, *3* crystalline lens, *4* maxillary sinus, *5* levator palpebrae superioris, *6* inferior oblique, *7* inferior rectus, *8* medial rectus, *9* lateral rectus, *10* lacrimal gland

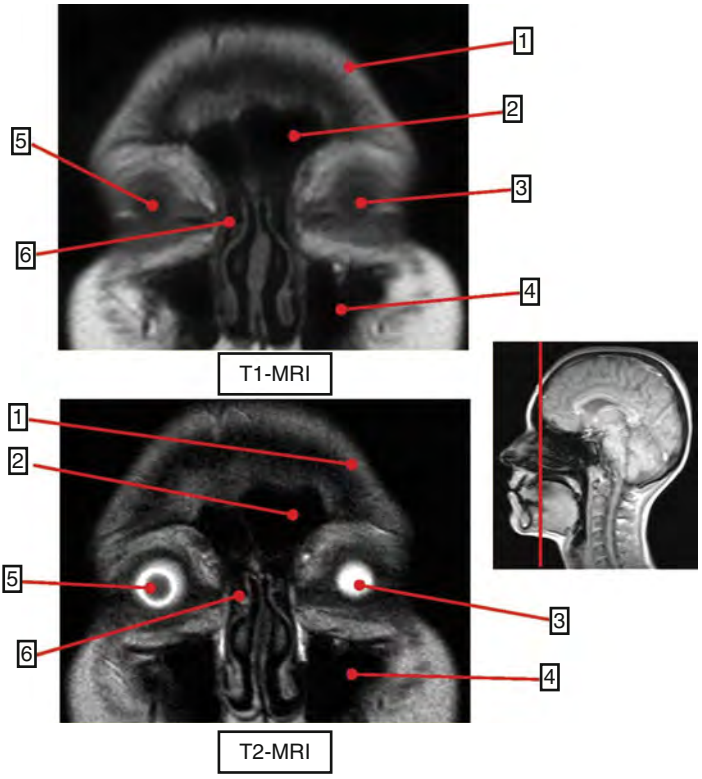

Fig. 2.37 Coronal MRI scan of the orbit: *1* frontal bone, *2* frontal sinus, *3* eye ball, *4* maxillary sinus, *5* crystalline lens, *6* ethmoidal air cells

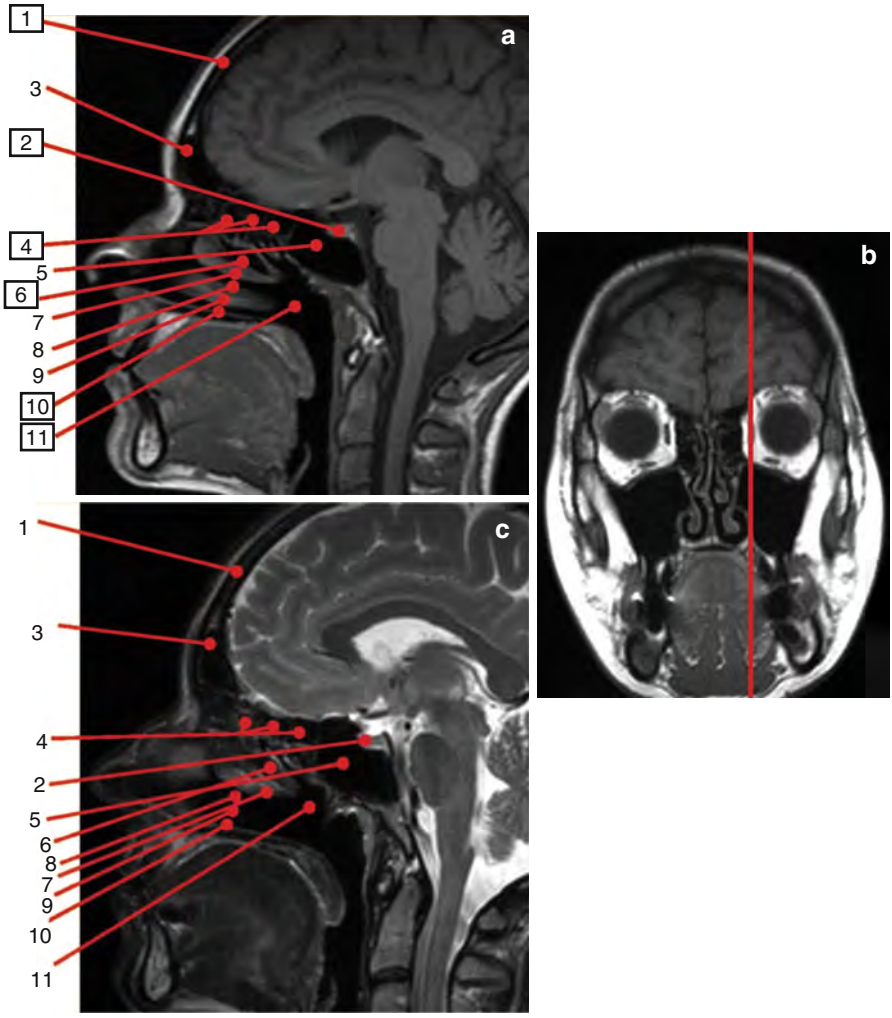

Fig. 2.38 Sagittal MRI scan of the orbit: *1* frontal bone, *2* pituitary gland, *3* frontal sinus, *4* ethmoidal labyrinth, *5* sphenoidal sinus, *6* superior nasal meatus, *7* middle nasal concha, *8* middle nasal meatus, *9* inferior nasal concha, *10* inferior nasal meatus, *11* nasopharynx. (**a**) T1-MRI, (**b**) Imaging plane, (**c**) T2-MRI

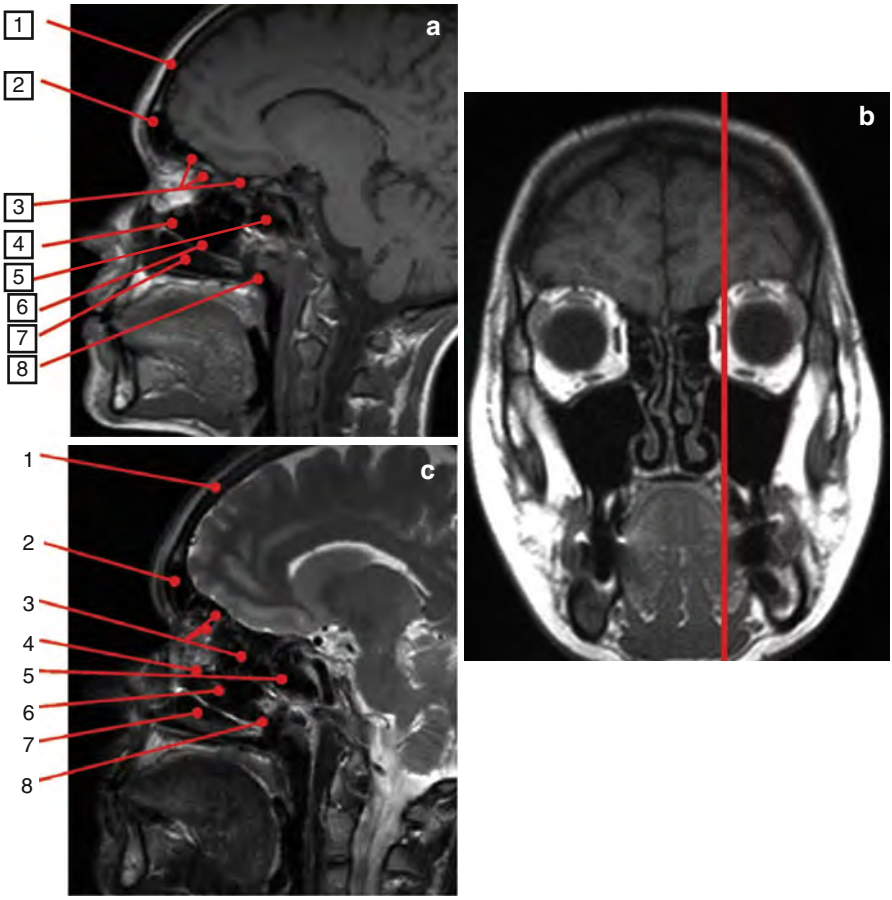

Fig. 2.39 Sagittal MRI scan of the orbit: *1* frontal bone, *2* frontal sinus, *3* ethmoidal labyrinth, *4* inferior nasal meatus, *5* sphenoidal sinus, *6* inferior nasal concha, *7* maxillary sinus, *8* nasopharynx. (**a**) T1-MRI, (**b**) Imaging plane, (**c**) T2-MRI

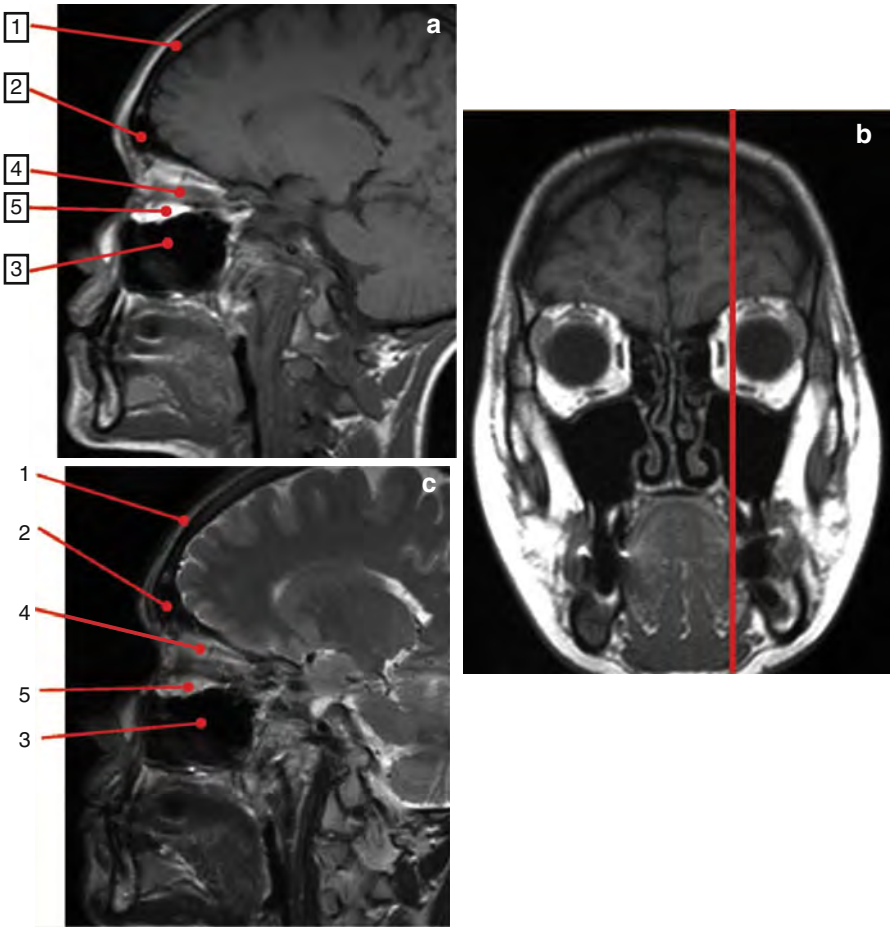

Fig. 2.40 Sagittal MRI scan of the orbit: *1* frontal bone, *2* frontal sinus, *3* maxillary sinus, *4* medial rectus, *5* orbital fat. (**a**) T1-MRI, (**b**) Imaging plane, (**c**) T2-MRI

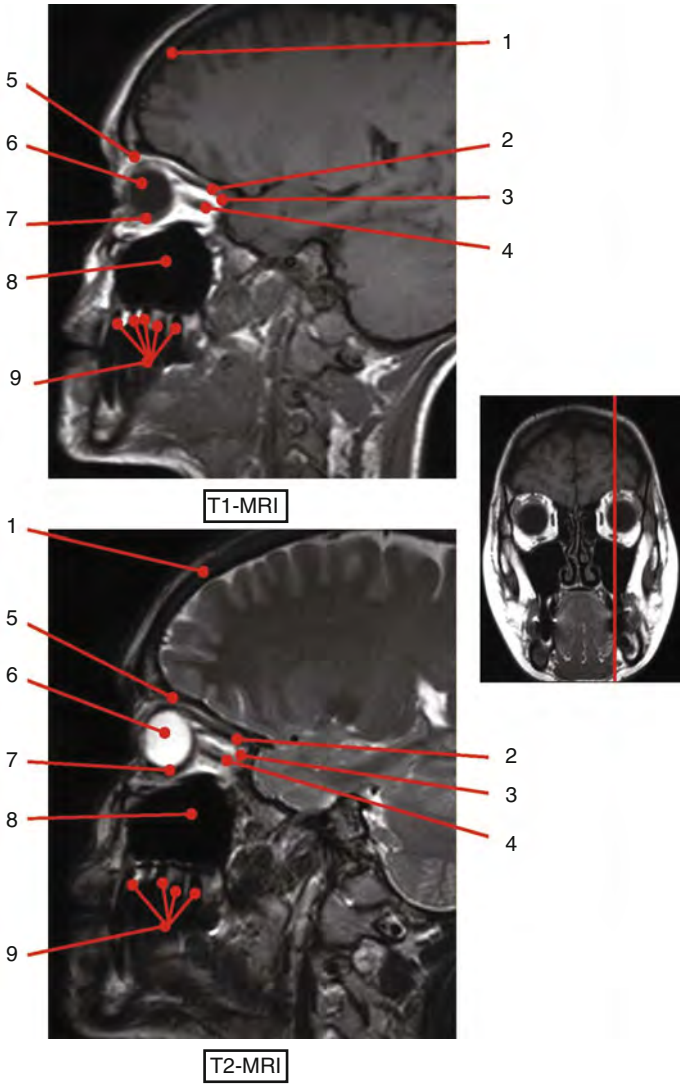

Fig. 2.41 Sagittal MRI scan of the orbit: *1* frontal bone, *2* superior rectus, *3* optic nerve, *4* medial rectus, *5* levator palpebrae superioris, *6* eye ball, *7* inferior rectus *8* maxillary sinus, *9* alveoar cavities and maxillary teeth

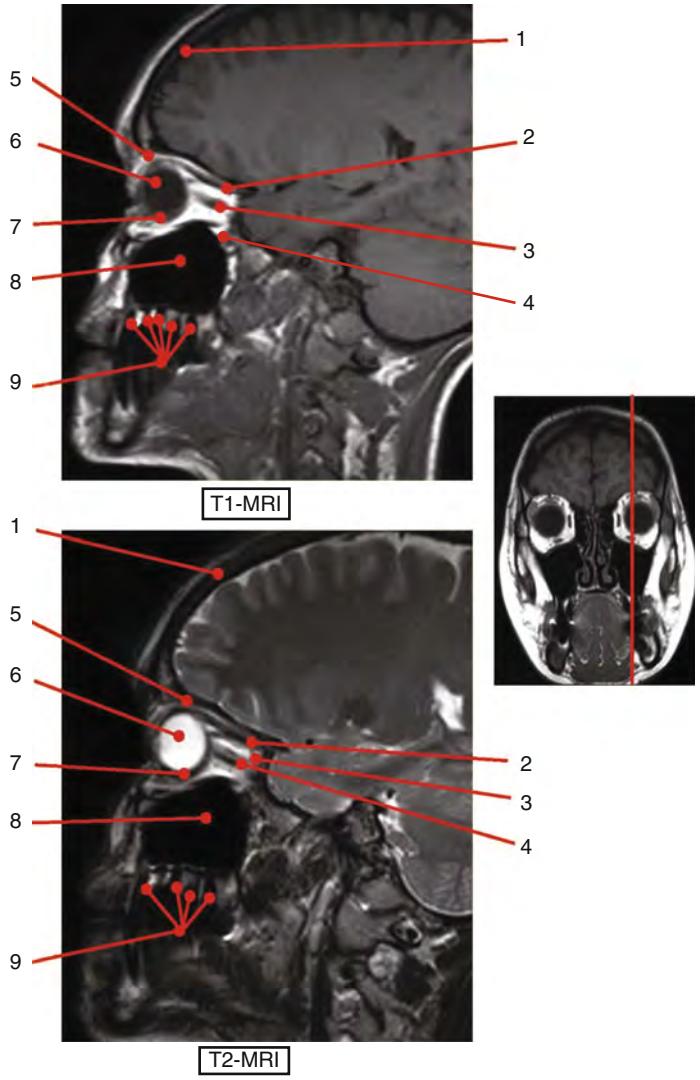

Fig. 2.42 Orbits. MRI scans. Sagittal cross sections: *1* frontal bone, *2* superior rectus, *3* optic nerve, *4* inferior rectus, *5* levator palpebrae superioris, *6* eye ball, *7* inferior rectus *8* maxillary sinus, *9* alveoar cavities and maxillary teeth

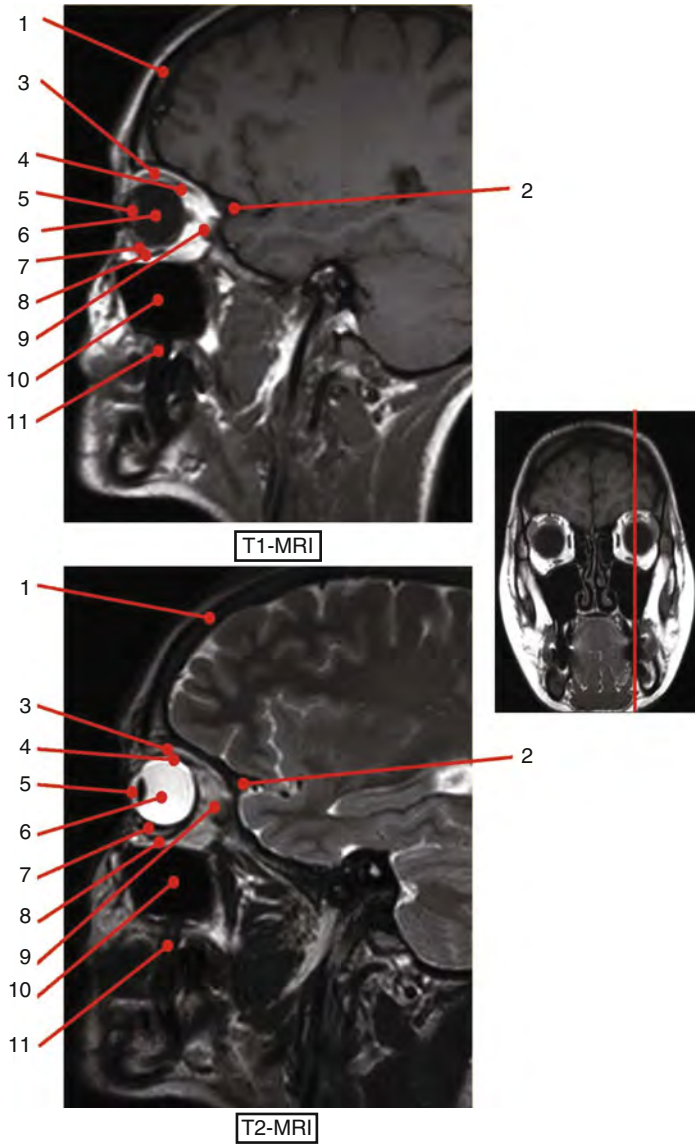

Fig. 2.43 Sagittal MRI scan of the orbit: *1* frontal bone, *2* medial cerebral artery, *3* levator palpebrae superioris, *4* superior rectus, *5* crystalline lens, *6* eye ball, *7* inferior rectus, *8* inferior oblique, *9* medial rectus, *10* maxillary sinus, *11* alveolar cavity of the 27th tooth

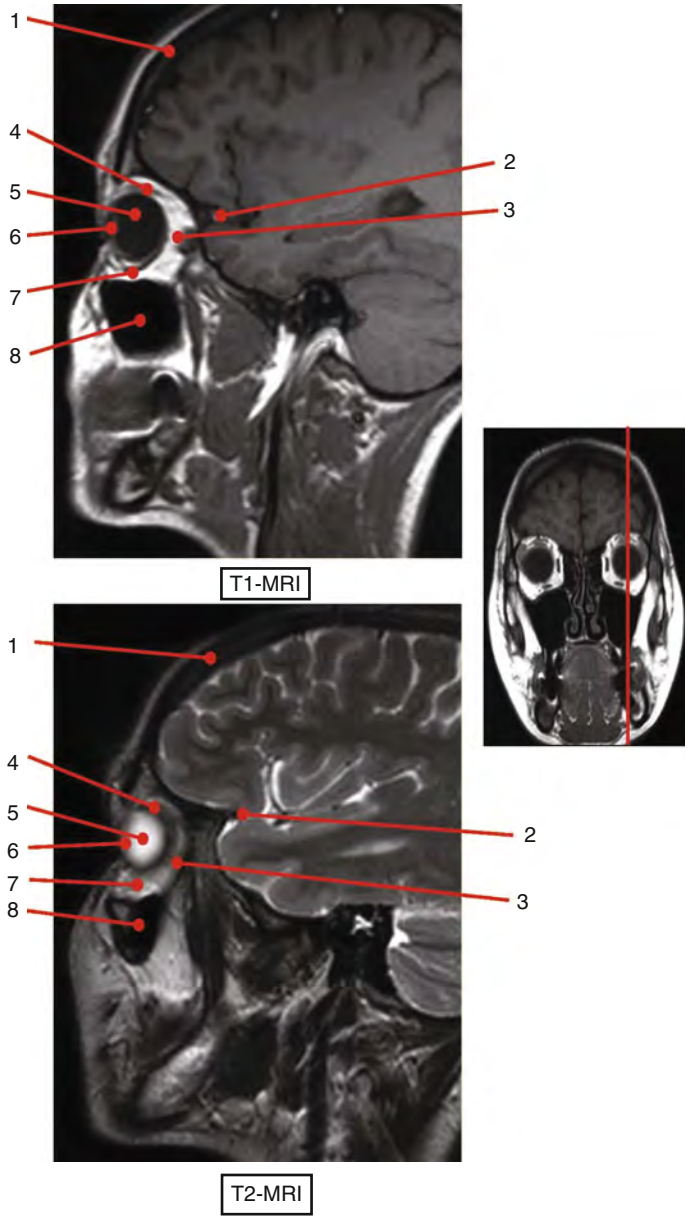

Fig. 2.44 Sagittal MRI scan of the orbit: *1* frontal bone, *2* medial cerebral artery, *3* retrobulbar fat, *4* superior rectus, *5* eye ball, *6* crystalline lens, *7* inferior rectus, *8* maxillary sinus

References

1. Yanagisawa, E., Smith, H. W., & Thaler, S. (1968). Radiologic anatomy of the paranasal sinuses. II. Lateral view. *Archives of Otolaryngology, 87*(2), 196–209.
2. Yanagisawa, E., & Smith, H. M. (1968). Radiographic anatomy of the paranasal sinuses. IV. Caldwell view. *Archives of Otolaryngology, 87*(3), 311–322.
3. Lloyd, G. A. (1966). Orbital emphysema. *The British Journal of Radiology, 39*, 933–938.
4. Kim, S. H., Ahn, K. J., Lee, J. M., et al. (2000). The usefulness of orbital lines in detecting blow-out fracture on plain radiography. *The British Journal of Radiology, 73*, 1265–1269.
5. Gas, C., Sidjilani, B.-M., Dodart, L., & Boutault, F. (1999). Fractures isolées du plancher orbitaire. *Revue de Stomatologie et de Chirurgie Maxillo-Faciale, 100*(1), 27–33.
6. Sanders, R., MacEwen, C. J., & McCulloch, A. S. (1994). The value of skull radiography in ophthalmology. *Acta Radiologica, 35*(5), 429–433.
7. Anderson, P. J., & Poole, M. D. (1995). Orbital floor fractures in young children. *Journal of Cranio-Maxillo-Facial Surgery, 23*(3), 151–154.
8. Iinuma, T., Hirota, Y., & Ishio, K. (1994). Orbital wall fractures: Conventional views and CT. *Rhinology, 32*(2), 81–83.
9. Kaltreider, S. A. (1996). Orbital fractures. In S. Bosniak (Ed.), *Principles and practice of ophthalmic plastic and reconstructive surgery* (Vol. 2, pp. 1085–1102). Philadelphia: Saunders.
10. Kubal, W. S. (2008). Imaging of orbital trauma. *Radiographics, 28*(6), 1729–1739.
11. Soparkar, C. N. S., & Patrinely, J. R. (2007). The eye examination in facial trauma for the plastic surgeon. *Plastic and Reconstructive Surgery, 120*(7 suppl. 2), 49–56.
12. Freund, M., Hahnel, S., & Sartor, K. (2002). The value of magnetic resonance imaging in the diagnosis of orbital floor fractures. *European Radiology, 12*(5), 1127–1133.
13. Hopper, R. A., Salemy, S., & Sze, R. W. (2006). Diagnosis of midface fractures with CT: What the surgeon needs to know. *Radiographics, 26*(3), 783–793.
14. Kontio, R., & Lindqvist, C. (2009). Management of orbital fractures. Oral Maxillofac. *The Surgical Clinics of North America, 21*(2), 209–220.
15. Holmgren, E. P., Dierks, E. J., Homer, L. D., & Potter, B. E. (2004). Facial computed tomography use in trauma patients who require a head computed tomogram. *Journal of Oral and Maxillofacial Surgery, 62*(8), 913–918.
16. Lee, H. J., Jilani, M., Frohman, L., & Baker, S. (2004). CT of orbital trauma. *Emergency Radiology, 10*(4), 168–172.
17. Lewandowski, R. J., Rhodes, C. A., McCarroll, K., & Hefner, L. (2004). Role of routine non-enhanced head computed tomography scan in excluding orbital, maxillary, or zygomatic fractures secondary to blunt head trauma. *Emergency Radiology, 10*(4), 173–175.
18. Rothfus, W. E., Curtin, H. D., Slamovits, T. L., & Kennerdell, J. S. (1984). Optic nerve/sheath enlargement: A differential approach based on high resolution CT morphology. *Radiology, 150*(2), 409–415.
19. Forbes, G. S., Earnest, F., & Waller, R. R. (1982). Computed tomography of orbital tumors, including late-generation scanning techniques. *Radiology, 142*(2), 387–394.
20. Leib, M. L. (1986). Computed tomography of the orbit. *International Ophthalmology Clinics, 26*(3), 103–121.
21. Krohel, G. B., Stewart, W. B., & Chavis, R. M. (1981). *Orbital disease. A practical approach* (p. 160). New York: Grune & Stratton.
22. Langen, H. J., Daus, H. J., Bohndorf, K., & Klose, K. (1989). Konventionelle Rontgenuntersuchung und Computertomographie bei der Diagnostik von Orbitafrakturen. *Fortschritte auf dem Gebiete der Röntgenstrahlen und der Nuklearmedizin, 150*(5), 582–587.
23. Elsas, T., & Anda, S. (1990). Orbital CT in the management of blow-out fractures of the orbital floor. *Acta Ophthalmologica, 68*(6), 710–714.
24. Rake, P. A., Rake, S. A., Swift, J. Q., & Schubert, W. (2004). A single reformatted oblique sagittal view as an adjunct to coronal computed tomography for the evaluation of orbital floor fractures. *Journal of Oral and Maxillofacial Surgery, 62*(4), 456–459.

25. Kwon, J., Barrera, J. E., Jung, T. Y., & Most, S. P. (2009). Measurements of orbital volume change using computed tomography in isolated orbital blowout fractures. *Archives of Facial Plastic Surgery, 11*(6), 395–398.
26. Tello, R., Suojanen, J., Costello, P., & McGinnes, A. (1994). Comparison of spiral CT and conventional CT in 3D visualization of facial trauma: Work in progress. *Computerized Medical Imaging and Graphics, 18*(6), 423–427.
27. Fox, L. A., Vannier, M. W., West, O. C., et al. (1995). Diagnostic performance of CT, MPR and 3DCT imaging in maxillofacial trauma. *Computerized Medical Imaging and Graphics, 19*(5), 385–395.
28. Kolk, A., Pautke, C., Wiener, E., et al. (2005). A novel high-resolution magnetic resonance imaging microscopy coil as an alternative to the multislice computed tomography in postoperative imaging of orbital fractures and computer-based volume measurement. *Journal of Oral and Maxillofacial Surgery, 63*(4), 492–498.
29. Kolk, A., Stimmer, H., Klopfer, M., et al. (2009). High resolution magnetic resonance imaging with an orbital coil as an alternative to computed tomography scan as the primary imaging modality of pediatric orbital fractures. *Journal of Oral and Maxillofacial Surgery, 67*(2), 348–356.
30. Dortzbach, R. K., Kronish, J. W., & Gentry, L. R. (1989). Magnetic resonance imaging of the orbit. Part I. Physical principles. *Ophthalmic Plastic and Reconstructive Surgery, 5*(3), 151–159.
31. Dortzbach, R. K., Kronish, J. W., & Gentry, L. R. (1989). Magnetic resonance imaging of the orbit. Part II. Clinical applications. *Ophthalmic Plastic and Reconstructive Surgery, 5*(3), 160–170.
32. Smith, F. W., & Crosher, G. A. (1985). Mascara: Unsuspected cause of magnetic resonance imaging artifact. *Magnetic Resonance Imaging, 3*(3), 287–289.
33. Bilaniuk, L. T., Atlas, S. W., & Zimmerman, R. A. (1987). Magnetic resonance imaging of the orbit. *Radiologic Clinics of North America, 25*(3), 509–528.
34. Ross, J. S., Masaryk, T. J., Modic, M. T., et al. (1990). Intracranial aneurysms: Evaluation by MR angiography. *American Journal of Neuroradiology, 11*(3), 449–455.
35. Jay, W. M. (1989). Advances in magnetic resonance imaging. *American Journal of Ophthalmology, 108*(5), 592–596.
36. Zimmerman, C. F., Schatz, N. J., & Glaser, J. S. (1990). Magnetic resonance imaging of optic nerve meningiomas. Enhancement with gadolinium-DTPA. *Ophthalmology, 97*(5), 585–591.
37. Kelly, W. M., Paglen, P. G., Pearson, J. A., et al. (1986). Ferromagnetism of intraocular foreign body causes unilateral blindness after MR study. *American Journal of Neuroradiology, 7*(2), 243–245.

Orbital Floor Fractures

3

Vadim P. Nikolaenko and Yury S. Astakhov

Contents

3.1 Epidemiology of Orbital Traumas 122
3.2 Classification of Orbital Fractures 123
3.3 Blow-Out Orbital Floor Fractures 124
3.3.1 Mechanisms of a Blow-Out Fracture of the Orbital Floor 124
3.3.2 Classification of Blow-Out Fractures of the Orbital Floor 127
3.3.3 Diagnosis of Blow-Out Orbital Floor Fractures 128
3.3.4 Management of Blow-Out Fractures of the Orbital Floor 144
3.3.5 Subsequent Surgery Steps 156
3.3.6 Characteristics of Different Graft Materials 161
3.4 Complications of Blow-Out Fractures of the Orbital Floor and Their Surgical Repair 176
3.4.1 Orbital Hematoma 176
3.4.2 Orbital Emphysema 179
3.4.3 Infectious Complications 179
3.4.4 Late Implant Infection 183
3.4.5 Optic Neuropathy 183
3.4.6 Diplopia 184
3.4.7 Enophthalmos 190
3.4.8 Infraorbital Nerve Neuropathy 193

V.P. Nikolaenko, MD, PhD (✉)
Department of Ophthalmology, Saint Petersburg State Hospital No. 2, Saint-Petersburg, Russia

Department of Otolaryngology and Ophthalmology, Medical Faculty, Saint-Petersburg State University, Saint-Petersburg, Russia
e-mail: dr.nikolaenko@mail.ru

Y.S. Astakhov, MD, PhD
Department of Ophthalmology, I.P. Pavlov First Saint Petersburg State Medical University, Saint-Petersburg, Russia

City Ophthalmologic Center at Saint Petersburg State Hospital No. 2, Saint-Petersburg, Russia
e-mail: astakhov73@mail.ru

© Springer-Verlag Berlin Heidelberg 2015

V.P. Nikolaenko, Y.S. Astakhov (eds.), *Orbital Fractures: A Physician's Manual*,
DOI 10.1007/978-3-662-46208-9_3

3.4.9 Cyst Formation Around an Implant. 194
3.4.10 Sino-orbital Fistula 195
3.4.11 Implant Migration 196
3.4.12 Dislocation of the Globe into the Maxillary Sinus 196
3.4.13 Upper Eyelid Retraction 197
3.4.14 Complications Caused by Using the Approach to the Orbital Floor. 198
3.5 Linear-Type Fracture of the Orbital Floor 200
3.5.1 The Mechanism of Trapdoor Fracture Formation 200
3.5.2 Clinical Presentation 202
3.5.3 Treatment. 202
3.6 Blow-In Orbital Floor Fracture 204
3.6.1 Treatment. 207
References 207

3.1 Epidemiology of Orbital Traumas

Orbital traumas typically occur during the first 30 years of life [1–3]. Orbital pathologies that are more common than orbital traumas are endocrine ophthalmopathy in adults and dermoid tumors in children. Fractures of orbital walls account for ~85 % of all orbital traumas requiring hospitalization [4].

Orbital fractures are a common midfacial trauma, the incidence being inferior only to injuries of nasal bones [5, 6]. Siritongtaworn and Siritongtaworn et al. [7, 8] reported that orbital fractures account for 40 % of all fractures of the facial skeleton. Men constitute three-quarters of all the injured individuals [1, 9–12].

Isolated orbital fractures are observed in ~35–40 % of cases, while 30–33 % of injured patients have two walls damaged. Fractures of three or all four orbital walls are found in 15–20 % and 5–10 % of patients, respectively [13].

In children, orbital fractures account for 23 % of all facial traumas, following only mandibular fractures (34 %) in terms of the rate of incidence [14]. Trapdoor-type fractures constitute 25–70 % of all orbital fractures in the pediatric population [15, 16].

It should be mentioned that orbital fractures are often combined with globe injuries, including penetrating traumas and ruptures of the sclera [17–22]. According to Ioannides et al. [23] and Cook [24], injuries of the globe or periocular soft tissues are observed in 26 % of patients with orbital fractures; however, conditions requiring surgical repair are observed much less frequently (6.5 % of cases).

The most severe globe injuries occur after fractures of the lateral orbital wall, its apex, and Le Fort III fractures. Isolated fractures of the orbital floor cause less severe globe injuries [25]. The reason for this is that the threshold energy for giving a blow-out fracture of the orbital floor is lower than that of rupture of the fibrous capsule of the globe [26, 27]. Much of the energy of the trauma is absorbed by the orbital floor when it is fractured, thus reducing the amount of energy which could be delivered to the globe. This loss of energy reduces the probability of serious globe injuries (mostly in the form of scleral rupture) 1.5-fold [28].

Literature data suggest that up to 70 % of all orbital fractures are combined with certain injuries of the globe, other facial bones, and head trauma [13, 21, 29, 30].

Meanwhile, the presence of an orbital fracture in a patient is associated with an increased risk of head trauma three- to fourfold (up to 50 %) [12, 13]; the

probability of head trauma significantly increases even more if two or more orbital walls were injured.

The major causes of orbital traumas include road accidents[1] and assaults (each of these causes accounts for 40 % of fractures) [1, 2, 12, 19, 33–35]. The traumas may also result from sport activities [9, 36–38]. Thus, 15–20 % of facial fractures are caused by sport activities in Italy, Australia, and New Zealand [39–42]. Single cases of orbital floor fractures by forceful nose blowing have also been reported [43].

3.2 Classification of Orbital Fractures

Orbital fractures are typically classified according to their anatomy. However, it is important for clinical practice that both localization of the injury and the degree to which the integrity of bone structures are disrupted (which is mainly determined by the impact on these structures) should be evaluated.

Numerous types of orbital fractures can be either isolated or combined with other facial injuries. The most common types of orbital fractures are:

- Blow-out and blow-in fractures of the orbital floor
- Blow-out and blow-in fractures of the medial orbital wall
- Naso-orbito-ethmoidal (NOE) fractures
- Fractures of the zygomatic orbital complex
- Le Fort II and III maxillary fractures
- Frontobasal fractures (including injuries of the walls of the frontal sinus; blow-out and blow-in fractures of the roof; fractures of the orbital apex, including those involving the optic canal; local fractures caused by sharp objects entering the orbit; supraorbital, glabellar, and isolated fractures of the supraorbital rim).

Furthermore, it is reasonable to distinguish between three varieties of fractures when evaluating each fracture: low-, middle-, and high-energy ones [44].

A low-energy fracture is an incomplete (“greenstick”) fracture with minimal displacement of fragments and typically does not require surgical management.

A middle-energy fracture is characterized by clinical symptoms typical of this form and moderate displacement of bone fragments. It requires open reposition and rigid fixation of bone fragments through the typical approaches. This group of patients is the largest one; standard treatment algorithms are used to manage them.

Finally, the high-energy type of fractures is the rarely observed. These comminuted fractures are characterized by extreme dislocation, pronounced instability of bone fragments, and disturbance of facial architecture. Multiple imaging approaches

[1] Duma and Jernigan [31] reported that the incidence rate of orbital fractures among the injured individuals (mostly in head-on collisions) is 0.22 %. The use of airbags and seatbelts reduces this figure to 0.09 % and considerably decreases the risk of open and multiple fractures with significant displacement of bone fragments [32]. However, the activated airbags may damage the globe themselves.

are required to obtain the proper anatomical diagnosis, and the repositioning of the injured bone structures necessitates that a personalized surgical strategy is used in each particular case.

3.3 Blow-Out Orbital Floor Fractures

Blow-out orbital floor fractures are the most common type of orbital fractures[2] [45] and rank second (after nasal traumas) in frequency among all midfacial injuries [5]. In most cases, these fractures are unilateral, although appreciably frequent cases (up to 5 %) of bilateral blow-out fractures of the orbital floor have also been reported [9, 22, 46, 47].

3.3.1 Mechanisms of a Blow-Out Fracture of the Orbital Floor

Although the first case description and photo recording of traumatic enophthalmos in a 12-year-old boy caused by blunt trauma was made by Lang in 1889, it was only in 1943 that Pfeiffer established the cause-and-effect relationship between enophthalmos and orbital fracture. The term "blow-out" was proposed by Smith and Converse [48] to denote fracturing of the orbital floor without the involvement of the infraorbital rim. A year later, Smith and Regan [49] proposed their "hydraulic" theory for the formation of a blow-out fracture.

An injuring agent that is larger than the orbital opening deforms and displaces the globe deep into the orbit, compressing its contents and abruptly increasing the intraorbital pressure, which in turn causes inferior orbital tissue to press through the weakest inferior wall into the maxillary sinus [26]. The prolapsed soft tissues return to their original position slower than bone fragments; hence, they are usually entrapped in the fracture zone (usually the fracture is linear in this case[3]) (Fig. 3.1). In patients with extensive fragmentation injuries of the orbital floor, soft tissues are displaced downward due to gravity and reactive edema rather than being entrapped.

There are fewer supporters of the buckling theory formulated by R. Le Fort [53] who believe that wavelike deformations transmitted from the infraorbital rim is the main mechanism of blow-out fracturing of the orbital floor [54]. Depending on the direction of the force vector, the orbital floor (mostly its interior half) undergoes either a horizontal or rotational deformation [55]. The fracture area will be maximal when an injuring agent is moving upward at an angle of 30° to the infraorbital rim (Fig. 3.2) [56].

[2] They account for 85 % of all orbital fractures.

[3] However, although it is very logical, the "hydraulic" theory cannot explain why it is the posteromedial area of the orbital floor (which ranks second in thickness and strength among the six areas of the orbital floor distinguished by Jones and Evans [50]) that is most frequently fractured. Kersten [51] reported a case of an orbital floor fracture when the eye subjected to cataract surgery 5 days prior to the trauma remained intact. Hence, it follows that neither compression of orbital tissues nor pressure exerted by the eyeball on the orbital floor played a significant role in fracture genesis.

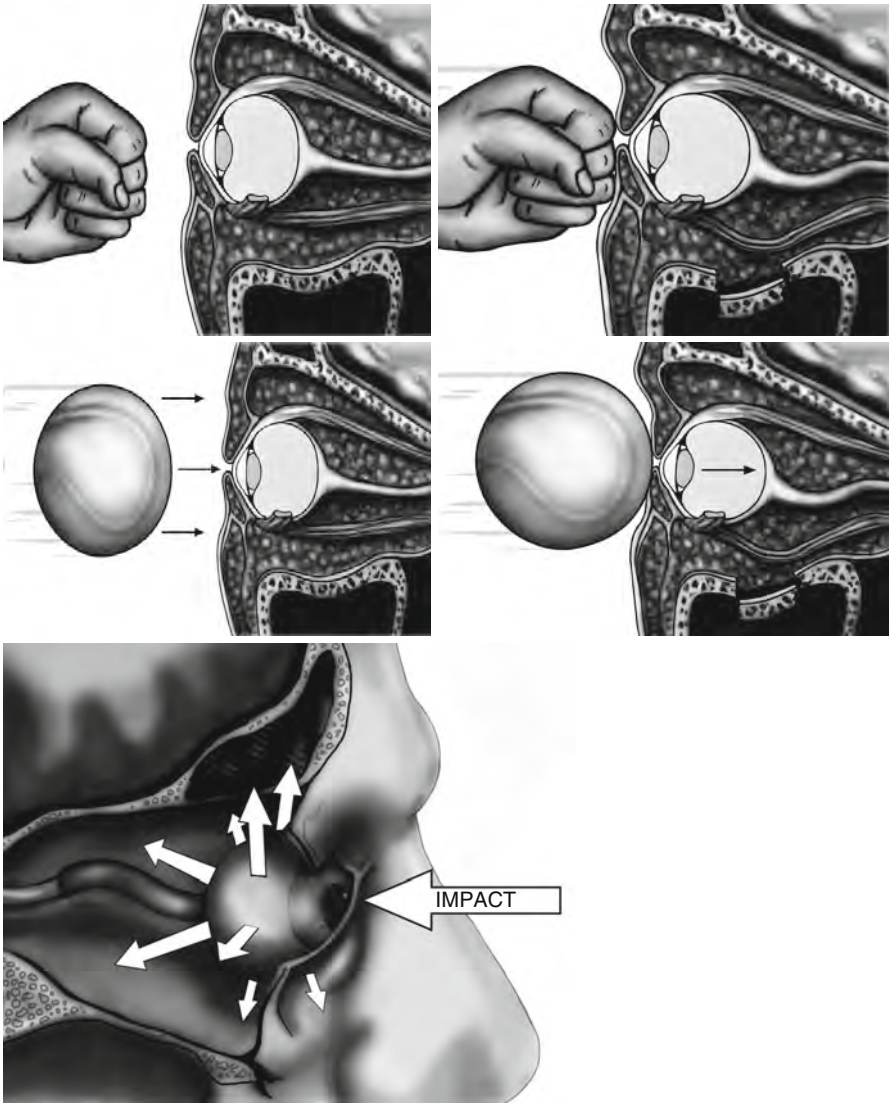

Fig. 3.1 The "hydraulic" theory of the orbital floor fracture (citation from Della Rocca [52]). See explanation in the text: It is an interesting fact that, contrary to the established opinion, a tennis ball striking the eye does not cause a fracture although it may damage the globe. The deformation of a hollow ball during the contact and the suction effect when the ball bounces off the periorbital area presumably dampen the increase in intraorbital pressure. A fracture can be caused by the impact of an injuring agent incapable of transitory deformation (e.g., a fist)

The kinetic energies required to damage the orbital floor via wavelike deformation and hydraulic shock are almost identical [57–60], but localization and extension of the "hydraulic" and "buckling" fractures differ considerably [61]. Cadaveric studies of the orbits demonstrated that fractures caused by wavelike deformation mostly localize in the anterior half of the orbital floor, do not affect the medial wall,

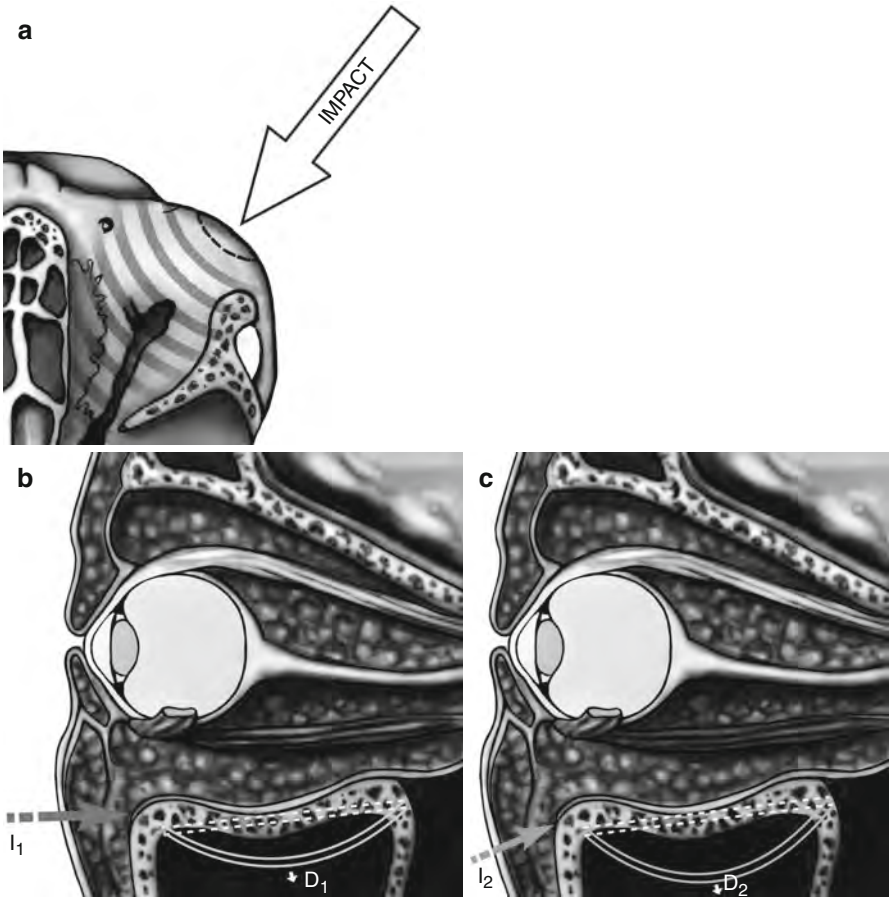

Fig. 3.2 The buckling theory of the formation of an orbital floor fracture: (**a**) The dorsal view of the inferior wall of the right orbit. The main mechanisms of blow-out fracturing of the orbital floor are wavelike deformations (shown with *dashed lines*) that are transmitted from the intraorbital rim to the orbital floor. (**b**, **c**) A horizontal impact (I_1) causes less significant deformation (D_1) compared to impact (I_2) that is parallel to the orbital floor plane (D_2)

and are not accompanied by soft tissue entrapment in the bone defect area. The hydraulic mechanism causes significantly more extensive fractures affecting both the entire orbital floor and the medial orbital wall and results in soft tissue prolapse and enophthalmos [60, 62].

Some authors [17, 52, 60] believe that both mechanisms contribute to fracture formation and it is fundamentally wrong to contrapose them. The variety and complexity of orbital fractures sometimes can be explained only by the simultaneous presence of both trauma mechanisms and with predominance of one over the other giving the individual pathological appearance in each specific case [62].

Another mechanism of fracture formation has been propose before: "pressing against" the orbital floor by the equator of the eyeball abruptly deformed at the

moment of globe trauma. Some authors support this hypothesis of Pfeiffer [63] even today [62, 64]. However, cadaver studies of the orbits relying on advanced mathematical models have demonstrated that it is soft tissues adjacent to the orbital floor that act as a direct injuring agent rather than the globe itself [65].

An isolated blow-out fracture of the orbital floor requires less energy compared to the damage of the medial wall or formation of an inferomedial fracture [65].

This fact, which may seem to be unreasonable at first glance, is well known among clinicians and was explained by Takizawa et al. [66]. The authors used experiments and subsequent computer simulation to demonstrate that both the thickness and the contour (profile) of orbital walls play a crucial role. In particular, the arch-shaped orbital roof is much more resistant to deformation as compared to the virtually planar floor, which can be deformed and fractured more easily. The medial wall is even thinner but it is reinforced by ethmoidal air cells. Hence, the fracture of the medial wall requires greater mechanical energy compared to that of the orbital floor [67, 68].

Such anatomical structures as the inferior orbital fissure, the infraorbital groove, and infraorbital canal [66], as well as reflexive contraction of the m. orbicularis oculi and presence of a large air-bearing cavity [17, 27] under the orbit, also facilitate the damage secondary to trauma to the orbital floor. The rarity of orbital floor fractures in children younger than 7–8 years is caused by underdevelopment of the maxillary sinus and continuing growth of the orbit [1, 69–72]. Even if a fracture is formed, it requires surgical management less often compared to adults [71].

3.3.2 Classification of Blow-Out Fractures of the Orbital Floor

According to radiologic classification proposed by Fueger et al. [73], blow-out fractures are subdivided into six main types, with some of them containing subtypes:

1. *Classical blow-out fracture*: a low-energy fracture of the medial half of the orbital floor medial to the infraorbital canal (Fig. 3.3). This variety is the most common because this is the weakest area of the orbital floor [74] and is observed in 50 % of cases [75].
2. *Fracture involving the infraorbital canal* (Fig. 3.4a, b).
3. *Inferomedial fracture*, i.e., a fracture of the inferior and medial walls. A number of authors [75, 76] reported that this middle-energy variant of trauma accounts for 20–40 % of all orbital floor fractures (Fig. 3.4c, d). Thus, the two most frequent orbital floor fractures are the classical and inferomedial ones. The share of all other variants is less than 10 % of cases.
4. *Total fracture* of the orbital floor (Fig. 3.5). Propagation of the fracture lateral to the infraorbital canal is typically caused by the effect of an injuring agent having an appreciably high kinetic energy, which results in fracturing of the entire orbital floor.

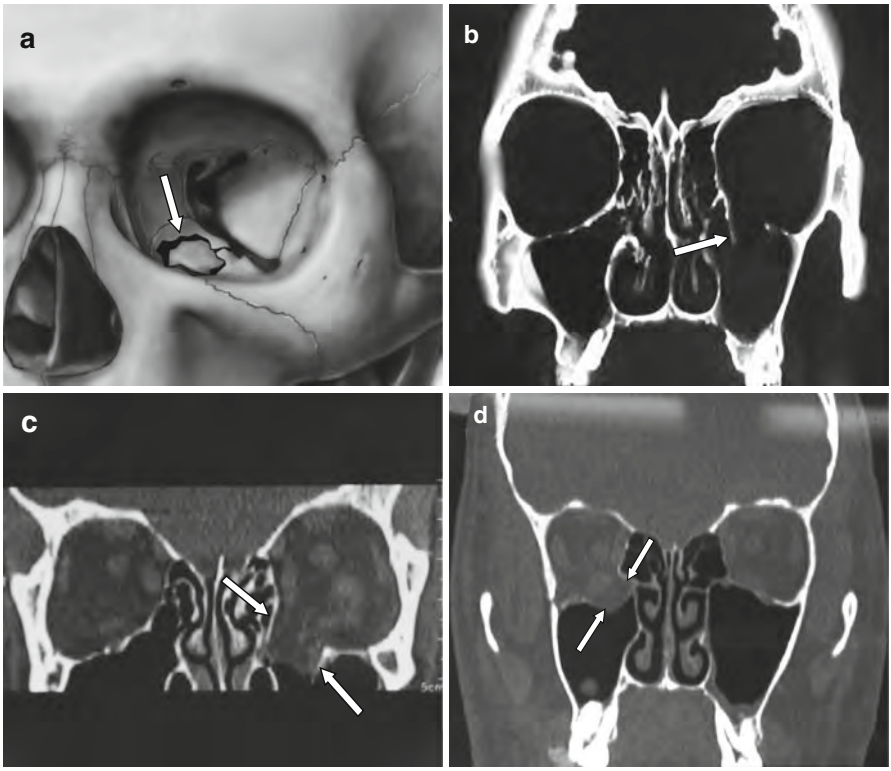

Fig. 3.3 Typical forms of orbital floor fractures according to Fueger et al. [73]: (**a**) Classical fracture, confined to the orbital lamina of the ethmoidal bone and infraorbital canal. The inferior orbital fissure often acts as the posterior border. (**b**) In most cases, a coronal CT scan shows the bony "cusp" with its base oriented toward the nose (an *arrow*), which illustrates the origin of the term "open-door fracture." (**c**, **d**) Less frequently, the fracture is formed by two bony "cusps" (an *arrows*)

5. *Atypical forms of blow-out fractures:*
   (a) Rectangular fracture
   (b) Triangular fracture
   (c) Stellate fracture
6. *Linear fractures of the orbital floor without fragment displacement:*
   (a) Y-shaped fracture
   (b) Lateral linear fracture (Fig. 3.6)

3.3.3 Diagnosis of Blow-Out Orbital Floor Fractures

Diagnosis of the blow-out orbital floor fracture is often facilitated by the presence of typical *complaints.* Diplopia during vertical eye movement is the key finding and is observed in 58 % of patients [78].

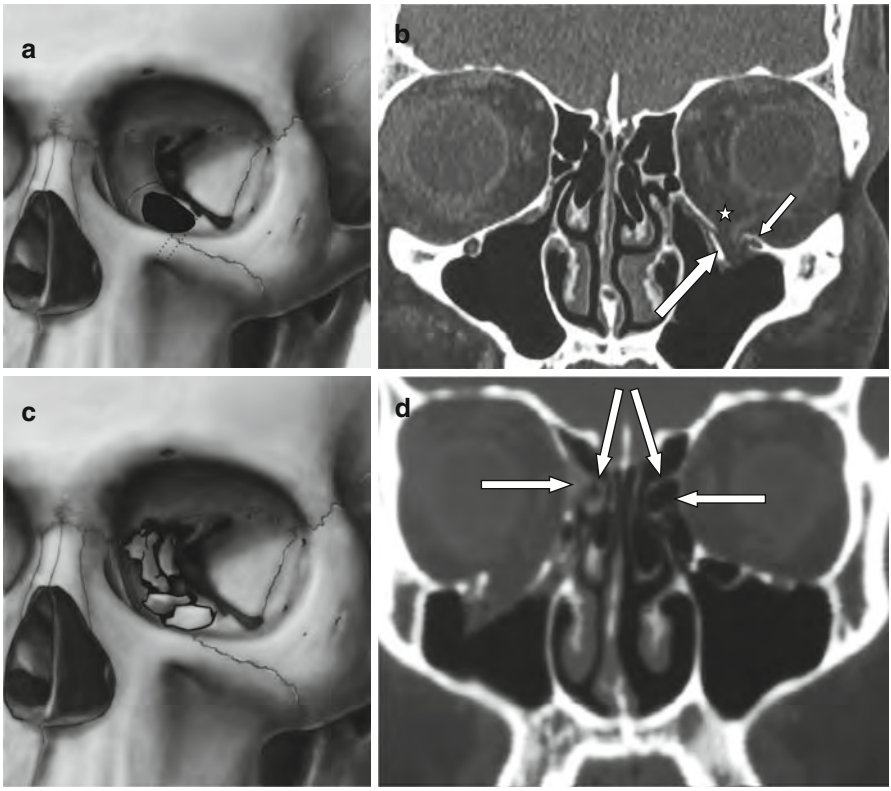

Fig. 3.4 Typical forms of orbital floor fractures: (**a**) Schematic representation of a fracture involving the infraorbital canal. Anterolateral view. (**b**) Coronal CT scan. *Thick* and *thin arrows* show the bony "cusp" and the infraorbital canal, respectively. The canal is adjacent to the belly of the inferior rectus muscle (shown with an *asterisk*). (**c**) Fracture of the inferior and medial walls (inferomedial fracture). Anterolateral view. (**d**) Coronal CT scan. Prolapse of orbital tissues into the maxillary sinus is indicative of orbital floor fracture; discontinued contour of the medial wall and opacity of ethmoidal air cells are indicative of medial wall fracture

The primary position of gaze and changes in diplopia intensity during eye movement help to localize the inferior rectus entrapment site.

Lerman [79] formulated rather interesting rules related to diplopia in patients with blow-out fractures:

1. Thus, if diplopia is aggravated with upward gaze and improved with downward gaze, while the eyeball in the injured orbit is slightly deviated downward in the primary position of gaze, the inferior rectus muscle is entrapped in the preequatorial zone (Fig. 3.7).
2. If limited mobility and diplopia have the same intensity both for the upward and downward gaze, while the eye is oriented centrally in the primary position of gaze, the muscle is entrapped in the equator of the eyeball (Fig. 3.8).

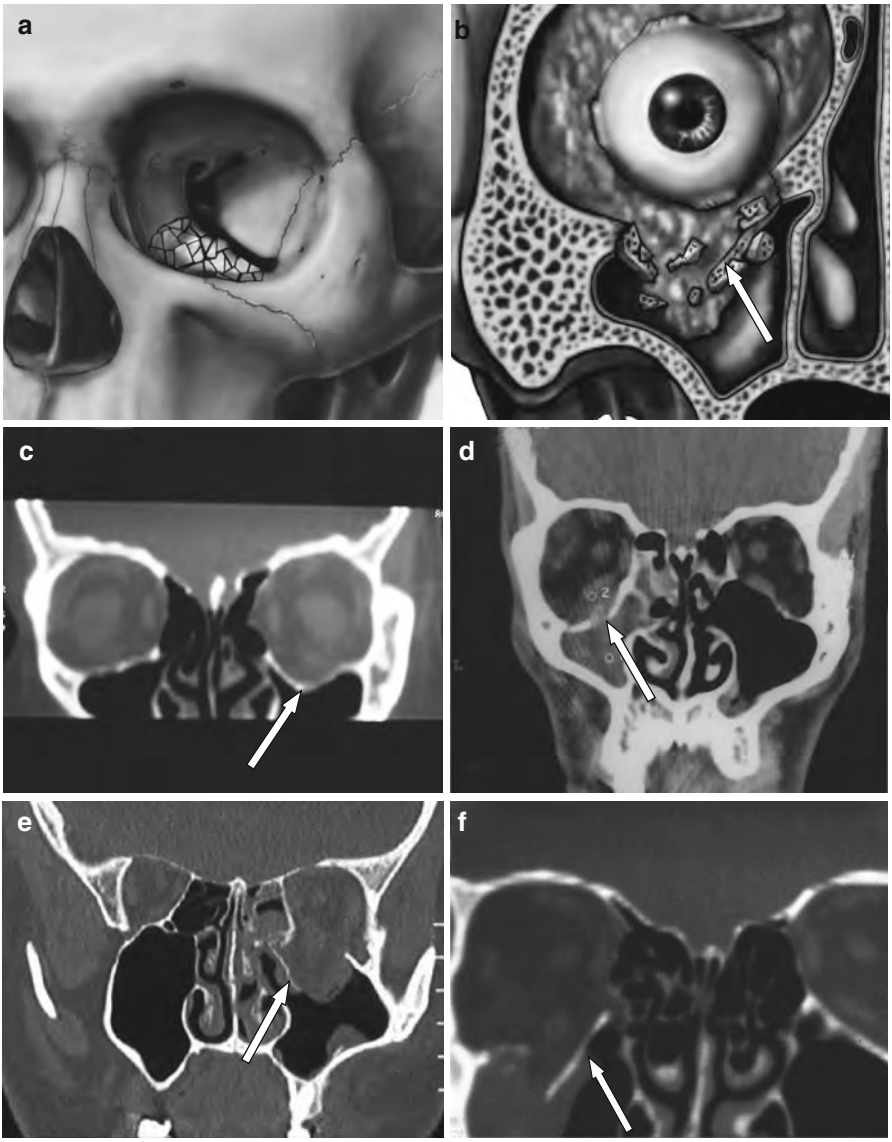

Fig. 3.5 Total fracture (i.e., the fracture spreading outward from the infraorbital canal): (**a**, **b**) Schematic representation of the fracture in the anterolateral (**a**) and coronal (**b**) views. (**c**) Total saucer-like fracture (*arrow*); (**d**) comminuted total fracture (*arrow*); (**e**, **f**) total open-door fracture (*arrow*)

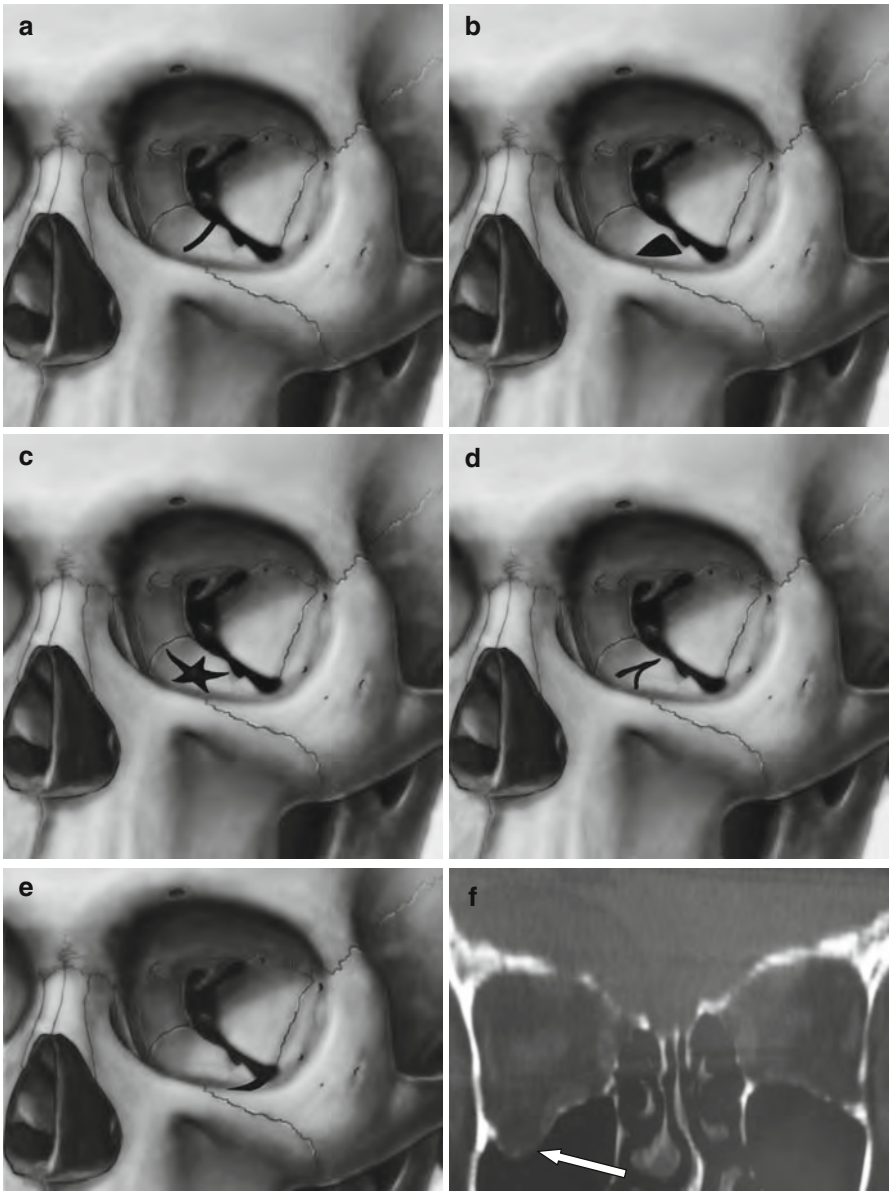

Fig. 3.6 Atypical forms of orbital floor fractures (on the example of left orbit, anterolateral view) (citation from Fueger et al. [73]): (**a**) Rectangular fracture running parallel to the infraorbital canal. (**b**) Triangular fracture. (**c**) Stellate fracture. (**d**) Y shaped. (**e**) Lateral linear fracture connecting the inferior orbital fissure with the infraorbital rim (Cited from Greenwald et al. [77]). (**f**) Coronal CT of the fracture of the lateral half of the orbital floor (shown with *arrows*)

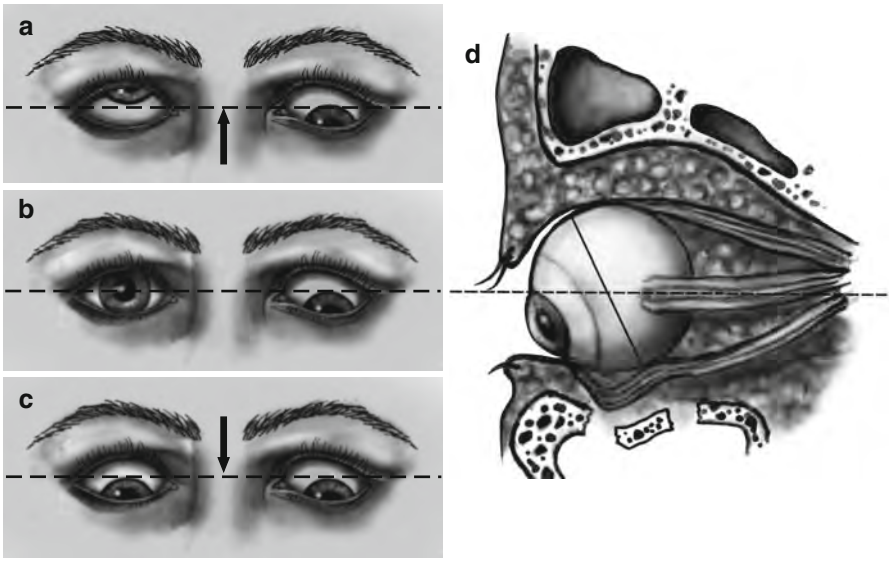

Fig. 3.7 Vertical eye movement problems (for the left eye) when a fracture localizes in the pre-equatorial zone (the equator is shown in (**d**) with a *black line*). The left eyeball is slightly deviated downward in primary position of gaze (**b**); diplopia is aggravated with upward gaze (**a**) and improved with downward gaze (**c**). *Black arrows* - direction of gaze (citation from Lerman [79])

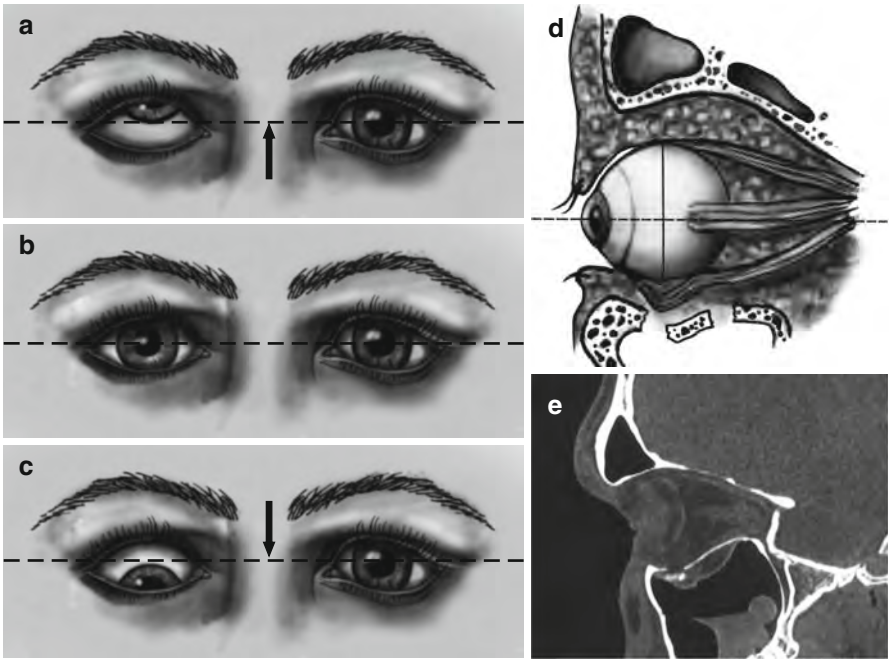

Fig. 3.8 Vertical eye movement problems (for the left eye) when a fracture localizes in the equatorial zone of the left eyeball (the equator is shown in (**d**) with a *black line*). The left eyeball is oriented centrally in primary position of gaze (**b**); limited mobility and diplopia have the same intensity both for upward (**a**) and downward (**d**) gaze (citation from Lerman [79])

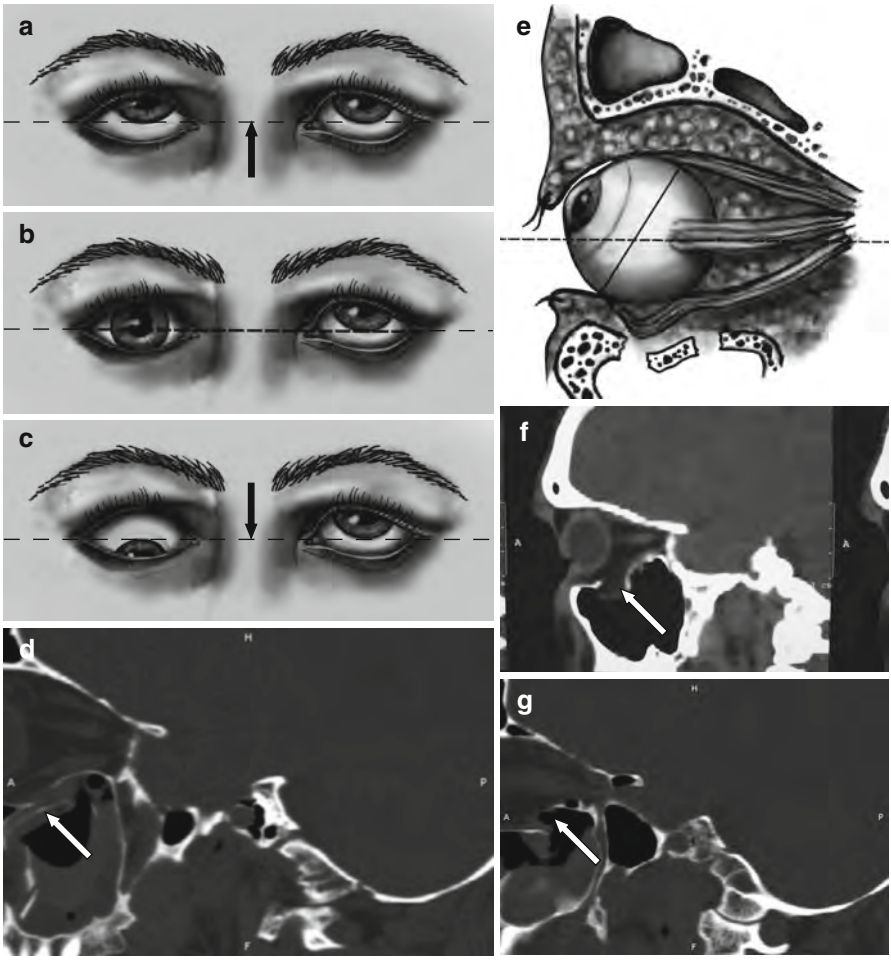

Fig. 3.9 Eye movement problems when the fracture (shown with *arrows* on the CT scan) localizes behind the equator of the eyeball (the equator is shown in (**d**) with a *black line*). The eyeball is slightly deviated upward in primary position of gaze (**b**); diplopia is aggravated with downward gaze (**a**) and improved with upward gaze (**c**) (citation from Lerman [79]). Posterior fractures of the orbital floor are accompanied by the most severe and persistent diplopia caused by the entrapment of posteroinferior portions of the adipose body of the orbit, which are permeated by numerous connective tissue intersections that are interwoven into the sheaths of extraocular muscles, in the bone defect

3. Finally, if diplopia is aggravated with downward gaze and improved with upward gaze, while the eyeball is slightly deviated upward in the primary position of gaze, the inferior rectus muscle is entrapped postequatorially[4] (Fig. 3.9).

[4] An upward deviation of the eyeball in patients with posterior fractures of the orbital floor was first reported by Cole and Smith back in 1963; however, the authors did not interpret the origin of this symptom.

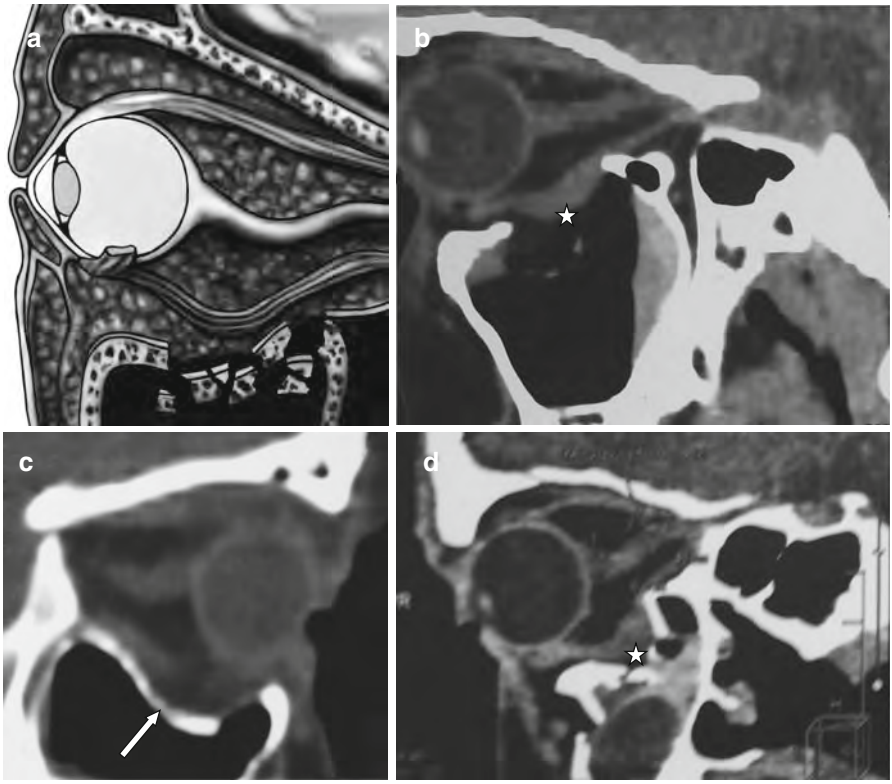

Fig. 3.10 A tentative mechanism of eyeball tropia in patients with posterior fractures of the orbital floor: (**a**) Schematic representation. (**b–d**) A CT scan contains an extensive (stretching up to the posterior wall of the maxillary sinus) defect (shown with an *asterisk*) or depression (shown with an *arrow*) of the orbital floor. The inferior rectus muscle is displaced downward. It should be mentioned that the muscle is not entrapped in the fracture zone and the traction test will be negative prior to surgery (Fig. 3.14). Hypofunction of the inferior rectus muscle is caused by other reasons: attachment to the sclera at an angle more obtuse than the physiological one (up to the *right angle*); displacement of the muscle origin from the orbital apex to the point where the muscle is "detached" from the orbital floor displaced downward; impaired motility of the muscle as it passes over a sharp edge of the defect, thus the effect of faden operation (muscle relaxation by suturing its belly to the sclera 13 mm away from its attachment site) is imitated

Paralysis of the inferior rectus complex [80], displacement of the inferior muscular complex into the fracture zone [81], and the abnormal angle of attachment of the dislocated inferior rectus muscle to sclera [82] are considered to be possible reasons for upward deviation of the eyeball (Fig. 3.10).

Complaints of hypoesthesia in the distribution of the infraorbital nerve occur in 70 % of patients [84] (Fig. 3.11). The combination of neurological impairments with vertical diplopia and enophthalmos allows one to almost for certain make a clinical diagnosis of orbital floor fracture [85].

A meticulous history to discover the *mechanism of trauma* is helpful for making the proper diagnosis. One should pay attention to two major factors that

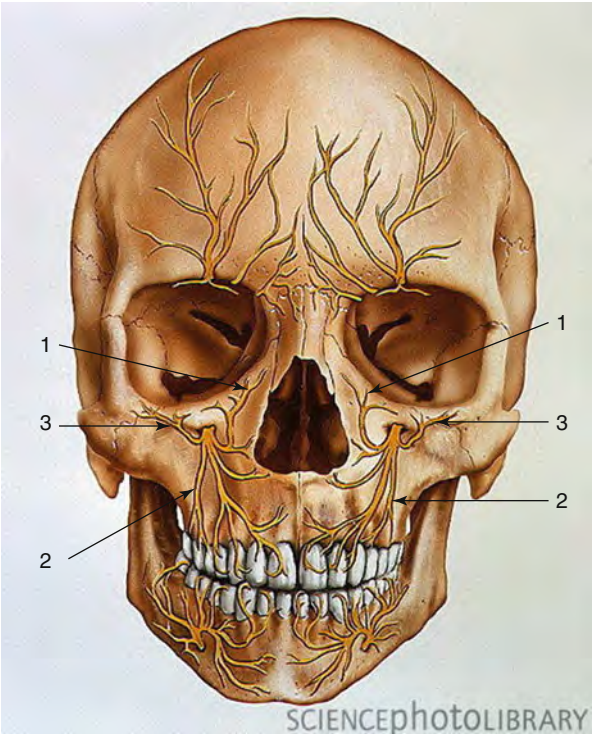

Fig. 3.11 The region innervated by the infraorbital nerve: *1* nasal branch (nasal skin and septum), *2* labial branch (upper lip skin and the oral mucosa), *3* palpebral branch (skin and conjunctiva of the lower eyelid)

determine the clinical presentation of a fracture: the size of an injuring agent and the energy component of the trauma. If the surface area of a blunt object is smaller than the size of the orbital opening, the patient may have rupture of the sclera. If the size of the injuring body is larger than that of the orbital opening, two alternative outcomes are possible. If the injuring object has a relative low speed and, therefore, low kinetic energy, the low-energy blow-out orbital floor fracture occurs. A rather strong impact results in a middle-energy trauma that may combine a fracture of the infraorbital rim and the orbital floor (Fig. 3.12a–d) [49]. Finally, a large injuring object with high kinetic energy may cause a fracture of the orbital rim, orbital floor, and other facial bones. And if enough energy is present, panfacial fractures may occur (Fig. 3.12e, f) [44]. These situations are usually caused by car accidents. Thus, the analysis of the traumatic circumstances is of practical importance as it allows one to predict the type of injury and question the signs of periocular edema and hematoma found during the primary examination that may hide a more serious underling injury.

An objective examination starts with external inspection. Possible orbital floor fracture is indicated by such findings as pronounced palpebral edema and hematoma, subconjunctival hemorrhage, and chemosis of the bulbar conjunctiva (Fig. 3.13a, b) [2, 86].

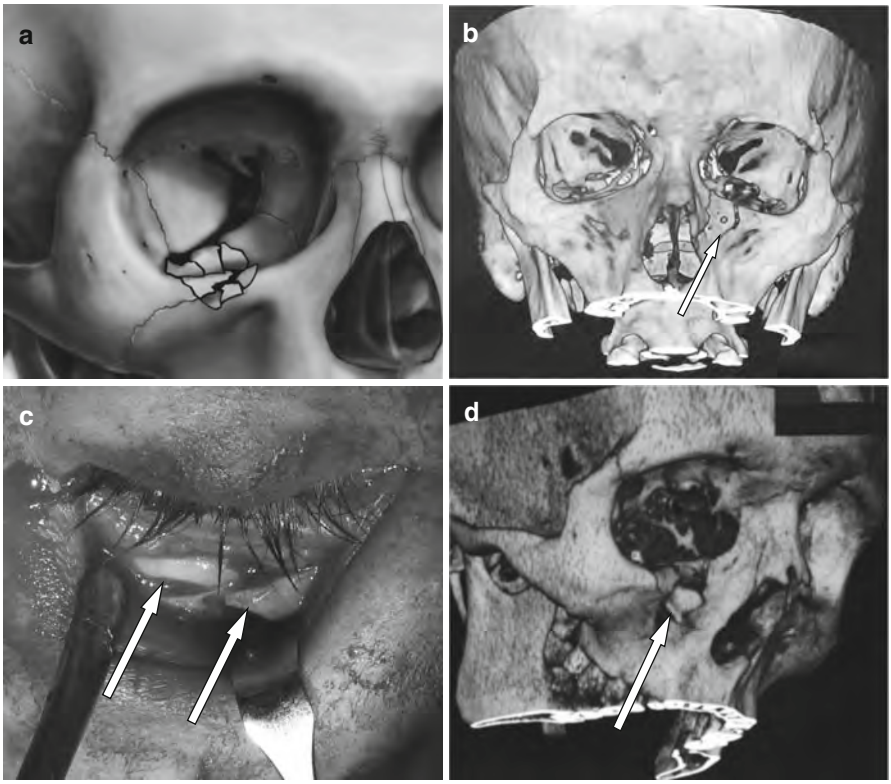

Fig. 3.12 Middle- and high-energy orbital fractures: (**a**–**d**) Middle-energy fracture of the infraorbital rim and inferior wall of the orbit (bone fragments are shown with *arrows*)

The concomitant findings and symptoms of orbital floor fractures are listed in the order of decreasing incidence: periorbital ecchymosis (75 %), diplopia (50–60 %), subconjunctival hemorrhage (40 %), and enophthalmos (33 %) [2, 9].

It is commonly believed that if a patient has these findings, it is possible to reliably assess the eyeball position in the orbit (in three views) and scope of its movements only 2–3 weeks after the injury [87], since reactive edema and hematoma of orbital soft tissues may disguise enophthalmos up to 3 mm in size[5].

Axial dystopia (eno- or exophthalmos) is determined with respect to the relatively healthy eye using a Hertel/Krahn exophthalmometer. A basis is selected so that the supports are tightly pressed against the anterior surface of the lateral orbital rims. An ophthalmologist uses his/her left eye to assess the protrusion of the patient's right eye and vice versa. When assessing the patient's right eye, the ophthalmologist's left eye is supposed to be open, while the patient looks at the ophthalmologist's closed right eye. The ophthalmologist uses his/her left eye to

[5] However, Yab et al. [88], relying on CT data, claim that edema of soft tissues has no significant effect on eyeball position in the orbit as soon as 10 days after trauma.

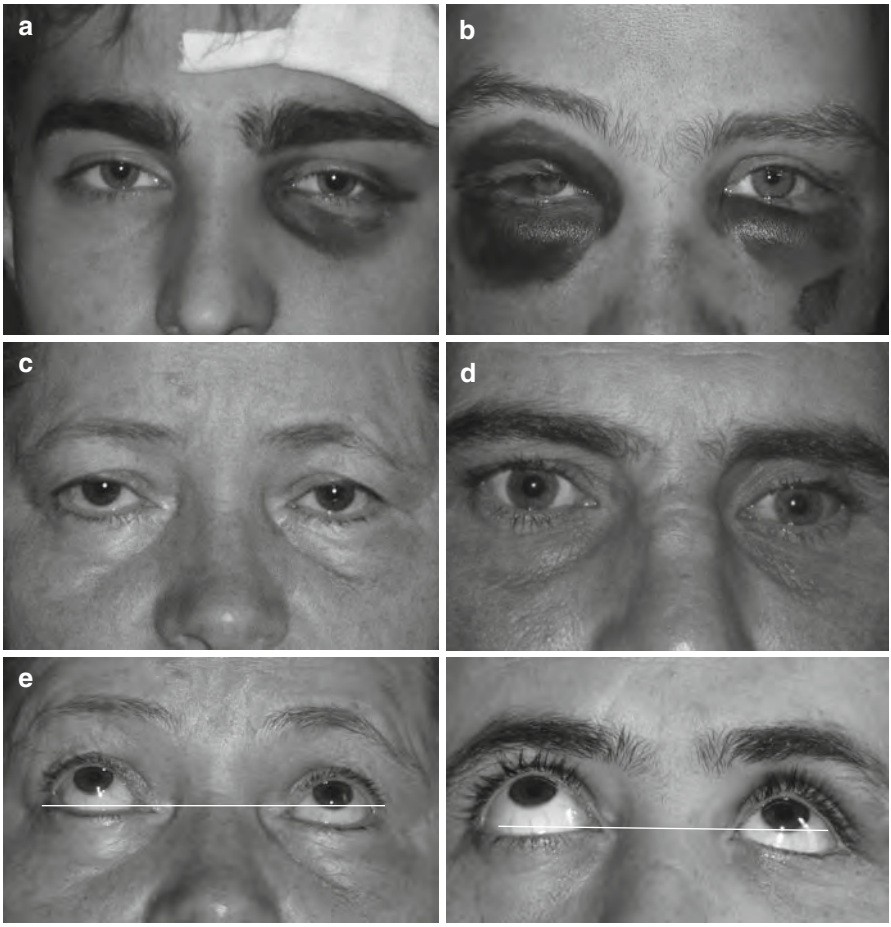

Fig. 3.13 Clinical presentation of orbital floor fracture (*white line* demonstrates movement restriction): (**a**, **b**) Periorbital ecchymosis, subconjunctival hemorrhage, palpebral edema, and hematoma. (**c**) Narrowing of the left orbital fissure that is clearly seen by comparing the positions of the lower eyelid on both sides. (**d**) Left-sided enophthalmos manifesting as deepening of the upper eyelid crease. (**e**, **f**) Ipsilateral restriction of supraduction (upward movements of the eyeball)

converge parallel lines into one line in a mirror and evaluates corneal protrusion using the scale drawn on the mirror [89].

Exophthalmos in the presence of injury to the orbital floor is possible only during the acute phase of trauma and is caused by edema and/or hematoma of orbital tissues. Globe retraction (sunken eye) is a typical symptom of blow-out fracture (Fig. 3.13c, d). Enophthalmos is indicative of increased orbital volume, which is typical of blow-out fractures with significant displacement of bone fragments (the classical, inferomedial, and total ones).

One to two millimeter dystopia is considered to be mild; 3–4 mm dystopia is regarded as moderate; enophthalmos greater than 5 mm is considered to be pronounced [90].

Yab et al. [88] analyzed CT scans of patients with orbital fractures and found that enophthalmos remains ~1 mm if the orbital volume increase is less than 2 mL.

The degree of enophthalmos subsequently increases in proportion to increasing orbital volume; however, it is never greater than 4 mm for an isolated orbital floor fracture.

Vertical dystopia (hypoglobus) is assessed with respect to a horizontal line running through the center of the pupil of the healthy eye [91, 92]. Eyeball prolapse is usually indicative of the extensive orbital floor fracture. Sporadic cases of dislocation of the eyeball into the maxillary sinus are the most marked variants of hypoglobus.

Lateral dystopia (in the frontal view) is measured by comparing the distance between the midpoint of the nasal bridge and the nasal portion of the limbus. The difference between the healthy and the injured sides is indicative of concomitant fracture of the medial orbital wall [89].

An *analysis of eye movements* is the next step of examination. The position of the eyeballs in primary gaze is first evaluated followed by assessment of ocular excursions across the horizontal and vertical meridians. The ocular motility in the six main directions of gaze is then inspected: rightward, leftward, upward and outward, upward and inward, downward and outward, and downward and inward. Total restriction of ocular motility is usually indicative of orbital edema or hematoma. Ipsilateral reduction of supraduction or infraduction is a diagnostically valuable finding (Fig. 3.13e, f). One should bear in mind that obvious restrictions of ocular motility are rather rare [93]. An induced diplopia test based on evaluation of the relative spatial position of the images produced by the normal and deviated (injured) eye is conducted to detect less evident ocular motility disorders.

Diplopia is induced by placing a red lens in front of an eye. This allows one to simultaneously find out which of the double images belongs to the right and left eye, respectively. The distance between an ophthalmologist and a patient facing one another should be 1.5–2 m. The ophthalmologist holds a flashlight and moves it rightward, leftward, upward, and downward, as well as in intermediate directions. The patient is asked whether he/she sees one or two lights. If the patient sees two lights, he/she is asked to tell how they are oriented with respect to each other, what the distance between them is, and when the distance increases or decreases.

The results are assessed using the following rules: (1) the injured muscle corresponds to the eye producing an image located further from the median horizontal or vertical line; this image is referred to as the ghost image; (2) the ghost image is always projected toward the paralyzed muscle; hence, homonymous diplopia emerges when abductor muscles are affected, while heteronymous diplopia is caused by damage to the adductor muscles; and (3) the distance between double images increases as gaze moves toward the injured muscle.

Differential diagnosis between the main reasons for ocular motility disorders (paresis of the oculomotor nerve branchlet or muscle entrapment in the fracture area) is performed using the *traction test (forced duction)* [94, 95].

The patient is asked to look at his/her left arm outstretched in the direction of suspected displacement of the eyeball (i.e., upward)[6]. After epibulbar anesthesia, the limbal conjunctiva at 6 o'clock meridian is fixed with corneal (colibri) forceps, and the eyeball is displaced in a direction opposite to the vector of traction of the inferior rectus that is suspected to be entrapped (i.e., upward). It is important that the eyeball is not pressed against the orbit, which may create an illusion that there is normal ocular motility with muscle entrapment [83].

A positive traction test is the impeded passive upward displacement of the eyeball, while its downward motility remains normal. According to clinical observation, ocular motility is limited both in up- and downward directions. The positive traction test indicates that either the inferior rectus or the inferior rectus and inferior oblique muscles are entrapped in the fracture area. In a number of cases, only the inferior portion of the anterior suspensory system is entrapped (Fig. 1.35); however, its close connection with the muscles also causes diplopia [94, 96] and requires surgical intervention.

A negative traction test (unimpeded passive upward displacement of the eyeball) is observed in 18 % of cases [17, 97, 98] and is indicative of rectus superior paralysis (Fig. 3.14) [83] or injured muscle (contusive edema, hematoma, or muscle detachment from the sclera) [99].

The so-called *generation test* (*muscular effort generation test*) is used in this instance [100]. After epibulbar anesthesia, the limbal conjunctiva at 6 o'clock meridian is fixed with corneal forceps, and the eyeball is held in the primary gaze direction. The patient is asked to look in the direction of action of the examined inferior rectus (i.e., downward). If innervation is retained, the ophthalmologist will feel the effect of the muscle trying to move the eyeball down (the positive test). The negative result of the test cannot be easily and unambiguously interpreted as it can be caused both by paralysis of the oculomotor nerve and by injury to the muscle. In most cases, the reason for the negative test is secondary to muscular dysfunction that typically disappears within 1–2 weeks. Chronic oculomotor disorders show that they are of neurogenic origin.

The contraindications to performing the traction test include acute pain, blepharospasm, orbital hematoma, or tissue edema because the risk of obtaining false-positive results is high [52].

Despite the fact that a blow-out fracture partially absorbs increased intraorbital pressure, these traumas are accompanied by various eye injuries in 30–40 % of cases

[6] This approach significantly increases the examination accuracy. For example, if the patient is looking downward prior to the test, the ophthalmologist will inevitably be experiencing resistance from the contracted inferior rectus. As a result, passive eye movements are restricted, and there is an illusion of muscle entrapment.

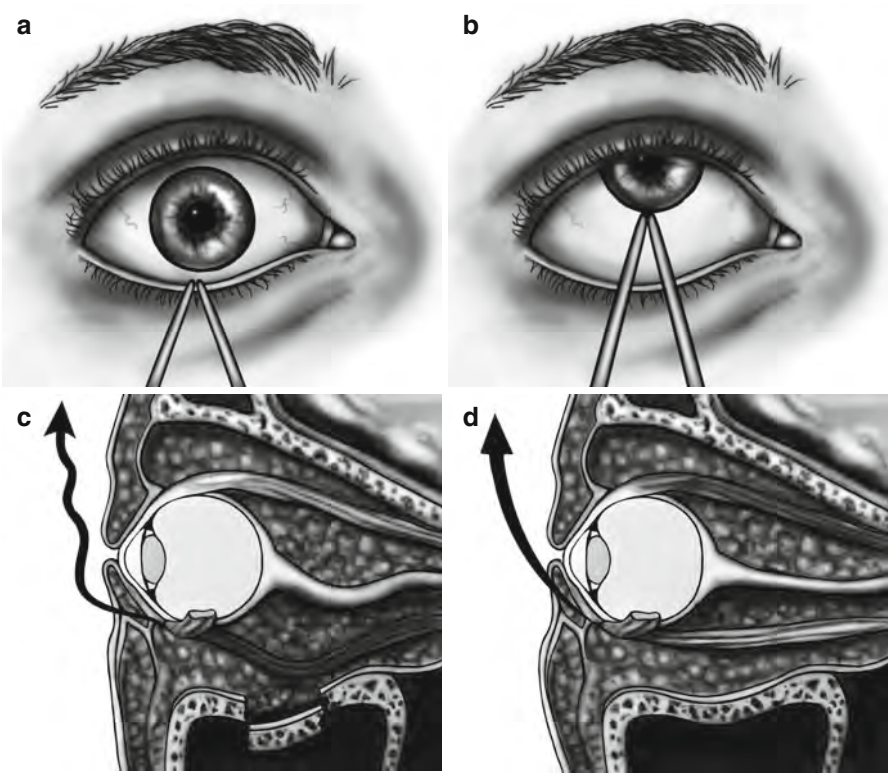

Fig. 3.14 The traction test procedure (citation from von Noorden [83]; Della Rocca [52]): (**a**) After epibulbar anesthesia, the limbal conjunctiva at 6 o'clock position is immobilized with corneal forceps. (**b**) The eyeball is displaced upward. (**c**) Positive traction test corresponds to impeded passive upward displacement of the eyeball (shown with a *curly arrow*), which is indicative of entrapment of the inferior rectus muscle (shown with *dark*) in the fracture area. (**d**) Negative traction test corresponds to unimpeded passive upward displacement of the eyeball (shown with a *curved arrow*), which is indicative of paralysis of the levator (the superior rectus muscle shown with *dark*)

[21, 28]. Severe intraocular injury occurs rather frequently (20–30 %) [12, 33, 101]. Tong et al. [9] reported that 40 % of these injuries are scleral ruptures. In 38 % of cases, orbital floor fractures are accompanied by injuries affecting structures other than facial bones (first of all, cranial and cerebral traumas). The risk of suffering an eyeball trauma for blow-out fracture is 2.5 times as high as that for zygomatic orbital fracture [33]. It is always mandatory that the integrity of the eyeball is established prior to any orbital floor reconstruction [102]. Unfortunately, traumas of the eyeball and periorbital area often go unnoticed at the primary inspection of patients with midfacial fractures [29].

The first parameters to be assessed in a newly admitted injured patient are visual acuity and pupillary responses [103].

Complete evaluation of the visual system in the emergency department is often unfeasible. Accurate evaluation of visual acuity when the patient is examined at the

hospital may be caused by a variety of reasons: an altered mental state either from trauma or intoxication, the absence of corrective lenses including the loss of contact lenses, tears admixed with blood, pain, poisoning, fear, or anxiety, which may prevent the patient from focusing. While the absolute accurate assessment of visual acuity may not contribute to the treatment decision making at that time, it is very important to document the reason why the complete evaluation was not possible. However, the finding of profound loss of vision clearly indicates that the visual pathway has been seriously damaged.

In the absence of central vision, either real or apparent, an ophthalmologist should perform a light sensitivity test comparing the light sensitivity of the traumatized eye to the normal eye. The test for distinguishing the red color is performed to assess the status of the optic nerve. An unfavorable prognostic factor is if the patient perceives the tested object (either a distal phalanx of the index finger or a red cap from the vial of a mydriatic agent) as having an orange or brownish tint.

Regardless of the patient's consciousness, the pupillary status, and evaluation for a relative afferent pupillary defect (RAPD) must be done. If the patient is unconscious or uncooperative, this may be the only test of the visual system that can be done. Particular attention should also be given to the shape and size of pupils [12].

Corectopia or a peaked pupil is a sign of penetrating eye injury or scleral rupture.

When performing evaluation of the pupils, one should bear in mind that pupil diameter does not closely correlate with visual acuity, because the pupil size depends on interaction between sympathetic fibers of the ophthalmic division of the trigeminal nerve (n. V_1) and parasympathetic fibers located in the inferior branch of the oculomotor nerve (n. III).

As a result, a blind eye may have a normal pupil diameter, and vice versa, a patient with the maximum degree of mydriasis may have high visual acuity.

Pupillary responses to the bright light are then analyzed. The afferent pupillary defect, or the Marcus Gunn pupil (impaired direct pupillary response to the light with the retained consensual response), confirms the presence of optic nerve trauma. The pupil in this case exhibits a paradoxical response to the light beam being rapidly moved from a healthy eye to the injured one. The pupil of the injured eye does not constrict under direct exposure to light; instead, it widens as it loses the direct response due to the impairment of the afferent portion of the pupillary reflex arc.

The next stage involves examination of the central visual field using the Amsler grid (Fig. 3.15) and estimation of visual field borders. After that, the anterior segment is examined using a flashlight. The final stage of examination is ophthalmoscopy of the fundus under drug-induced mydriasis. The pharmacological effect on the pupil and meticulous description of the initial state of the pupil must be reported in patient's medical history prior to dilation. Unless necessary, the pupil of the contralateral healthy eye should not be dilated.

The only symptom specific of orbital floor fracture that can be detected by visual inspection of the eyeball is pupil dilation to 5–8 mm persisting from several weeks to several months after the trauma. The pupil does not respond to light but is

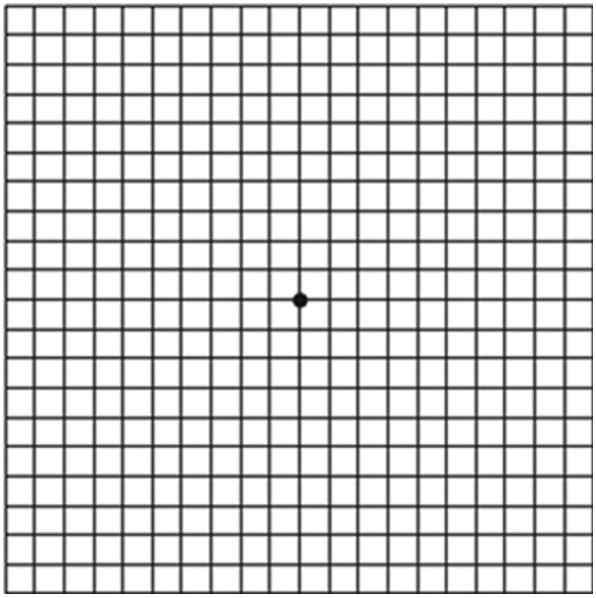

Fig. 3.15 Amsler grid for examining the central (20°) visual field: The 200×200 grid consists of squares with a side length of 5 mm formed by intercepting vertical and horizontal lines. The *fixation point* is placed in the center of the grid. A patient looks at the *fixation point* and sees the *lines* either as smooth and uniformly colored or distorted and partially obscure depending on his/her retinal status. The patient draws the pattern he/she sees on the Amsler grid

narrowed after pilocarpine instillation, which allows one to differentiate between this pathology and contusion-induced mydriasis[7] [105].

The obvious CT signs of the orbital floor fracture include muscle entrapment in the fracture area and extensive prolapse of the orbital adipose tissue into the maxillary sinus (Fig. 3.16a, b).

The indirect signs of the fracture are as follows (Fig. 3.16c, d):

- The muscle is adjacent to the seemingly uninjured orbital floor. The combination of this sign with the typical clinical presentation indicates that the sheath of the extraocular muscle and the surrounding connective tissue intersections in the area of linear fracture are subjected to trapdoor entrapment [95, 106, 107].

[7] A. Hornblass [104] was the first to pay attention to mydriasis in patients with posterior fracture of the orbital wall and to hypothesize the pupil dilation is caused by entrapment of the inferior oblique muscle in the area of the defect of the inferior orbital wall.

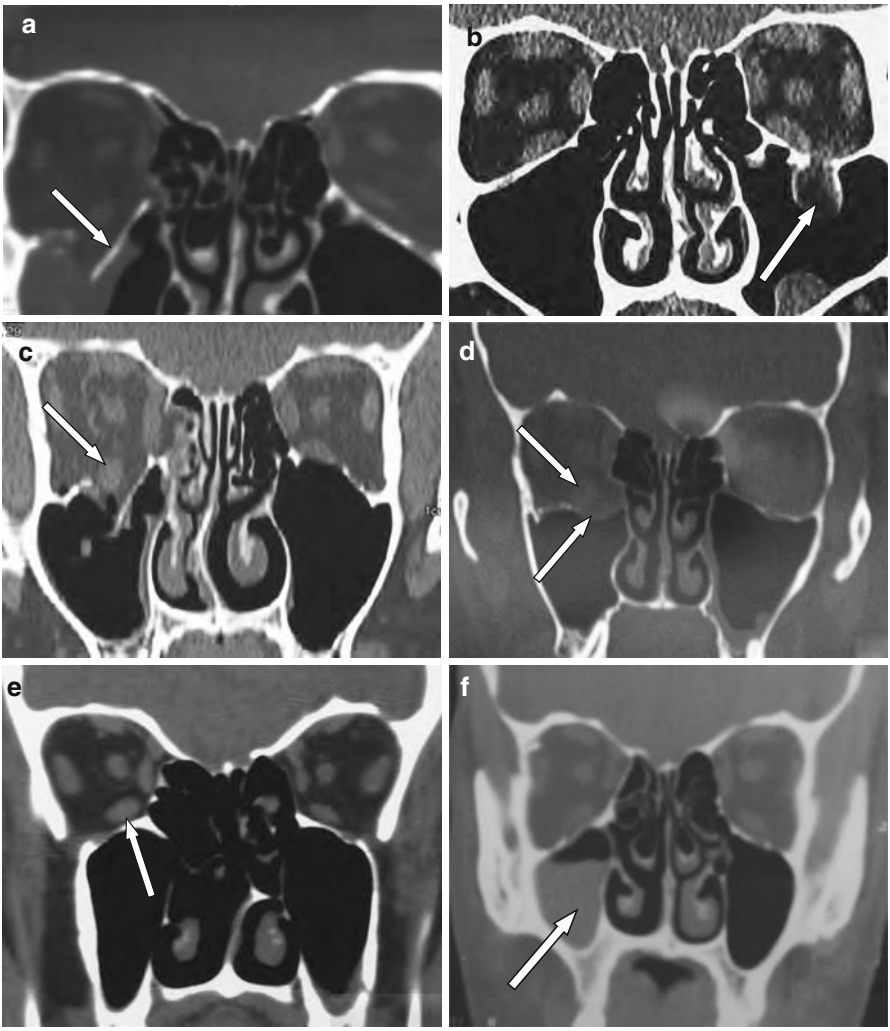

Fig. 3.16 CT signs of the orbital floor fracture: (**a**) An extensive bone defect with displacement of a bone fragment (shown with an *arrow*) into the sinus. (**b**) Prolapse of the orbital fat entrapped in the trapdoor fracture into the maxillary sinus (*arrow*). (**c**–**e**) Rounding of the normally flat belly of the inferior rectus muscle (shown with an *arrow*). The sign does not have a significant prognostic value in evident fractures (**c**) but is rather informative for small defects of the orbital floor (**d**, **e**). (**f**) Massive hemorrhage into the maxillary sinus, which facilitates diagnosis of a fracture with minimal displacement of bone fragments

- The missing inferior rectus muscle syndrome, when the muscle is entrapped in the bone defect area in patients with trapdoor fractures in such a way that it is imaged neither in the orbit nor in the maxillary sinus in coronal CT scans [108–110].
- Rounding of the normally flattened belly of the rectus muscle that is clearly discernible on a coronal CT scan (Fig. 3.16c–e) [12, 111]. This indicates that the muscle is no longer supported by the bones and connective tissue [112, 113]. It was found in cadaver studies using orbits that when the fracture area is less than 1 cm^2, rounding of the belly of the inferior rectus is caused only by periosteal rupture. This leads to a high risk of late enophthalmos and requires early surgical management. When the fracture area is 4 cm^2, the belly becomes round even if the periosteum is not ruptured; however, the symptom is more marked in case of periosteal rupture [112].
- The presence of free fluid in the paranasal sinus (Fig. 3.16f) [114].

If patient's general status is serious and coronal CT scanning is unfeasible, one can use transantral endoscopy via the approach to the maxillary sinus using the Caldwell–Luc procedure. This can be performed under local anesthesia in hospital and is a very helpful method to evaluate and treat the patient [115].

3.3.4 Management of Blow-Out Fractures of the Orbital Floor

3.3.4.1 Indications for Surgery

Blow-out fractures that make a patient suffer neither functionally nor aesthetically do not require surgical management [116]. All other cases are managed surgically. Conservative management or delayed surgery are not used any longer [117].

Management of the orbital floor fracture is aimed at restoring the original shape and volume of the orbit, repositioning its contents, and recovering ocular motility [117–119]. The formula for success consists in adequate exposure of the fracture area, clear visualization of its posterior edge, and compensation for the defect within its entire area [74].

Regardless of the fact that no prospective randomized studies focused on management of the orbital floor fractures have yet been conducted, much clinical experience has led to clear indications for surgery [120, 121].

The intervention needs to be early, single stage, and definitive. *Indications for reconstruction of the orbital floor during the first 3 days after trauma include:*

- *Early hypo- and enophthalmos indicating the total fracture of the orbital floor* (Figs. 3.5 and 3.17a)
- *Trapdoor orbital floor fracture in children*[8] (Fig. 3.17f)
- *Oculocardiac reflex showing no tendency toward spontaneous regression*[9] [12, 20, 120–126]

[8] A separate section is devoted to this fracture type.

[9] The oculocardiac reflex includes a triad of symptoms: bradycardia, nausea, and faintness. The first division of the trigeminal nerve transmitting signals from parasympathetic fibers of n. III and proprioceptors residing in the entrapped inferior oblique muscle is the afferent neuron. Then the impulse reaches the vagus nerve via the reticular formation; then the efferent signal travels to

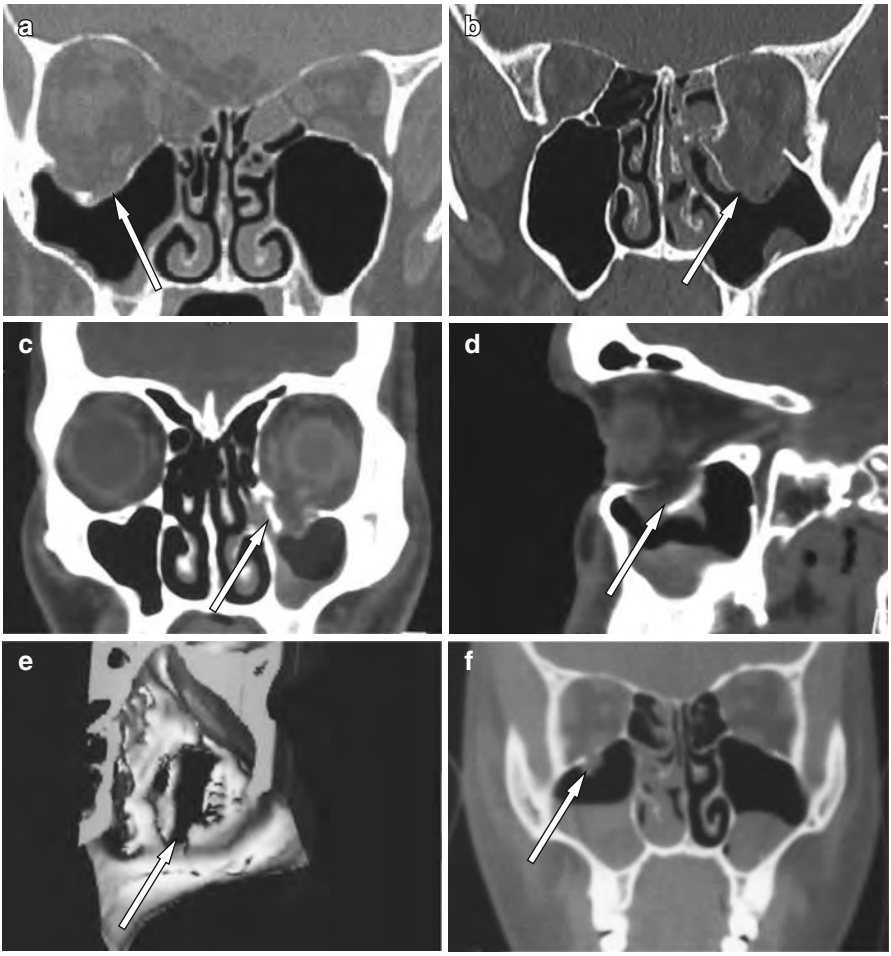

Fig. 3.17 Indications for reconstruction of the orbital floor: (**a**) Total fracture. (**b**) The volume of the injured orbit is significantly increased. (**c**–**e**) Orbital floor defect occupying a half of the orbital area in the coronal (**c**) and sagittal (**d**) views and on a 3D reconstruction (**e**); (**f**) entrapment of the inferior rectus muscle in the zone of the linear trapdoor fracture has a high rate of development of strangulation necrosis

In other cases of acute concomitant injuries of the orbit and midfacial area, the integrity of the orbit should be restored on day 3–9, when there is neither life hazard nor risk of vision loss or serious vision impairment [124]. More than two-thirds of American plastic surgeons perform this intervention within the first 14 days [84], while half of British surgeons operate on the orbital floor fracture 6–10 days after trauma [127].

cardiac and gastric receptors along the vagal trunk. Although the risk of fatal cardiac dysrhythmia in oculocardiac reflex is less than 1:3,500, this condition still requires an urgent intervention. The oculocardiac reflex is typical of fractures of the posterior segments of the orbital floor. Sires et al. [122] were the first to describe the oculocardiac reflex in patients with trapdoor fractures.

Each of the criteria listed below or their combination is an indication for surgery:

- *Diplopia in the functionally crucial gaze directions (e.g., for downward gaze*[10] *(within 30° of the primary gaze direction)* [12, 123] *or for direct gaze outward) persisting for 2 weeks after trauma in patients with radiologically verified fracture and positive traction test* [120].
- *An enophthalmos greater than 2 mm* [128, 129].
- *An orbital floor defect larger than half of the area of the orbital floor* (Fig. 3.17c) [87, 130–132]. This is associated with an increased risk of developing late hypo- and enophthalmos [120].
- *Significant downward displacement of the orbital contents and enophthalmos greater than 3 mm emerging in patients with a radiologically confirmed increase in orbital volume by at least 20 %* (Fig. 3.17b) [133–135].

Enucleation with insertion of an orbital implant in patients with a concomitant extensive orbital floor defect needs to include osteoplasty as the final stage. Otherwise, the patient will develop an anophthalmic enophthalmos and hypoglobus (Fig. 3.18) [136, 137].

The intervention is regarded as *early* if it was performed in the acute phase of trauma, i.e., within the first 14 days [87, 138]. This term is considered to be optimal for reconstructing the damaged orbit and recovering ocular motility [16, 118, 130, 139, 140], although chances of success do not decrease if the repair is done later within a month after an injury [141].

A surgery performed between 3 weeks to 4 months after the trauma, during the so-called gray period, is regarded as delayed surgery [142]. In this case, the fused bone fragments still can be mobilized without performing osteotomy [17], and the prolapsed soft tissues can be detached from the fracture margin [143]. Finally, an intervention performed 4 and more months after the trauma and requiring osteotomy is considered to be late intervention [134, 144]. Neither good aesthetic nor functional results can be achieved in this period [140] as the soft tissues covering the fracture area are inevitably cicatrized after the trauma [145, 146].

3.3.4.2 Approaches to the Orbital Floor

An intervention should be performed under intravenous or endotracheal anesthesia avoiding pronounced arterial hypotension.

It is reasonable to start the surgery with a peritomy and placing an inferior rectus bridle suture (Fig. 3.19).

[10] Both upper and lower portions of the visual field are functionally crucial for a school teacher, a librarian, and a basketball player.

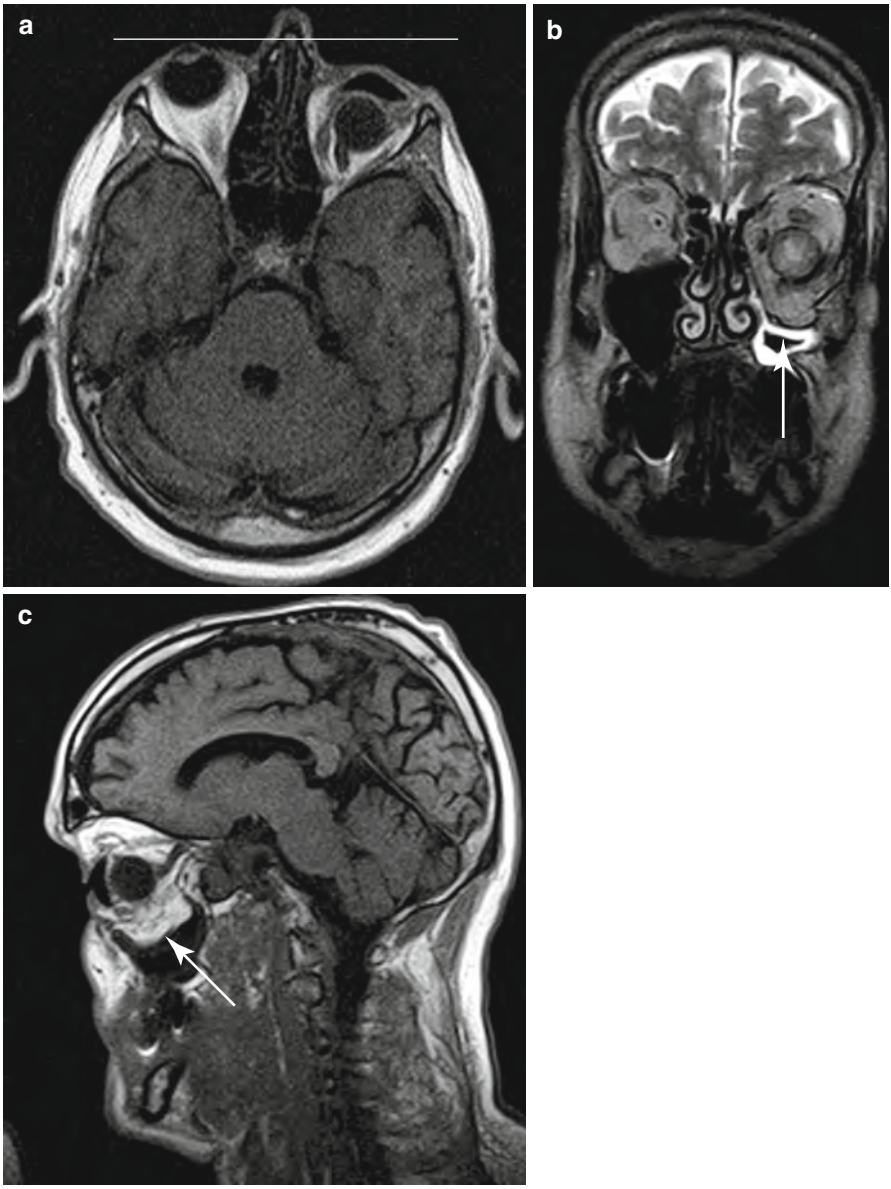

Fig. 3.18 MR image of an anophthalmic "enophthalmos" in a patient with a total orbital floor fracture: (**a**) Pronounced retraction of a cosmetic prosthesis on an axial MR image. (**b**) The coronal view shows the downward displacement of the orbital contents into the maxillary sinus. (**c**) Prolapse of orbital fat and orbital implant malposition that are clearly seen in the sagittal view

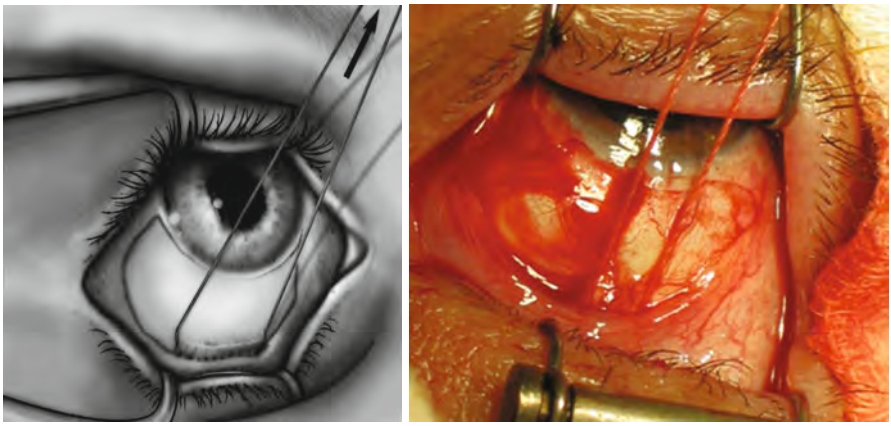

Fig. 3.19 Bridle suture placed on the inferior rectus

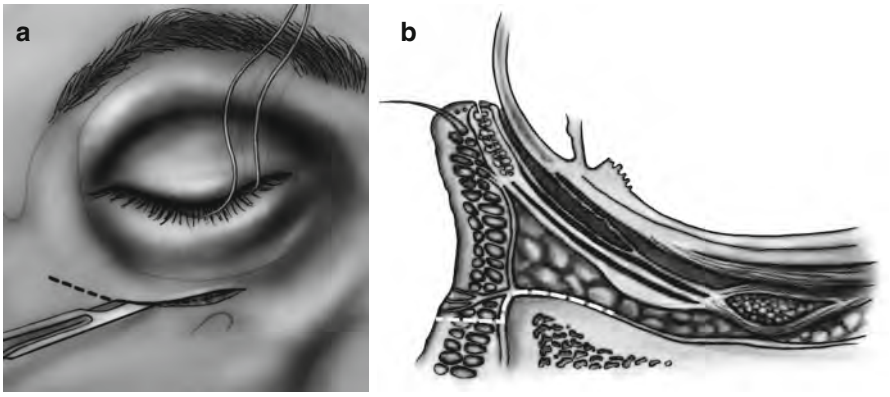

Fig. 3.20 Infraorbital approach to the orbital floor: (**a**) Front view. (**b**) The incision profile (see explanations in text)

An approach to the orbital floor can be performed through a transcutaneous (infraorbital or subtarsal) or subciliary incision with various modifications, as well as through a transconjunctival incision (either with or without cutting the lateral palpebral ligament). Each of these methods has its own advantages and drawbacks [147–152].

The transcutaneous approach along the infraorbital rim (the infraorbital approach) (Fig. 3.20) is the technically simplest one; however, there is a high risk of complications from cicatrix formation. If the incision is displaced toward the temple, persistent lymphostasis may occur the large lymph node basins are transected. If the incision is displaced toward the nose, persistent lacrimation may result because of disruption of the lacrimal pump function [94].

The *subtarsal approach* is recommended for elderly patients having folded skin of the lower eyelid [153]. This approach is a variant of the subciliary approach described below with formation of a skin–muscle flap.

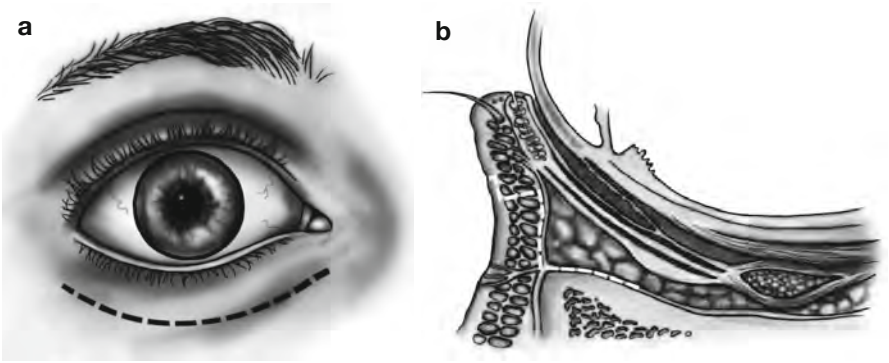

Fig. 3.21 Subtarsal approach to the orbital floor: (**a**) Front view. (**b**) The incision profile (see explanations in text)

After local subcutaneous anesthesia, an incision is made along the inferior edge of the *tarsal plate* on the subtarsal skinfold (Fig. 3.21). If the edema impedes its visualization, an incision is made 5–7 mm below the palpebral edge. The incision is started at a level of the inferior lacrimal punctum and ends 5–7 mm outward from the lateral margin of the orbital fissure. Skin is separated from the m. orbicularis oculi (2–3 mm in the downward direction) followed by its incision and exposure of the anterior surface of tarso-orbital fascia.

The stepwise profile of the approach prevents coarse cicatrix formation; furthermore, innervation of the pretarsal and preseptal portions of the m. orbicularis oculi is not affected. The dissection is continued in the preseptal plane, i.e., along the orbital septum up to the infraorbital rim.

The subtarsal incision is associated with a lower risk of vertical shortening and eversion of the eyelid; however, it still leaves a visible cicatrix and the risk of lymphostasis is higher than that of the subciliary approach [12]. This approach cannot be used in young patients. The subtarsal approach is recommended for inexperienced oculoplastic surgeons.

The *subciliary approach* was proposed by J. Converse in 1944 (citation from [148]). After subcutaneous infiltration with lidocaine supplemented with adrenaline, an incision is made along the skinfold 1.5–2 mm below the ciliary edge and parallel to it[11] starting from the medial corner of the orbital fissure (Fig. 3.22a, b). The skin is separated from the m. orbicularis oculi down to the inferior edge of the tarsal plate. At this level, the fibers of the m. orbicularis oculi are bluntly separated with exposure of the tarso-orbital fascia, which is subsequently transected near the infraorbital rim (Fig. 3.22c). An obvious advantage of the subciliary approach is that it provides sufficient visualization of the inferior and medial orbital walls and an almost indiscernible cicatrix is formed [154].

[11] Infiltration anesthesia is useful even if general anesthesia is employed, as it is useful for hydrodissection and helps control bleeding in the highly vascularized lid.

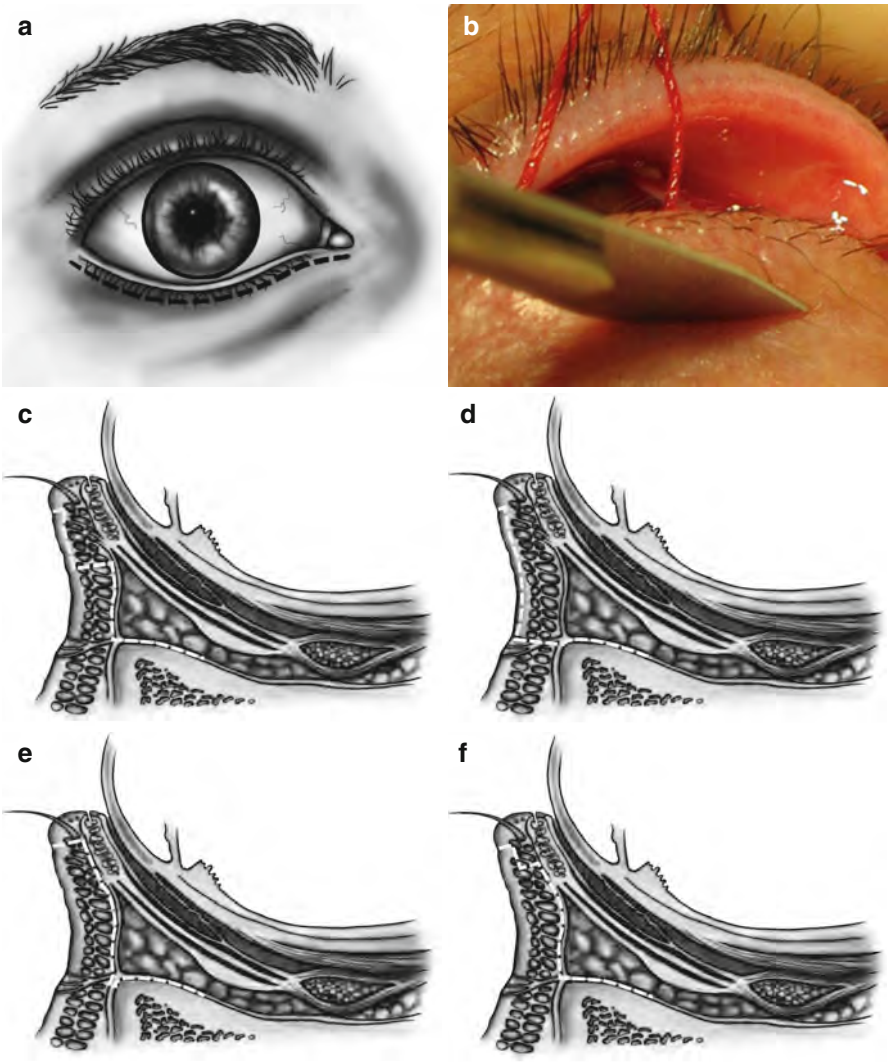

Fig. 3.22 Subciliary approaches to the orbital floor: (**a**, **b**) Front view. (**c**) The classical approach proposed by J. Converse (1944). (**d**) The "skin-only" procedure including formation of an isolated skin flap. (**e**) The "non-stepped skin–muscle flap" procedure. (**f**) Dissection of a "stepped skin–muscle flap"

The "skin-only" modification was proposed by aesthetic plastic surgeons in the late 1960s. A typical incision is made, and a skin flap is separated from the m. orbicularis oculi in the downward direction, down to the level of the infraorbital rim where the fibers of the m. orbicularis oculi, the tarso-orbital fascia, and the periosteum are subsequently separated (Fig. 3.22d). The drawbacks of this approach

include possible skin flap necrosis and development of transient ectropion in up to 40 % of cases.

The *Non-stepped Skin–Muscle Flap Procedure.* Incision of the skin and m. orbicularis oculi 2 mm below the eyelash line is followed by a separation of the eyelid along the surface of the tarsal plate and tarso-orbital fascia up to the infraorbital rim where it is dissected along with periosteum (Fig. 3.22e). In order to prevent shortening of the lower eyelid, it is important that the periosteum is cut on the anterior surface of the infraorbital rim, i.e., several millimeters below the site where the tarso-orbital fascia is attached to the bone [155].

A "stepped skin–muscle flap" procedure has been proposed because a subciliary incision is sometimes complicated by denervation of the pretarsal portion of the m. orbicularis oculi. This may lead to atonic eversion of an eyelid with sclera exposure near the inferior limbus.

An incision is made 2 mm below the eyelash line and is followed by dissection of the skin from the m. orbicularis oculi for 2–3 mm downward and then dissection of the m. orbicularis oculi and exposure of the anterior surface of the tarso-orbital fascia below the tarsal plate. Separation is then performed along the tarso-orbital fascia up to the infraorbital rim. The fascia and periosteum of the orbital floor are incised within the same plane (Fig. 3.22f). As a result, the strip of pretarsal orbicularis muscle continues to maintain the proper position of the lower eyelid.

More recently, others [52, 156, 157] have refined the procedure. Local injection of anesthesia in the subconjunctival and subcutaneous layers of the lower eyelid will result in hydrodissection of the subconjunctival and the precapsulopalpebral space. A 5-mm-long horizontal incision of the lateral canthus and transection of the inferior crus of the lateral ligament are then performed (Fig. 3.23a–d). This procedure mobilizes the lower eyelid and facilitates making an incision along the inferior conjunctival fornix. The lower eyelid is pulled away with a Desmarres lid retractor; a Jaeger lid plate is used to push the eyeball deeper inside the orbit. The palpebral conjunctiva and the lower lid retractor are dissected 3 mm above the conjunctival fold along the entire eyelid to end slightly medially from the projection of the lacrimal point (Fig. 3.23e–g). Thorough hemostasis is performed using diathermy. The periosteum is dissected along the infraorbital rim above the exit of the infraorbital nerve (Fig. 3.23i, j) and followed by dissection of the periosteum from the orbital floor (Fig. 3.23k, l).

The preseptal transconjunctival approach is preferred over the retroseptal approach, since the former approach provides minimal damage to the connective tissue network of the orbit, provides good visualization, and has an insignificant complication rate [12, 158–160].

The main advantage of the transconjunctival approach, in particular when combined with lateral canthotomy, is the absence of cutaneous scars and access to the infraorbital and lateral orbital edges, the lower portion of the medial orbital wall, the upper portion of the anterior wall of the maxillary sinus, the infraorbital nerve, and the medial half of the zygomatic bone [161]. The complication rate is lower than

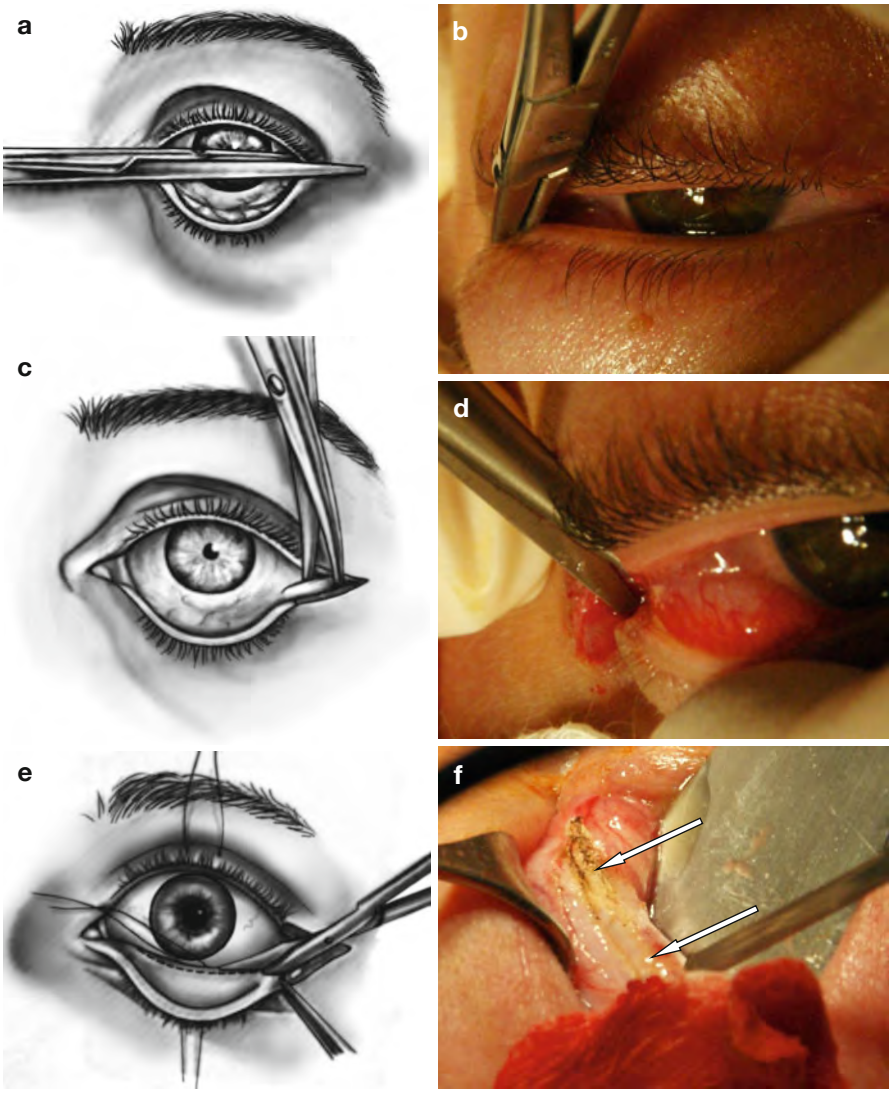

Fig. 3.23 Preseptal transconjunctival approach with transection of the lateral palpebral ligament (the initial stages): (**a**, **b**) Anemization and horizontal incision of the lateral palpebral commissure. (**c**, **d**) Transection of the inferior crus of the lateral palpebral ligament. (**e**, **f**) Dissection of the conjunctiva using scissors (**e**) or electrosurgery (**f**). The lower eyelid is pulled away with Desmarres lid retractors; a Jaeger lid plate is used to protect the eyeball. (**g**) Separation of the lower eyelid retractor (shown with an *arrow*). (**h**) Isolation and transection of the tarso-orbital fascia (shown with an *arrow*). (**i**, **j**) Dissection of the periosteum of the infraorbital rim (shown with *arrows*). (**k**, **l**) Periosteum of the orbital floor

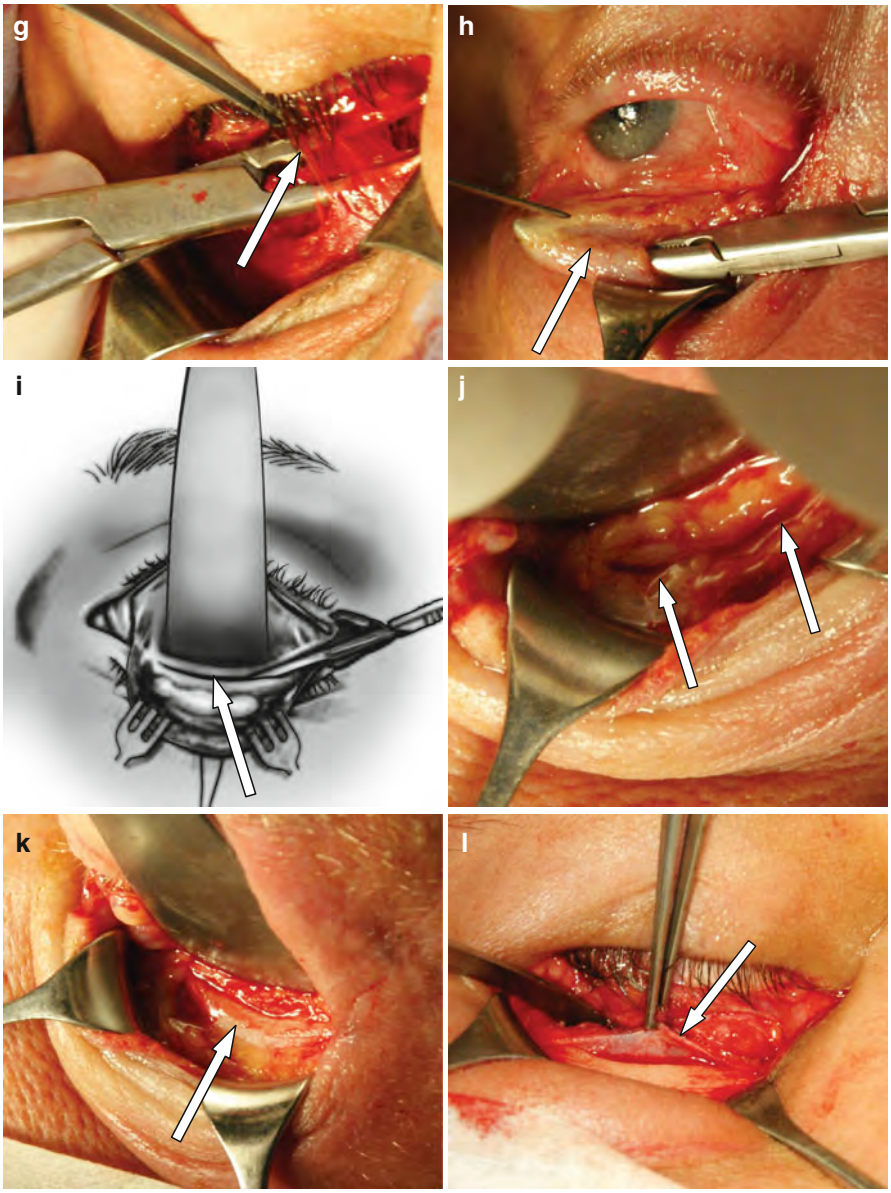

Fig. 3.23 (continued)

that for the subciliary approach [46, 149, 162, 163], particularly in young patients [12]. The drawbacks of this approach include transection of the lower eyelid retractor and persistent chemosis of bulbar conjunctiva[12]. Furthermore, a surgeon needs to perfectly know the lower eyelid anatomy; otherwise, there is a risk of "getting lost" in eyelid layers [156].

Endoscopic Approaches to the Orbital Floor

The main drawback of the transconjunctival and subciliary approaches to the orbital floor is difficulty visualizing the posterior edge of a fracture due to its distance (remoteness) and prolapse of adipose tissue. The elevation of the orbital floor toward the orbital apex by 15° is an additional impeding factor. Transantral or transnasal endoscopic approaches are indispensable in these cases [74, 164–169]. Endoscopy provides good illumination and visualization of the fracture for all surgery participants. It allows one to evaluate the completeness of release of the entrapped orbital tissues and the position of the posterior edge of the implant. This approach also makes it possible to trace the course of the infraorbital nerve to avoid its damage[13] [170–174]. The procedure is indispensable in cases when a fracture extends to the posterior wall of the maxillary sinus because it allows for better securing of the implant and its distal edge on a small bony spur, orbital process of the palatine bone (Fig. 3.24a–c).

Video-assisted endoscopic surgery can be performed even shortly after trauma in patients with persistent palpebral edema which would impede subciliary and transcutaneous approaches [174, 175].

The endoscopic procedures, compared to the transconjunctival approach, in terms of adequate recovery of the initial orbital volume has been shown in cadaver experiments [176, 177] and appreciably numerous clinical studies to be very effective [168, 178–181].

The Transantral Approach

A 4-cm-long incision along the gingivobuccal fold is made to expose the anterior wall of the maxillary sinus. An aperture with the area of 1–1.5 cm^2 is formed (Fig. 3.24d); a 4-mm endoscope is introduced into the sinus through the aperture to evaluate fracture length and configuration. While holding the endoscope with his/her left hand and using his/her right hand to hold the instruments, the surgeon carefully removes bony structures entrapping the orbital tissues until the negative traction test is obtained. A rolled flexible implant is placed through the surgical aperture and the orbital floor defect. After being placed in the orbit, the plate is deployed, rotated, and placed over the anterior, medial, and lateral margins of the fracture. If the fracture margins are unstable, the implant is fixed with a screw on the side of the sinus; the orbital floor is supported with an antral balloon, such as a Foley catheter, for 10–14 days [123, 164, 175, 182–184].

[12] Some authors believe that lymphostasis is caused by prolonged compression of orbital tissues during surgery. Hence, it is reasonable to reduce pressure exerted on soft tissues every 5 min to avoid this complication.

[13] Nevertheless, infraorbital nerve hypesthesia is among the main complications of endoscopic osteoplasty of the orbital floor.

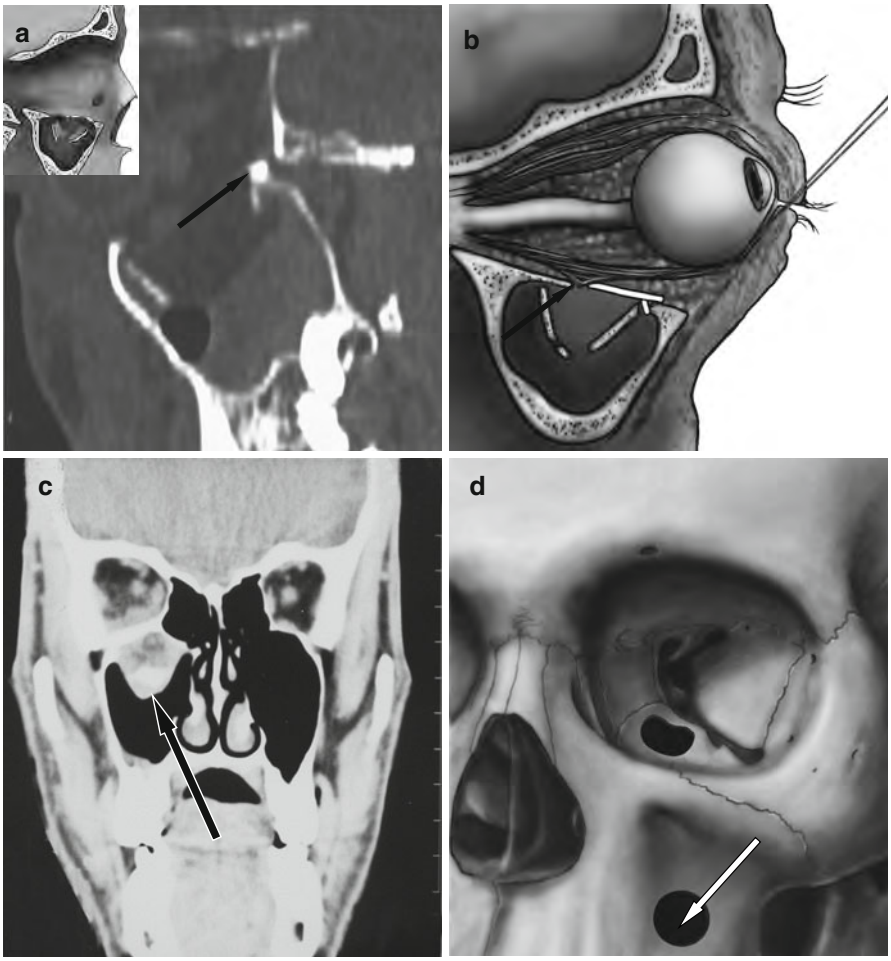

Fig. 3.24 Indications for endoscopic approaches: (**a**) Extensive posterior fracture with its distal margin confined to the small orbital process of the palatine bone. A CT scan showing the typical length of the fracture is shown for the sake of comparison. (**b**, **c**) A typical complication accompanying the attempt to place the distal margin of the implant on the posterior margin of the fracture under insufficient visibility conditions: entrapment of the muscle that used to be released (**b**) or the orbital fat (**c**) by the posterior margin of the implant. (**d**) Transantral approach (an *arrow* shows the foramen in the anterior wall of the maxillary sinus for placing an endoscope)

The transnasal approach is performed through the extended maxillary sinus ostium while adhering to the same strategy as transantral approach.

It is reasonable to use a combination of subciliary or transconjunctival incisions to assist endonasal or transantral endoscopic approaches to manage extensive posterior fractures of the orbital floor over 4 cm^2 in size and to correct long-term enophthalmos after trauma [5, 123, 163, 173, 184–189]. The transpalpebral approach is used to place an implant, while the endoscopic approach is used to visualize the rear margin of the fracture [171].

Although developed rather recently, the endoscopic methods are being continuously improved and are now used as alternative approaches to the fractured area as they provide good visualization and complete anatomic recovery of the orbital floor and eliminate improper position of the lower eyelid in postoperative period [20, 74, 165, 169, 190].

However, endoscopic methods require specific equipment and skills in video-assisted endoscopic surgery; they should be used only by experienced surgeons who know the orbital anatomy well and who are proficient in the conventional methods of orbital reconstructive surgery [172, 191, 192]. The share of endoscopic interventions in a level 1 American regional trauma center is less than 20 % and is confined to managing fractures of the orbital floor, the anterior wall of the frontal sinus, and the zygomatic arch [193]. Based on the survey of 400 American maxillofacial surgeons, Barone and Gigantelli [194] found that only 21.3 % of the respondents use endoscopic methods to manage facial fractures. These were mostly experienced surgeons engaged in private practice. The lack of access to specialized instruments was cited as the main limiting factor.

The two main disadvantages of the endoscopic method are the need for providing temporary antral support to bone fragments and the need for removing a balloon 2 weeks later which is associated with the risk of recurrent prolapse of the orbital floor. The alternative of maxillary sinus tamponade with a gauze sponge is a less suitable method because it is often complicated by orbital cellulitis, hematoma, and persistent diplopia in the postoperative period.

3.3.5 Subsequent Surgery Steps

3.3.5.1 The Release of the Entrapped Tissues and Closing the Bone Defect

Periosteum of the orbital floor is separated along the entire depth of the fracture (Fig. 3.25a). The prolapsed soft tissues are returned to the orbit with a spatula placed in the bone defect zone (Fig. 3.25b, c). When performing this step, it is extremely important to identify the infraorbital nerve as promptly as possible (Fig. 3.25d) to avoid damaging it [195]. Furthermore, it is important to avoid bringing the maxillary sinus mucous membrane into the orbit as it may cause cyst development around the implant. Finally, one needs to avoid excessive pressure exerted on the eye and the optic nerve.

The completeness of releasing entrapped tissues is controlled using the traction test (Fig. 3.25e).

The next surgical decision is the choice of an implant[14] that would overlap the bone defect by 2–3 mm in all directions (Fig. 3.25f). Plates with minimal (0.5–1 mm) thickness are used in patients without vertical dystopia [196]. If a patient has hypoglobus, the thickness of the implant is equal to the degree of eyeball depression.

[14] Numerous materials are used to close the defect (a separate subchapter is devoted to description thereof) [119].

The foil packaging of Vicryl suture can be employed to determine the fracture size and contour. The foil sheet is placed into the orbit and pressed against the fractured area. The indent of the bone defect is obtained [93]. After the excess foil around the indent is cut off with scissors, the resulting template is placed on the

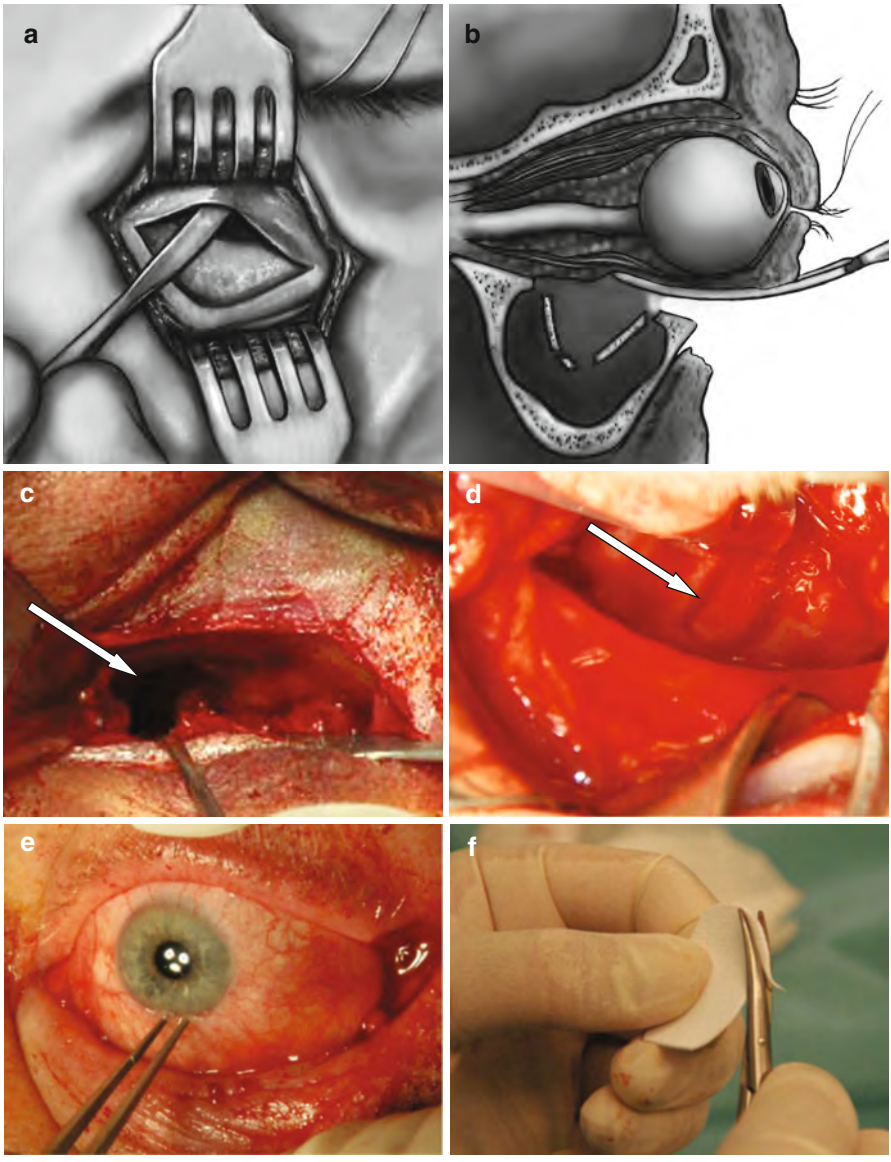

Fig. 3.25 The subsequent steps of surgery orbital floor reconstruction: (**a**–**c**) Separation of periosteum along the entire fracture depth (shown with an *arrow*). (**d**) The infraorbital nerve (shown with an *arrow*). (**e**) Vertical traction test. (**f**) Forming an implant ("Ecoflon" e-PTFE plate used as an example). (**g**, **h**) A straight raspatory is used as a guide to place the implant on the posterior margin of the fracture. (**i**) The plate is fixed with Beyer incisure (shown with an *arrow*). (**j**) Closing the periosteum. (**k**) Continuous suture of the conjunctiva. (**l**) Suture of the lateral canthus

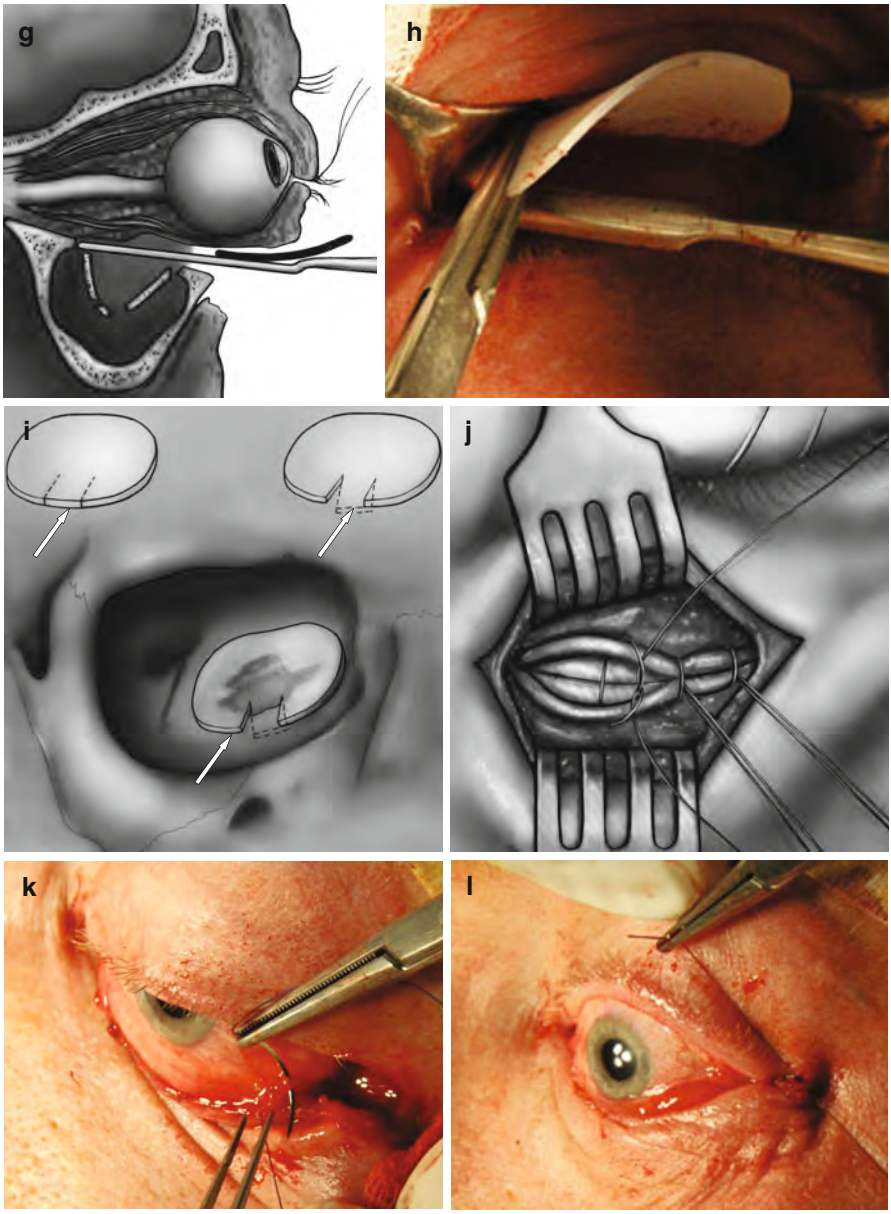

Fig. 3.25 (continued)

plate and outlined. Then the plate is used to form an implant. Sometimes it is reasonable to make the implant U shaped by cutting a fragment off its rear edge to prevent infraorbital nerve compression [195].

When closing extensive fractures, one should bear in mind that the rear portions of the orbital floor are angled upward. It is reasonable to use a simple procedure to prevent the rear edge of the implant placed in the orbit from resting in the maxillary sinus. A straight raspatory elevator is placed in the sinus until it reaches the posterior wall of the sinus and is subsequently moved upward until it reaches a bony spur (Fig. 3.25g, h). The raspatory acts as a guide helping the surgeon to achieve proper position of the rear edge of the plate [12]. A repeated traction test is conducted after the orbital implant is placed. If necessary, the plate is fixed on the anterior margin of the fracture with Beyer incisures (Fig. 3.25i).

The final stage of intervention during the subciliary approach includes thorough layered closure of the periosteum (Fig. 3.25j), tarso-orbital fascia, orbicularis oculi muscle, and skin, which prevents implant migration. To prevent postoperative lower eyelid retraction, the length of the tarso-orbital fascia needs to remain unchanged during closure.

Closure of the transconjunctival approach does not require mandatory suturing of the conjunctiva (Fig. 3.25k); this fact does not increase the risk of infectious complications and implant migration or rejection [149, 160]. However, the reconstruction of the lateral ligament and the canthus should be performed very accurately (Fig. 3.25l).

Postoperative treatment includes short-term bed rest (5–6 h), a head-elevated position, a cold pack applied to the orbital zone, and if indicated, analgesic and antiemetic drugs. There is no need in using a compressive bandage; however, if a bandage was used, it must be removed the day after surgery or even earlier in case the patient complains of undue pain. Traction sutures of the lower eyelid margin can be left for several days to prevent its cicatricial contraction. The duration of inpatient postoperative treatment usually depends on the patient's overall condition and typically is 4–10 days [197].

After discharge, the patients should avoid blowing their nose for at least 2 weeks [198]. Physical activity should be eliminated for a longer period, in particular for people engaged in physically demanding jobs. The physical activity restrictions for patients with blow-out fractures usually lasts for 6 weeks based on the general concept of wound healing and the rate of osteogenesis in patients with orbital fractures [199]. However, Gilliland et al. [200] used an experimental model to find that that as soon as 3 weeks after osteoplasty, the orbital floor which was covered with an implant had the same mechanical strength as that of the intact orbital floor.

***

The question whether antibiotic treatment is required in patients with blow-out fractures of the orbital floor needs special consideration. There have not been any standardized regimens of antibiotics for this category of patients that have been described in the literature [127, 161, 201].

There is only one reference that showed the use of broad-spectrum antibiotics such as co-amoxiclav or clindamycin to be effective in controlling postoperative infections [202]. Since there is no generally accepted opinion regarding antibiotic

use for this problem, Westfall and Shore [161] proposed to use the general surgery standards for prescribing antibiotics depending on wound type:

Type I: clean wound; risk of bacterial infection is less than 1.5 %. The effectiveness and need for preventive antibiotic therapy have not been proved.
Type II: clean-contaminated wound contacting with the upper respiratory tract without massive bacterial contamination. The risk of bacterial complications is 7.7 %; preventive antibiotic therapy is recommended.
Type III: contaminated wound connected with the gastrointestinal tract. The risk of complications is as high as 15.2 %; preventive antibiotic therapy is recommended.
Type IV: infected wound (an old injury, underlying infection, presence of purulent discharge, devitalized tissues or foreign bodies). The risk of wound infection is 40 %; antibiotic therapy is recommended both as a preventive and therapeutic measure.

The presence of a graft or a foreign body in the wound, which is the case if the orbital floor is reconstructed with a graft, significantly increases the risk of infection and is an indication for preventive antibiotic therapy.

The classification of the blow-out fracture wound depends of the affected anatomy. Paranasal sinuses are considered to be sterile. Hence, a blow-out fracture communicating with an intact sinus can be regarded as a clean wound (type I). If a fracture developed in a patient with sinusitis, the wound would then be considered as infected (type IV). The nasopharynx is not considered to be sterile; therefore, a fracture communicating with the nasopharynx should be classified as a clean-contaminated wound (type II). Thus, the *blow-out fracture* can be classified as any of the four types of surgical wounds (except for type III). *Antibacterial treatment is often required immediately after trauma and is mandatory after a surgery using an implant.*

Antibiotic therapy should, ideally, be started within the first 3 h after an injury; however, this is often infeasible. Intravenous intraoperative antibiotic therapy started at the time of anesthetic induction very effectively prevents purulent complications [203]. If surgery lasts more than 4 h, a second dose of the drug is given.

The choice of antibiotic agent, duration, and route of administration are extremely important. The absence of past medical history of sinusitis and contact with the oropharynx allows one to use an intravenous infusion of a first-generation cephalosporin (cefazolin).

Third-generation cephalosporins are recommended in all other cases. If there is a risk of saliva contacting the fractured area (i.e., for zygomatic orbital fractures), the recommended drugs include *aminoglycosides*, amoxicillin, or clindamycin. 2 g of amoxicillin or 600 mg of clindamycin is to be given intravenously during the surgery. 1 g of amoxicillin or (if a patient is allergic to penicillin) 600 mg of clindamycin is continued intravenously for the first 2 days after surgery followed by i.v. infusion of 600 and 300 mg of the drug three times per day, respectively, for 5 days [202].

It is reasonable to include glucocorticoids in the treatment of orbital fractures, since these drugs accelerate regression of orbital edema and the diplopia caused by

it without slowing down osteogenesis [93, 203]. Also, posttraumatic enophthalmos can be visualized much earlier and help with the decision whether further surgery is indicated [204].

Injection of 250 mg of methylprednisolone (20-mg dexamethasone) prior to intervention followed by i.v. infusion of the drug three times per day in the same dose (or the dose reduced twice for dexamethasone) every 6–8 h is recommended [12, 205, 206].

***

Final assessment of surgical outcomes in terms of such criteria as ocular motility and eyeball position in the orbit and presence or absence of diplopia is performed at least 6 months after the repair [75, 76]. In order to avoid additional radiation exposure of a patient, CT scanning should not be performed if an obvious clinical improvement is present.

Proper position of the eyeball in the orbit and the absence of diplopia are considered to be the fundamental indicators of long-term success.

3.3.6 Characteristics of Different Graft Materials

3.3.6.1 Autografts

A number of autograft materials can be used in orbital wall reconstruction (Fig. 3.26) [207, 208]. Full-thickness or split-thickness grafts of the membranous bone of the cranial vault are used most frequently [209, 210], since they are less susceptible to lysis and better retain their initial shape and volume [211, 212]. However, these grafts fail to take the shape of the orbit and therefore are often displaced and need to be fixed to the infraorbital margin [213].

The widely used graft structures include the internal plate of the anterior iliac crest bone [213–216], a fragment of the bony portion of the rib [217], or a fragment of patient's mandible [218, 219]. In order to achieve the required congruence with the orbital floor profile, a 2–3-mm-thick fragment of the external layer of compact osseous tissue is harvested from the chin region, behind the homonymous foramen, near the mandibular arch [219], or the mandibular symphysis [220].

The authors believe that the advantages of this method for closing the orbital floor bony defects are as follows: simplicity of harvesting graft material, simplicity of subsequent graft shaping, appropriate size and curvature of the bone plate, the absence of functional disorders when breathing or walking that often occur when the bony portion of the rib or iliac bone are harvested, and the absence of scars or other cosmetic defects at the graft harvest site.

Many different graft sites have been proposed when only a small thin flexible graft is needed. Anderson and Poole [69] used the patient's periosteal flap; Constantian [221] and Castellani et al. [222] used the conchal cartilage graft (Fig. 3.26c); Johnson and Raftopoulos [223] and Ozyazgan et al. [224] used the cartilaginous portion of a rib (Fig. 3.26d); and M. Kraus et al. [132, 225] and Talesh et al. [226] used the nasal septal cartilage.

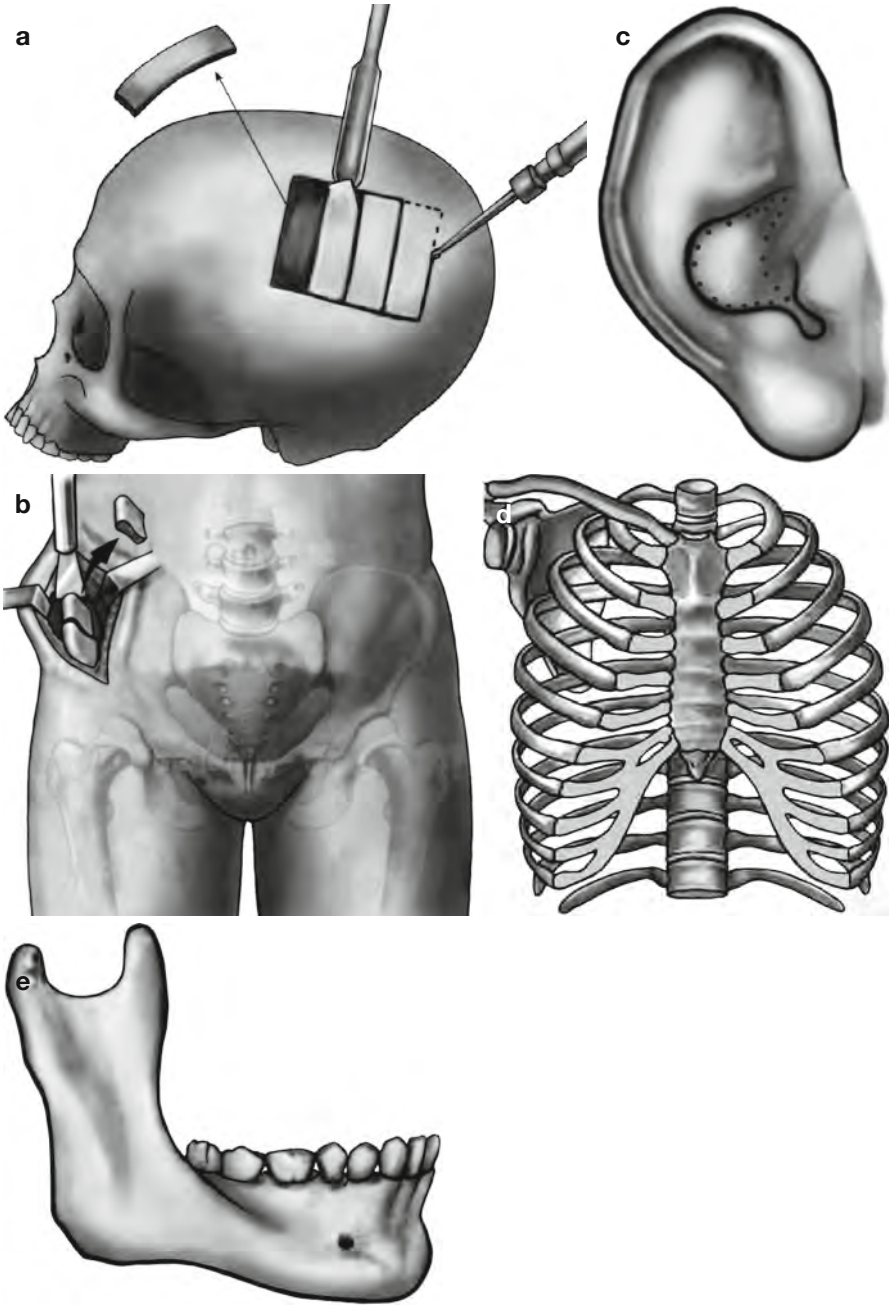

Fig. 3.26 Autografts used for closing orbital wall defects: (**a**) Cranial vault bones. (**b**) Internal plate of the iliac anterior crest bone. (**c**) Conchal cartilage (tissue harvesting site is shown with *dashed line*). (**d**) Bony portion of a rib (the cartilaginous portion of the ribs is hatched). (**e**) Mandible

A fragment of the anterior wall of the ipsi- or contralateral maxillary sinus can also be used to close small (up to 2 cm in size) orbital floor defects [185, 212, 227–229]; it is implanted into the orbit via the transantral approach using an endoscope [183]. The advantages of the procedure proposed by Kaye [230] include graft harvesting in close proximity to the graft site and the possibility of single-step maxillary sinus cleansing and thorough transantral repositioning of bone fragments in patients with extensive fractures. Other advantages include the absence of cutaneous scars and no risk of perforating the pleura and the dura mater that may occur when harvesting a rib or a cranial vault bone.

A literature review revealed that autografts are still used rather commonly, in particular by neurosurgeons[15] [207, 208, 232]. An obvious advantage of bone autografts is that they stimulate osteoconduction, osteoinduction, osteogenesis, and revascularization [213, 233]. Furthermore, autologous tissues are favorably characterized by biocompatibility and the minimal risk of graft infection, migration, or rejection [234]. Hence, this type of graft is primarily used to treat extensive orbital floor fractures when there is a risk of infection at the surgical site [211, 235, 236].

Significant drawbacks of autografting include increased surgical time, additional surgical trauma, graft harvesting complications[16], and lysis of one-third of the transplanted autologous tissue resulting in long-term development of enophthalmos, and difficulty associated with forming small grafts [211, 213, 238, 239]. The complexity of graft shaping makes correction of prolapse of the posterior retrobulbar portions of the orbit difficult, while the anterior portions of the reconstructed orbit sometimes turn out to be noticeably smaller than those in the contralateral healthy orbit [240]. As a result, the autologous bone graft does not always adequately substitute for the orbital volume that has increased after the fracture, and therefore does not lead to a high-precision anatomical reconstruction.

3.3.6.2 Allografts

It is more reasonable to use donor tissues, decalcified bone [69, 93, 241], and cartilage [242]. These materials are characterized by good tolerability and simplicity of shaping. Decalcified bone stimulates chemotaxis in the fracture area and transformation of mesenchymal cells to chondroblasts followed by ossification [93, 243].

The cartilage can be located either sub- or supraperiosteally in the orbital adipose tissue fat. A serious drawback of cartilaginous grafts having no epichondrium[17] is that they undergo gradual resorption within 1–1.5 years. This reabsorption has been confirmed by CT data. Hence, when using cartilaginous tissue, one needs to achieve intraoperative overcorrection of the enophthalmos by

[15] Thus, autologous bone grafts remain the main material used to close orbital floor defects in Australia and New Zealand [231].

[16] The rate of complications accompanying autograft bone harvesting (rupture of the dura mater, pneumothorax, hematoma, intercostal nerve injury, etc.) is 5–9 % [237].

[17] Similar drawbacks are typical of allografts harvested from plantar derma, cranial vault brephobone, and subcutaneous adipose tissue of fetal planta.

1.5–3 mm. However, this may be associated with the risk of developing hypertopia of the eyeball.

Closing bone defects using a composite consisting of lyophilized cartilage and heterogeneous (bovine) bone morphogenetic protein is more reasonable alternative to solving the problem of cartilage graft resorption. Addition of protein inducing osteogenesis significantly accelerates the slow process of calcification/ossification of the donor cartilage tissue, and it overcomes the process of cartilage tissue resorption [244]. Osteogenetic activity of recombinant bone morphogenetic protein and fibroblast growth factor has been confirmed experimentally [245, 246].

The dura mater [209, 247–249] and thigh fascia lata [250, 251] are used for orbital floor reconstruction in patients with small fractures up to 2 cm^2; these grafts can be easily shaped and implanted into the orbit. However, the use of these materials is limited, since balloon support on the side of the maxillary sinus is required when using these tissues to close a larger orbital floor defect.

The use of decalcified bone, cartilage, and the dura mater as donor tissue has declined significantly primarily due to the increasing risk of transmitting causative agents of numerous diseases with the graft. Thus, although the dura mater is one of the main osteoplastic materials in Europe, it has not been used in the United States because of the risk of contaminating a recipient with prions, the causative agents of Creutzfeldt–Jakob disease [209].

The cost of using allografts is also considerable because of the necessity for the establishment of tissue banks to conduct bacteriological and virological testing of donor material following of the rules for its preservation and storage [241]. In this regard, synthetic materials have considerable merit over donor tissues.

3.3.6.3 Exgrafts

Nonbiological materials such as resorbable and nonresorbable solid and porous polymers as well as 0.3–1.0-mm-thick titanium mesh constructs are most commonly used for surgical management of orbital floor fractures [7, 46, 87, 232, 252–254]. The choice of a material for closing bone defects primarily depends on the area of defect.

Resorbable polymer grafts are the main material to close small bone defects up to 2×2 cm in size without evident enophthalmos and hypoglobus [231, 255, 256]. A linear-type trapdoor fracture that can occur in children is a typical example of such an injury. Films “Gelfilm” [75, 257–259], “Seprafilm”[18] [260], polydioxanone[19] [118, 158, 209, 238, 255, 261], and Vicryl[20] [262] are used in these cases. Review of published data shows that the two latter materials are used most commonly.

Polydioxanone (PDS) has recently been widely used in clinical practice [231, 263]. An implant made of 0.15-mm-thick perforated polydioxanone foil less than 20 mm in diameter is not inferior to a 0.3-mm-thick titanium mesh in terms of its mechanical strength [264]. Hence, PDS is used to close bone defects up to 2 cm^2 in size [265].

The attempts to use 0.25- and 0.5-mm-thick plates to manage larger fractures were unsuccessful because intense PDS resorption started after 2–3 months and the

[18] The hybrid of carboxymethylcellulose and sodium hyaluronate.

[19] Poly(p-dioxanone). The empirical formula of the polymer is $C_4H_6O_3$.

[20] The copolymer of the derivatives of glycolic and lactic acids, polyglactin 910.

implant lost its mechanical strength. The newly formed connective and osseous tissues that replaced the biodestructed PDS [265] fail to perform the tectonic function even in medium-length fractures because they bulge into the maxillary sinus and cause late enophthalmos [266]. As a result, if these agents were used to repair a large fracture, one needs to overcorrect and that will lead to inevitable diplopia in the early postoperative period [265].

Other complications of using PDS are the development of diplopia and exophthalmos which seems to be caused by pronounced response of tissue to the material [255], plate displacement [267], and severe cicatrization in the implantation zone. MRI can often show the formation of liquid- and gas-containing cavities [268].

Closure of a small orbital floor defect up to 2 cm^2 with an ETHISORB Dura Patch[21] is associated with a much smaller rate of diplopia and enophthalmos [255, 261].

The serially produced 4-mm-thick *Vicryl plate* consists of 24 layers; thus, it can be separated into thinner implants that can be easily shaped and do not need to be fixed in the orbit. Vicryl is characterized by unique physical/mechanical properties that prevent compression of the optic nerve, lacrimal sac, or the extraocular muscles. The material is well tolerated by orbital tissues, bones, and the mucous membrane of paranasal sinuses and does not impede osteogenesis [269]. However, this material can cause an inflammatory response of the lower eyelid tissues in 14 % of cases, which may lead to cicatrization of the lower eyelid [270]. Furthermore, polyglactin should not be used to close large orbital floor defects and to perform contour reconstruction of the orbit because it starts to lose its original strength as soon as 1 week after implantation. Only traces are observable 1 month later and 4 month after surgery Vicryl is completely resorbed.

Caution is needed in choosing a mesh made of *polyglycolic acid–polylactic acid copolymer* (*LactoSorb*)[22] to close extensive orbital fractures [271], since the inevitable hydrolytic destruction of the implant causes enophthalmos. In addition, the mandatory rigid fixation of the plate to the infraorbital margin is associated with the risk of developing local inflammatory response that forces one to remove the implant at a later date [272]. The next generations of these implants (Resorb X(®), SonicWeld Rx-System®) and the *composite consisting of polylactide and hydroxyapatite* may be more applicable.

Lactic acid homopolymers with resorption duration ranging from 1 to 5 years are promising osteoplastic materials [273–277]. Despite their small thickness, polylactide implants with added trimethylene carbonate exhibit sufficient mechanical strength, can be easily shaped when heated to 55 °C to duplicate the orbital profile, and are also biocompatible. The resorbable properties of the materials do not require reoperation to remove them [271]. The above listed properties of polylactide make

[21] ETHISORB Dura Patch is a synthetic resorbable implant intended for closing dura mater defects. ETHISORB consists of a porous Vicryl and poly-p-dioxanone (PDS) layer that provides connective tissue ingrowth; the solid PDS matrix is used to seal the dura mater defect. The implant is almost completely resorbed within 90 days.

[22] The material was introduced into clinical practice in 1996. LactoSorb® trademark includes plates, meshes, and screws that are completely resorbed within a year after implantation. The initial mechanical strength of the material is not inferior to that of titanium mesh; 2 months later, LactoSorb® loses one-third of its original strength. However, the manufacturer believes that this process is compensated for by osteogenesis in the surgical area.

favorable comparison with the nonresorbable implants HAp and coral. The latter implants, HAp and coral, have a disadvantage because they need to have an increased thickness due to their fragility. They also have a rough surface, and the implant shape and curvature are determined by the manufacturer and cannot be changed. Finally, there is a need for special equipment for titanium constructs as well.

Experiments with using polylactide to close extensive bone defects showed that it is biocompatible with insignificant inflammation and capsule formation around the implant and osteogenesis in the bone defect area after 9 months. However, the implant lost its initial mechanical strength after 16 weeks, and by the end of the experiment, 40 % of plates were completely resorbed. The rest of the implants were severely deformed because of encapsulation and osteogenesis occurring in the adjacent areas [278]. Threefold thickening of the material 1–1.5 years after it was placed in the orbital tissues is another disadvantage [279]. Furthermore, because polylactide is radiologically transparent, CT monitoring of the implant position in the orbital floor forces one to use more expensive MRI for monitoring [274, 275, 279, 280]. There is an additional drawback in that the polylactide implants are very expensive.

1.5-mm-thick screws intended for fixing serially manufactured Inion polylactide plates turned out to be extremely fragile, and the 2.5-mm-thick ones are too thick (Fig. 3.27). In addition, their biodestruction by-products cause significant tissue response in the implantation zone which limits the number of screws that can be used during a surgery.

Thus, because polylactide has so many negative attributes, and there is no comprehensive data that shows it is better than titanium implants, it will not be used as the main material for closing extensive orbital floor defects in the near future [281]. However, the use of polylactide and polyglycolic acid meshes, plates, and screws may show promise for orthognathic surgery and pediatric cases. The slow hydrolytic destruction of the plate which occurs over several months allows for unimpeded growth of facial and cranial bones, whereas metal constructs would decelerate this process and cause facial asymmetry [1, 277, 282, 283].

Solid nonresorbable polymers have been used for over 40 years. They include *polymethyl methacrylate* (PMMA) [284], *polyethylene* (PE) [94], and *Supramid* [75, 285–287].

Solid Teflon has been mentioned as a material that can be used for orbital floor reconstruction [211, 235, 288]; Hardin [289] has performed 500 surgeries using this polymer.

Silicone implants are still used rather commonly [214, 290, 291]. According to Courtney et al. [127], polydimethylsiloxane is used in 66 % of orbital floor reconstruction surgeries performed in Great Britain.

Tercan's proposition [292] to use steel wire to reinforce a 0.6-mm-thick silicone plate makes it suitable for closing extensive fractures of the orbital floor and facilitates its fixation to the infraorbital margin. Furthermore, the mesh implant is visible on CT scans.

The disadvantages of using silicone, which has a nonporous, solid structure, include the risk of implant migration under the lower eyelid skin, to the nasal cavity or into the maxillary sinus [293, 294]. Another serious complication of using

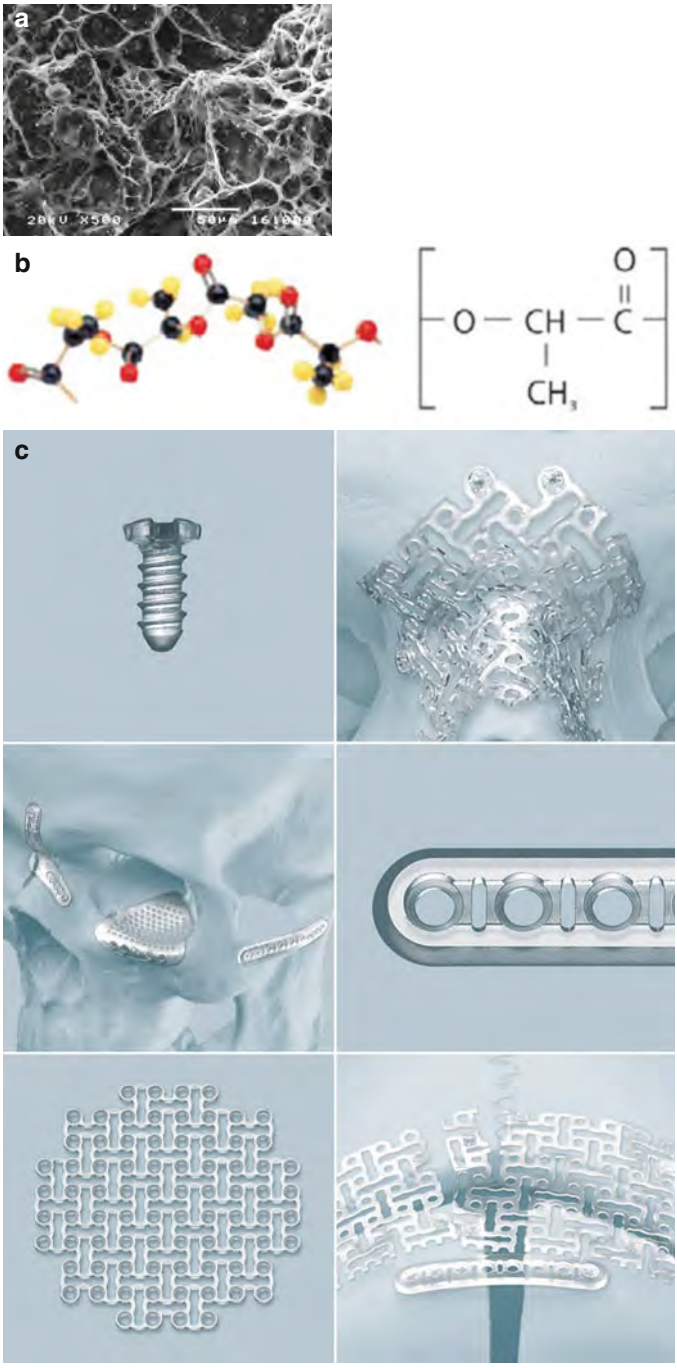

Fig. 3.27 Polylactide implants (using products manufactured by Swiss company "Synthes" as an example): (**a**, **b**) The amorphous ultrastructure of the copolymer based on D-lactide and DL-lactide monomers. The material undergoes hydrolytic destruction whose rate depends on copolymer composition. (**c**) Absorbable miniplates and screws

silicone is development of chronic perifocal inflammation impeding osteogenesis in the bone defect area [200, 269] and formation of a pseudocapsule lined with stratified squamous epithelium of the conjunctiva around the silicon. Implant encapsulation may result in formation of a cutaneous or sino-orbital fistula, persistent diplopia, vertical and axial dystopia, or cellulitis [295]. When staying in the orbital floor for a long time, silicone causes bone tissue resorption which may lead to maxillary sinus involvement in the pathological process in up to 70 % of patients.

Twenty-year follow-up of large patient cohorts has shown that silicone implants had to be removed because of complications in 13–14 % of cases [296]. Explantation was performed on average 4.3 years after surgery, although complications can emerge 10, 15, and even 25 years after osteoplasty [293, 297, 298]. Because of the high rate of late complications, many authors prefer using autologous conchal cartilage rather than silicone to close small fractures up to 1.5 cm^2 and using autologous bone grafts to substitute in larger defects.

Titanium is another common material for orbital floor reconstruction [240, 299]. The biocompatibility of titanium is attributed to the fact that its atomic number (22) is close to that of calcium (20), the main mineral component of bone [300]. Furthermore, titanium is characterized by the absence of evoked potentials on the surface, which makes it "invisible" for immunocompetent cells and eliminates the risk of metallosis. Unlike steel, titanium is capable of osseointegration; this fact explains the low risk of infection even when titanium is implanted in the oral cavity. Due to rigid fixation to the adjacent bone structures, there is zero probability of migration and rejection of titanium constructs. Furthermore, they ensure more accurate reconstruction of the orbital wall contour compared to bone grafts [240]. However, titanium constructs are believed to impede rapid callus formation, since the rigidly fixed fragments do not undergo compression required for it [277].

The relative simplicity of graft shaping, hypoallergenicity, corrosion resistance, nontoxicity, and non-carcinogenicity have made titanium an osteoplastic material that has been successfully used for the past 40 years [239, 301]. Coating the surface of titanium implants with mesenchymal stem cells which accelerates biointegration seems to be rather promising.

Titanium miniplates (Fig. 3.28a) proposed by Champy are poorly applicable for managing orbital fractures because these implants are difficult to be properly shaped and their linear size is inconsistent with the thin orbital walls. Furthermore, miniplates placed on the orbital margins increase sensitivity to cold, are easily palpable, and can deform the periorbital contour in patients with thin skin, which is the reason for explantation in 5–6 % of patients[23] [277, 303–306].

The drawbacks of miniplates have stimulated design of *microplates* as thin as 0.4–0.6 mm. They cannot be palpated under the skin, do not deform the orbital contours, and securely fix small fragments. Miniplates however cannot immobilize these small fragments due to screw diameter of 1.2–1.3 mm and the distance between the holes of 4 mm. Unfortunately, when implanted onto the infraorbital margin, microplates cannot resist cicatricial contraction of soft tissues in the zygomatic area [307].

[23] According to the data reported by Nagase et al. [302], miniplates are explanted in one-third of all patients operated on. Another one-third of plates have to be removed during reoperations.

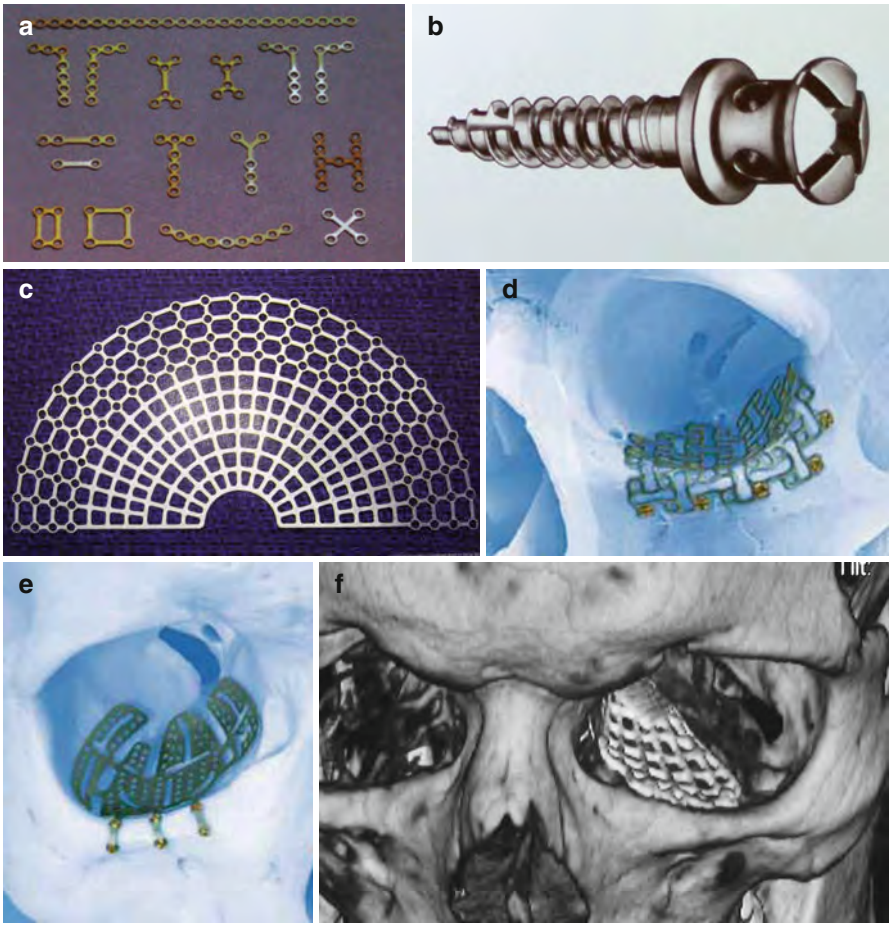

Fig. 3.28 Titanium implants for orbital reconstruction: (**a**) Miniplates. (**b**) Modern modifications of screws for fixing mini- and microplates whose use does not require drilling. (**c**, **d**) Titanium plate (**c**) and mesh (**d**) for closing extensive bone defects. (**e**) Titanium orbital implant manufactured by Synthes company (Switzerland). Due to its small thickness (0.2–0.4 mm) and numerous preformed cuts, the plate can be easily shaped. Three bulges rigidly attach the implant to the infraorbital margin. (**f**) A 3D CT image of the plate

Because it is extremely difficult to provide rigid fixation of laminar grafts for fractures of 2–4 orbital walls (Fig. 3.28c–g), these are the main indication for using *titanium mesh*. In these cases, titanium acts as a platform to host the grafts [308]. A significant drawback of the mesh is that it is very difficult to implant it because of sharp edges that hook soft tissues (Fig. 3.28e). Mesh explantation is also a challenging procedure as the mesh becomes interwoven with cicatricial tissue [12].

The attempts to implement *vitallium* (the cobalt–chromium–molybdenum alloy) in clinical practice failed as this material has no benefits compared to titanium [309]. *Tantalum* is not used, as its strength is lower than that of titanium.

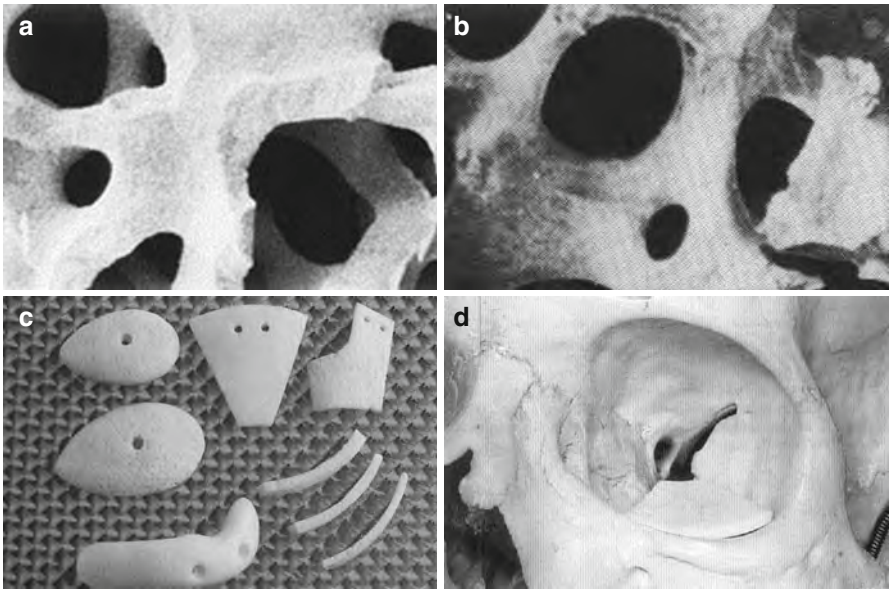

Fig. 3.29 Implants made of coral-derived hydroxyapatite: (**a**) The labyrinth-arch network of interconnected pores 150–500 μm in diameter, which resembles the haversian system (**b**) of human compact bone and provides rapid tissue colonization of hydrophilic coral. (**c**, **d**) Biocoral coral-derived osteoplastic implants (manufactured by Inoteb)

Silicon nitride has shown biocompatibility and good physical/mechanical properties in experimental studies. As opposed to titanium, it does not generate artifacts during radiological examination and can be attached to bones lined with mucous membrane. Carbon implants are currently undergoing preclinical trials.

Thus, nonresorbable and resorbable nonbiological implants for orbital floor reconstruction are extensively used by surgeons due to their biocompatibility, chemical stability, and commercial availability. Complications observed in clinical use such as implant migration, rejection, recurrent hemorrhage into the subcapsular space, and infection of the material occur because the newly formed connective tissue does not grow into this type of implants [310]. The risk of purulent complications when using solid implants is especially high in patients with traumatic anastomosis with the maxillary sinus [272]. Hence, porous synthetic materials have recently been becoming more common [207, 208].

Salyer and Hall [311], Mercier et al. [312], and Gas et al. [238] have successfully used implants made of aragonite. It is the skeleton of marine reef-building coral belonging to the genus *Madrepora* which has been subjected to hydrothermal treatment according to the procedure proposed by Roy and Linnehan [313]. The rigidity of the resulting *hydroxyapatite* (*HAp*) makes it possible to close even large orbital floor defects (Fig. 3.29). After fragment reposition, hydroxyapatite blocks can also be implanted in the maxillary sinus where they will support the reconstructed orbital floor [314].

Secure fixation of the coral-derived HAp to the underlying bone is observed as early as 3 months after implantation. Tissue colonization ends 4 months after osteoplasty; however, the newly formed osseous and connective tissues occupy less than 20–30 % of the porous space volume of HAp [315]. As a result, an implant staying in the tissues for over a year is partially resorbed via hydrolytic destruction [315–319]. This presumably accounts for the frequent development of enophthalmos in the long-term period after implantation using HAp [320]. For example, the total rate of complications accompanying bone defect closure using Biocoral hydroxyapatite was found to be 9.4 % [320].

To process coral, the operating room needs to be equipped with a diamond drill burr. After shaping, dust needs to be removed from the plate using normal saline solution and a brush, which causes a certain inconvenience during the surgery. The attempts of rigidly fixing HAp with wire or screws fail because of the fragility of the material. The use of coral for facial areas with thin layer of superficial soft tissues is also a challenge. Thus, the difficulties associated with shaping, fixating, and tissue coverage are responsible for the fact that coral-derived HAp remains an auxiliary osteoplastic material that can be used only in some situations, which are mainly for substituting large defects.

Less expensive implants made of *synthetic HAp* are also used for orbital wall repair [321]; however, they are characterized by even higher fragility.

Cement based on calcium phosphate β-$Ca_3[PO_4]_2$ with pore size of 100–300 μm and porosity of 36 % is a promising material for reconstruction of damaged orbital walls [322]. Strength of this material is 2.5-fold higher than that of coral [323]. It was found in an experiment involving rabbits that a ceramic implant is resorbed within several months and is replaced by newly formed compact bone [324]. Osteoinductive properties of β-$Ca_3[PO_4]_2$ can be enhanced by passivating its surface with recombinant bone morphogenetic protein [325]. The material is already being used in neurosurgery to separate the cranial cavity and accessory sinuses of the nose where it has demonstrated biocompatibility and ability of epithelialization [323].

Hoffmann et al. [326] used implants made of *Bioverit*, the nonresorbable porous glass ionomer cement with the formula SiO_2–Al_2O_3–MgO–Na_2O–K_2O, for orbital reconstruction. Klein and Glatzer [327] have reported in a small series the use of individual Bioverit II bioceramic implants to correct enophthalmos. They found that a high-speed drill needs to be used for cement shaping. The implant needs to be at least 3 mm thick for the planned use of titanium screws. Furthermore, the plate needs to be placed subperiosteally.

The Neuro-Patch dura mater prosthesis made of microporous nonwoven aliphatic polyester urethane can be used to close small orbital floor defects up to 1 cm^2 in size [328].

However, *porous polyethylene implants* manufactured by Porex Inc. (United States) and Synthes (Switzerland) (Fig. 3.30) are now most commonly used [35, 172, 178, 197, 329].

High biocompatibility and porous structure of PE provides rapid fusion of the implant and the adjacent tissues [310] provided that the implantation site is well vascularized [330]. Dougherty and Wellisz [331] examined a model of zygomatic

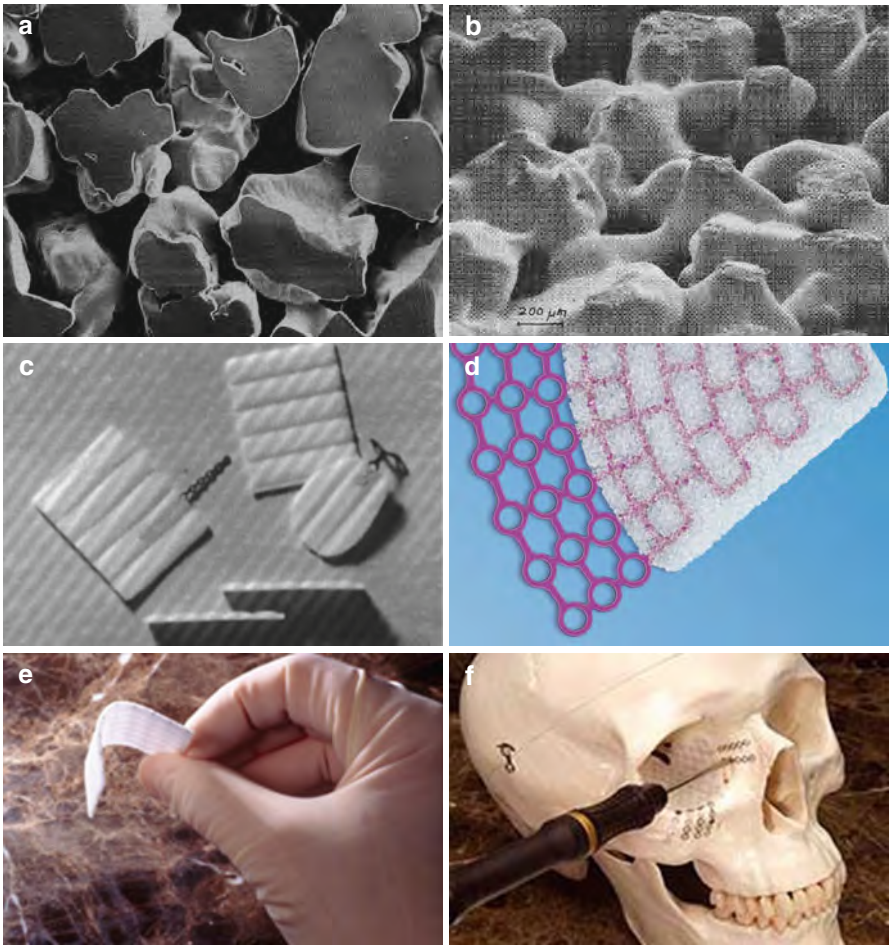

Fig. 3.30 Implants made of Medpor porous polyethylene (manufactured by Porex) and Synpor porous polyethylene (manufactured by Synthes): (**a**) The pore space, which is a system of unordered pores 150–500 µm in diameter occupying ~50 % of the implant volume. (**b**) Rough surface of porous PE. (**c**) Tunnel implants for closing extensive orbital floor defects. (**d–f**) Polyethylene plates reinforced with a titanium mesh

orbital fracture and found rapid epithelialization within 1 week and intergrowth of PE with fibrovascular tissue, as well as signs of osteogenesis inside the implant as soon as 3 weeks after the surgery. Reliable fusion with the adjacent anatomical structures was confirmed by subsequent clinical and morphological findings [332].

Since the volume of PE staying in the orbit for a long time is constant, there is no need to overcorrect during surgery. The risk of infection is significantly reduced due to the possibility of saturating the implant in an antibiotic solution and tissue colonization of polyethylene [202]. As a result, the rate of complications for using PE as an orbital implant is no higher than 5.5–6 % [320, 333].

0.85- and 1.5-mm-thick preforms are characterized by elasticity and can be easily processed using a scalpel and scissors [334, 335]. A 3-mm-thick plate can also be processed but needs to be preheated in hot water.

It can be rather difficult to achieve a stable position of the conventional implant model in patients with fractures of the posterior portion of the orbital floor or its extensive defects larger than 2 cm^2. Su and Harris [336] used 2–3 polyethylene plates placed in a shingle-like manner without any fixation to close extensive inferomedial fractures. Furthermore, modified laminar implants having internal canals, which allows one to reliably fix them using mini- and microplates, are used to treat this complex class of fractures [337] (Fig. 3.30c). Titanium-reinforced polyethylene implants are the most recent successful development for closing this type of fracture [338–340] (Fig. 3.30d–f).

The drawbacks of polyethylene include its radiotransparence: this material can be visualized in CT scans only after the vascularization process is finished [202]. It turned out that implantation of PE directly under skin without using proper periosteal or fascial coating is fraught with early and, in particular, late exposure, with its frequency being higher than 10 % [341]. Furthermore, polyethylene fails to duplicate facial contours because of its excessive rigidity [330].

Implants made of various configurations of *polytetrafluoroethylene* (*PTFE*)—nonporous films and porous plates—have recently been extensively used in craniofacial surgery. The modern applications of PTFE include facial contouring surgery, suspension surgeries in patients with facial nerve paralysis, and malar-, mento-, and rhinoplasty [342, 343].

Elasticity, ease of shaping, chemical and biological inertness, availability, and inexpensiveness of PTFE make it a promising material for closing the orbital floor defect [344]. PTFE film may be used to close small bone defects up to 1.5 cm. Furuta et al. [345] used PRECLUDE polytetrafluoroethylene dura mater substitute (manufactured by Gore & Ass. company) to compensate for periosteal deficits. Ma et al. [346] successfully used 2-mm-thick plates made of Proplast I, a composite material consisting of the mixture of PTFE and carbon fibers to close a blow-out fracture.

Six-month experiments involving repair of bone defects with Ecoflon porous polytetrafluoroethylene implants manufactured in Russia have demonstrated stability of the implant position, minimal phagocytic response (Fig. 3.31a) and delicate capsule formation around the polymer (Fig. 3.31b) and ingrowth of newly formed connective (Fig. 3.31c) and osseous (Fig. 3.31d, e) tissue into its pore space. This occurred in some areas even with hematopoietic bone marrow (Fig. 3.31f) (Astakhov and Nikolaenko 1999–2005).

The 8-year experience of using PTFE in clinical practice demonstrated that a PTFE plate can be easily shaped using scissors and a scalpel due to physicochemical properties of this porous material (Fig. 3.32a–d). Elasticity of the polymer allows the polymer to duplicate all the curvatures of the S-shaped profile of the orbital floor (Fig. 3.32e). Rough surface provides certain adhesion to the adjacent tissues and eliminates the need for rigid fixation of the implant to the infraorbital margin. Formation of clear images on CT slices allowing

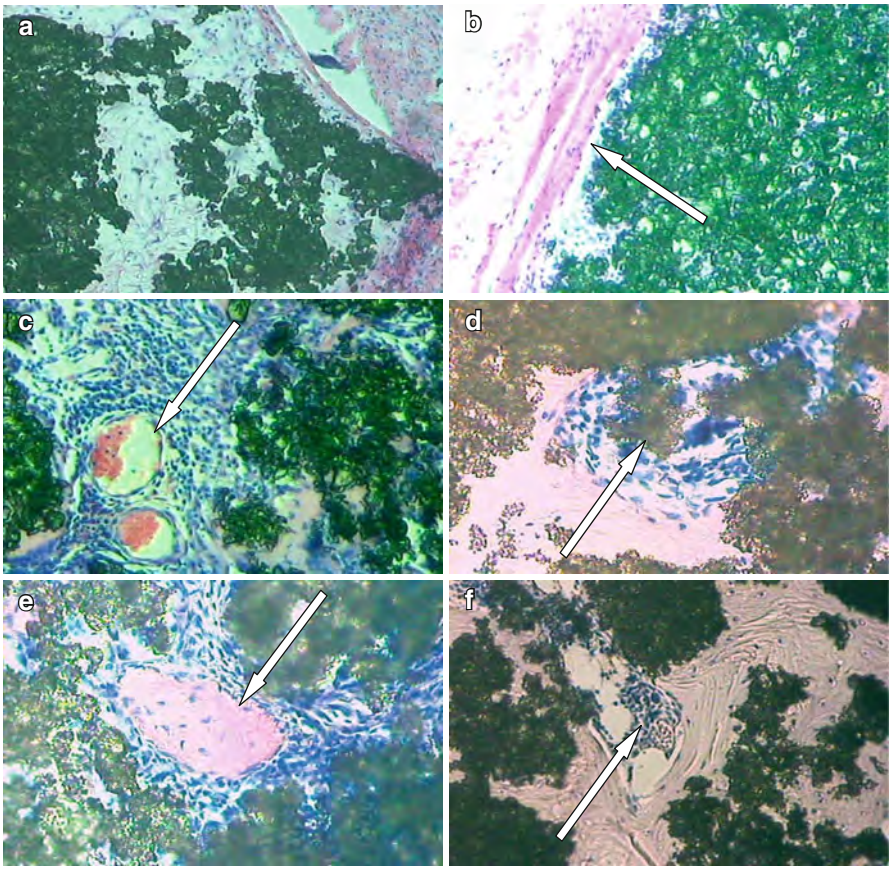

Fig. 3.31 Tissue responses accompanying implantation of Ecoflon porous PTFE manufactured in Russia into the orbit. Hematoxylin and eosin staining: (**a**) The absence of macrophagal response 1 week after surgery, ×100. (**b**) Encapsulation of the implant 2 weeks after the experiment was started, ×100. (**c**) Mature connective tissue inside PTFE 1 month after implantation, ×125. (**d**, **e**) Osteoblast proliferation in PTFE micropores (**d**) giving rise to an islet of newly formed osseous tissue (**e**) 6 months after surgery, ×200. (**f**) Hematopoietic bone marrow in the newly formed bone tissue (6 months after implantation of PTFE)

one to easily control the insertion position is an obvious advantage of the polymer (Fig. 3.32e, f).

Thus, high biocompatibility, no risk of infection transmission, approved manufacture, and acceptable costs gradually make porous polymers the main material for orbital floor reconstruction.

3.3.6.4 Xenografts

Cheung et al. [347] reported the first experience of using Permacol porcine dermal collagen xenograft to reconstruct the orbital floor. No complications were observed

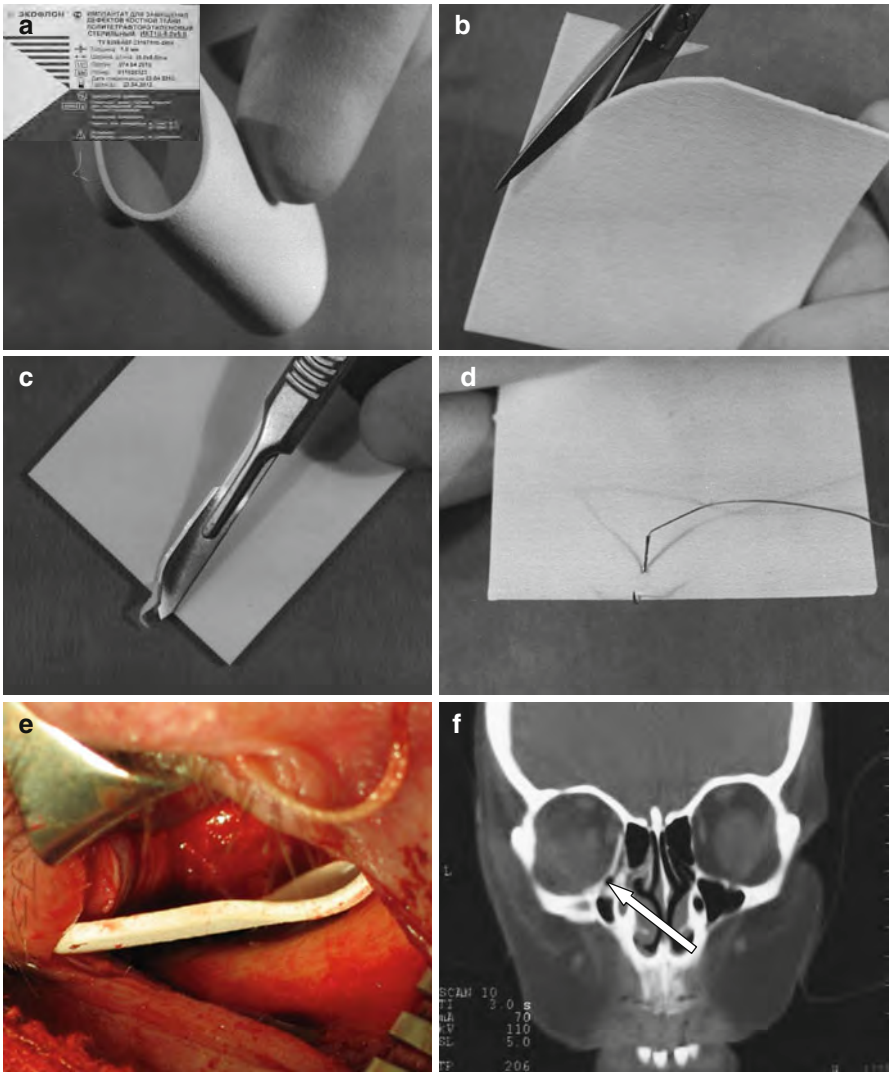

Fig. 3.32 Physical/mechanical properties of Ecoflon porous polytetrafluoroethylene (manufactured in Russia): (**a**) Elasticity and capability of reversible deformation. (**b**, **c**) Shaping using scissors and a scalpel. (**d**) Possibility of applying sutures using surgical needles. (**e**) Plate location on the orbital floor. (**f**) PTFE is clearly visualized on CT scans

during the surgery and in early postoperative period. However, there was a late onset of hypertopia and restriction of infraduction.

Implant removal did not significantly improve the condition of the orbital tissues. Gross scarring of the inferior rectus muscle was detected during a repeated orbitotomy. Histological examination showed an inflammatory response with pronounced giant cell reaction. Thus, despite such advantages of the xenograft as mechanical

strength and easy processing, it is unreasonable to use for managing orbital fractures. Better results will probably be achieved when using bovine and porcine pericardium, hydroxyapatite carbonate derived from porcine compact bone tissue [348], Surgisis ES lyophilized acellular matrix of submucosal tissue of porcine intestine [349], or Bio-Oss bovine bone matrix for this purpose.

***

Summarizing all the facts mentioned above, we would like to draw a conclusion that early and thorough single-stage treatment needs to be used to manage blow-out fractures. The implant used needs to fulfill a number of requirements, including:

1. Simplicity of the shaping and subsequent implantation procedures
2. Ability of the implant to support the orbital structures
3. Stability of the initial position due to rapid integration with the surrounding tissues
4. Resistance to bacterial contamination
5. Clear visualization of the implant on CT or MRI imaging

Modern nonbiological porous materials such as porous polyethylene, coral-derived hydroxyapatite, and porous polytetrafluoroethylene that has been designed by us and is highly competitive with the best international analogues in terms of its chemical and physical/mechanical properties meet these requirements to a great extent.

3.4 Complications of Blow-Out Fractures of the Orbital Floor and Their Surgical Repair

According to Folkestad and Westin [350], more than 80 % of patients have certain sensory or visual disturbances even 5 years subsequent to the trauma. The most conservative estimates show that the complications are associated with the surgical repair in 10–15 % of cases. Potential causes include the approach used, the material selected to close the bone defect, the foreign body reaction to the implant, or the inadequate scope of the surgical repair [237, 351]. Thorough description of the various complications that can develop in patients with blow-out orbital floor fracture is presented below.

3.4.1 Orbital Hematoma

There are five orbital compartments that can potentially accumulate blood: the intraconal, the extraconal, the subperiosteal compartments, the sub-Tenon's space, and the space below the optic nerve sheaths.

Blunt orbital trauma most typically results in a retrobulbar (intraconal) hematoma that is located within the muscular funnel and is caused by rupture of short posterior ciliary arteries [352] or, less frequently, in a subperiosteal hematoma [353]. The hemorrhage into the orbital cavity can also be delayed [354–356].

The first case of blindness caused by retrobulbar *hematoma which developed during repair of an orbital fracture* was reported in 1950. The current rate of this complication is 0.3–0.5 % [287, 356].

The main reason behind *intraoperative, or early postoperative*, *hemorrhagic complications* is disturbance of the orbital branchlet, which runs from the infraorbital artery 13–17 mm below the orbital margin and anastomoses with the vessels of the inferior rectus and inferior oblique muscles, as well as the lacrimal and dorsal nasal arteries. Sometimes 2–3 orbital branchlets run from the infraorbital artery every 3–4 mm. They can be cauterized without any risk to the orbital circulation. The orbital branchlet can be easily mistaken for the infraorbital artery when the orbital floor is displaced downward and the adipose tissue surrounds the infraorbital neurovascular bundle [357].

In patients with extensive orbital fractures, the effused blood is easily evacuated into the paranasal sinuses and the nasal cavity [356]. In a fracture without fragment displacement, blood remains in a closed space limited by the bones and the tarso-orbital fascia, which risks the development of the orbital compartment syndrome. This risk is higher in young people who have a well-developed network of connective tissue orbital bundles (Figs. 1.9, 1.10, 1.11, 1.12, and 1.13) that retains blood in the retrobulbar orbital compartment.

The orbital portion of the optic nerve is 25 mm in length. This is 7 mm longer that the distance from the posterior pole of the eye to the orbital apex. This extra 7 mm give it an S shape and thus is mobile. This and the mobility of the tarso-orbital fascia can compensate for the increase in intraorbital pressure to a certain extent but cannot protect the optic nerve and the globe against pronounced intraorbital and intraocular hypertension in patients who have a massive hematoma [358].

The rapidly increasing intraorbital pressure causes pronounced pain, diplopia, exophthalmos, periorbial ecchymosis, chemosis of the bulbar conjunctiva, subconjunctival hemorrhage, corneal edema caused by ocular hypertension, optic disk swelling, and external and internal ophthalmoplegia with afferent pupillary defect [358–360]. The raised orbital pressure caused by the bleeding may result in *compression of the optic nerve and the central retinal artery which then leads to* a risk of *irreversible loss of visual acuity up to complete blindness* [352, 356, 361, 362]. Since 100–120 min of ischemia cause retinal cell death, *early diagnosis and emergency surgical and therapeutic assistance are extremely important* [361].

The *diagnosis* of this condition relies on the following symptoms: *sudden onset, pronounced strain in the orbital tissues, acute pain, and abrupt reduction of acuity*.

In patients with intraoperative development of hematoma, the main signs include *strain in the orbital tissues, an abrupt increase in ocular pressure, and pupillary dilation*.

CT is a mandatory diagnostic tool that allows one to evaluate the hematoma location and size, the accompanying injuries to bones and the cerebrum, and the presence of foreign bodies in the eyeball, orbit, or the cranial cavity. When used as an urgent method of examination, CT is superior to MRI as it provides better visualization of bone structures and is more informative in terms of evaluating the condition of soft tissues. It also and does not have the risk of an MRI causing an additional injury by affecting an undiagnosed metallic foreign body [362].

3.4.1.1 The Treatment Algorithm

Patients with suspected retrobulbar hematoma need to undergo an urgent ophthalmological examination, lie with their head elevated, and have an ice pack placed on the orbital area.

Conservative treatment needs to be started *immediately* (without waiting for CT or ultrasonography results):

- Intravenous bolus injection of 8 mg of dexamethasone
- Intravenous bolus injection of 80–100 ml of 20 % mannitol solution for 3–5 min followed by a 24-h infusion (2 g mannitol/kg body weight)
- Oral administration of 250 mg of acetazolamide twice per day with a 12-h interval
- Instillation of 0.5 % timolol solution

In addition, blood pressure needs to be thoroughly controlled, and because the Valsalva maneuver can exacerbate the problem by increasing blood, ocular, and intracranial pressure, it needs to be avoided by eliminating nose blowing and vomiting.

Increased ocular pressure and/or pronounced vision loss (up to no light perception) in addition to the tense orbital tissues and the lack of effect of conservative treatment are an indication for performing emergency orbital decompression using various surgical approaches to prevent compression of the optic nerve and orbital vessels [360, 363]. According to the survey performed among 288 British maxillofacial surgeons, *retrobulbar hematoma requires surgical management in 90 % of cases* [359]. It should be mentioned that loss of light perception is not a contraindication for the emergent surgery, because even in cases where all light perception has been lost, there can be restoration of central vision if the surgery is done promptly [361, 364].

Lateral canthotomy with inferior cantholysis and orbitotomy are the simplest procedures for orbital decompression.

Lateral canthotomy is performed under local (infiltration) anesthesia (Fig. 3.23a–d). The palpebral commissure is incised up to the lateral orbital margin using straight scissors; the inferior crus of the lateral palpebral ligament is then transected.

Inferolateral orbitotomy is performed if the initial decompression is insufficient. In addition to dissection of the tarso-orbital fascia, one needs to open the 3D network of well-developed 0.5-mm-thick connective tissue membranes

around the inferior rectus and oblique muscles, as well as at the level of the eyeball equator [106].

The membranes have a round orientation in the plane where the oblique muscles are attached and are mostly oriented radially at the level of rectus extraocular muscles. Thus, dissection should be performed along connective tissue bundles in order to separate them without disturbing the 3D structure. Taking into account the risk of recurrent orbital hematoma, no sutures are placed on the orbitotomy incision.

Opening of the subperiosteal hematoma assumes that the targeted access to it, both from the orbit and through the adjacent sinus, is used.

3.4.2 Orbital Emphysema

Clinically significant emphysema of the orbit and periorbital tissues, defined as causing disturbances of extraocular muscle function and vision, caused by repeated sneezing or nose blowing is a rather rare[24] complication of blow-out orbital floor fractures [12, 366–368]. Rupture of the mucous membrane of the maxillary sinus is a prerequisite of the development of this complication, which is indicated by the fact that emphysema is accompanied by blood in the sinus [369].

In addition to keeping a patient informed about the recommended behavior, it is reasonable to plug the ipsilateral nasal passage, thus preventing air from getting into the orbit [370].

Emergency drainage is recommended for patients with pronounced orbital emphysema (the procedure is thoroughly described in Chap. 4 devoted to fractures of the medial orbital wall).

3.4.3 Infectious Complications

The reasons for development of orbital infection include sinusitis, dental and periodontal pathology, hematogenous dissemination, penetrating orbital injury, and inadequate asepsis and antisepsis during surgery [161, 371–373]. Maxillary sinus tamponade considerably increases the risk of infectious complications although the reasons for that are not clear [235].

Underlying or accompanying sinusitis is responsible for 70–90 % of all orbital infection cases. Therefore, thorough examination of the sinuses is essential when evaluating orbital trauma [374].

Purulent complications are most frequently associated, in descending order, with the ethmoidal labyrinth (75–90 %) or the frontal and maxillary sinuses. Isolated

[24] Brasileiro et al. [365] reported that the rate of subcutaneous emphysema in a large cohort (390 patients, 458 sinus wall fractures) was 7.43 %. Sixty percent of those were injuries to the maxillary sinus. One-third of patients had multi-trauma of the ethmoidal labyrinth and the maxillary sinus. In most cases, emphysema affected only the periorbital area and did not spread to the orbit.

inflammation of the sphenoidal sinus is a very rare condition, and if present, it usually is a complication of ethmoiditis.

The prevalence of ethmoidal labyrinth pathology is caused by insignificant thickness of the medial orbital wall, presence of two ethmoidal foramina (the preformed route), and sometimes additional perforations, which are normal variants [375]. The orbital floor may also have congenital defects or dehiscences, while the fracture caused by trauma allows the infection to directly enter the orbit from the sinus. Valveless facial veins facilitate transmission of microflora from the sinuses.

The microbial population in paranasal sinuses is typically represented by *Streptococcus* (*pneumoniae*, *agalactiae*, *equinus*), α-hemolytic *Streptococcus*, less frequently, *Haemophilus influenzae* and *Staphylococcus aureus*. The combination of both aerobic and anaerobic bacteria (bacteroides, peptostreptococci, peptostaphylococci, *Pseudomonas aeruginosa*, and *Haemophilus influenzae*) as well as rare Gram-negative bacteria, which sometimes are insusceptible to antibiotic therapy, is typical of adult patients [184]. Blood in the sinus accompanying the fracture provides a favorable environment for bacterial growth.

Chronic dental and periodontic pathology is the second most common reason for infectious complications. For example, tooth extraction is the reason for 22.5 % of all purulent inflammations of the maxillary sinus.

Nasopharyngeal infections in high-risk patients (AIDS, diabetes, chronic diarrhea with metabolic acidosis) are the third most common infections. Administration of glucocorticoids, immunosuppressants, and chemotherapy drugs is associated with a high risk of rhinocerebral fungal infection caused by phycomycetes, ascomycetes, and other nasopharyngeal saprophytes. In ~5 % of cases, when sinus aeration is disturbed, inflammatory complications are caused by *Aspergillus* fungi in combination with other causative agents.

3.4.3.1 Clinical Presentation

The orbital septum plays a crucial role in the presentation, course, and treatment of orbital infections. It is attached to palpebral cartilages and orbital margins and separates the orbit into two compartments, the anterior preseptal and posterior, postseptal. The eyelids and the lacrimal sac are located in the anterior compartment. The eyeball, the optic nerve, the extraocular muscles, neurovascular structures of the orbit, and adipose tissue are located behind the orbital septum. *The fascia to a certain extent impedes inflammation spreading from the anterior compartment to the posterior one and vice versa.*

There are five clearly defined forms of orbital infection: *preseptal cellulitis, postseptal cellulitis, subperiosteal abscess, orbital abscess, and cavernous sinus thrombosis* (Fig. 3.33) [376].

Preseptal (periorbital) cellulitis, in the posttraumatic setting, develops when infection spreads through a bone defect; periorbital swelling results from impeded blood outflow along the superior ophthalmic vein. The clinical examination is limited by palpebral swelling closing the palpebral opening and hyperemia of periorbital skin. *The main difference of this pathology from a postseptal process is that it is not characterized by involvement of the patient's systemic condition, exophthalmos, limited ocular motility, or reduced visual acuity.*

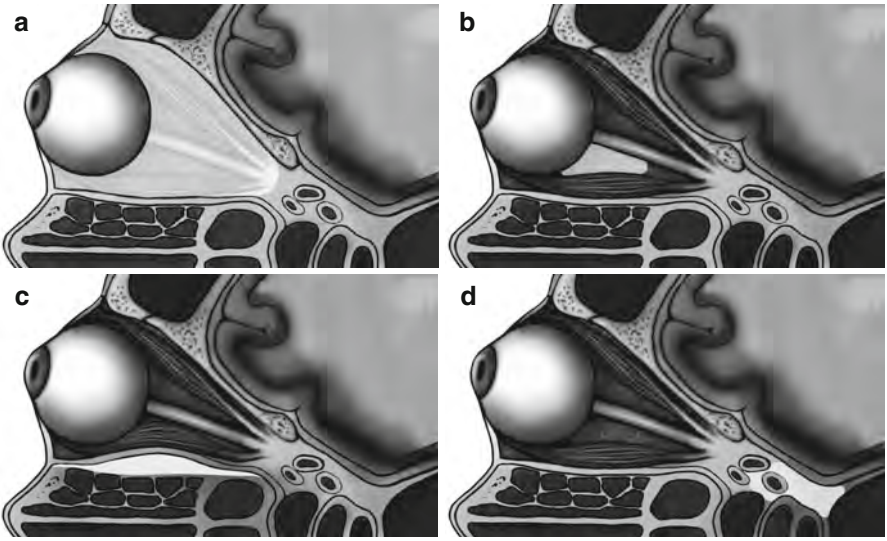

Fig. 3.33 Clinical forms of orbital infection (the axial cross-section of the orbit): (**a**) Postseptal cellulitis. (**b**) Orbital abscess. (**c**) Subperiosteal abscess. (**d**) Cavernous sinus thrombosis

Postseptal cellulitis is the acute diffuse purulent inflammation of orbital tissue behind the tarso-orbital fascia. Fortunately it is a rare complication of orbital fractures. Its rate is usually less than 1 %. Recent sphenoethmoiditis (1–2 weeks prior to trauma) or sphenoethmoiditis developed during the early period after trauma (no later than within 5 weeks) is the inciting factor; however, cellulitis cases have also been described in patients without past history of this disease [371]. Forceful nose blowing aggravates the emergence of the pathological process [368].

In most cases, the pathology is *unilateral* and is characterized by acute onset. The patients complain of general fatigue, orbital pain aggravated by eyelid palpation and eye movements, and diplopia accompanied by *fever and the characteristic changes in blood in patients with infections, leukocytosis, shift in band neutrophil count, toxic granulosity of neutrophils, aniso- and poikilocytosis, and elevated ESR*. After several hours, the general symptoms of infection are accompanied by hyperemia and *marked palpebral swelling*, conjunctival chemosis, *exophthalmos with partially or completely limited ocular motility*, *and sudden vision loss* caused by compression of the optic nerve secondary to swollen tissues occluding the central retinal artery.

In almost half of cases, postseptal cellulitis causes *orbital or subperiosteal abscess* formation that requires drainage along with intensive antibiotic therapy.

In addition to the past medical history and the characteristic clinical presentation, diagnosis is facilitated by X-ray imaging of the orbital and paranasal sinuses.

In 10–20 % of cases, the course of orbital cellulitis is aggravated by maxillary osteomyelitis, decreased vision caused by toxic optic neuropathy (3–11 %), superior orbital fissure syndrome, and orbital apex syndrome. Purulent processes in the orbit can be complicated by thrombophlebitis of the veins in the orbit,

pterygopalatine plexus, cavernous sinus, and internal jugular vein which subsequently may be followed by development of severe intracranial complications.

Orbital abscess is an encapsulated purulent cavity located in the muscular funnel. For an appreciably large abscess, the clinical presentation resembles that of postseptal cellulitis; thus, differential diagnosis requires performing CT and MRI.

Subperiosteal abscess is characterized by accumulation of pus between the bony orbital wall and the periosteum. In 80 % of cases, it is localized in the superomedial quadrant of the orbit. Its symptoms are marked edema and hyperemia of the upper eyelid, disturbed upper eyelid motility, and eyeball displacement in the direction opposite to the abscess location accompanied by limited ocular motility and exophthalmos. In patients with injured posterior ethmoidal air cells and the sphenoidal sinus, the clinical presentation also includes the orbital apex syndrome.

Septic encephalopathy is common for this condition; cerebral meninges can also be involved in the pathological process. Diagnosis verification and differential diagnosis with the orbital abscess and cavernous sinus thrombosis require performing CT scanning or preferably MRI.

Cavernous sinus thrombosis is caused by septic embolism of cerebral sinuses and *is often bilateral*.

Fever, chills, marked changes in mental status, and elevated leukocytes are all signs and symptoms of brain involvement. The impeded venous outflow from the orbit is associated with marked chemosis, dilated episcleral veins, increased ocular pressure, optic disk congestion, tortuosity and congestion of retinal veins, and exophthalmos. Dysfunction of trigeminal nerve branches I and II and sequential palsy of the abducent, oculomotor, and trochlear nerves are also classic signs of cavernous sinus thrombosis.

Cavernous sinus thrombosis is characterized by rapid progression leading to loss of consciousness and coma.

3.4.3.2 Treatment

Purulent complications involving orbital soft tissues require urgent intensive therapy; it is only preseptal cellulitis that requires using conservative treatment. In all other cases, urgent opening and drainage of paranasal sinuses by an otolaryngologist and a maxillofacial surgeon is required in addition to intravenous injection of broad-spectrum antibiotics (co-amoxiclav, ceftriaxone, meropenem), anticoagulation, and stabilization of blood pressure. Taking this into account, *it seems most reasonable that these patients are admitted to the otolaryngology or the maxillofacial surgery unit*.

The following measures may be needed in addition to surgical drainage of the primary focus such as sinusitis:

- Opening of subperiosteal abscess via the exo- or endonasal approach
- Canthotomy, cantholysis, and orbitotomy aimed at orbital decompression or opening and drainage of the orbital abscess

It is clear that treatment of orbital fractures, especially using grafting material, should be postponed in these cases [377].

The vision and oculomotor functions may return entirely to normal provided that treatment of the infectious state was initiated in a timely and thorough manner [378].

3.4.4 Late Implant Infection

The reasons for late implant infection include dental surgeries, rhinoplasty, implant migration into the paranasal sinus causing a sino-orbital fistula, dacryocystitis caused by medial displacement of the graft, drug abuse, or acute respiratory viral infection [379]. According to the published data, infection of a porous implant inevitably causes explantation [202, 270, 334]. *Staphylococcus aureus* and *epidermidis* are the bacterial species typically detected by microbiological examination in this case.

3.4.5 Optic Neuropathy

Trauma-induced optic neuropathy can result in either partial or complete vision loss without external or primary ophthalmoscopic signs of damage to the globe after the trauma [24].

Blindness after optic nerve trauma can be caused by the direct impact of the kinetic energy of a wounding agent, by rupture of pial sheath vessels, or by development of the compartment syndrome secondary to retrobulbar or subperiosteal hemorrhage. Since the optic nerve is rarely affected in patients with the classical blow-out fracture of the orbital floor, diagnosis and treatment of neuropathy caused by blunt orbital trauma is provided in the subsequent chapters of this handbook.

Loss of central vision after osteoplasty indicates that the optic nerve or vessels feeding it were compressed by the implant, or ischemic optic neuropathy resulted from uncontrolled intraoperative arterial hypotension [237, 380]. Retrobulbar or subperiosteal hemorrhage and marked edema of orbital fat can also occur because of the severity of surgical wound [381, 382]. Fortunately, the risk of this disastrous complication is less than 0.07 % [84].

Urgent orbital decompression, removal of the implant compressing the nerve, and hematoma drainage combined with megadose glucocorticoid therapy may lead to some improvement of visual functions [202, 381].

Prevention of postoperative vision impairment includes elimination of excessive pressure exerted onto the eye and the optic nerve during osteoplasty, periodic intraoperative measurement of blood pressure to monitor for severe arterial hypotension, the use of the smallest implant that is sufficient to close the defect for subperiosteal implantation, and reliable fixation of the implant. If a compression bandage is used, it should be removed the next morning to test visual acuity and pupillary responses and to perform ophthalmoscopy.

Special care is needed when performing tamponade of the maxillary sinus, since this procedure may significantly increase the intraorbital pressure [237]. The development of compressive optic neuropathy can be caused by deliberate or accidental placement of a hemostatic sponge in the posterior portions of the orbit after surgical repair [383].

Meanwhile, it seems unlikely that the optic nerve can be directly damaged with surgical instruments, since the orbital floor is characterized by 15° elevation and S-shaped profile that prevent accidental placing raspatory into the deep orbital compartments. Furthermore, the distance between the infraorbital margin and the orbital apex of 45 mm also plays a protective role [12]. There is no reliable evidence

demonstrating that manipulations in the orbit cause increased intraorbital pressure that is dangerous for blood circulation [380].

As opposed to the commonly held belief, bone fragment repositioning does not increase ocular pressure. This was demonstrated by the use of intraoperative tonometry reported by Paton et al. [384]. Placement of large implants during late orbital reconstruction may cause short-term ophthalmic hypertension, but it does not affect the ocular functions at all [93, 380, 385].

3.4.6 Diplopia

3.4.6.1 Definition and Classification

It is reasonable to start describing one of the most severe complications of both the fracture itself and its surgical management by discussing which type of diplopia should actually be regarded as a complication. The diplopia should also be graded as mild, moderate, or significant.

Theoretically, osteoplasty of the orbital floor should not cause diplopia. However, since not every diplopia type is an indication for surgical management, not every postoperative diplopia should be regarded as a complication.

In particular, *diplopia in extreme positions of gaze* (referred to as mild by Hammer and Prein [386]) *is not a complication and does not require treatment* [12].

Primary gaze diplopia is considered severe and requires therapy.

It would seem reasonable to consider upward-gaze diplopia to be of moderate severity, since the absence of diplopia in the lower visual fields allows the patient to walk and perform visual activity at a short working distance. However, there are a number of occupations for which upward-gaze diplopia interferes with professional competency, hence in this case would be considered as being severe.

Synonymous terms, such as "diplopia in functionally important gaze directions," "disturbing diplopia," and "clinically significant diplopia," seem to be more appropriate for these cases[25].

When performing mathematical and statistic calculations, researchers can use the gradation of diplopia and oculomotor disorders proposed by Grant et al. [387].

Degree of oculomotor disorders:

0—The range of movements is identical to that of a healthy eye.
1—For the maximum supraduction, the inferior limbus of the damaged eye is diverged from that of the healthy eye by less than 1 mm.
2—1–2-mm divergence.
3—The divergence fluctuates within 2–3 mm.
4—Divergence of the injured eye is over 3 mm.

[25] Within 30° from the point of fixation [320].

3.4.6.2 Degree of Diplopia

0—No diplopia.
I—The horizontal divergence angle at which diplopia emerges is 45° or more.
II—The horizontal divergence angle at which diplopia emerges is 15–45°.
III—The angle of gaze divergence is less than 15°.
IV—Diplopia in primary gaze position.

3.4.6.3 Epidemiology of Diplopia

Preoperative diplopia is observed in 60–85 % of patients [75, 76, 238].

Both a surgeon and a patient should bear in mind that even a perfect surgery can be accompanied by emergence or aggravation of the already existing diplopia early after the intervention. It is transient diplopia that requires no special treatment [8, 213].

One should not make any judgments as to the degree of severity of diplopia for at least 30 days after surgery. Complete regression of diplopia and concomitant paresthesia of the infraorbital nerve may take 2–6 months [175, 320, 386].

Late oculomotor disorders after osteoplasty are observed approximately in 50 % of patients [388], while diplopia remains persistent in 5–37 % of patients who had long-term follow-up followed up [75, 76, 213, 238, 350, 389].

3.4.6.4 Risk Factors of Persistent Diplopia

The obvious risk factors of persistent postoperative diplopia include extensive (e.g., inferomedial) fracture [76], its spread to the so-called deep orbit defined as being behind the inferior orbital fissure which is an anatomical border of the orbital floor [390], tamponade of the maxillary sinus[26] [350], advanced age of a patient [75], and delayed surgical management [118, 238, 391]. Full ocular motility is obtained in 80 % of patients operated on during the first week after trauma, 50 % if operated on during the second week, and in less than 25 % of patients if the surgery is delayed longer than 2 weeks.

The *mechanisms* of transient or permanent diplopia in patients with blow-out fracture can vary [390].

Muscle edema and/or hematoma are clearly visualized on high-resolution CT scans [99]. The negative traction test result facilitates diagnosis. The outcome is complete recovery without surgical intervention.

Muscle entrapment in the fracture site [118] is observed in only 5–10 % of cases [387] but is an unfavorable prognostic factor associated with the risk of persistent diplopia. The contact between muscle belly and the bone at two points seen in sequential CT scans is the CT sign of muscle entrapment [345].

[26] It is not surprising that the most recent publication describing tamponade of the sinus as the main procedure for orbital floor augmentation dates back to 1985 (Gray et al.) although the double approach is still occasionally described in literature.

Fibrosis or entrapment of fat and connective tissue interconnections of the orbit [107, 118, 392], which are a passive component of the oculomotor system and comprise the integral locomotor system together with the muscles [106].

Dislocation of extraocular muscles accompanying enophthalmos and hypoglobus changes their traction vector and results in muscular imbalance and diplopia. The hypothesis relies on cases when diplopia disappeared after surgical correction of hypoglobus without any interventions on extraocular muscles [387].

Volkmann's ischemic contracture in patients with trapdoor fractures [393]. Smith et al. [394] performed direct intraoperative measurements to demonstrate a significant increase in pressure in the sheath of the inferior rectus entrapped at the fracture site. The microcirculation in muscular tissue is impaired, resulting in the development of the "Volkmann's ischemic contracture."

This mechanism most typically occurs in hypotensive patients with pronounced edema of orbital tissues. As opposed to the trapdoor fracture, swollen tissues in patients with an extensive bone defect can migrate to the sinus, thus preventing a significant increase in orbital pressure.

Although not denying that a certain compartment syndrome can be caused by a fracture, N. Iliff et al. [392] cast doubts on its role in the emergence of oculomotor disorders, since neither microangiographic nor histological examination revealed regions with ischemic necrosis of muscular or connective tissue structures of the orbit.

Paresis/paralysis of vertical motor muscles caused by central or peripheral pathology is associated with impairment of the orbital portion of the oculomotor nerve.

Paresis of the oculomotor muscle entrapped in the fractured area [395, 396]. Limited motility of the injured eye both in the field of action of the entrapped paretic muscle and of the antagonist muscle in the same eye (i.e., both for the down- and upward directions) is observed in patients after orbital fracture. The CT scan shows that the muscle is adjacent to the fracture site. Eyeball deviation in primary gaze position is observed in 20 % of patients before surgery (see the Lerman's regularities presented in the beginning of this chapter). After the muscle is released from the fracture site, its paresis manifests as muscle underaction in the direction of its action and overaction in the direction of its antagonist (Fig. 3.34).

Spontaneous regression of oculomotor disorders with complete recovery or minimal diplopia impeding neither professional nor everyday activity occurs in most cases. Obvious deviation requires either prism correction or surgical management. Thus, an ophthalmologist needs to identify patients with paresis of the entrapped extraocular muscle in a timely manner and warn them that another type of diplopia may develop after the surgery which may require additional treatment.

Rupture of the muscle belly or detachment of the inferior rectus tendon from the sclera at the moment of trauma [397, 398]. Usually the primary surgery shows that the peripheral portion of the muscle attached to the sclera is thin, while the central portion of the belly is fused with the connective tissue and adipose tissue of the orbit. As a result, in two-thirds of cases, oculomotor disorders resemble the presentation of inferior rectus muscle palsy with limited motility in the direction of action of this muscle. The presentation resembling muscle entrapment at the fracture site with limited motility in the direction opposite to action of this muscle

Fig. 3.34 Eye movement disorders in patients with orbital floor fractures: (**a**, **b**) upward deviation (**a**) and absence of infraduction (**b**) of left eyeball caused by paresis of the inferior rectus muscle released from the fracture site. (**c**–**d**) An identical clinical case. The upward deviation of the right eyeball in primary gaze position (**c**) is caused by the overaction of the antagonist of the inferior rectus muscle (the superior rectus muscle of the right eyeball). (**d**) The overaction of the superior rectus muscle is also observed for the upward gaze. (**e**, **f**) Limited infraduction (downward rotation of an eye)

is rarer. A formula for success in treating this pathology is the early, single-stage, and thorough surgical management including reconstruction of both osseous and muscular structures [399]. The main limitation is associated with the fact that it is difficult to timely diagnose muscular involvement. MRI is an indispensable technique in this situation; however, it is usually not performed when a patient is admitted to hospital. If reconstruction of the integrity of the inferior rectus muscle has no effect, the muscle is resected; the inferior oblique muscle is shortened by 6 mm and sewn in a lateral position with respect to the external edge of the inferior rectus muscle [400].

Blow-out fractures with inferior rectus muscle detached from the sclera either partially or completely and entrapped in a bone defect are even rarer and are extremely challenging to diagnose [398, 401]. The detached muscle that retained its

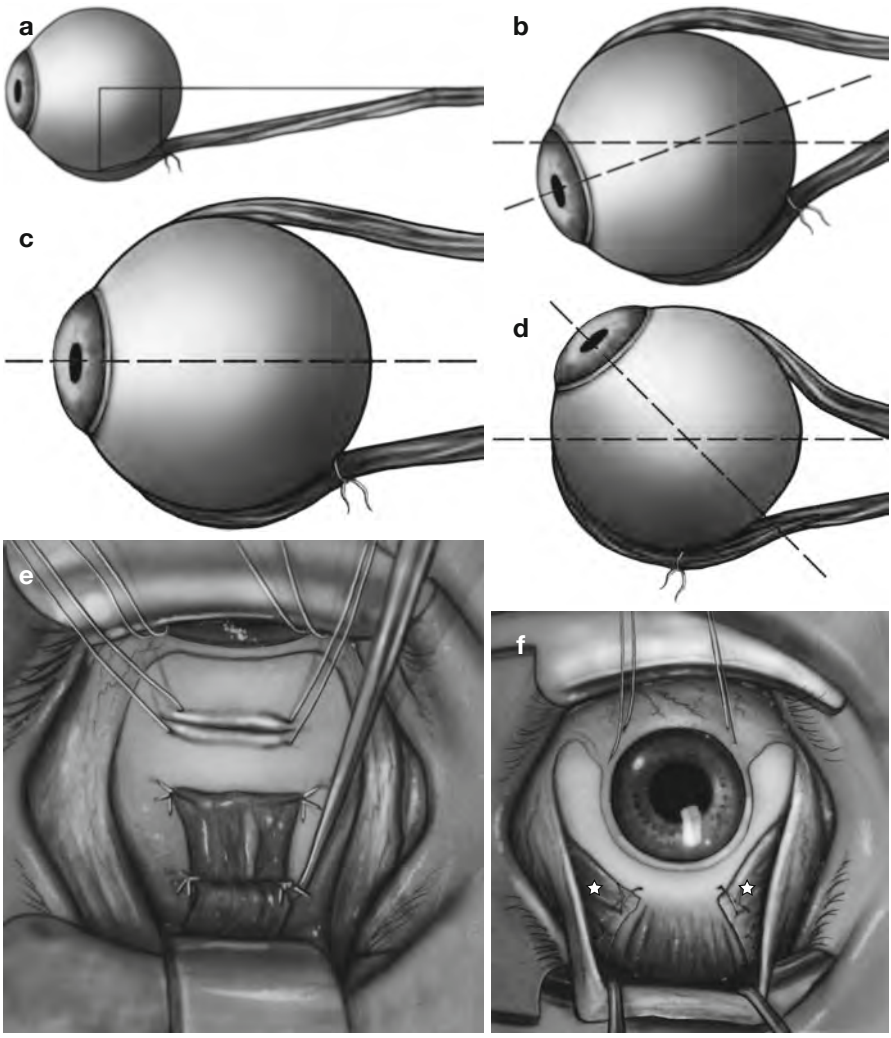

Fig. 3.35 Surgical management of diplopia: (**a**) The faden operation (surgical weakening of the contralateral inferior rectus muscle by fixing its belly to the sclera with two 5-0 sutures 13 mm away from the anatomical attachment site). (**b**) The result is reduction of infraduction of the healthy eye and reduction of downward-gaze diplopia. (**c**) Proper position of the eyeball in primary gaze position. (**d**) Retention of full excursions of the eye in upgaze position. (**e**) A combination of faden operation and recession of the inferior rectus muscle. (**f**) Complete inferior transposition of horizontal muscles (inverse Knapp procedure). *Asterisks* horizontal rectus muscles

contractile capacity needs to be sewn back in place. Transposition of the adjacent horizontal muscles or the faden operation is recommended for patients with neurogenic paralysis (Fig. 3.35).

Casuistic cases of *implant fusion with the inferior rectus muscle* were reported [347, 402].

3.4.6.5 Treatment of Diplopia

Depending on the reason of severe diplopia, either recurrent intervention on the orbital floor to release the residual entrapment of the muscle or orbital adipose tissue in the fractured area or surgery on vertical motor muscles is recommended. The use of prism glasses is recommended for patients with minimal diplopia.

Diplopia in downgaze caused by the underaction of the inferior rectus muscle can be almost always eliminated or reduced using optic, surgical, or combined procedures [80]. In some cases, it is easier for patients to use monocular reading.

Correcting diplopia using prism glasses is used to neutralize the minimal downward diplopia. It is extremely difficult to select prism glasses for people with presbyopia, especially those with concomitant ametropia. Bifocal lenses are used in this case: their upper segment is a stigmatic lens (because there is no primary gaze diplopia), while the lower section is a prism lens. Unfortunately, people with presbyopia and ametropia are often dissatisfied with their vision. Compromise can be reached by wearing two pairs of glasses (distance spectacles with spherical lenses and reading spectacles with prism lenses); however, many people do not feel comfortable with the need to change their glasses all the time. Another acceptable solution is to use reading spectacles where the lower segment border corresponds to the inferior pupillary margin. Regular bifocal lenses are recommended to be worn when outside and while driving. Fresnel prism glasses are now not as popular as they used to be since they cannot provide a clear image and a wide field of view for binocular vision. Anti-strabismic interventions to recover binocular vision in primary and downward gaze are performed at least 6–8 months after trauma [403]. The choice of intervention depends on deviation type and the degree of muscle imbalance. Paralysis or weakness of the inferior rectus muscle requires intervention on ipsilateral vertical motor muscles by recession of the superior and resection of the inferior rectus muscle or strengthening of the opposite synergist along with weakening of the contralateral antagonist [404, 405]. Recession 3–5 mm of the inferior rectus muscles is recommended for patients with restricted supraduction caused by its entrapment.

In 10–15 % of cases, after 4–6 weeks, the surgery is complicated by overcorrection manifested by ipsilateral hypertropia of 12–25 prism diopters, hypofunction of the inferior rectus muscle, and lower eyelid shortening because of natural anatomical connections between the inferior rectus muscle and the lid retractor.

Cicatrization and fusion of the inferior rectus muscle with the transverse Lockwood's ligament is detected during repeated surgical intervention. It results in forward displacement of the extraocular muscle and prolapse of its anterior portion. This weakens muscle traction and causes pseudoparesis of the muscle manifested by disappearance of downward excursions of the eye from the normal central position [406]. Primary infratarsal lower eyelid retractor lysis is the only method to prevent this complication [391].

The faden operation is the surgical weakening of the contralateral inferior rectus muscle by applying two posterior fixing sutures 13–15 mm behind its insertion site [407]. It is used for 18 % of patients with orbital floor fractures whose oculomotor disorders are caused by muscle paralysis rather than by muscle entrapment (Fig. 3.35a–d) [97, 98]. Sewing the muscle to the sclera weakens its action in a dosed manner without changing the primary gaze position of the eyeball. As a result, slight

restriction of infraduction emerges on the healthy side, thus reducing downgaze diplopia. The faden operation is used as an independent tool rather rarely; it is usually supplemented with small recession of the inferior rectus muscle (Fig. 3.35e) [408]. The faden operation is ineffective if there is no infraduction of the affected eye.

Complete inferior transposition of horizontal rectus muscles by the transposition of tendons of horizontal muscles to the insertion site of the inferior rectus muscle (the inverse Knapp procedure) can be used in individual, accurately selected cases of marked underaction of the inferior rectus muscle (Fig. 3.35f) [403, 405, 409]. One should bear in mind that there is a high risk of achieving overcorrection if one underestimates the degree of integrity of the inferior rectus muscle [410].

3.4.7 Enophthalmos

3.4.7.1 Epidemiology of Enophthalmos

Globe retraction (axial dystopia, enophthalmos) is the main *late complication* of both untreated blow-out fractures and unsuccessful orbital floor repairs [12, 411, 412].

Prior to surgery, cosmetically significant globe retraction of at least 2 mm is observed in one in three patients [75, 320] and persists in 7–11 % of patients in the late period after surgical repair [75, 413, 414]. In patients with small fractures less than 2×2 cm, the risk of enophthalmos 2 years after the intervention is less than 1 % [388].

According to experimental and clinical data, *the main reasons for posttraumatic enophthalmos include the increase in orbital volume caused by prolapse of the posteromedial portion of the orbital floor and disturbance of the regular anatomical relationship between the orbital adipose tissue and the suspensory apparatus of the eyeball* (Figs. 1.5b, c and 3.36) [415–417].

The loss of osseous support predetermines gravity-induced dislocation of orbital tissue backward and downward [418]. Dislocation of the eyeball is aggravated by remodeling processes in the injured orbit transforming the cone shape of soft tissues to a spherical one [416]. Meanwhile, the ultrastructure, volume, and radiological density of retrobulbar adipose tissue remain unchanged.

Since enophthalmos is caused only by fractures localized behind the equator of the eyeball [419], the surgical procedures displacing the retroequatorial fat correct globe retraction very well.

Since the volume of orbital soft tissues remains unchanged after trauma, *it is most reasonable to perform procedures aimed at recovering the shape and spatial arrangement of soft tissues via their mobilization and reconstruction of bones which support these tissues*.

When choosing an approach to the orbital cavity, one should take into account the previously used surgical approaches. Thus, it is not recommended to use a subciliary incision twice, since the eyelid is often shortened to some extent and the repeated incision would worsen the outcome. In this situation, the subtarsal approach is preferred.

To correct late enophthalmos, the orbital periosteum needs to be circumferentially incised and thoroughly separated for at least 3 cm deep inside the orbit [420]. Deeper dissection is dangerous because of individual variations in orbital depth, and

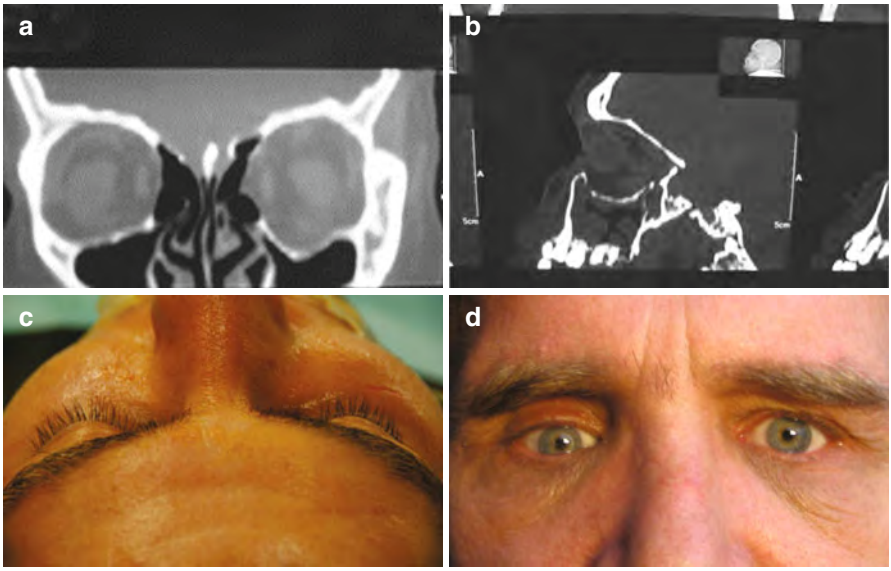

Fig. 3.36 Posttraumatic increase in orbital volume: (**a**) Prolapse of the posteromedial portion of the orbital floor is clearly visualized by coronal CT imaging. (**b**) Depression of the orbital floor and the previously mentioned prolapse of the inferior rectus muscle are seen in an axial CT scan. The conical shape of the orbital apex is transformed to the spherical shape. (**c**) Retraction of the right globe (enophthalmos). In patients with blow-out fractures, the retraction is never severe. (**d**) Prolapse (hypoglobus) of the right globe

the superior orbital fissure structures can be damaged [421]. The task is complicated even more by coarse cicatrization involving the periosteum [93]; however, there are no other methods to adequately displace the retracted eyeball forward.

The completeness of orbital tissue mobilization is tested using the "anterior" traction test [422]. Tendons of the horizontal muscles are fixed with forceps, and the eyeball is pulled forward. If the eyeball is displaced easily, one can proceed to the next stage of orbit repair. If the eye cannot be displaced forward, separation of soft tissues from the bones needs to be continued. Otherwise, the implant will not be able to return the eyeball in its proper position; the eye will be compressed and the ocular pressure will increase [105].

Osteoplasty is the next stage of enophthalmos correction following the separation and dissection of the cicatricial tissue.

The CAD/CAM (computer-aided design and computer-aided machinery) technology [203, 321, 414, 423–427] borrowed from the industry has recently been widely used instead of stereolithography to manufacture 3D implants identical to a missing bone fragment [428, 429].

Spiral CT data are processed using specialized software (e.g., Mimics software package developed by Materialise) to obtain a 3D virtual model of the damaged orbit and superimpose it into the mirror image of the contralateral intact orbit.

Thus, a virtual template for a future implant can be designed [430]. The next stage involves formation of the 3D construct made of titanium [423–425, 431] or Bioverit II [327], which is an identical copy of the missing bone fragment. The final step is implantation of the construct under telemonitoring, which allows one to repair the damaged orbit with less than 1 mm deviation from the calculated values [432–435]. Drawbacks of the CAD/CAM procedure include its high cost (USD 3500) and long production time (48 h). These problems should be solved due to the industrial production of preformed 3D titanium implants of several nominal sizes [436–438].

If complete reconstruction of orbital walls under telemonitoring cannot be performed, the increased orbital volume is replaced by subperiosteal implantation of the donor or synthetic material [422, 439].

Matsuo et al. [420] proposed a simple procedure for semiquantitative correction of posttraumatic enophthalmos. A latex form is made of the patient's face, and molding compound is dropped using a syringe onto the imprint of the enophthalmic orbit until the imprints of the orbital areas become symmetrical. The syringe scale demonstrates the volume of autologous costal cartilage that needs to be placed subperiosteally onto the orbital floor (or, if needed, onto the lateral and medial walls as well) behind the equator of the eye. The surgery is expected to provide a mild 1–2 mm overcorrection; otherwise, enophthalmos will develop once the reactive edema of orbital tissues subsides [197].

Recently, mathematical calculations based on CT scans have demonstrated a clear linear relationship between the traumatic increase in orbital volume and the degree of enophthalmos [440]. In particular, each cubic centimeter of orbital volume augmentation causes 0.8–0.9 mm enophthalmos [90, 337, 411, 418, 441, 442]. The orbital volume in patients with extensive fractures of the orbital floor increases by 3–4 cm^3 on average [335, 337], and the volume of orbital fat prolapsed through the fractured area is ~3 cm^3 [443].

Hence, having measured the orbital volume using CT and the corresponding software, one can select the required volume of a wedge-shaped implant for primary osteoplasty to prevent late onset enophthalmos which would require secondary orbital repair [20, 291, 444].

Another procedure can be used if even the maximum possible implant size fails to correct enophthalmos or there is a high risk of ocular hypertension or distortion. In this case, some contralateral orbital adipose tissue can be removed to achieve facial symmetry by deepening the contralateral upper eyelid sulcus.

If a patient has cosmetically apparent enophthalmos, accompanied by no or poor vision in that eye, a convex magnifying lens may be worn in front of that eye.

Correction of concomitant hypoglobus is a simpler procedure. A special implant is placed under the equator of the eyeball [202]. A simple procedure for determining the thickness of the implant for hypoglobus correction was proposed. After orbitotomy, the globe and the surrounding adipose tissue were lifted above the orbital floor. Legs of the ophthalmic calipers were placed in the resulting space at a depth of 12–14 mm. The caliper legs were expanded until the eyeball being displaced acquired the proper position. The caliper scale was used to determine the required thickness of a wedge-shaped graft.

Rare Reasons for Late Enophthalmos

Enophthalmos after orbital floor fracture can be caused by obturation of the maxillary sinus ostium by prolapsed orbital adipose tissue. In this case, the mechanism of enophthalmos development is identical to that of the silent sinus syndrome[27] [445–448]. The orbital floor, like other walls of the maxillary sinus, is misshaped, thus increasing the orbital volume. After diagnosis is verified using CT, recovery of sinus aeration and osteoplasty of the orbital floor are recommended [446].

3.4.8 Infraorbital Nerve Neuropathy

The most common late complications of orbital floor fracture, observed in 18–32 % of patients, include sensory disturbances in the innervation zone of the infraorbital nerve [93, 202, 238, 389, 391].

The degree of posttraumatic neuropathy depends on fracture location and type, as well as by displacement of bone fragments. The most unfavorable situation is when the nerve trunk is in the fractured area. In this case, neuropathy develops in 100 % of cases and does not recover even 1 year after trauma manifested as persistent hypesthesia. Displaced fractures cause persistent and long-term paresthesia in almost 90 % of patients. Non-displaced fractures are associated with the risk of developing transient neuropathy in 50 % of patients [449].

The risk of long-term infraorbital nerve dysfunction significantly increases if surgical management of the fracture is delayed.

3.4.8.1 Infraorbital Nerve Hyperesthesia

Tengtrisorn et al. [450] described a rare complication of infraorbital nerve hyperesthesia that persisted for 1–2 years after blunt trauma of the orbit. Orbital nerve decompression completely eliminated this complication. Thus, persistent infraorbital nerve hyperesthesia is an indication for late orbital floor reconstruction including single-stage nerve decompression.

3.4.8.2 Abnormal Pupillary Response

Stromberg and Knibbe [451] reported transient anisocoria that developed after orbital floor reconstruction that lasted for 2 h. The reason for it was short-term blockade of parasympathetic postganglionic fibers located deep in the inferior oblique muscle (Fig. 3.37). Bodker et al. [452] believe that along with manipulations on the inferior oblique muscles, mydriasis and the absence of pupillary response can be caused by traumatic injury of the ciliary ganglion when closing the posterior orbital floor fracture.

[27] The silent sinus syndrome was first described by Montgomery in 1964. About 125 cases have been reported. The syndrome is characterized by progressive painless reduction of the maxillary sinus size and resorption (osteopenia) of its walls in patients with ostium blockade and chronic hypoventilation. Sinus atelectasis is seen on CT scans. Surgeries enhancing sinus ventilation provide a favorable effect.

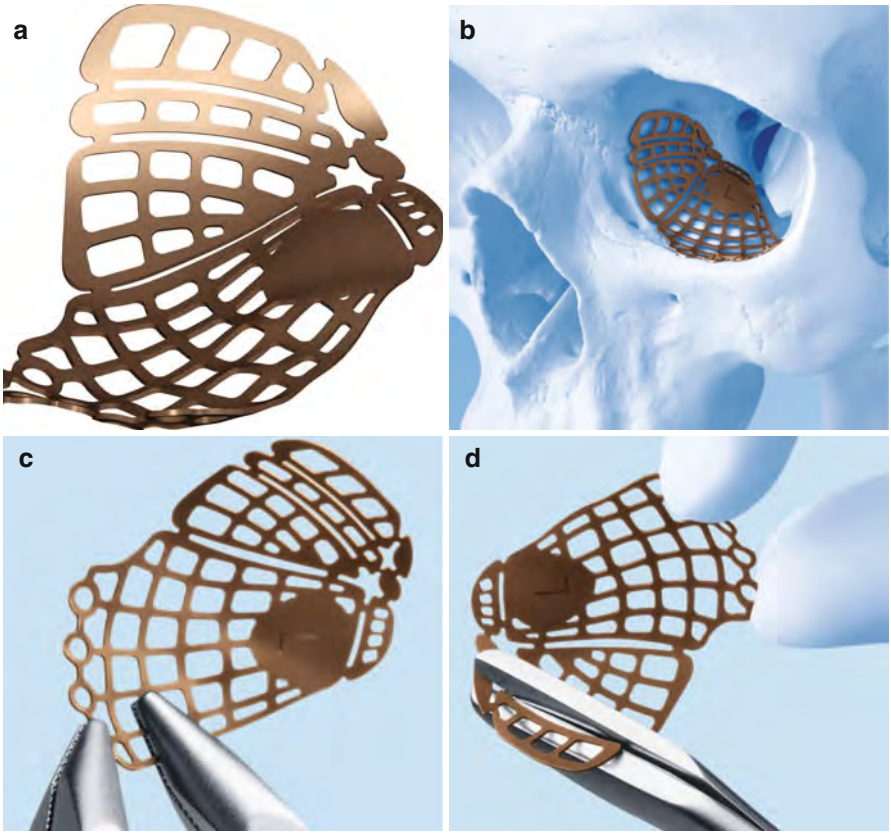

Fig. 3.37 Preformed 3D titanium implants (using products of the Synthes company (Switzerland) as an example): (**a**, **b**) An implant designed by digital processing of CT scans duplicates the contour of the inferior and medial orbital walls to a maximum possible extent, thus making it possible to close even the extensive inferomedial fractures. (**c**, **d**) Possibility to shape a plate using special tools

3.4.9 Cyst Formation Around an Implant

Formation of an inclusion cyst around an implant made of nonporous polymers such as silicone [295, 453–456] or less frequently Teflon[28] [289, 457] and Supramid [458] is a rare late complication of orbital floor reconstruction.

The clinical presentation includes complaints of impaired vision, fullness sensation in the orbit, and diplopia. Ophthalmic examination reveals chemosis of the inferior conjunctival fornix, hypertopia, exophthalmos, impeded retropulsion of the eyeball to the orbit, and marked oculomotor disorders. A fistula connecting the

[28] The rate of this complication was 3.8 % when monolithic Teflon was used [289].

pseudocapsule cavity around the implant with the inferior conjunctival fornix can be found [459].

The effect of the cyst may be seen by ophthalmoscopy which may show scleral invagination in the lower quadrants secondary to compression caused by the cyst [455, 460]. A structure with soft tissue optical density and rather clear contours which is adjacent to the orbital floor and displaces the eyeball upward can be seen around the implant in a CT scan [461]. A thick pseudocapsule was found around the plate during diagnostic orbitotomy. Cyst contents with volume of 1–2 ml are usually of hemorrhagic origin [462–465].

The clinical presentation is nonspecific; therefore, one must differentiate between the cyst and inflammation caused by implant infection and cellulitis and vascular orbital pathologies such as orbital venous varix, carotid–cavernous fistula, and other orbital pathologies. Mucocele and sino-orbital fistulas can have similar symptoms as well [259].

The management includes cyst puncture, aspiration of cyst contents, implant removal, and partial dissection of the capsule without opening the paranasal sinus. Explantation of the monolithic monomer is not associated with any technical complications because the orbital floor defect is already replaced by newly formed osseous tissue. This tissue is covered by a thick pseudocapsule so that neither functional nor cosmetic disorders occur at the time of implant removal [235, 289].

Histological examination of the dissected tissues reveals that the cyst can be lined with one of three tissue types: stratified non-squamous conjunctival epithelium that was introduced during the transconjunctival approach, stratified squamous epithelium introduced during the transcutaneous approach, and ciliary respiratory tract epithelium that was introduced to the orbit when soft tissues prolapsed into the maxillary sinus were repositioned [457–462, 465].

3.4.10 Sino-orbital Fistula

The formation of a sino-orbital fistula is a rare late complication of orbital floor repair [366, 466]. The clinical presentation includes complaints of full bursting pain in the orbit, diplopia, intermittent hypertopia, proptosis, and limited retropulsion of the eyeball caused by air that penetrated into the orbit during nose blowing. Rapid regression of symptoms within several days after the air stops penetrating into the orbit is a significant diagnostic factor [463]. An *air-bearing* soft tissue structure that closely communicates with the paranasal sinus is seen around the implant on a CT scan, which allows one to easily differentiate between the sino-orbital fistula and inclusion cyst or orbital venous varix, which is another potential reason for transient exophthalmos.

Osteoplasty using synthetic nonporous materials, primarily silicone, is found in the past medical history of these patients [467]. While the rigid plate supports the orbital tissues, it cannot seal the bone defect because it cannot duplicate all the curvatures of the orbital floor. As a result, any increase in intranasal pressure may cause air

penetration into the orbital cavity through the maxillary sinus and the bone defect. It is clear that an implant needs a certain amount of elasticity to both to have a supporting function and to seal the opening in the orbital floor. The management includes implant removal, partial dissection of its pseudocapsule and the adjacent paranasal sinus epithelium, and sealing the orbital floor defect with a more elastic implant [468].

3.4.11 Implant Migration

The implant most typically migrates forward (under the lower eyelid skin) and is subsequently exposed or, less frequently, migrates posteriorly resulting in optic nerve compression or medially causing chronic dacryocystitis [469].

Massaro-Giordano et al. [470] reported a very unusual case of migration of an orbital implant that was used to close a traumatic orbital floor defect 25 years previously. The patient sought medical assistance because the implant migrated through the ethmoidal labyrinth and the nasal septum causing sinusitis and impaired nasal respiration.

Liu and Al-Sadhan [471] reported a similar complication 7 years after the use of a silicone orbital floor osteoplasty. The implant migrated into the nasal meatus and reached the nasal septum. The clinical presentation included impaired nasal respiration, discharge from nasal meatus, induration in the lower eyelid and its poor mobility, shortening of the inferior conjunctival fornix, and a cutaneous fistula. This complication was easily diagnosed by endoscopy of the nasal meatus and CT scanning.

The main reasons for these complications include the large size and improper fixation of a solid synthetic, usually silicone. The management includes explantation and surgical elimination of the cicatricial deformation of the lower eyelid, dacryocystitis, fistula, etc.

3.4.12 Dislocation of the Globe into the Maxillary Sinus

In rare cases, the total orbital floor fracture may cause dislocation[29] of the globe into the maxillary sinus, which is often complicated by rupture of the extraocular muscles [472, 473] (Fig. 3.38). Globe repositioning, closure of the bone defect, and suturing the damaged extraocular muscles are feasible procedures and must be performed; however, ocular motility and central vision usually cannot be restored [474, 475]. Ophthalmic examination reveals a pale optic disk in these patients, which is indicative of its severe injury [476].

[29] Classification of traumatic dislocation of the globe: luxation, forward protrusion of the eyeball from the orbit; dislocation, migration of the eyeball into the paranasal sinuses or the nasal cavity; and avulsion, forward protrusion of the globe accompanied by rupturing of the extraocular muscle or the optic nerve.

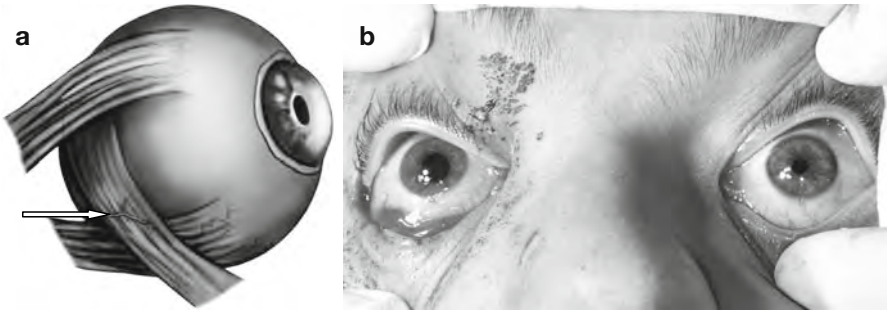

Fig. 3.38 Parasympathetic postganglionic fibers (**a**) localizing deep in the inferior oblique muscle; intraoperative damage to these fibers causes short-term mydriasis (**b**)

Dislocation of the globe into the maxillary sinus is sometimes mistaken for traumatic enucleation [473, 477]. This mistake can be avoided by performing computed tomography.

Smit et al. [478] reported a rare case from their own practice. A male patient who had a diagnosis of "anophthalmic syndrome" on the right side sought their medical assistance because he was dissatisfied with his aesthetic appearance. The past medical history showed that the patient had a car accident 5 years previously resulting in a severe midfacial fracture and primary traumatic enucleation of the globe. According to the original surgical repair operative report, the eyeball remnants were removed and facial bones were repositioned. CT scanning performed 5 (!) years later showed a total orbital floor fracture and the eyeball (without phthisical signs) located in the maxillary sinus.

3.4.13 Upper Eyelid Retraction

Enophthalmos and pseudoptosis are typical of blow-out fractures; however, extremely rare cases of upper eyelid retraction 1–2 months after trauma have been reported [479–481].

One of the tentative mechanisms is the overactivity of the superior rectus muscle and the levator palpebrae superioris muscle caused by a hypotropic eye trying to obtain its proper position.

Reifler [479] believes that deepening of the upper eyelid groove and eyelid retraction are caused by enophthalmos induced by orbital fat atrophy. Recession of the levator palpebrae superioris muscle is the operation of choice.

The hypothesis that the inferior rectus muscle prolapsed into the fractured area pulls the superior rectus muscle and the levator palpebrae superioris muscle through the system of orbital septa does not sound convincing. The hypothesis that this phenomenon is based on hyperfunction of the Müller's muscle also raises doubts, since pathogenetically reasonable interventions have no effect in similar situations.

3.4.14 Complications Caused by Using the Approach to the Orbital Floor

Any existing approach to the orbital floor—either the transcutaneous (infraorbital or subtarsal), or the subciliary, or the transconjunctival one—is associated with unique potential complications.

The infraorbital approach is associated with the worst functional and aesthetic outcomes because lymphostasis, lacrimation disorders, and gross scarring may occur (Fig. 3.39a) [162].

The subciliary incision appears to be preferable as it provides good visualization of the orbital floor and leaves a negligible cutaneous scar (Fig. 3.39b). However, the subciliary approach can be complicated by lower eyelid malposition manifested by rounding of the lateral margin of the palpebral fissure, with retraction and eversion being two variants (Fig. 3.39c–e) [149, 186, 482]. While the latter complication develops in 3 % of cases, eyelid shortening is observed in about 20 % of patients [482].

The reason for rounding of the lateral angle of the palpebral fissure is the loss of tone of the lower eyelid caused by iatrogenic denervation of pretarsal fibers of the orbicularis oculi muscle (see the description of the subciliary approach procedure) [483]. The so-called snapback test is used to evaluate eyelid tone: the eyelid should snap back quickly and firmly after being pulled down by an index finger. Atony is diagnosed if the eyelid fails to provide firm contact or its snapping back is rather slow.

To eliminate rounding of the lateral angle, it is sufficient to shorten the lateral palpebral ligament so that it returned in its original position so that the lateral canthal angle is located 2 mm above the medial angle.

Lower eyelid eversion is caused by cicatricial shortening of the anterior musculocutaneous palpebral plate. Isolated shortening of the posterior plate (the retractor muscle and the conjunctiva) results in entropion, which is a more rare complication [151, 152]. The median plate (the tarso-orbital fascia) is most commonly cicatrized, which results in retraction of the atonic lower eyelid [149, 155, 202] by the excessive surgical trauma and fascial traction during sewing the periosteum.

The exposure of the normally covered sclera at the inferior limbus develops during the second postoperative week [93, 484] and usually is transient. If exposure is present in the early postoperative period, the patient is recommended to regularly perform forceful blinking and palpebral massage during this period. Corticosteroid injection into the deep tissues has a positive effect [12]. However, surgical treatment is required in 6–9 % of cases and should only be performed if the exposure persists after 6 months of observation and conservative therapy [162].

The *vertical traction test* needs to be performed to determine the scope of intervention. The lower eyelid elasticity normally allows one to pull its ciliary edge up to the superior limbus. If only the skin is contracted by scar tissue (the anterior plate), the eyelid still can be pulled up onto the cornea although it is rather difficult. Cicatrization of the median plate (the tarso-orbital fascia) significantly limits eyelid

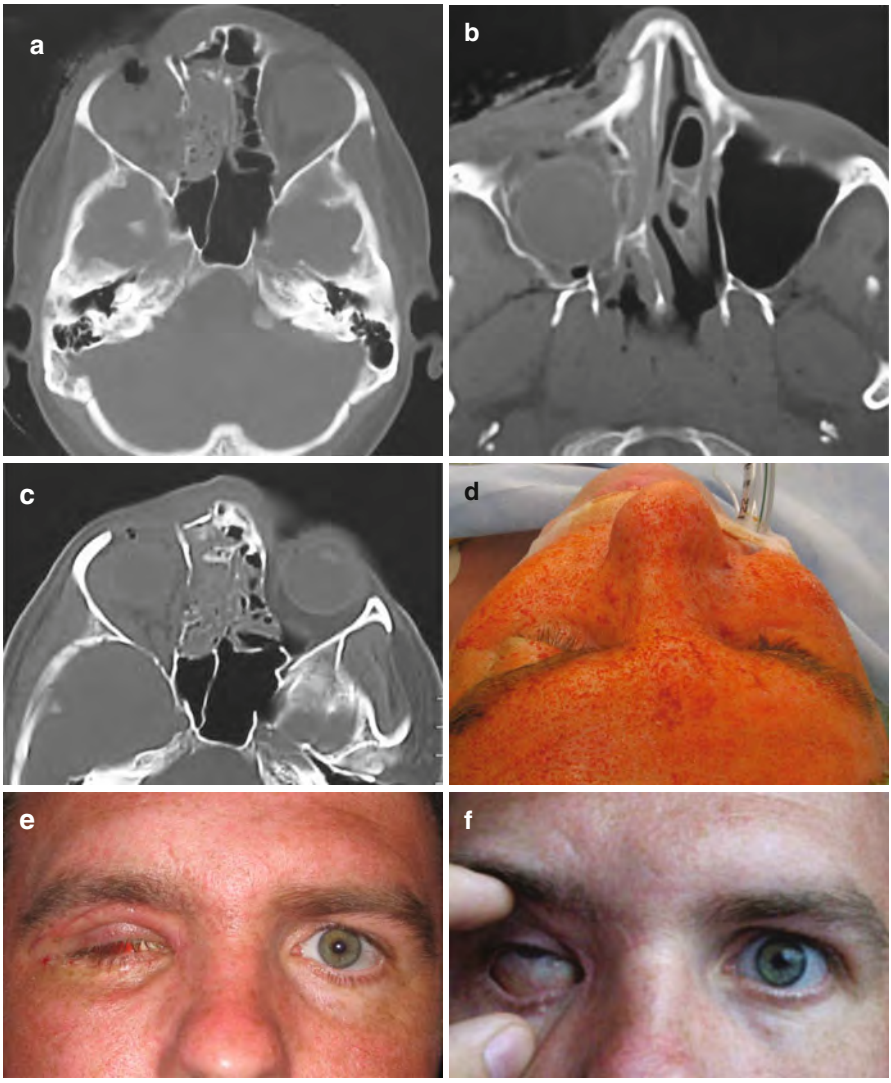

Fig. 3.39 Dislocation of the globe into the maxillary sinus (authors' own observation): (**a**) Axial CT scanning shows that there is no eye in the orbit. (**b**) The eyeball is located in the sinus. (**c**) CT control after eye repositioning into the orbit (single-stage reconstruction of the inferomedial fracture was not performed because the operation was urgent and patient's general condition was critical). (**d**) Enophthalmos. (**e**) Ptosis. (**f**) Restrictive strabismus, the absence of vertical excursions of the eyeball in the outcome of multistage surgical treatment

mobility, and its surgical correction is very challenging. The tarso-orbital fascia is dissected through the transconjunctival approach and lengthened by grafting a flap harvested from the hard palate mucous membrane [12, 482, 485]. The final stage of the intervention is shortening the lateral palpebral ligament.

Park and Meyer [486] reported a case of lower eyelid epiblepharon that developed in a child after the subciliary approach to a zygomatic orbital fracture. Such a rare complication was caused by excessive surgical trauma followed by extensive scarring of the lower eyelid retractor, fibers of the orbicularis oculi muscle, and the orbital septum.

The main complications of the transconjunctival approach occur less than 4 % of the time and include shortening of the lower conjunctival fornix, eversion and retraction of the lower eyelid, pyogenic granuloma, conjunctival cyst, and epiphora [149, 155, 186, 202, 487]. Transient chemosis of the bulbar conjunctiva, transection of lacrimal canaliculi and damage to the lower eyelid, up to complete avulsion, and lacrimal sac injury have been reported [155, 161, 487].

Eyelid malposition does not require surgical correction in most cases. The so-called pyogenic granuloma results from disrupted regeneration of the conjunctival tissue surrounding the sutures; hence, treatment starts with suture removal and local glucocorticoid therapy; the excess granulation tissue is dissected if these measures have no effect.

3.5 Linear-Type Fracture of the Orbital Floor

The linear-type trapdoor or "greenstick" fracture was first described by Soll and Poley in 1965 [488]. It is the most common type of pediatric orbital fractures as children have elastic osseous tissue [70, 387, 489–491] and is observed in 30 % of adult patients.

3.5.1 The Mechanism of Trapdoor Fracture Formation

The trapdoor fracture is initiated by moderate impact exerted onto the infraorbital rim causing wavelike deformation propagating through the orbital floor [387, 491]. It gives rise to a linear or an arc-shaped fracture along the infraorbital rim and displacement of the anteromedial portion of the orbital floor under the posterolateral portion (Fig. 3.40a–c) [387, 491]. The superimposed osseous plates form the jaws of the trapdoor for orbital tissues. After the initial impact, the orbital rim returns in its original position; the orbital floor fragments return to normal position; however, the soft tissues that did not return into the orbital cavity remain entrapped in the fractured area (Fig. 3.40d, e).

In addition to entrapment of the muscle or connective tissue intersections, in case of the lateral linear-type trapdoor fracture, oculomotor disorders may also be caused by entrapment of the oculomotor nerve branchlet running to the inferior oblique muscle [492].

Fig. 3.40 The outcomes of using various approaches to the orbital floor: (**a**) A coarse cicatrix after using the infraorbital approach, which caused long-term lymphostasis. (**b**) A negligible cicatrix when using the subciliary incision. (**c**) Atonic eversion of the lower eyelid caused by denervation of the pretarsal portion of the orbicularis oculi muscle after the inadequately performed subciliary approach. (**d**) Retraction of the lower eyelid of the right eye caused by excessive scarring of the tarso-orbital fascia that developed after the repeated subciliary approach to the orbital floor. Retraction of the lower eyelid of the left eye that complicated the traumatic subciliary incision comes under notice. (**e**) Eversion of the lower eyelid caused by cicatricial shortening of the anterior (musculocutaneous) palpebral plate. (**f**) Good aesthetic outcome of using the transconjunctival approach

Since the fracture occupies less than 5–15 % of the surface area of the orbital floor, the pressure, both in the orbit and in the connective tissue sheath of the inferior rectus muscle, may increase abruptly at the moment of trauma. This results in strangulation necrosis or, in milder cases, ischemic contracture of muscular fibers entrapped in the fractured area [110, 489].

3.5.2 Clinical Presentation

Complaints of painful eye movements and diplopia are typical of the trapdoor fracture [493, 494]. The former symptom unequivocally indicates that a muscle is entrapped in the fractured area, while the latter one can be caused by isolated entrapment of connective tissue intersections [387]. Seventy-five percent of patients have nausea and vomiting. These symptoms are much less frequent for the classical blow-out fracture, known as the open-door fracture as opposed to the trapdoor one. Pain and diplopia are present in 64 % of cases, with nausea and vomiting, in only 14 and 7 % of cases, respectively [495].

The cooperation of a pediatric patient is very limited in this circumstance and impede the possibility of the traction test; therefore, objective examination and CT data are necessary to make a reliable diagnosis [490].

Criden and Ellis [491] found limited upward eye movement in all the patients with entrapped muscles and additional limited eye movement downward in 50 % of cases.

P*ronounced oculomotor disorders are a cardinal symptom of the trapdoor fracture* [387]. *Meanwhile, enophthalmos is three times less frequent than oculomotor disorders* [493]. *Periorbital edema is less severe than that in adult patients and regresses twice as rapidly*: on average within 3 days instead of seven [490]. Fifty percent of children have eye blunt globe injury, which suggests that a thorough ophthalmic examination if required [496].

The incongruence between the clinical presentation of the trauma and its severity is a feature of the trapdoor fracture, which impedes timely diagnosis and treatment of this pathology [139, 494, 495, 497]. Since the clinical symptoms are vague and often misleading for a surgeon, these fractures are known in English-language literature as “the white-eye blow-out fracture” [139], as opposed to the conventional “red-eye blow-out fracture.”

The CT presentation of the trapdoor fracture is also characterized by lack of symptoms [16, 498]. Local entrapment of the muscle in the fractured area can be seen on a CT scan in only 25 % of cases; in the remaining cases, the muscle is only adjacent to the bone defect area, being indicative of entrapment of connective tissue intersections [387]. MRI is useful in such cases as it visualizes even the minimal volume of soft tissues that were displaced to the fractured area [499].

3.5.3 Treatment

The 2-week observation period, reasonable for adult patients, should not be used for this type of fracture in the pediatric population [10, 110, 489, 490, 494]. Due to good blood circulation and rapid healing response in children, callus is formed rapidly and embeds the soft tissues entrapped in the fractured area [164]. Hence, operative management within the first 2–7 days needs to be performed to avoid irreversible oculomotor disorders [70, 139, 387, 440, 500].

Each of the criteria listed below or their combination is an indication for surgery [501]:

- Limited vertical eye movement, in particular when combined with pain, nausea, and vomiting.
- Diplopia (if a child can identify it).
- CT signs of entrapment of the muscle or its connective tissue sheath in the fractured area are indications for surgical intervention only if the *proper clinical symptoms are observed*.

Thirty-three to fifty percent of patients need surgical management [16, 70, 496, 501, 502].

3.5.3.1 Surgical Strategy for the Trapdoor Fracture

The absence of orbital floor defect allows one to manage without grafting [255].

In order to release the soft tissues entrapped in a trapdoor fracture, a surgeon needs to push the leaflet and move it upward from the maxillary sinus with a hook (Fig. 3.41a). Lined with the periosteum on one side and with the mucous membrane on its other side, the leaflet is a vital bone graft. Once the leaflet is moved upward and a surgeon makes sure that its pedicle is strong enough, it is sufficient to fix its free edge with a titanium microplate or a mesh (Fig. 3.41b–d). Repositioning of the

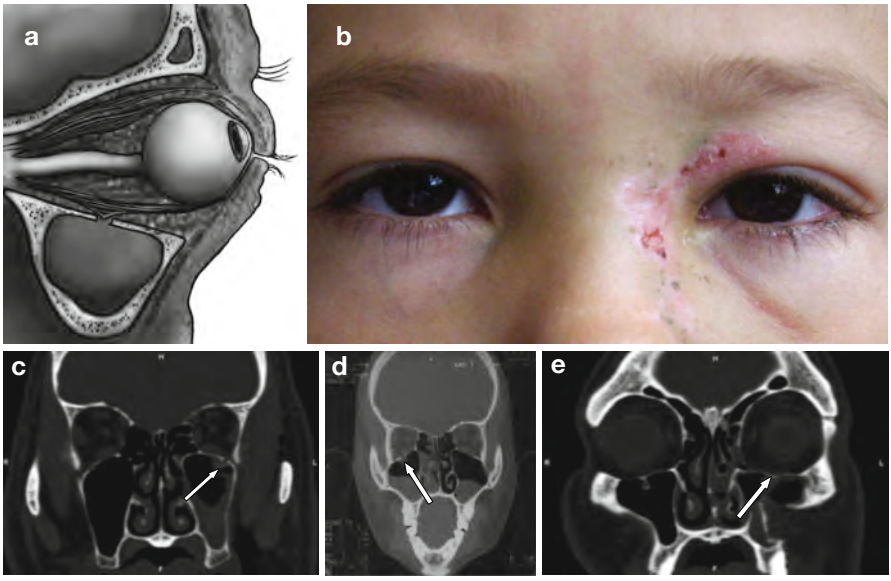

Fig. 3.41 Linear-type orbital floor fracture: (**a**) Schematic representation. (**b**) The minimal changes in the auxiliary apparatus of the eye. Skin abrasion in the periorbital area indicates that the fracture was induced by direct impact of a wounding agent on the orbital rim. (**c**) Displacement of the anteromedial leaflet under the posterolateral one, which is typical of this type of fracture. (**d**, **e**) Minimal entrapment of soft tissues in the trapdoor fracture zone

osteomucoperiosteal flap provides fast healing of the orbital floor, proper sinus drainage, and the absence of complications associated with implant use.

The release of the entrapped muscle rapidly eliminates bradycardia, nausea, and vomiting [10, 493]. The rates of regression of diplopia and oculomotor disorders are determined by the period during which surgical management is performed.

The oculomotor function is restored within 4 days if surgery was performed within the first week after trauma, or on average within 10–18 days if surgery was performed during the second week after trauma. A 15-day delay in surgical management increases the rehabilitation duration up to 50 days [504]. Complete, although slow, recovery of ocular motility and elimination of diplopia can be expected even 1 month after trauma [10]. All other conditions being equal, regression of diplopia in children below 9 years of age takes twice as long as in 10–15-year-old adolescents [70].

3.6 Blow-In Orbital Floor Fracture

Blow-in orbital floor fractures are rare. The first case of a blow-in orbital floor fracture in a patient with extensive injury of the anterior wall of the maxillary sinus and infraorbital rim was reported in 1964 [505].

Fractures of this type are most commonly caused by car accidents. The other mechanisms such as falls from a height, violence, household, or sports-related injuries play a secondary role. Since blow-in orbital fractures are high-energy injuries, the fracture also affects the other facial structures in 73 % of patients and is aggravated by concomitant head injury in every other patient [505].

Fractures are differentiated into isolated blow-in fractures and combined ones (i.e., fractures of the infraorbital rim and the orbital floor). While the emergence of a combined fracture of the infraorbital rim and the orbital floor can be attributed to the direct impact of a wounding agent moving upward into the anterior wall of the maxillary sinus, it is much more difficult to explain the genesis of an isolated blow-in fracture of the orbital floor. There is skepticism about the hypothesis that pressure in the maxillary sinus is abruptly increased because of transient deformation of facial bones at the moment of impact; however, no other suggestions have been made so far.

As opposed to blow-out fracture, fragments of the infraorbital rim and/or the orbital floor are displaced upward, thus causing the characteristic and clearly defined complex of symptoms for reduction of orbital volume (Fig. 3.42) [506, 507]. The clinical presentation is determined by the degree to which the orbital volume is reduced and consists of the following typical symptoms:

- *Vertical dystopia* (hypertopia of the globe) indicates that the blow-in fracture of the orbital floor has an anterior localization. *Axial dystopia* (proptosis or exophthalmos) indicates that the blow-in fracture has a post-equatorial localization and is observed more commonly. Other signs of globe dystopia include widening of the palpebral fissure, visible scleral strip near the limbus at the 6 and 12 o'clock positions, conjunctival injection, chemosis, and epiphora.

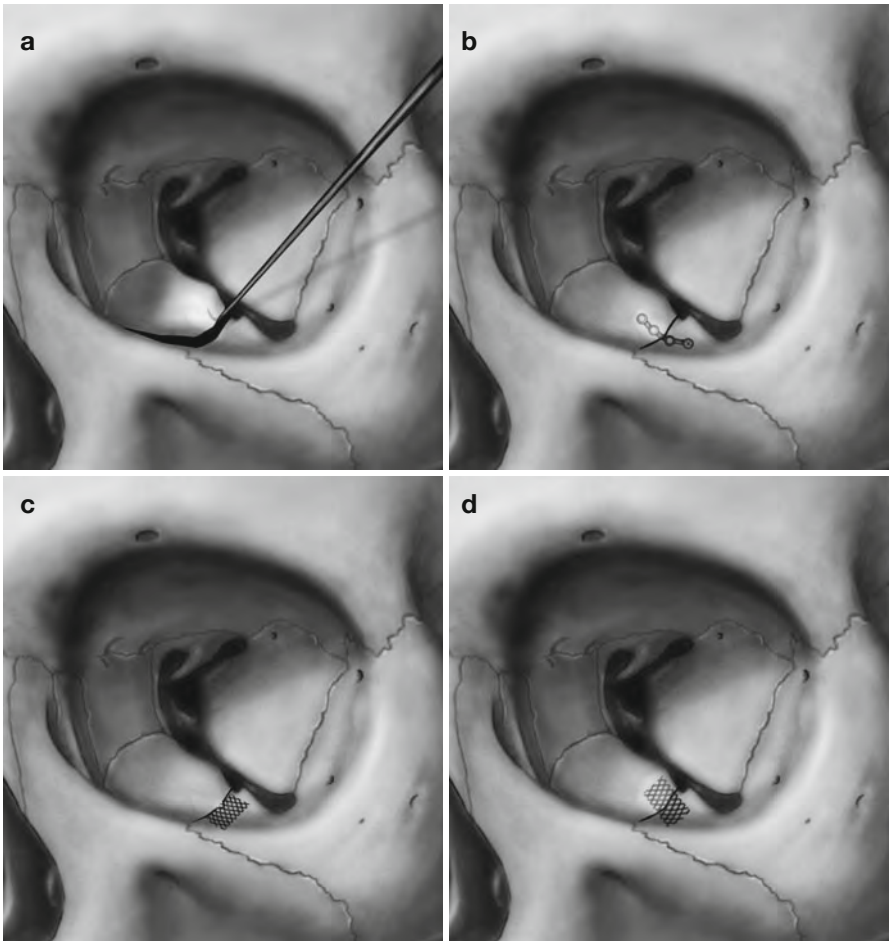

Fig. 3.42 Surgical strategy in patients with trapdoor fractures (Adapted from Burm et al. [503]): (**a**) The leaflet is carefully (!) moved forward from the maxillary sinus with a hook. (**b**) The bone fragment is fixed with a titanium microplate placed below it (12–15 mm long, 5 mm wide, and 0.2 mm thick). The plate needs to lie not in the maxillary sinus but in a specially formed submucosal pocket. The other edge of the titanium construct is carefully (to avoid damaging the infraorbital nerve) fixed with a 2-mm screw 1.2 mm in diameter to the thick anterior portion of the orbital floor (the cantilever fixation procedure). (**c**) If the leaflet has a small protrusion (a ledge), immobilization is achieved by placing a 15×6 mm titanium mesh below it. No rigid mesh fixation is required (the ledge fixation procedure). (**d**) If there is no ledge, leaflet is fixed by placing a mesh below it (the cantilever fixation procedure)

- *Oculomotor disorders and diplopia* are observed in 25 and 30 % of cases, respectively, and are mostly caused by an abrupt increase in orbital pressure or the mechanical impact exerted by a bone fragment/subperiosteal hematoma on the inferior muscle complex [506]. Muscle imbalance is a sign of the superior orbital fissure syndrome in 10 % of patients or the orbital apex syndrome in 3 % of patients.
- *Posttraumatic neuropathy of the optic and infraorbital nerves.*

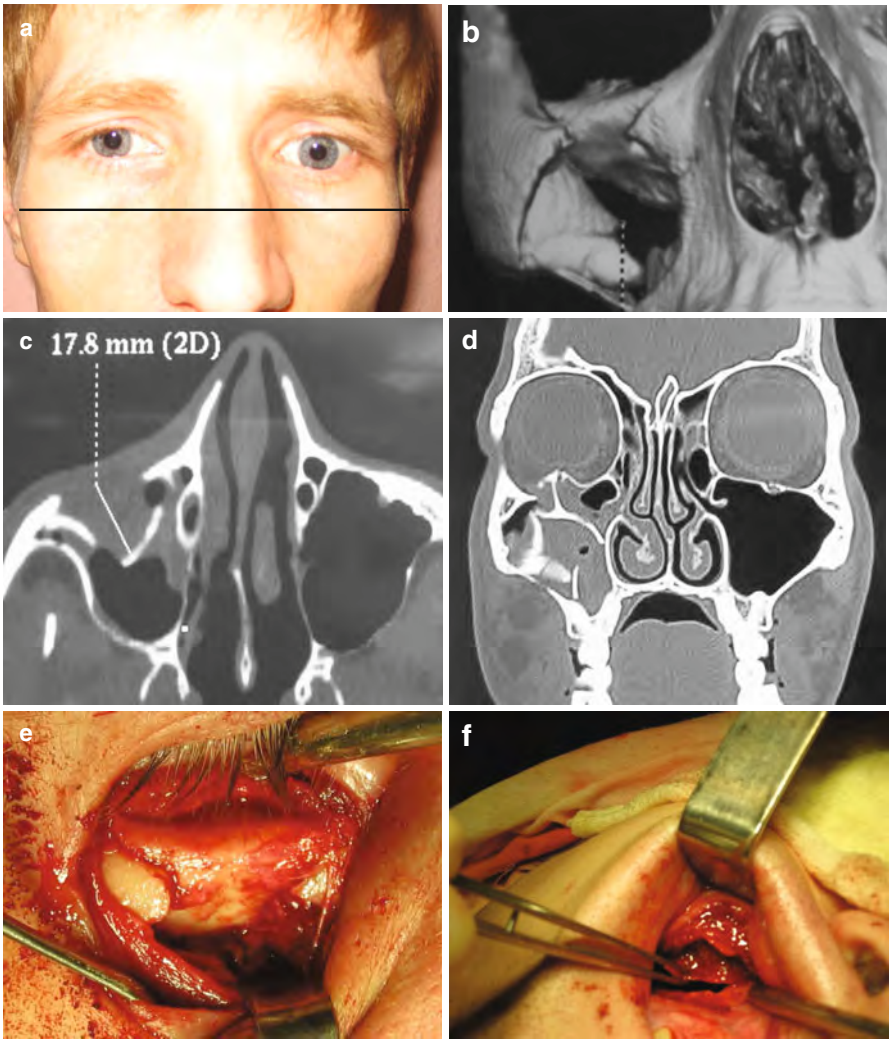

Fig. 3.43 Blow-in fracture of the right orbit (patient S.): (**a**) Patient's appearance. Depression of the right infraorbital area and hypertopia of the right globe were revealed during examination. (**b**) 3D reconstruction of the comminuted blow-in fracture of the anterior wall of the maxillary sinus. (**c**–**d**) Displacement of bone fragments into the orbit inducing hypertopia and compression of the globe. (**e**) Intraoperative presentation of the fracture. (**f**) The detached fragment of the anterior wall of the maxillary sinus (Courtesy of M.M. Solovyev)

The diagnosis is made based on the typical signs of acute traumatic orbital compartment syndrome listed above and the coronal and sagittal CT data. Meticulous preoperative ophthalmic examination is required because of the high (12 %) risk of eyeball injury by bone fragments.

3.6.1 Treatment

All patients with blow-in orbital floor fractures require early, single-stage, and meticulous surgical management.

Infraorbital rim fragments are repositioned and fixed with titanium miniplates. Displacement of large orbital rim fragments usually destroys the adjacent orbital floor, making it necessary to perform orbital floor repair using titanium or porous synthetic implants.

Thorough fracture reconstruction minimizes the risk of developing early and late complications caused by inadequate reconstruction of the orbital floor and orbital volume [506] (Fig. 3.43).

References

1. Ferreira, P., Marques, M., Pinho, C., et al. (2004). Midfacial fractures in children and adolescents: A review of 492 cases. *British Journal of Oral and Maxillofacial Surgery, 42*(6), 501–505.
2. Chi, M. J., Ku, M., Shin, K. H., & Baek, S. (2010). An analysis of 733 surgically treated blowout fractures. *Ophthalmologica, 224*(3), 167–175.
3. Hwang, K., You, S. H., & Sohn, I. A. (2009). Analysis of orbital bone fractures: A 12-year study of 391 patients. *The Journal of Craniofacial Surgery, 20*(4), 1218–1223.
4. de Concilis, C. (1996). Epidemiology of orbital pathology. In S. Bosniak (Ed.), *Principles and practice of ophthalmic plastic and reconstructive surgery* (2nd ed., Vol. 2, pp. 853–859). Philadelphia: Saunders.
5. Chang, E. W., & Manolidis, S. (2005). Orbital floor fracture management. *Facial Plastic Surgery, 21*(3), 207–213.
6. Repanos, C., Carswell, A. J., & Chadha, N. K. (2010). Manipulation of nasal fractures under local anaesthetic: A convenient method for the Emergency Department and ENT clinic. *Emergency Medicine Journal, 27*(6), 473–474.
7. Siritongtaworn, P. (2001). Correction of severe enophthalmos with titanium mesh. *Journal of the Medical Association of Thailand, 84*(Suppl 2), 485–490.
8. Siritongtaworn, P., Tongsawas, S., & Siltharm, S. (2001). Diplopia in facial fractures. *Journal of the Medical Association of Thailand, 84*(Suppl 2), 491–494.
9. Tong, L., Bauer, R. J., & Buchman, S. R. (2001). A current 10-year retrospective survey of 199 surgically treated orbital floor fractures in a nonurban tertiary care center. *Plastic and Reconstructive Surgery, 108*(3), 612–621.
10. Baek, S. H., & Lee, E. Y. (2003). Clinical analysis of internal orbital fractures in children. *Korean Journal of Ophthalmology, 17*(1), 44–49.
11. Shahim, F. N., Cameron, P., & McNeil, J. J. (2006). Maxillofacial trauma in major trauma patients. *Australian Dental Journal, 51*(3), 225–230.
12. Cole, P., Boyd, V., Banerji, S., & Hollier, L. H. (2007). Comprehensive management of orbital fractures. *Plastic and Reconstructive Surgery, 120*(7 suppl 2), 57S–63S.
13. Manolidis, S., Weeks, B. H., Kirby, M., et al. (2002). Classification and surgical management of orbital fractures: Experience with 111 orbital reconstructions. *The Journal of Craniofacial Surgery, 13*(6), 726–737.
14. Posnick, J. C., Wells, M., & Pron, G. E. (1993). Pediatric facial fractures: Evolving patterns of treatment. *Journal of Oral and Maxillofacial Surgery, 51*(8), 836–844.
15. Koltai, P. J., Amjad, I., Meyer, D., & Feustel, P. J. (1995). Orbital fractures in children. *Archives of Otolaryngology – Head & Neck Surgery, 121*(12), 1375–1379.

16. Bansagi, Z. C., & Meyer, D. R. (2000). Internal orbital fractures in the pediatric age group: Characterization and management. *Ophthalmology, 107*(5), 829–836.
17. Kaltreider, S. A. (1996). Orbital fractures. In S. Bosniak (Ed.), *Principles and practice of ophthalmic plastic and reconstructive surgery* (2nd ed., Vol. 2, pp. 1085–1102). Philadelphia: Saunders.
18. Hatton, M. P., Thakker, M. M., & Ray, S. (2002). Orbital and adnexal trauma associated with open-globe injuries. *Ophthalmic Plastic and Reconstructive Surgery, 18*(6), 458–461.
19. Gewalli, F., Sahlin, P., Guimaraes-Ferreira, J., & Lauritzen, C. (2003). Orbital fractures in craniofacial trauma in Goteborg: Trauma scoring, operative techniques, and outcome. *Scandinavian Journal of Plastic and Reconstructive Surgery and Hand Surgery, 37*(2), 69–74.
20. Chang, E. L., & Bernardino, C. R. (2004). Update on orbital trauma. *Current Opinion in Ophthalmology, 15*(5), 411–415.
21. Shere, J. L., Boole, J. R., Holtel, M. R., & Amoroso, P. J. (2004). An analysis of 3599 midfacial and 1141 orbital blowout fractures among 4426 United States Army Soldiers, 1980–2000. *Otolaryngology – Head and Neck Surgery, 130*(2), 164–170.
22. He, D., Blomquist, P. H., & Ellis, E. (2007). Association between ocular injuries and internal orbital fractures. *Journal of Oral and Maxillofacial Surgery, 65*(4), 713–720.
23. Ioannides, C., Treffers, W., Rutten, M., & Noverraz, P. (1988). Ocular injuries associated with fractures involving the orbit. *Journal of Cranio-Maxillo-Facial Surgery, 16*(4), 157–159.
24. Cook, T. (2002). Ocular and periocular injuries from orbital fractures. *Journal of the American College of Surgeons, 195*(6), 831–834.
25. Read, R. W., & Sires, B. S. (1998). Association between orbital fracture location and ocular injury: A retrospective study. *The Journal of Cranio-Maxillofacial Trauma, 4*(3), 10–15.
26. Gilliland, G. D., Gilliland, G., Fincher, T., et al. (2005). Assessment of biomechanics of orbital fracture: A study in goats and implications for oculoplastic surgery in humans. *American Journal of Ophthalmology, 140*(5), 868–876.
27. Kellman, R. M., & Schmidt, C. (2009). The paranasal sinuses as a protective crumple zone for the orbit. *Laryngoscope, 119*(9), 1682–1690.
28. Kreidl, K. O., Kim, D. Y., & Mansour, S. E. (2003). Prevalence of significant intraocular sequelae in blunt orbital trauma. *The American Journal of Emergency Medicine, 21*(7), 525–528.
29. Pelletier, C. R., Jordan, D. R., Braga, R., & McDonald, H. (1998). Assessment of ocular trauma associated with head and neck injuries. *Journal of Trauma, 44*(2), 350–354.
30. Nagase, D. Y., Courtemanche, D. J., & Peters, D. A. (2006). Facial fractures – Association with ocular injuries: A 13-year review of one practice in a tertiary care centre. *The Canadian Journal of Plastic Surgery, 14*(3), 167–171.
31. Duma, S. M., & Jernigan, M. V. (2003). The effects of airbags on orbital fracture patterns in frontal automobile crashes. *Ophthalmic Plastic and Reconstructive Surgery, 19*(2), 107–111.
32. Stacey, D. H., Doyle, J. F., & Gutowski, K. A. (2008). Safety device use affects the incidence patterns of facial trauma in motor vehicle collisions: An analysis of the National Trauma Database from 2000 to 2004. *Plastic and Reconstructive Surgery, 121*(6), 2057–2064.
33. Brown, M. S., Ky, W., & Lisman, R. D. (1999). Concomitant ocular injuries with orbital fractures. *The Journal of Cranio-Maxillofacial Trauma, 5*(3), 41–46.
34. Motamedi, M. H. (2003). An assessment of maxillofacial fractures: A 5-year study of 237 patients. *Journal of Oral and Maxillofacial Surgery, 61*(1), 61–64.
35. Cruz, A. A., & Eichenberger, G. C. (2004). Epidemiology and management of orbital fractures. *Current Opinion in Ophthalmology, 15*(5), 416–421.
36. Hwang, K., You, S. H., & Lee, H. S. (2009). Outcome analysis of sports-related multiple facial fractures. *The Journal of Craniofacial Surgery, 20*(3), 825–829.
37. Procacci, P., Ferrari, F., Bettini, G., et al. (2009). Soccer-related facial fractures: Postoperative management with facial protective shields. *The Journal of Craniofacial Surgery, 20*(1), 15–20.

38. Tuli, T., Haechl, O., Berger, N., et al. (2010). Facial trauma: How dangerous are skiing and snowboarding? *Journal of Oral and Maxillofacial Surgery, 68*(2), 293–299.
39. Lim, L. H., Moore, M. H., Trott, J. A., & David, D. J. (1993). Sports-related facial fractures: A review of 137 patients. *Australian and New Zealand Journal of Surgery, 63*(10), 784–789.
40. Rocchi, G., Fadda, M. T., Marianetti, T. M., et al. (2007). Craniofacial trauma in adolescents: Incidence, etiology, and prevention. *Journal of Trauma, 62*(2), 404.
41. Antoun, J. S., & Lee, K. H. (2008). Sports-related maxillofacial fractures over an 11-year period. *Journal of Oral and Maxillofacial Surgery, 66*(3), 504–508.
42. Reehal, P. (2010). Facial injury in sport. *Current Sports Medicine Reports, 9*(1), 27–34.
43. García de Marcos, J. A., del Castillo-Pardo de Vera, J. L., & Calderón-Polanco, J. (2008). Orbital floor fracture and emphysema after nose blowing. *Oral and Maxillofacial Surgery, 12*(3), 163–165.
44. Manson, P. N., Markowitz, B., Mirvis, S., et al. (1990). Toward CT-based facial fracture treatment. *Plastic and Reconstructive Surgery, 85*(2), 202–212.
45. Lee, H. J., Jilani, M., Frohman, L., & Baker, S. (2004). CT of orbital trauma. *Emergency Radiology, 10*(4), 168–172.
46. Mackenzie, D. J., Arora, B., & Hansen, J. (1999). Orbital floor repair with titanium mesh screen. *The Journal of Cranio-Maxillofacial Trauma, 5*(3), 9–16.
47. Swinson, B., Amin, M., Nair, P., et al. (2004). Isolated bilateral orbital floor fractures: A series of 3 cases. *Journal of Oral and Maxillofacial Surgery, 62*(11), 1431–1435.
48. Smith, B., & Converse, J. M. (1957). Early treatment of orbital floor fractures. *Transaction of the American Academy of Ophthalmology and Otolaryngology, 61*(5), 602–608.
49. Smith, B., & Regan, W. F. (1957). Blow-out fracture of the orbit. *American Journal of Ophthalmology, 44*(6), 733–739.
50. Jones, D. E., & Evans, J. N. (1967). "Blow-out" fractures of the orbit: An investigation into their anatomical basis. *The Journal of Laryngology and Otology, 81*(10), 1109–1120.
51. Kersten, R. C. (1987). Blowout fractures of the orbital floor with entrapment caused by isolated trauma to the orbital rim. *American Journal of Ophthalmology, 103*(2), 215–220.
52. Della Rocca, R. C. (1990). Orbital surgery. In H. M. Clayman (Ed.), *Atlas of contemporary ophthalmic surgery* (pp. 879–1020). St. Louis: Mosby.
53. Le Fort, R. (1901). Etude experimental sur les fractures de la mechoire superieure. Parts I, II, III. *Review Chirurgia Paris, 23*, 201–360, 470.
54. Kulvin, D. R., & Leadbetter, M. G. (1989). Orbital rim trauma causing a blowout fracture. *Plastic and Reconstructive Surgery, 84*(6), 969–970.
55. Al-Sukhun, J., Kontio, R., & Lindqvist, C. (2006). Orbital stress analysis – Part I: Simulation of orbital deformation following blunt injury by finite element analysis method. *Journal of Oral and Maxillofacial Surgery, 64*(3), 434–442.
56. Nagasao, T., Miyamoto, J., Nagasao, M., et al. (2006). The effect of striking angle on the buckling mechanism in blowout fracture. *Plastic and Reconstructive Surgery, 117*(7), 2373–2380.
57. Green, R. P., Peters, D. R., Shore, J. W., et al. (1990). Force necessary to fracture the orbital floor. *Ophthalmic Plastic and Reconstructive Surgery, 6*(3), 211–217.
58. Bullock, J. D., Warwar, R. E., Ballal, D. R., & Ballal, R. D. (1999). Mechanisms of orbital floor fractures: A clinical, experimental, and theoretical study. *Transactions of the American Ophthalmological Society, 97*, 87–110.
59. Warwar, R. E., Bullock, J. D., Ballal, D. R., & Ballal, R. D. (2000). Mechanisms of orbital floor fractures: A clinical, experimental, and theoretical study. *Ophthalmic Plastic and Reconstructive Surgery, 16*(3), 188–200.
60. Ahmad, F., Kirkpatrick, N. A., Lyne, J., et al. (2006). Buckling and hydraulic mechanisms in orbital blowout fractures: Fact or fiction? *The Journal of Craniofacial Surgery, 17*(3), 438–441.
61. Ahmad, F., Kirkpatrick, W. N., Lyne, J., et al. (2003). Strain gauge biomechanical evaluation of forces in orbital floor fractures. *British Journal of Plastic Surgery, 56*(1), 3–9.

62. Waterhouse, N., Lyne, J., Urdang, M., & Garey, L. (1999). An investigation into the mechanism of orbital blowout fractures. *British Journal of Plastic Surgery, 52*(8), 607–612.
63. Pfeiffer, R. L. (1943). Traumatic enophthalmos. *Transactions of the American Ophthalmological Society, 41*, 293–306.
64. Erling, B. F., Iliff, N., Robertson, B., & Manson, P. N. (1999). Footprints of the globe: A practical look at the mechanism of orbital blowout fractures, with a revisit to the work of Raymond Pfeiffer. *Plastic and Reconstructive Surgery, 103*(4), 1313–1316.
65. Rhee, J. S., Kilde, J., Yoganadan, N., & Pintar, F. (2002). Orbital blowout fractures: Experimental evidence for the pure hydraulic theory. *Archives of Facial Plastic Surgery, 4*(2), 98–101.
66. Takizawa, H., Sugiura, K., Baba, M., et al. (1988). Structural mechanics of the blowout fracture: Numerical computer simulation of orbital deformation by the finite element method. *Neurosurgery, 6*(pt 1), 1053–1055.
67. Jo, A., Rizen, V., Nikolic, V., & Banovic, B. (1989). The role of orbital wall morphological properties and their supporting structures in the etiology of "blow-out" fractures. *Surgical and Radiologic Anatomy, 11*(3), 241–248.
68. Song, W. K., Lew, H., Yoon, J. S., et al. (2009). Role of medial orbital wall morphologic properties in orbital blow-out fractures. *Investigative Ophthalmology & Visual Science, 50*(2), 495–499.
69. Anderson, P. J., & Poole, M. D. (1995). Orbital floor fractures in young children. *Journal of Cranio-Maxillo-Facial Surgery, 23*(3), 151–154.
70. Cope, M. R., Moos, K. F., & Speculand, B. (1999). Does diplopia persist after blow-out fractures of the orbital floor in children. *British Journal of Oral and Maxillofacial Surgery, 37*(1), 46–51.
71. Klenk, G., & Kovacs, A. (2003). Blow-out fracture of the orbital floor in early childhood. *The Journal of Craniofacial Surgery, 14*(5), 666–671.
72. Vyas, R. M., Dickinson, B. P., Wasson, K. L., et al. (2008). Pediatric facial fractures: Current national incidence, distribution, and health care resource use. *The Journal of Craniofacial Surgery, 19*(2), 339–349.
73. Fueger, G. F., Milauskas, A. T., & Britton, W. (1966). The roentgenologic evaluation of orbital blow-out injuries. *The American Journal of Roentgenology, Radium Therapy and Nuclear Medicine, 97*(3), 614–617.
74. Strong, E. B. (2004). Endoscopic repair of orbital blow-out fractures. *Facial Plastic Surgery, 20*(3), 223–230.
75. Hosal, B. M., & Beatty, R. L. (2002). Diplopia and enophthalmos after surgical repair of blowout fracture. *Orbit, 21*(1), 27–33.
76. Biesman, B. S., Hornblass, A., Lisman, R., & Kazlas, M. (1996). Diplopia after surgical repair of orbital floor fractures. *Ophthalmic Plastic and Reconstructive Surgery, 12*(1), 9–16.
77. Greenwald, H. S., Jr., Keeney, A. H., & Shannon, G. M. (1974). A review of 128 patients with orbital fractures. *American Journal of Ophthalmology, 78*(4), 655–664.
78. al-Qurainy, I. A., Stassen, L. F., Dutton, G. N., et al. (1991). The characteristics of midfacial fractures and the association with ocular injury: A prospective study. *British Journal of Oral and Maxillofacial Surgery, 29*(5), 291–301.
79. Lerman, S. (1970). Blowout fracture of the orbit, diagnosis and treatment. *British Journal of Ophthalmology, 54*(2), 90–98.
80. Kushner, B. J. (1995). Management of diplopia limited to down gaze. *Archives of Ophthalmology, 113*(11), 1426–1430.
81. Nardi, M. (1996). Hypertropia and the posterior blowout fracture. *Ophthalmology, 103*(1), 152–156.
82. Seiff, S. R., & Good, W. V. (1996). Hypertropia and the posterior blowout fracture: Mechanism and management. *Ophthalmology, 103*(1), 152–156.
83. Von Noorden, G. K. (1983). *Atlas of strabismus* (4th ed., p. 223). St. Louis: Mosby.
84. Wilkins, R. B., & Havins, W. E. (1982). Current treatment of blow-out fractures. *Ophthalmology, 89*(5), 464–466.
85. Bedford, M. A. (1976). *A colour atlas of ophthalmological diagnosis* (p. 190). London: Wolfe Publishing.

86. Anderson, R., & Teague, D. A. (1963). Blowout fractures of the orbital floor: The use of a stent in their repair. *American Journal of Ophthalmology, 56*(1), 46–50.
87. Rubin, P. A., Bilyk, J. R., & Shore, J. W. (1994). Orbital reconstruction using porous polyethylene sheets. *Ophthalmology, 101*(10), 1697–1708.
88. Yab, K., Tajima, S., & Ohba, S. (1997). Displacements of eyeball in orbital blowout fractures. *Plastic and Reconstructive Surgery, 100*(6), 1409–1417.
89. Krohel, G. B., Stewart, W. B., & Chavis, R. M. (1981). *Orbital disease. A practical approach* (p. 160). New York: Grune & Stratton.
90. Fan, X., Li, J., Zhu, J., et al. (2003). Computer-assisted orbital volume measurement in the surgical correction of late enophthalmos caused by blowout fractures. *Ophthalmic Plastic and Reconstructive Surgery, 19*(3), 207–211.
91. Putterman, A. M., & Chalfin, J. (1979). Ocular asymmetry measuring device. *Ophthalmology, 86*(6), 1203–1208.
92. Hatt, M. (1986). *Ophthalmic plastic and reconstructive surgery* (p. 166). Stuttgart: Thieme.
93. Yavuzer, R., Tuncer, S., Basterzi, Y., et al. (2004). Reconstruction of orbital floor fracture using solvent-preserved bone graft. *Plastic and Reconstructive Surgery, 113*(1), 34–44.
94. Browning, C. W., & Walker, R. V. (1965). The use of alloplastics in 45 cases of orbital floor reconstruction. *American Journal of Ophthalmology, 60*(4), 684–699.
95. Grove, A. S., Tadmor, R., New, P. F., & Momose, K. J. (1978). Orbital fracture evaluation by coronal computed tomography. *American Journal of Ophthalmology, 85*(5 pt 1), 679–685.
96. Harris, G. J., Garcia, G. H., Logani, S. C., et al. (1998). Orbital blow-out fractures: Correlation of preoperative computed tomography and postoperative ocular motility. *Transactions of the American Ophthalmological Society, 96*, 329–347.
97. Metz, H. S. (1983). Restrictive factors in strabismus. *Survey of Ophthalmology, 28*(2), 71–83.
98. Wojno, T. H. (1987). The incidence of extraocular muscle and cranial nerve palsy in orbital floor blow-out fractures. *Ophthalmology, 94*(6), 682–687.
99. Lyon, D. B., & Newman, S. A. (1989). Evidence of direct damage to extraocular muscles as a cause of diplopia following orbital trauma. *Ophthalmic Plastic and Reconstructive Surgery, 5*(2), 81–91.
100. Metz, H. S. (1976). Forced duction, active force generation, and saccadic velocity tests. *International Ophthalmology Clinics, 16*(3), 47–73.
101. Mellema, P. A., Dewan, M. A., Lee, M. S., et al. (2009). Incidence of ocular injury in visually asymptomatic orbital fractures. *Ophthalmic Plastic and Reconstructive Surgery, 25*(4), 306–308.
102. Lelli, G. J., Milite, J., & Maher, E. (2007). Orbital floor fractures: Evaluation, indications, approach, and pearls from an ophthalmologist's perspective. *Facial Plastic Surgery, 23*(3), 190–199.
103. Soparkar, C. N. S., & Patrinely, J. R. (2007). The eye examination in facial trauma for the plastic surgeon. *Plastic and Reconstructive Surgery, 120*(7 suppl 2), 49S–56S.
104. Hornblass, A. (1979). Pupillary dilatation in fractures of the floor of the orbit. *Ophthalmic Surgery, 10*(11), 44–46.
105. Flanagan, J. C., Kapustiak, J. F., & Nowinski, T. (1988). Orbital fractures. In S. R. Waltman et al. (Eds.), *Surgery of the eye* (2nd ed., Vol. 2, pp. 695–718). New York: Churchill Livingstone.
106. Koornneef, L. (1988). Eyelid and orbital fascial attachments and their clinical significance. *Eye, 2*(pt 2), 130–134.
107. Ortube, M. C., Rosenbaum, A. L., Goldberg, R. A., & Demer, J. L. (2004). Orbital imaging demonstrates occult blow out fracture in complex strabismus. *Journal of AAPOS, 8*(3), 264–273.
108. Anda, S., Elsas, T., & Harstad, H. K. (1987). The missing rectus: A CT observation from blow-out fracture of the orbital floor. *Journal of Computer Assisted Tomography, 11*(5), 895–897.
109. Wachler, B. S., & Holds, J. B. (1998). The missing muscle syndrome in blowout fractures: An indication for urgent surgery. *Ophthalmic Plastic and Reconstructive Surgery, 14*(1), 17–18.
110. Yano, H., Minagawa, T., Masuda, K., & Hirano, A. (2009). Urgent rescue of 'missing rectus' in blowout fracture. *Journal of Plastic, Reconstructive & Aesthetic Surgery, 62*(9), 301–304.

111. Levine, L. M., Sires, B. S., Gentry, L. R., & Dortzbach, R. K. (1998). Rounding of the inferior rectus muscle: A helpful radiologic findings in the management of orbital floor fractures. *Ophthalmic Plastic and Reconstructive Surgery, 14*(2), 141–143.
112. Banerjee, A., Moore, C. C., Tse, R., & Matic, D. (2007). Rounding of the inferior rectus muscle as an indication of orbital floor fracture with periorbital disruption. *Journal of Otolaryngology, 36*(3), 175–180.
113. Matic, D. B., Tse, R., Banerjee, A., & Moore, C. C. (2007). Rounding of the inferior rectus muscle as a predictor of enophthalmos in orbital floor fractures. *The Journal of Craniofacial Surgery, 18*(1), 127–132.
114. Lambert, D. M., Mirvis, S. E., Shanmuganathan, K., & Tilghman, D. L. (1997). Computed tomography exclusion of osseous paranasal sinus injury in blunt trauma patients: The "clear sinus" sign. *Journal of Oral and Maxillofacial Surgery, 55*(11), 1207–1210.
115. Sandler, N. A., Carrau, R. L., Ochs, M. W., & Beatty, R. L. (1999). The use of maxillary sinus endoscopy in the diagnosis of orbital floor fractures. *Journal of Oral and Maxillofacial Surgery, 57*(4), 399–403.
116. Back, C. P., McLean, N. R., Anderson, P. J., & David, D. J. (2007). The conservative management of facial fractures: Indications and outcomes. *Journal of Plastic, Reconstructive & Aesthetic Surgery, 60*(2), 146–151.
117. Roncevic, R., & Roncevic, D. (1999). Extensive, traumatic fractures of the orbit in war and peace time. *The Journal of Craniofacial Surgery, 10*(4), 284–300.
118. Roth, A., Desmangles, P., & Rossillion, B. (1999). Le traitement précose des impotences musculaires secondaires aux fractures du plancher de I'orbite. *Journal Francais D Ophtalmologie, 22*(6), 645–650.
119. Rinna, C., Ungari, C., Saltarel, A., et al. (2005). Orbital floor restoration. *The Journal of Craniofacial Surgery, 16*(6), 968–972.
120. Burnstine, M. A. (2002). Clinical recommendations for repair of isolated orbital floor fractures: An evidence-based analysis. *Ophthalmology, 109*(7), 1207–1210.
121. Burnstine, M. A. (2003). Clinical recommendations for repair of orbital facial fractures. *Current Opinion in Ophthalmology, 14*(5), 236–240.
122. Sires, B. S., Stanley, R. B., & Levine, L. M. (1998). Oculocardiac reflex caused by orbital floor trapdoor fracture: An indication for urgent repair. *Archives of Ophthalmology, 116*(7), 955–956.
123. Koide, R., Ueda, T., Takano, K., et al. (2003). Surgical outcome of blowout fracture: Early repair without implants and the usefulness of balloon treatment. *Japanese Journal of Ophthalmology, 47*(4), 392–397.
124. Matteini, C., Renzi, G., Becelli, R., et al. (2004). Surgical timing in orbital fracture treatment: Experience with 108 consecutive cases. *The Journal of Craniofacial Surgery, 15*(1), 145–150.
125. Hopper, R. A., Salemy, S., & Sze, R. W. (2006). Diagnosis of midface fractures with CT: What the surgeon needs to know. *Radiographics, 26*(3), 783–793.
126. Worthington, J. P. (2010). Isolated posterior orbital floor fractures, diplopia and oculocardiac reflexes: A 10-year review. *British Journal of Oral and Maxillofacial Surgery, 48*(2), 127–130.
127. Courtney, D. J., Thomas, S., & Whitfield, P. H. (2000). Isolated orbital blowout fractures: Survey and review. *British Journal of Oral and Maxillofacial Surgery, 38*(5), 496–504.
128. Catone, G. A., Morrissette, M. P., & Carlson, E. R. (1988). A retrospective study of untreated orbital blow-out fractures. *Journal of Oral and Maxillofacial Surgery, 46*(12), 1033–1038.
129. Yano, H., Nakano, M., Anraku, K., et al. (2009). A consecutive case review of orbital blowout fractures and recommendations for comprehensive management. *Plastic and Reconstructive Surgery, 124*(2), 602–611.
130. Hawes, M. J., & Dortzbach, R. K. (1983). Surgery on orbital floor fractures. Influence of time of repair and fracture size. *Ophthalmology, 90*(9), 1066–1070.
131. Boush, G. A., & Lemke, B. N. (1994). Progressive infraorbital nerve hypesthesia as a primary indication for blow-out fracture repair. *Ophthalmic Plastic and Reconstructive Surgery, 10*(4), 271–275.

132. Kraus, M., Gatot, A., & Fliss, D. M. (2001). Repair of traumatic inferior orbital wall defects with nasoseptal cartilage. *Journal of Oral and Maxillofacial Surgery, 59*(12), 1397–1400.
133. Manson, P. N., Grivas, A., Rosenbaum, A., et al. (1986). Studies of enophthalmos: II. The measurement of orbital injuries and their treatment by quantitative computed tomography. *Plastic and Reconstructive Surgery, 77*(2), 203–214.
134. Wojno, T. H. (1989). Blowout fractures. In G. L. Spaeth et al. (Eds.), *Current therapy in ophthalmic surgery* (pp. 298–301). Toronto: Decker.
135. Raskin, E. M., Millman, A. L., Lubkin, V., et al. (1998). Prediction of late enophthalmos by volumetric analysis of orbital fractures. *Ophthalmic Plastic and Reconstructive Surgery, 14*(1), 19–26.
136. Ataullah, S., Whitehouse, R. W., Stelmach, M., et al. (1999). Missed orbital wall blow-out fracture as a cause of post-enucleation socket syndrome. *Eye, 13*(pt 4), 541–544.
137. Honda, T., Sakurai, H., Nakazawa, H., et al. (2006). Correction of late post-traumatic enophthalmos using a tissue expander. *Annals of Plastic Surgery, 56*(6), 686–688.
138. Choi, J. C., Fleming, J. C., Aitken, P. A., & Shore, J. W. (1999). Porous polyethylene channel implants: A modified porous polyethylene sheet implant designed for repairs of large and complex orbital wall fractures. *Ophthalmic Plastic and Reconstructive Surgery, 15*(1), 56–66.
139. Jordan, D. R., Allen, L. H., White, J., et al. (1998). Intervention within days for some orbital floor fractures: The white-eyed blowout. *Ophthalmic Plastic and Reconstructive Surgery, 14*(6), 379–390.
140. Becelli, R., Renzi, G., Perugini, M., & Iannetti, G. (2000). Craniofacial traumas: Immediate and delayed treatment. *The Journal of Craniofacial Surgery, 11*(3), 265–269.
141. Dal Canto, A. J., & Linberg, J. V. (2008). Comparison of orbital fracture repair performed within 14 days versus 15 to 29 days after trauma. *Ophthalmic Plastic and Reconstructive Surgery, 24*(6), 437–443.
142. Whitaker, L. A., & Yaremchuk, M. J. (1990). Secondary reconstruction of posttraumatic orbital deformities. *Annals of Plastic Surgery, 25*(6), 440–449.
143. Hinohira, Y., Yumoto, E., Hyodo, M., & Shiraishi, A. (2008). Reduction surgeries for delayed cases with isolated blowout fractures. *Otolaryngology – Head and Neck Surgery, 138*(2), 252–254.
144. Carr, R. M., & Mathog, R. H. (1997). Early and delayed repair of orbitozygomatic complex fractures. *Journal of Oral and Maxillofacial Surgery, 55*(3), 253–258.
145. Yaremchuk, M. J. (1999). Orbital deformity after craniofacial fracture repair: Avoidance and treatment. *The Journal of Cranio-Maxillofacial Trauma, 5*(2), 7–16.
146. Clauser, L., Galiè, M., Pagliaro, F., & Tieghi, R. (2008). Posttraumatic enophthalmos: Etiology, principles of reconstruction, and correction. *The Journal of Craniofacial Surgery, 19*(2), 351–359.
147. Eppley, B. L., Custer, P. L., & Sadove, A. M. (1990). Cutaneous approaches to the orbital skeleton and periorbital structures. *Journal of Oral and Maxillofacial Surgery, 48*(8), 842–854.
148. Rohrich, R. J., Janis, J. E., & Adams, W. P. (2003). Subciliary versus subtarsal approaches to orbitozygomatic fractures. *Plastic and Reconstructive Surgery, 111*(5), 1708–1714.
149. De Riu, G., Meloni, S. M., Gobbi, R., et al. (2008). Subciliary versus swinging eyelid approach to the orbital floor. *Journal of Cranio-Maxillo-Facial Surgery, 36*(8), 439–442.
150. Luppens, D. P., & Codner, M. A. (2009). Discussion. The incidence of lower eyelid malposition after facial fracture repair: A retrospective study and meta-analysis comparing subtarsal, subciliary, and transconjunctival incisions. *Plastic and Reconstructive Surgery, 124*(5), 1587–1589.
151. Ridgway, E. B., Chen, C., Colakoglu, S., et al. (2009). The incidence of lower eyelid malposition after facial fracture repair: A retrospective study and meta-analysis comparing subtarsal, subciliary, and transconjunctival incisions. *Plastic and Reconstructive Surgery, 124*(5), 1578–1586.
152. Ridgway, E. B., Chen, C., & Lee, B. T. (2009). Acquired entropion associated with the transconjunctival incision for facial fracture management. *The Journal of Craniofacial Surgery, 20*(5), 1412–1415.

153. Baqain, Z. H., Malkawi, Z., Hadidi, A., & Rajab, L. D. (2008). Subtarsal approach for orbital floor repair: A long-term follow-up of 12 cases in a Jordanian teaching hospital. *Journal of Oral and Maxillofacial Surgery, 66*(1), 45–50.
154. Salgarelli, A. C., Bellini, P., Landini, B., et al. (2010). A comparative study of different approaches in the treatment of orbital trauma: An experience based on 274 cases. *Oral and Maxillofacial Surgery, 14*(1), 23–27.
155. Goldberg, R. A., Lessner, A. M., Shorr, N., & Baylis, H. I. (1990). The transconjunctival approach to the orbital floor and orbital fat. A prospective study. *Ophthalmic Plastic and Reconstructive Surgery, 6*(4), 241–246.
156. Silkiss, R. Z., & Carroll, R. P. (1992). Transconjunctival surgery. *Ophthalmic Surgery, 23*(4), 288–291.
157. Appling, W. D., Patrinely, J. R., & Salzer, T. A. (1993). Transconjunctival approach vs subciliary skin-muscle flap approach for orbital fracture repair. *Archives of Otolaryngology – Head & Neck Surgery, 119*(9), 1000–1007.
158. Baumann, A., & Ewers, R. (2001). Use of the preseptal transconjunctival approach in orbit reconstruction surgery. *Journal of Oral and Maxillofacial Surgery, 59*(3), 287–291.
159. Schmäl, F., Basel, T., Grenzebach, U. H., et al. (2006). Preseptal transconjunctival approach for orbital floor fracture repair: Ophthalmologic results in 209 patients. *Acta Oto-Laryngologica, 126*(4), 381–389.
160. Lane, K. A., Bilyk, J. R., Taub, D., & Pribitkin, E. A. (2009). "Sutureless" repair of orbital floor and rim fractures. *Ophthalmology, 116*(1), 135–138.
161. Westfall, C. T., & Shore, J. W. (1991). Isolated fractures of the orbital floor: Risk of infection and the role of antibiotic prophylaxis. *Ophthalmic Surgery, 22*(7), 409–411.
162. Bahr, W., Bagambisa, F. B., Schlegel, G., & Schilli, W. (1992). Comparison of transcutaneous incisions used for exposure of the infraorbital rim and orbital floor: A retrospective study. *Plastic and Reconstructive Surgery, 90*(4), 585–591.
163. Patel, P. C., Sobota, B. T., Patel, N. M., et al. (1998). Comparison of transconjunctival versus subciliary approaches for orbital fractures: A review of 60 cases. *The Journal of Cranio-Maxillofacial Trauma, 4*(1), 17–21.
164. Otori, N., Haruna, S., & Moriyama, H. (2003). Endoscopic endonasal or transmaxillary repair of orbital floor fracture: A study of 88 patients treated in our department. *Acta Oto-Laryngologica, 123*(6), 718–723.
165. Malhotra, R., Selva, D., Wormald, P. J., & Davis, G. (2005). Video-endoscope assisted teaching during sub-periosteal orbital surgery. *Orbit, 24*(2), 113–116.
166. Farwell, D. G., & Strong, E. B. (2006). Endoscopic repair of orbital floor fractures. *Facial Plastic Surgery Clinics of North America, 14*(1), 11–16.
167. Schubert, W., & Jenabzadeh, K. (2009). Endoscopic approach to maxillofacial trauma. *The Journal of Craniofacial Surgery, 20*(1), 154–156.
168. Hinohira, Y., Yumoto, E., & Shimamura, I. (2005). Endoscopic endonasal reduction of blow-out fractures of the orbital floor. *Otolaryngology – Head and Neck Surgery, 133*(5), 741–747.
169. Strong, E. B., Kim, K. K., & Diaz, R. C. (2004). Endoscopic approach to orbital blowout fracture repair. *Otolaryngology – Head and Neck Surgery, 131*(5), 683–695.
170. Mohammad, J. A., Warnke, P. H., & Shenaq, S. M. (1998). Endoscopic exploration of the orbital floor: A technique for transantral grafting of floor blowout fractures. *The Journal of Cranio-Maxillofacial Trauma, 4*(2), 16–19.
171. Woog, J. J., Hartstein, M. E., & Gliklich, R. (1998). Paranasal sinus endoscopy and orbital fracture repair. *Archives of Ophthalmology, 116*(5), 688–691.
172. Chen, C. T., & Chen, Y. R. (2003). Endoscopic orbital surgery. *Atlas of Oral & Maxillofacial Surgery Clinics of North America, 11*(2), 179–208.
173. Mohadjer, Y., & Hartstein, M. E. (2006). Endoscopic orbital fracture repair. *Otolaryngologic Clinics of North America, 39*(5), 1049–1057.
174. Ducic, Y., & Verret, D. J. (2009). Endoscopic transantral repair of orbital floor fractures. *Otolaryngology – Head and Neck Surgery, 140*(6), 849–854.

175. Miki, T., Wada, J., Haraoka, J., & Inaba, I. (2004). Endoscopic transmaxillary reduction and balloon technique for blowout fractures of the orbital floor. *Minimally Invasive Neurosurgery, 47*(6), 359–364.
176. Wallace, T. D., Moore, C. C., Bromwich, M. A., & Matic, D. B. (2006). Endoscopic repair of orbital floor fractures: Computed tomographic analysis using a cadaveric model. *Journal of Otolaryngology, 35*(1), 1–7.
177. Maturo, S. C., Wiseman, J., & Mair, E. (2008). Transantral endoscopic repair of orbital floor fractures with the use of a flexible endoscope holder: A cadaver study. *Ear, Nose, and Throat Journal, 87*(12), 693–695.
178. Fernandes, R., Fattahi, T., Steinberg, B., & Schare, H. (2007). Endoscopic repair of isolated orbital floor fracture with implant placement. *Journal of Oral and Maxillofacial Surgery, 65*(8), 1449–1453.
179. Jin, H. R., Yeon, J. Y., Shin, S. O., et al. (2007). Endoscopic versus external repair of orbital blowout fractures. *Otolaryngology – Head and Neck Surgery, 136*(1), 38–44.
180. Kim, J. H., Kook, M. S., Ryu, S. Y., et al. (2008). A simple technique for the treatment of inferior orbital blow-out fracture: A transantral approach, open reduction, and internal fixation with miniplate and screws. *Journal of Oral and Maxillofacial Surgery, 66*(12), 2488–2492.
181. Ikeda, K., Suzuki, H., Oshima, T., & Takasaka, T. (1999). Endoscopic endonasal repair of orbital floor fracture. *Archives of Otolaryngology – Head & Neck Surgery, 125*(1), 59–63.
182. Batchvarova, Z., & Athmani, B. (2005). The antral balloon catheter: A simple, fast, and inexpensive method for reconstruction of the orbital floor fracture. *Plastic and Reconstructive Surgery, 116*(7), 2048–2049.
183. Nishiike, S., Nagai, M., Nakagawa, A., et al. (2005). Endoscopic transantral orbital floor repair with antral bone grafts. *Archives of Otolaryngology – Head & Neck Surgery, 131*(10), 911–915.
184. Ikeda, K., Oshima, T., Suzuki, H., et al. (2003). Surgical treatment of subperiosteal abscess of the orbit: Sendai's ten year experience. *Auris, Nasus, Larynx, 30*(3), 259–262.
185. Hayasaka, S., Aikawa, Y., Wada, M., et al. (1994). Transconjunctival and transantral approaches are combined with antral wall bone graft to repair orbital floor blow-out fractures. *Ophthalmologica, 208*(5), 284–288.
186. Chen, C. T., & Chen, Y. R. (2001). Endoscopically assisted repair of orbital floor fractures. *Plastic and Reconstructive Surgery, 108*(7), 2011–2018.
187. Ploder, O., Oeckher, M., Klug, C., et al. (2003). Follow-up study of treatment of orbital floor fractures: Relation of clinical data and software-based CT-analysis. *International Journal of Oral and Maxillofacial Surgery, 32*(3), 257–262.
188. Kakibuchi, M., Fukazawa, K., Fukuda, K., et al. (2004). Combination of transconjunctival and endonasal-transantral approach in the repair of blowout fractures involving the orbital floor. *British Journal of Plastic Surgery, 57*(1), 37–44.
189. Kwon, J. H., Kim, J. G., Moon, J. H., & Cho, J. H. (2008). Clinical analysis of surgical approaches for orbital floor fractures. *Archives of Facial Plastic Surgery, 10*(1), 21–24.
190. Cheong, E. C., Chen, C. T., & Chen, Y. R. (2009). Endoscopic management of orbital floor fractures. *Facial Plastic Surgery, 25*(1), 8–16.
191. Farwell, D. G., Sires, B. S., Kriet, J. D., & Stanley, R. B. (2007). Endoscopic repair of orbital blowout fractures: Use or misuse of a new approach? *Archives of Facial Plastic Surgery, 9*(6), 427–433.
192. Moore, C. C., Bromwich, M., Roth, K., & Matic, D. B. (2008). Endoscopic anatomy of the orbital floor and maxillary sinus. *The Journal of Craniofacial Surgery, 19*(1), 271–276.
193. Forrest, C. R. (1999). Application of endoscope-assisted minimal-access techniques in orbitozygomatic complex, orbital floor, and frontal sinus fractures. *The Journal of Cranio-Maxillofacial Trauma, 5*(4), 7–12.
194. Barone, C. M., & Gigantelli, J. W. (1998). Endoscopic repair of posttraumatic enophthalmos using medial transconjunctival approach: A case report. *The Journal of Cranio-Maxillofacial Trauma, 4*(1), 22–26.

195. Hwang, K., & Hwang, J. H. (2009). Do we have to dissect infraorbital nerve from periorbita in orbital floor fracture? *The Journal of Craniofacial Surgery, 20*(4), 1260–1262.
196. Theologie-Lygidakis, N., Iatrou, I., & Alexandridis, C. (2007). Blow-out fractures in children: Six years' experience. *Oral Surgery, Oral Medicine, Oral Pathology, Oral Radiology, and Endodontics, 103*(6), 757–763.
197. Xu, J. J., Teng, L., Jin, X. L., et al. (2009). Porous polyethylene implants in orbital blow-out fractures and enophthalmos reconstruction. *The Journal of Craniofacial Surgery, 20*(3), 918–920.
198. Vairaktaris, E., Moschos, M. M., Vassiliou, S., et al. (2008). Delayed appearance of diplopia due to orbital emphysema after repair of orbital fractures. *Oral Surgery, Oral Medicine, Oral Pathology, Oral Radiology, and Endodontics, 106*(1), 8–10.
199. Rever, L. J., Manson, P. N., Randolph, M. A., et al. (1991). The healing of facial bone fractures by the process of secondary union. *Plastic and Reconstructive Surgery, 87*(3), 451–458.
200. Gilliland, G. D., Gilliland, G., Fincher, T., et al. (2007). Timing of return to normal activities after orbital floor fracture repair. *Plastic and Reconstructive Surgery, 120*(1), 245–251.
201. Martin, B., & Ghosh, A. (2003). Antibiotics in orbital floor fractures. *Emergency Medicine Journal, 20*(1), 66.
202. Villarreal, P. M., Monje, F., Morillo, A. J., et al. (2002). Porous polyethylene implants in orbital floor reconstruction. *Plastic and Reconstructive Surgery, 109*(3), 877–885.
203. Eufinger, H., Wehmöller, M., Machtens, E., et al. (1995). Reconstruction of craniofacial bone defect with individual alloplastic implants based on CAD/CAM-manipulated CT-data. *Journal of Cranio-Maxillo-Facial Surgery, 23*(3), 175–181.
204. Millman, A. L., Della Rocca, R. C., Spector, S., et al. (1987). Steroids and orbital blowout fractures – A new systematic concept in medical management and surgical decision-making. *Advances in Ophthalmic, Plastic, and Reconstructive Surgery, 6*, 291–300.
205. Flood, T. R., McManners, J., el-Attar, A., & Moos, K. F. (1999). Randomized prospective study of the influence of steroids on postoperative eye-opening after exploration of the orbital floor. *British Journal of Oral and Maxillofacial Surgery, 37*(4), 312–315.
206. Thorén, H., Snäll, J., Kormi, E., et al. (2009). Does perioperative glucocorticosteroid treatment correlate with disturbance in surgical wound healing after treatment of facial fractures? A retrospective study. *Journal of Oral and Maxillofacial Surgery, 67*(9), 1884–1888.
207. Gosain, A. K., & Persing, J. A. (1999). Biomaterials in the face: Benefits and risks. *The Journal of Craniofacial Surgery, 10*(5), 404–414.
208. Cho, Y. R., & Gosain, A. K. (2004). Biomaterials in craniofacial reconstruction. *Clinics in Plastic Surgery, 31*(3), 377–385.
209. Friesenecker, J., Dammer, R., Moritz, M., & Niederdellmann, H. (1995). Long-term results after primary restoration of the orbital floor. *Journal of Cranio-Maxillo-Facial Surgery, 23*(1), 31–33.
210. Laure, B., Tranquart, F., Geais, L., & Goga, D. (2010). Evaluation of skull strength following parietal bone graft harvest. *Plastic and Reconstructive Surgery, 126*(5), 1492–1499.
211. Polley, J. W., & Ringler, S. L. (1987). The use of Teflon in orbital floor reconstruction following blunt facial trauma: A 20-year experience. *Plastic and Reconstructive Surgery, 79*(1), 39–43.
212. Lee, H. H., Alcaraz, N., Reino, A., & Lawson, W. (1998). Reconstruction of orbital floor fractures with maxillary bone. *Archives of Otolaryngology – Head & Neck Surgery, 124*(1), 56–59.
213. Kontio, R. K., Laine, P., Salo, A., et al. (2006). Reconstruction of internal orbital wall fracture with iliac crest free bone graft: Clinical, computed tomography, and magnetic resonance imaging follow-up study. *Plastic and Reconstructive Surgery, 118*(6), 1365–1374.
214. Newell, F. W. (1982). *Ophthalmology. Principles and concepts* (5th ed., p. 559). St. Louis: Mosby.
215. Kakibuchi, M., Fukuda, K., Yamada, N., et al. (2003). A simple method of harvesting a thin iliac bone graft for reconstruction of the orbital wall. *Plastic and Reconstructive Surgery, 111*(2), 961–962.

216. Sakakibara, S., Hashikawa, K., Terashi, H., & Tahara, S. (2009). Reconstruction of the orbital floor with sheets of autogenous iliac cancellous bone. *Journal of Oral and Maxillofacial Surgery, 67*(5), 957–961.
217. Chen, C. T., Chen, Y. R., Tung, T. C., et al. (1999). Endoscopically assisted reconstruction of orbital medial wall fractures. *Plastic and Reconstructive Surgery, 103*(2), 714–720.
218. Mintz, S. M., Ettinger, A., Schmakel, T., & Gleason, M. J. (1998). Contralateral coronoid process bone grafts for orbital floor reconstruction: An anatomic and clinical study. *Journal of Oral and Maxillofacial Surgery, 56*(10), 1140–1144.
219. Kosaka, M., Matsuzawa, Y., Mori, H., et al. (2004). Orbital wall reconstruction with bone grafts from the outer cortex of the mandible. *Journal of Cranio-Maxillo-Facial Surgery, 32*(6), 374–380.
220. Krishnan, V., & Johnson, J. V. (1997). Orbital floor reconstruction with autogenous mandibular symphyseal bone grafts. *Journal of Oral and Maxillofacial Surgery, 55*(4), 327–330.
221. Constantian, M. B. (1982). Use of auricular cartilage in orbital floor reconstruction. *Plastic and Reconstructive Surgery, 69*(6), 951–953.
222. Castellani, A., Negrini, S., & Zanetti, U. (2002). Treatment of orbital floor blowout fractures with conchal auricular cartilage graft: A report on 14 cases. *Journal of Oral and Maxillofacial Surgery, 60*(12), 1413–1417.
223. Johnson, P. E., & Raftopoulos, I. (1999). In situ splitting of a rib graft for reconstruction of the orbital floor. *Plastic and Reconstructive Surgery, 103*(6), 1709–1711.
224. Ozyazgan, I., Eskitascioglu, T., Baykan, H., & Coruh, A. (2006). Repair of traumatic orbital wall defects using conchal cartilage. *Plastic and Reconstructive Surgery, 117*(4), 1269–1276.
225. Kraus, M., Gatot, A., Kaplan, D. M., & Fliss, D. M. (2002). Post-traumatic orbital floor reconstruction with nasoseptal cartilage in children. *International Journal of Pediatric Otorhinolaryngology, 64*(3), 187–192.
226. Talesh, K. T., Babaee, S., Vahdati, S. A., & Tabeshfar, S. (2009). Effectiveness of a nasoseptal cartilaginous graft for repairing traumatic fractures of the inferior orbital wall. *British Journal of Oral and Maxillofacial Surgery, 47*(1), 10–13.
227. Copeland, M., & Meisner, J. (1991). Maxillary antral bone grafts for repair of orbital fractures. *The Journal of Craniofacial Surgery, 2*(1), 18–21.
228. Cieślik, T., Skowronek, J., Cieślik, M., & Cieślik-Bielecka, A. (2009). Bone graft application from anterior sinus maxillary wall in orbital floor reconstruction. *The Journal of Craniofacial Surgery, 20*(2), 512–515.
229. Morong, S., Snell, L., Nishtar, S., et al. (2010). Maxillary bone grafts for the repair of traumatic orbital floor defects. *Journal of Otolaryngology – Head & Neck Surgery, 39*(5), 579–585.
230. Kaye, B. L. (1966). Orbital floor repair with antral wall bone grafts. *Plastic and Reconstructive Surgery, 37*(1), 62–65.
231. Lynham, A. J., Chapman, P. J., Monsour, F. N., et al. (2004). Management of isolated orbital floor blow-out fractures: A survey of Australian and New Zealand oral and maxillofacial surgeons. *Clinical and Experimental Ophthalmology, 32*(1), 42–45.
232. Jordan, D. R., St. Onge, P., Anderson, R. L., et al. (1992). Complications associated with alloplastic implants used in orbital fracture repair. *Ophthalmology, 99*(10), 1600–1608.
233. Slade, C. S. (1995). Bone grafts in orbital reconstruction. *International Ophthalmology Clinics, 35*(1), 47–56.
234. Lai, A., Gliklich, R. E., & Rubin, P. A. (1998). Repair of orbital blow-out fractures with nasoseptal cartilage. *Laryngoscope, 108*(5), 645–650.
235. Aronowitz, J. A., Freeman, B. S., & Spira, M. (1986). Long-term stability of teflon orbital implants. *Plastic and Reconstructive Surgery, 78*(2), 166–173.
236. Goldberg, R. A., Garbutt, M., & Shorr, N. (1993). Oculoplastic uses of cranial bone grafts. *Ophthalmic Surgery, 24*(3), 190–196.
237. Marin, P. C., Love, T., Carpenter, R., et al. (1998). Complications of orbital reconstruction: Misplacement of bone grafts within the intramuscular cone. *Plastic and Reconstructive Surgery, 101*(5), 1323–1327.

238. Gas, C., Sidjilani, B.-M., Dodart, L., & Boutault, F. (1999). Fractures isolées du plancher orbitaire. *Revue de Stomatologie et de Chirurgie Maxillo-Faciale, 100*(1), 27–33.
239. Gear, A. J., Lokeh, A., Aldridge, J. H., et al. (2002). Safety of titanium mesh for orbital reconstruction. *Annals of Plastic Surgery, 48*(1), 1–7.
240. Ellis, E., & Tan, Y. (2003). Assessment of internal orbital reconstructions for pure blowout fractures: Cranial bone grafts versus titanium mesh. *Journal of Oral and Maxillofacial Surgery, 61*(4), 442–453.
241. Chen, T. M., & Wang, H. J. (2002). Cranioplasty using allogenic perforated demineralized bone matrix with autogenous bone paste. *Annals of Plastic Surgery, 49*(3), 272–279.
242. Bevivino, J. R., Nguyen, P. N., & Yen, L. J. (1994). Reconstruction of traumatic orbital floor defects using irradiated cartilage homografts. *Annals of Plastic Surgery, 33*(1), 32–37.
243. Neigel, J. M., & Ruzicka, P. O. (1996). Use of demineralized bone implants in orbital and craniofacial reconstruction and a review of the literature. *Ophthalmic Plastic and Reconstructive Surgery, 12*(2), 108–120.
244. Sailer, H. F., & Kolb, E. (1994). Application of purified bone morphogenetic protein (BMP) preparations in cranio-maxillo-facial surgery. Reconstruction in craniofacial malformations and post-traumatic or operative defects of the skull with lyophilized cartilage and BMP. *Journal of Cranio-Maxillo-Facial Surgery, 22*(4), 191–199.
245. Mackenzie, D. J., Sipe, R., Buck, D., et al. (2001). Recombinant human acidic fibroblast growth factor and fibrin carrier regenerates bone. *Plastic and Reconstructive Surgery, 107*(4), 989–996.
246. Ripamonti, U., Crooks, J., & Rueger, D. C. (2001). Induction of bone formation by recombinant human osteogenic protein-1 and sintered porous hydroxyapatite in adult primates. *Plastic and Reconstructive Surgery, 17*(4), 977–988.
247. Waite, P. D., & Clanton, J. T. (1988). Orbital floor reconstruction with lyophilized dura. *Journal of Oral and Maxillofacial Surgery, 46*(9), 727–730.
248. Guerra, M. F., Perez, J. S., Rodriguez-Campo, F. J., & Gias, L. N. (2000). Reconstruction of orbital fractures with dehydrated human dura mater. *Journal of Oral and Maxillofacial Surgery, 58*(12), 1361–1366.
249. Iatrou, I., Theologie-Lygidakis, N., & Angelopoulos, A. (2001). Use of membrane and bone grafts in the reconstruction of orbital fractures. *Oral Surgery, Oral Medicine, Oral Pathology, Oral Radiology, and Endodontics, 91*(3), 281–286.
250. Bedrossian, E. H. (1993). Banked fascia lata as an orbital floor implant. *Ophthalmic Plastic and Reconstructive Surgery, 9*(3), 66–70.
251. Celikoz, B., Duman, H., & Selmanpakoglu, N. (1997). Reconstruction of the orbital floor with lyophilized tensor fascia lata. *Journal of Oral and Maxillofacial Surgery, 55*(3), 240–244.
252. Browning, C. W. (1967). Alloplast materials in orbital repair. *American Journal of Ophthalmology, 63*(5 pt 1), 955–962.
253. Nguyen, P. N., & Sullivan, P. (1992). Advances in the management of orbital fractures. *Clinics in Plastic Surgery, 19*(1), 87–98.
254. Janecka, I. P. (2000). New reconstructive technologies in skull base surgery: Role of titanium mesh and porous polyethylene. *Archives of Otolaryngology – Head & Neck Surgery, 126*(3), 396–401.
255. Jank, S., Emshoff, R., Schuchter, B., et al. (2003). Orbital floor reconstruction with flexible Ethisorb patches: A retrospective long-term follow-up study. *Oral Surgery, Oral Medicine, Oral Pathology, Oral Radiology, and Endodontics, 95*(1), 16–22.
256. Kontio, R., & Lindqvist, C. (2009). Management of orbital fractures. *Oral and Maxillofacial Surgery Clinics of North America, 21*(2), 209–220.
257. Osguthorpe, J. D. (1991). Orbital wall fractures: Evaluation and management. *Otolaryngology – Head and Neck Surgery, 105*(5), 702–707.
258. Mermer, R. W., & Orban, R. E. (1995). Repair of orbital floor fractures with absorbable gelatin film. *The Journal of Cranio-Maxillofacial Trauma, 1*(4), 30–34.

259. Stewart, M. G., Patrinely, J. R., Appling, W. D., & Jordan, D. R. (1995). Late proptosis following orbital floor fracture repair. *Archives of Otolaryngology – Head & Neck Surgery, 121*(6), 649–652.
260. Taban, M., Nakra, T., Mancini, R., et al. (2009). Orbital wall fracture repair using Seprafilm. *Ophthalmic Plastic and Reconstructive Surgery, 25*(3), 211–214.
261. Buchel, P., Rahal, A., Seto, I., & Iizuka, T. (2005). Reconstruction of orbital floor fracture with polyglactin 910/polydioxanon patch (ethisorb): A retrospective study. *Journal of Oral and Maxillofacial Surgery, 63*(5), 646–650.
262. Mauriello, J. A., Wasserman, B., & Kraut, R. (1993). Use of Vicryl (polyglactin-910) mesh implant for repair of orbital floor fracture causing diplopia: A study of 28 patients over 5 years. *Ophthalmic Plastic and Reconstructive Surgery, 9*(3), 191–195.
263. Jaquiéry, C., Aeppli, C., Cornelius, P., et al. (2007). Reconstruction of orbital wall defects: Critical review of 72 patients. *International Journal of Oral and Maxillofacial Surgery, 36*(3), 193–199.
264. Dietz, A., Ziegler, C. M., Dacho, A., et al. (2001). Effectiveness of a new perforated 0.15 mm poly-p-dioxanon-foil versus titanium-dynamic mesh in reconstruction of the orbital floor. *Journal of Cranio-Maxillo-Facial Surgery, 29*(2), 82–88.
265. Iizuka, T., Mikkonen, P., Paukku, P., & Lindqvist, C. (1991). Reconstruction of orbital floor with polydioxanone plate. *International Journal of Oral and Maxillofacial Surgery, 20*(2), 83–87.
266. Baumann, A., Burggasser, G., Gauss, N., & Ewers, R. (2002). Orbital floor reconstruction with an alloplastic resorbable polydioxanone sheet. *International Journal of Oral and Maxillofacial Surgery, 31*(4), 367–373.
267. Kolk, A., Pautke, C., Wiener, E., et al. (2005). A novel high-resolution magnetic resonance imaging microscopy coil as an alternative to the multislice computed tomography in postoperative imaging of orbital fractures and computer-based volume measurement. *Journal of Oral and Maxillofacial Surgery, 63*(4), 492–498.
268. Kontio, R., Suuronen, R., Salonen, O., et al. (2001). Effectiveness of operative treatment of internal orbital wall fracture with polydioxanone implant. *International Journal of Oral and Maxillofacial Surgery, 30*(4), 278–285.
269. Morain, W. D., Colby, E. D., Stauffer, M. E., et al. (1987). Reconstruction of orbital wall fenestrations with polyglactin 910 film. *Plastic and Reconstructive Surgery, 80*(6), 769–774.
270. Ng, J. D., Huynh, T. H., & Burgett, R. (2004). Complications of bioabsorbable orbital implants and fixation plates. *Ophthalmic Plastic and Reconstructive Surgery, 20*(1), 85–86.
271. Enislidis, G., Pichorner, S., Kainberger, F., & Ewers, R. (1997). Lactosorb panel and screws for repair of large orbital floor defects. *Journal of Cranio-Maxillo-Facial Surgery, 25*(6), 316–321.
272. Hollier, L. H., Rogers, N., Berzin, E., & Stal, S. (2001). Resorbable mesh in the treatment of orbital floor fractures. *The Journal of Craniofacial Surgery, 12*(3), 242–246.
273. Cordewener, F. W., Bos, R. R., Rozema, F. R., & Houtman, W. A. (1996). Poly(L-lactide) implants for repair of human orbital floor defects: Clinical and magnetic resonance imaging evaluation of long-term results. *Journal of Oral and Maxillofacial Surgery, 54*(1), 9–13.
274. Al-Sukhun, J., & Lindqvist, C. (2006). A comparative study of 2 implants used to repair inferior orbital wall bony defects: Autogenous bone graft versus bioresorbable poly-L/DL-lactide (P[L/DL]LA 70/30) plate. *Journal of Oral and Maxillofacial Surgery, 64*(7), 1038–1048.
275. Al-Sukhun, J., Tornwall, J., Lindqvist, C., & Kontio, R. (2006). Bioresorbable poly-L/DL-lactide (P[L/DL]LA 70/30) plates are reliable for repairing large inferior orbital wall bony defects: A pilot study. *Journal of Oral and Maxillofacial Surgery, 64*(1), 47–55.
276. Landes, C. A., Ballon, A., & Roth, C. (2006). Maxillary and mandibular osteosyntheses with PLGA and P(L/DL)LA implants: A 5-year inpatient biocompatibility and degradation experience. *Plastic and Reconstructive Surgery, 117*(7), 2347–2360.

277. Wood, G. (2006). Inion biodegradable plates: The first century. *British Journal of Oral and Maxillofacial Surgery, 44*(1), 38–41.
278. Kontio, R., Suuronen, R., Konttinen, Y. T., et al. (2004). Orbital floor reconstruction with poly-L/D-lactide implants: Clinical, radiological and immunohistochemical study in sheep. *International Journal of Oral and Maxillofacial Surgery, 33*(4), 361–368.
279. Heidemann, W., & Gerlach, K. L. (2002). Imaging of biodegradable osteosynthesis materials by ultrasound. *Dento Maxillo Facial Radiology, 31*(3), 155–158.
280. Wiener, E., Kolk, A., Neff, A., et al. (2005). Evaluation of reconstructed orbital wall fractures: High-resolution MRI using a microscopy surface coil versus 16-slice MSCT. *European Radiology, 15*(6), 1250–1255.
281. Dorri, M., Nasser, M., & Oliver, R. (2009). Resorbable versus titanium plates for facial fractures. *Cochrane Database of Systematic Reviews, 21*(1), CD007158.
282. Eppley, B. L. (2005). Use of resorbable plates and screws in pediatric facial fractures. *Journal of Oral and Maxillofacial Surgery, 63*(3), 385–391.
283. Cançado, R. P., Cardoso, E. S., Bourguignon Filho, A. M., et al. (2006). Effects of the LactoSorb bioabsorbable plates on the craniofacial development of rabbits: Direct morphometric analysis using linear measurements. *International Journal of Oral and Maxillofacial Surgery, 35*(6), 528–532.
284. Miller, G. R., & Tenzel, R. R. (1969). Orbital fracture repair with methylmethacrylate implants. *American Journal of Ophthalmology, 68*(4), 717–719.
285. Majmundar, M. V., & Hamilton, J. S. (2007). Repair of orbital floor fractures with SupraFOIL smooth nylon foil. *Archives of Facial Plastic Surgery, 9*(1), 64–65.
286. Nunery, W. R., Tao, J. P., & Johl, S. (2008). Nylon foil "wraparound" repair of combined orbital floor and medial wall fractures. *Ophthalmic Plastic and Reconstructive Surgery, 24*(4), 271–275.
287. Park, D. J., Garibaldi, D. C., et al. (2008). Smooth nylon foil (SupraFOIL) orbital implants in orbital fractures: A case series of 181 patients. *Ophthalmic Plastic and Reconstructive Surgery, 24*(4), 266–270.
288. Ouadah, A., Gerard, M., Malpuech, F., et al. (1998). Le traitement des fractures du plancher de l'orbite: Réfection par lame de Téflon. Analyse des résultats sur 5 ans. *Revue de Stomatologie et de Chirurgie Maxillo-Faciale, 99*(suppl 1), 120–121.
289. Hardin, J. C. (1996). Blowout fractures of the orbit. *Plastic and Reconstructive Surgery, 97*(6), 856–859.
290. Goldman, R. J., & Hessburg, P. C. (1973). Appraisal of surgical correction in 130 cases of orbital floor fracture. *American Journal of Ophthalmology, 76*(1), 152–155.
291. Putterman, A. M., & Millman, A. L. (1989). Custom orbital implant in the repair of late posttraumatic enophthalmos. *American Journal of Ophthalmology, 108*(2), 153–159.
292. Tercan, M. (1995). Thin Silastic sheet for orbital floor repair. *Plastic and Reconstructive Surgery, 96*(5), 1238–1239.
293. Brown, A. E., & Banks, P. (1993). Late extrusion of alloplastic orbital floor implants. *British Journal of Oral and Maxillofacial Surgery, 31*(3), 154–157.
294. Groombridge, C., & McGuinness, J. (2006). Interesting case: Foreign body in the nose: An orbital Silastic sheet had migrated into the nasal cavity. *British Journal of Oral and Maxillofacial Surgery, 44*(1), 33.
295. Schmidt, B. L., Lee, C., Young, D. M., & O'Brien, J. (1998). Intraorbital squamous epithelial cyst: An unusual complication of Silastic implantation. *The Journal of Craniofacial Surgery, 9*(5), 452–455.
296. Morrison, A. D., Sanderson, R. C., & Moos, K. F. (1995). The use of silastic as an orbital implant for reconstruction of orbital wall defects: Review of 311 cases treated over 20 years. *Journal of Oral and Maxillofacial Surgery, 53*(4), 412–417.
297. Dancey, A. L., & Perry, M. J. (2004). Late presentation of alloplastic implant extrusion. *Plastic and Reconstructive Surgery, 113*(3), 1081–1082.
298. Warrier, S., Prabhakaran, V. C., Davis, G., & Selva, D. (2008). Delayed complications of silicone implants used in orbital fracture repairs. *Orbit, 27*(3), 147–151.

299. Janecka, I. P. (1996). Correction of ocular dystopia. *Plastic and Reconstructive Surgery, 97*(5), 892–899.
300. Yaremchuk, M. J. (2003). Facial skeletal reconstruction using porous polyethylene implants. *Plastic and Reconstructive Surgery, 111*(6), 1818–1827.
301. Beals, S., & Munro, I. R. (1987). The use of miniplates in craniomaxillofacial surgery. *Plastic and Reconstructive Surgery, 79*(1), 33–38.
302. Nagase, D. Y., Courtemanche, D. J., & Peters, D. A. (2005). Plate removal in traumatic facial fractures: 13-year practice review. *Annals of Plastic Surgery, 55*(6), 608–611.
303. Rallis, G., Mourouzis, C., Papakosta, V., et al. (2006). Reasons for miniplate removal following maxillofacial trauma: A 4-year study. *Journal of Cranio-Maxillo-Facial Surgery, 34*(7), 435–439.
304. Thorén, H., Snäll, J., Hallermann, W., et al. (2008). Policy of routine titanium miniplate removal after maxillofacial trauma. *Journal of Oral and Maxillofacial Surgery, 66*(9), 1901–1904.
305. Hanson, J., Lovald, S., Cowgill, I., et al. (2011). National hardware removal rate associated with internal fixation of facial fractures. *Journal of Oral and Maxillofacial Surgery, 69*(4), 1152–1158.
306. Rauso, R., Tartaro, G., Stea, S., et al. (2011). Plates removal in orthognathic surgery and facial fractures: When and why. *The Journal of Craniofacial Surgery, 22*(1), 252–254.
307. Yaremchuk, M. J., Del Vecchio, D. A., Fiala, T. G., & Lee, W. P. (1993). Microfixation of acute orbital fractures. *Annals of Plastic Surgery, 30*(5), 385–397.
308. Glassman, R. D., Manson, P. N., Vanderkolk, C. A., et al. (1990). Rigid fixation of internal orbital fractures. *Plastic and Reconstructive Surgery, 86*(6), 1103–1109.
309. Sargent, L. A., & Fulks, K. D. (1991). Reconstruction of internal orbital fractures with vitallium mesh. *Plastic and Reconstructive Surgery, 88*(1), 31–38.
310. Jacono, A. A., & Moskowitz, B. (2000). Alloplastic implants for orbital wall reconstruction. *Facial Plastic Surgery, 16*(1), 63–68.
311. Salyer, K. E., & Hall, C. D. (1989). Porous hydroxyapatite as an onlay bone-graft substitute for maxillofacial surgery. *Plastic and Reconstructive Surgery, 84*(2), 236–244.
312. Mercier, J., Piot, B., Gueguen, P., et al. (1996). Le plancher orbitaire en corail. Son intérêt en traumatologie. Résultats d'une étude multicentrique portant sur 83 cas. *Revue de Stomatologie et de Chirurgie Maxillo-Faciale, 97*(6), 324–331.
313. Roy, D. M., & Linnehan, S. K. (1974). Hydroxyapatite formed from coral skeletal carbonate by hydrothermal exchange. *Nature, 247*(5438), 220–222.
314. Lemke, B. N., & Kikkawa, D. O. (1999). Repair of orbital floor fractures with hydroxyapatite block scaffolding. *Ophthalmic Plastic and Reconstructive Surgery, 15*(3), 161–165.
315. Gosain, A. K., Riordan, P. A., Song, L., et al. (2005). A 1-year study of hydroxyapatite-derived biomaterials in an adult sheep model: III. Comparison with autogenous bone graft for facial augmentation. *Plastic and Reconstructive Surgery, 116*(4), 1044–1052.
316. Holmes, R. E. (1979). Bone regeneration within a coralline hydroxyapatite implant. *Plastic and Reconstructive Surgery, 63*(5), 626–633.
317. Piecuch, J. F. (1982). Extraskeletal implantation of porous hydroxyapatite ceramic. *Journal of Dental Research, 61*(12), 1458–1460.
318. Roux, F. X., Brasnu, D., Loty, B., et al. (1988). Madreporic coral: A new bone graft substitute for cranial surgery. *Journal of Neurosurgery, 69*(4), 510–513.
319. Reedy, B. K., Pan, F., Kim, W. C., et al. (1999). Properties of coralline hydroxyapatite and expanded polytetrafluoroethylene membrane in the immature craniofacial skeleton. *Plastic and Reconstructive Surgery, 103*(1), 20–26.
320. Nam, S. B., Bae, Y. C., Moon, J. S., & Kang, Y. S. (2006). Analysis of the postoperative outcome in 405 cases of orbital fracture using 2 synthetic orbital implants. *Annals of Plastic Surgery, 56*(3), 263–267.
321. Ono, I., Gunji, H., Suda, K., et al. (1994). Orbital reconstruction with hydroxyapatite ceramic implants. *Scandinavian Journal of Plastic and Reconstructive Surgery and Hand Surgery, 28*(3), 193–198.

322. Siniković, B., Kramer, F. J., Swennen, G., et al. (2007). Reconstruction of orbital wall defects with calcium phosphate cement: Clinical and histological findings in a sheep model. *International Journal of Oral and Maxillofacial Surgery, 36*(1), 54–61.
323. Nakajima, T., Yoshimura, Y., Nakanishi, Y., et al. (1995). Anterior cranial base reconstruction using a hydroxyapatite-tricalciumphosphate composite (Ceratite®) as a bone substitute. *Journal of Cranio-Maxillo-Facial Surgery, 23*(2), 64–67.
324. Chuang, E. L., & Bensinger, R. E. (1982). Resorbable implant for orbital defects. *American Journal of Ophthalmology, 94*(4), 547–549.
325. Ferraz, F. H., Schellini, S. A., Schellini, R. C., et al. (2008). BMP implant associated with platelet-rich plasma in orbit fracture repair. *Current Eye Research, 33*(3), 293–301.
326. Hoffmann, J., Cornelius, C. P., Groten, M., et al. (1998). Orbital reconstruction with individually copy-milled ceramic implants. *Plastic and Reconstructive Surgery, 101*(3), 604–612.
327. Klein, M., & Glatzer, C. (2006). Individual CAD/CAM fabricated glass-bioceramic implants in reconstructive surgery of the bony orbital floor. *Plastic and Reconstructive Surgery, 117*(2), 565–570.
328. Chew, M., Lim, T. C., Lim, J., & Tan, W. T. (1998). New synthetic orbital implant for orbital floor repair. *Plastic and Reconstructive Surgery, 101*(6), 1734.
329. Lin, I. C., Liao, S. L., & Lin, L. L. (2007). Porous polyethylene implants in orbital floor reconstruction. *Journal of the Formosan Medical Association, 106*(1), 51–57.
330. Frodel, J. L., & Lee, S. (1998). The use of high-density polyethylene implants in facial deformities. *Archives of Otolaryngology – Head & Neck Surgery, 124*(11), 1219–1223.
331. Dougherty, W. R., & Wellisz, T. (1994). The natural history of alloplastic implants in orbital floor reconstruction: An animal model. *The Journal of Craniofacial Surgery, 5*(1), 26–32.
332. Patel, P. J., Rees, H. C., & Olver, J. M. (2003). Fibrovascularization of porous polyethylene orbital floor implants in humans. *Archives of Ophthalmology, 121*(3), 400–403.
333. Choi, J. C., Sims, C. D., Casanova, R., et al. (1995). Porous polyethylene implant for orbital wall reconstruction. *The Journal of Cranio-Maxillofacial Trauma, 1*(3), 42–49.
334. Romano, J. J., Iliff, N. T., & Manson, P. N. (1993). Use of Medpor porous polyethylene implants in 140 patients with facial fractures. *The Journal of Craniofacial Surgery, 4*(3), 142–147.
335. Ozturk, S., Sengezer, M., Isik, S., et al. (2005). Long-term outcomes of ultra-thin porous polyethylene implants used for reconstruction of orbital floor defects. *The Journal of Craniofacial Surgery, 16*(6), 973–977.
336. Su, G. W., & Harris, G. J. (2006). Combined inferior and medial surgical approaches and overlapping thin implants for orbital floor and medial wall fractures. *Ophthalmic Plastic and Reconstructive Surgery, 22*(6), 420–423.
337. Ye, J., Kook, K. H., & Lee, S. Y. (2006). Evaluation of computer-based volume measurement and porous polyethylene channel implants in reconstruction of large orbital wall fractures. *Investigative Ophthalmology & Visual Science, 47*(2), 509–513.
338. Garibaldi, D. C., Iliff, N. T., Grant, M. P., & Merbs, S. L. (2007). Use of porous polyethylene with embedded titanium in orbital reconstruction: A review of 106 patients. *Ophthalmic Plastic and Reconstructive Surgery, 23*(6), 439–444.
339. Hanu-Cernat, L. M., James, G., & Barnard, N. A. (2009). Perforated, custom-shaped, porous, polyethylene-coated titanium mesh implants in the treatment of large defects of the orbital wall. *British Journal of Oral and Maxillofacial Surgery, 47*(3), 220–221.
340. Nowinski, D., Messo, E., & Hedlund, A. (2010). Treatment of orbital fractures: Evaluation of surgical techniques and materials for reconstruction. *The Journal of Craniofacial Surgery, 21*(4), 1033–1037.
341. Menderes, A., Baytekin, C., Topcu, A., et al. (2004). Craniofacial reconstruction with high-density porous polyethylene implants. *The Journal of Craniofacial Surgery, 15*(5), 719–724.
342. Steinsapir, K. D. (2003). Aesthetic and restorative midface lifting with hand-carved, expanded polytetrafluoroethylene orbital rim implants. *Plastic and Reconstructive Surgery, 111*(5), 1727–1737.

343. Panossian, A., & Garner, W. (2004). Polytetrafluoroethylene facial implants: 15 years later. *Plastic and Reconstructive Surgery, 113*(1), 347–349.
344. Hanson, L. J., Donovan, M. G., Hellstein, J. W., & Dickerson, N. C. (1994). Experimental evaluation of expanded polytetrafluoroethylene for reconstruction of orbital floor defects. *Journal of Oral and Maxillofacial Surgery, 52*(10), 1050–1055.
345. Furuta, M., Yago, K., & Iida, T. (2006). Correlation between ocular motility and evaluation of computed tomography in orbital blowout fracture. *American Journal of Ophthalmology, 142*(6), 1019–1025.
346. Ma, L., Wong, S. P., Wu, C. Y., & Yao, S. J. (1987). Orbital reconstruction with proplast. *Ophthalmic Plastic and Reconstructive Surgery, 3*(3), 151–157.
347. Cheung, D., Brown, L., & Sampath, R. (2004). Localized inferior orbital fibrosis associated with porcine dermal collagen xenograft orbital floor implant. *Ophthalmic Plastic and Reconstructive Surgery, 20*(3), 257–259.
348. Rinna, C., Reale, G., Foresta, E., & Mustazza, M. C. (2009). Medial orbital wall reconstruction with swine bone cortex. *The Journal of Craniofacial Surgery, 20*(3), 881–884.
349. Seymour, P. E., Krein, H. M., Leventhal, D. D., et al. (2008). Orbital floor reconstruction using porcine small intestinal submucosa. *Medical Science Monitor, 14*(11), 227–230.
350. Folkestad, L., & Westin, T. (1999). Long-term sequelae after surgery for orbital floor fractures. *Otolaryngology – Head and Neck Surgery, 120*(6), 914–921.
351. Dufresne, C. R., Manson, P. N., & Iliff, N. T. (1988). Early and late complications of orbital fractures. *Clinics in Plastic Surgery, 15*(2), 239–253.
352. Pigadas, N., & Lloyd, R. E. (2005). Haematoma of anterior ethmoidal artery after reduction of fracture of zygomatic complex. *British Journal of Oral and Maxillofacial Surgery, 43*(5), 417–419.
353. Ganesan, K., Fabbroni, G., Loukota, R., & Craggs, L. (2008). Traumatic subperiosteal hematoma of the orbit: A report of 2 cases. *Journal of Oral and Maxillofacial Surgery, 66*(6), 1266–1269.
354. Wood, C. M. (1989). The medical management of retrobulbar haemorrhage complicating facial fractures: A case report. *British Journal of Oral and Maxillofacial Surgery, 27*(4), 291–295.
355. Yazici, B., & Taner, P. (2007). Delayed orbital subperiosteal hemorrhage after blunt trauma. *Ophthalmic Plastic and Reconstructive Surgery, 23*(4), 315–316.
356. Rosdeutscher, J. D., & Stadelmann, W. K. (1998). Diagnosis and treatment of retrobulbar hematoma resulting from blunt periorbital trauma. *Annals of Plastic Surgery, 41*(6), 618–622.
357. Coulter, V. L., Holds, J. B., & Anderson, R. L. (1990). Avoiding complications of orbital surgery: The orbital branches of the infraorbital artery. *Ophthalmic Surgery, 21*(2), 141–143.
358. Bains, R. A., & Rubin, P. A. (1995). Blunt orbital trauma. *International Ophthalmology Clinics, 35*(1), 37–46.
359. Bater, M. C., Ramchandani, P. L., & Brennan, P. A. (2005). Post-traumatic eye observations. *British Journal of Oral and Maxillofacial Surgery, 43*(5), 410–416.
360. Chen, C. H., Chen, C. T., & Huang, F. (2009). Retrobulbar hematoma as a rare complication after secondary correction of enophthalmos. *The Journal of Craniofacial Surgery, 20*(3), 963–967.
361. Schick, B., Weber, R., Keerl, R., et al. (1996). Orbital hematomas. *Laryngo- Rhino- Otologie, 75*(6), 363–367.
362. Gerbino, G., Ramieri, G. A., & Nasi, A. (2005). Diagnosis and treatment of retrobulbar haematomas following blunt orbital trauma: A description of eight cases. *International Journal of Oral and Maxillofacial Surgery, 34*(2), 127–131.
363. Korinth, M. C., Ince, A., Banghard, W., et al. (2002). Pterional orbita decompression in orbital hemorrhage and trauma. *Journal of Trauma, 53*(1), 73–78.
364. Lee, K. Y., Tow, S., & Fong, K. S. (2006). Visual recovery following emergent orbital decompression in traumatic retrobulbar haemorrhage. *Annals of the Academy of Medicine, Singapore, 35*(11), 831–832.

365. Brasileiro, B. F., Cortez, A. L., Asprino, L., et al. (2005). Traumatic subcutaneous emphysema of the face associated with paranasal sinus fractures: A prospective study. *Journal of Oral and Maxillofacial Surgery, 63*(8), 1080–1087.
366. Levine, M. R., & Perla, B. (1995). Maxillary sinus orbital fistula secondary to repair of an orbital floor fracture. *Ophthalmic Plastic and Reconstructive Surgery, 11*(1), 66–69.
367. Weber, D., Shaw, S., & Winslow, J. (2009). Traumatic eye swelling. Subconjunctival and orbital emphysema with orbital floor fracture. *Annals of Emergency Medicine, 54*(4), 635, 642.
368. Oluwole, M., & White, P. (1996). Orbital floor fracture following nose blowing. *Ear, Nose, and Throat Journal, 75*(3), 169–170.
369. Shinohara, H., Shirota, Y., & Fujita, K. (2004). Implication of differences in the incidence of orbital emphysema in ethmoidal and maxillary sinus fractures. *Annals of Plastic Surgery, 53*(6), 565–569.
370. Reeves, D. L., Lucarelli, M. J., & Rose, J. G. (2005). Severe subcutaneous emphysema following orbital blowout fracture. *Ophthalmic Plastic and Reconstructive Surgery, 21*(6), 465–467.
371. Goldfarb, M. S., Hoffman, D. S., & Rosenberg, S. (1987). Orbital cellulitis and orbital fractures. *Annals of Ophthalmology, 19*(3), 97–99, 115.
372. Paterson, A. W., Barnard, N. A., & Irvine, G. H. (1994). Naso-orbital fracture leading to orbital cellulitis, and visual loss as a complication of chronic sinusitis. *British Journal of Oral and Maxillofacial Surgery, 32*(2), 80–82.
373. Kwon, H., Kim, S. W., Jung, S. N., et al. (2011). Cellulitis related to bioabsorbable plate and screws in infraorbital rim fracture. *The Journal of Craniofacial Surgery, 22*(2), 625–627.
374. Rumelt, S., & Rubin, P. A. D. (1996). Potential sources for orbital cellulitis. *International Ophthalmology Clinics, 36*(3), 207–221.
375. Jayamanne, D. G. R., Bell, R. W. D., & Allen, E. D. (1994). Orbital cellulitis – An unusual presentation and late complication of severe facial trauma. *British Journal of Oral and Maxillofacial Surgery, 32*(3), 187–189.
376. Chandler, J. R., Langenbrunner, D. J., & Stevens, E. R. (1970). The pathogenesis of orbital complications in acute sinusitis. *Laryngoscope, 80*(9), 1414–1428.
377. Ben Simon, G. J., Bush, S., Selva, D., & McNab, A. A. (2005). Orbital cellulitis: A rare complication after orbital blowout fracture. *Ophthalmology, 112*(11), 2030–2034.
378. Karslioglu, S., Serin, D., & Simsek, I. B. (2006). Anterior limbal approach in the treatment of a late and extensive post-traumatic retrobulbar abscess. *Ophthalmic Surgery, Lasers & Imaging, 37*(6), 490–493.
379. Mauriello, J. A., Hargrave, S., Yee, S., et al. (1994). Infection after insertion of alloplastic orbital floor implants. *American Journal of Ophthalmology, 117*(2), 246–252.
380. Forrest, C. R., Khairallah, E., & Kuzon, W. M. (1999). Intraocular and intraorbital compartment pressure changes following orbital bone grafting: A clinical and laboratory study. *Plastic and Reconstructive Surgery, 104*(1), 48–54.
381. McCartney, D. L., & Char, D. H. (1985). Return of vision following orbital decompression after 36 hours of postoperative blindness. *American Journal of Ophthalmology, 100*(4), 602–604.
382. Liu, D. (1994). Blindness after blow-out fracture repair. *Ophthalmic Plastic and Reconstructive Surgery, 10*(3), 206–210.
383. Arat, Y. O., Dorotheo, E. U., Tang, R. A., et al. (2006). Compressive optic neuropathy after use of oxidized regenerated cellulose in orbital surgery: Review of complications, prophylaxis, and treatment. *Ophthalmology, 113*(2), 333–337.
384. Paton, G. J., Aquilina, P. J., Lynham, A., & Lee, G. A. (2006). Intraocular pressure changes secondary to reduction of orbito-zygomatic complex fractures. *Journal of Oral and Maxillofacial Surgery, 64*(1), 100–103.
385. Zhou, H., Fan, X., & Xiao, C. (2007). Direct orbital manometry in normal and fractured orbits of Chinese patients. *Journal of Oral and Maxillofacial Surgery, 65*(11), 2282–2287.

386. Hammer, B., & Prein, J. (1995). Correction of posttraumatic orbital deformities: Operative techniques and review of 26 patients. *Journal of Craniomaxillofacial Surgery, 23*(2), 81–90.
387. Grant, J. H., Patrinely, J. R., Weiss, A. H., et al. (2002). Trapdoor fracture of the orbit in a pediatric population. *Plastic and Reconstructive Surgery, 109*(2), 482–499.
388. Jank, S., Schuchter, B., Emshoff, R., et al. (2003). Clinical signs of orbital wall fractures as a function of anatomic location. *Oral Surgery, Oral Medicine, Oral Pathology, Oral Radiology, and Endodontics, 96*(2), 149–153.
389. Aitasalo, K., Kinnunen, I., Palmgren, J., & Varpula, M. (2001). Repair of orbital floor fractures with bioactive glass implants. *Journal of Oral and Maxillofacial Surgery, 59*(12), 1390–1395.
390. Sleep, T. J., Evans, B. T., & Webb, A. A. (2007). Resolution of diplopia after repair of the deep orbit. *British Journal of Oral and Maxillofacial Surgery, 45*(3), 190–196.
391. Meyer, D. R., Simon, J. W., & Kansora, M. (1996). Primary infratarsal lower eyelid retractor lysis to prevent eyelid retraction after inferior rectus muscle recession. *American Journal of Ophthalmology, 122*(3), 331–339.
392. Iliff, N., Manson, P. N., Katz, J., et al. (1999). Mechanisms of extraocular muscle injury in orbital fractures. *Plastic and Reconstructive Surgery, 103*(3), 787–799.
393. Okinaka, Y., Hara, J., & Takahashi, M. (1999). Orbital blowout fracture with persistent mobility deficit due to fibrosis of the inferior rectus muscle and perimuscular tissue. *Annals of Otology, Rhinology and Laryngology, 108*(12), 1174–1176.
394. Smith, B., Lisman, R. D., Simonton, J., & Della Rocca, R. (1984). Volkmann's contracture of the extraocular muscles following blowout fracture. *Plastic and Reconstructive Surgery, 74*(2), 200–216.
395. Mauriello, J. A., Antonacci, R., Mostafavi, R., et al. (1996). Combined paresis and restriction of the extraocular muscles after orbital fracture: A study of 16 patients. *Ophthalmic Plastic and Reconstructive Surgery, 12*(3), 206–210.
396. Jin, H. R., Lee, H. S., Yeon, J. Y., & Suh, M. W. (2007). Residual diplopia after repair of pure orbital blowout fracture: The importance of extraocular muscle injury. *American Journal of Rhinology, 21*(3), 276–280.
397. Sloan, B., & McNab, A. A. (1998). Inferior rectus rupture following blowout fracture. *Australian and New Zealand Journal of Ophthalmology, 26*(2), 171–173.
398. Ameerally, P. J., Ormiston, I. W., & Avery, C. (2007). Partial avulsion of the inferior rectus: An unusual cause of diplopia after blunt orbital trauma. *British Journal of Oral and Maxillofacial Surgery, 45*(3), 240–241.
399. Ludwig, I. H., & Brown, M. S. (2002). Flap tear of rectus muscles: An underlying cause of strabismus after orbital trauma. *Ophthalmic Plastic and Reconstructive Surgery, 18*(6), 443–449.
400. Godeiro, K. D., Pinto, A. G., Souza Filho, J. P., et al. (2005). Traumatic tear of the inferior rectus muscle treated with inferior oblique anterior transposition. *International Ophthalmology, 26*(4–5), 185–189.
401. Yip, C. C., Jain, A., McCann, J. D., & Demer, J. L. (2006). Inferior rectus muscle transection: A cause of diplopia after non-penetrating orbital trauma. *Graefe's Archive for Clinical and Experimental Ophthalmology, 244*(12), 1698–1700.
402. Mauriello, J. A. (1990). Inferior rectus muscle entrapped by Teflon implant after orbital floor fracture repair. *Ophthalmic Plastic and Reconstructive Surgery, 6*(3), 218–220.
403. Lipton, J. R., Page, A. B., & Lee, J. P. (1990). Management of diplopia on down-gaze following orbital trauma. *Eye, 4*(pt 4), 535–537.
404. Van Eeckhoutte, L., De Clippeleir, L., Apers, R., et al. (1998). A protocol for extraocular muscle surgery after orbital floor fracture ("blow-out"). *Binocular Vision & Strabismus Quarterly, 13*(1), 29–36.
405. Hong, S., Lee, S. J., Lee, H. K., et al. (2008). Surgical management for large hypertropia and exotropia after disinsertion of inferior rectus muscle. *Ophthalmic Surgery, Lasers & Imaging, 39*(6), 505–507.

406. Wright, K. W. (1996). Late overcorrection after inferior rectus recession. *Ophthalmology, 103*(9), 1503–1507.
407. Buckley, E. G., & Meekins, B. B. (1988). Fadenoperation for the management of complicated incomitant vertical strabismus. *American Journal of Ophthalmology, 105*(3), 304–312.
408. Saunders, R. A. (1984). Incomitant vertical strabismus. Treatment with posterior fixation of the inferior rectus muscle. *Archives of Ophthalmology, 102*(8), 1174–1177.
409. Burke, J. P., & Keech, R. V. (1995). Effectiveness of inferior transposition of the horizontal rectus muscles for acquired inferior rectus paresis. *Journal of Pediatric Ophthalmology and Strabismus, 32*(3), 172–177.
410. Maurino, V., Kwan, A. S., & Lee, J. P. (2001). Review of the inverse Knapp procedure: Indications, effectiveness and results. *Eye, 15*(pt 1), 7–11.
411. Chen, C. T., Huang, F., & Chen, Y. R. (2006). Management of posttraumatic enophthalmos. *Chang Gung Medical Journal, 29*(3), 251–261.
412. Ahn, H. B., Ryu, W. Y., Yoo, K. W., et al. (2008). Prediction of enophthalmos by computer-based volume measurement of orbital fractures in a Korean population. *Ophthalmic Plastic and Reconstructive Surgery, 24*(1), 36–39.
413. Folkestad, L., & Granstrom, G. (2003). A prospective study of orbital fracture sequelae after change of surgical routines. *Journal of Oral and Maxillofacial Surgery, 61*(9), 1038–1044.
414. Metzger, M. C., Schön, R., Zizelman, C., et al. (2007). Semiautomatic procedure for individual performing of titanium meshes for orbital fractures. *Plastic and Reconstructive Surgery, 119*(3), 969–976.
415. Stasior, O. G., & Roen, J. L. (1982). Traumatic enophthalmos. *Ophthalmology, 89*(11), 1267–1273.
416. Manson, P. N., Clifford, C. M., Su, C. T., et al. (1986). Mechanisms of global support and posttraumatic enophthalmos: I. The anatomy of the ligament sling and its relation to intramuscular cone orbital fat. *Plastic and Reconstructive Surgery, 77*(2), 193–202.
417. Ramieri, G., Spada, M. C., Bianchi, S. D., & Berrone, S. (2000). Dimensions and volumes of the orbit and orbital fat in posttraumatic enophthalmos. *Dento Maxillo Facial Radiology, 29*(5), 302–311.
418. Kolk, A., Pautke, C., Schott, V., et al. (2007). Secondary post-traumatic enophthalmos: High-resolution magnetic resonance imaging compared with multislice computed tomography in postoperative orbital volume measurement. *Journal of Oral and Maxillofacial Surgery, 65*(10), 1926–1934.
419. Pearl, R. M. (1992). Treatment of enophthalmos. *Clinics in Plastic Surgery, 19*(1), 99–111.
420. Matsuo, K., Hirose, T., Furuta, S., et al. (1989). Semiquantitative correction of posttraumatic enophthalmos with sliced cartilage grafts. *Plastic and Reconstructive Surgery, 85*(5), 826–828.
421. Evans, B. T., & Webb, A. A. (2007). Post-traumatic orbital reconstruction: Anatomical landmarks and the concept of the deep orbit. *British Journal of Oral and Maxillofacial Surgery, 45*(3), 183–189.
422. Lee, J. (2000). Preplanned correction of enophthalmos using diced cartilage grafts. *British Journal of Plastic Surgery, 53*(1), 17–23.
423. Metzger, M. C., Schön, R., Weyer, N., et al. (2006). Anatomical 3-dimensional pre-bent titanium implant for orbital floor fractures. *Ophthalmology, 113*(10), 1863–1868.
424. Metzger, M. C., Schön, R., Weyer, N., et al. (2006). Computer-assisted extracorporeal orbital reconstruction after optic nerve decompression by removal of sphenoid bone. *Annals of Plastic Surgery, 57*(2), 223–227.
425. Metzger, M. C., Schön, R., Schulze, D., et al. (2006). Individual preformed titanium meshes for orbital fractures. *Oral Surgery, Oral Medicine, Oral Pathology, Oral Radiology, and Endodontics, 102*(4), 442–447.
426. Collyer, J. (2010). Stereotactic navigation in oral and maxillofacial surgery. *British Journal of Oral and Maxillofacial Surgery, 48*(2), 79–83.
427. Tang, W., Guo, L., Long, J., et al. (2010). Individual design and rapid prototyping in reconstruction of orbital wall defects. *Journal of Oral and Maxillofacial Surgery, 68*(3), 562–570.

428. Yab, K., Tajima, S., & Imai, K. (1993). Clinical application of a solid three-dimensional model for orbital wall fractures. *Journal of Cranio-Maxillo-Facial Surgery, 21*(7), 275–278.
429. Holck, D. E., Boyd, E. M., Ng, J., & Mauffray, R. O. (1999). Benefits of stereolithography in orbital reconstruction. *Ophthalmology, 106*(6), 1214–1218.
430. Schramm, A., Suarez-Cunqueiro, M. M., Rücker, M., et al. (2009). Computer-assisted therapy in orbital and mid-facial reconstructions. *The International Journal of Medical Robotics, 5*(2), 111–124.
431. Kozakiewicz, M., Elgalal, M., Loba, P., et al. (2009). Clinical application of 3D pre-bent titanium implants for orbital floor fractures. *Journal of Cranio-Maxillo-Facial Surgery, 37*(4), 229–234.
432. Gellrich, N.-C., Schramm, A., Hammer, B., et al. (2002). Computer-assisted secondary reconstruction of unilateral posttraumatic orbital deformity. *Plastic and Reconstructive Surgery, 110*(6), 1417–1429.
433. Schön, R., Metzger, M. C., Zizelmann, C., et al. (2006). Individually preformed titanium mesh implants for a true-to-original repair of orbital fractures. *International Journal of Oral and Maxillofacial Surgery, 35*(11), 990–995.
434. Pham, A. M., Rafii, A. A., Metzger, M. C., et al. (2007). Computer modeling and intraoperative navigation in maxillofacial surgery. *Otolaryngology – Head and Neck Surgery, 137*(4), 624–631.
435. Stuehmer, C., Essig, H., Schramm, A., et al. (2008). Intraoperative navigation assisted reconstruction of a maxillo-facial gunshot wound. *Oral and Maxillofacial Surgery, 12*(4), 199–203.
436. Andrades, P., Hernandez, D., Falguera, M. I., et al. (2009). Degrees of tolerance in posttraumatic orbital volume correction: The role of prefabricated mesh. *Journal of Oral and Maxillofacial Surgery, 67*(11), 2404–2411.
437. Scolozzi, P., Momjian, A., & Heuberger, J. (2009). Accuracy and predictability in use of AO three-dimensionally preformed titanium mesh plates for posttraumatic orbital reconstruction: A pilot study. *The Journal of Craniofacial Surgery, 20*(4), 1108–1113.
438. Scolozzi, P., Momjian, A., & Heuberger, J. (2010). Computer-aided volumetric comparison of reconstructed orbits for blow-out fractures with nonpreformed versus 3-dimensionally preformed titanium mesh plates: A preliminary study. *Journal of Computer Assisted Tomography, 34*(1), 98–104.
439. Coban, Y. K., & Kabalci, S. K. (2008). Surgical treatment of posttraumatic enophthalmos with diced medpor implants through mini-lateral canthoplasty incision. *The Journal of Craniofacial Surgery, 19*(2), 539–541.
440. McNab, A. A. (2001). Orbital and optic nerve trauma. *World Journal of Surgery, 25*(8), 1084–1088.
441. Whitehouse, R. W., Batterbury, M., Jackson, A., & Noble, J. L. (1994). Prediction of enophthalmos by computed tomography after 'blow out' orbital fracture. *British Journal of Ophthalmology, 78*(8), 618–620.
442. Kolk, A., Pautke, C., Wiener, E., et al. (2008). Isotropic proton-density-weighted high-resolution MRI for volume measurement of reconstructed orbital fracture – A comparison with multislice CT. *Magnetic Resonance Imaging, 26*(8), 1167–1174.
443. Kwon, J., Barrera, J. E., Jung, T. Y., & Most, S. P. (2009). Measurements of orbital volume change using computed tomography in isolated orbital blowout fractures. *Archives of Facial Plastic Surgery, 11*(6), 395–398.
444. Kempster, R., Beigi, B., & Galloway, G. D. (2005). Use of enophthalmic implants in the repair of orbital floor fractures. *Orbit, 24*(4), 219–225.
445. Gagnon, M. R., Yeatts, R. P., Williams, Z., & Matthews, B. (2004). Delayed enophthalmos following a minimally displaced orbital floor fracture. *Ophthalmic Plastic and Reconstructive Surgery, 20*(3), 241–243.
446. Ross, J. J., & Kersten, R. C. (2005). Late enophthalmos mimicking silent sinus syndrome secondary to orbital trauma. *The Journal of Craniofacial Surgery, 16*(5), 840–843.

447. Baujat, B., Derbez, R., Rossarie, R., et al. (2006). Silent sinus syndrome: A mechanical theory. *Orbit, 25*(2), 145–148.
448. Montezuma, S. R., Gopal, H., Savar, A., et al. (2008). Silent sinus syndrome presenting as enophthalmos long after orbital trauma. *Journal of Neuro-Ophthalmology, 28*(2), 107–110.
449. Renzi, G., Carboni, A., Perugini, M., et al. (2004). Posttraumatic trigeminal nerve impairment: A prospective analysis of recovery patterns in a series of 103 consecutive facial fractures. *Journal of Oral and Maxillofacial Surgery, 62*(11), 1341–1346.
450. Tengtrisorn, S., McNab, A. A., & Elder, J. E. (1998). Persistent infra-orbital nerve hyperaesthesia after blunt orbital trauma. *Australian and New Zealand Journal of Ophthalmology, 26*(3), 259–260.
451. Stromberg, B. V., & Knibbe, M. (1988). Anisocoria following reduction of bilateral orbital floor fractures. *Annals of Plastic Surgery, 21*(5), 486–488.
452. Bodker, F. S., Cytryn, A. S., Putterman, A. M., & Marschall, M. A. (1993). Postoperative mydriasis after repair of orbital floor fracture. *American Journal of Ophthalmology, 115*(3), 372–375.
453. Kang, S. J., & Kwak, I. H. (1996). Hematic cyst formation after repair of blow-out fracture. *Korean Journal of Ophthalmology, 10*(1), 60–62.
454. Coyle, J. T. (1997). Hemorrhage into an intraorbital pseudocyst. *Archives of Ophthalmology, 114*(9), 1156–1157.
455. Tahhan, M., Alkhardaji, F., Durrani, O. M., & Price, N. J. (2002). Intraorbital epithelial cyst formation: A rare complication of silastic implantation. *Archives of Ophthalmology, 120*(12), 1768–1769.
456. Tan, C. S., Ang, L. P., Choo, C. T., et al. (2006). Orbital cysts lined with both stratified squamous and columnar epithelia: A late complication of silicone implants. *Ophthalmic Plastic and Reconstructive Surgery, 22*(5), 398–400.
457. Mauriello, J. A., Flanagan, J. C., & Peyster, R. G. (1984). An unusual late complication of orbital floor fracture repair. *Ophthalmology, 91*(1), 102–107.
458. Rosen, C. E. (1996). Late migration of an orbital implant causing orbital hemorrhage with sudden proptosis and diplopia. *Ophthalmic Plastic and Reconstructive Surgery, 12*(4), 260–262.
459. Klisovic, D. D., Katz, S. E., & Lubow, M. (2002). The wayward implant: Orbital silicone plate extrusion associated with squamous epithelial downgrowth and infection. *Orbit, 21*(2), 149–154.
460. Hillier, R. J., Osborne, S. F., & Leatherbarrow, B. (2009). Epithelial inclusion cyst associated with a porous polyethylene orbital floor implant. *Ophthalmic Plastic and Reconstructive Surgery, 25*(3), 238–239.
461. Glavas, I., Lissauer, B., & Hornblass, A. (2005). Chronic subperiosteal hematic cyst formation twelve years after orbital fracture repair with alloplastic orbital floor implant. *Orbit, 24*(1), 47–49.
462. Marks, M. W., & Yeatts, R. P. (1994). Hemorrhagic cyst of the orbit as a long-term complication of prosthetic orbital floor implant. *Plastic and Reconstructive Surgery, 93*(4), 856–859.
463. McCannel, C. A., Weinberg, D. A., Glasgow, B. J., & Goldberg, R. A. (1996). Intracapsular hemorrhage as a late complication of an orbital floor implant. *Archives of Ophthalmology, 114*(9), 1156–1157.
464. Gilhotra, J. S., McNab, A. A., McKelvie, P., & O'Donnell, B. A. (2002). Late orbital haemorrhage around alloplastic orbital floor implants: A case series and review. *Clinical & Experimental Ophthalmology, 30*(5), 352–355.
465. Jones, D. F., & Wilson, M. W. (2008). Respiratory epithelial ingrowth and hemorrhage as late complications of orbital floor fracture repair with silicone sheet implant. *Ophthalmic Plastic and Reconstructive Surgery, 24*(6), 498–499.
466. McNab, A. A. (2000). Sino-orbital fistula: Two case reports. *Clinical and Experimental Ophthalmology, 28*(4), 324–325.
467. Joughin, K., Antonyshyn, O., Wilson, K. L., & Riding, M. (1993). Persistent posttraumatic orbital-antral fistula. *Annals of Plastic Surgery, 30*(1), 77–79.

468. Neves, R. B., Yeatts, R. P., & Martin, T. J. (1998). Pneumo-orbital cyst after orbital fracture repair. *American Journal of Ophthalmology, 125*(6), 879–880.
469. Mauriello, J. A., Fiore, P. M., & Kotch, M. (1987). Dacryocystitis. Late complication of orbital floor fracture repair with implant. *Ophthalmology, 94*(3), 248–250.
470. Massaro-Giordano, M., Kirschner, R. A., & Wulc, A. E. (1998). Orbital floor implant migration across the ethmoidal sinuses and nasal septum. *American Journal of Ophthalmology, 126*(6), 848–850.
471. Liu, D., & Al-Sadhan, Y. (1999). Orbital floor implant migration across the ethmoidal sinuses and nasal septum. *American Journal of Ophthalmology, 128*(1), 122–123.
472. Ziccardi, V. B., Patterson, G. T., Ramasastry, S., & Sotereanos, G. C. (1993). Management of a severe zygomatico-orbital fracture with dislocation of the globe into the antrum. *The Journal of Craniofacial Surgery, 4*(2), 95–101.
473. Pelton, R. W., Rainey, A. M., & Lee, A. G. (1998). Traumatic subluxation of the globe into the maxillary sinus. *American Journal of Neuroradiology, 19*(8), 1450–1451.
474. Kiratli, H., Tumer, B., & Bilgic, S. (1999). Management of traumatic luxation of the globe. A case report. *Acta Ophthalmologica Scandinavica, 77*(3), 340–342.
475. Abrishami, M., Aletaha, M., Bagheri, A., et al. (2007). Traumatic subluxation of the globe into the maxillary sinus. *Ophthalmic Plastic and Reconstructive Surgery, 23*(2), 156–158.
476. Kim, S., & Baek, S. (2005). Traumatic dislocation of the globe into the maxillary sinus associated with extraocular muscle injury. *Graefe's Archive for Clinical and Experimental Ophthalmology, 243*(12), 1280–1283.
477. Saleh, T., & Leatherbarrow, B. (1999). Traumatic prolapse of the globe into the maxillary sinus diagnosed as traumatic enucleation of the globe. *Eye, 13*(pt 5), 678–680.
478. Smit, T. J., Koornneef, L., & Zonneveld, F. W. (1990). A total orbital floor fracture with prolapse of the globe into the maxillary sinus manifesting as postenucleation socket syndrome. *American Journal of Ophthalmology, 110*(5), 569–570.
479. Reifler, D. M. (1988). Lid retraction following blow-out fracture of the orbit. *Ophthalmic Surgery, 19*(11), 825.
480. Conway, S. T. (1988). Lid retraction following blow-out fracture of the orbit. *Ophthalmic Surgery, 19*(4), 279–281.
481. Kwon, S. I., & Kim, Y. J. (2008). Upper eyelid retraction after periorbital trauma. *Korean Journal of Ophthalmology, 22*(4), 255–258.
482. Patel, B. C., Patipa, M., Anderson, R. L., & McLeish, W. (1997). Management of postblepharoplasty lower eyelid retraction with hard palate grafts and lateral tarsal strip. *Plastic and Reconstructive Surgery, 99*(5), 1251–1260.
483. Kim, Y. K., & Kim, J. W. (2010). Evaluation of subciliary incision used in blowout fracture treatment: Pretarsal flattening after lower eyelid surgery. *Plastic and Reconstructive Surgery, 125*(5), 1479–1484.
484. Tuncer, S., Yavuzer, R., Kandal, S., et al. (2007). Reconstruction of traumatic orbital floor fractures with resorbable mesh plate. *The Journal of Craniofacial Surgery, 18*(3), 598–605.
485. Patipa, M., Patel, B. C., McLeish, W., & Anderson, R. L. (1996). Use of hard palate grafts for treatment of postsurgical lower eyelid retraction: A technical overview. *The Journal of Cranio-Maxillofacial Trauma, 2*(3), 18–28.
486. Park, R. I., & Meyer, D. R. (1996). Acquired lower eyelid epiblepharon. *American Journal of Ophthalmology, 122*(3), 449–451.
487. Mullins, J. B., Holds, J. B., Branham, G. H., & Thomas, J. R. (1997). Complications of the transconjunctival approach. A review of 400 cases. *Archives of Otolaryngology – Head & Neck Surgery, 123*(4), 385–388.
488. Soll, D. B., & Poley, B. J. (1965). Trapdoor variety of blowout fracture of the orbital floor. *American Journal of Ophthalmology, 60*(2), 269–272.
489. de Man, K., Wijngaarde, R., Hes, J., & de Jong, P. T. (1991). Influence of age on the management of blow-out fractures of the orbital floor. *International Journal of Oral and Maxillofacial Surgery, 20*(6), 330–336.

490. Kwon, J. H., Moon, J. H., Kwon, M. S., & Cho, J. H. (2005). The differences of blowout fracture of the inferior orbital wall between children and adults. *Archives of Otolaryngology – Head & Neck Surgery, 131*(8), 723–727.
491. Criden, M. R., & Ellis, F. J. (2007). Linear nondisplaced orbital fractures with muscle entrapment. *Journal of AAPOS, 11*(2), 142–147.
492. Kakizaki, H., Zako, M., Iwaki, M., et al. (2005). Incarceration of the inferior oblique muscle branch of the oculomotor nerve in two cases of orbital floor trapdoor fracture. *Japanese Journal of Ophthalmology, 49*(3), 246–252.
493. Egbert, J. E., May, K., Kersten, R. C., & Kulwin, D. R. (2000). Pediatric orbital floor fracture: Direct extraocular muscle involvement. *Ophthalmology, 107*(10), 1875–1879.
494. Mehanna, P., Mehanna, D., & Cronin, A. (2009). White-eyed blowout fracture: Another look. *Emergency Medicine Australasia, 21*(3), 229–232.
495. Lane, K., Penne, R. B., & Bilyk, J. R. (2007). Evaluation and management of pediatric orbital fractures in a primary care setting. *Orbit, 26*(3), 183–191.
496. Hatton, M. P., Watkins, L. M., & Rubin, P. A. (2001). Orbital fractures in children. *Ophthalmic Plastic and Reconstructive Surgery, 17*(3), 174–179.
497. Cobb, A., Murthy, R., Manisali, M., et al. (2009). Oculovagal reflex in paediatric orbital floor fractures mimicking head injury. *Emergency Medicine Journal, 26*(5), 351–353.
498. Parbhu, K. C., Galler, K. E., Li, C., & Mawn, L. A. (2008). Underestimation of soft tissue entrapment by computed tomography in orbital floor fractures in the pediatric population. *Ophthalmology, 115*(9), 1620–1625.
499. Kolk, A., Stimmer, H., Klopfer, M., et al. (2009). High resolution magnetic resonance imaging with an orbital coil as an alternative to computed tomography scan as the primary imaging modality of pediatric orbital fractures. *Journal of Oral and Maxillofacial Surgery, 67*(2), 348–356.
500. Salvin, J. H. (2007). Systematic approach to pediatric ocular trauma. *Current Opinion in Ophthalmology, 18*(5), 366–372.
501. Cohen, S. M., & Garrett, C. G. (2003). Pediatric orbital floor fractures: Nausea/vomiting as signs of entrapment. *Otolaryngology – Head and Neck Surgery, 129*(1), 43–47.
502. Losee, J. E., Afifi, A., Jiang, S., et al. (2008). Pediatric orbital fractures: Classification, management, and early follow-up. *Plastic and Reconstructive Surgery, 122*(3), 886–897.
503. Burm, J. S., Chung, C. H., & Oh, S. J. (1999). Pure orbital blowout fracture: new concepts and importance of medial orbital blowout fracture. *Plastic and Reconstructive Surgery, 103*(7), 1839–49.
504. Yoon, K. C., Seo, M. S., & Park, Y. G. (2003). Orbital trapdoor fracture in children. *Journal of Korean Medical Science, 18*(6), 881–885.
505. Raflo, G. T. (1984). Blow-in and blow-out fractures of the orbit: Clinical correlations and proposed mechanisms. *Ophthalmic Surgery, 15*(2), 114–119.
506. Antonyshyn, O., Gruss, J. S., & Kassel, E. E. (1989). Blow-in fractures of the orbit. *Plastic and Reconstructive Surgery, 84*(1), 10–20.
507. Nkenke, E., Amann, K., Maier, T., et al. (2005). Untreated 'blow-in' fracture of the orbital floor causing a mucocele: Report of an unusual late complication. *Journal of Cranio-Maxillo-Facial Surgery, 33*(4), 255–259.

Medial Wall Fractures

4

Vadim P. Nikolaenko, Yury S. Astakhov,
and Sergei A. Karpischenko

Contents

4.1 Isolated "Trap-Door" Fracture 232
4.2 Isolated Comminuted and Punched-Out Fractures 234
4.3 Inferomedial Fracture 238
4.4 Radiological Signs 238
4.5 Treatment of the Medial Wall Fractures 240
4.6 Further Surgical Steps 244
References 246

Medial orbital wall fractures are less common than blowout orbital floor fractures [1, 2]. Isolated medial wall fractures occur in only 4 % of cases [3, 4] and most commonly are a part of inferomedial or nasoorbitoethmoidal fractures [5–7]. While pediatric medial wall fractures are always isolated, in 1/3 of adult cases, they accompany other facial fractures [7], 50 % of which usually are nasal fractures [8].

V.P. Nikolaenko, MD, PhD, DSc (✉)
Department of Ophthalmology, Saint Petersburg State Hospital No. 2,
Saint-Petersburg, Russia

Department of Otolaryngology and Ophthalmology, Medical Faculty,
Saint-Petersburg State University, Saint-Petersburg, Russia
e-mail: dr.nikolaenko@mail.ru

Y.S. Astakhov, MD, PhD, DSc
Department of Ophthalmology, I.P. Pavlov First Saint Petersburg State Medical University,
Saint-Petersburg, Russia

City Ophthalmologic Center at Saint Petersburg State Hospital No. 2,
Saint-Petersburg, Russia
e-mail: astakhov73@mail.ru

S.A. Karpischenko, MD
ENT Department, First Pavlov State Medical University of Saint Petersburg,
Saint-Petersburg, Russia
e-mail: karpischenkos@mail.ru

© Springer-Verlag Berlin Heidelberg 2015

V.P. Nikolaenko, Y.S. Astakhov (eds.), *Orbital Fractures: A Physician's Manual*,
DOI 10.1007/978-3-662-46208-9_4

Medial wall fractures typically result from direct trauma (accidents, physical assault, and contact sport activities) [9, 10]. There are individual reports of medial wall fractures due to barotrauma [11], sneezing [12], and repeated forceful nose blowing [13–17].

Inferior and medial wall fractures have similar mechanisms. W. Fuchs et al. (1901) theorized that the fracture was caused by lateral displacement of the globe (similar to the hypothesis of orbital floor fracture due to inferior globe displacement proposed by R. Pfeiffer). There are two major theories regarding blowout fractures—*hydraulic theory* (blowout fracture due to increase in intraorbital or intranasal pressure) and *mechanical ("buckling") theory* (transmission of the external force from the medial orbital rim to the walls) [18, 19]. Different clinical types of medial wall fractures may be associated with the predominance of one of these mechanisms.

Blunt trauma to the bridge of the nose causes the so-called blow-in fractures. The pressure transmitted through medial orbital rim causes the expansion of the ethmoidal cells and displacement of the medial wall into the orbital cavity [3, 20].

The main fracture site is the weakest anterior part of the orbital lamina (lamina papyracea), which forms the middle third of the medial orbital wall (Fig. 4.1a) [21, 22].

Sneezing may cause not only a blow-in fracture (which is quite logical) but also a blow-out fracture. The possible mechanism underlying bone fragments being displaced into the ethmoidal cells may be explained by the rapid increase in intranasal pressure, passage of air into the orbit, and acute orbital emphysema. Air reflux into paranasal sinuses displaces the fragments of orbital lamina of the ethmoidal bone resulting in a blowout pattern [12]. This fracture type is a good illustration of the hydraulic theory as there is no pressure to on the orbital rim or direct impact of the deformed globe on the medial wall [14].

The majority (90 %) of isolated medial wall injuries occur in the pediatric age group and are linear "trap-door" or tongue-shaped fractures (∩–formed fractures) [8, 23–25]. This is due to high bone elasticity which allows for transient deformation. While the vast majority of this type of fracture is seen in the pediatric population, it is also possible in adults [4, 26].

The mechanism of "trap-door" fracture is similar to that of the orbital floor injury. Medial wall fragments are pushed outwards (into the ethmoidal cells) and after the impact return to their initial position entrapping less mobile soft tissue [26].

Comminuted fractures or fractures with one detached ("punched-out") bone fragment are observed in 7 % of cases due to a very low thickness (0.27 mm) and fragility of medial orbital wall in the elderly [8, 23, 24, 27–29].

Thus, the main types of medial wall injuries are isolated (linear or ∩–formed "trap-door," comminuted, and "punched-out" fracture), inferomedial, and nasoorbitoethmodial fractures (Figs. 3.4 and 4.1) each with its specific clinical manifestation.

4.1 Isolated "Trap-Door" Fracture

This fracture is clinically characterized by the immediate onset of diplopia and limitation of horizontal globe motion, often accompanied by nausea, minimal edema and hematoma of the eyelids, and absence of enophthalmos [4].

Diplopia during adduction/abduction may be considered the pathognomonic sign of this fracture [6, 9, 30]. One third of the patients complain of diplopia in the

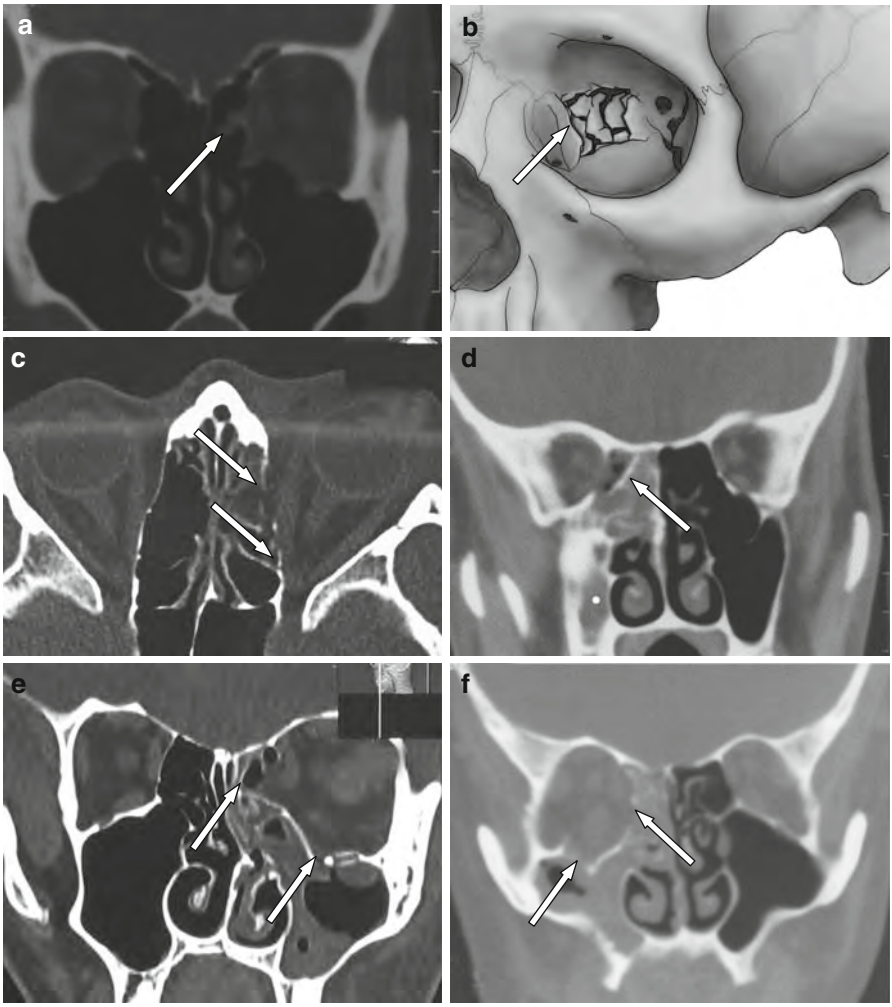

Fig. 4.1 Medial wall fractures: (**a**) "trap-door" fracture. There is some adipose tissue entrapped in the fracture site (*arrow*), (**b**) comminuted fracture of the medial wall, (**c**) comminuted fracture on axial CT, (**d**) "punched-out" fracture with single separated bone fragment, (**e**, **f**) inferomedial fracture

primary gaze position, but others develop this sign within 30° from fixation point [31]. One should remember that diplopia with an isolated medial wall fracture may be clinically evident in only 50 % of cases [23], and its absence does not rule out orbital injury.

Occasionally "trap-door" fractures may entrap the medial rectus [25, 26, 32]. Before 1975 only six cases were reported [33], and only six more cases were reported in the following years. Interestingly, all reported patients were black, which may be interpreted as an anatomical predisposition to such injuries due to ethnical

differences in midface anatomy [34]. This hypothesis is supported by other case reports on Asian patients, in which medial wall fractures are more commonly seen compared to orbital floor fractures [9, 30, 35]. The incidence of medial wall fractures in patients from Southeast Asia is shown to be higher due to thinner medial wall, weaker nasofrontal suture, lower nasal bridge, and weaker orbital rim compared to Caucasians [4].

Limitation of globe movements is present in 10–25 % of cases and, according to S. Lerman rules, is determined by the site of medial rectus muscle entrapment (preequatorial or postequatorial) [8, 23, 36]. When the anterior portion of the muscle is entrapped, Duane[1] pseudosyndrome is observed. Posterior portion entrapment results in exotropia with significant limitation of adduction and normal abduction of the globe[2] [3, 4, 25, 37, 38].

Positive duction test (limitation of abduction), sometimes accompanied by nausea and the oculocardiac reflex, confirms muscle or muscle sheath entrapment and rules out other possible causes of globe movement restriction such as injury to the oculomotor nerve and/or contusion of the medial rectus [25].

4.2 Isolated Comminuted and Punched-Out Fractures

Isolated, comminuted, and punched-out fractures are characterized by a vivid clinical picture. The key diagnostic triad includes diplopia, limitation of horizontal globe motion, and positive abduction test and is commonly accompanied by periorbital edema, ecchymosis, and subconjunctival hemorrhage (Fig. 4.2e) [4, 5, 18, 34, 39].

In one third of patients, the area of the isolated fracture exceeds 4 cm^2 which causes mild enophthalmos (up to 2 mm) [8].

Nasal bleeding (epistaxis) is an obvious sign of fracture [21, 40]. The source of bleeding is the anterior ethmoidal artery which is frequently damaged even after minimal displacement of the bone fragments of the medial orbital wall. Small anterior ethmoidal cells are quickly filled with blood, which then flows from the hiatus semilunaris into the middle nasal meatus and obturates it. Difficulties in nasal breathing force a patient to blow his/her nose which leads to orbital emphysema. This characteristic sign of the medial wall injuries [41] was first described by R. Berlin in 1880.

According to radiological findings, emphysema is diagnosed in approximately 50 % of patients with orbital fractures [42] and indicates the involvement of the

[1] Esotropia, limitation of abduction, narrowing of palpebral fissure, pseudoptosis, and retraction enophthalmos (posterior displacement of the globe in abduction). The last symptom may be absent when medial rectus becomes entrapped in the posterior part of medial orbital wall (Fig. 4.2a).

[2] Entrapment of the posterior part of medial rectus clinically manifests as a pseudoparalysis with intact lateral rectus (the anterior portion of the entrapped muscle fails to rotate the globe to the nose, while holding it in abduction). This uncommon syndrome can be falsely interpreted and delay surgical intervention (Fig. 4.2b–d).

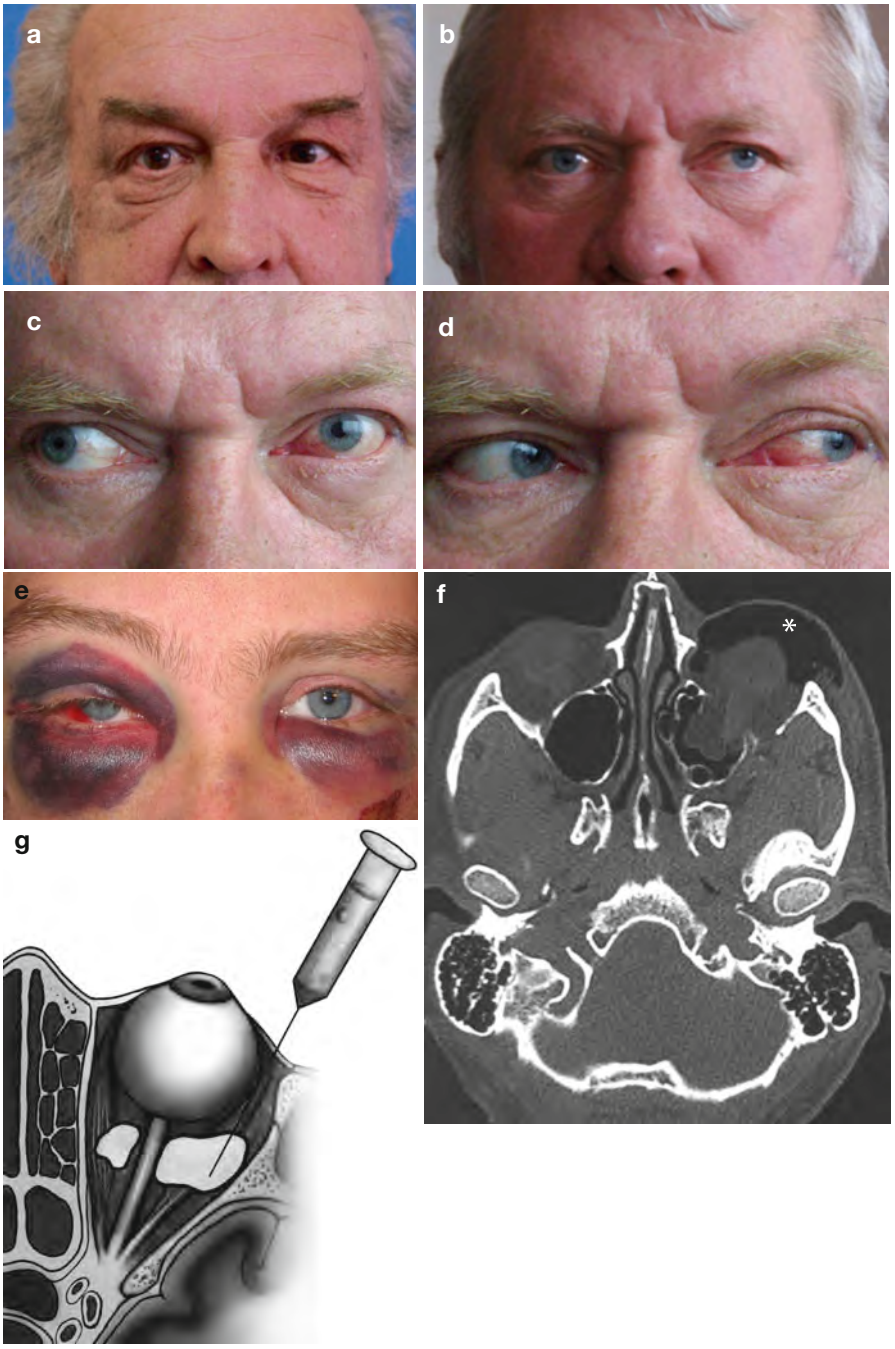

Fig. 4.2 Clinical signs of medial wall fracture: (**a**) esotropia of the left eye in an anterior medial wall fracture; (**b**–**d**) exotropia of the left eye (**b**) with significant limitation of adduction (**c**) and normal abduction (**d**), suggesting the entrapment of the posterior part of the medial rectus; (**e**) eyelid hematoma and subconjunctival hemorrhage, indirect signs of medial wall fracture; (**f**) orbital emphysema (*) and its drainage technique (**g**) (see explanation in the text)

paranasal sinuses [43]. Orbital emphysema is particularly common in medial wall injuries[3] [17, 41, 44].

Emphysema in orbital fractures[4] is associated with the communication between orbital cavity and ethmoidal cells, which in 100 % of cases follows the disruption of sinus mucosa. Thus, orbital emphysema is always accompanied by blood in the sinus [17].

Forceful expiratory effort (sneezing, nose blowing, etc.) elevates the intranasal pressure up to 115 mmHg and presses the air into the orbit. If the periosteum is intact, the air can accumulate in the subperiosteal space causing dystopia of the globe and blindness in extreme cases. In most cases, mild emphysema spontaneously resolves in 7–14 days [12, 13].

If the periosteum is ruptured, air passes into the orbit and spreads along the fascia into subconjunctival, preseptal, and postseptal spaces. Generally, it accumulates at the injured orbital wall. Orbital tissues in this case sometimes are pushed against the wall and block the communication, acting as a valve which can lead to the development of tension emphysema [42]. Clinical signs include axial, vertical, or horizontal dystopia. Tension emphysema and valve mechanism are especially characteristic of "trap-door" fractures [45].

Acute increase in intraorbital pressure is usually absorbed by elastic orbital tissues, allowing the displacement of the globe. In the majority of cases, emphysema spontaneously resolves without any sequelae [45, 46].

Rarely, emphysema leads to irreversible loss of vision due to the impairment of vascular supply to the optic nerve or occlusion of the central retinal artery. This clinical scenario is seen predominantly in younger patients whose orbital septum begins to deform at a pressure of only 70–100 mmHg (according to the experimental data of Ch. F. Heerfordt (1904)). This deformation may cause compression of the optic nerve.

Because the perfusion pressure of the retina and optic nerve is only 60–70 mmHg, the increased orbital pressure caused by the deformation of the orbital septum may be greater than the perfusion pressure to the nerve and retina. If that occurs, blood flow to the retina will stop, and if that continues for more than 100 min, it will cause irreversible damage to the retina.

In this case urgent surgical intervention is required [15, 17, 45, 47].

Medical history of recent blunt trauma to the bridge of the nose or orbit or forceful expiratory effort (sneezing and nose blowing) may be helpful in the diagnosis of emphysema. Routine physical examination is also very informative (edema of the eyelids increasing while blowing the nose, crepitus in the periocular soft tissues [35]). Visual acuity and pupil reaction should be a part of the initial evaluation.

[3] One should remember that emphysema can also be the sign of pulmonary barotrauma [47], pneumomediastinum, tumor growth, or gas-producing microorganisms and even Munchausen syndrome.

[4] The first descriptions of the pathogenesis of orbital emphysema were published by E. Fuchs (1901) and Ch. F. Heerfordt (1904).

Other recommended investigations include ophthalmoscopy, intraocular pressure measurement, and CT of the orbit [45].

Staging of orbital emphysema:

Stage I—small radiologically diagnosed asymptomatic air mass in the orbit. The treatment is limited to prophylactic oral antibiotics and vasoconstrictive nasal drops for the congestion relief.

Stage II—increase in air mass leads to dystopia and thereby diplopia. In addition to standard treatment, CT scan is recommended to diagnose injuries requiring delayed surgical intervention.

Stage I and stage II are not accompanied by the loss of vision.

Stage III—the increasing air mass causes the failure of the absorbing mechanism of orbital soft tissues. There is an increase in intraocular pressure and obstruction of the blood flow in the smallest vessels of the optic nerve. Severe loss of vision with ophthalmoscopically normal retinal circulation may be observed.

Stage IV—intraocular pressure due to tension emphysema increases up to 60–70 mmHg leading to central retinal artery occlusion and blindness in 100 min. Severe loss of vision with the ophthalmoscopical picture of a central retinal artery occlusion is observed.

Stage III and stage IV cause severe loss of vision[5]; therefore immediate medical treatment is needed.

In case of emphysema with significant increase in intraocular pressure and loss of vision, orbital decompression should be considered.

After the localization of the air mass on CT scans, drainage of the orbit is performed according to the J. V. Linberg technique (1982). The air mass is drained with a 25-gauge needle attached to a saline-filled syringe with the plunger removed [48]. Proper placement of the needle is confirmed by the appearance of water bubbles in the syringe (Fig. 4.2g). If there is loss of light perception, drainage is combined with canthotomy and cantholysis (Fig. 3.25).

A timely and successful drainage results in rapid return of intraorbital and intraocular pressure to normal and restoration of the blood flow and visual acuity [17, 42, 49, 50].

In the absence of contraindications, single intravenous injection of 30 mg/kg prednisolone is given followed by 15 mg/kg prednisolone every 6 h for 24 h. Symptomatic therapy includes administration of analgesics and antiemetics [45].

Theoretically, emphysema with underlying sinusitis may cause infection of the orbital soft tissues [47]. Therefore broad-spectrum antibiotics in prophylactic doses are indicated, although the necessity and benefit of such treatment is yet to be proved [12].

[5] It should be mentioned that such severe injury is uncommon. From 1900 to 1994 only 85 such cases were described [47].

Emphysema of the face, neck, or mediastinum are uncommon for medial wall fractures, but these complications should be kept in mind, because they may be misleading and interpreted as a clinical sign of thorax or abdominal injury [43, 51, 52].

S. J. Garg et al. (2005) [10] first described the unique case of asymptomatic "blowout" medial orbital wall fracture with a bone fragment penetrating the globe.

4.3 Inferomedial Fracture

If medial wall injury is a part of inferomedial fracture, all patients develop diplopia (Fig. 4.1e, f), and 40 % of patients experience globe movement restriction. If the area of the fracture exceeds 4 cm^2 (approximately 80 % of cases), clinically significant enophthalmos (more than 2 mm) is observed.

Nasal congestion causing repetitive nose blowing and orbital emphysema is less common in inferomedial fractures, since blood accumulates in the more spacious maxillary sinus compared to the ethmoidal cells.

Extensive inferomedial fracture is very rarely complicated by globe dislocation into the ethmoidal cells [53, 54]. The first description of the globe dislocation into ethmoidal cells is thought to be published by Raghav et al. [55]. In some cases globe dislocation may still have a favorable functional outcome [56, 57]; however, more commonly it causes irreversible loss of vision and restricted globe mobility in spite of successful globe reposition and reconstruction of muscles and orbital walls [54].

Another rare condition after inferomedial fracture resembles Brown syndrome (superior oblique tendon sheath syndrome with the limitation of globe supraduction during adduction). In this case, the patient experiences diplopia in a primary gaze position and ipsilateral hypotropia. The recommended treatment is the recession of the inferior rectus of the ipsilateral eye [58].

Clinical signs of nasoorbitoethmoidal fracture are discussed in corresponding chapters.

4.4 Radiological Signs

X-ray gives a clear view of the medial wall fracture only in 15 % of cases [44] due to superimposition of multiple anatomical structures in the nasoorbitoethmoidal region [59]. Generally, the diagnosis of medial wall fracture is based on indirect clinical signs including orbital emphysema and ethmoidal cells opacification [60].

Introduction of high-sensitive CT scanners brought the diagnosis of medial wall fractures to a higher level [21, 59]. Thus, the number of medial wall surgical procedures has doubled in the past decade [61].

Axial and coronal views are especially useful in this pathology [34]. CT signs of medial orbital wall fracture besides obvious displacement of bone fragments include [9]:

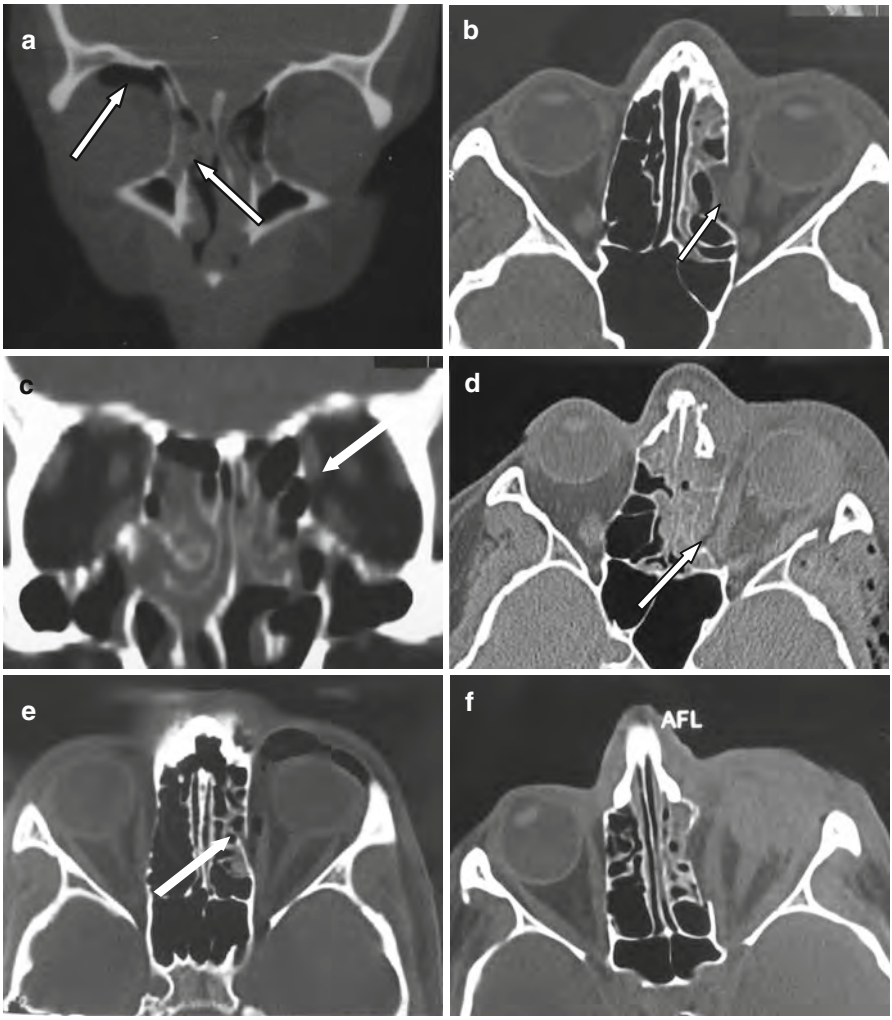

Fig. 4.3 CT signs of medial orbital wall fracture: (a) air mass under the roof of the orbit and blood in the ethmoidal cells (*arrows*) on coronal CT indicate medial orbital wall fracture regardless of the seemingly intact medial wall contour. (**b**) Medial wall fracture with thickening and dislocation of medial rectus belly (*arrow*). (**c**) Displacement of medial rectus into ethmoidal sinus, the muscle seems to be absent both in the orbit and in the sinus. *Arrow* shows contralateral medial rectus. (**d**) Entrapment of the posterior portion of the medial rectus (*arrow*). (**e**) Bone fragment. (**f**) Extensive blowout fracture of the medial wall

- Entrapment of the orbital fat in the ethmoidal cells (Fig. 4.1a)
- Orbital emphysema and hemosinus (Fig. 4.3a)
- Edema and/or displacement of the medial rectus in the nasal direction [9, 62]
- Adjoining muscles pressed to the medial orbital wall or prolapse of the muscle belly into the ethmoidal cells (rarely) [25, 26, 62] (Fig. 4.3b–d)

4.5 Treatment of the Medial Wall Fractures

Surgical treatment of the "blowout" medial orbital wall fracture is aimed at the restoration of a normal orbital wall, reconstruction of the initial orbital shape and volume, and normalization of ethmoidal ventilation [23].

It should be remembered that not all patients with medial orbital wall fractures need surgical treatment [1, 2, 29, 63].

Indications for medial orbital wall reconstruction [28, 63] are:

- Enophthalmos > 2 mm
- Globe movement restriction
- Persistent horizontal diplopia
- Bone defect >2 cm^2 with fragment displacement ≥3 mm
- Accompanying orbital floor fracture
- "Rounding" of medial rectus (height to width ratio >0.7 according to coronal CT) which is a sign of late enophthalmos

Surgical Timing. "Trap-door" fracture of the orbital wall is a medical emergency [4][6]; other medial wall injuries should be surgically treated 7–14 days after acute symptoms are controlled [23].

Surgery should be carried out under endotracheal or intravenous anesthesia.

The surgical approach to the medial orbital wall is determined by the localization and extent of the fracture. The different approaches are transcutaneous, transconjunctival, microscopic transnasal, and endoscopic [23, 64].

Transcutaneous approaches include subciliary, upper lid, medial eyebrow, medial canthal, and bicoronal incisions.

The subciliary incision is described in detail in the previous chapter and is considered the optimal transcutaneous approach [9, 38, 39] but gives a suboptimal view of the upper third of the medial wall.

In contrast, the *bicoronal approach* (Fig. 4.4a) exposes the whole medial wall leaving the medial canthal ligament intact but requires extensive dissection and may cause a significant bleeding. Postoperatively this incision may be complicated by persisting forehead skin anesthesia.

The incision along the medial half of the fold of the upper eyelid poorly exposes deep parts of the orbit and does not allow the placement of a large implant. The *medial eyebrow approach may* also lead to the permanent numbness of the forehead skin due to the supratrochlear nerve injury (Fig. 4.4a).

The ethmoidal Lynch incision provides a good view of all areas of the medial wall (Fig. 4.4b), but it is made perpendicular to the Langer's skin tension lines. This leads to excessive scarring and deformation of the medial canthus [23, 65]. To avoid this complication, not only the well-known *medial and upper medial Z incisions* can

[6] Surgery in the first 4 days after injury guarantees complete regression of symptoms in 4–6 weeks. After delayed surgical treatment residual symptoms may persist for up to 10 months [4].

be used (Fig. 4.4c) [68] but also the W modification of this incision as proposed by Burns et al. [23].

Upper Medial W-Formed Approach. After temporary tarsorrhaphy, the 3-cm-long W-formed incision is made along the upper medial edge of the orbit, starting

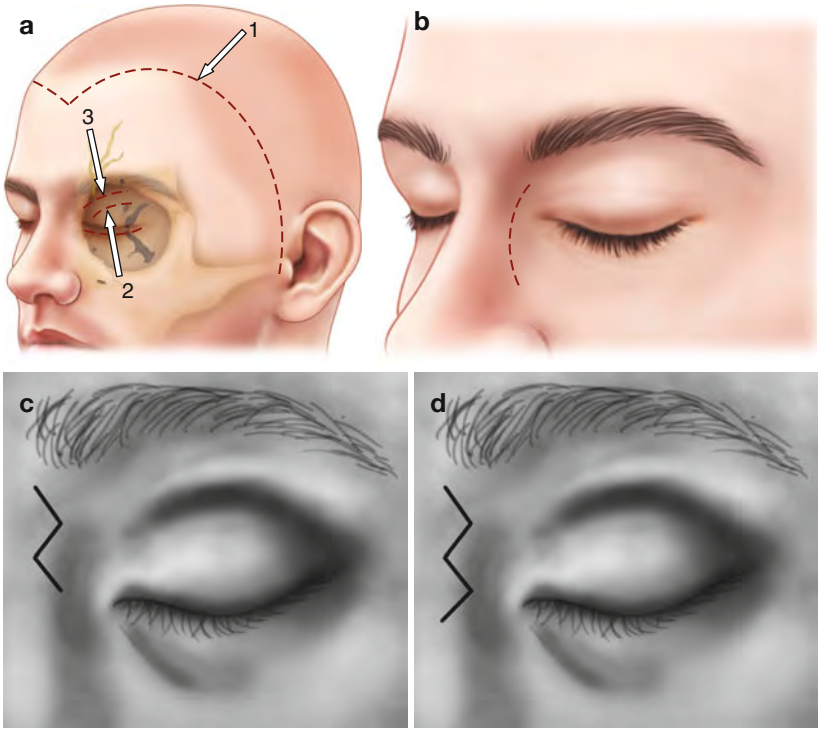

Fig. 4.4 Surgical approaches to the medial orbital wall (transcutaneous): (**a**) coronal (*1*), along the inner half of the fold of the upper eyelid (*2*), and medial eyebrow approach (*3*). The course of supratrochlear nerve is shown with the *dashed line*. (**b**) Lynch approach (2.5-cm curvilinear skin incision made 10 mm medial to the insertion of medial canthal ligament, followed by the division and blunt dissection of the periosteum of the medial orbital wall up to the middle third of the lamina papyracea). (**c**) Upper medial Z-formed approach. *Arrows* show the location of the medial canthal ligament and trochlea of superior oblique that should be avoided during skin incision. (**d**) Upper medial W-formed approach (see description in text). (**e**) (*1*) Inferior (preseptal and postseptal) transconjunctival approach without lateral canthal ligament dissection; (*2*) medial transconjunctival (transcaruncular or retrocaruncular) approach. The incision is begun in the sulcus between the lacrimal caruncle and plica semilunaris and continued up to 20 mm along the inferior conjunctival fornix. Subconjunctival dissection to the posterior lacrimal crest is made in the avascular zone parallel to the medial wall behind Horner's muscle. Division of periosteum is made behind the posterior lacrimal crest; (*3*) inferior transconjunctival approach with the division of lateral canthal ligament; combinations of inferior and medial approaches, with dissection of lateral palpebral ligament if necessary, are also used. (**f**) The line of transcaruncular incision. (**g**) Transcaruncular approach in coronal plane. (**h**) Orbital zones exposed by different methods (*1*) coronal approach, (*2*) approach along the upper eyelid, (*3*) medial eyebrow approach (Illustration materials from www.aofoundation.org)

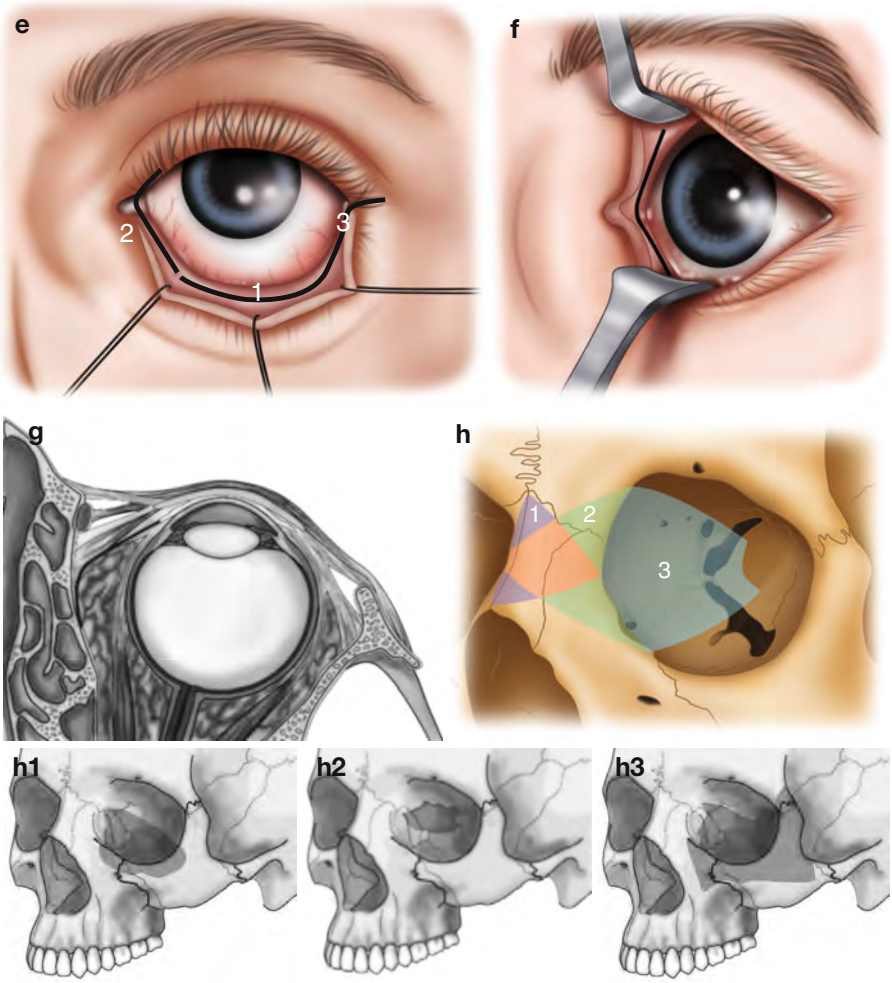

Fig. 4.4 (continued)

1 cm medial from the insertion of medial canthal ligament to the lower medial edge of the eyebrow (Fig. 4.4d). The angles between the cuts are approximately 110–120°. Because all four cuts run parallel or at an acute angle to the Langer's skin tension lines, this incision results in a very cosmetic scar. The lateral part of the W-formed incision may be continued laterally along the lower edge of the medial third of the eyebrow, if necessary, providing good view of the whole medial wall and a placement of larger implant (up to 3 cm in length) to close total wall defect.

A careful splitting (parallel to the orbital edge) of the orbicularis oculi is then performed to avoid supratrochlear nerve injury.

Division of the periosteum is made at the upper edge of palpebral canthal ligament (partially cutting it off, if necessary) and carried out to the upper medial orbital edge 3–4 mm from the rim. It is important to preserve the inferior part of the medial canthal ligament to avoid the subsequent telecanthus formation. Periosteum is then separated from the medial wall up to the lacrimal bone.

To avoid injuries to the trochlea which will result in diplopia due to acquired Brown's syndrome and injuries of the lacrimal sac, adjacent periosteum is not dissected. After the dissection of periosteum from the medial orbital wall and inner part of the orbital roof, the fracture, entrapped soft tissues, and anterior ethmoidal neurovascular bundle become clearly visible. Anterior ethmoidal vessels should be cauterized to prevent profuse bleeding. Dissection is generally extended up to the middle third of the lamina papyracea. When the posterior ethmoidal artery becomes exposed, further dissection should be immediately stopped due to high risk of optic nerve injury.

Transconjunctival approaches include inferior and medial incisions [40, 69], extended transcaruncular approach [70], and a combination of transcaruncular and inferior transconjunctival approaches (Fig. 4.4e, f) [31, 71].

Inferior conjunctival incision was already described in detail in previous chapter(s). The main disadvantage of this approach is poor exposure of upper areas of the medial wall [22].

Medial Conjunctival (Retrocaruncular) Approach (Fig. 4.4f–h). In this approach the 10–14-mm-long incision is made behind the lacrimal caruncle followed by blunt dissection to reach the suture between the lacrimal and ethmoidal bones. After the dissection of the periosteum, the fracture zone becomes visible and the anterior ethmoidal artery is cauterized if necessary [66].

Disadvantages of this approach include difficult dissection of soft tissues and poor exposure of extensive fractures. Besides, due to the small size of incision, it is not possible to cover the extensive fracture with one implant. One has to use several small implants that could later migrate into the ethmoidal labyrinth. This approach is best used with endoscopic equipment by an experienced otolaryngologist.

The combination of inferior and medial conjunctival approaches allows the exposure of the whole medial wall, but it may be complicated by excessive scarring with the involvement of lacrimal points and canaliculi, extropion or entropion, and intraoperative injury of the inferior oblique, medial canthal ligament, or lacrimal apparatus [22].

Extended transcaruncular approach involves the extension of the incision on the lacrimal caruncle for 10–12 mm to the inferior and superior conjunctival fornix [72]. The soft tissues are the bluntly dissected in the anteroposterior direction. The dissection of the periosteum behind the posterior lacrimal crest allows optimal exposure of the fracture [73].

The advantages of this approach include the absence of excessive scarring, the possibility for implant plates up to 2 cm in height [6], and good exposure of the whole medial orbital wall and orbital floor with the extended incision along inferior conjunctival fornix [31, 74, 75]. One serious disadvantage is the high risk (80 %) of cutting the inferior oblique off its attachment [6].

Endoscopic Endonasal Approach. The procedure is performed under general anesthesia. The fracture is visualized by means of a digital video camera attached to the endoscope that projects the enlarged image to the screen.

After the resection of middle nasal concha and removal of uncinate process, the ethmoidal bulla is incised. The ethmoidal septum and mucosa are then removed; the fragments of the broken medial orbital wall are left in place. Prolapsed soft tissues are put back into the orbital cavity, and the medial wall defect is closed with a 2-mm silicone plate placed into the ethmoidal labyrinth for 2 months [1, 27, 30, 76, 77].

Instead of a silicone plate iodoform-impregnated swab, a Foley catheter (removed in 2–3 weeks postoperatively), resected uncinate process, Merocel or lyophilized human dura mater, or automucosal graft (for small defects) may be used [59, 78]. Sometimes the medial orbital wall defect may be closed by means of endoscopically rotating the displaced bone fragment by 90° [79].

Indications for transnasal endoscopic approach are limited to small isolated medial orbital wall fractures (<2 cm^2). When the defect exceeds 2 cm^2 or the bone fragment is displaced more than 3 mm or in the case of inferomedial fracture, transnasal endoscopic approach is possible only in combination with transcutaneous approach [22].

Among other disadvantages of transnasal endoscopic approaches are higher risk of infection due to temporary nasal tamponade, the need to remove the implant or catheter, and increased hospital stay and cost of treatment [80]. Moreover, the approach to the posterior part of medial orbital wall puts the optic nerve at high risk of injury. And finally, this method needs significant clinical experience in otolaryngological techniques and special instrumentation [1, 22].

Several other authors have proposed an alternative endoscopic approach through the medial transconjunctival and retrocaruncular incision with the use of 30-degree 2.7-mm endoscope [65, 66, 81].

4.6 Further Surgical Steps

Soft tissues prolapsing into the ethmoidal sinus are gently put backwards into the orbital cavity [23]. The tissue release is controlled by means of a horizontal duction test.

Further steps are determined by the fracture type. In the case of a ∩–formed "trap-door" fracture, fixing this flap, as described in the previous chapter, is appropriate (Fig. 3.47).

Osteoplasty with the use of autogenous [65, 66], donor [67], or synthetic grafts is a viable option in case of comminuted fractures [4, 6, 39, 82]. The authors'

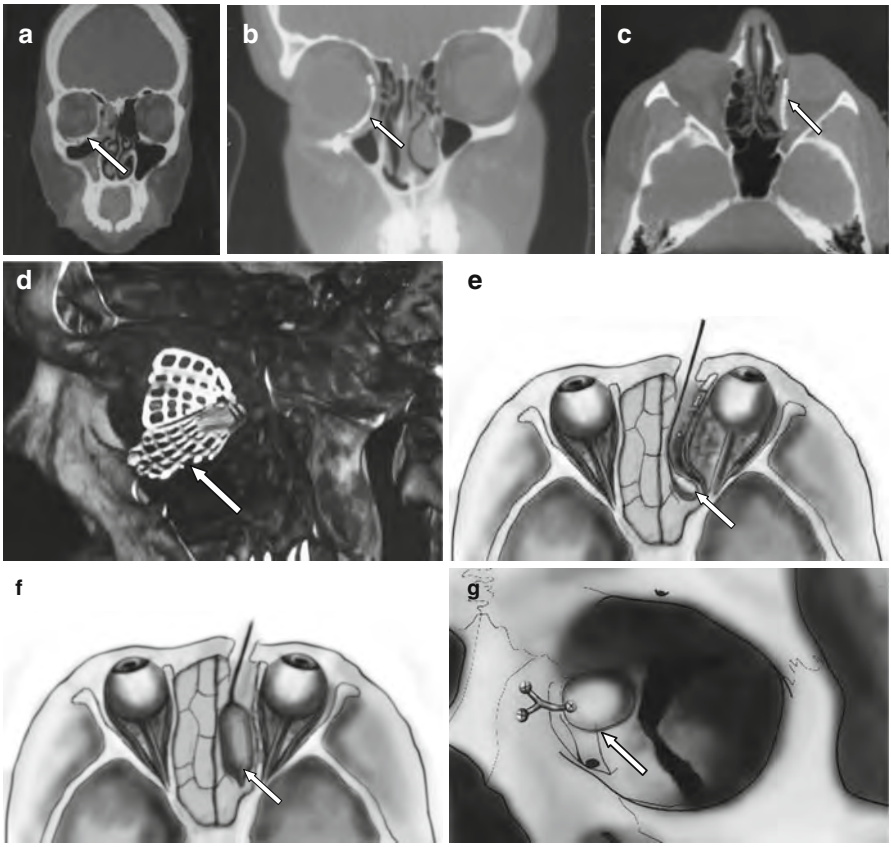

Fig. 4.5 Medial orbital wall defect closing (a) with porous polytetrafluoroethylene sheets (*arrow*). (**b–d**) With titanium mesh (*arrow*) that covers inferomedial fracture. (**e**) Silicone balloon (*arrow*) inserted into the ethmoidal labyrinth. (**f**) Filling the balloon with saline to achieve reposition of bone fragments. (**g**) Fixation of Y-formed titanium microimplant

preferred graft is titanium mesh (Fig. 4.5b–d). The implant should be precisely placed so its anterior part would not obstruct the lacrimal passage and its posterior part would not compress the orbital branches of the trigeminal nerve.

If there is a large bone fragment, the hole is made 5 mm above the medial canthal ligament and 5 mm medial to the orbital rim. After the insertion of elevator into ethmoidal cells (no more than 3 cm due to the proximity of the optic nerve!), the fracture is then reduced. A balloon is then inserted into the sinus and filled with 2–3 ml of saline to achieve hemostasis and support of the medial wall. A preformed implant is placed subperiosteally and fixed with screws to the orbital rim, the balloon is then extracted, and the wound is closed (Fig. 4.5e–g).

Postoperative management (nasal breathing control, antibiotic therapy, and steroids) follows the principles described in the previous chapter.

The most common complications are sinusitis and transient globe mobility disturbances. The late complications include enophthalmos, caused by inadequate surgical technique, and diplopia requiring prism or surgical correction according to the methods described in the previous chapter.

References

1. Lee, H. M., Han, S. K., Chae, S. W., et al. (2002). Endoscopic endonasal reconstruction of blowout fractures of the medial orbital walls. *Plastic and Reconstructive Surgery, 109*(3), 872–876.
2. Belli, E., Matteini, C., & Mazzone, N. (2009). Evolution in diagnosis and repairing of medial orbital wall fractures. *The Journal of Craniofacial Surgery, 20*(1), 191–193.
3. Brannan, P. A., Kersten, R. C., & Kulwin, D. R. (2006). Isolated medial orbital wall fractures with medial rectus muscle incarceration. *Ophthalmic Plastic and Reconstructive Surgery, 22*(3), 178–183.
4. Tse, R., Allen, L., & Matic, D. (2007). The white-eyed medial blowout fracture. *Plastic and Reconstructive Surgery, 119*(1), 277–286.
5. Scassellati-Sforzolini, G., Cavina, C., Scassellati-Sforzolini, B., et al. (1997–1998). Isolated lesion of the medial orbital wall following endonasal surgery. Isolated fractures of the medial orbital wall. *International Ophthalmology, 21*(6), 353–358.
6. Baumann, A., & Ewers, R. (2000). Transcaruncular approach for reconstruction of medial orbital wall fracture. *International Journal of Oral and Maxillofacial Surgery, 29*(4), 264–267.
7. Tse, R., Allen, L., & Matic, D. (2007). The white-eyed medial blowout fracture. *Plastic and Reconstructive Surgery, 119*(1), 277–286.
8. Burm, J. S., Chung, C. H., & Oh, S. J. (1999). Pure orbital blowout fracture: New concepts and importance of medial orbital blowout fracture. *Plastic and Reconstructive Surgery, 103*(7), 1839–1849.
9. Tanaka, T., Morimoto, Y., Kito, S., et al. (2003). Evaluation of coronal CT findings of rare cases of isolated medial orbital wall blow-out fractures. *Dento Maxillo Facial Radiology, 32*(5), 300–303.
10. Garg, S. J., Benson, W., Fineman, M., & Bilyk, J. R. (2005). Bone from an orbital floor fracture causing an intraocular foreign body. *American Journal of Ophthalmology, 139*(3), 543–545.
11. Bolognini, A., Delehaye, E., Cau, M., & Cosso, L. (2008). Barotraumatic orbital emphysema of rhinogenic origin in a breath-hold diver: A case report. *Undersea & Hyperbaric Medicine, 35*(3), 163–167.
12. Chiu, T. W., Chung, C. K., Chan, S. H., et al. (2006). Sneezing and orbital fracture. *Plastic and Reconstructive Surgery, 117*(3), 1049–1050.
13. Hunts, J. H., Patrinely, J. R., Holds, J. B., & Anderson, R. L. (1994). Orbital emphysema. Staging and acute management. *Ophthalmology, 101*(5), 960–966.
14. Suzuki, H., Furukawa, M., Takahashi, E., & Matsuura, K. (2001). Barotraumatic blowout fracture of the orbit. *Auris, Nasus, Larynx, 28*(3), 257–259.
15. Monaghan, A. M., & Millar, B. G. (2002). Orbital emphysema during air travel: A case report. *Journal of Cranio-Maxillo-Facial Surgery, 30*(6), 367–368.
16. Dunn, C. (2003). Surgical emphysema following nose blowing. *The Journal of Laryngology and Otology, 117*(2), 141–142.
17. Garcia-Medina, J. J., Garcia-Medina, M., & Pinazo-Duran, M. D. (2006). Severe orbitopalpebral emphysema after nose blowing requiring emergency decompression. *European Journal of Ophthalmology, 16*(2), 339–342.
18. Leone, C. R., Lloyd, W., & Rylander, G. (1984). Surgical repair of medial wall fractures. *American Journal of Ophthalmology, 97*(3), 349–356.

19. Ducroz, V., Divaris, M., Franchi, G., et al. (1995). Fracture de la paroi mediale de l`orbite. A propos de 4 observations. *Revue de Stomatologie et de Chirurgie Maxillo-Faciale, 96*(3), 137–141.
20. Daly, B. D., Russell, J. L., Davidson, M. J., & Lamb, J. T. (1990). Thin section computed tomography in the evaluation of naso-ethmoidal trauma. *Clinical Radiology, 416*(4), 272–275.
21. Sanderov, B., & Viccellio, P. (1988). Fractures of the medial orbital wall. *Annals of Emergency Medicine, 17*(9), 973–976.
22. Kim, K. S., Kim, E. S., & Hwang, J. H. (2006). Combined transcutaneous transethmoidal/transorbital approach for the treatment of medial orbital blowout fractures. *Plastic and Reconstructive Surgery, 117*(6), 1947–1955.
23. Burm, J. S., & Oh, S. J. (2001). Direct local approach through a W-shaped incision in moderate or severe blowout fractures of the medial orbital wall. *Plastic and Reconstructive Surgery, 107*(4), 920–928.
24. Burm, J. S. (2005). Internal fixation in trapdoor-type orbital blowout fracture. *Plastic and Reconstructive Surgery, 116*(4), 962–970.
25. McCulley, T. J., Yip, C. C., Kersten, R. C., & Kulwin, D. R. (2004). Medial rectus muscle incarceration in pediatric medial orbital wall trapdoor fractures. *European Journal of Ophthalmology, 14*(4), 330–333.
26. Kakizaki, H., Zako, M., Katori, N., & Iwaki, M. (2006). Adult medial orbital wall trapdoor fracture with missing medial rectus muscle. *Orbit, 25*(1), 61–63.
27. Jin, H. R., Shin, S. O., Choo, M. J., & Choi, Y. S. (2000). Endonasal endoscopic reduction of blowout fractures of the medial orbital wall. *Journal of Oral and Maxillofacial Surgery, 58*(8), 847–851.
28. Jin, H. R., Shin, S. O., Choo, M. J., & Choi, Y. S. (2000). Relationship between the extent of fracture and the degree of enophthalmos in isolated blowout fractures of the medial orbital wall. *Journal of Oral and Maxillofacial Surgery, 58*(6), 617–620.
29. Yano, H., Nakano, M., Anraku, K., et al. (2009). A consecutive case review of orbital blowout fractures and recommendations for comprehensive management. *Plastic and Reconstructive Surgery, 124*(2), 602–611.
30. Sanno, T., Tahara, S., Nomura, T., & Hashikawa, K. (2003). Endoscopic endonasal reduction for blowout fracture of the medial orbital wall. *Plastic and Reconstructive Surgery, 112*(5), 1228–1237.
31. Kim, S., Helen, L. M., Chung, S. H., et al. (2005). Repair of medial orbital wall fracture: Transcaruncular approach. *Orbit, 24*(1), 1–9.
32. Turko, A., Talbot, S., & Pomahac, B. (2009). Medial orbital wall fracture with associated medial rectus entrapment and retrobulbar hematoma. *Plastic and Reconstructive Surgery, 123*(3), 108e–109e.
33. Davidson, T. M., Olesen, R. M., & Nahum, A. M. (1975). Medial orbital wall fracture with rectus entrapment. *Archives of Otolaryngology, 101*(1), 33–35.
34. Merle, H., Gerard, M., & Raynaud, M. (1998). Isolated medial orbital blow-out fracture with medial rectus entrapment. *Acta Ophthalmologica Scandinavica, 76*(3), 378–379.
35. Nam, S. B., Bae, Y. C., Moon, J. S., & Kang, Y. S. (2006). Analysis of the postoperative outcome in 405 cases of orbital fracture using 2 synthetic orbital implants. *Annals of Plastic Surgery, 56*(3), 263–267.
36. Shetty, T. T., Sami, A. S., Clark, D. R., & Bearn, M. A. (1995). Posterior medial wall blow out fracture. *The British Journal of Ophthalmology, 79*(4), 390.
37. Duane, T. D., Schatz, N. J., & Caputo, A. R. (1976). Pseudo-Duane's retraction syndrome. *Transactions of the American Ophthalmological Society, 74*, 122–132.
38. Segrest, D. R., & Dortzbach, R. K. (1989). Medial orbital wall fractures: Complications and management. *Ophthalmic Plastic and Reconstructive Surgery, 5*(2), 75–80.
39. Bae, Y. C., Choi, S. J., Moon, J. S., & Nam, S. B. (2007). Comparison of the postoperative outcome in pure medial orbital fracture among three groups: Using porous polyethylene or hydroxyapatite through subciliary approach and transnasal endoscopic correction. *Annals of Plastic Surgery, 59*(3), 287–290.

40. Barone, C. M., & Gigantelli, J. W. (1998). Endoscopic repair of posttraumatic enophthalmos using medial transconjunctival approach: A case report. *The Journal of Cranio-Maxillofacial Trauma, 4*(1), 22–26.
41. Shinohara, H., Shirota, Y., & Fujita, K. (2004). Implication of differences in the incidence of orbital emphysema in ethmoidal and maxillary sinus fractures. *Annals of Plastic Surgery, 53*(6), 565–569.
42. Dobler, A. A., Nathenson, A. L., Cameron, J. D., et al. (1993). A case of orbital emphysema as an ocular emergency. *Retina, 13*(2), 166–168.
43. Roccia, F., Griffa, A., Nasi, A., & Baragiotta, N. (2003). Severe subcutaneous emphysema and pneumomediastinum associated with minor maxillofacial trauma. *The Journal of Craniofacial Surgery, 14*(6), 880–883.
44. Langen, H. J., Daus, H. J., Bohndorf, K., & Klose, K. (1989). Konventionelle Rontgenuntersuchung und Computertomographie bei der Diagnostik von Orbitafrakturen. *Fortschritte auf dem Gebiete der Röntgenstrahlen und der Nuklearmedizin, 150*(5), 582–587.
45. Muhammad, J. K., & Simpson, M. T. (1996). Orbital emphysema and the medial orbital wall: A review of the literature with particular reference to that associated with indirect trauma and possible blindness. *Journal of Cranio-Maxillo-Facial Surgery, 24*(4), 245–250.
46. Cartwright, M. J., Ginsburg, R. N., & Nelson, C. C. (1992). Tension pneumoorbitus. *Ophthalmic Plastic and Reconstructive Surgery, 8*(4), 303–304.
47. Zimmer-Galler, I. E., & Bartley, G. B. (1994). Orbital emphysema: Case reports and review of the literature. *Mayo Clinic Proceedings, 69*(2), 115–121.
48. Vairaktaris, E., Moschos, M. M., Vassiliou, S., et al. (2008). Delayed appearance of diplopia due to orbital emphysema after repair of orbital fractures. *Oral Surgery, Oral Medicine, Oral Pathology, Oral Radiology, and Endodontics, 106*(1), 8–10.
49. Al-Shammari, L., Majithia, A., Adams, A., & Chatrath, P. (2008). Tension pneumo-orbit treated by endoscopic, endonasal decompression: Case report and literature review. *The Journal of Laryngology and Otology, 122*(3), 8.
50. Key, S. J., Ryba, F., Holmes, S., & Manisali, M. (2008). Orbital emphysema — the need for surgical intervention. *Journal of Cranio-Maxillo-Facial Surgery, 36*(8), 473–476.
51. Almog, Y., Mayron, Y., Weiss, J., et al. (1993). Pneumomediastinum following blowout fracture of the medial orbital wall: A case report. *Ophthalmic Plastic and Reconstructive Surgery, 9*(4), 289–291.
52. Bars, N., Atlay, Y., Tülay, E., & Tanju, G. (2008). Extensive subcutaneous emphysema and pneumomediastinum associated with blowout fracture of the medial orbital wall. *The Journal of Trauma, 64*(5), 1366–1369.
53. Moon, M., Pietris, G., & Shapter, M. (1997). Dislocation of the globe into the ethmoid sinuses. *Australian and New Zealand Journal of Ophthalmology, 25*(2), 175–176.
54. Kang, B. D., & Jang, M. H. (2003). A case of blowout fracture of the orbital wall with eyeball entrapped within the ethmoid sinus. *Korean Journal of Ophthalmology, 17*(2), 149–153.
55. Raghav, B., Vashisht, S., Keshav, B. R., & Berry, M. (1991). The missing eyeball — CT evaluation (a case report). *Indian Journal of Ophthalmology, 39*(4), 188–189.
56. Tranfa, F., Di Matteo, G., Di Salle, F., et al. (2000). Traumatic displacement of the globe into the ethmoid sinus. *American Journal of Ophthalmology, 130*(2), 253–254.
57. Okabe, H., Kimura, K., Sonoda, S., & Sakamoto, T. (2005). Displacement of globe into ethmoid sinus by medial orbital wall fracture with good recovery of vision. *Japanese Journal of Ophthalmology, 49*(5), 426–428.
58. Hwang, J. U., & Lim, H. T. (2005). Acquired simulated Brown syndrome following surgical repair of medial orbital wall fracture. *Korean Journal of Ophthalmology, 19*(1), 80–83.
59. Lee, M. J., Kang, Y. S., Yang, J. Y., et al. (2002). Endoscopic transnasal approach for the treatment of medial orbital blow-out fracture: A technique for controlling the fractured wall with a balloon catheter and Merocel. *Plastic and Reconstructive Surgery, 110*(2), 417–426.
60. de Visscher, J. G. A. M., & van der Wal, K. G. H. (1988). Medial orbital floor fracture with enophthalmos. *Journal of Cranio-Maxillo-Facial Surgery, 16*(2), 55–59.

61. Folkestad, L., & Granstrom, G. (2003). A prospective study of orbital fracture sequelae after change of surgical routines. *Journal of Oral and Maxillofacial Surgery, 61*(9), 1038–1044.
62. Ortube, M. C., Rosenbaum, A. L., Goldberg, R. A., & Demer, J. L. (2004). Orbital imaging demonstrates occult blow out fracture in complex strabismus. *Journal of AAPOS, 8*(3), 264–273.
63. Seiff, S. R. (1989). Cyanoacrylate fixed silicone sheet in medial blowout fracture repair. *Ophthalmic Surgery, 20*(9), 674–676.
64. Cruz, A. A., Akaishi, P. M., & Baccega, A. (2008). Upper eyelid crease approach to the medial orbital wall. *Plastic and Reconstructive Surgery, 122*(1), 25–26.
65. Chen, C. T., Chen, Y. R., Tung, T. C., et al. (1999). Endoscopically assisted reconstruction of medial orbital wall fractures. *Plastic and Reconstructive Surgery, 103*(2), 714–720.
66. Mun, G. H., Song, Y. H., & Bang, S. I. (2002). Endoscopically assisted transconjunctival approach in medial orbital wall fractures. *Annals of Plastic Surgery, 49*(4), 337–343.
67. Ballin, C. R., Sava, L. C., Maeda, C. A., et al. (2009). Endoscopic transnasal approach for treatment of the medial orbital blowout fracture using nasal septum graft. *Facial Plastic Surgery, 25*(1), 3–7.
68. Arthurs, B., Silverstone, P., & Della Rocca, R. C. (1987). Medial wall fractures. *Advances in Ophthalmic Plastic and Reconstructive Surgery, 6*, 393–401.
69. Kim, D. W., Choi, S. R., Park, S. H., & Koo, S. H. (2009). Versatile use of extended transconjunctival approach for orbital reconstruction. *Annals of Plastic Surgery, 62*(4), 374–380.
70. Malhotra, R., Saleh, G. M., de Sousa, J. L., et al. (2007). The transcaruncular approach to orbital fracture repair: Ophthalmic sequelae. *The Journal of Craniofacial Surgery, 18*(2), 420–426.
71. Lee, C. S., Yoon, J. S., & Lee, S. Y. (2009). Combined transconjunctival and transcaruncular approach for repair of large medial orbital wall fractures. *Archives of Ophthalmology, 127*(3), 291–296.
72. Shorr, N., Baylis, H. I., Goldberg, R. A., & Perry, J. D. (2000). Transcaruncular approach to the medial orbit and orbital apex. *Ophthalmology, 107*(8), 1459–1463.
73. Oh, J. Y., Rah, S. H., & Kim, Y. H. (2003). Transcaruncular approach to blowout fractures of the medial orbital wall. *Korean Journal of Ophthalmology, 17*(1), 50–54.
74. Garcia, G. H., Goldberg, R. A., & Shorr, N. (1998). The transcaruncular approach in repair of orbital fractures: A retrospective study. *The Journal of Cranio-Maxillofacial Trauma, 4*(1), 7–12.
75. Edgin, W. A., Morgan-Marshall, A., & Fitzsimmons, T. D. (2007). Transcaruncular approach to medial orbital wall fractures. *Journal of Oral and Maxillofacial Surgery, 65*(11), 2345–2349.
76. Hinohira, Y., Takahashi, H., Komori, M., & Shiraishi, A. (2009). Endoscopic endonasal management of medial orbital blowout fractures. *Facial Plastic Surgery, 25*(1), 17–22.
77. Park, C. H., Choi, D. J., Lee, J. H., et al. (2009). Endoscopic reduction of medial orbital wall fractures using the rolled silastic sheet technique. *The Journal of Trauma, 66*(5), 1421–1424.
78. Moore, C., & Conlin, A. (2008). Endoscopic transnasal repair of a medial wall orbital blowout fracture using a balloon catheter. *Journal of Otolaryngology - Head & Neck Surgery, 37*(1), 22–25.
79. Naraghi, M., & Kashfi, A. (2002). Endonasal endoscopic treatment of medial orbital wall fracture via rotational repositioning. *American Journal of Otolaryngology, 23*(5), 312–315.
80. Kim, S. H., Kang, D., & Park, J. (2009). Comparison of endoscopic endonasal reduction and transcaruncular reduction for the treatment of medial orbital wall fractures. *Annals of Plastic Surgery, 62*(3), 258–264.
81. Meningaud, J. P., Pitak-Arnnop, P., & Bertrand, J. C. (2007). Endoscope-assisted repair of medial orbital wall fractures using a retrocaruncular approach. *Journal of Oral and Maxillofacial Surgery, 65*(5), 1039–1043.
82. Kontio, R., Suuronen, R., Salonen, O., et al. (2001). Effectiveness of operative treatment of internal orbital wall fracture with polydioxanone implant. *International Journal of Oral and Maxillofacial Surgery, 30*(4), 278–285.

Naso-Orbito-Ethmoid Fractures

5

Vadim P. Nikolaenko, Yury S. Astakhov,
and Sergei A. Karpischenko

Contents

5.1 Introduction to Midface (Naso-Orbito-Ethmoid) Fractures 252
5.2 Definition of a Naso-Orbito-Ethmoid Fracture 252
5.3 Classification of NOE Fractures 253
5.4 Clinical Presentation of Type I NOE Fractures 253
5.5 Clinical Presentation of Type II and III NOE Fractures 255
5.6 Diagnosis of NOE Fractures 256
5.7 Treatment of NOE Fractures 258
5.8 Main Stages of the Surgery 259
5.8.1 Surgical Approach 259
5.9 Late Reconstruction of the NOE Region 267
5.10 Lacrimal Outflow Pathology 267
5.11 Pathology of Perinasal Sinuses 268
References 269

V.P. Nikolaenko, MD, PhD, DSc (✉)
Department of Ophthalmology, Saint Petersburg State Hospital No. 2,
Saint-Petersburg, Russia

Department of Otolaryngology and Ophthalmology, Medical Faculty,
Saint-Petersburg State University, Saint-Petersburg, Russia
e-mail: dr.nikolaenko@mail.ru

Y.S. Astakhov, MD, PhD, DSc
Department of Ophthalmology, I.P. Pavlov First Saint Petersburg State Medical University,
Saint-Petersburg, Russia

City Ophthalmologic Center at Saint Petersburg State Hospital No. 2,
Saint-Petersburg, Russia
e-mail: astakhov73@mail.ru

S.A. Karpischenko, MD
ENT Department, First Pavlov State Medical University of Saint Petersburg,
Saint-Petersburg, Russia
e-mail: karpischenkos@mail.ru

© Springer-Verlag Berlin Heidelberg 2015

V.P. Nikolaenko, Y.S. Astakhov (eds.), *Orbital Fractures: A Physician's Manual*,
DOI 10.1007/978-3-662-46208-9_5

5.1 Introduction to Midface (Naso-Orbito-Ethmoid) Fractures

The naso-orbito-ethmoid (NOE) region occupies the middle third of the face and is formed by numerous nasal and orbital bones including the zygomatic bone and maxilla (Fig. 5.1a). As a consequence, NOE fractures are the most difficult facial injuries to diagnose and treat and are often missed or overlooked. More than that, even if diagnosed properly, oftentimes the surgical repair is not adequate because the complexity of the anatomical interrelations in the region is not precisely understood [1–3]. And finally, to compound the situation, these fractures often are associated with injuries of the soft tissues that play a vital role in the formation of the profile of this part of the face [4, 5].

5.2 Definition of a Naso-Orbito-Ethmoid Fracture

NOE fractures in essence are broken nasal bones and cartilages telescoped backward into the interorbital space (Fig. 5.1b) usually as a result of an assault or a motor vehicle accident [6, 7]. The force vector resulting in a NOE fracture is usually

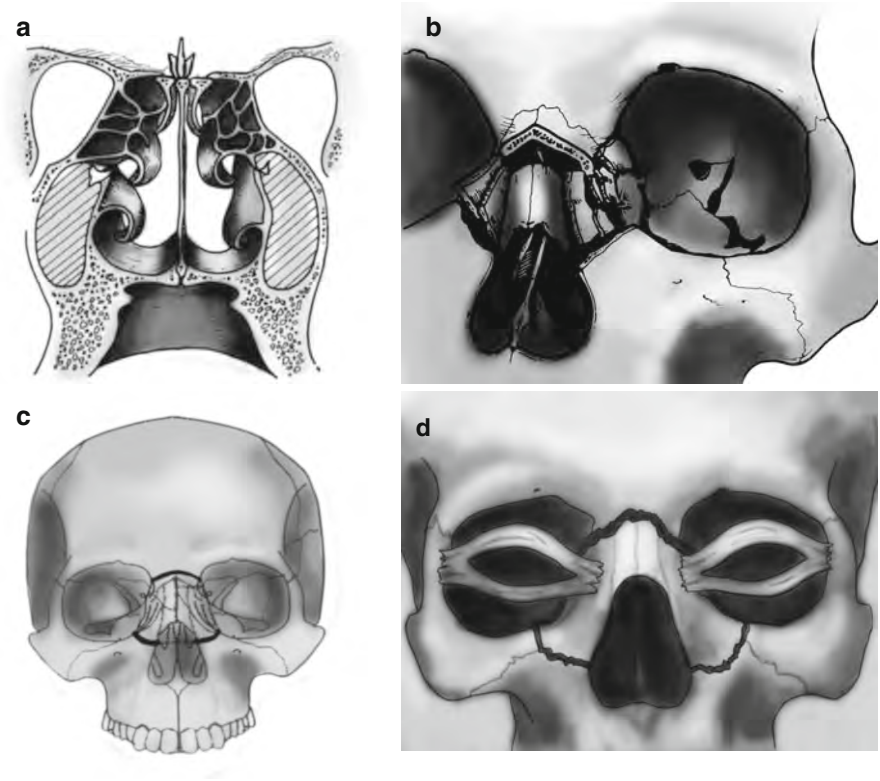

Fig. 5.1 Types of NOE fractures: (**a**) anatomy of the NOE region. (**b**) Telescopic displacement of nasal bones into the interorbital space. (**c**) Trajectory of a NOE fracture. (**d**) Complete bilateral type I NOE fracture. (**e**, **f**) Incomplete unilateral comminuted type I NOE fracture. (**g**) Test for motility of the central fragment

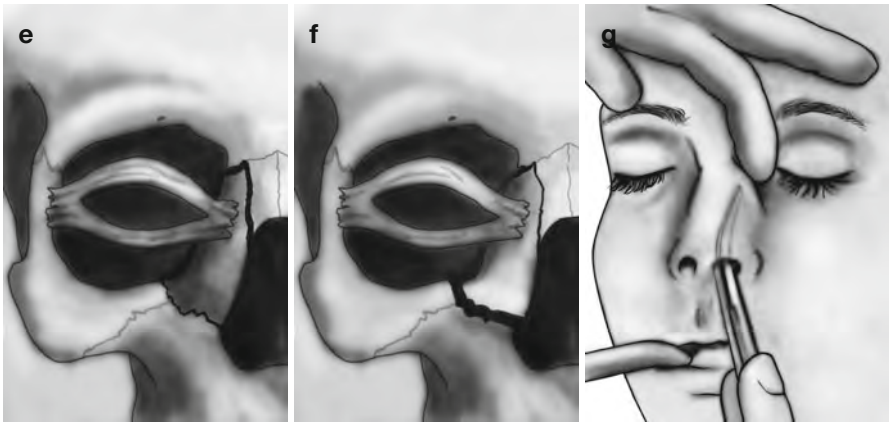

Fig. 5.1 (continued)

transmitted through and thus fracturing five sutures, the frontal process of the maxilla in the place where it joins the internal angular process of the frontal bone, then the medial orbital wall, the infraorbital rim, the lateral nasal wall, and the nasomaxillary suture of piriform aperture (Fig. 5.1c) [8]. The resulting segment (namely, the frontal process of the maxilla, forming the lower two-thirds of medial orbital rim) is the *central fragment* of the NOE fracture, to which the medial canthal tendon (MCT) is attached. Formation of one or several movable fragments of the medial orbital rim with the attached MCT is the key factor in pathogenesis of NOE fracture.

5.3 Classification of NOE Fractures

Classification of NOE fractures is based on the integrity of the central fragment [9]. According to Markowitz et al. [10], there are three types of fractures:

Type I – isolated fracture resulting in one large fragment which is also the central fragment (Fig. 5.1d–f).
Type II – fracture of the central fragment resulting in comminuted fragments with fracture lines going around the MCT attachment site so that the latter remains intact (Fig. 5.2a, b).
Type III – fracture of the central fragment involves comminuted fragments with destruction of the MCT attachment site to the extent of its avulsion (Fig. 5.2c–e).

5.4 Clinical Presentation of Type I NOE Fractures

This group of fractures accounts for 18 % of all fractures in this region [11]. Complete bilateral type I NOE fractures resulting in an isolated central fragment, detached from the surrounding osseous structures by all five fracture lines, are more

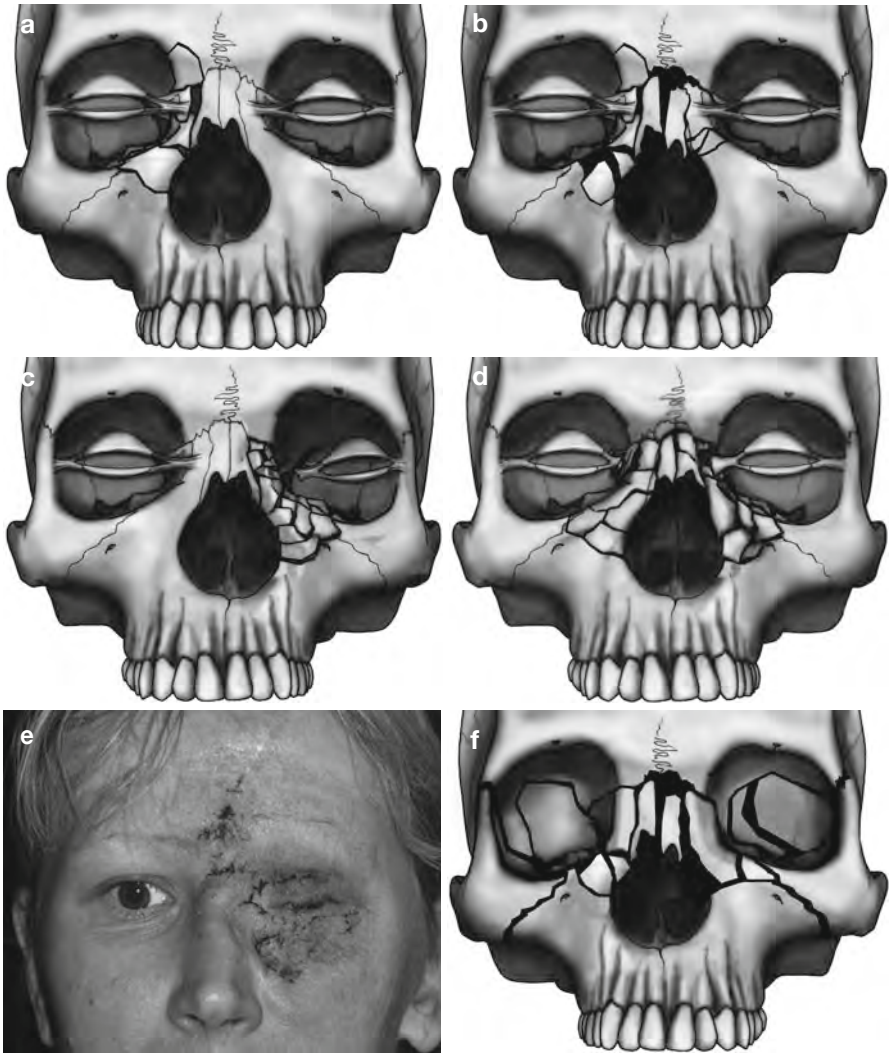

Fig. 5.2 Types of NOE fractures: (**a**, **b**) the unilateral (**a**) and bilateral (**b**) type II NOE fractures. (**c**, **d**) Unilateral (**c**) and bilateral (**d**) type III NOE fractures. (**e**) Shortening of the palpebral fissure and widening of the nasal bridge due to displacement of central fragment. (**f**) Combination of a NOE fracture and a zygomatic orbital fracture. Materials from www.aofoundation.org were used for this illustration

typically an exclusion rather than a rule. It is usually a low-energy unilateral "green-stick" fracture located in the site of the junction of the frontal process of maxilla and the internal angular process of the frontal bone above the MCT attachment site (Fig. 5.1e) [11].

As the central fragment moves downward, it affects the medial palpebral commissure, which causes lengthening of the palpebral fissure and prolapse of the

medial canthus. Sagging of the inner infraorbital rim alongside deformation of the piriform aperture is very likely, but it is usually disguised by edema and hematoma of the soft tissues. Injury of the lateral nasal wall causes ipsilateral face asymmetry and obstruction of the lacrimal pathways. Meanwhile, the length of the nasal bridge and intercanthal distance usually do not change, which may give an illusion of the intact NOE complex. In such case, palpating the MCT attachment site or testing central fragment for flexibility under general anesthesia makes diagnosis considerably easier (Fig. 5.1g). Crepitation or flexibility of the bone fragment unmistakably indicates a fracture that requires open repositioning or rigid fixation.

5.5 Clinical Presentation of Type II and III NOE Fractures

These are moderate-energy fractures that comprise 72 % of all the fractures in this region [11].

Since the only difference between type II and type III fractures is the condition of bones around the MCT attachment site, the respective symptoms are very similar. The detailed clinical presentation of a typical comminuted NOE fracture of both types includes:

- *Symptoms determined by lateral displacement of the central fragment caused, in turn, by the orbicularis oculi strain* (flattening and widening of the nasal bridge, shortening of the palpebral fissure and rounding of its medial angle, and the increase in intercanthal distance – traumatic telecanthus) (Fig. 5.2e)
- *Symptoms determined by telescopic displacement of fractured nasal bones* (saddle nose deformity, epicanthus caused by displacement of nasal skin on the medial palpebral commissure, epiphora caused by obstruction of the lacrimal pathways with bone fragments, epistaxis, anosmia, and obstruction of nasal passages) [12, 13]

Fractures can be either unilateral (the so-called hemi-NOE-fracture) or bilateral (Fig. 5.2b, d). The latter, observed in two-thirds of injured patients, is often asymmetrical and combines types I and II.

Only 10 % of NOE fractures are isolated; more commonly a NOE fracture is a part of the extensive fracture that engages other facial bones or the skull base (Fig. 5.2f) [5, 13, 14]. Fragments of the vomer, ethmoid, and nasal bones may penetrate into the cranial cavity as they are telescoped backward. As a consequence, 50 % of the time this type of fracture involves brain injury; in 40 %, cerebral spinal fluid (CSF) leak; and in 30 %, vision-threatening injuries of the eyeball and optic nerve.[1]

A CSF leak is usually caused by propagation of the fracture to the walls of the frontal sinus associated with dura mater rupture. The leak can be detected

[1] No other type of midface injury bears such a high risk of blindness [7, 15]

through visual examination; sometimes a patient himself/herself senses a metallic taste in the nasopharynx. CSF fluid may also gather under the periosteum of the orbital wall either as palpable fluctuating formation or intermittent swelling of orbital tissues worsening at straining and coughing or squeezing of the jugular veins [6].

In 4.5 % of cases, a high-energy fracture of NOE complex is accompanied by a circular fracture of both orbits (3–4 walls), types I and III Le Fort fractures of the zygomatic bones maxilla and mandible that lead to lateral transposition, increase in orbital volume, and divergence of orbits.[2] Widening of the face, lateral dislocation of both eyeballs, increase in interorbital, interpupillary, and intercanthal distances are the classic signs of traumatic hypertelorism. While this condition accounts for only 1.5 % of all midfacial traumas, the incidence is probably much higher because of the high mortality rate secondary to severe brain injury and other life-threatening injuries caused by the original trauma. In every second patient, injury of the optic nerve causes bilateral blindness. Half of the patients surviving this trauma have bilateral blindness secondary to optic nerve damage. Ruptured globes are often found in these traumas as well [10].

5.6 Diagnosis of NOE Fractures

It would not seem difficult to diagnose a NOE fracture for its pathognomonic symptoms such as flattened nasal bridge and telecanthus. However, the difficulty is that in the early days following injury, the obvious signs of fracture are disguised by swelling, ecchymosis, and emphysema of midfacial soft tissues [14, 16].

CSF leak, epistaxis, and epiphora are typical, yet not pathognomonic symptoms. This is where a clinician should be especially suspicious. As bones of the NOE complex endure the load of up to 30 g/cm^2, any nasal fracture may be a part of a more extensive injury [7]. That is why *every midfacial trauma should be treated as a potential NOE fracture*.

When making the final diagnosis, CT scanning of 1.5-mm sections is very important (Fig. 5.3) [5, 17]. Axial CT signs indicating a NOE fracture are as follows: spread of the nasomaxillary suture, asymmetrical nasolacrimal ducts, shadowing and destruction of ethmoid air cells, depression and displacement of nasal bones, displaced fracture of the medial orbital wall accompanied by displacement of segments, and orbital emphysema. Coronal CT scans can reveal both inferomedial spread of the nasomaxillary suture and fracture of the infraorbital rim with posterior displacement.

[2] The interorbital distance normally is 25 mm; the divergence angle of optical nerves at the level of optical canal is 45°

Fig. 5.3 CT scan of a NOE fracture: (**a**, **b**) telescopic displacement of broken nasal bones backward into the interorbital space (denoted with *arrows*). (**c**) Fracture line crosses both nasolacrimal ducts (*long arrows*). (**d**) Unilateral (hemi-) NOE fracture. (**e**) Unilateral disruption of the nasomaxillary suture in an axial scan (*long arrow*). *Short arrow* indicates zone of diastasis of the zygomaticomaxillary suture, verifying that the patient has a combination of NOE and maxilloorbital fractures. (**f**) The same combination of two fractures. The nasolacrimal duct is destroyed (*long arrow*), a fracture of the zygomatic arch (*short arrow*). (**g**) Combination of a bilateral (*long arrows*) NOE fracture and depressed fracture of anterior wall of maxillary sinus (*short arrows*). (**h**) 3D reconstruction of the same injury of facial bones. (**i**, **j**) 3D reconstruction of a combination of NOE (*long arrows*) and zygomatic orbital (*short arrows*) fractures

Fig. 5.3 (continued)

5.7 Treatment of NOE Fractures

Considering that the overwhelming majority of NOE fractures are very complex, treating them often requires the multidisciplinary approach involving a neurosurgeon, a maxillofacial surgeon, and an ophthalmologist [4, 13].

The *treatment* begins with stabilization of vital signs and evaluation of the neurological status. The surgical treatment of a NOE fracture can be started only after the risk of penetrating brain injury or open globe injury has been eliminated [18]. In the situation where there is either open brain injury or an open globe, neurosurgical and ophthalmic surgical interventions are performed first, followed by reduction of the NOE fracture.

On condition that the patient's neurological status is stable, a CSF leak should not prevent early fracture repositioning, because the intervention may stop the leak [6].

The goal of the treatment is to reconstruct the initial appearance of the palpebral fissure and nose, which involves restoration of the intercanthal distance, height, and contour of the nasal bridge and symmetry of medial palpebral commissures [19].

A key to success is an experienced surgeon knowledgeable of the complex midface anatomy, the use and interpretation of appropriate ancillary tests, as well as training in the surgical repair of midfacial trauma [20–23].

Delayed surgical treatment of a NOE fracture is extremely inadvisable because it is much more difficult to eliminate all functional and esthetic problems with late surgery [5, 24, 25] especially with NOE region [7].

5.8 Main Stages of the Surgery

5.8.1 Surgical Approach

Five incisions are used to give proper exposure of the NOE region: subciliary, upper gingivobuccal, coronal, limited median vertical, and the gull-wing approach (Figs. 5.4a–c and 5.5a–c).

The subciliary approach exposes the infraorbital rim and the orbital floor; upper gingivobuccal incision provides access to stabilize the nasomaxillary suture and piriform aperture. Gull-wing incisions give the best exposure of the entire NOE region; coronal incisions are essential for fractures extending to the frontal sinus, anterior, and lateral orbital walls. A nasal or glabellar injury provides an additional approach to the fracture and is used in about one third of the cases [26, 27].

Choice of the incision (or their combination) is determined by the characteristics of the fracture (uni- or bilateral, coarse or comminuted, isolated or extended) [5, 10, 28].

Subciliary and gingivobuccal incisions will suffice to deglove a unilateral type I NOE fracture with inferior displacement [11]. All other cases (superior dislocation of the central fragment, type I bilateral fractures, comminuted fractures) require a combination of the *superior* and *inferior* (subciliary and gingivobuccal) approaches. A coronal incision is used for extended fractures, and median vertical and the gull-wing incisions for isolated fractures.

Identification of the MCT and central fragment sometimes poses a serious challenge, as there is a risk of complete avulsion of the former from the central fragment if one is not careful. In order to avoid this iatrogenic complication, one should start the surgical dissection at the nasal bones to identify the anatomy. The Eyelash traction test is another way to evaluate this situation (Furnas and Bircoll 1973); it is used to determine whether MCT is detached by means of pulling the eyelashes of the upper eyelid.

Restoration of the medial orbital rim via open repositioning and rigid fixation of the central fragment[3] is the key stage of surgery whose technique is defined by the fracture type [10, 21, 23].

[3] Nowadays, closed repositioning of a NOE fracture with alignment of nasal bones with aid of instruments through the nasal passage as well as medial displacement of the central fragment with finger pressure and closed wire transnasal canthopexy are not used because of unsatisfactory results

In patients with *complete bilateral types I NOE fractures*, the central fragment which is displaced posteroinferiorly is fixed with 1.5- and 2-mm titanium microplates to the supraorbital rim and piriform aperture (Fig. 5.4e) Lateral displacement of the fragment can be effectively treated by a transnasal reduction by the technique presented below.

If *a fracture is incomplete*, the plate is applied only over the fragment area including the infraorbital rim, the edge of the piriform aperture or the frontomaxillary suture (Fig. 5.4f–h). It is recommended that titanium constructs are not placed in the immediate proximity to the MCT as they may deform the nasal bridge contour [26].

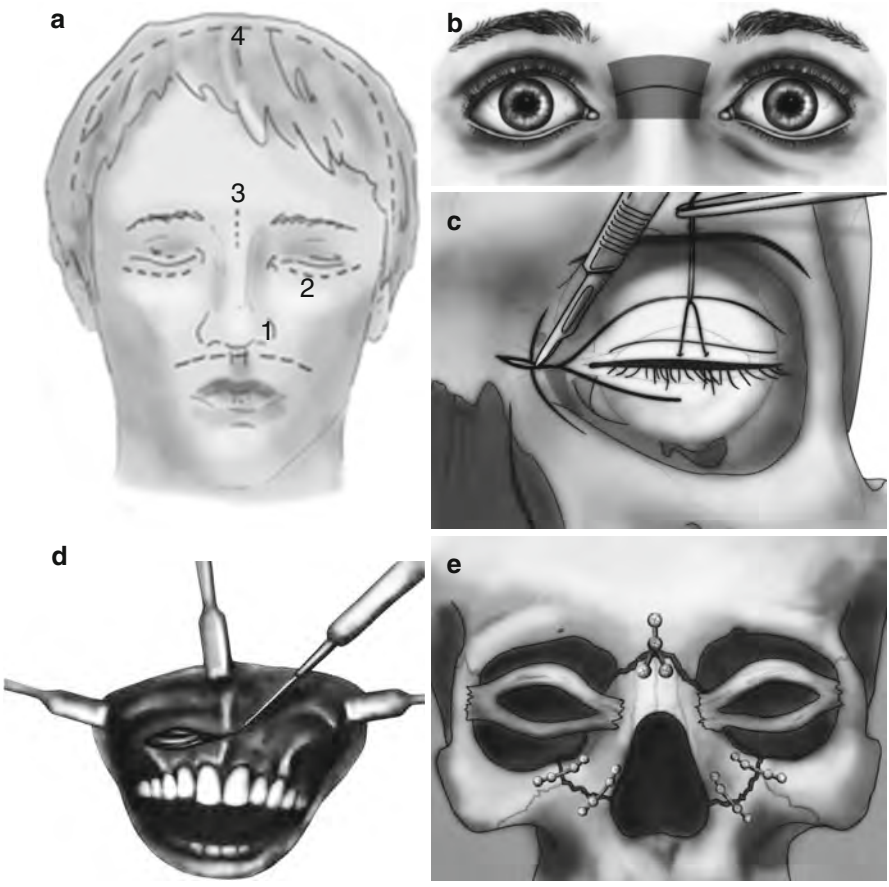

Fig. 5.4 Treatment of NOE fractures: (**a**–**c**) approaches to the NOE region: *1* – upper gingivobuccal (a detailed image is given in figure "**d**"), *2* – subciliary, *3* – limited median vertical, *4* – coronal. (**b**, **c**) glabellar, (**b**) and extended glabellar (**c**) approaches. (**e**–**h**) Fixation of central fragment at complete bilateral (**e**), incomplete unilateral, (**f**, **g**) and complete (**h**) type I NOE fractures

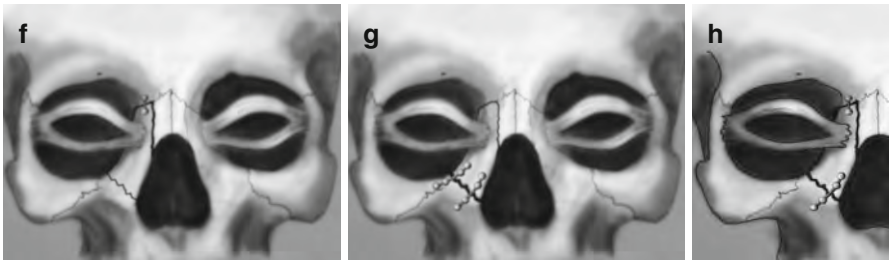

Fig. 5.4 (continued)

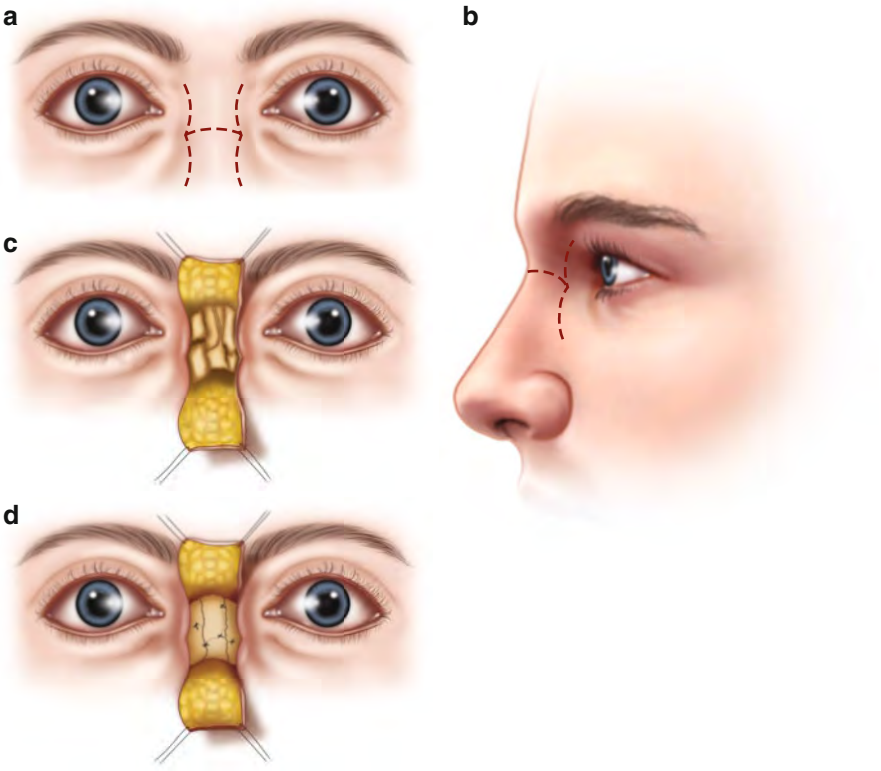

Fig. 5.5 Stages of surgical treatment of a NOE fracture: (**a**–**c**) degloving of comminuted fracture through gull-wing incision. (**d**–**e**) Fixation of fragments with wire (**d**) or titanium microplates (**e**). Comminuted fracture requires placing some plates in the immediate proximity to the medial canthal tendon, which is an undesirable but compulsory measure

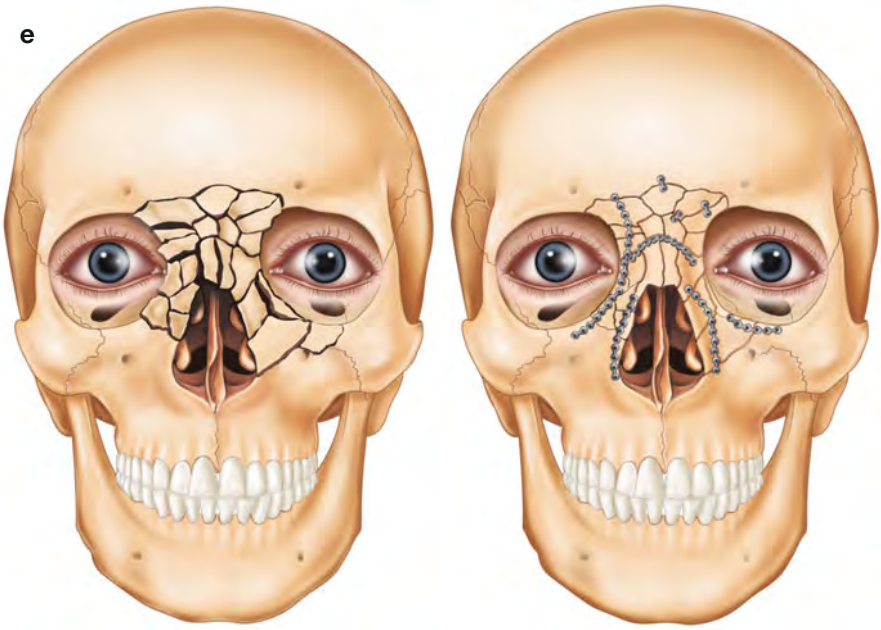

Fig. 5.5 (continued)

The surgical approach to a type II fracture implies separating the fragment with the attached MCT from the periosteum followed by wire fixation through holes made posterosuperiorly to the lacrimal sac fossa. After that, all fragments surrounding the tendon are gathered together, and the reconstructed central fragment is attached to the adjacent bones with titanium microplates (Fig. 5.5e) [10].

There are two possible ways of treating the rare *type III fractures* involving avulsion of the MCT. If fragments are so small that it is impossible to make two holes 4 mm away from each other in a single fragment, and glue fixation failed [29, 30], bone autografting is needed [13]. Fortunately, such cases are very rare. More often, it is possible to fix the detached canthal tendon to a large fragment of the medial orbital rim and then perform transnasal canthopexy for each tendon alone.

Transnasal canthopexy is an important stage of the surgery without which it is impossible to restore the nasal bridge and medial orbital rim [11, 21, 31, 32]. Canthopexy comes within the purview of surgeons experienced in repairing midfacial traumas.

The specific canthopexy technique depends on the type of fracture. Immobilization using transnasal wiring is recommended in patients with bilateral avulsion of the MCTs, whereas ipsilateral canthopexy will suffice for unilateral injuries (Fig. 5.6c).

While the technical details dramatically vary from author to author, we would like to draw the readers' attention to one aspect. The normal anatomical features of the MCT have a thick anterior pedicle attached to the frontal process of maxilla at the level of the frontomaxillary suture and a thin posterior pedicle attached to the posterior lacrimal crest. In order to prevent ectropion, while repositioning the MCT, it should be pulled not only medially, but also posteriorly, to the anterior lacrimal crest. This surgical maneuver will approximate the normal anatomical anchors of the MCT and thus reduce the likelihood of postoperative ectropion (Fig. 1.18b). If this aspect is ignored and wiring holes are made too anterior, the ideal intercanthal distance will not be achieved (31–33 mm) [11, 32]. In general, one should try to make the nasal bridge as thin as possible keeping in mind that due to certain reasons it is impossible to hypercorrect telecanthus [1].

A simplified technique for fixation of the MCT has recently been proposed. It consists in attaching the MCT to the long leg of a Y-shaped titanium miniplate that is oriented toward the depth of the orbit and attached to nasal bones with its short legs (Fig. 5.7a) [31] or to a special fixing system [33].

The medial orbital wall and the orbital floor are reconstructed as described in the previous chapters.

Repositioning/restoration of the nasal septum and dorsum. A NOE fracture is defined by telescoped fragments and, consequently, the loss of bone support for the middle and distal thirds of the nose. This results in the typical sign of an upturned nose.

The typical shortened and upturned nose is the sign of a NOE fracture. This is caused by telescoped fragments and, consequently, the loss of bone support for the middle and distal thirds of the nose. A nasal tip droop sometimes seen in the injured patients also indicates the loss of septal support. Because of the trauma to the support system, without bone grafting in these cases, it is impossible to restore the normal nasal contour (Fig. 5.7b, c) [34]. Early intervention is extremely important as reconstruction in the later post-operative period is a very difficult task [5, 15].

Reapposition of soft tissues is the final and the most difficult stage of NOE fracture treatment. There is no other facial zone where both alignment of bones and covering tissues plays such an important role. It is where cicatricial contraction may nullify a surgeon's best efforts to restore the original contour of the NOE region [1, 5, 35]. Even if the bone fragments have been perfectly aligned, cicatrization in the canthal tendon area may pull the skin off the bone and create an impression of telecanthus.

A number of techniques minimizing this complication have been described, the gull-wing incision being among them. Furthermore, it is recommended that titanium plates are not placed in the immediate proximity to the MCT. Enhanced repair of the tendon with thicker wire or 3/0 suture also has a beneficial effect. The final closure of the wound should be the suturing of the skin to the periosteum 10 mm anteriorly from the tendon. This will prevent the soft tissues from

being pulled off the bone due to the postoperative swelling, hematoma, or cicatrization. Finally, soft pads or gauze bandages are applied over the palpebral commissure and nasal bones. These have no effect on the position of the bones and can enhance the postoperative esthetics by helping keep the soft tissues in the proper position [21].

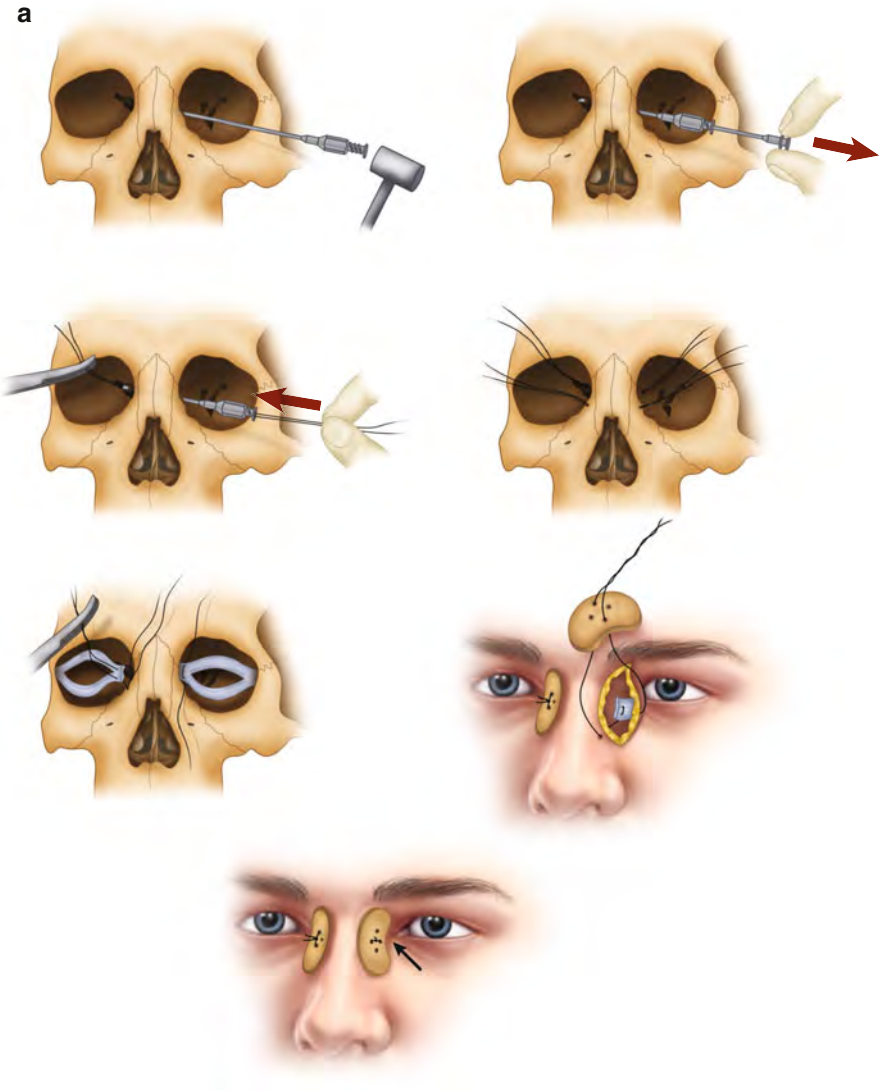

Fig. 5.6 General notion on the technique of transnasal canthopexy: (**a**) main stages of the surgery. (**b**) Fixation of the medial tendon to the central fragment. (**c**) Ipsilateral canthopexy at unilateral telecanthus

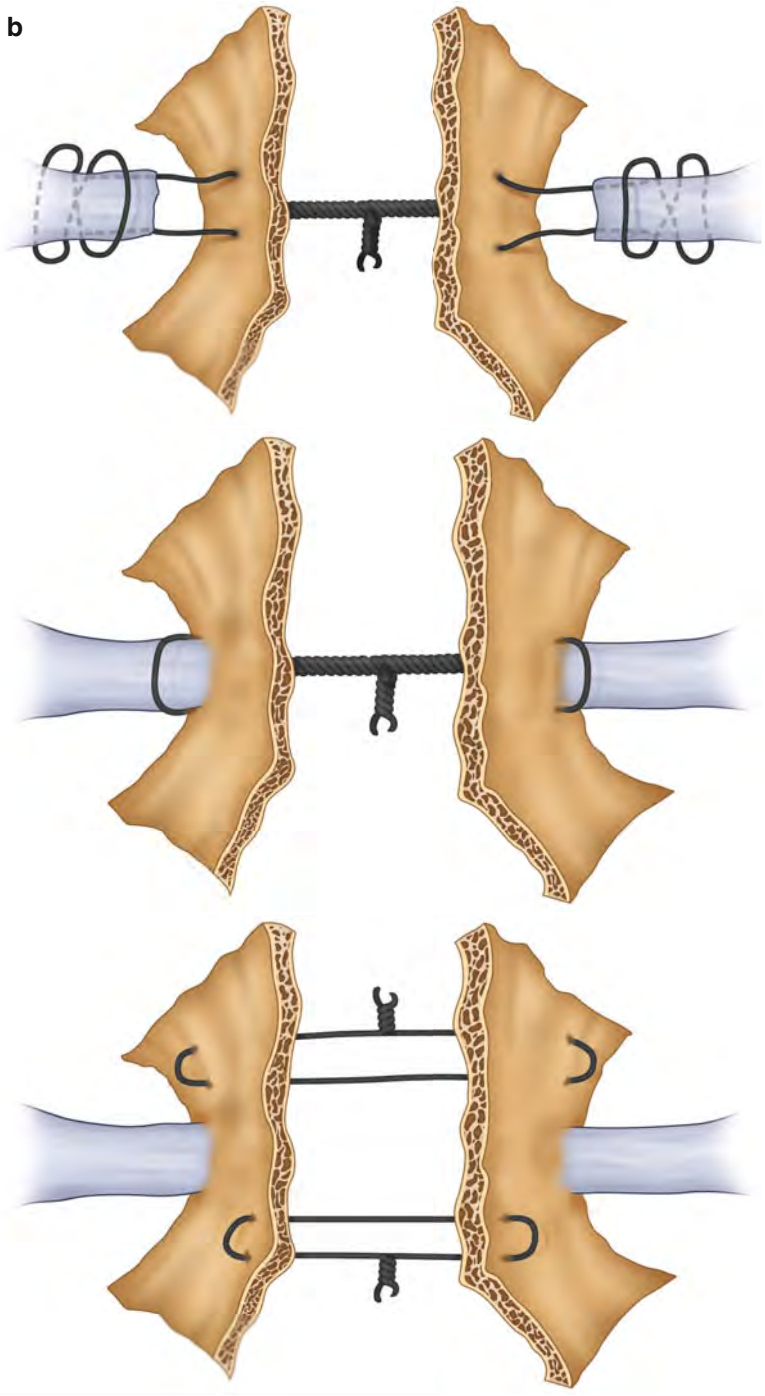

Fig. 5.6 (continued)

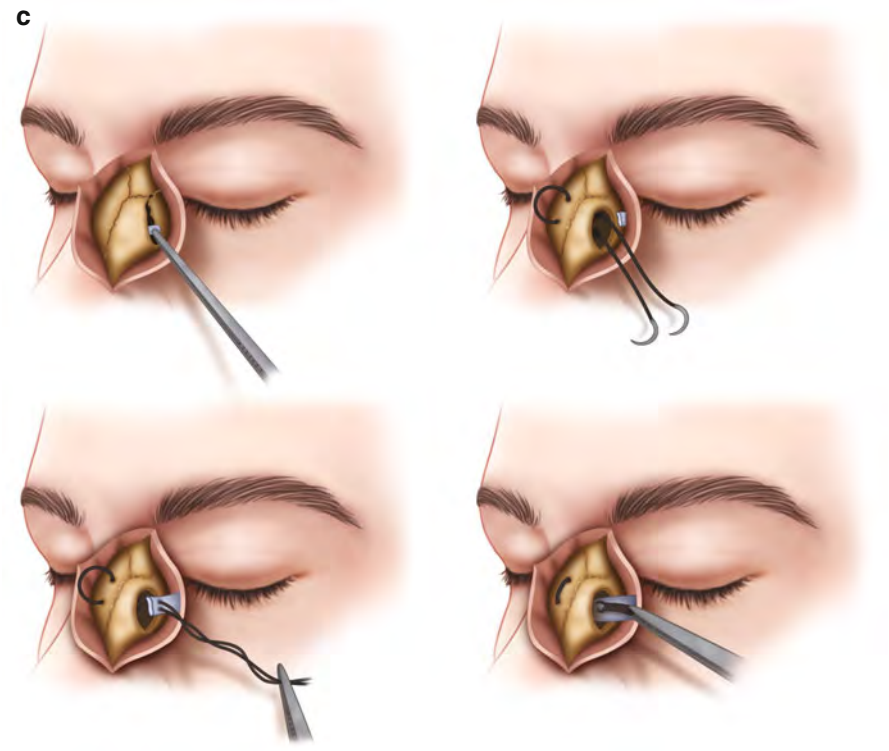

Fig. 5.6 (continued)

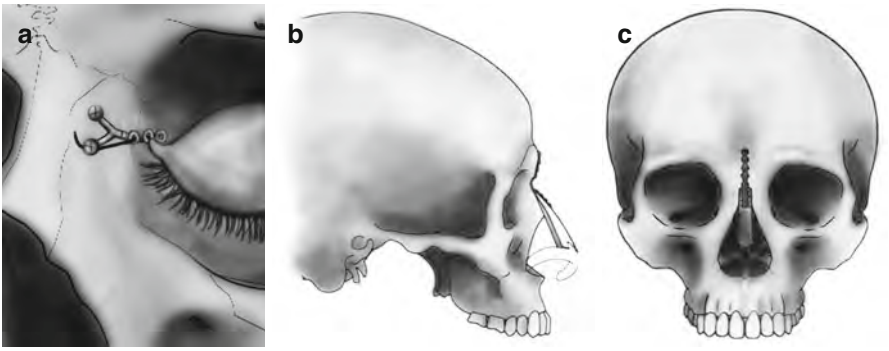

Fig. 5.7 Final stages of treatment of a NOE fracture: (**a**) fixation of the medial canthal tendon using a titanium miniplate; (**b**, **c**) rhinoplasty

5.9 Late Reconstruction of the NOE Region

Late reconstruction of the NOE region is possible only on condition that blood supply and lymph drainage are restored. This is manifested by regression of swelling and induration of soft tissue in the fractured area. The surgery includes four key stages [36]:

1. *Mobilization of soft tissues* by separating them from the periosteum. Aside from the already mentioned incisions, other ones can also be used (e.g., Y-U- and Z-shaped); the choice is defined by the type of cicatricial deformity of the NOE region.
2. *Restoration of osseous structures*. Osteotomy is typically accompanied by elements of autografting and contour osteoplasty.
3. *Restoration of the shape of the palpebral fissure and location of the palpebral commissure* require overcorrection in the course of repositioning of the central fragments combined with transnasal canthopexy.
4. *Reapposition of soft tissues* requires the surgical removal of subcutaneous scar tissue in order to make the skin thinner, fixing it, and using soft compression pads.

In addition, it might be necessary to *restore the nose with the aid of cranial vault bone grafting*, *to remove the titanium microplates set over the nasal bridge, and to correct enophthalmos*. Late reconstruction typically requires at least two surgeries. Almost half of the surgical cases take place in the zone of the previous operation in order to fix defects caused by unpredictable behavior of transplanted bone grafts and coarse cicatrization of soft tissues. While bone deformations can be corrected successfully, the problem associated with scarring, thickening, and loss of elasticity of soft tissues covering the NOE region remains unsolved. That is why late reconstruction, although providing considerable improvement to a patient's appearance, cannot restore the original contour of the NOE region and is less efficient than early surgical treatment [20, 25].

One should keep in mind that rehabilitation of a patient with a NOE fracture implies not only repositioning of the midfacial bones, but also restoration of the lacrimal outflow and functions of the frontal sinus and ethmoidal labyrinth [4].

5.10 Lacrimal Outflow Pathology

Epiphora occurring in the acute trauma period can be a result of rupture of lacrimal pathways caused by the trauma or more often by obstruction of the bone segment of the nasolacrimal duct by dislocated fragments [12, 17, 37–39]. In the late post-trauma period, one of the possible reasons for epiphora is cicatricial eversion of the lacrimal punctum and or cicatricial ectropion [6, 38, 40]. The treatment technique depends on the reason for the epiphora.

In the acute trauma period, lacrimal pathways pathology is handled only when it is evident that those structures are injured. Primary surgical management of injuries of the lacrimal ducts or lacrimal sac is performed according to the conventional methods.

Because one third of patients who have post-trauma epiphora recover spontaneously, if there is no clear indication of injury to the lacrimal pathway, surgery can be delayed for 3–5 months [37, 40]. Such wait-and-see policy is especially reasonable after early repositioning and rigid fixation of a NOE fracture, because the risk of lacrimal pathway obstruction is only 5 %. Untreated fractures are associated with epiphora in 90 % of cases [38], and closed repositioning and external compression of bone fragments that have not aligned properly have a rate as high as 60 % [40]. Delayed surgical treatment of a NOE fracture or late reconstruction of this region leaves the lacrimal pathways little chance to recover patency [24, 37].

Tear overflow persisting for 3–5 months is a signal to perform X-ray examination of the lacrimal pathways, which usually reveals an obstruction of the nasolacrimal duct. The operation of choice is classic external dacryocystorhinostomy, which is successful in 94 % of cases [37].

The question not answered yet is the order of surgical treatment for the telecanthus associated with chronic dacryocystitis. Single-stage intervention is technically difficult. Dacryocystorhinostomy performed as the first stage poses a risk of obstruction of the anastomosis in the course of subsequent correction of telecanthus. Canthoplasty with subsequent external dacryocystorhinostomy appears to be the optimal variant, although the transcutaneous approach to the lacrimal sac may worsen the aesthetic outcome achieved at the previous treatment stage.

5.11 Pathology of Perinasal Sinuses

Two thirds of patients with NOE fractures experience difficulties related to paranasal sinuses, primarily the ethmoidal sinus. Since broken ethmoidal air cells are prone to spontaneous ventilation and draining, such injuries are usually not treated surgically.

The only exception to the above is fracture of the anterior ethmoidal labyrinth because in 25 % of these cases, there is obstruction of the frontal ostium which can cause frontal sinusitis. Also, about 30 % of the time, patients will have changes in the maxillary sinus from profound swelling to trauma-induced mucocele. Trauma in a patient who already has a chronic infectious process is at a higher risk of developing cellulitis and subperiostal abscess [41].

If the patient with a NOE fracture has a history of chronic sinusitis, it is reasonable to combine the primary surgical treatment with endonasal microinvasive surgery restoring aeration of the paranasal sinuses. Such a patient needs regular follow-up monitoring by an ENT specialist and CT control for at least three months after trauma.

The indications for surgical treatment of the frontal sinus are limited as only 1 % of patients have delayed complications [41]. If the frontonasal duct is injured,

surgical obliteration of the sinus is required to avoid mucocele formation [9]. Fracture of the anterior or both sinus walls is to be treated according to principles described in the respective chapter.

References

1. Hammer, B., & Prein, J. (1995). Correction of posttraumatic orbital deformities: Operative techniques and review of 26 patients. *Journal of Cranio-maxillo-facial Surgery, 23*(2), 81–90.
2. Young, P. A., & Rice, D. H. (2007). Management of a type II nasoethmoid orbital fracture and near-penetration of the intracranial cavity with transnasal canthopexy. *Ear, Nose, and Throat Journal, 86*(6), 344–347, 360.
3. Papadopoulos, H., & Salib, N. K. (2009). Management of naso-orbital-ethmoidal fractures. *Oral and Maxillofacial Surgery Clinics of North America, 21*(2), 221–225.
4. Fedok, F. G. (1995). Comprehensive management of nasoethmoid-orbital injuries. *The Journal of Cranio-Maxillofacial Trauma, 1*(4), 36–48.
5. Sargent, L. A. (2007). Nasoethmoid orbital fractures: Diagnosis and treatment. *Plastic and Reconstructive Surgery, 120*(7 Suppl. 2), S16–S31.
6. Beyer, C. K., Fabian, R. L., & Smith, B. (1982). Naso-orbital fractures, complications, and treatment. *Ophthalmology, 89*(5), 456–463.
7. Heine, R. D., Catone, G. A., Bavitz, J. B., & Grenadier, M. R. (1990). Naso-orbital-ethmoid injury: Report of a case and review of the literature. *Oral Surgery, Oral Medicine, and Oral Pathology, 69*(5), 542–549.
8. Evans, B. T., & Webb, A. A. (2007). Post-traumatic orbital reconstruction: Anatomical landmarks and the concept of the deep orbit. *The British Journal of Oral & Maxillofacial Surgery, 45*(3), 183–189.
9. Hopper, R. A., Salemy, S., & Sze, R. W. (2006). Diagnosis of midface fractures with CT: What the surgeon needs to know. *Radiographics, 26*(3), 783–793.
10. Markowitz, B. L., Manson, P. N., Sargent, L., et al. (1991). Management of the medial canthal tendon in nasoethmoid orbital fractures: The importance of the central fragment in classification and treatment. *Plastic and Reconstructive Surgery, 87*(5), 843–853.
11. Manson, P. N., Markowitz, B., Mirvis, S., et al. (1990). Toward CT-based facial fracture treatment. *Plastic and Reconstructive Surgery, 85*(2), 202–212.
12. Ellis, E. (1993). Sequencing treatment for naso-orbito-ethmoid fractures. *Journal of Oral and Maxillofacial Surgery, 51*(5), 543–558.
13. Chou, E. K., Wu, C. I., Yu, J. C., & Chang, S. C. (2009). Epistaxis as the only initial symptom in pediatric naso-orbital-ethmoid fracture complicated with meningitis. *The Journal of Craniofacial Surgery, 20*(3), 953–955.
14. Daly, B. D., Russell, J. L., Davidson, M. J., & Lamb, J. T. (1990). Thin section computed tomography in the evaluation of naso-ethmoidal trauma. *Clinical Radiology, 41*(4), 272–275.
15. Ioannides, C., Freihofer, H. P., & Bruaset, I. (1984). Trauma of the upper third of the face. Management and follow-up. *Journal of Maxillofacial Surgery, 12*(6), 255–261.
16. Gruss, J. S. (1985). Naso-ethmoid-orbital fractures: Classification and role of primary bone grafting. *Plastic and Reconstructive Surgery, 75*(3), 303–317.
17. Almousa, R., Amrith, S., Mani, A. H., et al. (2010). G. Radiological signs of periorbital trauma – the Singapore experience. *Orbit, 29*(6), 307–312.
18. Ioannides, C., Treffers, W., Rutten, M., & Noverraz, P. (1988). Ocular injuries associated with fractures involving the orbit. *Journal of Cranio-Maxillo-Facial Surgery, 16*(4), 157–159.
19. Hoffmann, J. F. (1998). Naso-orbital-ethmoid complex fracture management. *Facial Plastic Surgery, 14*(1), 67–76.
20. Iliff, N. T. (1991). The ophthalmic implications of the correction of late enophthalmos following severe midfacial trauma. *Transcation of the American Ophthalmological Society, 89*, 477–548.

21. Leipziger, L. S., & Manson, P. N. (1992). Nasoethmoid orbital fractures. Current concepts and management principles. *Clinics in Plastic Surgery, 19*(1), 167–193.
22. Sargent, L. A., & Rogers, G. F. (1999). Nasoethmoid orbital fractures: Diagnosis and management. *The Journal of Cranio-Maxillofacial Trauma, 5*(1), 19–27.
23. Herford, A. S., Ying, T., & Brown, B. (2005). Outcomes of severely comminuted (type III) nasoorbitoethmoid fractures. *Journal of Oral and Maxillofacial Surgery, 63*(9), 1266–1277.
24. Merkx, M. A., Freihofer, H. P., Borstlap, W. A., & van Hoff, M. A. (1995). Effectiveness of primary correction of traumatic telecanthus. *International Journal of Oral and Maxillofacial Surgery, 24*(5), 344–347.
25. Nowinski, D., Di Rocco, F., Roujeau, T., et al. (2010). Complex pediatric orbital fractures combined with traumatic brain injury: Treatment and follow-up. *The Journal of Craniofacial Surgery, 21*(4), 1054–1059.
26. Kim, M. G., Kim, B. K., Park, J. L., et al. (2008). The use of bioabsorbable plate fixation for nasal fractures under local anaesthesia through open lacerations. *Journal of Plastic, Reconstructive & Aesthetic Surgery, 61*(6), 696–699.
27. Jeong, H. S., Moon, M. S., Lee, H. K., & Kim, K. S. (2010). Use of fibrin glue for open comminuted nasal bone fractures. *The Journal of Craniofacial Surgery, 21*(1), 75–78.
28. Nunery, W. R., & Tao, J. P. (2008). Medial canthal open nasal fracture repair. *Ophthalmic Plastic and Reconstructive Surgery, 24*(4), 276–279.
29. Dadaş, B., Alkan, S., Cifci, M., & Başak, T. (2007). Treatment of tripod fracture of zygomatic bone by N-2-butyl cyanoacrylate glue fixation, and its effects on the tissues. *European Archives of Oto-Rhino-Laryngology, 264*(5), 539–544.
30. Endres, K., Marx, R., Tinschert, J., et al. (2008). A new adhesive technique for internal fixation in midfacial surgery. *Biomedical Engineering Online, 19*(7), 16.
31. Shore, J. W., Rubin, P. A., & Bilyk, J. R. (1992). Repair of telecanthus by anterior fixation of cantilevered miniplates. *Ophthalmology, 99*(7), 1133–1138.
32. Freihofer, H. P. (1995). Effectiveness of secondary post-traumatic periorbital reconstruction. *Journal of Cranio-Maxillo-Facial Surgery, 23*(3), 143–150.
33. Kosins, A. M., Kohan, E., Shajan, J., et al. (2010). Fixation of the medial canthal tendon using the Mitek anchor system. *Plastic and Reconstructive Surgery, 126*(6), E309–E310.
34. Gentile, P., & Cervelli, V. (2009). Nasal dorsum reconstruction with 11th rib cartilage and auricular cartilage grafts. *Annals of Plastic Surgery, 62*(1), 63–66.
35. Imola, M. J., Ducic, Y., & Adelson, R. T. (2008). The secondary correction of post-traumatic craniofacial deformities. *Otolaryngology - Head and Neck Surgery, 139*(5), 654–660.
36. Whitaker, L. A., & Yaremchuk, M. J. (1990). Secondary reconstruction of posttraumatic orbital deformities. *Annals of Plastic Surgery, 25*(6), 440–449.
37. Becelli, R., Renzi, G., Mannino, G., et al. (2004). Posttraumatic obstruction of lacrimal pathways: A retrospective analysis of 58 consecutive naso-orbitoethmoid fractures. *The Journal of Craniofacial Surgery, 15*(1), 29–33.
38. Uraloglu, M., Erkin Unlu, R., Ortak, T., & Sensoz, O. (2006). Delayed assessment of the nasolacrimal system at naso-orbito-ethmoid fractures and a modified technique of dacryocystorhinostomy. *The Journal of Craniofacial Surgery, 17*(1), 184–189.
39. Jordan, D. R., Ziai, S., Gilberg, S. M., & Mawn, L. A. (2008). Pathogenesis of canalicular lacerations. *Ophthalmic Plastic and Reconstructive Surgery, 24*(5), 394–398.
40. Gruss, J. S., Hurwitz, J. J., Nik, N. A., & Kassel, E. E. (1985). The pattern and incidence of nasolacrimal injury in naso-orbital-ethmoid fractures: The role of delayed assessment and dacryocystorhinostomy. *British Journal of Plastic Surgery, 38*(1), 116–121.
41. Paterson, A. W., Barnard, N. A., & Irvine, G. H. (1994). Naso-orbital fracture leading to orbital cellulitis, and visual loss as a complication of chronic sinusitis. *The British Journal of Oral & Maxillofacial Surgery, 32*(2), 80–82.

Zygomaticoorbital Fractures

6

Vadim P. Nikolaenko, Yury S. Astakhov,
Mikhail M. Soloviev, G. Khatskevich, and Igor G. Trofimov

Contents

6.1 Definition . . . 272
6.2 Epidemiology . . . 272
6.3 Mechanisms of Fracture Development . . . 274
6.4 Fracture Classification . . . 274
6.5 Diagnosis of the Zygomaticoorbital Fracture . . . 274
6.6 Radiological Diagnosis . . . 283
6.7 Management of Zygomaticoorbital Fractures . . . 284
6.8 Complications of Zygomaticoorbital Fractures . . . 291
6.8.1 Enophthalmos . . . 292
6.8.2 Infraorbital Nerve Neuropathy . . . 293
6.8.3 Diplopia . . . 294
6.8.4 Retrobulbar Hematoma . . . 294
References . . . 294

V.P. Nikolaenko, MD, PhD, DSc (✉)
Department of Ophthalmology, Saint Petersburg State Hospital No. 2,
Saint-Petersburg, Russia

Department of Otolaryngology and Ophthalmology, Medical Faculty,
Saint-Petersburg State Hospital, Saint-Petersburg, Russia
e-mail: dr.nikolaenko@mail.ru

Y.S. Astakhov, MD, PhD, DSc
Department of Ophthalmology, I.P. Pavlov First Saint Petersburg State Medical University,
Saint-Petersburg, Russia

City Ophthalmologic Center at Saint Petersburg State Hospital No. 2,
Saint-Petersburg, Russia

© Springer-Verlag Berlin Heidelberg 2015

V.P. Nikolaenko, Y.S. Astakhov (eds.), *Orbital Fractures: A Physician's Manual*,
DOI 10.1007/978-3-662-46208-9_6

M.M. Soloviev, MD, PhD • I.G. Trofimov
Department of Maxillo-facial and Plastic surgery, St. Petersburg State Hospital No. 2, Saint-Petersburg, Russia

Department of Maxilla-facial and oral surgery, I.P. Pavlov First Saint Petersburg State Medical University, Saint-Petersburg, Russia

Department of Maxilla-facial and oral surgery, St. Petersburg State University, Saint-Petersburg, Russia

G. Khatskevich, MD, PhD
Department of Pediatric Stomatology and Maxillo-facial surgery, I.P. Pavlov First Saint Petersburg State Medical University, Saint-Petersburg, Russia

6.1 Definition

The zygomatic bone forms the orbital floor and the lateral orbital wall and has two points where it contacts the maxilla and the cranium (Fig. 6.1a). *Fractures of the body of the zygomatic bone* are extremely rare and are usually caused by gunshot wounds. As for peacetime traumas, the term *zygomatic bone fracture* usually applies to trauma when the bone has been fractured at the sutures connecting the zygoma to the maxilla and cranium. Because of the complex anatomy and sutures of the zygoma, the pattern of fractures involving this bone is rather diverse. Zygomatic fractures are often accompanied by a NOE fracture or are a component of a more extensive craniofacial injury (Le Fort II and III fractures, the panfacial fracture).

Hence, it must be acknowledged that the term *zygomatic bone fracture* fails to provide the essence of the patient's trauma. The term *zygomaticoorbital fracture* appears more apt as it determines the key role played by the zygomatic bone in the formation of the orbital floor and the lateral orbital wall. Neither the normal orbital anatomy nor the original facial configuration can be recovered without meticulous repositioning of the zygomatic bone [1].

6.2 Epidemiology

Fractures of the zygomaticoorbital complex rank third in incidence among all bone injuries occurring in humans. The share of zygomaticoorbital fractures in children and adolescents is 60 % of all facial fractures; in adults, this figure is 24–33 %, with only mandibular fractures being more frequent (70 %) [2–5]. In 40 % of cases, the fractures affecting the zygomatic bone are accompanied by injuries to the maxilla, orbit, and nose as well as limb traumas [6–8]. Twenty-five percent of the patients have head injuries. As a result, zygomaticoorbital fractures are the most frequent reason for admission to trauma units [9, 10].

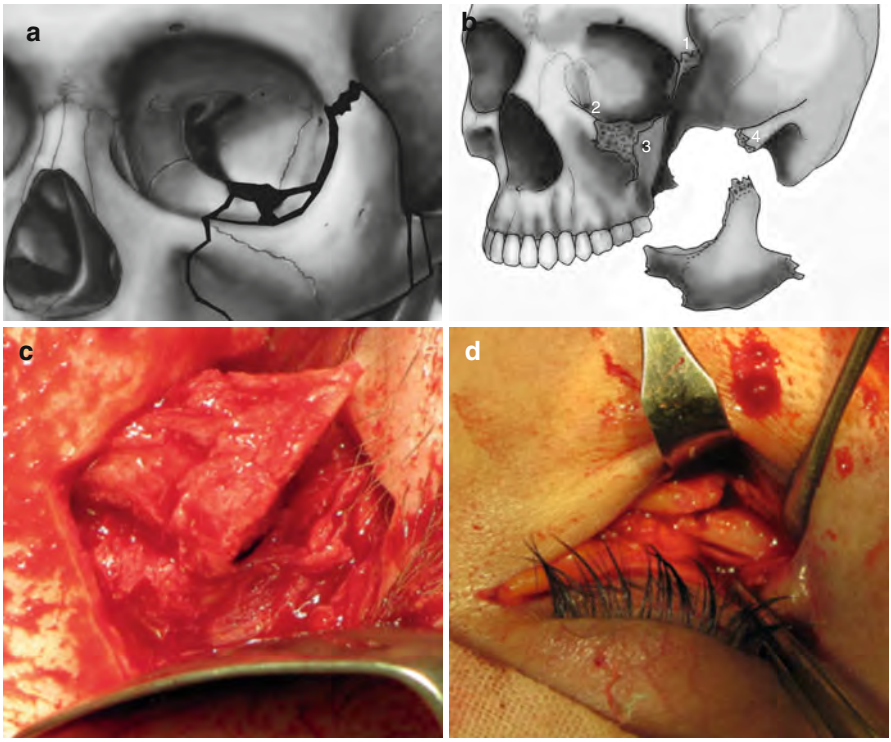

Fig. 6.1 Zygomaticoorbital fracture: (**a**) Isolation of the zygomatic bone with respect to four sutures. (**b**) Fracture lines in a typical zygomaticoorbital fracture: (*1*) the fracture line starting from the inferior orbital fissure and propagating upward along the sphenozygomatic suture to the frontozygomatic suture where it crosses the lateral orbital rim; (*2*) the fracture propagating from the inferior orbital fissure anteriorly along the orbital surface of the maxilla; it crosses the infraorbital rim and propagates downward along the anterior surface of the maxilla under the zygomaticomaxillary suture; (*3*) the fracture beginning at the inferior orbital fissure, running downward along the inferotemporal surface of the maxilla and continuing anteriorly under the zygomaticomaxillary suture until it merges with fracture no. 2; and (*4*) one or several fracture lines of the zygomatic arch fracture. (**c**) Spread of the frontozygomatic suture. (**d**) Orbital rim fracture

These types of fractures typically occur in individuals aged 21–40 years and are 3–4 times more frequently observed in males than in females [8]. The main causes of these injuries include car accidents (45–80 %), violence (20 %), falls (20 %), and sport activities (13–20 %) [11–13].

Unilateral fractures of the zygomaticoorbital complex are the vast majority; bilateral fractures are observed only in 5 % of patients. Despite the fact that the incidence of concomitant injuries of the visual system (*traumatic optic neuropathy, incomitant or restrictive strabismus*) is as high as 33–36 % [14–18], very few publications have been devoted to zygomaticoorbital fractures [19].

6.3 Mechanisms of Fracture Development

An impact of a sufficiently high-energy object that moves from the anterolateral in the posteromedial direction causes isolation of the zygomatic bone with respect to the four sutures, the superior (frontozygomatic), the medial (zygomaticomaxillary), the lateral (zygomaticotemporal), and the posterior (sphenozygomatic) (Fig. 6.1a) [20]. Dislocation of the isolated zygomatic bone usually additionally causes a fracture of the orbital floor and the anterior wall of the maxillary sinus (Fig. 6.1b). In the English-language literature, this condition is known as a *tetrapod (quadripod) fracture* [21, 22].

A rather frequent isolation of the zygomatic bone with respect to three sutures (the frontozygomatic, zygomaticomaxillary, and zygomaticotemporal ones) is known in the English-language literature as a *tripod fracture* [23] or a *zygomaticomaxillary fracture although a more accurate term would be "quadripod" as usually all four zygomatic sutures are usually involved*.

6.4 Fracture Classification

The *low-energy fractures* comprising 18 % of all zygomaticoorbital injuries are characterized by at least one incomplete fracture, most often, that of the frontozygomatic suture. No surgical management is required as bone fragments are either not displaced or displaced negligibly [24].

Moderate-energy complete zygomaticoorbital fractures comprise (77 %) of the fractures and are characterized by mild to moderate dislocation with respect to all the sutures and by disintegration of the fracture edges. The dislocation orientation (inferior, medial, posterior) depends on the applied force vector.

High-energy zygomaticoorbital fractures are usually components of the Le Fort or panfacial fractures. They can rarely be observed as an isolated entity (5 %).

6.5 Diagnosis of the Zygomaticoorbital Fracture

Since these patients are usually admitted to the hospital because of multiple trauma, it is necessary to include meticulous analysis of the vital signs, evaluation of the neurological status, and the condition of the thoracic and abdominal organs and extremities.

The clinical presentation of the fracture depends on the degree to which the zygomaticoorbital complex has been affected.

As mentioned previously, either the absence or minimal dislocation of bone fragments is typical of *low-energy incomplete fractures* [24]. As a result, the clinical presentation is limited to periorbital ecchymosis (over 70 % of cases), soft tissue edema (over 20 % of cases), and subconjunctival hemorrhage (~40 %) [25].

Moderate-energy complete zygomaticoorbital fractures (77 %) are the comminuted fractures and are accompanied by either mild or moderate dislocation with respect to all

the sutures. The isolation of the zygomaticoorbital complex starts in the area of the zygomaticomaxillary suture and the infraorbital rim; the frontal process (the frontozygomatic suture), greater wing of the sphenoid (the sphenozygomatic suture), and the zygomatic arch (the zygomaticotemporal suture) are affected in more severe cases (Fig. 6.2) [24].

The clinical presentation depends on the number of facial bones destroyed at the moment of injury (Fig. 6.9). Diagnosis is facilitated by the fact that each fracture type has its own typical complex of symptoms.

Signs of destruction of the zygomaticomaxillary suture include edema of facial soft tissues, sensation disorders in the area of the superior dental plexus, local palpation tenderness of the superior gingivobuccal fold, and deformation of the zygomaticoalveolar crest (Fig. 6.3).

The hematoma typical of zygomatic fractures, the "raccoon eye," develops at the moment of trauma and is caused by vessel injury in the fractured area and spreads beyond the orbicularis oculi muscle. The "raccoon eyes" appearance observed in patients with basilar skull fracture occurs late, showing several hours or sometimes the next day after trauma, and never spreads beyond the orbicularis oculi muscle.[1]

If an injury of the anterior wall of the maxillary sinus is complicated by rupture of the mucous membrane, moderate bleeding from the ipsilateral half nose is observed. Because of the fracture of the sinus wall and blood in the sinus, percussion of premolars generates a dull sound (the cracked pot symptom according to E.S. Malevich) on the side of injury.

Rare manifestations of the zygomaticoorbital fracture include orbital emphysema [26] and propagation of subcutaneous emphysema to the retropharyngeal space and the mediastinum. This rare finding may mislead a physician into searching for a nonexistent damage to the esophagus and other mediastinal structures [27, 28].

Along with chemosis, subconjunctival hemorrhage, periorbital edema, and "raccoon eyes" hematoma, the fracture of the infraorbital rim can be diagnosed by the easily palpated "bone step" in the middle third of the infraorbital rim (Fig. 6.3e) and dysesthesia in the distribution of the infraorbital nerve.[2]

In the acute aftermath of trauma, neuropathy is typically observed in 70–80 % of patients. Its incidence depends on the type of damage to the zygomaticoorbital complex. The following situations are associated with the highest risk for developing neuropathy: the fracture crosses the infraorbital canal, a comminuted type of fracture, and displacement of bone fragments which usually accompany moderate- and high-energy fractures of the zygomatic bone [29].

The main mechanisms contributing to the development of traumatic neuropathy include compression of the infraorbital nerve in the infraorbital canal; perineural edema or hematoma; and less frequently, ischemia and nerve rupture [30].

[1] One should not overestimate the diagnostic significance of the time when the "raccoon eyes" sign has emerged in patients with high-energy trauma, when facial fracture is often concomitant with the basilar skull fracture.

[2] In patients with the zygomaticoorbital fracture, the zygomaticofacial and zygomaticotemporal branches can be affected in addition to the infraorbital nerve (Govsa et al. [132]).

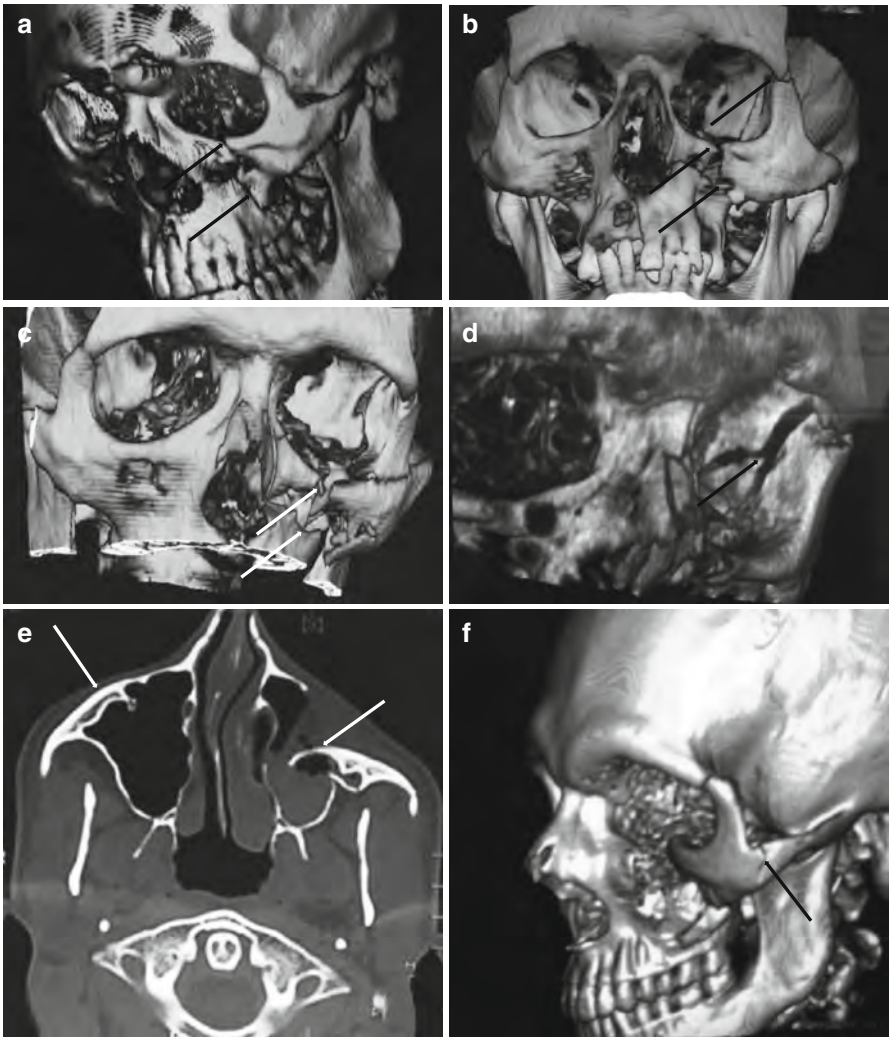

Fig. 6.2 Types of injuries of the zygomaticoorbital complex (according to the CT data): (**a**) The minimal diastasis of the zygomaticomaxillary junction (*an arrow*). (**b**, **c**) 3D reconstruction of a moderate-energy fracture with spread of the zygomaticomaxillary suture and the infraorbital rim (*arrows*). The minimal spread of the frontozygomatic suture is clearly observed (**b**). (**d**) Diastasis of the sphenozygomatic suture and formation of a comminuted fracture of the lateral orbital wall (an *arrow*). (**e**, **f**) A profound dislocation of the zygomatic bone and its separation at all the sutures, including the zygomaticotemporal one (*arrow*), which are clearly seen both in an axial CT scan (**e**) and in 3D reconstruction

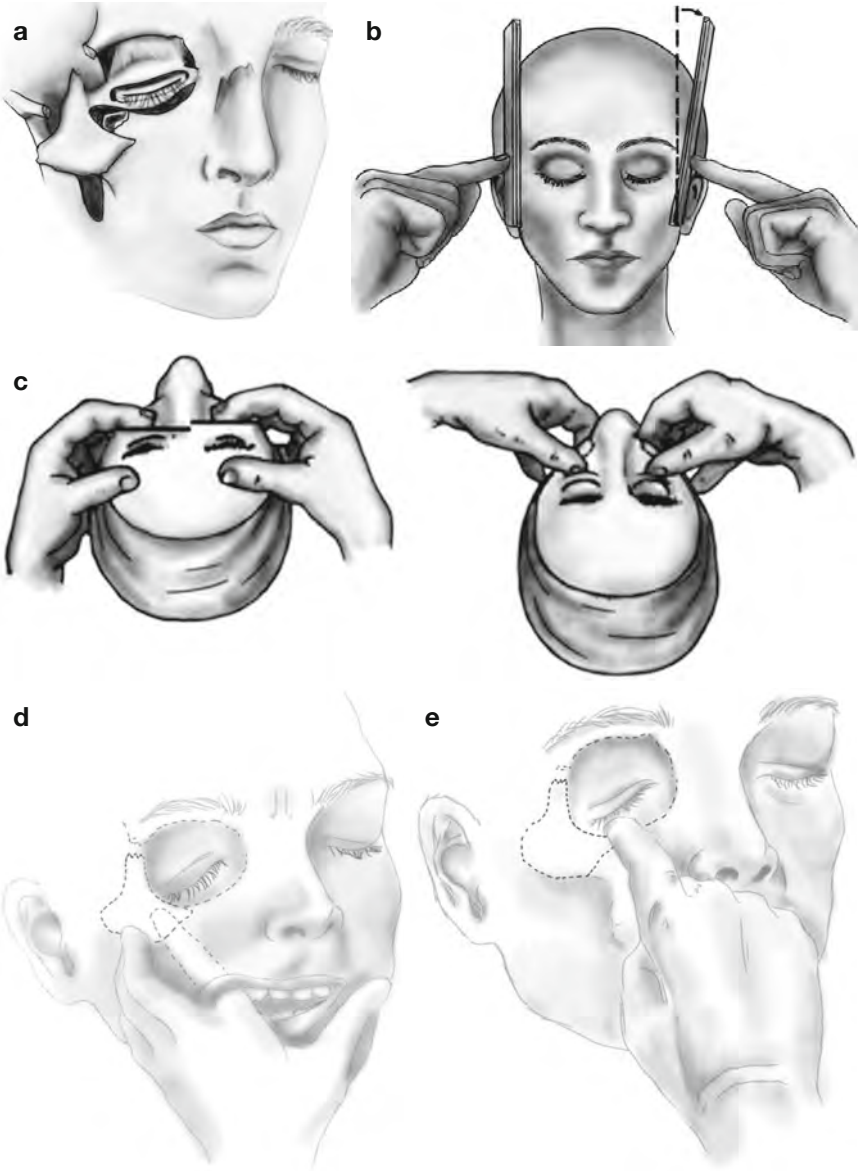

Fig. 6.3 Symptomatology of zygomaticoorbital fractures: (**a**) A typical moderate-energy fracture. (**b**) Typical antero-postero-inferior displacement of the zygomatic bone illustrated by a test with a ruler placed to the zygomatic arch and squama temporalis. Divergence of the ruler from the vertical position is indicative of displacement of the zygomatic bone. (**c**) Ipsilateral retraction of the zygomatic region and tenderness of buccal soft tissues. (**d**, **e**) "Bone step" symptom revealed by palpating the zygomaticoalveolar crest (**d**) and the infraorbital rim (**e**). (**f**) Appearance of a patient with a low-energy injury (ecchymosis and subconjuctival hemorrhage with the facial width and contour of the zygomatic region remaining intact and proper position of the lateral angle of the orbital fissure). (**g–i**) Facial changes typical of the moderate- and high-energy fractures. Prolapse of the lateral canthus, evident hypoglobus (**h**, **i**), and enophthalmos indicated by deepening of the upper eyelid groove (**i**). (**j**, **k**) Less evident but much more frequent aesthetic disorders (With the permission of professor G.A. Khatskevich and associate professor M.M. Solovyev)

Fig. 6.3 (continued)

The infraorbital nerve is completely anesthetized only if its trunk is anatomically interrupted, which is an extremely rare event. The patients most often have (in order of decreasing incidence) hypoesthesia, paresthesia, and hyperesthesia. Since Aβ myelinated fibers responsible for pressure and touch are more sensitive to compression and ischemia than Aδ myelinated and C unmyelinated fibers (heat and pain sensitivity), the patients may have mosaic neurosensory deficit [31].

Fracture of the infraorbital rim inevitably involves the orbital floor during the traumatic process. However, the orbital floor fracture as a component of the zygomaticoorbital fracture is significantly different from its isolated blowout fracture in terms of incidence (75 and 25 %, respectively) [25], clinical presentation, and treatment strategy (Fig. 6.4a–c).

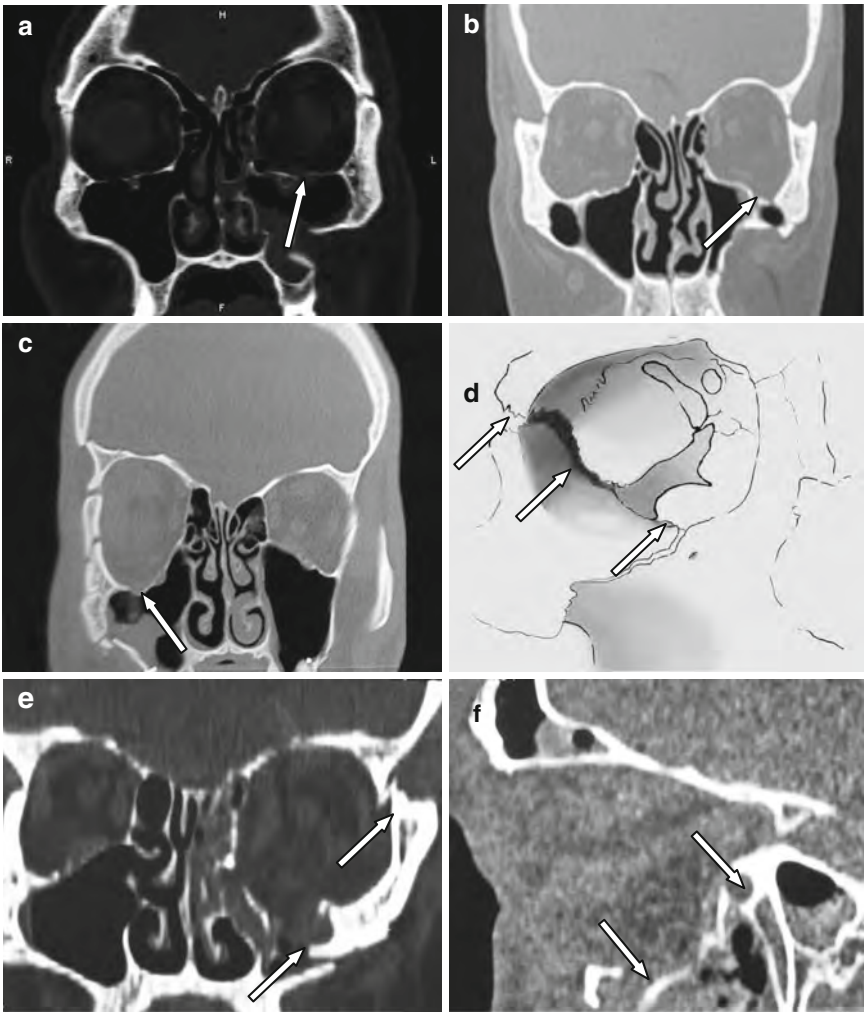

Fig. 6.4 Types of injuries of the orbital floor in patients with a zygomaticoorbital fracture (*arrows*): (**a**, **b**) A small linear-type defect without soft tissue entrapment (hence, without diplopia) accompanied by the minimal increase in orbital volume (**b**). (**c**) A "saucer-like" fracture causing a significant increase in the orbital volume and enophthalmos. (**d**, **e**) Spread of the sphenozygomatic suture. (**f**) Total orbital floor fracture caused by rotation of the zygomatic bone

In patients with a blowout fracture of the orbital floor, the probability of detecting another facial fracture is less than 4 %, while the converse is true with the facial skeleton when almost always there is a combined with injury of the orbital floor and rim. Because motor vehicle accidents are the most frequent causes of this type of trauma, these patients also have a sevenfold higher risk of concomitant trauma to the body and limbs.

Periorbital edema and hematoma in patients with zygomaticoorbital fractures occur 2.5 times more often as compared to those caused by isolated injury of the

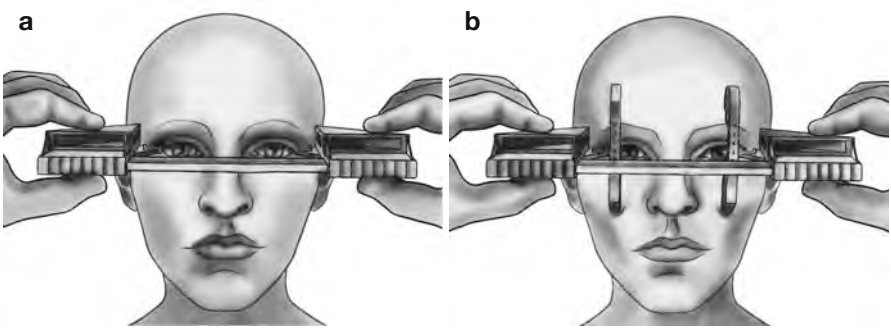

Fig. 6.5 Hertel exophthalmometer (**a**) and Naugle orbitometer (**b**)

orbital floor, while diplopia and oculomotor disorders are twofold less common (i.e., in 30–35 % of cases) [25].

If diplopia is caused by edema or hematoma of the inferior muscle complex or contusion of the inferior branch of the oculomotor nerve, one can expect spontaneous regression of diplopia within 3–6 months. However, the more frequent reasons for diplopia in patients with zygomaticoorbital fractures include entrapment of the muscle or adipose tissue in the fractured area. The vertical traction test is used to make this diagnosis.

In patients with *concomitant diastasis of the frontozygomatic suture*, the physical examination will reveal a depression when palpating the upper half of the lateral orbital rim. This finding demonstrates that the zygomatic bone has been profoundly dislocated.

Spread of the sphenozygomatic suture, which is almost identical to the diagnosis "*lateral orbital wall fracture*," plays a significant role in pathogenesis of functional and aesthetic problems. However, there is a paucity of literature on this type of fracture. The diastasis of the sphenozygomatic junction indicating that the zygomatic bone has rotated around its vertical axis results in a significant increase of the orbital volume, which leads to significant enophthalmos and hypoglobus (Fig. 6.4d–f) [32]. It is the zygomaticoorbital rather than the isolated blowout fracture that is the main reason of late enophthalmos [6, 25, 33].

As for the immediate post-traumatic period, exophthalmos is usually observed in patients due to edema of the orbital tissues, while the enophthalmos appears not earlier than 2 weeks after the trauma. Early enophthalmos indicates that the zygomaticoorbital complex has been severely damaged and requires urgent surgical intervention.

When evaluating the eyeball position in patients with zygomaticoorbital fractures, one should bear in mind that the Hertel exophthalmometer cannot be used because its point of fixation, the lateral orbital rim, has been destroyed or has been profoundly dislocated (Fig. 6.5a) [4, 34, 35]. The Naugle orbitometer (Fig. 6.5b) that uses the frontal arch and the malar eminence as points of fixation and the infraorbital rim as the reference point has been used for this purpose in clinical practice since 1992.

Sometimes the zygomatic bone is rotated inward, into the orbit, thus forming the pattern of the *blow-in fracture of the lateral wall* (Fig. 6.6) [36, 37].

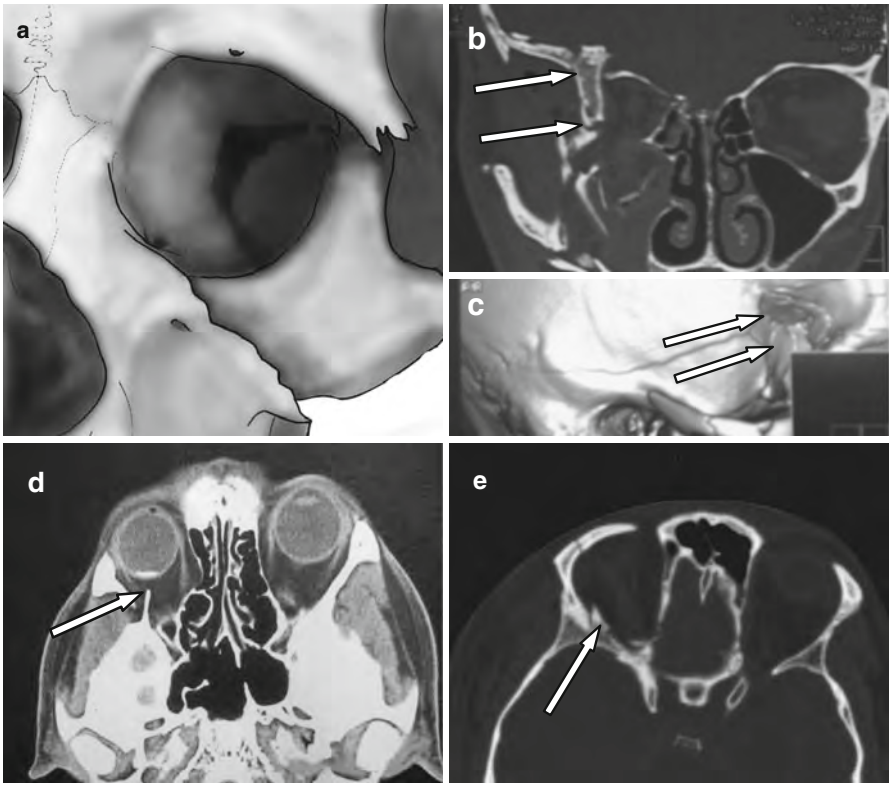

Fig. 6.6 Pattern of the blow-in fracture (*arrows*) of the zygomatic bone: (**a**–**c**) Dislocation of the lateral orbital wall secondary to the zygomatic bone pushed into orbital cavity. (**d**) Incorporation of a fragment of the greater wing of the sphenoid bone to the muscle cone. (**e**) Fracture of the trigone, i.e., the central third of the greater wing of the sphenoid bone near the sphenosquamosal suture indicating that the fracture is high-energy one

The first thing to do when examining these patients is to rule out any damage to the eyeball by a bone fragment (observed in 10 % of patients) and traumatic optic neuropathy (6 %) [18, 38–40].

The main mechanism of neuropathy is nerve compression in the so-called deep orbit by disturbed microcirculation in the minor pial vessels of the optic nerve leading to retrobulbar or optic nerve sheath hematoma [41–43]. The nerve can be compressed in the optic canal and also the development of the superior orbital fissure syndrome if the nerve is directly impacted by bone fragments [41, 44]. Furthermore, since the optic nerve dural tissue and the periosteum are continuous near the point where the nerve enters the optic canal, abrupt deceleration (e.g., in a frontal crash) may cause its avulsion.

Incorporation of a fragment of the frontal process of the zygomatic bone and/or the greater wing of the sphenoid into the muscular cone is highly likely to lead to permanent or intermittent compression of the optic nerve (Fig. 6.6d) [37, 44–46]. In the latter case, a patient has a typical symptom of sudden gaze-evoked amaurosis [47, 48]. Vision quickly recovers after the gaze returns to its primary position. Despite the intraconal type of injury, exophthalmos may be absent in this situation. However, ophthalmoscopic imaging always reveals changes in the optic disc or choroidal folds.

The degree of neuropathy varies over a broad range from mildly decreased color perception to full loss of vision. Instantaneous and total blindness is indicative of optic nerve avulsion or stroke and is an unfavorable prognostic factor [37]. Delayed onset and gradual or incomplete vision loss are typical of optic nerve compression and bring hope that it will be restored to some extent [49].

A zygomatic arch fracture is accompanied by flattening of the zygomatic area, facial widening, and disruption of the zygomatic arch at a point where the force was applied (the "depression" symptom). In a case of conventional inward and downward dislocation of fragments, additional signs include significant restriction in opening the mouth and impeded lateral movements of the mandible on the affected side. These restrictions of movement occur because of entrapment of the coronoid process of the mandible by a dislocated fragment of the zygomatic arch (Fig. 6.7c–e) [50]. A certain degree of trismus is typical of zygomatic arch fractures because of indirect injury of the muscle of mastication and damage to its attachment site.

High-energy fractures of the zygomatic bone. In addition to the aforementioned injuries of the zygomaticoorbital complex, high-energy fractures also involve comminuted fractures of the greater wing of the sphenoid, zygomatic arch, and the external angular process of the frontal bone. These fractures affect the glenoid fossa and cause the profound posterolateral dislocation of the zygomatic arch and the malar eminence. They result in such typical signs as flattening of the zygomatic region, facial widening, and enophthalmos because of the increased orbital volume.

***

Thus, the *full-scale clinical presentation of a classical zygomaticoorbital fracture with profound fragment dislocation* includes:

- Facial widening, flattening of the zygomatic area, inferior position of the lateral angle of the palpebral fissure, subconjunctival hemorrhage, and periorbital ecchymosis
- Dysesthesia along the infraorbital nerve
- The "bone step" symptom observed when palpating the upper half of the lateral and middle thirds of the infraorbital rim and the zygomaticoalveolar crest
- Emphysema of the orbit and facial tissues
- Trismus
- Ocular misalignment and/or diplopia [4, 5, 23].

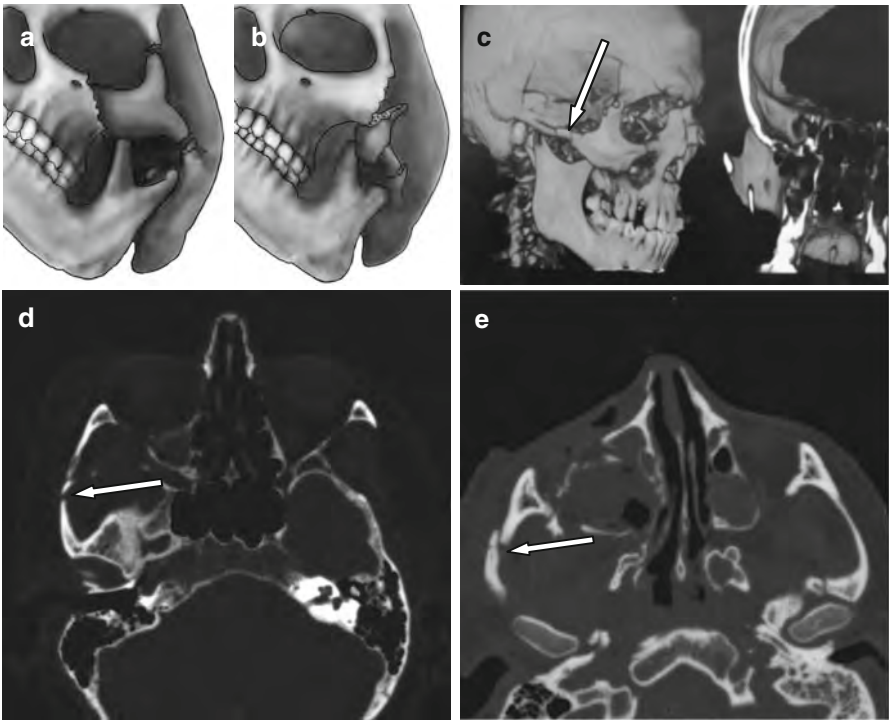

Fig. 6.7 Entrapment of the coronoid process of the mandible by a dislocated zygomatic bone fragment: (**a**–**b**) the entrapment mechanism for a zygomaticoorbital fracture (**a**) and fracture of the zygomatic arch (**b**). (**c**) 3D reconstruction of a zygomatic arch fracture (shown with an *arrow*). (**d**, **e**) Axial CT scan of a zygomatic arch fracture with fragment displacement (shown with an *arrow*)

It should be mentioned that rapidly developing edema in patients with facial injuries often disguises the typical symptoms of a zygomaticoorbital fracture. In this case, radiological methods are the best choice for accurate diagnosis.

6.6 Radiological Diagnosis

The radiological signs of zygomaticoorbital fractures are most clearly visualized on images in semiaxial view. These signs include diastasis and deformation of the contours of the frontozygomatic suture, steplike deformation or discontinuity of the infraorbital rim contour near the steplike deformation, disturbed configuration of the zygomaticoalveolar crest, asymmetry of orbital openings, ipsilateral thickening and compaction of facial soft tissues, blood in the sinus, and emphysema.

Despite clear visualization of the zygomaticoorbital fracture, radiology does not provide comprehensive information on the length and degree to which the fragments have been displaced in all three planes. That is why radiological examination is currently used only as a screening method [51]. Axial, coronal, and oblique sagittal CT scanning are needed to make a radiological diagnosis of a zygomaticoorbital fracture [52–54].

When analyzing the axial CT scans with cross sections 1.5 mm thick, the main focus is placed on the condition of the lateral orbital wall. In patients with typical zygomaticoorbital fractures, this wall is separated into two fragments along the sphenozygomatic suture: the zygomatic bone and the greater wing of the sphenoid (Fig. 6.8b, c). The condition of the zygomatic arch and zygomaticomaxillary suture are evaluated in the same view (Fig. 6.8d). The coronal and oblique parasagittal views are the optimal ones to analyze the degree of damage to the frontozygomatic suture and the infraorbital rim, respectively (Fig. 6.8e, f).

Three-dimensional CT reconstructions are crucial for the integral evaluation of the fracture, its length and orientation, and the degree of bone fragment dislocation in patients with severe damage to the zygomaticoorbital complex (Fig. 6.2) [55, 56].

6.7 Management of Zygomaticoorbital Fractures

No surgical treatment is needed for zygomatic bone fractures with no or with minimal bone fragment dislocation. In approximately 40 % of patients with zygomatic fractures, conservative management is sufficient with close follow-up for 3–4 weeks post trauma to evaluate the healing of the fracture [7, 57–61].

However, zygomaticoorbital fractures with bone fragment dislocation accompanied by functional and/or aesthetic disorders need surgical management. Usually this involves a joint effort of maxillofacial and plastic surgeons together with an ophthalmologist.

Time period for surgery. Taking into account the high rate of osteogenesis in patients with maxillofacial injuries [62], the optimal choice is to perform an intervention in the acute trauma period, i.e., within the first 14 days [63, 64]. If the surgical repair is delayed, there is a worse functional and aesthetic result because the repair usually requires osteotomy, distraction osteogenesis, facial contouring surgery, and sculpturing the cicatricial soft tissues [1, 65].

The surgical success relies on meticulous repositioning of the zygomaticoorbital complex. This requires complete exposure of the entire fracture site and apposition of the bone fragments using titanium supports[3] [4, 54, 67–69]. The number of open reposition and rigid fixation areas depends on the severity of a zygomaticoorbital fracture [70]. Titanium plates are placed with allowance for the positions of facial counterforces (Fig. 6.9).

[3] Wire fixation of the zygomatic bone, which used to be rather popular in the 1950s, is not currently used, since it cannot resist the tractional forces of the masseter which torques the zygomatic bone [6]. Resorbable stints do not provide proper mechanical strength of the restored zygomaticoorbital complex; therefore, they are used only in pediatric practice [78, 79].

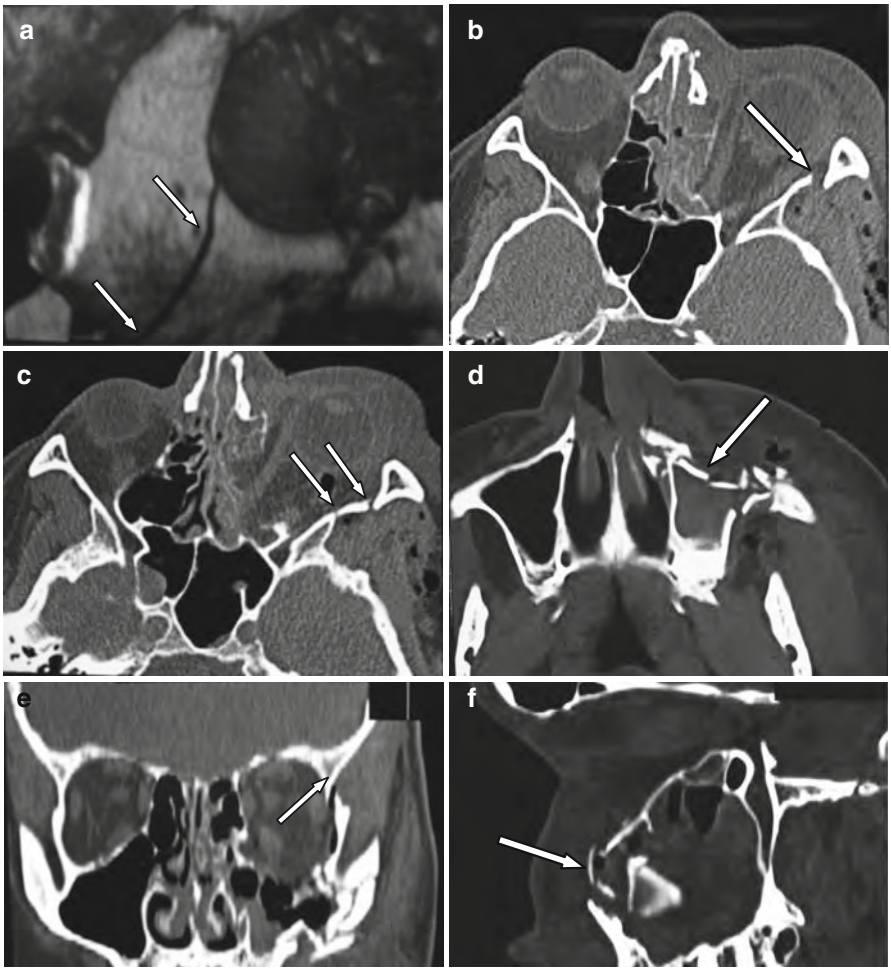

Fig. 6.8 Radiological diagnosis of a zygomaticoorbital fracture (the fracture line is shown with *arrows*) (**a**) Fracture of the zygomatic bone. (**b**) An axial CT scan that illustrates the spread of the sphenozygomatic suture. (**c**) CT presentation of diastasis of the sphenozygomatic suture combined with fracture of the greater wing of the sphenoid bone. (**d**) Destruction of the zygomaticomaxillary suture seen in an axial CT scan. (**e**) Spread of the frontozygomatic suture in an coronal CT scan. (**f**) Sagittal CT scanning allows one to detect a fracture of the infraorbital rim and the anterior wall of the maxillary sinus

Surgical approaches to the zygomaticoorbital fracture. Various combinations of the *upper gingivobuccal as well as periorbital and coronal approaches* are used to expose the zygomaticoorbital complex.

An upper gingivobuccal incision using the procedure proposed by Keen visualizes the zygomaticomaxillary suture very well (Fig. 5.4d) [71].

The intraoral approach is usually supplemented with one of the numerous incisions of the lower eyelid allowing one to reach the infraorbital rim. The preseptal transconjunctival approach combined with lateral canthotomy is preferred (Fig. 3.23).

Fig. 6.9 Facial counterforces

Dingman described approaching the fracture through the lateral portion of the eyebrow and this approach is typically used to expose the frontozygomatic suture. Since this approach is often complicated with severe cicatrization, an approach continuing the supratarsal fold outward has been proposed [72, 73]. Another alternative is to continue the subciliary or the transconjunctival incision of the lower eyelid laterally. The so-called extended C-shaped conjunctival approach allows one to reach the frontozygomatic suture, the lateral wall, the infraorbital rim, and the zygomatic arch. However, the incision is associated with a high risk of persisting edema of the upper eyelid [74, 75].

The combination of the upper gingivobuccal and lower transconjunctival incisions with approach through the lateral half of the superior conjunctival fornix allows one to avoid any complications typical of skin incisions [76, 77].

In the case of high-energy comminuted zygomaticoorbital injuries where visualization of the entire fractured area is crucial, a simple coronal incision is not sufficient. In this instance, the use of various modifications of bicoronal incisions (Fig. 6.10) combined with the transoral or transconjunctival approaches is necessary [80].

A combination of the upper gingivobuccal, lateral supratarsal, and preseptal transconjunctival approaches are most commonly used in practice.

Incisions and separation of soft tissues should be minimized to avoid late deformation of soft tissues but sufficient to adequately expose and reliably fix the fractures.

Zygomatic bone repositioning. If the zygomatic bone was slightly dislocated, closed repositioning according to the procedure proposed by Limberg [81–83] can be performed.

If the CT shows a significant dislocation in at least one point, especially when combined with comminuted fractures, open repositioning using instruments and approaches shown in Fig. 6.11a, b is needed. One should bear in mind that *incorrect repositioning of zygomatic bone is associated with more severe complications than closed repositioning, wire fixation of bone fragments, or delayed surgical intervention*.

Principles behind fixation of the zygomatic bone. High-precision reconstruction of the zygomaticoorbital complex implies that four points are fixed (the lateral and

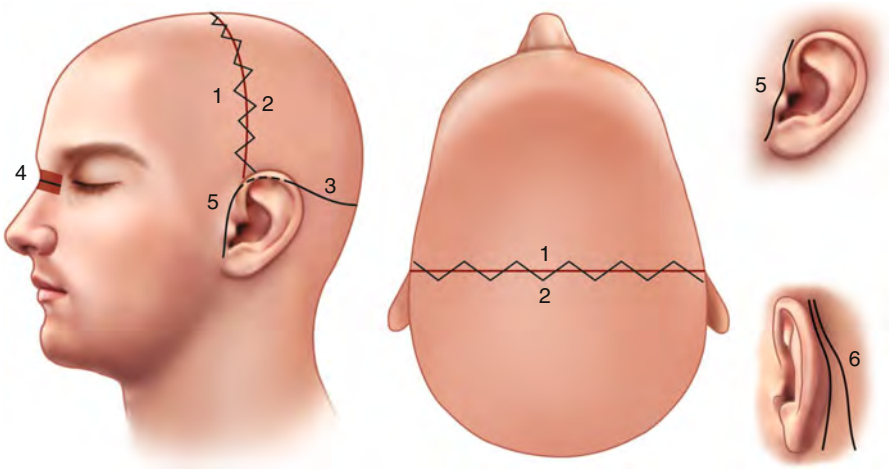

Fig. 6.10 Some approaches to the zygomaticoorbital fracture: (*1*) Conventional coronal incision and its modifications: zigzag "stealth" (*2*) and vertex (*3*) incisions used in patients with alopecia. (*4*) Limited or partial median horizontal approach used in patients with a combination of NOE and zygomaticoorbital fracture. (*5*) Preauricular approach. (*6*) Retroauricular approach. The figure does not show the periorbital and intraoral approaches that have been thoroughly described in the previous chapters

infraorbital rims, the zygomaticomaxillary suture, and the zygomatic arch); the lateral orbital wall is additionally fixed in patients with very severe fractures. However, three-point fixation, without exposure of the zygomatic arch, is usually used in practice; if properly performed, this procedure restores the facial symmetry [6, 79, 84, 85].

The initial step to surgical repair is the apposition of the edges of the frontozygomatic suture which will determine the vertical dimension of the zygomaticoorbital complex (Fig. 6.11c). Regardless of the fact that the frontozygomatic suture is formed by thick bones that ideally suit rigid fixation, rather thin and short plates need to be used because of the thin layer of overlying soft tissues.

Another important aspect is the need for meticulous shaping of a miniplate to duplicate the contour of the lateral orbital rim to avoid redislocation of the zygomatic bone during screw tightening. Taking this fact into account, it is reasonable to perform final fixation of the frontozygomatic suture after the second, third, and fourth plates have been already placed. The frontozygomatic suture is temporarily immobilized during the surgery with a plate non-tightly fixed with two screws or temporary elastic sutures (rubber bands stretched between screws mounted in fracture edges) [86, 87].

The evaluation of the quality of zygomatic bone repositioning does not play any significant role, since even an obvious rotation of the zygomatic bone virtually does not change the configuration of the frontozygomatic suture [24].

The next stage, apposition of the infraorbital rim, plays the key role in zygomatic bone *repositioning*; however, effective *rigid fixation* of this fracture line cannot be

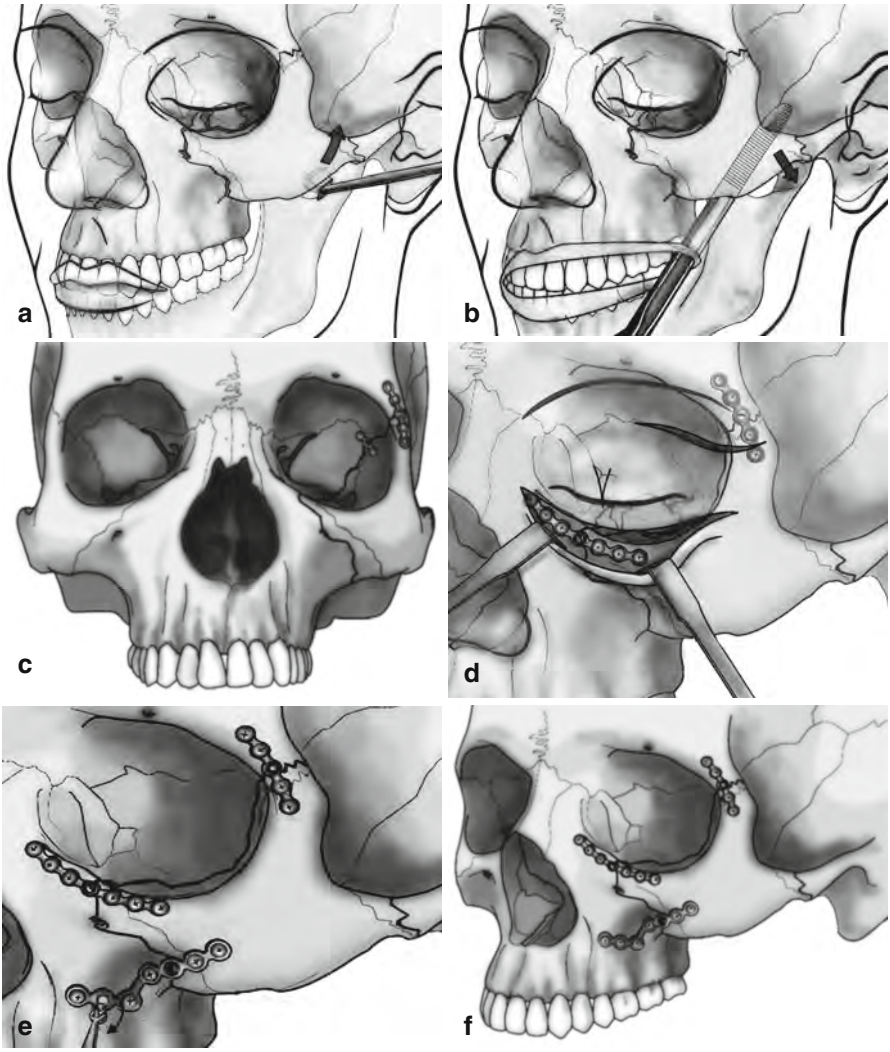

Fig. 6.11 Zygomatic bone repositioning and fixation: (**a**) Closed repositioning. (**b**) Open repositioning using an instrument placed under the zygomatic bone via the intraoral approach. (**c**) The first stages of zygomatic bone fixation. Apposition of the frontozygomatic suture is performed through an incision continuing the supratarsal fold outward followed by plate placement on the sphenozygomatic suture (if needed). (**d**) The infraorbital rim is reconstructed through the transconjunctival approach. (**e**) Fixation of the zygomaticomaxillary suture. (**f**) Surgical outcome. (**g**) Bottom view of the zygomatic arch. As opposed to its name, this anatomic structure has a virtually linear shape. (**h**) The reconstructed zygomatic arch having a linear shape. (**i**, **j**) Plastic surgery reconstruction of an orbital floor defect with a titanium plate and polytetrafluoroethylene. (**k**, **l**) Facial soft tissue resuspension (see explanation in the text) (Materials from www.aofoundation.org were used for this illustration)

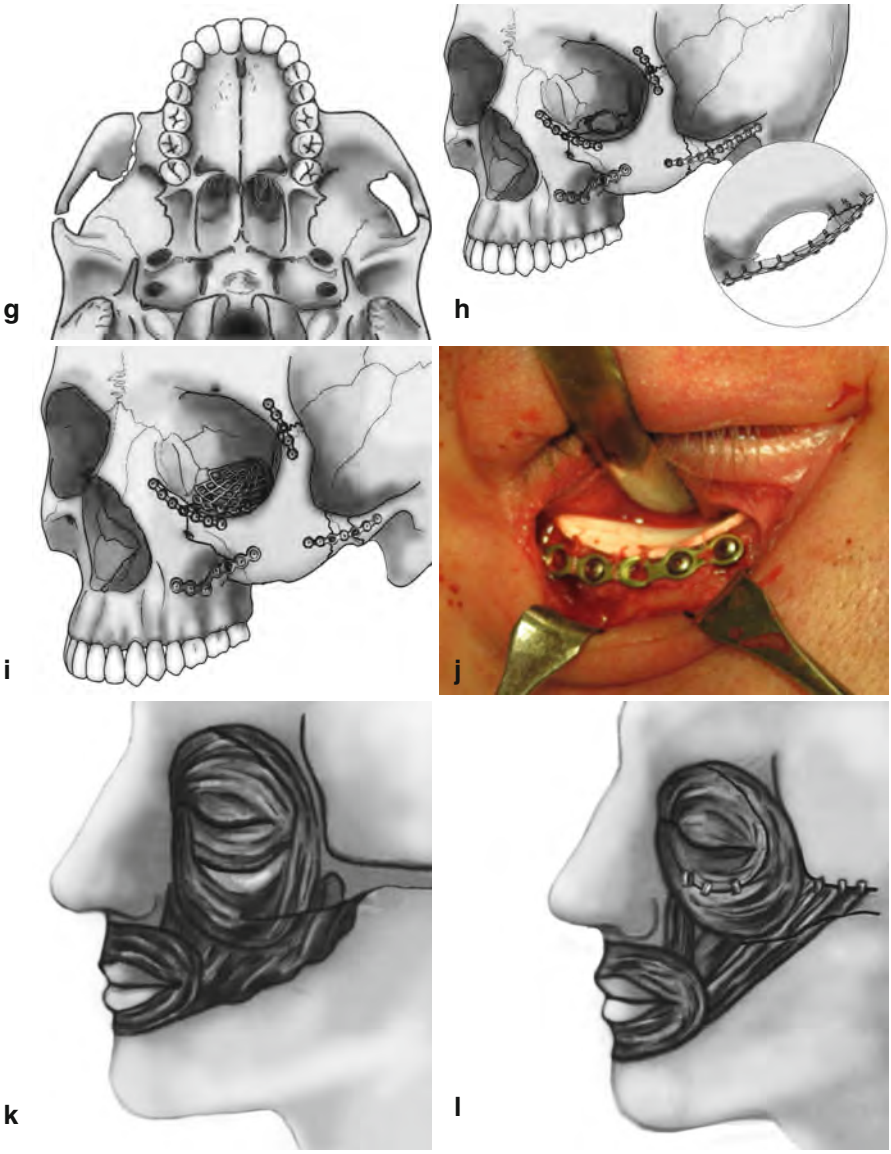

Fig. 6.11 (continued)

achieved. Hence, a small and thin plate needs to be implanted here to minimize the risk of cicatricial eyelid deformation [85]. It is recommended that a titanium plate is placed on the superior rather than on the anterior surface of the infraorbital rim, where it could be easily palpated (Fig. 6.11c).

The *zygomaticomaxillary suture* is the best place for fixation as it provides direct countereffect to tractional forces of the masseter and is covered with a thick soft tissue layer, making it possible to use long and thick (2 mm) titanium plates and screws (Fig. 6.11d).

Thus, the completeness of zygomatic bone repositioning should be primarily evaluated based on the infraorbital rim; reliable fixation is ensured by placing titanium plates near the zygomaticomaxillary and frontozygomatic sutures.

As the *sphenozygomatic suture* is the longest three-dimensional contact zone with other facial bones, it is the best indicator to evaluate the quality of zygomatic bone repositioning in three planes. Even a minor rotary dislocation of the zygomatic bone will result in a bad apposition of this suture. Because of its great thickness, the lateral orbital wall is rarely fragmented. This allows one to meticulously appose the sphenozygomatic suture. Along with revision of other landmarks, it provides high-precision repositioning and rigid fixation of the zygomatic bone [79].

Unfortunately, the typical periorbital (subciliary, transconjunctival, and upper blepharoplastic) approaches do not provide adequate exposure of this zone. Complete fixation of the fracture along the lateral orbital wall requires one to use the lateral orbitotomy approach or coronal incision with partial separation of the temporal muscle from the pterygopalatine fossa [36, 46, 88]. Taking into account the complexity of the approach to the sphenozygomatic suture, its use as a landmark when performing repositioning of the zygomaticoorbital complex is limited to high-energy extensive comminuted fractures. In this case, rigid fixation of the sphenozygomatic suture needs to be performed right after apposition of the frontozygomatic suture (Fig. 6.11e).

Blow-in comminuted fractures of the lateral orbital wall is another unambiguous indication for exposure of the sphenozygomatic suture through the coronal approach. In these cases, which are rather rare, the attempts to repose bone fragments through the conventional periorbital incisions are associated with a high risk of injury to the eye [46]. The coronal approach allows manipulation of the fragments of the lateral orbital wall under direct visual control without exerting mechanical impact on the eyeball. This intervention results in orbital wall reconstruction, restoration of eyeball motility, and regression of optic neuropathy [36].

Ten percent of the injured patients have zygomatic arch fractures [7, 89]. We would like to emphasize that zygomatic arch restoration is the key aspect in reconstruction of the zygomaticoorbital complex only when the main three fixation points are destroyed [32]. In these rare cases, zygomatic arch restoration through the preauricular, coronal, or endoscopic approaches is the first surgical stage that is aimed at recovering the original anteroposterior and transversal midfacial dimensions [90–93]. One should bear in mind that the zygomatic arch is an almost linear structure, and making it slightly curved during the reconstruction is a typical error that

causes flattening and broadening of the face (Fig. 6.11g, h). In order to avoid this complication, one should measure the distance between the inner surface of the reconstructed zygomatic arch and the temporal muscle; this distance must be shorter than 8 mm [94].

In patients with only a slight zygomatic bone deformation, one needs to seriously consider the indications for open repositioning. There should be concern for the possible complications of the coronal approach such as cicatricial alopecia, damage to the temporal branch of the facial nerve, and exaggeration of the normal anatomical depression any of which may mitigate the aesthetic effect of the surgery. The realization of all of these potential complications has led to a recent decrease in popularity of open repositioning and rigid fixation of the zygomatic arch in this condition.

The surgical stage following zygomatic arch fixation is *revision* and, if needed, *orbital floor reconstruction* (Fig. 6.11i, j) [95–97]. The indications, which are observed in 20 % of patients with moderate-energy injuries, include complaints of vertical diplopia or an extensive defect according to the coronal CT findings [81, 98, 99]. In most cases, the zygomaticoorbital fracture causes a linear orbital floor defect of only a small area that does not need to be closed [53, 100]. Zygomatic bone repositioning slightly increases the area of the existing defect, but an osteoplasty using a thin polyethylene, polytetrafluoroethylene, or titanium implant is necessary only if there is prolapse of adipose tissue to the maxillary sinus [95, 96, 99]. *Exposure of the orbital floor in every single patient with a zygomaticoorbital fracture is an unnecessary procedure* [7, 20, 101].

The final stage of the surgery includes meticulous closure of the periosteum and midface soft tissue resuspension. With this in mind, holes are drilled in the external half of the infraorbital rim and in the lateral orbital rim below the level of the canthus to place suspension sutures made of non-resorbable 2-0 suture material for anchoring the periosteum and muscles (Fig. 6.11k, l). This procedure prevents sagging of soft tissue covering the zygomatic bone, which is accompanied by ectropion of the external half of the lower eyelid, sometimes occurring together with drooping of the lateral canthus, flattening of the nasolabial fold, and reduced zygomatic prominence. The dissected lateral canthus is sutured to the internal surface of the lateral orbital rim slightly higher than its original attachment site [102].

The *postoperative management* is performed according to the principles described in the previous chapter. The follow-up period lasts for at least 40 days [103].

6.8 Complications of Zygomaticoorbital Fractures

Bergler et al. [104] insisted that almost half of patients have certain functional or aesthetic disorders even long after the fracture and surgical management [105]. Deformations of the zygomaticoorbital complex were observed in patients admitted to the hospital with multiple trauma much more often than in patients with an

isolated orbital fracture [106]. This fact can be explained by different circumstances of the trauma and energy of a wounding agent. Furthermore, the life-threatening aspects of multiple trauma impede both the thorough ophthalmic examination and adequate timely management of facial trauma.

Clinical presentation, diagnosis, and algorithms for managing a number of complications of zygomaticoorbital fractures have been described in previous chapters of this handbook, which allows us to avoid repetition and refer the readers to the corresponding sections. Only some aspects need to be discussed in more detail.

All the common complications such as facial asymmetry, enophthalmos, diplopia, infraorbital nerve neuropathy, and malocclusion are associated with only one reason and that is malposition of the zygomatic bone [107]. Experience has demonstrated that most patients are tolerant of some asymmetry of zygomatic prominence that can be as high as 2–4 mm.[4] However, they are more concerned with enophthalmos and hypoglobus, diplopia, and infraorbital nerve neuropathy [108].

6.8.1 Enophthalmos

Enophthalmos is the most common complications of both untreated and unsuccessfully operated on zygomaticoorbital fractures.

Edema of facial soft tissues and orbital hematoma, which disguise many facial deformities typical of a zygomaticoorbital fracture were often the reasons for patients' unreasonable refusal to undergo surgery.

The possible reasons for residual postoperative enophthalmos include:

- Malposition (usually postero-infero-exterior deviation) of the zygomatic bone [79]
- Fixation of the zygomatic bone to an undiagnosed hemi-NOE fracture
- Inadequate closure of the concomitant inferomedial orbital fracture by an implant displaced into the paranasal sinus

To correct the malposition of the zygomatic bone during the first month after surgery, it is sufficient to remove the titanium plates, displace the bone antero-supero-medially, and reanchor it (bearing in mind there is a risk of hypercorrection and development of exophthalmos).

In the late postoperative period, reconstruction of the zygomaticoorbital complex is associated with significant difficulties, and one needs to be even more cautious when making a decision about the advisability of the surgery [4, 5, 33, 70, 109, 110]. If osseous structures are slightly dislocated and there are no severe functional disorders, it is reasonable to perform only contouring of the orbital rims and to restore the orbital contents by subperiosteal implantation of porous synthetic material [66].

More extensive interventions are used in patients with profound functional and aesthetic disorders such as prolapse of the lateral canthus, entrapment of the

[4] In 30 % of healthy individuals, asymmetry of the position of zygomatic bones can reach 4 mm (Pape et al. [133]; citation from Freihofer [120]).

infraorbital nerve, and restricted mandibular excursions. Adequate dissection and mobilization of soft tissues; subperiosteal osteotomy of the fractured areas; and mobilization, repositioning, and reanchoring of the zygomatic bone (preferably performed under intraoperative CT control) are necessary [111–113]. The task is significantly facilitated by using stereolithographic three-dimensional models and preoperative computer-assisted planning followed by uploading the software to the control unit of the operating room video system – CAD/CAM and RP (rapid prototyping) methods and intraoperative CT control [114–120].

Another poorly known cause of postoperative enophthalmos is the *combination of a zygomaticoorbital fracture and undiagnosed hemi-NOE fracture* (Fig. 5.3d). It is clear that fixation of the zygomatic bone to the unstable infraorbital rim cannot eliminate the facial deformities typical of these fractures. Hence, the NOE fracture needs to be corrected before final repositioning of the zygomatic bone. A greenstick fracture of the nasofrontal suture does not require rigid fixation. Patients with an unstable nasofrontal suture should have rigid fixation of the suture edges via the coronal approach. Repositioning and fixation of the central fragment of the NOE fracture is performed by placing a thick titanium plate on the nasomaxillary suture. If needed, fixation can be enhanced by placing an implant on the infraorbital rim.

6.8.2 Infraorbital Nerve Neuropathy

The incidence of this complication in the long-term period varies from 15 to 50 %. Such a significant variance largely depends on study design and different patient selection criteria [29–31, 122].

Long-term persistence of neuropathy is determined both by the features of the fracture and the approaches used to manage it.

Single-stage comprehensive surgical treatment involving open repositioning and rigid fixation of fragments with titanium microplates plays a crucial role [30, 122]. However, even successful repositioning of the zygomatic bone is accompanied by dysesthesia in two-thirds of patients which may last up to 6 months [123]. Temporary dysfunction of the infraorbital nerve was observed in 100 % of cases after single-stage orbital floor reconstruction [124].

There was no long-term difference in infraorbital nerve neuropathy occurring in patients with a minimally dislocated zygomatic bone whether or not they underwent open repositioning and rigid fixation of the zygomatic bone.

The degree of late neurological disorders in patients subjected to single-stage orbital floor reconstruction holds an intermediate position between the groups of patients subjected to closed and open zygomatic bone repositioning [125, 126].

There are unquestionable risk factors for persisting neurological symptoms. For example, insufficiently rigid Kirschner wire fixation of the dislocated fragments and tamponade of the maxillary sinus with iodoform or a Foley catheter are accompanied by pronounced and long-lasting dysesthesia. This can occur in up to

50 % of the patients. Repositioning, especially closed repositioning, of the zygomatic bone in patients with a low-energy fracture, either without or with minimal dislocation, does not restore sensitivity; instead, it can aggravate neuropathy by increasing the perineural edema and the risk of hematoma development in direct proximity from the nerve [122]. Conservative management is justified in these cases, since sensitivity spontaneously recovers approximately one month after trauma.

In 25 % of patients, infraorbital nerve dysfunction persists up to 6–12 months after repositioning of the zygomaticoorbital complex. This usually indicates that the trunk has been entrapped in the fractured area [30, 31]. On the other hand, profound hypoesthesia is regarded only as a relative indication for surgical management [122, 127]; persistent hyperesthesia unambiguously shows that microsurgical decompression of the infraorbital nerve is needed and electrocautery of the nerve may be required if the intervention is unsuccessful.

6.8.3 Diplopia

Preoperative diplopia is observed in every third patient with a zygomatic fracture [25]; persisting diplopia is observed in the postoperative period in 3.4–8 % of cases. Diplopia persisting for 2 months is an indication for performing the traction test and high-resolution CT scanning. Dynamic follow-up is recommended if the traction test results are negative and there are no signs of entrapment or fusion of the muscle and the bone in the coronal MRI. If diplopia persists for 6 months, strabismus surgery is recommended.

6.8.4 Retrobulbar Hematoma

Retrobulbar hematoma is observed postoperatively in 0.1–0.3 % of cases [98, 128] and may cause central vision loss [129].

The development of massive retrobulbar hematoma complicated by the optic neuropathy is an indication for immediate injection of diuretic agents, megadose glucocorticoid therapy, and surgical decompression of the orbit by lateral canthotomy, cantholysis, and deep pterional (frontotemporal) decompression [41, 45, 130, 131]. Timely and adequate measures contribute to gradual vision recovery to a certain extent [38, 42].

References

1. Kelley, P., Hopper, R., & Gruss, J. (2007). Evaluation and treatment of zygomatic fractures. *Plastic and Reconstructive Surgery, 120*(7, Suppl. 2), S5–S15.
2. Motamedi, M. H. (2003). An assessment of maxillofacial fractures: A 5-year study of 237 patients. *Journal of Oral and Maxillofacial Surgery, 61*(1), 61–64.

3. Ferreira, P., Marques, M., Pinho, C., et al. (2004). Midfacial fractures in children and adolescents: A review of 492 cases. *The British Journal of Oral & Maxillofacial Surgery, 42*(6), 501–505.
4. Czerwinski, M., Martin, M., & Lee, C. (2005). Quantitative comparison of open reduction and internal fixation versus the Gillies method in the treatment of orbitozygomatic complex fractures. *Plastic and Reconstructive Surgery, 115*(7), 1848–1854.
5. Czerwinski, M., Martin, M., & Lee, C. (2005). Quantitative topographical evaluation of the orbitozygomatic complex. *Plastic and Reconstructive Surgery, 115*(7), 1858–1862.
6. Pearl, R. M. (1992). Treatment of enophthalmos. *Clinics in Plastic Surgery, 19*(1), 99–111.
7. Covington, D. S., Wainwright, D. J., Teichgraeber, J. F., & Parks, D. H. (1994). Changing patterns in the epidemiology and treatment of zygoma fractures: 10-year review. *The Journal of Trauma, 37*(2), 243–248.
8. Brasileiro, B. F., & Passeri, L. A. (2006). Epidemiological analysis of maxillofacial fractures in Brazil: A 5-year prospective study. *Oral Surgery, Oral Medicine, Oral Pathology, Oral Radiology, and Endodontics, 102*(1), 28–34.
9. Manolidis, S., Weeks, B. H., Kirby, M., et al. (2002). Classification and surgical management of orbital fractures: Experience with 111 orbital reconstructions. *The Journal of Craniofacial Surgery, 13*(6), 726–737.
10. Subhashraj, K., Nandakumar, N., & Ravindran, C. (2007). Review of maxillofacial injuries in Chennai, India: A study of 2748 cases. *The British Journal of Oral & Maxillofacial Surgery, 45*(8), 637–639.
11. Malara, P., Malara, B., & Drugacz, J. (2006). Characteristics of maxillofacial injuries resulting from road traffic accidents – a 5 year review of the case records from Department of Maxillofacial Surgery in Katowice, Poland. *Head & Face Medicine, 2*(2), 7.
12. Salonen, E. M., Koivikko, M. P., & Koskinen, S. K. (2008). Acute facial trauma in falling accidents: MDCT analysis of 500 patients. *Emergency Radiology, 15*(4), 241–247.
13. Shirani, G., Kalantar Motamedi, M. H., Ashuri, A., & Eshkevari, P. S. (2010). Prevalence and patterns of combat sport related maxillofacial injuries. *Journal of Emergencies, Trauma, and Shock, 3*(4), 314–317.
14. al-Qurainy, I. A., Titterington, D. M., Dutton, G. N., et al. (1991). Midfacial fractures and the eye: The development of a system for detecting patients at risk of eye injury. *The British Journal of Oral & Maxillofacial Surgery, 29*(6), 363–367.
15. al-Qurainy, I. A., Stassen, L. F., Dutton, G. N., et al. (1991). The characteristics of midfacial fractures and the association with ocular injury: A prospective study. *The British Journal of Oral & Maxillofacial Surgery, 29*(5), 291–301.
16. Ugboko, V. I., Udoye, C., Olateju, S. O., & Amole, A. O. (2006). Blindness and visual impairment from severe midface trauma in Nigerians. *International Journal of Oral and Maxillofacial Surgery, 35*(2), 127–131.
17. Barry, C., Coyle, M., Idrees, Z., et al. (2008). Ocular findings in patients with orbitozygomatic complex fractures: a retrospective study. *Journal of Oral and Maxillofacial Surgery, 66*(5), 888–892.
18. Jamal, B. T., Pfahler, S. M., Lane, K. A., et al. (2009). Ophthalmic injuries in patients with zygomaticomaxillary complex fractures requiring surgical repair. *Journal of Oral and Maxillofacial Surgery, 67*(5), 986–989.
19. Cruz, A. A., & Eichenberger, G. C. (2004). Epidemiology and management of orbital fractures. *Current Opinion in Ophthalmology, 15*(5), 416–421.
20. Pearl, R. M. (1990). Prevention of enophthalmos: A hypothesis. *Annals of Plastic Surgery, 25*(2), 132–133.
21. Folkestad, L., & Granstrom, G. (2003). A prospective study of orbital fracture sequelae after change of surgical routines. *Journal of Oral and Maxillofacial Surgery, 61*(9), 1038–1044.
22. Bogusiak, K., & Arkuszewski, P. (2010). Characteristics and epidemiology of zygomaticomaxillary complex fractures. *The Journal of Craniofacial Surgery, 21*(4), 1018–1023.

23. Della Rocca, R. C. (1990). Orbital surgery. In H. M. Clayman (Ed.), *Atlas of contemporary ophthalmic surgery* (pp. 879–1020). Mosby: St. Louis etc.
24. Manson, P. N., Markowitz, B., Mirvis, S., et al. (1990). Toward CT-based facial fracture treatment. *Plastic and Reconstructive Surgery, 85*(2), 202–212.
25. Tong, L., Bauer, R. J., & Buchman, S. R. (2001). A current 10-year retrospective survey of 199 surgically treated orbital floor fractures in a nonurban tertiary care center. *Plastic and Reconstructive Surgery, 108*(3), 612–621.
26. Harmer, S. G., Ethunandan, M., Zaki, G. A., & Brennan, P. A. (2007). Sudden transient complete loss of vision caused by nose blowing after a fracture of the orbital floor. *The British Journal of Oral & Maxillofacial Surgery, 45*(2), 154–155.
27. Ong, W. C., Lim, T. C., Lim, J., & Sundar, G. (2005). Cervicofacial, retropharyngeal and mediastinal emphysema: a complication of orbital fracture. *Asian Journal of Surgery, 28*(4), 305–308.
28. Raoul, G., Vanlergerghe, B., & Ferri, J. (2010). Massive pneumomediastinum and subcutaneous emphysema secondary to isolated zygomaticomaxillary complex fracture. *The Journal of Craniofacial Surgery, 21*(1), 266–268.
29. Renzi, G., Carboni, A., Perugini, M., et al. (2004). Posttraumatic trigeminal nerve impairment: a prospective analysis of recovery patterns in a series of 103 consecutive facial fractures. *Journal of Oral and Maxillofacial Surgery, 62*(11), 1341–1346.
30. Westermark, A., Jensen, J., & Sindet-Pedersen, S. (1992). Zygomatic fractures and infraorbital nerve disturbances. Miniplate osteosynthesis vs. other treatment modalities. *Oral Surgery, Oral Diagnosis, 3*, 27–30.
31. Vriens, J. P., & Moos, K. F. (1995). Morbidity of the infraorbital nerve following orbitozygomatic complex fractures. *Journal of Cranio-Maxillo-Facial Surgery, 23*(6), 363–368.
32. Hopper, R. A., Salemy, S., & Sze, R. W. (2006). Diagnosis of midface fractures with CT: What the surgeon needs to know. *Radiographics, 26*(3), 783–793.
33. Chen, C. T., Huang, F., & Chen, Y. R. (2006). Management of posttraumatic enophthalmos. *Chang Gung Medical Journal, 29*(3), 251–261.
34. Kratky, V., & Hurwitz, J. J. (1994). Hertel exophthalmometry without orbital rim contact. *Ophthalmology, 101*(5), 931–937.
35. Schmitz, J. P., Parks, W., Wilson, I. F., & Schubert, W. (1999). The use of the Naugle orbitometer in maxillofacial trauma. *The Journal of Cranio-Maxillofacial Trauma, 5*(1), 13–18.
36. Stanley, R. B., Sires, B. S., Funk, G. F., & Nerad, J. A. (1998). Management of displaced lateral orbital wall fractures associated with visual and ocular motility disturbances. *Plastic and Reconstructive Surgery, 102*(4), 972–979.
37. Gonzalez, M. G., Santos-Oller, J. M., de Vicente Rodriguez, J. C., & Lopez-Arranz, J. S. (1990). Optic nerve blindness following a malar fracture. *Journal of Cranio-Maxillo-Facial Surgery, 18*(7), 319–321.
38. Funk, G. F., Stanley, R. B., & Becker, T. S. (1989). Reversible visual loss due to impacted lateral orbital wall fractures. *Head and Neck, 11*(4), 295–300.
39. Gruss, J. S., & Hurwitz, J. J. (1990). Isolated blow-in fracture of the lateral orbit causing globe rupture. *Ophthalmic Plastic and Reconstructive Surgery, 6*(3), 221–224.
40. Koo, L., Hatton, M. P., & Rubin, P. A. (2007). Traumatic blindness after a displaced lateral orbital wall fracture. *The Journal of Trauma, 62*(5), 1288–1289.
41. Knox, B. E., Gates, G. A., & Berry, S. M. (1990). Optic nerve decompression via the lateral facial approach. *Laryngoscope, 100*(5), 458–462.
42. Lee, K. Y., Tow, S., & Fong, K. S. (2006). Visual recovery following emergent orbital decompression in traumatic retrobulbar haemorrhage. *Annals of the Academy of Medicine, Singapore, 35*(11), 831–832.
43. Popat, H., Doyle, P. T., & Davies, S. J. (2007). Blindness following retrobulbar haemorrhage – it can be prevented. *The British Journal of Oral & Maxillofacial Surgery, 45*(2), 163–164.
44. Yoshioka, N., Tominaga, Y., Motomura, H., & Muraoka, M. (1999). Surgical treatment for greater sphenoid wing fracture (orbital blow-in fracture). *Annals of Plastic Surgery, 42*(1), 87–91.

45. Lipkin, A. F., Woodson, G. E., & Miller, R. H. (1987). Visual loss due to orbital fracture. The role of early reduction. *Archives of Otolaryngology - Head and Neck Surgery, 113*(1), 81–83.
46. Stanley, R. B. (1988). The temporal approach to impacted lateral orbital wall fractures. *Archives of Otolaryngology - Head and Neck Surgery, 114*(5), 550–553.
47. Hampton, G. R., & Krohel, G. B. (1983). Gaze-evoked blindness. *Annals of Ophthalmology, 15*(1), 73–76.
48. Otto, C. S., Coppit, G. L., Mazzoli, R. A., et al. (2003). Gaze-evoked amaurosis: a report of five cases. *Ophthalmology, 110*(2), 322–326.
49. Amrith, S., Pham, T., Chee, C., & Chan, T. K. (1993). Visual recovery following transethmoidal optic nerve decompression in traumatic optic neuropathy. *Ophthalmic Surgery, 24*(1), 49–52.
50. Czerwinski, M., Ma, S., Motakis, D., & Lee, C. (2008). Economic analysis of open approach versus conventional methods of zygoma fracture repair. *The Canadian Journal of Plastic Surgery, 16*(3), 153–156.
51. Crighton, L. A., & Koppel, D. A. (2007). The value of postoperative radiographs in the management of zygomatic fractures: prospective study. *The British Journal of Oral & Maxillofacial Surgery, 45*(1), 51–53.
52. Mauriello, J. A., Lee, H. J., & Nguyen, L. (1999). CT of soft tissue injury and orbital fractures. *Radiologic Clinics of North America, 37*(1), 241–252.
53. Ellis, E., & Reddy, L. (2004). Status of the internal orbit after reduction of zygomaticomaxillary complex fractures. *Journal of Oral and Maxillofacial Surgery, 62*(3), 275–283.
54. Kaufman, Y., Stal, D., Cole, P., & Hollier, L., Jr. (2008). Orbitozygomatic fracture management. *Plastic and Reconstructive Surgery, 121*(4), 1370–1374.
55. Gillespie, J. E., Isherwood, I., Barker, G. R., & Quayle, A. A. (1987). Three-dimensional reformations of computed tomography in the assessment of facial trauma. *Clinical Radiology, 38*(5), 523–526.
56. Fox, L. A., Vannier, M. W., West, O. C., et al. (1995). Diagnostic performance of CT, MPR and 3DCT imaging in maxillofacial trauma. *Computerized Medical Imaging and Graphics, 19*(5), 385–395.
57. Rever, L. J., Manson, P. N., Randolph, M. A., et al. (1991). The healing of facial bone fractures by the process of secondary union. *Plastic and Reconstructive Surgery, 87*(3), 451–458.
58. Rohrich, R. J., Hollier, L. H., & Watumull, D. (1992). Optimizing the management of orbitozygomatic fractures. *Clinics in Plastic Surgery, 19*(1), 149–165.
59. Gomes, P. P., Passeri, L. A., & Barbosa, J. R. (2006). A 5-year retrospective study of zygomatico-orbital complex and zygomatic arch fractures in Sao Paulo State Brazil. *Journal of Oral and Maxillofacial Surgery, 64*(1), 63–67.
60. Antoun, J. S., & Lee, K. H. (2008). Sports-related maxillofacial fractures over an 11-year period. *Journal of Oral and Maxillofacial Surgery, 66*(3), 504–508.
61. Lee, K. H., & Antoun, J. (2009). Zygomatic fractures presenting to a tertiary trauma centre, 1996–2006. *The New Zealand Dental Journal, 105*(1), 4–7.
62. Stoll, P., & Schilli, W. (1988). Primary reconstruction with AO-miniplates after severe craniomaxillofacial trauma. *Journal of Cranio-Maxillo-Facial Surgery, 16*(1), 18–21.
63. Carr, R. M., & Mathog, R. H. (1997). Early and delayed repair of orbitozygomatic complex fractures. *Journal of Oral and Maxillofacial Surgery, 55*(3), 253–258.
64. Baek, M. K., Jung, J. H., Kim, S. T., & Kang, I. G. (2010). Delayed treatment of zygomatic tetrapod fracture. *Clinical and Experimental Otorhinolaryngology, 3*(2), 107–109.
65. Mitsukawa, N., Satoh, K., Morishita, T., & Hosaka, Y. (2006). Clinical application of distraction osteogenesis for traumatic maxillofacial deformities. *The Journal of Craniofacial Surgery, 17*(3), 431–437.
66. Eski, M., Sengezer, M., Turegun, M., et al. (2007). Contour restoration of the secondary deformities of zygomaticoorbital fractures with porous polyethylene implant. *The Journal of Craniofacial Surgery, 18*(3), 520–525.
67. Denny, A. D., & Gonnering, R. S. (1990). Early repair of complex orbital fractures. *Retina, 10*(Suppl. 1), 8–19.

68. Shaw, G. Y., & Khan, J. (1994). Precise repair of orbital maxillary zygomatic fractures. *Archives of Otolaryngology - Head and Neck Surgery, 120*(6), 613–619.
69. Ducic, Y. (1997). Midface reconstruction with titanium mesh and hydroxyapatite cement: A case report. *The Journal of Cranio-Maxillofacial Trauma, 3*(2), 35–39.
70. Hollier, L. H., Thornton, J., Pazmino, P., & Stal, S. (2003). The management of orbitozygomatic fractures. *Plastic and Reconstructive Surgery, 111*(7), 2386–2392.
71. Wales, C. J., & Carter, L. M. (2007). A safe and accurate technique for transbuccal incisions. *The British Journal of Oral & Maxillofacial Surgery, 45*(2), 177.
72. Kung, D. S., & Kaban, L. B. (1996). Supratarsal fold incision for approach to the superior lateral orbit. *Oral Surgery, Oral Medicine, Oral Pathology, Oral Radiology, and Endodontics, 81*(5), 522–525.
73. Gaia, B. F., Landgraf, H., Pardo-Kaba, S. C., & Shinohara, E. H. (2008). Access to the frontal sinus and zygomatico frontal suture through the supratarsal fold. *The British Journal of Oral & Maxillofacial Surgery, 46*(3), 226–228.
74. Uemura, T., Jinnai, T., Yokoyama, T., et al. (2001). C-shape extended transconjunctival approach for the exposure and osteotomy of traumatic orbitozygomaticomaxillary deformities. *The Journal of Craniofacial Surgery, 12*(6), 603–607.
75. Kharkar, V. R., Rudagi, B. M., Halli, R., & Kini, Y. (2010). Comparison of the modified lateral orbitotomy approach and modified hemicoronal approach in the treatment of unstable malunions of zygomatic complex fractures. *Oral Surgery, Oral Medicine, Oral Pathology, Oral Radiology, and Endodontics, 109*(4), 504–509.
76. Langsdon, P. R., Knipe, T. A., Whatley, W. S., & Costello, T. H. (2005). Transconjunctival approach to the zygomatico-frontal limb of orbitozygomatic complex fractures. *Facial Plastic Surgery, 21*(3), 171–175.
77. Langsdon, P. R., Rohman, G. T., Hixson, R., et al. (2010). Upper lid transconjunctival versus transcutaneous approach for fracture repair of the lateral orbital rim. *Annals of Plastic Surgery, 65*(1), 52–55.
78. Kasrai, L., Hearn, T., Gur, E., & Forrest, C. R. (1999). A biomechanical analysis of the orbitozygomatic complex in human cadavers: examination of load sharing and failure patterns following fixation with titanium and bioresorbable plating systems. *The Journal of Craniofacial Surgery, 10*(3), 237–243.
79. Rohner, D., Tay, A., Meng, C. S., et al. (2002). The sphenozygomatic suture as a key site for osteosynthesis of the orbitozygomatic complex in panfacial fractures: a biomechanical study in human cadavers based on clinical practice. *Plastic and Reconstructive Surgery, 110*(6), 1463–1471.
80. Zhang, Q. B., Dong, Y. J., Li, Z. B., & Zhao, J. H. (2006). Coronal incision for treating zygomatic complex fractures. *Journal of Cranio-Maxillo-Facial Surgery, 34*(3), 182–185.
81. Kovacs, A. F., & Ghahremani, M. (2001). Minimization of zygomatic complex fracture treatment. *International Journal of Oral and Maxillofacial Surgery, 30*(5), 380–383.
82. Mavili, M. E., Canter, H. I., & Tuncbilek, G. (2007). Treatment of noncomminuted zygomatic fractures with percutaneous screw reduction and fixation. *The Journal of Craniofacial Surgery, 18*(1), 67–73.
83. af Geijerstam, B., Hultman, G., Bergström, J., & Stjärne, P. (2008). Zygomatic fractures managed by closed reduction: An analysis with postoperative computed tomography follow-up evaluating the degree of reduction and remaining dislocation. *Journal of Oral and Maxillofacial Surgery, 66*(11), 2302–2307.
84. Hammer, B., & Prein, J. (1995). Correction of posttraumatic orbital deformities: Operative techniques and review of 26 patients. *Journal of Cranio-Maxillo-Facial Surgery, 23*(2), 81–90.
85. Yonehara, Y., Hirabayashi, S., Tachi, M., & Ishii, H. (2005). Treatment of zygomatic fractures without inferior orbital rim fixation. *The Journal of Craniofacial Surgery, 16*(3), 481–485.
86. Taglialatela Scafati, C., Facciuto, E., & Aliberti, F. (2004). The Elastic Internal Traction (EIT): An effective method to reduce the displaced facial fractures. *International Journal of Oral and Maxillofacial Surgery, 33*(7), 709–712.

87. Sood, V., & Lowe, T. (2010). Modification of the elastic internal traction method for temporary inter-fragment reduction prior to internal fixation. *The British Journal of Oral & Maxillofacial Surgery, 48*(4), E7–E8.
88. Evans, B. T., & Mourouzis, C. (2009). Lateral orbitotomy: A useful technique in the management of severe traumatic disruption of the lateral orbital skeleton. *International Journal of Oral and Maxillofacial Surgery, 38*(9), 984–987.
89. Gruss, J. S., Van Wyck, L., Phillips, J. H., & Antonyshyn, O. (1990). The importance of the zygomatic arch in complex midfacial fracture repair and correction of posttraumatic orbitozygomatic deformities. *Plastic and Reconstructive Surgery, 85*(6), 878–890.
90. Park, D. H., Lee, J. W., Song, C. H., et al. (1998). Endoscopic application in aesthetic and reconstructive facial bone surgery. *Plastic and Reconstructive Surgery, 102*(4), 1199–1209.
91. Chen, C. T., Lai, J. P., Chen, Y. R., et al. (2000). Application of endoscope in zygomatic fracture repair. *British Journal of Plastic Surgery, 53*(2), 100–105.
92. Czerwinski, M., & Lee, C. (2006). The rationale and technique of endoscopic approach to the zygomatic arch in facial trauma. *Facial Plastic Surgery Clinics of North America, 14*(1), 37–43.
93. Schubert, W., & Jenabzadeh, K. (2009). Endoscopic approach to maxillofacial trauma. *The Journal of Craniofacial Surgery, 20*(1), 154–156.
94. Song, W. C., Choi, H. G., Kim, S. H., et al. (2009). Topographic anatomy of the zygomatic arch and temporal fossa: a cadaveric study. *Journal of Plastic, Reconstructive & Aesthetic Surgery, 62*(11), 1375–1378.
95. Romano, J. J., Iliff, N. T., & Manson, P. N. (1993). Use of Medpor porous polyethylene implants in 140 patients with facial fractures. *The Journal of Craniofacial Surgery, 4*(3), 142–147.
96. Eski, M., Sahin, I., Deveci, M., et al. (2006). A retrospective analysis of 101 zygomatico-orbital fractures. *The Journal of Craniofacial Surgery, 17*(6), 1059–1064.
97. Yu, H., Shen, G., Wang, X., & Zhang, S. (2010). Navigation-guided reduction and orbital floor reconstruction in the treatment of zygomatico-orbital-maxillary complex fractures. *Journal of Oral and Maxillofacial Surgery, 68*(1), 28–34.
98. Lynham, A. J., Monsour, F. N., & Chapman, P. (2002). Management of orbitozygomatic fractures. *ANZ Journal of Surgery, 72*(5), 364–366.
99. Czerwinski, M., Izadpanah, A., Ma, S., et al. (2008). Quantitative analysis of the orbital floor defect after zygoma fracture repair. *Journal of Oral and Maxillofacial Surgery, 66*(9), 1869–1874.
100. Shumrick, K. A., & Campbell, A. C. (1998). Management of the orbital rim and floor in zygoma and midface fractures: Criteria for selective exploration. *Facial Plastic Surgery, 14*(1), 77–81.
101. al-Qurainy, I. A., Stassen, L. F., Dutton, G. N., et al. (1991). Diplopia following midfacial fractures. *The British Journal of Oral & Maxillofacial Surgery, 29*(5), 302–307.
102. Phillips, J. H., Gruss, J. S., Wells, M. D., & Chollet, A. (1991). Periosteal suspension of the lower eyelid and cheek following subciliary exposure of facial fractures. *Plastic and Reconstructive Surgery, 88*(1), 145–148.
103. Roccia, F., Diaspro, A., Nasi, A., & Berrone, S. (2008). Management of sport-related maxillofacial injuries. *The Journal of Craniofacial Surgery, 19*(2), 377–382.
104. Bergler, W., Hoffmann, A., & Hörmann, K. (1997). Late sequelae of lateral and central midfacial fractures after osteosynthesis with miniplates. *HNO, 45*(3), 128–132.
105. Lee, J. H., Chang, J. W., Choi, M. S., & Ahn, H. C. (2010). Delayed infection after a zygoma fracture fixation with absorbable plates. *The Journal of Craniofacial Surgery, 21*(6), 2018–2019.
106. Seider, N., Gilboa, M., Miller, B., et al. (2007). Orbital fractures complicated by late enophthalmos: higher prevalence in patients with multiple trauma. *Ophthalmic Plastic and Reconstructive Surgery, 23*(2), 115–118.
107. Nardi, M. (1996). Hypertropia and the posterior blowout fracture. *Ophthalmology, 103*(1), 152–156.

108. Folkestad, L., Aberg-Bengtsson, L., & Granström, G. (2006). Recovery from orbital floor fractures: A prospective study of patients' and doctors' experiences. *International Journal of Oral and Maxillofacial Surgery, 35*(6), 499–505.
109. Gasparini, G., Saponaro, G., Moro, A., et al. (2010). Zygomatic sagittal split osteotomy: A novel and simple surgical technique for use in midface corrections. *The Journal of Craniofacial Surgery, 21*(6), 1872–1875.
110. Holmes, S. (2011). Reoperative orbital trauma: Management of posttraumatic enophthalmos and aberrant eye position. *Oral and Maxillofacial Surgery Clinics of North America, 23*(1), 17–29.
111. Stanley, R. B. (1999). Use of intraoperative computed tomography during repair of orbitozygomatic fractures. *Archives of Facial Plastic Surgery, 1*(1), 25–26.
112. Clauser, L., Galiè, M., Pagliaro, F., & Tieghi, R. (2008). Posttraumatic enophthalmos: Etiology, principles of reconstruction, and correction. *The Journal of Craniofacial Surgery, 19*(2), 51–59.
113. Rodriguez, E. D., Bluebond-Langner, R., Park, J. E., & Manson, P. N. (2008). Preservation of contour in periorbital and midfacial craniofacial microsurgery: Reconstruction of the soft-tissue elements and skeletal buttresses. *Plastic and Reconstructive Surgery, 121*(5), 1738–1747.
114. Klug, C., Schicho, K., Ploder, O., et al. (2006). Point-to-point computer-assisted navigation for precise transfer of planned zygoma osteotomies from the stereolithographic model into reality. *Journal of Oral and Maxillofacial Surgery, 64*(3), 550–559.
115. Westendorff, C., Gülicher, D., Dammann, F., et al. (2006). Computer-assisted surgical treatment of orbitozygomatic fractures. *The Journal of Craniofacial Surgery, 17*(5), 837–842.
116. Pham, A. M., Rafii, A. A., Metzger, M. C., et al. (2007). Computer modeling and intraoperative navigation in maxillofacial surgery. *Otolaryngology – Head and Neck Surgery, 137*(4), 624–631.
117. Li, W. Z., Zhang, M. C., Li, S. P., et al. (2009). Application of computer-aided three-dimensional skull model with rapid prototyping technique in repair of zygomatico-orbito-maxillary complex fracture. *International Journal of Medical Robotics and Computer Assisted Surgery, 5*(2), 158–163.
118. Ogino, A., Onishi, K., & Maruyama, Y. (2009). Intraoperative repositioning assessment using navigation system in zygomatic fracture. *The Journal of Craniofacial Surgery, 20*(4), 1061–1065.
119. Bell, R. B., & Markiewicz, M. R. (2009). Computer-assisted planning, stereolithographic modeling, and intraoperative navigation for complex orbital reconstruction: A descriptive study in a preliminary cohort. *Journal of Oral and Maxillofacial Surgery, 67*(12), 2559–2570.
120. Pohlenz, P., Blake, F., Blessmann, M., et al. (2009). Intraoperative cone-beam computed tomography in oral and maxillofacial surgery using a C-arm prototype: First clinical experiences after treatment of zygomaticomaxillary complex fractures. *Journal of Oral and Maxillofacial Surgery, 67*(3), 515–521.
121. Freihofer, H. P. (1995). Effectiveness of secondary post-traumatic periorbital reconstruction. *Journal of Cranio-Maxillo-Facial Surgery, 23*(3), 143–150.
122. Peltomaa, J., & Rihkanen, H. (2000). Infraorbital nerve recovery after minimally dislocated facial fractures. *European Archives of Oto-Rhino-Laryngology, 257*(8), 449–452.
123. Zachariades, N., Papavassiliou, D., & Papademetriou, I. (1990). The alterations in sensitivity of the infraorbital nerve following fractures of the zygomaticomaxillary complex. *Journal of Cranio-Maxillo-Facial Surgery, 18*(7), 315–318.
124. Fogasa, W. C., Ferreira, M. C., & Dellon, A. L. (2004). Infraorbital nerve injury associated with zygoma fractures: Documentation with neurosensory testing. *Plastic and Reconstructive Surgery, 113*(3), 834–838.
125. Vriens, J. P., van der Glas, H. W., Bosman, F., et al. (1998). Information on infraorbital nerve damage from multitesting of sensory function. *International Journal of Oral and Maxillofacial Surgery, 27*(1), 20–26.

126. Vriens, J. P., van der Glas, H. W., Moos, K. F., & Koole, R. (1998). Infraorbital nerve function following treatment of orbitozygomatic complex fractures. A multitest approach. *International Journal of Oral and Maxillofacial Surgery, 27*(1), 27–32.
127. Boush, G. A., & Lemke, B. N. (1994). Progressive infraorbital nerve hypesthesia as a primary indication for blow-out fracture repair. *Ophthalmic Plastic and Reconstructive Surgery, 10*(4), 271–275.
128. Bater, M. C., Ramchandani, P. L., & Brennan, P. A. (2005). Post-traumatic eye observations. *The British Journal of Oral & Maxillofacial Surgery, 43*(5), 410–416.
129. Pigadas, N., & Lloyd, R. E. (2005). Haematoma of anterior ethmoidal artery after reduction of fracture of zygomatic complex. *The British Journal of Oral & Maxillofacial Surgery, 43*(5), 417–419.
130. Larsen, M., & Wieslander, S. (1999). Acute orbital compartment syndrome after lateral blow-out fracture effectively relieved by lateral cantholysis. *Acta Ophthalmologica Scandinavica, 77*(2), 232–233.
131. Korinth, M. C., Ince, A., Banghard, W., et al. (2002). Pterional orbita decompression in orbital hemorrhage and trauma. *The Journal of Trauma, 53*(1), 73–78.
132. Govsa, F., Celik, S., & Ozer, MA. (2009). Orbital restoration surgery in the zygomaticotemporal and zygomaticofacial nerves and important anatomic landmarks. *The Journal of Craniofacial Surgery, 20*(2), 540–544
133. Pape, H. D., Galanski, M., & Rothe, F. (1977). Metric and x-ray comparison of the middle face following periorbital fractures. *Fortschr Kiefer Gesichtschir, 22*, 128–131

Maxillary Fractures

7

Vadim P. Nikolaenko, Yury S. Astakhov,
Mikhail M. Soloviev, G. Khatskevich, and Igor G. Trofimov

Contents

7.1 Epidemiology of Maxillary Fractures 305
7.2 Fracture Classification 305
7.3 Clinical Presentation of Maxillary Fractures 308
7.3.1 Clinical Presentation of Le Fort I Fractures 308
7.3.2 Clinical Presentation of Le Fort II Fractures 309
7.3.3 Clinical Presentation of Le Fort III Fractures 311
7.4 Radiological Diagnosis 313
7.5 Treatment Principles in the Management of Maxillary Fractures 315
7.5.1 Indications for Surgical Management 315
7.5.2 Management of Le Fort I Fractures 318
7.5.3 Management of Le Fort II Fractures 318
7.5.4 Management of Le Fort III Fractures 318
7.5.5 Postoperative Treatment 319
7.5.6 Complications 319
References 320

V.P. Nikolaenko, MD, PhD, DSc (✉)
Department of Ophthalmology, Saint Petersburg State Hospital No. 2,
Saint-Petersburg, Russia

Department of Otolaryngology and Ophthalmology, Medical Faculty,
Saint-Petersburg State University, Saint-Petersburg, Russia
e-mail: dr.nikolaenko@mail.ru

Y.S. Astakhov, MD, PhD, DSc
Department of Ophthalmology, I.P. Pavlov First Saint Petersburg State Medical University,
Saint-Petersburg, Russia

City Ophthalmologic Center at Saint Petersburg State Hospital No. 2,
Saint-Petersburg, Russia
e-mail: astakhov73@mail.ru

© Springer-Verlag Berlin Heidelberg 2015

V.P. Nikolaenko, Y.S. Astakhov (eds.), *Orbital Fractures: A Physician's Manual*,
DOI 10.1007/978-3-662-46208-9_7

M.M. Soloviev, MD, PhD • I.G. Trofimov
Department of Maxillo-facial and Plastic surgery, St. Petersburg State Hospital No. 2, Saint-Petersburg, Russia

Associated professor, Department of Maxilla-facial and oral surgery, I.P.Pavlov First Saint Petersburg State Medical University, Saint-Petersburg, Russia

Associated professor, Department of Maxilla-facial and oral surgery, St. Petersburg State University, Saint-Petersburg, Russia

G. Khatskevich, MD, PhD
Professor, Head of Department of Pediatric Stomatology and Maxillo-facial surgery, I.P. Pavlov First Saint Petersburg State Medical University, Saint-Petersburg, Russia

The two maxilla bones form a framework for the facial skeleton. They combine the cranio-fronto-ethmoidal complex with the mandible and the occlusal plane and unite two zygomatico-orbital complexes.

The maxilla can be regarded as a four-faceted pyramid with the outer wall of the nasal cavity being its base and the four facets being formed by the orbital floor (superiorly), the alveolar ridge (inferiorly), the anterior wall of the maxillary sinus (anteriorly), and the anterior surface of the pterygopalatine fossa (posterior outwardly).

The maxilla and the adjacent midfacial bones play a crucial role as they dampen vertical compression caused by chewing or a wounding agent moving upward. Skull base protection is maintained due to the presence of seven vertical buttresses or "reinforcing ribs." They include three paired ones (nasomaxillary, zygomaticomaxillary, and pterygomaxillary) and an auxiliary non-paired median one, the ethmoid-vomerine buttress (Fig. 7.1).

Several soft tissue structures are tightly connected with the maxilla and are often affected in patients with maxillary fractures:

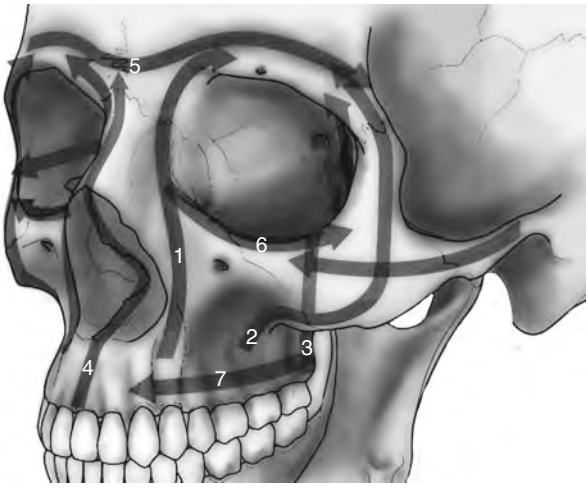

Fig. 7.1 Vertical and horizontal midfacial zygomaticomaxillary buttresses: *1* nasomaxillary buttress, *2* zygomaticomaxillary buttress, *3* pterygomaxillary buttress, *4* fronto-ethmoid-vomerine buttress, *5* frontal buttress, *6* infraorbital buttress, *7* inferior (U-shaped) buttress (Materials from www.aofoundation.org were used for this illustration)

- The infraorbital nerve
- Branches of the maxillary artery supplying the midface
- Orbital contents (the globe, the optic nerve, the extraocular muscles, and the lacrimal apparatus)

Since the maxilla is adjacent to the oral and nasal cavities, the orbit, and other anatomical structures, it is extremely significant both morphologically and functionally. Maxillary fractures are justly regarded as the most severe injuries.

7.1 Epidemiology of Maxillary Fractures

Maxillary fractures comprise 6–28 % of all facial fractures. Most of them occur in 20–40-year-old men; half of those acquire the trauma while intoxicated with alcohol [1–5]. Motor vehicle accidents, assaults, and falls are the major reasons for maxillary fractures [1, 3, 6, 7]. The percentage of maxillary fractures and the involvement of orbital bones secondary to motor vehicle accidents has significantly risen over the past several decades from 10 % in the 1950s to 50 % in the 1990s [8]. Furthermore, maxillary fractures affect the zygomatic bone in 80 % of patients [9]. The anterior visual pathway is affected to some extent in 90 % of patients, while severe damage such as globe rupture or optic neuropathy is observed in 12–20 % of cases [1, 10].

Finally, 30–40 % of patients have multiple traumas combined with brain injury and limb fractures [2, 6, 11–13].

7.2 Fracture Classification

The classification of non-gunshot maxillary fractures was proposed by French surgeon René Le Fort in 1901 [14]. Three main types of maxillary fractures have been described in experimental studies using cadaver skulls. The formation of a certain type of fracture depends on the degree, direction, and the point to which the vector force of the trauma is exerted.

Le Fort I fractures (also known as horizontal, floating, or Guérin's fractures) are formed when the vector force of the trauma moves downward and affects the maxillary alveolar process. The fracture line extends from the nasal septum toward the edges of the piriform aperture, runs posteriorly in the horizontal direction over the apex of the teeth above the level of the bottom of the maxillary sinus, crosses the zygomaticoalveolar crest, and passes through the tuber maxillae and the lower third of the pterygoid process of sphenoidal bone (Fig. 7.2a, b). Sometimes the fracture line stops near the sockets of the second or third molar teeth. It is accompanied by transverse fracture of the nasal septum. The floor of the nasal cavity and maxillary sinus is detached and their mucous membranes are inevitably damaged. This fracture type occurs in 14–24 % of patients [15, 16]; in 9 % of these cases, the fracture is unilateral and nondisplaced [17]. *Le Fort I fractures do not affect the orbit.*

Le Fort II (pyramidal) *fractures* are the most common type (55–64 %) of maxillary fractures. They result from a blow to the lower or mid-maxilla. Two variations are possible depending on the angle of trauma.

A *direct blow* results in a typical pyramidal fracture with or without injury to the hard palate. The fracture line crosses the nasofrontal suture and descends along the medial orbital wall (the lacrimal bone) and the orbital floor to reach the inferior orbital fissure where it turns forward. It crosses the infraorbital rim along the infraorbital foramen or in close proximity to it, extends along the anterior wall of the maxillary sinus above the zygomatic bone, and crosses the pterygomaxillary fissure to reach the pterygoid process of the sphenoidal bone. The nasal septum can be involved in bilateral fractures. The cribriform plate of the ethmoidal bone and the frontal sinus are damaged in more severe cases, and the pattern of the

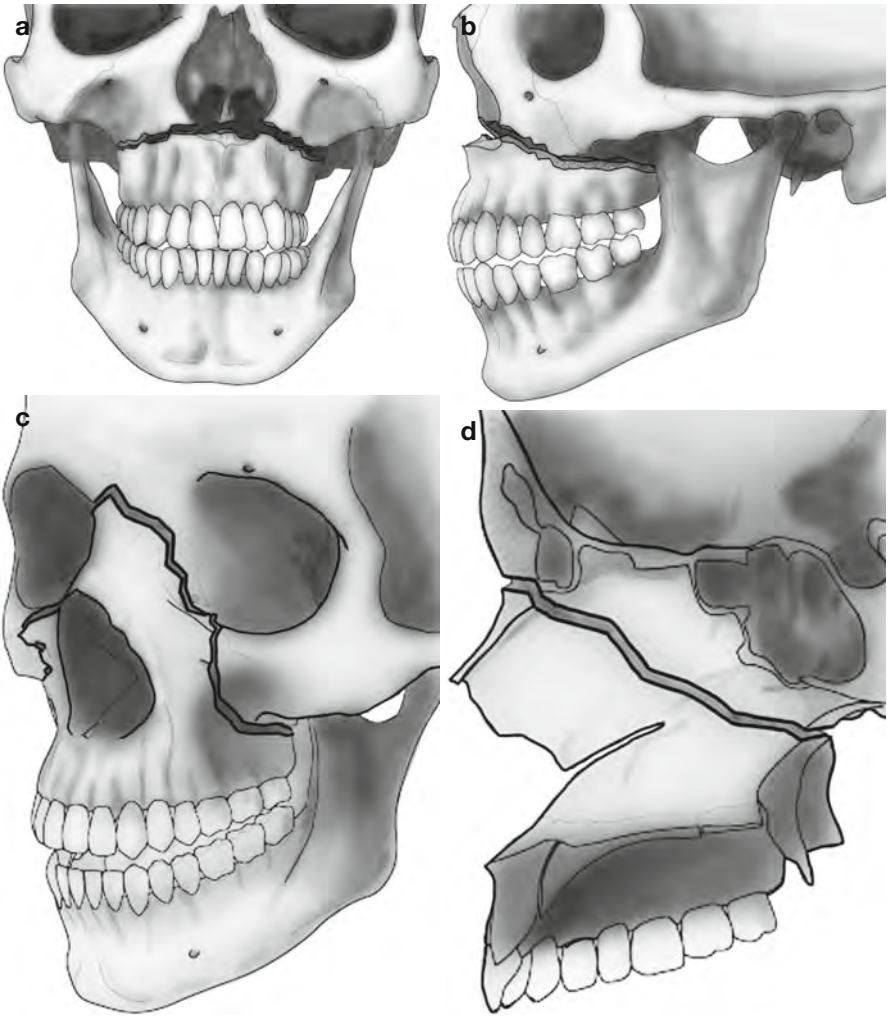

Fig. 7.2 Maxillary fractures: (**a**, **b**) Le Fort I fracture. (**c**, **d**) Le Fort II fracture. (**e**, **f**) Le Fort III fracture (see explanation in the text) (Materials from www.aofoundation.org were used for this illustration)

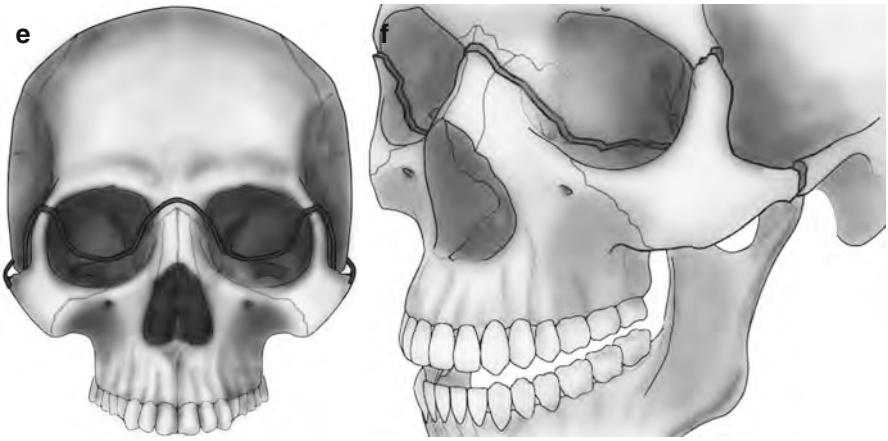

Fig. 7.2 (continued)

naso-orbito-ethmoidal fracture is formed (Fig. 7.2c, d). Thus, *the maxillary and nasal bones are detached from the zygomatic and neurocranial bones in Le Fort II fractures (complete detachment of the maxilla and nasal bones).*

A *side blow* gives rise to a unilateral zygomatico-orbital fracture combined with Le Fort I and/or II fractures [17].

Le Fort III fracture (also known as transverse fractures or craniofacial disjunction) results from a blow to the nasal dorsum or the upper third of the maxilla. The fracture line starts near the nasofrontal or frontomaxillary suture and extends posteriorly along the medial orbital wall through the lacrimal groove and the ethmoidal bone. Located posteriorly, the appreciably thick sphenoid bone usually (but not always) prevents the extension of the fracture line into the optic canal. Hence, the fracture turns toward the infraorbital fissure and extends posterolaterally through the lateral orbital wall, the frontozygomatic suture, and the zygomatic arch. It subsequently runs posteriorly and downward along the greater wing of the sphenoidal bone to reach the upper section of the pterygoid process and the body of the sphenoidal bone. In the nasal cavity, the fracture line runs through the base of the perpendicular plate of the ethmoidal bone and the vomer and between the pterygoid processes of the sphenoidal bone to its body (Fig. 7.2e, f). *Thus, the facial bones are detached from the neurocranial bones in this type of fracture.* Le Fort III fractures are observed in 8–12 % of patients with maxillary fractures [15, 16].

Although the practical significance of the Le Fort classification is obvious, one should bear in mind that it is not perfectly comprehensive. The reason is that the energy of the trauma sustained in motor vehicle accidents is much higher than that used by R. Le Fort in his experiments. In most cases, contemporary maxillary fractures are a combination of various Le Fort fractures (either I–II or II–III) (Fig. 7.6d) [18, 19]. The fracture lines frequently diverge from the trajectories described above to form unilateral (hemi-Le Fort) fractures, mixed fractures, and other atypical varieties of fractures [20]. Finally, extremely high-energy maxillary fractures can be combined with injuries to the mandible and cranial vault, thus forming panfacial fractures.

Furthermore, the Le Fort classification does not describe the two rather common types of maxillary injuries. The first type is a small isolated fracture that usually localizes near the alveolar process of the anterior wall of the maxillary sinus or the

nasomaxillary suture. This type of injury is caused by a strong local impact of an object (e.g., a hammer) (Fig. 7.6e, f). The rate of these fractures is as high as 9–10 % [16]. The second type comprises fractures resulting from an impact directed upward and damaging the horizontal "reinforcing ribs" of the face: the alveolar process, the infraorbital rim, and the zygomatic arc.

7.3 Clinical Presentation of Maxillary Fractures

7.3.1 Clinical Presentation of Le Fort I Fractures

The patient's general condition is usually fair. The main reasons for complaints are maxillary pain aggravated by biting and chewing, difficulty with biting off food using one's front teeth, numbness in teeth and gingival mucous membrane, abnormal occlusion, foreign body sensation in the throat, and blocked nasal breathing.

Examination reveals soft tissue swelling of the upper lip and cheek as well as flattened nasolabial folds. Elongation of the lower third of the face that is sometimes observed indicates that there is a significant downward displacement of the maxillary fragment.

Inspection of the oral cavity usually reveals a hematoma along the upper gingivobuccal fold. The soft palate seems to be elongated; the palatine uvula contacts the

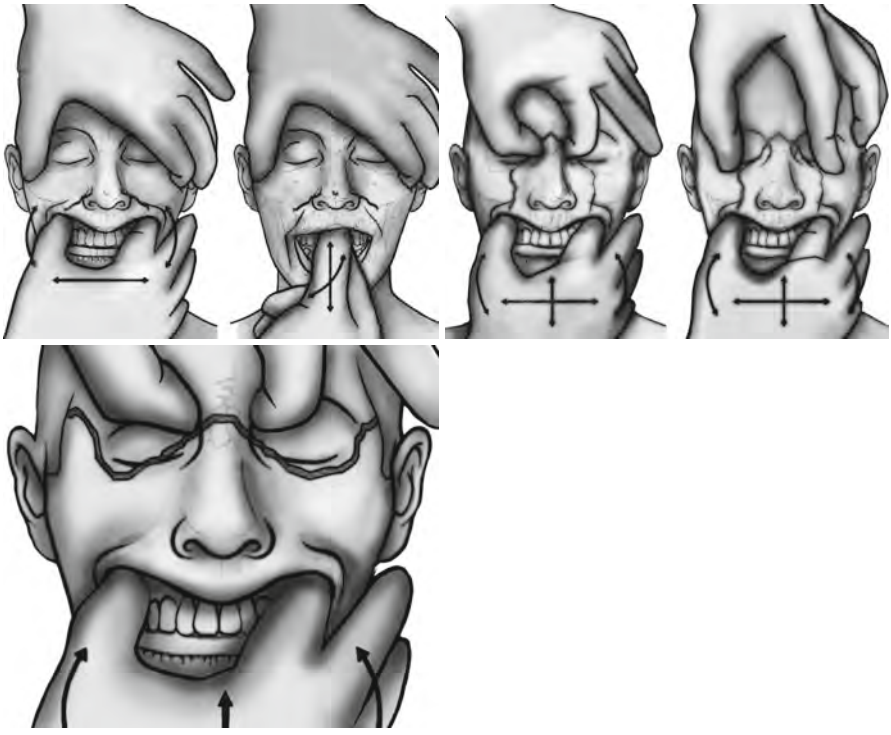

Fig. 7.3 Technique for palpation of the maxilla (see explanations in the text) (Materials from www.aofoundation.org were used for this illustration)

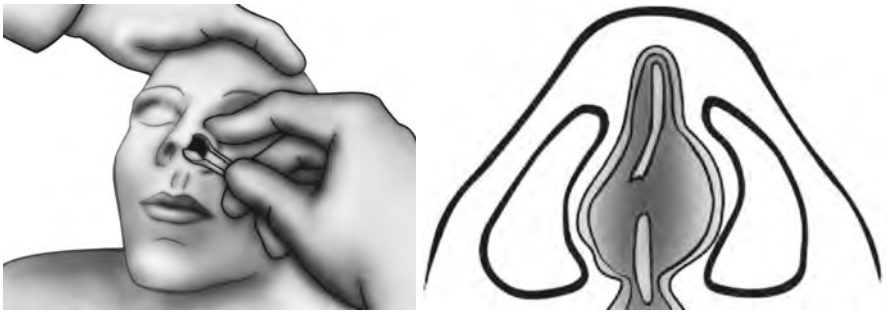

Fig. 7.4 Technique for examination of the nasal cavity (see explanations in the text) (Materials from www.aofoundation.org were used for this illustration)

posterior pharyngeal wall. Mobility of the alveolar process of the maxilla is revealed by palpation (Fig. 7.3).

There have been anecdotal reports of profuse hemorrhage from the nasal and oral cavities originating from the maxillary or the superior posterior alveolar artery [21–24].

7.3.2 Clinical Presentation of Le Fort II Fractures

Due to the concomitant brain injury, the overall patient status is from moderate to severe. In addition to the complaints listed above, conscious patients complain of numbness in the distribution of the infraorbital nerve; lack of olfactory ability or anosmia, indicating that the olfactory nerve fibers in cribriform plate orifices have been either disrupted or entrapped; and hemorrhage from the oral and nasal cavities (or lacrimal points if the nasolacrimal canal is damaged). Some patients also complain of diplopia.

Swelling of the periorbital tissues, the upper lip, and the nasal root causes typical alterations in facial configuration, which can change depending on patient's body position. The patient's face is flattened in the lying position as the fragment is displaced posteriorly. The face of a standing patient is elongated due to the downward displacement of the maxilla.

The clinical presentation also includes the "raccoon eyes" finding. The hematoma affects the lower eyelid, the medial canthus (spreading to the nasal root skin), and the medial portion of the upper eyelid. Chemosis and subconjunctival hemorrhage are rather frequent findings. Facial, cervical, and thoracic subcutaneous emphysema can also be observed.

The condition of the nasal and oral cavities is thoroughly assessed at the next stage.

Le Fort II fractures are characterized by mobile nasal bones. Examination of the nasal cavity allows one to identify fresh or old hematomas, nasal leak of CSF, and submucosal membrane hematoma of the nasal septum that is associated with a high risk of abscess and necrosis of the adjacent cartilage (Fig. 7.4b).

Examination of the oral cavity aims at evaluating the state and completeness of dental occlusion, stability of the hard palate, and condition of soft tissues. Intraoral palpation of the maxillary surface provides additional data on the condition of the

Fig. 7.5 Symptoms of maxillary fractures: (**a**, **b**) mesial occlusion, facial elongation, enophthalmos (indicated by deepening of the upper eyelid groove shown with an *arrow*), and flattening of the zygomatic area. (**c**) The frontal view of a patient. (**d**) Hemi-Le Fort I fracture (Reproduced with permission of professor G.A. Khatskevich and associate professor M.M. Solovyev)

nasomaxillary and zygomaticomaxillary buttresses and the anterior wall of the maxillary sinus.

Examination of the oral vestibule reveals mucous membrane hemorrhages near the molar and premolar teeth affecting the buccal mucosa. Open bite, caused by posterior and outward displacement of the maxilla and occlusion only at the level of molars, is quite typical (Fig. 7.5). Sensitivity of the gingival mucosa to pain is reduced near the incisors, canines, and premolars. As opposed to Le Fort I fracture, sensitivity of molar teeth and the corresponding gingival areas and the mucous membrane of the hard and soft palate is retained. Percussion of upper teeth results in cracked pot sound.

Protrusion of the lateral pharyngeal wall that is observed in some cases indicates that there is a hematoma in the peripharyngeal space.

The "bone step" finding is revealed by palpation of the infraorbital rim and the zygomaticoalveolar crest. This finding cannot be detected near the nasofrontal suture because of significant swelling of soft tissues. However, bony crepitus can be discovered here. To do so, the left index finger is placed on the infraorbital rim and the thumb is placed on the nasal root, while the maxilla is gently rocked in the anteroposterior direction with the right hand. Synchronous displacement of the bone fragment in both tested areas indicates that there is a fracture. When the supposed bone fragment is displaced up and down, the skin above the nasal root forms a fold or changes its color as its tension is altered (Fig. 7.3).

Pain is aggravated when pressing against the hooks of the pterygoid processes of the sphenoidal bone (Guérin's sign). The bone fragment displaced downward moves upward, thus reducing the length of the midface and nose.

The physical evaluation of the eyes and the orbit includes the following: integrity of the orbital rims and walls, visual acuity and pupillary responses, muscle balance, eyeball position in the orbit, and the intercanthal distance.

Orbital pathological conditions are very diverse and can include:

- Combination of symptoms typical of orbital floor fractures (vertical diplopia, eno- and hypoglobus, infraorbital neuropathy) [1, 25].
- Combination of findings typical of a naso-orbito-ethmoidal fracture caused by dislocation of the central fragment and telescopic posterior displacement of the broken nasal bones. Optic neuropathy and CSF leak caused by fracture of the perpendicular plane of ethmoidal bone are associated with the highest risk.

7.3.3 Clinical Presentation of Le Fort III Fractures

The serious condition of a patient is often aggravated by basilar skull fracture, brain injury, and traumatic shock [26].

Conscious patients complain of diplopia when being in a vertical position, swallowing difficulties, foreign body sensation in the throat, feeling of choking and nausea, malocclusion, and inability to open the mouth properly due to the pressure exerted by the coronoid process of the mandible on the displaced zygomatic bone.

Profound soft tissue swelling makes the patient's face moon shaped. While being flattened in a supine position, the face becomes elongated when the patient sits up, and the eyeballs are displaced downward, thus expanding the palpebral fissure and causing diplopia. During jaw closing, the eyeballs and the orbital floor are displaced upward.

It is usually difficult to evaluate the condition of facial bones by visual inspection because of the concomitant soft tissue swelling, ecchymosis, and continuous hemorrhage. Nevertheless, edema of periorbital tissues and facial flattening are indicative of extensive Le Fort III fracture.

The "bone step" sign and bony crepitus can hardly be detected by palpation of the tissues within the nasal root and the superior-outward edge of the orbit because of profound soft tissue swelling. Furthermore, the displaced fragments in patients with a high-energy fracture may seem immobile during palpation. Guérin's sign is also observed.

A CSF leak is easily disguised by often bleeding from the mouth, nose, and ears in this type of fracture [15]. Latent, intermittent CSF leak is identified by provocative tests including straining effort and compression of jugular veins, the test using double stains,[1] the handkerchief test,[2] and lumbar puncture (required to detect blood in CSF).

Ophthalmic symptoms and findings in Le Fort III fractures include the symptoms of all the fractures described in the previous chapters (inferomedial, NOE, and zygomatico-orbital ones). Severe enophthalmos and hypoglobus are observed in 90 % of cases.

There is a high risk of damaging the eyeball, the optic nerve, and structures in the superior orbital fissures (the oculomotor, trochlear, and abducent nerves), particularly in patients with the congenitally narrow superior orbital fissure. Reduced visual acuity is a sign of possible damage to the visual pathway. Other major factors also associated with high risk of injury to structures of the visual pathway are as follows: orbital floor fracture, comminuted facial fracture, diplopia, and amnesia. The acronym BAD ACT referring to blowout fracture, acuity, diplopia, amnesia, and comminuted trauma makes it easy to remember the high-risk factors of damage to the visual pathway [27].

Kiratli et al. [28] reported a case of luxation of the eyeball accompanied by rupture of the optic nerve and all extraocular muscles except for the medial rectus. Jellab et al. [29] reported two cases of eyeball displacement into the maxillary sinus. Tunçbilek and Işçi [30] reported midfacial trauma aggravated by traumatic enucleation.

The concomitant fracture of the petrous part of the temporal bone is accompanied by hearing impairment or loss, vestibular disorders, and facial nerve paralysis [31].

Hence, the *full-scale clinical presentation of classical Le Fort II and III fractures with profound fragment displacement* includes the following signs and symptoms:

- Severe pain when closing the jaw, open bite
- Facial elongation and flattening due to posterior and downward displacement of maxillary fragments
- Maxillary mobility
- Pain during palpation of the pterygoid process of the sphenoidal bone
- The “bone step” sign during palpation of the upper half of the lateral and mid-thirds of the infraorbital rim and the zygomaticoalveolar crest
- Orbital and facial emphysema
- Ocular dystopia and/or diplopia

[1] Nasal discharge is collected into a gauze napkin and divided into the zones: the central one is stained with blood; the yellowish rim around it indicates that CSF is also present.

[2] If the discharge from the nose is nasal secretion, a handkerchief moistened with it will stiffen after drying due to the high protein content. If it is CSF discharging from the nose, the handkerchief density will remain virtually unchanged after drying as protein content in CSF is much lower in this case.

7.4 Radiological Diagnosis

The usefulness of plain X-rays is limited because of the shielding effect of swollen soft tissues and overlapping projections of numerous midfacial bones [32]. Nevertheless, frontal and lateral radiography of the skull and targeted examination of the zygomatic bone are still used for screening.

X-rays of accessory nasal sinuses shed light on the condition of zygomatic arches, nasal bones, the anterior and lateral walls of the maxillary sinus, and the orbital rims. Radiography provides appreciably clear imaging of all maxillary buttresses. Lateral radiography of the skull allows one to evaluate the sagittal dimensions of the midface and the integrity of the anterior and posterior walls of the frontal sinus. Hemosinus, facial edema, and emphysema also have certain diagnostic values. Evaluation of the condition of the cervical spine makes it possible to rule out its injury (e.g., a whiplash fracture). However, CT scanning is an indispensable method for analyzing multiple fractures, evaluating the concomitant injuries to the cartilages and soft tissues, and revealing injuries involving the optic canal and remains the main diagnostic tool (Fig. 7.6).

Thin (2 mm) coronal and axial sections are used to obtain the desired data. The plan of actions for managing multiple maxillary fractures can be significantly facilitated by 3D reconstruction of the midface using the CAD/CAM method [18, 33, 34].

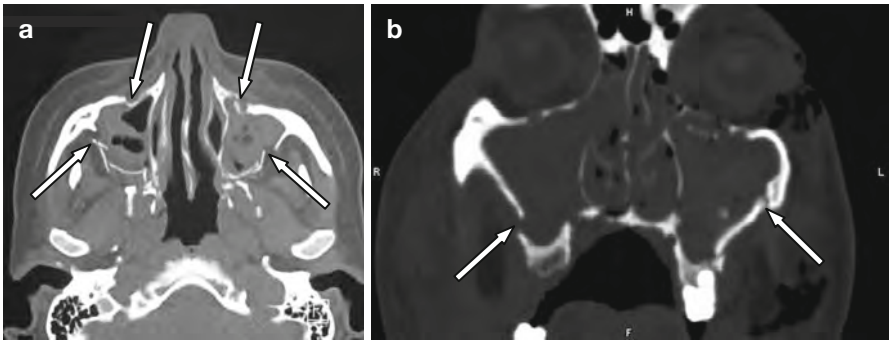

Fig. 7.6 Radiological signs of Le Fort II maxillary fractures: (**a**) a computed axial tomography (CAT) scan showing the fracture line of the anterior and lateral walls of the maxillary sinus (shown with *arrows*). (**b**) A coronal CT scan clearly visualizes the fracture of the lateral wall of the maxillary sinus. (**c**) 3D reconstruction of a pyramidal fracture (shown with *arrows*). (**d**) A combination of Le Fort I and II fractures (shown with *arrows*). (**e**, **f**) A blow-in fracture of the anterior wall of the maxillary sinus. (**g**) The fracture line of lateral orbital walls is seen in the CAT scan. (**h**, **i**) Sagittal (**h**) and coronal (**i**) CT scans clearly visualize the fracture of the body of the sphenoidal bone. (**j**) Axial CT scan of the fracture of greater wing of the sphenoidal bone. (**k**, **l**) Coronal (**k**) and sagittal (**l**) CT scans of the fracture of pterygoid process. (**e**–**l**) A blow-in fracture of the anterior wall of the maxillary sinus (shown with *arrows*) (Reproduced with permission of G.E. Trufanov and E.P. Burlachenko)

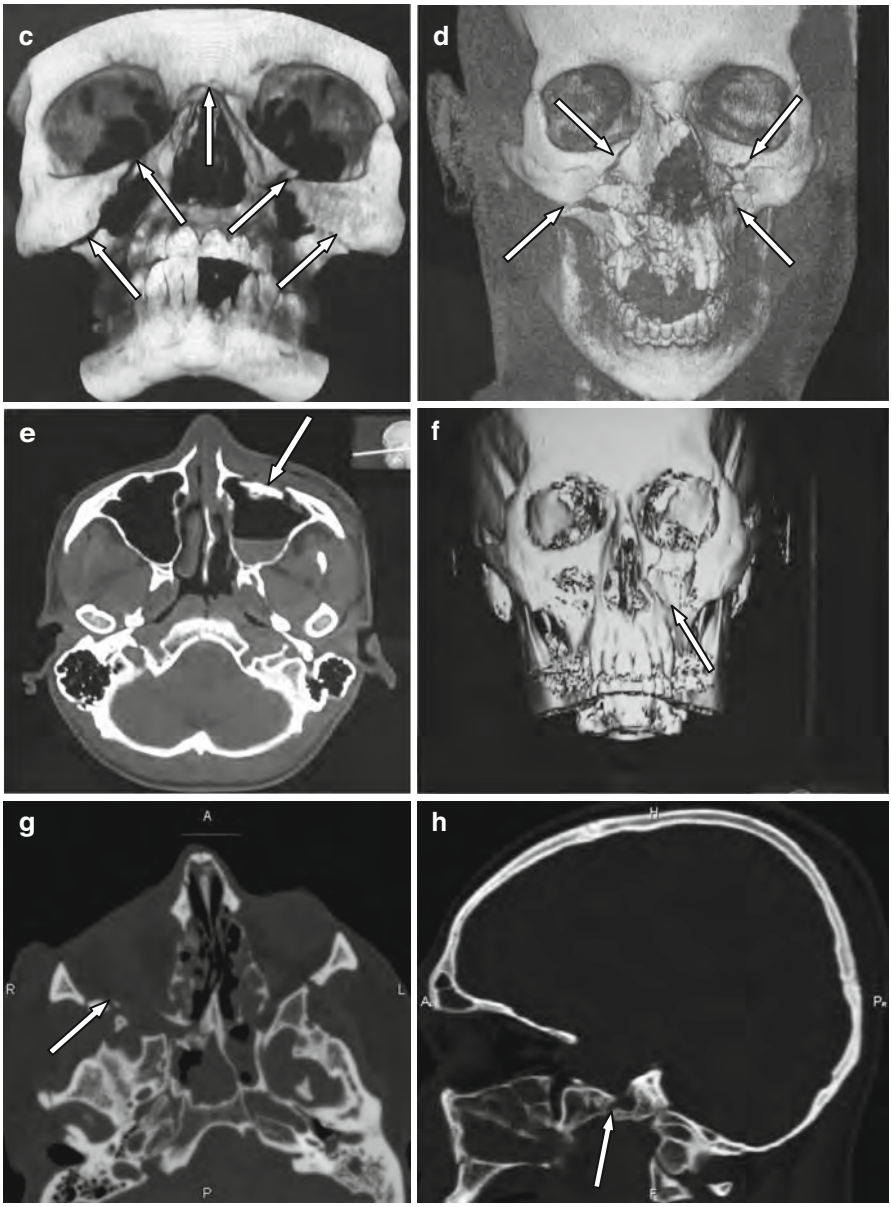

Fig. 7.6 (continued)

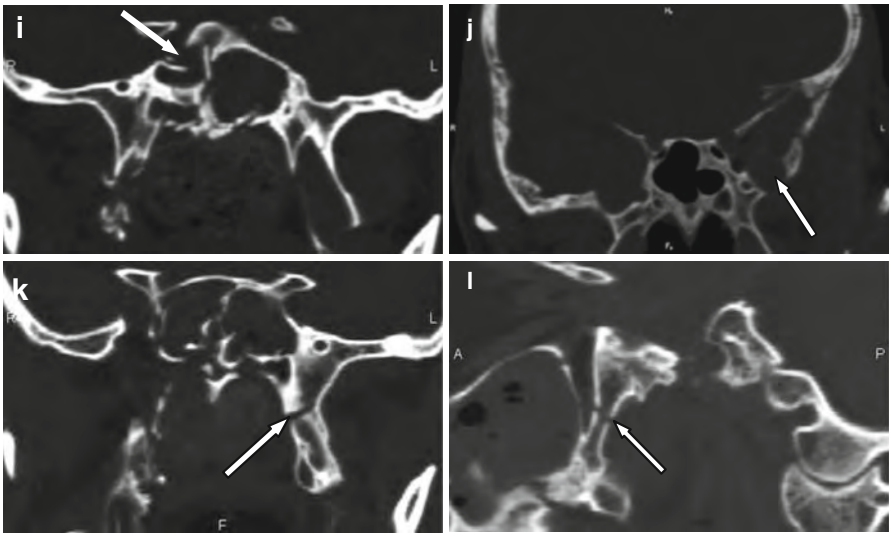

Fig. 7.6 (continued)

7.5 Treatment Principles in the Management of Maxillary Fractures

Because motor vehicle accidents are the main mechanism of maxillary fracture and are often accompanied by trauma to many other parts of the body, the conditions of the respiratory tract, cranium and spinal cord, thoracic and abdominal organs, and long bones are assessed first and foremost [35, 36].

7.5.1 Indications for Surgical Management

Treatment of maxillary fractures is started only after the vital functions are stabilized. However, it should be borne in mind that delayed management may well result in significantly poor postoperative functional and aesthetic outcomes [37, 38]. A multidisciplinary approach should be used to treat this cohort of patients [39].

Patients with local fractures that do not disturb the anatomy and functions of the maxilla (e.g., minor defects of the anterior wall of the maxillary sinus) do not require an operation.

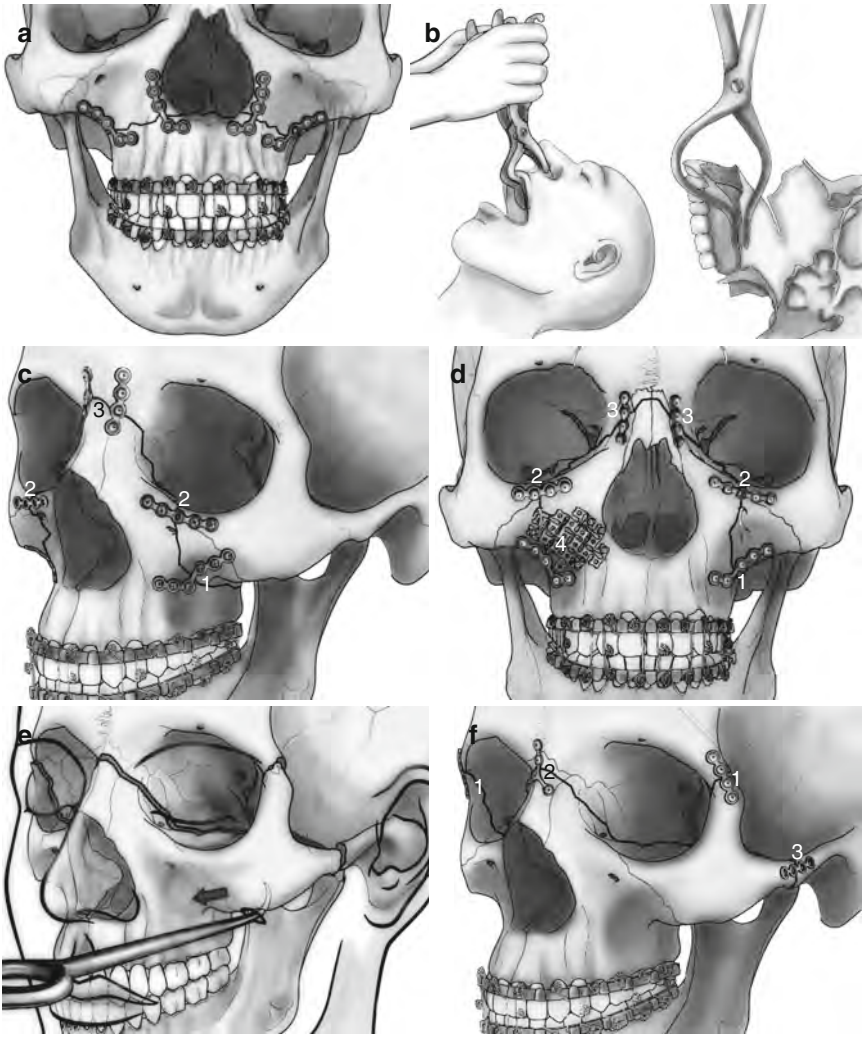

Fig. 7.7 Open reposition and rigid fixation of maxillary fractures: (**a**) Le Fort I fractures. (**b**) Reposition of a pyramidal fracture using Rowe forceps. (**c**, **d**) The order of placing titanium plates onto the edges of a Le Fort II fracture. (**e**) Reposition of the zygomatic bone in treatment of a Le Fort III fracture. (**f**) The order of placing titanium plates onto the edges of a Le Fort III fracture (Materials from www.aofoundation.org were used for this illustration)

Treatment of maxillary fractures aims both at reconstruction and repositioning of the maxilla with respect to the skull base and the mandible. Four out of seven vertical buttresses need to be reconstructed to attain this goal, namely, the anterior ones (two anterior medial, or the nasomaxillary ones, and two anterior lateral, or the zygomaticomaxillary ones) (Figs. 7.1 and 7.7). Clinical practice shows that there is

no need to reconstruct the two posterior (pterygomaxillary) and the medial (frontoethmoidal-vomerine) buttresses.

Thus, reconstruction of the anterior vertical buttresses allows the surgeons to restore the facial length and normal occlusion. However, full-fledged treatment of Le Fort I and III fractures requires the reconstruction of normal facial width, which cannot be attained without reconstructing the three horizontal (transverse) buttresses in the midface that connect the anterior medial and lateral vertical buttresses. Otherwise, flattening, widening, and asymmetry of the face, as well as crossbite, will persist.

The frontal arch, formed by massive supraorbital rims of the frontal bone, is the top reinforcing rib. The frontal buttress reinforces the superior, medial, and lateral walls of both orbits. Reconstruction of the frontal arch is the key step in treating Le Fort II and III comminuted orbital fractures.

The infraorbital buttress was referred to as the outer framework of the midface. It is formed by the zygomatic arch, the body of the zygomatic bone, and the appreciably strong infraorbital rim and is located below. The comminuted fractures of the infraorbital buttress accompany high-energy fractures rather frequently and require restoration. The original width and proper protrusion of the midface at the subcranial level cannot be achieved without restoring these fractures. Special focus should be placed on restoration of the original shape of the zygomatic arch, which actually is an almost linear structure in spite of its name [40].

Finally, the anterior portion of the massive U-shaped inferior transverse buttress, which lies in the plane of dental occlusion, is formed by the alveolar process, the bottom of the piriform aperture, and the strong anterior nasal spine. The posterior portion of the inferior buttress consists of the maxillary tuber, the hard palate, and the vomer.

The patient is transnasally intubated to perform interjaw wire fixation. The tube can also be inserted in the retromolar position or instead of missing teeth.

It is reasonable to start the surgery with interjaw wire fixation and then proceed to open reposition and rigid fixation of maxillary fragments [41]. The order of manipulations in patients with concomitant mandible fractures is as follows: osteosynthesis of the mandible, interjaw wire fixation, and reposition of the maxillary fracture. Care is needed when mobilizing fragments using the Rowe forceps to avoid damaging the nasolacrimal and infraorbital canals and the extraocular muscles. In patients with Le Fort III fractures, bone fragment reposition can be performed only after making sure that the fracture line does not intersect the optic canal.[3]

Once normal dental occlusion has been attained, final reposition and rigid fixation of the maxillary fragments with titanium miniplates are performed. Titanium constructs are now widely used in this segment of craniofacial surgery even though they have a number of drawbacks compared to wire fixation. The drawbacks include higher cost, longer surgery time due to the need to accurately shape and anchor the

[3] Shibuya et al. [42] reported that reposition of maxillofacial fractures in patients with traumatic optic neuropathy does not aggravate the condition of the optic nerve. However, the patients requiring optic nerve decompression and reposition of maxillary fractures have the worst visual prognosis compared to those needing conservative treatment or reposition of midfacial fractures only.

plate, and the necessity of higher surgical skill. The use of fragment wire fixation, suspension of the maxilla, and external osteosynthesis is currently limited because these methods do not give sufficient fragment immobilization and therefore lead to poor functional and aesthetic outcomes.

7.5.2 Management of Le Fort I Fractures

Interjaw wire fixation is enough to provide fixation of a nondisplaced Le Fort I fracture. Open reposition and rigid fixation with titanium miniplates are required to manage unstable fractures with fragment displacement.

Incision along the superior gingivobuccal fold according to Keen's procedure provides an adequate access to the nasomaxillary and zygomaticomaxillary buttresses, the piriform aperture, and the anterior nasal spine. To fix the classical Le Fort I fracture, it is enough to place one titanium miniplate on each side in the projection of the nasomaxillary or zygomaticomaxillary buttress (Fig. 7.7).

7.5.3 Management of Le Fort II Fractures

Adequate exposure of Le Fort II fractures is achieved through the intraoral and periorbital (transcutaneous or transconjunctival) incisions.

Surgical treatment of pyramidal fractures consists of repositioning and subsequent fixation of a bone fragment to the intact zygomatic bone. The first titanium miniplate secures the zygomaticomaxillary buttress. If the pyramidal fragment still remains unstable, additional plates are placed onto the infraorbital rim and the nasomaxillary reinforcing rib. The extensive defect of the anterior wall of the maxillary sinus is also reconstructed (Fig. 7.7b–d) [43]. If a Le Fort II fracture is accompanied by a significant injury to the orbital floor and the medial orbital wall, their reconstruction is the final stage of the surgery [44].

7.5.4 Management of Le Fort III Fractures

The surgery consists in fixation of maxillary fragments to the stable mandible from below and to the skull base from above. In patients with mandibular or basilar skull fractures, rigid fixation of these structures is performed first and foremost. It is followed by reposition of the maxilla and interjaw wire fixation.

Modifications of the trans-superciliary, glabellar, and bicoronal incisions are used along with the intraoral and periorbital ones to expose the fracture line; zygomatic arch defects are visualized by endoscopy [45].

The first titanium miniplates are placed onto the frontozygomatic sutures. Frontonasal buttresses and the zygomatic arch are the additional anchoring points (Fig. 7.7e, f). As few plates as possible should be used for fracture reduction. The final stage of the surgery includes suspension of midfacial soft tissues, staggered

layer surgical closure of the incisions, and application of a moderate compression bandage to minimize swelling.

7.5.5 Postoperative Treatment

Special attention should be paid to prevention of bleeding, vomiting, and airway obstruction during the first hours after surgery. After performing interjaw wire fixation, a surgeon needs to have tools ready to immediately cut the wire if nausea or vomiting occurs.

Taking into account the fact that the fracture zone communicates with the oral cavity and paranasal sinuses, 5–10-day preventive antibiotic therapy against Gram-positive and anaerobic bacteria is recommended.

The postoperative length of stay of patients without complications is 5–7 days. It is reasonable to perform follow-up examinations 2–4 and 3–8 weeks after surgery. A longer follow-up is required if late deformations are expected.

The main aim of the early postoperative period is to reliably immobilize bone fragments. Depending on patient's age and general condition, fracture length, degree of fragment displacement, and the surgical approach used, consolidation takes place after 4–8 weeks. Hence, maxillomandibular fixation is needed during this period and requires meticulous hygiene of the oral cavity in the morning, in the evening, and after each meal. Well-planned administration of nutrition via a feeding tube is extremely important; however, it has been found that even a well-balanced diet is accompanied by postoperative body weight loss of 4–6 kg [46].

Stability of the facial skeleton is assessed by palpating the maxillary teeth as a patient tenses and relaxes the muscles of mastication.

Minimal mobility is allowed, but noticeable displacement of teeth is indicative of improper healing. X-ray or CT scanning is recommended if inadequate bone fragment consolidation is suspected.

The interjaw wiring is removed once clinical and radiological signs of fracture healing and normal dental occlusion are achieved. The possible minimal vertical excursions of the maxilla are gradually eliminated on their own. The noticeable mobility of bone fragments indicates that either wiring was removed too early or one of the titanium miniplates has failed to perform its function.

7.5.6 Complications

Infection, abnormal occlusion, and facial asymmetry are the major complications of surgical management of maxillary fractures; the total rate of complications is 5–7.5 % [2, 16, 47].

Postoperative suppurative complications are mostly observed among patients with extensive infected soft tissue injuries, open fractures articulating with the oral and nasal cavities and the paranasal sinuses, and hemosinus.

Culture and sensitivity test and opening and drainage of the suppurative focus are recommended if broad-spectrum antibiotics show no effect. The torpid course of suppuration is associated with a high risk of osteomyelitis at anchoring points of titanium constructs, thus making it necessary to remove them.

Suppurative sinusitis can develop if the fracture line runs through the ostium of paranasal sinus because of impaired aeration.

Improper fusion of bone fragments resulting in malocclusion is caused either by inadequate intraoperative reposition of fragments or failure of the anchors during the postoperative period. These complications can be prevented by meticulously performed open reposition and rigid fixation of bone fragments with titanium miniplates.

The more serious problem is that patients do not adhere to the postoperative regimen (70 % of cases) [46]. Early chewing causes micromotions of bone fragments and leads to inconsistent callus formation. If improper fracture consolidation is detected in a timely manner, it is reasonable to attempt to normalize the occlusion by additional wire or elastic fixation. Titanium constructs should be removed and reapplied after meticulous reposition of bone fragments if no effect is observed. Delayed corrective interventions can be successful only by performing osteotomy along the fracture line followed by reposition and rigid fixation of its edges [48, 49].

Residual diplopia is another bothersome complication that is observed in 15 % of patients operated on for maxillary fractures [1, 50].

***

Theabsence of prospective studies among this cohort of patients makes it difficult to make any long-term prognosis for treatment outcomes in each particular case. The experience shows that reconstruction of isolated maxillary fractures usually facilitates the restoration of the anatomy and functions of the midface. Meanwhile, the outcomes of treating fractures that are a combination of Le Fort fractures and other facial injury types are often disappointing. Early one-stage exhaustive surgical management is the only way to attain good results in these situations. The use of navigation systems that allow one to control reposition and fixation of bone fragments shows promise, especially when the main facial landmarks have been dislocated or destroyed [51].

References

1. Amrith, S., Saw, S. M., Lim, T. C., & Lee, T. K. (2000). Ophthalmic involvement in craniofacial trauma. *Journal of Cranio-Maxillo-Facial Surgery, 28*(3), 140–147.
2. Brasileiro, B. F., & Passeri, L. A. (2006). Epidemiological analysis of maxillofacial fractures in Brazil: a 5-year prospective study. *Oral Surgery, Oral Medicine, Oral Pathology, Oral Radiology, and Endodontics, 102*(1), 28–34.
3. Cheema, S. A., & Amin, F. (2006). Incidence and causes of maxillofacial skeletal injuries at the Mayo Hospital in Lahore, Pakistan. *The British Journal of Oral & Maxillofacial Surgery, 44*(3), 232–234.

4. Eggensperger, N. M., Danz, J., Heinz, Z., & Iizuka, T. (2006). Occupational maxillofacial fractures: a 3-year survey in central Switzerland. *Journal of Oral and Maxillofacial Surgery, 64*(2), 270–276.
5. Lee, K. H., & Snape, L. (2008). Role of alcohol in maxillofacial fractures. *The New Zealand Medical Journal, 121*(1271), 15–23.
6. Eggensperger, N., Smolka, K., Scheidegger, B., et al. (2007). A 3-year survey of assault-related maxillofacial fractures in central Switzerland. *Journal of Cranio-Maxillo-Facial Surgery, 35*(3), 161–167.
7. Lee, K. H., Snape, L., Steenberg, L. J., & Worthington, J. (2007). Comparison between interpersonal violence and motor vehicle accidents in the aetiology of maxillofacial fractures. *ANZ Journal of Surgery, 77*(8), 695–698.
8. Friesenecker, J., Dammer, R., Moritz, M., & Niederdellmann, H. (1995). Long-term results after primary restoration of the orbital floor. *Journal of Cranio-Maxillo-Facial Surgery, 23*(1), 31–33.
9. Covington, D. S., Wainwright, D. J., Teichgraeber, J. F., & Parks, D. H. (1994). Changing patterns in the epidemiology and treatment of zygoma fractures: 10-year review. *The Journal of Trauma, 37*(2), 243–248.
10. al-Qurainy, I. A., Stassen, L. F., Dutton, G. N., et al. (1991). The characteristics of midfacial fractures and the association with ocular injury: a prospective study. *The British Journal of Oral & Maxillofacial Surgery, 29*(5), 291–301.
11. Zwahlen, R. A., Labler, L., Trentz, O., et al. (2007). Lateral impact in closed head injury: a substantially increased risk for diffuse axonal injury – a preliminary study. *Journal of Cranio-Maxillo-Facial Surgery, 35*(3), 142–146.
12. Mulligan, R. P., & Mahabir, R. C. (2010). The prevalence of cervical spine injury, head injury, or both with isolated and multiple craniomaxillofacial fractures. *Plastic and Reconstructive Surgery, 126*(5), 1647–1651.
13. Thorén, H., Snäll, J., Salo, J., et al. (2010). Occurrence and types of associated injuries in patients with fractures of the facial bones. *Journal of Oral and Maxillofacial Surgery, 68*(4), 805–810.
14. Le Fort, R. (1901). Etude experimental sur les fractures de la mechoire superieure. Parts I, II, III. *Revue de Chirurgie Paris, 23*, 201, 360, 470.
15. Lee, S. T. (1983). Management of severe maxillo-facial injuries. *Annals of the Academy of Medicine, Singapore, 12*(2 Suppl), 446–451.
16. Motamedi, M. H. (2003). An assessment of maxillofacial fractures: a 5-year study of 237 patients. *Journal of Oral and Maxillofacial Surgery, 61*(1), 61–64.
17. Manson, P. N., Markowitz, B., Mirvis, S., et al. (1990). Toward CT-based facial fracture treatment. *Plastic and Reconstructive Surgery, 85*(2), 202–212.
18. Chen, W. J., Yang, Y. J., Fang, Y. M., et al. (2006). Identification and classification in Le Fort type fractures by using 2D and 3D computed tomography. *Chinese Journal of Traumatology, 9*(1), 59–64.
19. Hopper, R. A., Salemy, S., & Sze, R. W. (2006). Diagnosis of midface fractures with CT: what the surgeon needs to know. *Radiographics, 26*(3), 783–793.
20. Salonen, E. M., Koivikko, M. P., & Koskinen, S. K. (2010). Violence-related facial trauma: analysis of multidetector computed tomography findings of 727 patients. *Dento Maxillo Facial Radiology, 39*(2), 107–112.
21. Chen, C. C., Jeng, S. F., Tsai, H. H., et al. (2007). Life-threatening bleeding of bilateral maxillary arteries in maxillofacial trauma: report of two cases. *The Journal of Trauma, 63*(4), 933–937.
22. Dean, N. R., Ledgard, J. P., & Katsaros, J. (2009). Massive hemorrhage in facial fracture patients: definition, incidence, and management. *Plastic and Reconstructive Surgery, 123*(2), 680–690.
23. Hwang, K., & Choi, H. G. (2009). Bleeding from posterior superior alveolar artery in Le Fort I fracture. *The Journal of Craniofacial Surgery, 20*(5), 1610–1612.

24. Singam, P., Thanabalan, J., & Mohammed, Z. (2011). Superselective embolisation for control of intractable epistaxis from maxillary artery injury. *Biomedical Imaging and Intervention Journal, 7*(1), e.3.
25. Siritongtaworn, P., Tongsawas, S., & Siltharm, S. (2001). Diplopia in facial fractures. *Journal of the Medical Association of Thailand, 84*(Suppl 2), 491–494.
26. Salonen, E. M., Koivikko, M. P., & Koskinen, S. K. (2007). Multidetector computed tomography imaging of facial trauma in accidental falls from heights. *Acta Radiologica, 48*(4), 449–455.
27. al-Qurainy, I. A., Titterington, D. M., Dutton, G. N., et al. (1991). Midfacial fractures and the eye: the development of a system for detecting patients at risk of eye injury. *The British Journal of Oral & Maxillofacial Surgery, 29*(6), 363–367.
28. Kiratli, H., Tumer, B., & Bilgic, S. (1999). Management of traumatic luxation of the globe. A case report. *Acta Ophthalmologica Scandinavica, 77*(3), 340–342.
29. Jellab, B., Baha, A. T., Moutaouakil, A., et al. (2008). Management of a severe cranio-orbito-facial trauma with a dislocation of the globe into the maxillary sinus. *Bulletin de la Société Belge d'Ophtalmologie, 309–310*, 37–41.
30. Tunçbilek, G., & Işçi, E. (2008). Traumatic avulsion of the globe: a very rare complication of maxillofacial trauma. *The Journal of Craniofacial Surgery, 19*(2), 313–315.
31. Bento, R. F., Salomone, R., Brito, R., et al. (2008). Partial lesions of the intratemporal segment of the facial nerve: graft versus partial reconstruction. *The Annals of Otology, Rhinology, and Laryngology, 117*(9), 665–669.
32. Avery, L. L., Susarla, S. M., & Novelline, R. A. (2011). Multidetector and three-dimensional CT evaluation of the patient with maxillofacial injury. *Radiologic Clinics of North America, 49*(1), 183–203.
33. Fan, X., Zhou, H., Lin, M., et al. (2007). Late reconstruction of the complex orbital fractures with computer-aided design and computer-aided manufacturing technique. *The Journal of Craniofacial Surgery, 18*(3), 665–673.
34. Kim, J. J., & Huoh, K. (2010). Maxillofacial (midface) fractures. *Neuroimaging Clinics of North America, 20*(4), 581–596.
35. Chen, J. W. (2008). Cervical spine injuries. *Oral and Maxillofacial Surgery Clinics of North America, 20*(3), 381–391.
36. Jamal, B. T., Diecidue, R., Qutub, A., & Cohen, M. (2009). The pattern of combined maxillofacial and cervical spine fractures. *Journal of Oral and Maxillofacial Surgery, 67*(3), 559–562.
37. Triana, R. J., & Shockley, W. W. (1998). Pediatric zygomatico-orbital complex fractures: the use of resorbable plating systems. A case report. *The Journal of Cranio-Maxillofacial Trauma, 4*(4), 32–36.
38. Cole, P., Kaufman, Y., & Hollier, L. (2009). Principles of facial trauma: orbital fracture management. *The Journal of Craniofacial Surgery, 20*(1), 101–104.
39. Holmes, S. (2009). Facial trauma – who should provide care? *The British Journal of Oral & Maxillofacial Surgery, 47*(3), 179–181.
40. Gruss, J. S., Van Wyck, L., Phillips, J. H., & Antonyshyn, O. (1990). The importance of the zygomatic arch in complex midfacial fracture repair and correction of posttraumatic orbitozygomatic deformities. *Plastic and Reconstructive Surgery, 85*(6), 878–890.
41. Pigadas, N., Whitley, S. P., Roberts, S. A., et al. (2008). A randomized controlled trial on cross-infection control in maxillofacial trauma surgery: a comparison of intermaxillary fixation techniques. *International Journal of Oral and Maxillofacial Surgery, 37*(8), 716–722.
42. Shibuya, T. Y., Feinberg, S. M., Mathog, R. H., et al. (2006). Visual risks of facial fracture repair in the setting of traumatic optic neuropathy. *Archives of Otolaryngology – Head & Neck Surgery, 132*(3), 258–264.
43. Ballon, A., Landes, C. A., Zeilhofer, H. F., et al. (2008). The importance of the primary reconstruction of the traumatized anterior maxillary sinus wall. *The Journal of Craniofacial Surgery, 19*(2), 505–509.

44. Ellis, E., & Reddy, L. (2004). Status of the internal orbit after reduction of zygomaticomaxillary complex fractures. *Journal of Oral and Maxillofacial Surgery, 62*(3), 275–283.
45. Schubert, W., & Jenabzadeh, K. (2009). Endoscopic approach to maxillofacial trauma. *The Journal of Craniofacial Surgery, 20*(1), 154–156.
46. Behbehani, F., Al-Aryan, H., Al-Attar, A., & Al-Hamad, N. (2006). Perceived effectiveness and side effects of intermaxillary fixation for diet control. *International Journal of Oral and Maxillofacial Surgery, 35*(7), 618–623.
47. Gomes, P. P., Passeri, L. A., & Barbosa, J. R. (2006). A 5-year retrospective study of zygomatico-orbital complex and zygomatic arch fractures in Sao Paulo State, Brazil. *Journal of Oral and Maxillofacial Surgery, 64*(1), 63–67.
48. Becking, A. G., Zijderveld, S. A., & Tuinzing, D. B. (2007). The surgical management of post-traumatic malocclusion. *Clinics in Plastic Surgery, 34*(3), 37–43.
49. Güler, N., Cabbar, F., & Duygu, G. (2009). Correction of malocclusion by anterolateral osteotomy in a traumatized maxilla. *Dental Traumatology, 25*(4), 447–450.
50. Iliff, N. T. (1991). The ophthalmic implications of the correction of late enophthalmos following severe midfacial trauma. *Transactions of the American Ophthalmological Society, 89*, 477–548.
51. Holmes, S., Goldner, S., Bridle, C., et al. (2006). Evaluation of complex craniomaxillofacial fractures by a new three-dimensional planning system. *The British Journal of Oral & Maxillofacial Surgery, 44*(5), 416–417.

Frontobasilar Fractures

8

Vadim P. Nikolaenko, Yury S. Astakhov,
Yury A. Shulev, and Sergei A. Karpischenko

Contents

8.1 Epidemiology of Frontobasilar Fractures 326
8.2 Classification of Frontobasilar Fractures 326
8.3 Fractures of Walls of the Frontal Sinus. 328
8.3.1 Classification of Fractures of Frontal Sinus Walls 329
8.3.2 Clinical Presentation of Fractures of Frontal Sinus Walls 332
8.3.3 Radiological Diagnosis 334
8.3.4 Treatment of Fractures of Frontal Sinus Walls 334
8.3.5 Complications of Fractures of Frontal Sinus Walls 338

V.P. Nikolaenko, MD, PhD, DSc (✉)
Department of Ophthalmology, Saint Petersburg State Hospital No. 2,
Saint-Petersburg, Russia

Department of Otolaryngology and Ophthalmology, Medical Faculty,
Saint-Petersburg State University, Saint-Petersburg, Russia
e-mail: dr.nikolaenko@mail.ru

Y.S. Astakhov, MD, PhD, DSc
Department of Ophthalmology, I.P. Pavlov First Saint Petersburg State Medical University,
Saint-Petersburg, Russia

City Ophthalmologic Center at Saint Petersburg State Hospital No. 2,
Saint-Petersburg, Russia
e-mail: astakhov73@mail.ru

Y.A. Shulev, MD, PhD
Department of Neurosurgery, I.I. Mechnikov North-West State Medical University,
Saint-Petersburg City Hospital No 2, Saint-Petersburg, Russia
e-mail: vlshamanin@gmail.com

S.A. Karpischenko, MD
ENT Department, First Pavlov State Medical University of Saint Petersburg,
Saint-Petersburg, Russia
e-mail: karpischenkos@mail.ru

© Springer-Verlag Berlin Heidelberg 2015

V.P. Nikolaenko, Y.S. Astakhov (eds.), *Orbital Fractures: A Physician's Manual*,
DOI 10.1007/978-3-662-46208-9_8

8.4 Orbital Roof Fractures 343
8.4.1 Epidemiology of Orbital Roof Fractures 344
8.4.2 Classification of Fractures 345
8.4.3 Clinical Presentation of Orbital Roof Fractures 345
8.4.4 Diagnosis 349
8.4.5 Treatment of Orbital Roof Fractures 349
8.4.6 Complications of Orbital Roof Fractures 350
8.5 Orbital Apex Fractures 352
8.5.1 Clinical Presentation of Orbital Apex Fractures 352
8.5.2 Radiological Diagnosis 355
8.5.3 Treatment of Orbital Apex Fractures 355
8.6 Local Orbital Roof Fractures 358
References 358

The frontobasilar region of the upper craniofacial skeleton is divided into two anatomical areas. The *frontal* area *F* is comprised of the anterior cranial vault. The *basilar* area *B* is comprised of the superior and lateral orbital walls, the orbital apex, and the ethmoidal labyrinth. The anterior cranial vault is twice as strong as the adjacent bone structures [1, 2].

The frontal region is then subdivided into the *central and two lateral zones*. The central zone is the projection of the frontal sinus and the inner third of the supraorbital region lying medial to the supraorbital neurovascular bundle. The two *lateral zones*, the fronto-temporo-orbital, consist of the outer two-thirds of the supraorbital region and the squama of the temporal bone (Fig. 8.1).

The basilar region is also subdivided into the *central* and two *lateral zones*. The superior NOE complex, cribriform plate of the ethmoid bone, and planum sphenoidale form the central zone, and two *lateral zones are comprised of* the superior and lateral orbital walls and the orbital apex.

8.1 Epidemiology of Frontobasilar Fractures

Injuries involving the frontobasilar region comprise 5–28 % of all facial fractures [3–6]. The main reasons include motor vehicle accidents (55 %) and falls (35 %) [5, 7, 8]. This variety of fracture occurs 95 % of the time in 30–40-year-old men.

These fractures are also associated with an extremely high (25–90 %) risk of damaging the eye [1, 3, 9, 10].

8.2 Classification of Frontobasilar Fractures

The classification of frontobasilar fractures proposed by Burstein et al. [2] relies on CT data and is based on the anatomical subdivision of the frontobasilar region (Table 8.1 and Figs. 8.1 and 8.2).

Thus, the 1F fracture combines fractures of frontal sinus walls and glabellar fractures, while the 2B fractures include fractures of the orbital roof and apex and local fractures of the orbital roof.

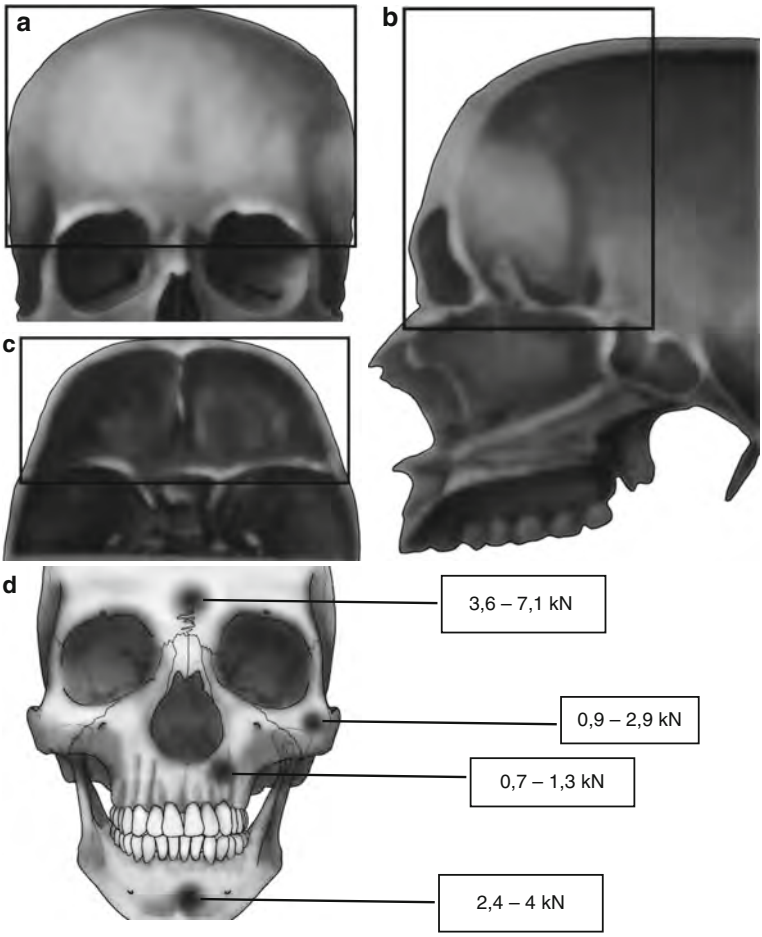

Fig. 8.1 The frontobasilar region: (**a**–**c**) Borders of the frontobasilar region. (**d**) Energy required for different facial segments to fracture [150]

Table 8.1 Classification of frontobasilar fractures

Injured area	Central zone (type 1)	Lateral zone (type 2)	Their combination (type 3)
Frontal (F)	*Frontal bone*	Lateral two-thirds of the supraorbital region	1F+2F
	Frontal sinuses; The medial third of the supraorbital region	Squama of the temporal bone	
Basilar (B)	*NOE complex* Cribriform plate Planum sphenoidale	Orbital roof Lateral orbital wall Orbital apex	1B+2B
Frontobasilar (FB)	1F+1B	2F+2B	Any combination of F and B fractures

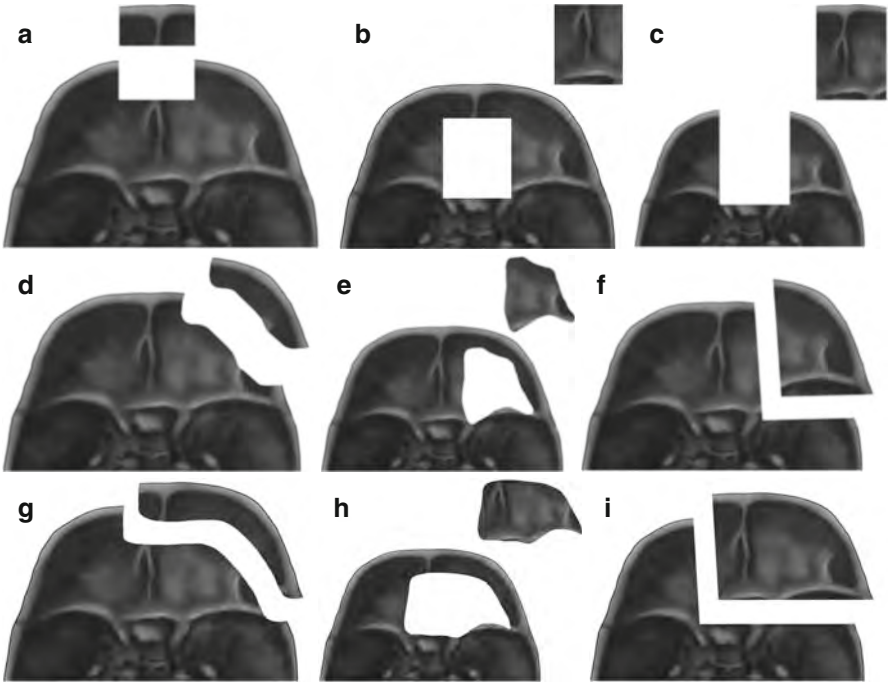

Fig. 8.2 Classification of frontobasilar fractures proposed by Burstein et al. [2]: *Type I (central) fractures* are confined to the superior naso-ethmoidal complex, the midfrontal bone, and the medial third of supraorbital rims medial to the supraorbital notch. The frontal sinus is bilaterally involved (**a**, 1F type; **b**, 1B type; **c**, 1F+1B type). *Type II (unilateral) fractures* involve the entire supraorbital rim and the upper portion of the lateral orbital wall. They spread to the squama of the temporal bone and the ipsilateral frontal bone and affect the frontal sinus. The NOE complex remains unaffected (**d**, 2F type; **e**, 2B type; **f**, 2F+2B type). *Type III (bilateral) fractures* include fractures of the upper portion of the naso-ethmoid complex, bilateral fractures of the supraorbital rim, fractures of the upper portion of the lateral orbital wall, and bilateral fractures of the frontal bone (**g**, 1F+2F type; **h**, 1B+2B type; **i**, F+B type)

The combined fracture (Type 3) is the most frequent variety.

Low- and medium-energy frontobasilar injuries are isolated in 40–50 % of patients. Midfacial fractures such as NOE fractures, fractures of the medial orbital wall and orbital floor, and Le Fort II maxillary fractures are involved in high-energy traumatic processes in the remaining cases [11–13].

8.3 Fractures of Walls of the Frontal Sinus

Fractures of walls of the frontal sinus comprise 5–15 % of all facial fractures. They are accompanied by severe head injury 50 % of the time and with other maxillofacial injuries 70–80 % of the time [5, 11, 13]. This variety of fractures is usually a component of multiple traumatic injuries and accounts for the relatively high (5 %) mortality rate among this cohort of patients [5, 8].

Both sinus walls are affected in 70 % of these injuries; the frontonasal duct is involved in ~10 % of patients [7]. Fracture of the posterior wall of the sinus is much more serious because of the higher risk of CSF leak and concomitant brain damage. While the incidence of open and closed fractures is virtually identical, the complication rate accompanying open fractures is three times higher than that for a closed fracture.

Fractures of frontal sinus walls in children typically affect the orbital roof. The NOE complex is involved in 30 % of patients, while nasal bones are affected in 60 % of cases [14]. The injury is accompanied by a higher (60–70 %) risk of CSF leak and intracranial damage, such as hemorrhage to the cranial parenchyma and cranial floor, and pneumocephalus compared to adults [7, 14, 15].

8.3.1 Classification of Fractures of Frontal Sinus Walls

The classification is based on three criteria: conditions of the anterior and posterior walls and the frontonasal duct [5, 7].

- Type 1: linear fractures of the anterior wall with minimal displacement of bone fragments or without any displacement.
- Type 2: comminuted or blow-in fractures of the anterior wall involving or not involving the frontonasal duct. Approximately 30 % of all injuries are type I and type II fractures [16].
- Type 3: comminuted fractures of both walls of the frontal sinus.
- Type 4: comminuted fractures of both walls with injury to the dura mater and CSF leak. Type 4 comprises almost 40 % of all the injuries [7].
- Type 5: the same with damage to soft tissues and/or bones (Fig. 8.3).

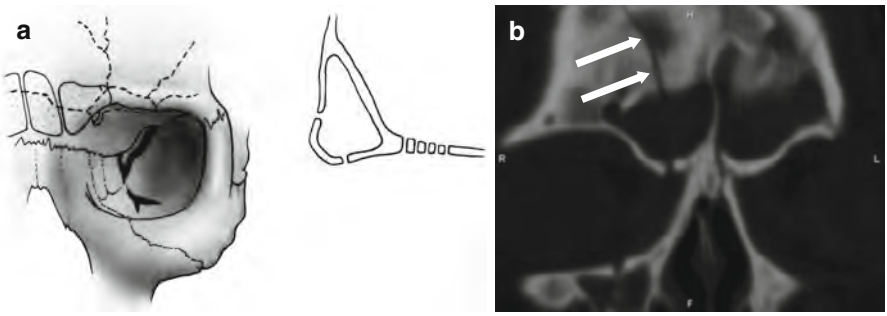

Fig. 8.3 Fractures of frontal sinus walls (frontal and lateral view): (**a**, **b**) A linear fracture of the anterior sinus wall with or without the minimal displacement of bone fragments (type I). The posterior wall and the cribriform plate were not affected (shown with *arrows*). (**c**, **d**) A comminuted fracture of the anterior wall, while the posterior wall and the cribriform plate were not affected (type 2). (**e**–**h**) A fracture of both sinus walls (type 3). The absence of a CSF leak is caused by the fracture of the posterior sinus wall without displacement of bone fragments (shown with *arrows*) (Cited from Bell et al. [5]; Montovani et al. [7]). (**i**, **j**) A comminuted fracture of both sinus walls with CSF leak (shown with *arrows*) through the damaged posterior wall and the cribriform plate (type 4). (**k**–**n**) A comminuted fracture of both sinus walls with CSF leak and the concomitant defect of soft tissues and bones (type 5) (shown with *arrows*) (citation from Bell et al. [5]; Montovani et al. [7]). (**o**, **p**) An isolated fracture of the posterior wall of the frontal sinus

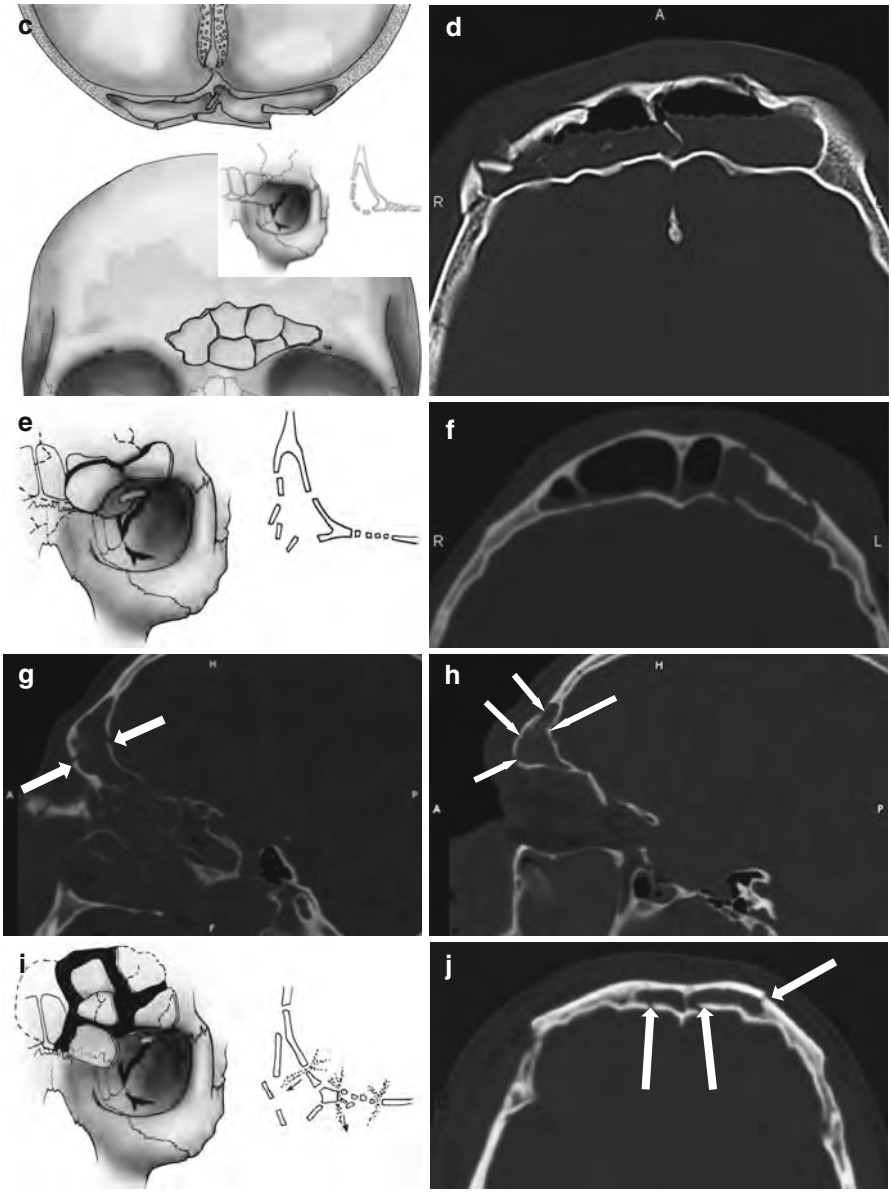

Fig. 8.3 (continued)

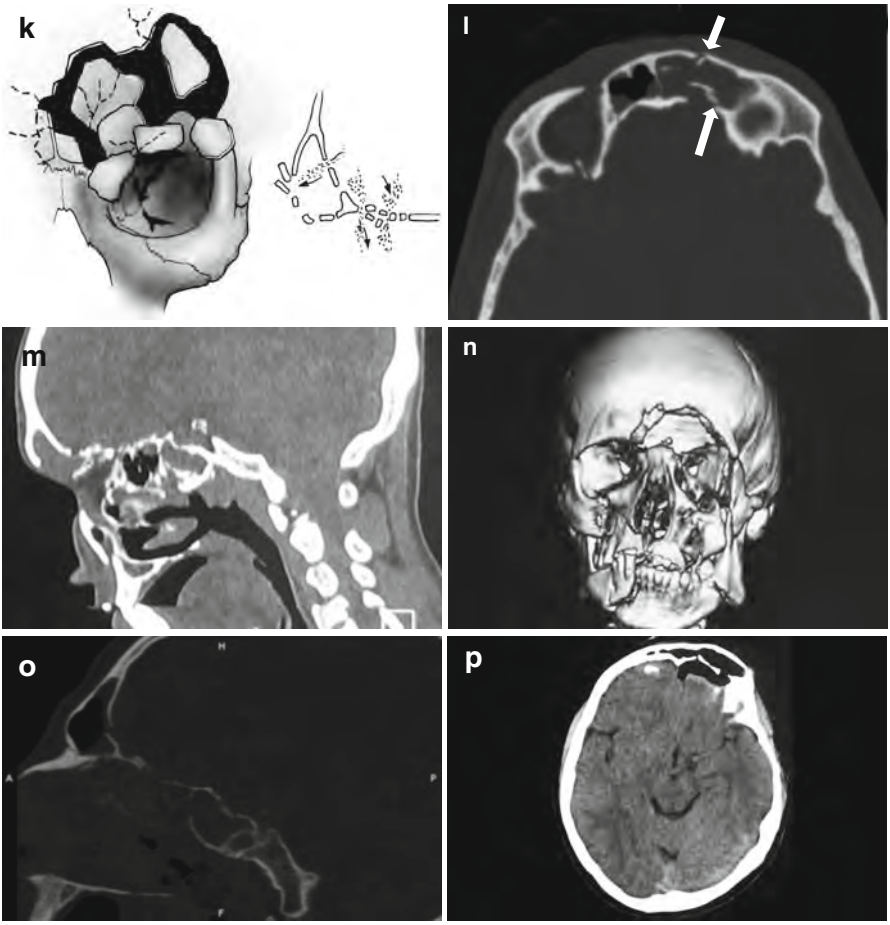

Fig. 8.3 (continued)

One should bear in mind that:

- There have been anecdotal reports of isolated fractures of the posterior wall of the frontal sinus (less than 1 % of cases) (Fig. 8.3o, p).
- Fractures of both sinus walls, as well as involvement of the NOE complex or the medial orbital rim into the fracture, explicitly indicate that the frontonasal duct is injured.
- The traumatic impact is sometimes confined to wavelike deformation of the anterior wall with the energy transmission to the frontonasal duct, thus affecting its function of aeration. The force may also be transmitted to the optic canal or the superior orbital fissure, resulting in the superior orbital fissure syndrome or the orbital apex syndrome.

8.3.2 Clinical Presentation of Fractures of Frontal Sinus Walls

Eighty-two percent of conscious patients complain of pain in the fracture area. Fifty percent of patients have skin defects in this area; 25 % of them have an obvious depression [17] (Fig. 8.4).

Approximately half of patients have neurological findings. These may be secondary to brain concussions or sub- and epidural hematomas requiring emergency drainage in 10 % of cases. The most severe fractures (2.5–13 % of all sinus injuries) are complicated by open head injury.

A third of the fractures of frontal sinus walls are accompanied by leakage of CSF from the skin wound [18]. Leak of CSF fluid from only one naris usually, but not always, indicates the side of rupture in the dura mater. A CSF leak is sometimes disguised as lacrimation[1] or massive edema of the upper eyelid that is disproportional to the "minimal" injury to the frontal region. This is a sign that CSF has accumulated in soft tissues [19–22]. One should bear in mind that a nasal CSF leak can be absent within the first several hours or even days after trauma because of occlusion of the rupture of the dura mater by swollen brain tissue or obstruction of the ethmoidal labyrinth by a blood clot [1, 11].

CT cisternography and/or nasal endoscopy with preliminary intrathecal (subarachnoidal) injection of fluorescein may be required in patients with the minimal trauma of the sinus to diagnose a CSF leak [11]. Concomitant anosmia indicates that the defect of the dura mater fused to the cribriform plate of the ethmoid bone is the most likely source of CSF leak. Injury to the posterior wall of the frontal sinus is a source of a leak much less often. The olfactory ability remains unaffected in this case.

In some cases the only sign of penetrating head trauma is pneumocephalus, an accumulation of air in the epidural, subdural, subarachnoidal, or intraventricular spaces. This is caused by a combination of a valve effect in the fracture area and the negative intracranial pressure in patients with a profound CSF leak. Unlike a CSF leak which involves the frontal sinus, the presence of pneumocephalus only

[1] Differential diagnosis of cerebrospinal and lacrimal fluids is performed by measuring the glucose level. Glucose content over 30 mg/ml is typical of CSF.

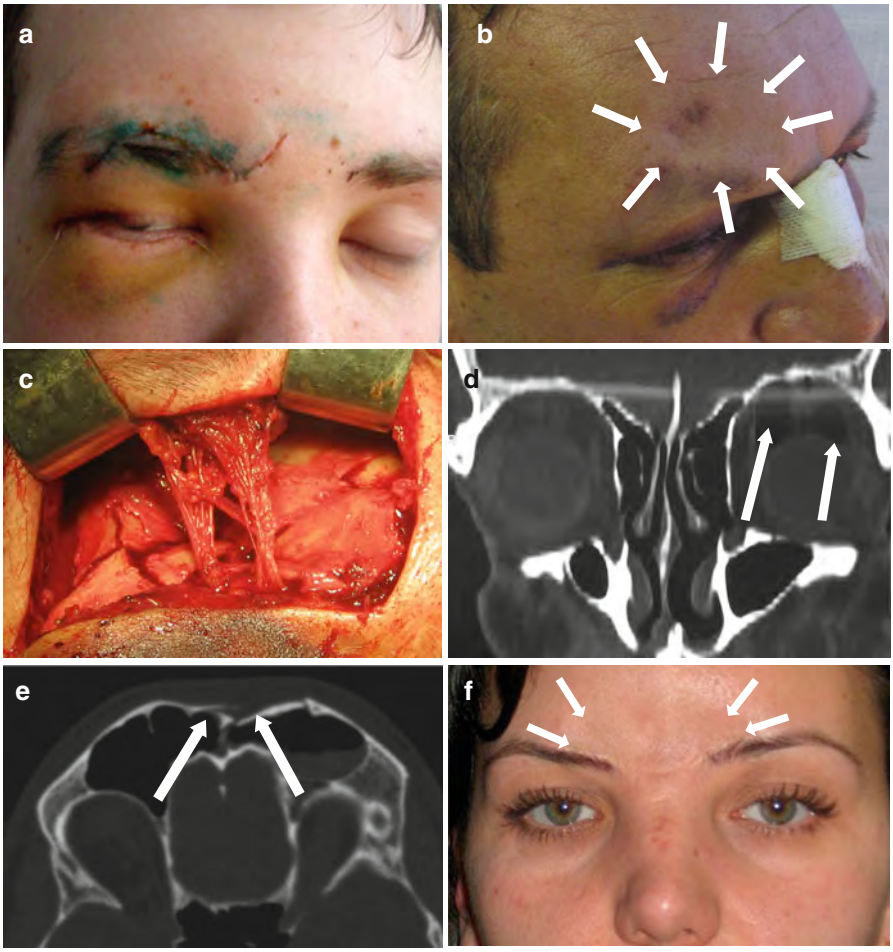

Fig. 8.4 Clinical presentation of the fracture of frontal sinus walls: (**a**) Skin wound in the frontal region. (**b**) Depression of the frontal region (shown with *arrows* along its perimeter). (**c**) A comminuted fracture of the anterior wall (type 3); the supraorbital neurovascular bundle is shown with an *arrow*. (**d**) Orbital emphysema (shown with *arrows*) causing hypoglobus and exophthalmos. (**e**) A CT scan of a glabellar (type 1F) fracture. (**f**) Appearance of a female patient with a glabellar defect; its borders are shown with *arrows* (Reproduced with permission of professor G.A. Khatskevich)

indicates that there is a cranial fracture but does not necessarily localize it to the frontal sinus [23]. Furthermore, presence of pneumocephalus does not predict a prolonged leak. Since there are no characteristic clinical signs, pneumocephalus is typically diagnosed radiologically [24].

At least of 25 % of injured patients have defects of the visual system, such as traumatic optic neuropathy, damage in the optic chiasm, oculomotor nerves palsy, or, less frequently, scleral rupture, intraocular hemorrhage, and retinal detachment.

Infrequently the fracture may spread along the floor of the anterior cranial fossa to the middle fossa and have corresponding symptoms, or it may spread along the

squama of the temporal bone, accompanied by dysfunction of the facial and vestibulocochlear nerves.

8.3.3 Radiological Diagnosis

Extensive injuries to frontal sinus walls, such as composite or comminuted fractures, are seen quite easily in panoramic X-ray images or seen in more detail in images in the nasomental view. Isolated injuries to the supraorbital rim are imaged as an angular stepwise deformity or fragmentation; shadowing of the sinus is usually seen because of blood in the sinus. Pneumocephalus is sometimes detected. A fracture of the posterior wall of the frontal sinus, in particular a linear one, may not be visible by plain radiological examination. Hence, plain radiological examination should be used for diagnosis only if computed tomography is unavailable[2]. Otherwise, CT scanning of all cranial segments should be carried out.

Coronal CT scanning allows the surgeon to diagnose an injury to the frontal recess. Axial CT scanning is indispensable for verifying fractures of sinus walls. Sagittal CT scanning is the most informative method as it shows all the signs of frontal sinus injury listed above (Fig. 8.3) [25]. Multiplanar reconstructions are used to assess the spatial arrangement of the dislocated bone fragments.

Neurological symptoms and ophthalmic disorders are indications for examining the brain, orbital apex, optic canals, and sella turcica [20, 26–28].

Since the treatment strategy largely depends on the extent of damage to the frontonasal duct, special attention should paid to such radiological signs as destruction of the anterior ethmoidal air cells and fracture of the floor of the frontal sinus when analyzing X-rays.

One should bear in mind that only 80 % of frontobasilar fractures can be visualized by neuroradiological methods.

8.3.4 Treatment of Fractures of Frontal Sinus Walls

There are four treatment regimens: (1) the watch-and-wait approach, (2) open reposition and rigid fixation of the fracture without obliteration/cranialization of the frontal sinus, (3) obliteration, and (4) cranialization. The choice for the specific treatment strategy relies on two criteria: damage to the nasofrontal duct and presence of persisting CSF leak.

Sixty percent of the time, the *watch-and-wait approach* is appropriate because there is minimal, less than 2 mm, displacement of bone fragments (type 1) [1, 5, 6, 29]. Surgical intervention is required in all other cases.

Surgical management of frontal sinus fractures aims at:

- Preventing immediate or early cerebral complications of trauma (CSF leak, meningitis)

[2] Planned intraoperative use of a non-magnified image as a template during sinus obliteration/cranialization is the only indication for X-ray imaging of the frontal sinus (Fig. 8.7c, d).

- Restoring nasofrontal duct patency
- Preventing late complications, such as osteomyelitis of the frontal bone, chronic frontal sinusitis, mucocele, mucopyocele, and cerebral abscess
- Restoration of the frontal contour

8.3.4.1 Optimal Surgery Time

Selecting the optimal surgery time can be rather challenging, especially if the frontobasilar fracture is accompanied by other head and midfacial injuries [7, 30]. In this situation, the brain injury can be life-threatening, and it is extremely important not to aggravate patient's condition by early surgical management of the facial injury. On the other hand, taking into account the suboptimal outcomes of secondary reconstructions, frontobasilar fractures should be operated on as early as possible. It is important to use the individualized and multidisciplinary approach in this case, which would allow the surgeons to choose the optimal strategy in each particular case [14, 15, 27].

First and foremost, neurosurgical management of penetrating head injuries with extensive tissue damage and exposure of the brain parenchyma or other life-threatening injuries or other injuries with a high risk of neurological deficit is performed [31, 32]. It is followed by surgical management of open-globe injury and optic nerve decompression. The frontal sinus walls are reconstructed only after 10–14 days.

Delayed surgical intervention is significantly complicated by the formation of granulation tissue between bone fragments, development of persistent soft tissue swelling, and high risk of infectious complications caused by inadequate drainage of the injured paranasal sinuses [1, 20].

Hence, a tendency toward early one-stage and thorough surgical management of frontobasilar and orbitofacial fractures has recently been described [31]. The practice has demonstrated that early one-stage surgeries are technically simpler, have less complications, and have better aesthetic outcomes. Contrary to what one might expect, if the multidisciplinary approach is used, the one-stage surgery may not aggravate preexisting neurological deficits [33, 35, 36].

8.3.4.2 The Main Surgical Stages

Approaches to the frontal sinus. The choice of an approach depends on fracture length and the degree of involvement of the brain and meninges in the traumatic process.

The approach through the wound, as well as the superciliary, trans-superciliary and superior supratarsal incisions, can be used in patients with an isolated fracture of the anterior wall not affecting the frontonasal duct and/or the medial orbital rim and having no concomitant craniofacial pathologies (type 2) (Fig. 8.5) [37–40]. The *endoscopic approach* can be used in some cases [41–45]. The *bicoronal or vertex approaches* that provide good overview of the entire frontobasilar region are recommended for all other types of frontal sinus fractures [15, 46].

Reposition of bone fragments without frontal sinus obliteration is recommended only for type 2 fractures that do not affect the frontonasal duct. This situation is found in about 25 % of patients [5]. The surgery in this case consists in mobilization and reposition of fragments of the anterior sinus wall followed by rigid fixation with low-profile titanium constructs and keeping the mucous membrane intact (Fig. 8.6)

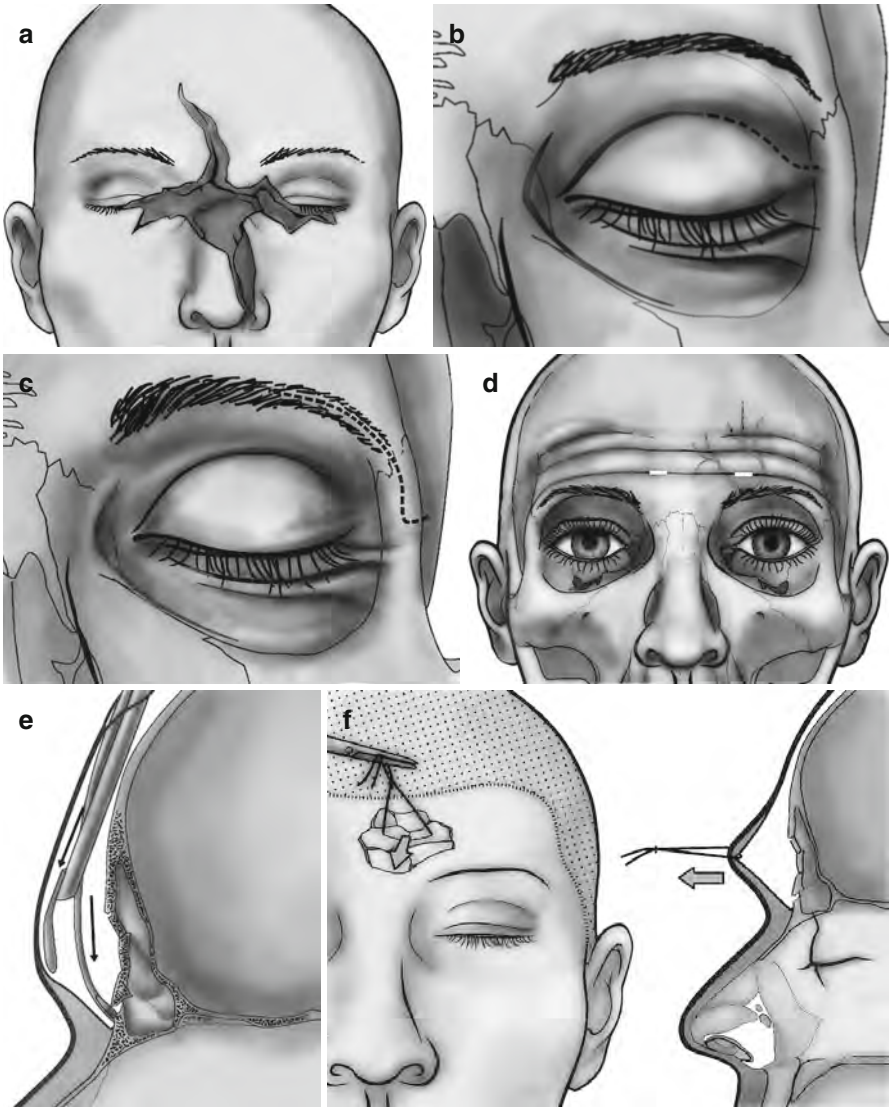

Fig. 8.5 Some approaches to the frontal sinus: (**a**) Approach through the existing wound. (**b**) The superior supratarsal approach. (**c**) The superciliary approach. (**d**) Skin incisions to place an endoscope and an elevator. (**e**) Visualization of the fracture area. (**f**) The suture running through all the layers of external soft tissues (skin, mimic muscles, and periosteum) that improves the view (Materials from www.aofoundation.org were used for this illustration)

[5, 47]. Closed repositioning proposed by Piccolino et al. [6] can be used in some cases of type 2 fractures. Using CT guidance, a percutaneous screw is placed into the center of a depressed bone fragment which is then used to lift the fragment to its original position (Fig. 8.6d).

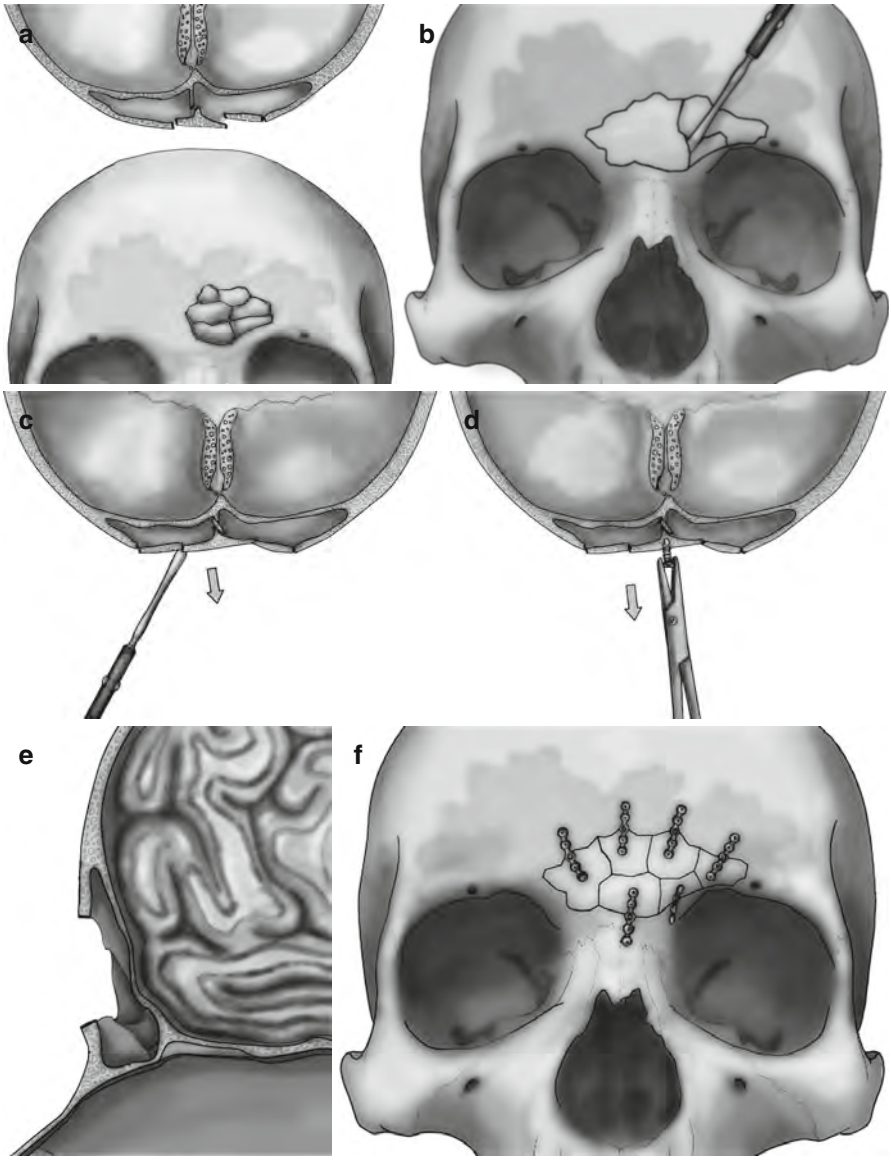

Fig. 8.6 Management of the isolated fracture of the anterior frontal sinus wall: (**a**) Schematic view of the fracture. (**b**, **c**) Bone fragment repositioning with an elevator. (**d**) Distraction of the bone fragment using a screw placed in it. (**e**) Intraoperative evaluation of the integrity of sinus floor. (**f**) Rigid fixation of bone fragments with low-profile titanium constructs (Materials from www.aofoundation.org were used for this illustration)

Type 2 fractures involving the NOE complex and/or the superomedial orbital rim explicitly indicate that the frontonasal duct has been injured and there is a need for *sinus obliteration* [31, 48]. Sinus obliteration is also required for all type

3–5 fractures. The borders of the frontal sinus should be meticulously identified at the first stage of the surgery using one of the four methods: (1) bayonet forceps can be used as a probe determining the borders of the sinus cavity; (2) direct observation can be done using endoscopic illumination; (3) an unmagnified X-ray of the frontal sinus can be displayed to compare with the surgical field; and (4) a tele-imaging system can also be utilized (Fig. 8.7a–e). The frontal wall is removed with a drill and bone-cutting forceps; the mucous membrane is then detached (Fig. 8.7f–i). The mucosa and periosteum are then removed from all the sinus segments using a drill and various burs (Fig. 8.7j, k) [49]. If a fracture of the posterior sinus wall is less than 25 % of its surface area, the fragments are removed and the dura mater is inspected to find any lesions that require meticulous closure (Fig. 8.7l–p).

The next stage is obliteration of the frontonasal duct to prevent contamination from the nasal cavity and to prevent the ingrowth of the mucous membrane of the ethmoidal labyrinth into the frontal sinus. The duct is broadened by carefully destructing the upper ethmoidal air cells, the mucosal remnants are removed, and the duct is tightly plugged with autologous fascia or muscle (Fig. 8.7q).

The sinus cavity can be left empty relying on subsequent osteogenesis. However, it is usually filled with autologous fascia or adipose tissue, pericranium, muscular tissue, milled bone, hydroxyapatite, or carbon (Fig. 8.7r) [50, 51].

Cranialization of the frontal sinus has been described especially for extensive fractures of its posterior wall occupying over 25 % of its surface area and accompanied by a CSF leak and/or soft tissue and bone defect (*types 4 and 5*). The procedure is identical to obliteration but there is one exception: the posterior wall of the frontal sinus is completely removed during the surgery for injuries to the brain [52]. Treatment of the rupture of the dura mater and obliteration of the frontonasal duct is then performed. The final stage of the surgery includes repositioning and rigid fixation of anterior wall fragments performed according to the conventional procedures.

The CAD/CAM method provides precise reconstruction of the supraorbital rim and the anterior sinus wall with a titanium implant that is a mirror reflection of the contralateral healthy orbit. It renders invaluable help in patients with unilateral comminuted fractures [53]. In much more severe bilateral injuries, meticulous repositioning of bone fragments, which can be put together both on the operating field and on an instrument tray holder, is the only practical solution [15]. Reconstruction of an extensive defect of the anterior wall is performed if needed.

The fragments of NOE and other orbital fractures are anchored to the stabilized frontal bone at the final stage of the surgery.

Postoperative treatment includes a 2-week antibiotic therapy [34].

8.3.5 Complications of Fractures of Frontal Sinus Walls

Complications of fractures of frontal sinus walls can be caused by either the injury itself or through the surgical manipulation. Traumatic complications include

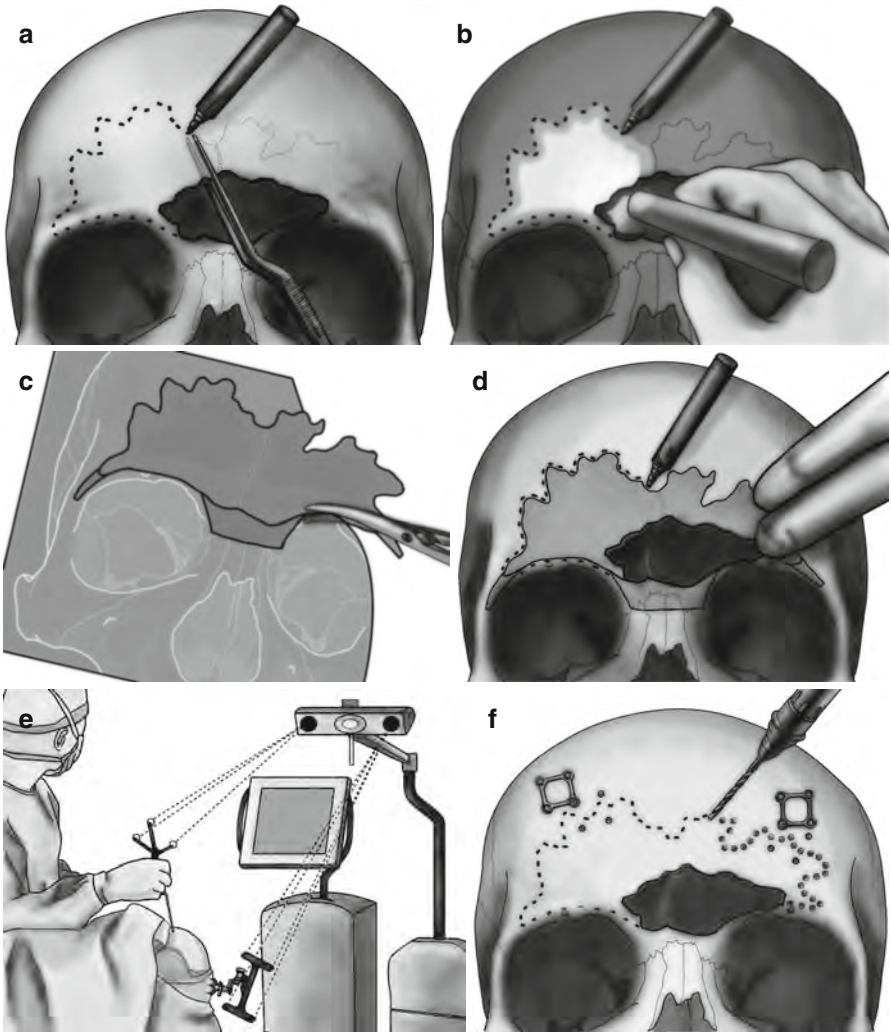

Fig. 8.7 Obliteration of the frontal sinus. Its borders are identified at the first stage: (**a**) Using a bayonet forceps. (**b**) Using endoscopic illumination. (**c**, **d**) Using a template made of the unmagnified X-ray of the frontal sinus. (**e**) Using a tele-imaging system. (**f**) Drilling multiple perforations in the bone. (**g**, **h**) The frontal sinus with anterior wall is removed. (**i**–**k**) The mucosa and inner osteal layer are meticulously removed. (**l**) Treatment of a small defect in the posterior sinus wall. (**m**, **n**) The posterior wall of the frontal sinus is removed. (**o**) Nibbling away at fracture edges with bone-cutting forceps; the brain parenchyma is protected by retractors. (**p**) Occlusion of the frontonasal duct. (**q**) Filling the sinus lumen with autologous fat tissue. (**r**) Rigid fixation of fragments of the anterior sinus walls with titanium constructs (Materials from www.aofoundation.org were used for this illustration)

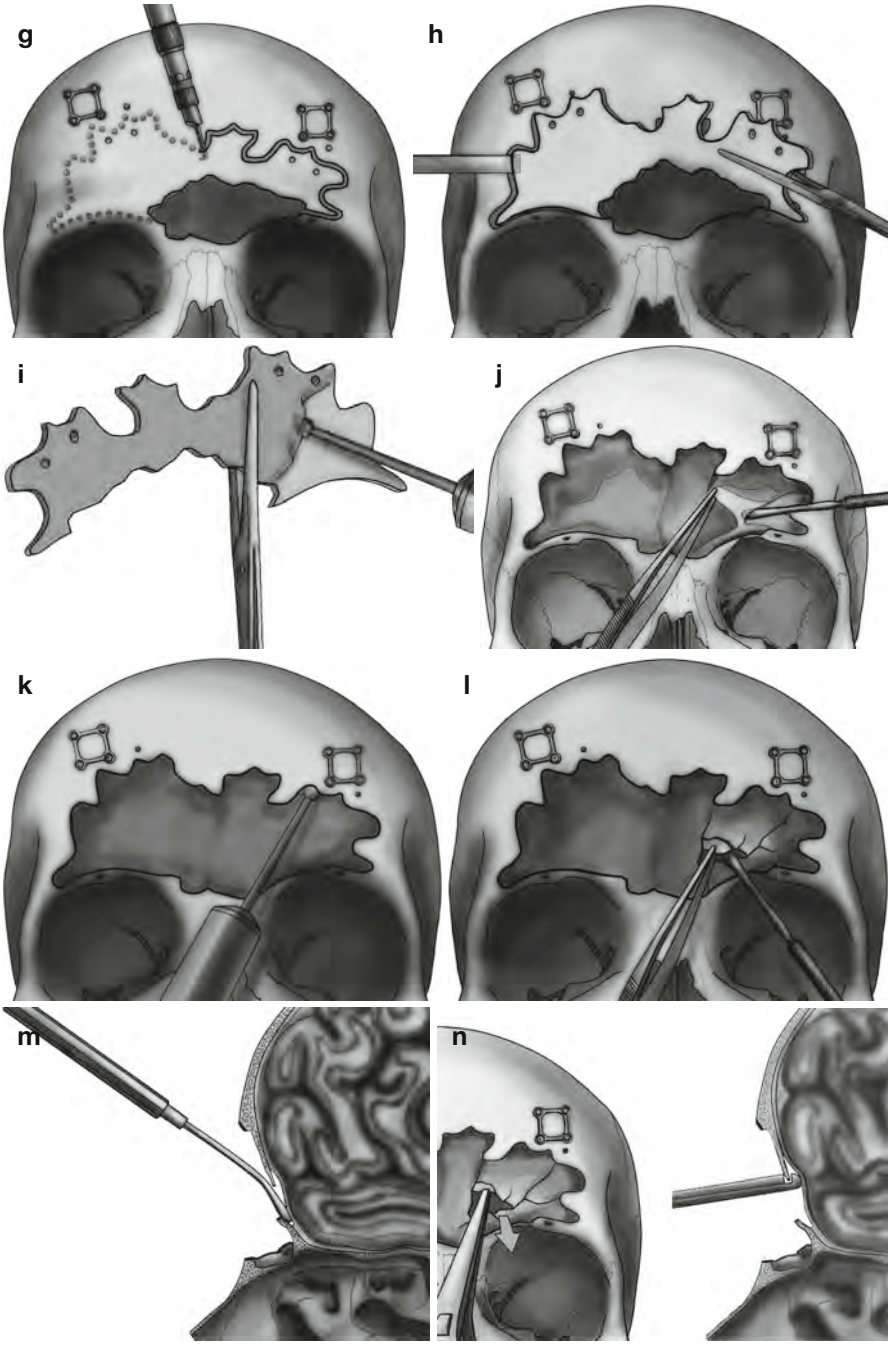

Fig. 8.7 (continued)

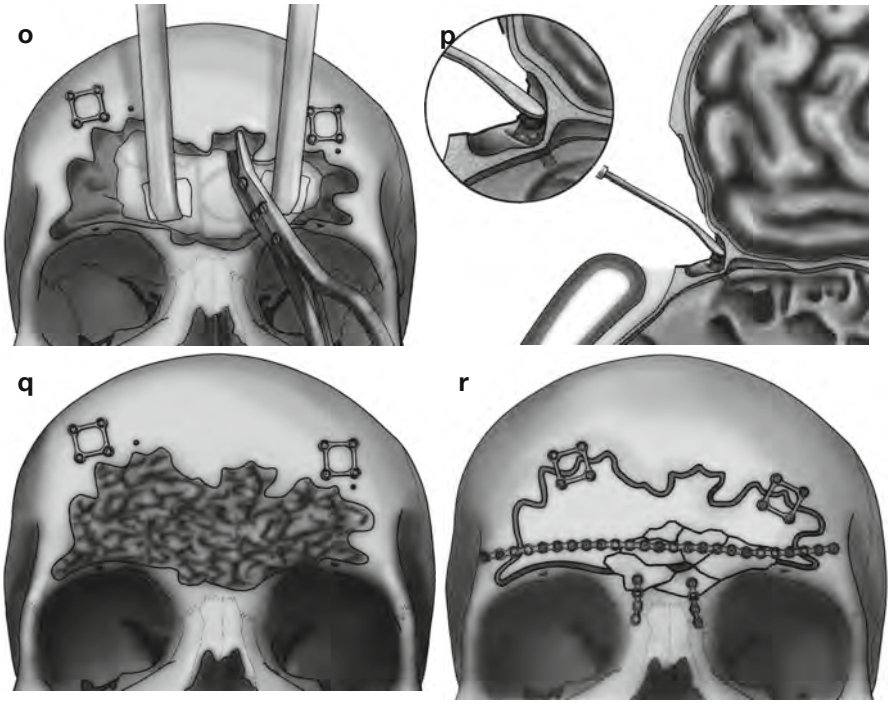

Fig. 8.7 (continued)

obstruction of the frontonasal duct, CSF leak, or infections secondary to a contaminated wound. Possible complications include an inappropriate surgical approach, untimely and/or inadequate range of surgical repair, the graft material used, etc. [8, 17]. According to the time of onset, the complications can be subdivided into early, within the first month after trauma, and late, after 1 month.

The reported incidence of early complications of a fracture of frontal sinus walls is 2.5–24 % [11, 13]. Such a high discrepancy between the figures is because some authors have reported transient complications such as hypoesthesia of the supraorbital nerve or transient vertical diplopia that spontaneously resolve within 2–3 weeks.

Since the injuries requiring surgical management are severe, the risk of complications among these patients is 15–16 % [5, 8].

CSF leak is the most serious early complication of a frontal sinus fracture. Fifty to eighty percent of the time, the leak can be managed by nonoperative measures which aim to reduce the risk of increased intracranial pressure (e.g., bed rest, elevated head position, prevention of coughing and sneezing, normalization of stool frequency and consistency, the use of diuretics and antibiotics, lumbar drainage placement) [54, 55].

The watch-and-wait approach is justified if the CT shows that the degree of displacement of fragments of the posterior sinus wall is less than its thickness. However, one should bear in mind that persistent CSF leak for 7 days increases the

risk of meningitis two- to eightfold, thus necessitating surgical intervention. Emergency surgery is needed when the degree of displacement of the posterior wall fragments is higher than its thickness, because a CSF leak does not stop spontaneously in these cases [11].

A CSF leak, and a persistent CSF leak in particular, is closely associated with infectious complications [1, 34] that affect both the frontal sinus (frontal sinusitis and mucopyocele) and the brain. The incidence of meningitis, encephalitis, or frontal lobe abscess can be up to 6 % [33, 56].

The symptoms of *meningitis* include high fever, pronounced headache caused by intracranial hypertension, nuchal rigidity, the Kernig's sign, and upper and lower Brudziński's sign, secondary to meningeal irritation and progressive depression of consciousness. If a patient has high intracranial pressure, during a lumbar puncture, CSF quickly trickles or there may be a sudden rush of fluid. Pleocytosis and high CSF protein level are reliable laboratory signs of meningitis. MRI reveals meningeal thickening.

Treatment of meningitis includes intravenous, or sometimes intrathecal, injection of antibiotics, depending on the results of CSF culture and the patient's symptoms.

Encephalitis occurs when the process affects the brain parenchyma and cranial nerves. Focal symptoms—cranial nerve III, IV, VI, and VII palsy, hemiparesis or generalized muscle weakness, and aphasia—are observed in addition to meningitis signs.

Infection spread through the area of the fracture of the posterior frontal sinus wall has a high risk of developing *subperiosteal (Pott's puffy tumor) and/or epidural abscess* located between the bone and the dura mater. The abscess manifests itself as infection-induced encephalopathy with headache, fever, and abnormal blood tests. The treatment includes immediate lavage of the frontal sinus and abscess drainage simultaneously with targeted antibiotic therapy.

The *subdural empyema* develops in the space between the dura mater and the arachnoid mater as infection is spread through the perforant veins in the frontal sinus. Because the clinical presentation is very nonspecific, the diagnosis is based on CT and MRI findings. These findings reveal the low-density crescent or ribbon-shaped contents along the cranial bones. Therapy is performed in accordance with the principles listed above. Subdural empyema has a rather serious prognosis, since the disease is characterized by a severe torpid course and high mortality rate.

Frontal lobe abscess is a rare but potentially fatal complication accompanied by nonspecific symptoms: persistent headache, fever, psychic changes, and hypersomnia. The concomitant brain injury makes the neurological signs not so evident; hence, CSF analysis and timely CT scanning and MRI are very important.

Intravenous contrast-enhanced CT scans show the abscess as a low-density round focus (0–30 HU) with an unclear contour surrounded by a narrow zone (capsule) intensively accumulating the contrast.

T1-weighted MRI images show a ring-shaped structure whose central portion generates a hypointense signal, while the peripheral portion generates a hyper- or an

isointense signal. T2-weighted MRI images show the abscess as a focus with a hyperintense signal in its central portion and a hypointense signal from its peripheral portion.

Treatment of a frontal lobe abscess at early stages is confined to the timely parenteral administration of antibiotics that can easily penetrate through the blood–brain barrier and selection of the appropriate antibiotic based on the CSF culture results. The third- and fourth-generation cephalosporins, carbapenems (ceftriaxone, cefotaxime, cefepime, meropenem), and vancomycin are typically used.

Surgical management of an abscess with a dense capsule is indicated in addition to medical treatment.

The treatment regimen should be continually monitored by evaluating clinical signs, laboratory test results, and CT and MRI findings. The duration of treatment often ranges from 3 to 9 months. The osteoplastic surgery is postponed until the patient fully recovers. The prognosis depends on early diagnosis and timely onset of treatment.

Late complications of mucocele and/or mucopyocele result after fractures located medial to the supraorbital notch affecting the NOE complex lead to obstruction of the frontonasal duct. Although they are rare, they progress very slowly and are accompanied by few symptoms. These complications are very severe as they damage the orbital walls, sinuses, and the skull [11, 57]. Treatment includes complete excision of pathological tissues and reconstruction of bone defects.

Complications caused by the surgical approach. Incisions along the lower edge of the eyebrow extending medially are associated with a high risk of rough scar formation.

An incorrect coronal incision is complicated by transection of the frontal branches of the facial nerve and devascularization of the temporal fat pad. This may result in an aesthetically unappealing depression in this region. Finally, even with a perfectly performed coronal approach, alopecia may also lead to a poor aesthetic appearance.

The *outcomes of fronto-orbital fractures* depend on the degree of brain damage and cerebral complications [31].

8.4 Orbital Roof Fractures

Second only to the lateral wall, the orbital roof is the strongest orbital wall. It is formed by the orbital lamina of the frontal bone and the lesser wing of the sphenoid[3] [58]. The additional factors reinforcing the orbital roof include its arc-shaped profile, the dura mater that is significantly thick and tightly fused with the bone, and the cerebrospinal fluid and the medullary substance counteracting the intraorbital pressure that increases in the moment of trauma [59]. The frontal sinus also plays a crucial role in the clinical presentation and treatment strategy of orbital roof fractures.

[3] A 57–157 kg/cm^2 effort is needed to facture the frontal bone.

8.4.1 Epidemiology of Orbital Roof Fractures

Orbital roof fractures are the least common orbital fractures [60]. A meta-analysis of the English-language literature published from 1970 to 2000 revealed that orbital roof fractures are observed in 1–9 % of all facial traumas but 60–93 % of other craniofacial injuries [54, 55, 61, 62]. A typical adult patient is a 30-year-old man (89–93 %) who has experienced a high-energy blow and has multiple concomitant injuries to other organs and systems (57–77 %) [63], including fractures of long bones (26–30 %) and spine (12 %), and non-penetrating injuries to the thoracic, abdominal, and pelvic organs. The high mortality rate of 12 % is attributable to these accompanying injuries [54, 55].

The major causes of trauma include motor vehicle accidents, falls, blows to the face with heavy objects, or penetrating orbital injuries [63].

An almost equal sex distribution is observed in the pediatric population. In 53–93 % of patients, the orbital roof fracture is a component of a frontobasilar fracture without or with an insignificant displacement of bone fragments and accompanied by multiple other trauma sites. Bilateral fractures are observed in 5–10 % of cases [54, 64]. The pediatric traumas are caused by falls and motor vehicle accidents in half and third of cases, respectively [54].

Orbital roof fractures, both as an independent entity and as a component of a more extensive craniofacial trauma, typically occur in young children, which is due to the specific features of their skull anatomy [65].

The anthropometric parameters of a newborn's head are a balance between the size of the maternal passages, the disproportionately large brain, and a comparatively small face. The ratio between the face and skull size is 1:8; hence, fractures of facial bones in infants are tenfold less frequent than in adults (0.6–1.2 % and 10 %, respectively) [66, 67]. On the contrary, the protruding orbital roof is injured much more frequently compared to adults because a newborn's skull does not reach 80 % of its final dimension until the age of 2 and does not reach its final size until the age of 7. The situation is worsened by physiological hypoplasia of the frontal sinus that does not have the ability to dampen blows.

As opposed to the skull, the facial skeleton continues to grow during the second decade of one's life. The "face/skull" ratio eventually decreases to 1:2, thus increasing the incidence rate of fractures of facial bones, including the inferior orbital wall. Furthermore, pneumatization of the frontal sinus reduces the incidence rate of orbital roof fractures [68].

As a result, the orbital roof fractures, both isolated and combined with injuries to the other wall, in 3–7-year-old children comprise 60 % of all orbital injuries, while the orbital floor fractures comprise less than 25 % of fractures. Six- to eight-year-old children have an equal risk of fracturing the orbital floor and roof. In 12-year-old children, the distribution of the different types of orbital fractures does not differ from the adult population, since growth of facial bones and pneumatization of paranasal sinuses makes inferomedial fractures the most common type [65, 68, 69].

8.4.2 Classification of Fractures

Messinger et al. [54] used the CT findings to subdivide orbital roof fractures into three types:

1. *Nondisplaced fractures* (Fig. 8.8a–e) comprise 40 % of all fractures [55].
2. Isolated *blow-out* fractures with one or several bone fragments displaced upward, into the frontal cranial fossa, along with the orbital adipose tissue. The dura mater and medullary substance can be either unaffected or affected (Fig. 8.8f–h) [70–72]. The bone fragments may also be displaced into the large frontal sinus, which illustrates the dampening effect of the sinus in such injuries [54, 73]. The large expanse of the frontal sinus contributes to an anatomically weak orbital roof [74]. A blow-out fracture of the orbital roof is caused by a sudden and abrupt increase in intraorbital pressure or, less frequently, by a penetrating orbital injury.
3. Isolated *blow-in* fractures can occur with one or several bone fragments displaced downward into the orbit, either with or without periosteal damage. The bone fragments in this type of fracture may be forced into the orbital adipose tissue (Fig. 8.8i–k). This type of fracture results from a high-energy impact to the supraorbital region of the frontal bone followed by deformation and fracture of the thin orbital roof [26, 59, 75]. A more unusual mechanism of a blow-in fracture is a remote cranial injury that transmits increased intracranial pressure to the orbital roof with a resulting fracture [76]. Isolated blow-in fractures occur more often than the blow-out types in the adult population and are typically accompanied by brain injury [77].

Furthermore, each of these fracture varieties may involve the supraorbital rim.

Isolated supraorbital rim fractures are extremely rare (Fig. 8.9). A literature search found only one report of a supraorbital rim fracture with a bone fragment displaced under the scalp as a consequence of a motor vehicle accident [78]. The fracture line usually spreads from the orbital rim to the orbital roof or the squamous part of the frontal bone. This injury pattern is typical of patients with undeveloped frontal sinuses [54].

8.4.3 Clinical Presentation of Orbital Roof Fractures

In addition to massive swelling of the eyelids and ecchymosis, the clinical presentation of a typical orbital roof fracture includes several signs and symptoms.

These include a subperiosteal hematoma, with a bone fragment, or a leptomeningeal cyst in the upper orbital area [77, 79–81]. Hypoglobus is observed in a third of patients and indicates that the orbital roof fracture has an anterior localization and is a blow-in type (Fig. 8.10). Proptosis is typical of a posterior blow-in fracture and is found in 60–65 % of patients [54].

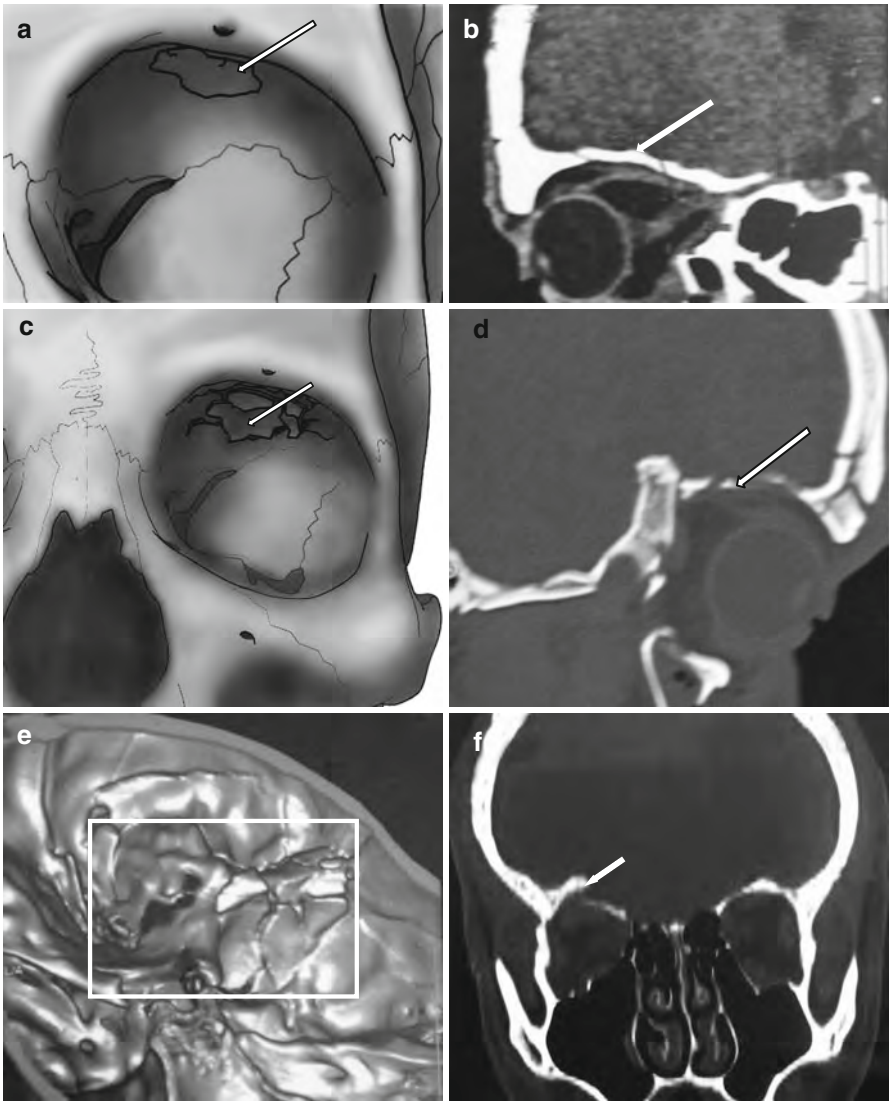

Fig. 8.8 Types of orbital roof fractures: (**a**–**d**) Without displacement of bone fragments. (**e**) 3D reconstruction of a comminuted fracture (*white box*) shown in Fig. 8.8c (*top view*, view from the anterior cranial fossa). (**f**–**h**) A blow-out fracture of the orbital roof (shown with an *arrow*). (**i**–**l**) Blow-in fracture. The bone fragment displaces the globe downward (**k**)

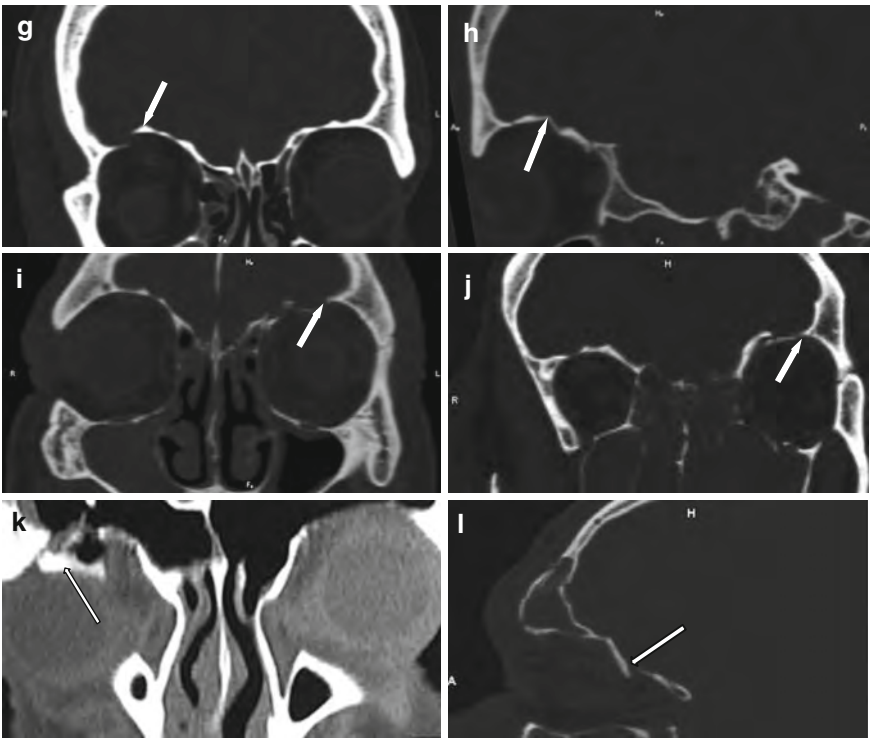

Fig. 8.8 (continued)

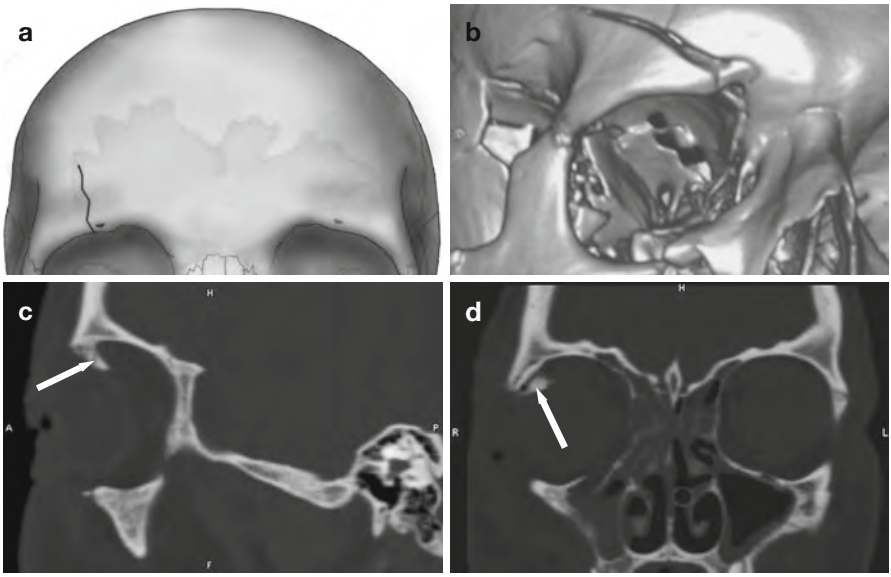

Fig. 8.9 Supraorbital rim fracture: (**a**) Schematic view of an isolated fracture. (**b**) A much more common type: the supraorbital rim fracture as a component of a more extensive injury. (**c**, **d**) Blow-in fracture of the supraorbital rim

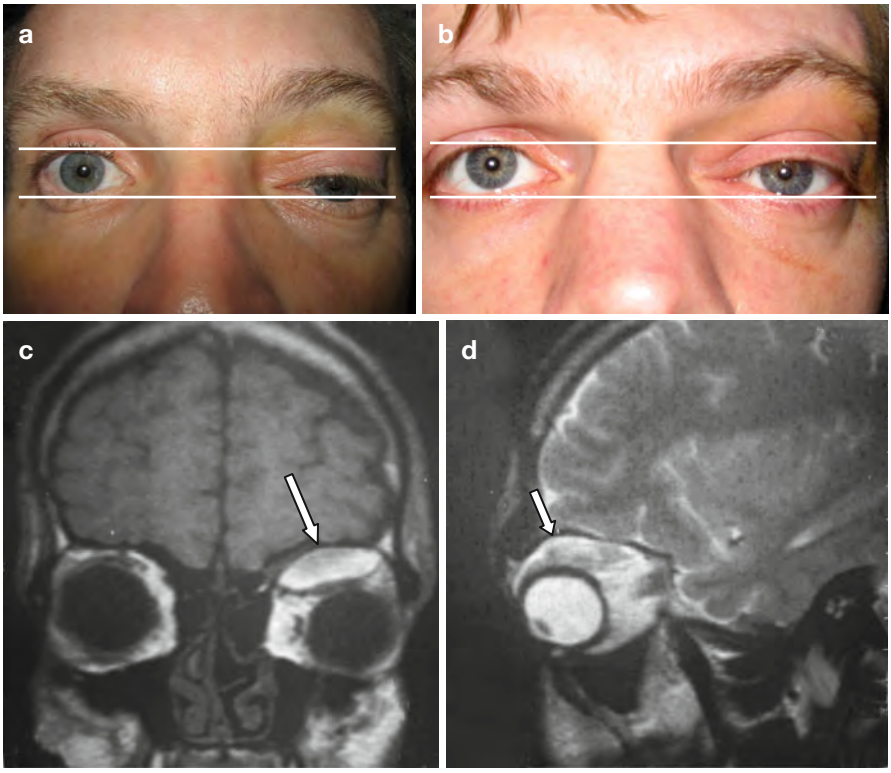

Fig. 8.10 Clinical presentation of a subperiosteal hematoma in a patient with a fracture of the left orbital roof: (**a**, **b**) Small palpebral hematoma (**a**, patient's appearance before surgery; **b**, after drainage of the hematoma narrowing of the orbital fissure caused by ptosis and downward displacement of the globe). (**c**, **d**) MRI scans before treatment was started (the hematoma is shown with an *arrow*)

Ocular motility disorders (17 %) and ptosis of the upper eyelid (25 %). In the case of an anterior fracture, the mechanical effect of a bone fragment or subperiosteal hematoma on the superior muscle complex is the main reason for motility disorders and ptosis [44, 79, 82, 83]. In patients with posterior blow-in orbital wall fractures, the ocular motility disorders may be a sign of the superior orbital fissure or orbital apex syndromes [54, 84]. In these cases, the external and internal ophthalmoplegia is accompanied by dysesthesia in the innervation zone of the first branch of the trigeminal nerve. One should be aware that brain stem injuries can also lead to limited ocular motility in these patients as well [84].

Limited vertical movements of the globe in patients with orbital roof fracture should be differentiated from supraduction deficit in patients with Brown's syndrome. This syndrome is caused by a restriction of the tendon of the superior oblique

muscle, usually in the region of the trochlear notch, and is most notable during adduction[4] [85].

The triad of nasal CSF leak, pneumocephalus, and pulsating exophthalmos is caused by combined injury to the orbital roof and dura mater and occurs in 3–9 % of cases [55]. A number of factors contribute to this triad:

- The relatively thin orbital plate can be easily fractured under mechanical impact. This leads to a traumatic communication between the frontal sinus and ethmoidal labyrinth cavities with the anterior cranial fossa.
- Nasal bone fractures, which are often associated with the orbital injury, displace the perpendicular plate of the ethmoidal bone upward, damage the cribriform plate, and rupture the dura mater which is tightly fused with the crista galli.

The orbital roof fracture is combined both with subperiosteal and epi- or subdural hematoma in 15–20 % of cases [55, 65, 82, 87].

Pulsating exophthalmos is a pathognomonic but rare sign of an orbital roof defect of 1–2 cm^2 that requires surgical management to avoid the late development of an encephalocele [54]. Cranio-orbital fistulae accompanied by CSF leak from the palpebral fissure are even less common [19, 71, 88].

Posterior roof fractures can cause traumatic optic neuropathy with or without the fracture extending to the orbital apex and occurs in 16 % of patients[5] [55].

8.4.4 Diagnosis

A complete ophthalmic examination cannot be performed in 75 % of patients due to severity of their physical condition [20, 27, 28]. Hence, a complete diagnosis depends on neurological assessment and computed tomography (Figs. 8.3 and 8.8). Coronal and sagittal CT scanning and 3D reconstruction allow one to assess the fracture length, location of bone fragments, entrapment of orbital tissues, and involvement of the optic nerve and the brain [82, 89].

8.4.5 Treatment of Orbital Roof Fractures

Haug et al. [61] analyzed the English-language literature published over the past 30 years and found that treatment of orbital roof fractures in children was mostly by nonsurgical measures (53–86 %). The only exclusion was extensive blow-in fractures.

[4] However, there have been anecdotal reports of the involvement of the trochlear notch in the supraorbital rim fracture line and entrapment of the superior oblique muscle tendon between the bone fragments, which resulted in development of clinical presentation of Brown's syndrome in patients with orbital roof fractures [86].

[5] The pathogenesis, clinical presentation, diagnosis, and treatment of this condition are described in detail in Sect. 8.5.1.2 and 8.5.3.

The treatment of adults is individualized depending on the following factors: displacement of bone fragments, involvement of the cranial vault, the status of the frontal sinus bone and the dura mater, and the presence of cerebral hematomas.

Fractures without any displacement or with the minor displacement of bone fragments require no surgical management [54], while interventions are needed for the rest of the injuries.

The goals of *treatment* are restoring the orbital volume by repositioning and rigid fixation of bone fragments (using osteoplasty, if needed), separating the cranial cavity from the orbit, and eliminating ocular motility disorders [20, 27, 28].

Indications for early one-stage exhaustive surgery performed by a multidisciplinary medical team include:

- Significant displacement of bone fragments and formation of an extensive orbital roof defect
- Intracranial displacement of the orbital contents
- Profound or persistent CSF leak
- Ocular motility disorders caused by dislocation of a bone fragment
- Encephalocele [46, 54, 83, 90]

Indications for emergency surgery include the need for optic nerve decompression most frequently secondary to an impinging bone fragment or hematoma or secondary to the bleeding from the infraorbital or ethmoidal arteries [91]. In all other cases, restoration of orbital roof integrity should be performed on day 1–10, after life-threatening conditions are eliminated. The problems of waiting longer include resorption of the fracture edges, cicatricial tissue in the fracture zone, and suppurative inflammation in the injured paranasal sinuses.

In only about 6 % of cases is there an indication for surgical intervention for an isolated fracture of the orbital roof. It is usually corrected subsequent to surgery for brain injuries and after repair of the frontal sinus walls [20, 27, 28].

Three methods for reconstructing the orbital roof are used depending on fracture type. Fragments can be repositioned without fixation if the fractures are small and the orbital roof is stable and the periosteum has not been injured (46 % of cases). Repositioning of the orbital fat, watertight suturing of periosteal ruptures, and osteosynthesis with titanium mini- or microplates are recommended for extensive fractures (34 % of surgeries). Finally, the methods listed above are supplemented with osteal and dural reconstruction using autograft, allograft, and explants if the fractures are extensive with tissue defects (20 % of patients) [90, 92–95].

The anatomical and functional success is achieved in the primary surgery 80 % of the time. In 20 % of patients, reoperation is necessary.

8.4.6 Complications of Orbital Roof Fractures

As with other types of craniofacial injuries, complications of orbital roof fractures can be subdivided into those induced by the trauma and those secondary to the

surgical management. CSF leak, pneumocephalus, frontal lobe contusion, epidural hematoma, meningitis, infectious complications, ocular motility disorders, globe dislocation, and encephalocele can all be a direct result of the trauma. The surgical approach, timing, scope of surgical repair, and the use of implants all have effects of the final success as well [20, 27, 28, 71, 91].

We would like to pay special attention to *traumatic orbital encephalocele*. It is a rather rare complication of orbital roof fractures [95, 96]. Only 15 cases [71] have been reported over the 50 years after this entity was first described [151].

This complication is primarily in children as they have an undeveloped frontal sinus and the fracture inevitably spreads to the floor of the anterior cranial fossa, while the dura mater is ruptured[6].

The development of an encephalocele is induced by a seemingly insignificant blunt orbital trauma that usually results from child's fall from his own height [98]. The clinical signs can appear several months or even years after trauma [99, 100]. The gradual increase in surface area of the bone defect (the so-called growing fracture) is caused by growth of the skull and brain, CSF pulsation, and the absence of a counterforce. This leads to prolapse of the arachnoid mater and the medullary substance through the fracture site of the frontal bone [101]. The formation of a leptomeningeal cyst is caused by increased intracranial pressure secondary to contusion of the frontal lobes which leads to an increased pressure gradient between the cranial cavity and the orbit [102, 103].

The clinical picture includes persistent eyelid swelling, ecchymosis, hypoglobus, or, less frequently, pulsating exophthalmos and diplopia caused by limited supraduction [22, 97, 99]. Idiopathic "lacrimation" is sometimes observed, which turns out to be a CSF leak on closer examination [19, 88]. Some patients may have pulsating swelling of the upper eyelid caused by traumatic fistula between the cyst in the eyelid and the subarachnoid space [104].

CT scans show an extensive orbital roof defect, usually the anterior portion, which explains why hypoglobus prevails over exophthalmos in these patients. MRI clearly shows contusion foci in the frontal lobes, rupture of the dura mater, and protrusion of the brain parenchyma into the orbit [22, 99].

Treatment includes uni- or bilateral frontobasilar craniotomy through the coronal approach, complete resection of the injured brain parenchyma that has lost its function, watertight closure of the dura mater defect, and reconstruction of the orbital roof with an autograft, allograft, or explants [71, 98, 105].

Even though the incidence rate of encephalocele among children with orbital roof fractures is 8–14 % and as high as 100 % in patients with blow-in fractures >2 cm^2 [54, 96], it is reasonable to perform early surgical management of the orbital roof with these large tissue defects. The intervention should be performed 5–25 days after trauma, depending on the patient's general health status and the indications for surgical management of the accompanying brain trauma. Ideally, it should be performed after clear demarcation of the contusion focus of the frontal lobe [71, 100]. NOE and zygomatico-orbital fractures should also be dealt with

[6] Nine cases have been reported in adults [71, 95, 97].

appropriately. Despite the severity of the trauma, significant improvement in the general condition and extraocular muscle functions is attained, and exophthalmos is eliminated in most patients.

8.5 Orbital Apex Fractures

Orbital apex fractures are one of the high-energy traumas caused by motor vehicle accidents, falls, or head blows [106–108]. Most orbital apex fractures are the continuation of the orbital, NOE, maxillary, or panfacial fractures in young men with multiple trauma. Thirty-three percent of the time, the orbital apex fractures are bilateral [106].

The complex anatomy of bones and their intimate connection with numerous vascular and neural structures require special care in the diagnosis and treatment of orbital apex fractures.

8.5.1 Clinical Presentation of Orbital Apex Fractures

The anatomical structures passing through the two apertures, the optic foramen and the superior orbital fissure, determine the clinical presentation of the fractures in the superior orbital fissure and the orbital apex [109–111].

8.5.1.1 The Superior Orbital Fissure Syndrome

The clinical presentation includes ptosis of the upper eyelid, external and internal ophthalmoplegia (mydriasis and the absence of pupil response), anesthesia in the distribution of the first branch of the trigeminal nerve (globe, skin of the upper eyelid and forehead), disturbance in venous outflow from the orbit (exophthalmos, congested retinal and iris vessels, conjunctival vessel dilation, and increased intraocular pressure), and sometimes corneal anesthesia. *The full-scale clinical presentation of the superior orbital fissure is rather rare*[7] *as it usually includes only some symptoms* (Fig. 8.11).

8.5.1.2 The Orbital Apex Syndrome

The orbital apex syndrome is a combination of the superior orbital fissure syndrome and optic neuropathy.

Traumatic optic neuropathy is trauma-induced vision loss, either complete or partial, without any external or ophthalmoscopic signs of globe or optic nerve injury (Walsh and Hoyt 1969; cited from [112, 113]). Its incidence is one case per one million population [114].

Traumatic optic neuropathy is subdivided into those affecting the *anterior portion of the optic nerve* (intraocular and orbital), the *canalicular portion,* and the *chiasm*. Injury to the intracanalicular portion is the most common.

[7] So is the syndrome: its incidence rate among patients with craniofacial trauma is 1.2 %.

Fig. 8.11 Clinical presentation of the partial superior orbital fissure syndrome: (**a**–**c**) Complete (external and internal) ophthalmoplegia without ptosis and corneal anesthesia in patient A. (**d**) Downward deviation of the globe caused by superior rectus palsy. (**e**) Impaired abduction. (**f**) A rare combination of the clinical presentations of the superior orbital fissure syndrome and traumatic carotid-cavernous fistula (external and internal ophthalmoplegia, exophthalmos, profound chemosis, and dilated vessels of the eye)

Hippocrates described the cause-and-effect relationship between a wound of the lateral half of the eyebrow and vision loss [115]. It was suggested that the reason for blindness induced by blunt injury of the frontal region is optic nerve damage.

In rare cases, the damage to the orbital portion of the optic nerve is caused by direct impact of a bone fragment or object that has penetrated into the orbit [116].

Indirect trauma to the optic nerve can occur with a blow on the forehead that induces inertial displacement of the eyeball forward. This results in abrupt tension of the intraocular and canal portions of the optic nerve and rupture of the supplying pial vessels; the ophthalmic artery and the central retinal artery usually remain

unaffected [113, 115, 118]. Furthermore, the force of the trauma is transmitted through bones to the orbital apex and optic canal, where it causes compression of the optic nerve as a result of hemorrhage into the intraconal or subdural space.

Traumatic optic neuropathy is characterized by decreased visual acuity up to total blindness, disrupted perception of red color, superior altitudinal visual field defects, and afferent pupillary defects [115, 117, 119]. Optic nerve damage should be highly suspected if a patient has at least one of these symptoms. The visual acuity should be constantly monitored as sometimes there is a delay in visual loss.

The circumstances of trauma, as well as the degree and rate of progression of visual acuity loss, play a key role in making proper diagnosis and for choosing the optimal treatment. The probability of visual improvement after therapy in patients with contusion is twice as high as that in patients with a penetrating orbital injury or a fracture of the posterior third portion of its walls [112, 120, 121].

Sudden vision loss typically indicates a direct injury to the nerve or disrupted circulation and is an unfavorable sign [115]. The probability of restoring light perception in these cases is less than 25 % [120, 122].

Visual acuity of at least 0.001 (1/800) in these traumatic patients significantly increases the chance of visual recovery, even if the fracture affects the optic canal. However, it is possible only if medical and surgical treatment is initialed in a timely manner [123].

The patients with injury to the orbital portion of the optic nerve and visual acuity of 0.05 (20/400) and higher, especially the younger patients, have a good chance of attaining the original level of vision after the reconstruction of the orbital apex fracture. The visual results of patients with vision less than 0.05 (20/400) or with injury to the canal portion of the optic nerve are quite variable. The visual recovery after repositioning bone fragments can range from no improvement at all to partial recovery of vision acuity but with significant visual field defects [124].

Gradual loss of central vision that was initially present immediately after trauma indicates that the optic nerve has been compressed by a hematoma, air, or edema in the orbital tissues. Its regression can be achieved with adequate and timely treatment including decompression [125].

In anecdotal cases, frontal contusion is complicated by eye luxation and rupture of the optic nerve at the level of the lamina cribrosa or 30–50 mm away from the posterior pole (incomplete avulsion) [118, 126]. The simultaneous detachment of conjunctiva from the limbus and rupture of extraocular muscles (medial, inferior, superior, lateral rectus, and oblique muscles—listed in descending order of incidence) make the diagnosis a complete avulsion [127, 128]. Ma and Nerad [74], as well as [152], have reported a case of eyeball dislocation into the frontal lobe after severe craniofacial trauma.

Optic nerve avulsion is often accompanied by rupture of the ophthalmic artery with subarachnoid hemorrhage, disruption of the optic chiasm, meningitis, CSF leak, and life-threatening thalamic lesions.

8.5.2 Radiological Diagnosis

Since X-rays provide little information on orbital apex fractures, the diagnosis of this type of fracture relies on high-resolution multispiral CT scanning with 1.5 mm thickness of the slices.

Significant CT findings correlating with the optic nerve trauma include optic nerve avulsion (visualized in 15 % of patients with traumatic optic neuropathy), displacement of bone fragments into the orbit (15 %), fractures of the optic canal (15–25 %) and the lesser wing of the sphenoid, a foreign body in close proximity to the optic nerve, and hemorrhage under its sheath [84, 129, 130]. The indirect signs of neuropathy include blood accumulation in the posterior ethmoidal air cells and the sphenoid sinus (Fig. 8.12e, f) [131] and in the orbit (23 %).

The absence of findings on a CT scan does not contradict the orbital apex fracture diagnosis, since even the modern CT scanners sometimes fail to show these injuries and not allow assessment of their length [129].

8.5.3 Treatment of Orbital Apex Fractures

Treatment of traumatic optic neuropathy is of primary importance. It starts with early intravenous injection of megadose methylprednisolone, the drug of choice according to the National Acute Spinal Cord Injury Study 2 (USA).

The approved Boston scheme for optic nerve decompression (1993) suggests methylprednisolone infusion (30 mg/kg body weight) within 8 h after trauma. The subsequent continuous methylprednisolone infusion (5.4 mg/kg body weight/h) continues for 23 h. Two hundred and fifty milligrams of the drug is infused every 6 h over the next 2 days. The final stage of steroid therapy is oral administration of prednisolone for 15 days.

Corticosteroid therapy reduces contusion-induced edema, optic nerve necrosis, and vasospasm. Inhibition of free radicals and lipid peroxidation is also a part of the neuroprotective effect of methylprednisolone and dexamethasone.

The use of other medical managements to reduce optic neuropathy caused by posttraumatic ischemia, cellular calcium accumulation, neurofilament degradation, inhibition of hydrolysis of membrane lipids, and release of arachidonic acid has not been studied as much.

Surgical decompression is indicated only for patients with obvious compression of the orbital portion of the optic nerve (e.g., with a fragment of the greater wing of the sphenoid). Urgent reduction and/or repositioning of the fragment using both the modern microsurgical transnasal or transconjunctival-endonasal endoscopic approaches and the conventional approaches to the orbital apex that are more traumatic (transfrontal craniotomy, external ethmoidectomy, and transantral transethmoidal approach) is performed in these cases [45, 122, 132]. It is reasonable to use the computer-assisted surgery (CAS) method to minimize the risk of damaging the internal carotid artery and the optic nerve [133, 134].

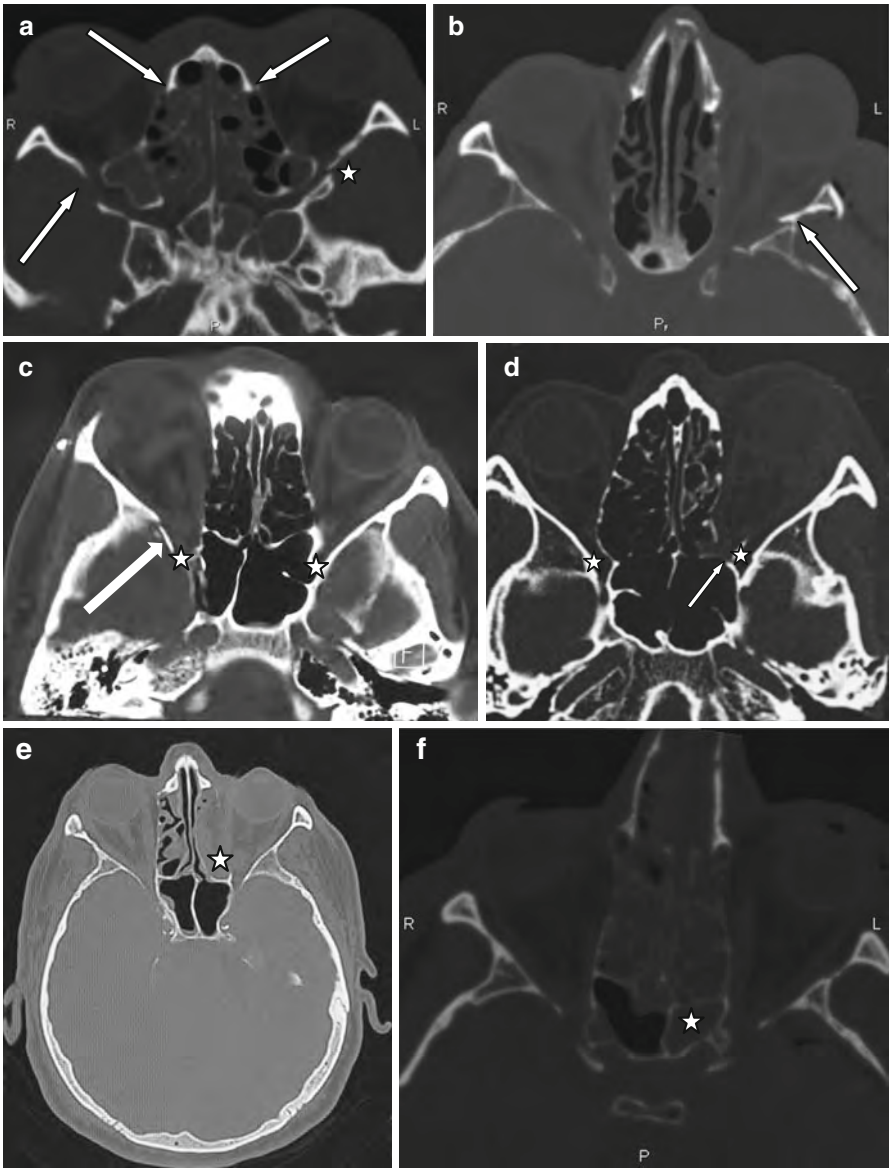

Fig. 8.12 A CT pattern of the orbital apex fracture: (**a**) A component of Le Fort III maxillary fracture. The fracture line is shown with *arrows*; the orbital apex fracture is shown with an *asterisk*. (**b**) A blow-in fracture of the lateral orbital wall with the fracture line spreading to the orbital apex (shown with an *arrow*). (**c**) The bone fragment (shown with an *arrow*) adjacent to the optic foramen (shown with an *asterisk*). (**d**) A fracture of the posterior portion of the medial orbital wall. The fracture line is shown with an *arrow*; the optic canals are shown with *asterisks*. (**e**, **f**) Blood accumulation (shown with an *asterisk*) in posterior ethmoidal air cells (**e**, **f**) and in the sphenoid sinus (**f**) — an indirect sign of optic canal fracture

The rationale for decompressing the canal portion of the optic nerve is currently subject to debate [31, 113, 135], although there is a tendency more recently toward the more active surgical intervention [122, 134].

Radiologically verified compression of the optic nerve in the optic canal is an indication for surgical treatment, especially if the 48-h steroid therapy has no effect or amaurosis has developed and the visual evoked potentials are reduced despite the therapy [64, 117, 129, 134]. Urgent surgery is required [20, 48], although visual acuity can be improved even 13 days after the trauma [136].

The operation of choice is a modern modification of Fukado's decompression (1972) which does not have the drawbacks typical of the external transethmoidal, transfrontal, or pterional approaches [1, 137, 138]. The endonasal transethmoidal-transorbital and the transethmoidal-sphenoidal approaches allow the surgeon to remove at least half of the circumference of the optic canal without using skin incisions, craniotomy, or retraction of the frontal lobes [131]. Meticulous preoperative examination searching for a possible traumatic carotid-cavernous fistula, the use of microsurgical instrumentation, and knowledge of the anatomy of orbital apex allow one to prevent serious complications, such as perforation of the carotid artery or rupture of the dura mater.

In patients *who have an epidural hematoma of the optic nerve* verified by oblique paracoronal MRI in projection perpendicular to the optic nerve, treatment consists of a 3-day intravenous injection of 250 mg of methylprednisolone four times daily followed by oral administration of 80 mg of prednisolone daily for the next week. The indications for optic nerve sheath fenestration include the rather rare occurrence of a subdural hematoma [113].

Other manifestations of the orbital apex syndrome such as cranial nerve III, IV, and VI palsies and anesthesia in the distribution of the first branch of n. V, including the cornea, typically do not require urgent surgical treatment. Corticosteroid therapy and 1-year follow-up is adequate, but the neuro-ophthalmic symptoms are expected to regress to some extent [84, 139]. Surgery may be performed if persistent ptosis and diplopia last for more than 1 year after trauma [140].

***

Unfortunately, there is little success in treating traumatic optic neuropathy [113, 141]. If patients had some light perception after the trauma, there may be partial restoration of visual function after several months of therapy and in only 50 % of patients who had surgery after the development of total loss of vision [64, 120, 129].

Prospective clinical trials have not been possible because of the small patient sample sizes and variability of the actual trauma. Therefore, the advantage of any particular surgical or medical strategy—megadose glucocorticoid monotherapy, surgical decompression, or their combination—has not been scientifically proven [114, 141]. However, it has been found that the nonsurgical approach in general has a worse outcome [112].

8.6 Local Orbital Roof Fractures

Although these fractures are rather small in size, they impose a serious diagnostic and therapeutic challenge. Suffice it to say that the death rate in patients with penetrating orbitocranial injuries during the World War II was 12 %, which was twice as high as the death rate from penetrating cranial injuries in any other location [21].

The traumatic circumstances and appearance of a patient admitted to the hospital may seem harmless, but should not be underestimated [21, 142].

The history and determination of what kind of object penetrated the orbit and cranium are extremely important. *Any object that is small enough to penetrate into the orbit should be also be regarded as possibly actually penetrated the orbit*. Particular attention should be given as to whether the object was vegetable matter such a tree branch, a pencil, a wooden paint brush handle, etc. [38, 143–145].

Meticulous visual inspection is performed after a detailed history is obtained. Close attention should be paid even to a minor palpebral skin injury as it can be accompanied by a severe penetrating cranial injury [109, 142]. A conjunctival wound can easily go unnoticed due to the presence of chemosis and subconjunctival hemorrhage [21]. One should be particularly alert to any unexplained findings, such as palpebral edema disproportionate to the severity of the injury, rhinorrhea and epiphora developing after trauma, or profound bleeding that cannot be explained by damage to orbital vessels [146].

The next stage is meticulous ophthalmic examination searching for signs of the superior orbital fissure or orbital apex syndromes: reduced vision acuity, narrowed visual field, afferent pupil defect, and color vision deficiency [109, 147].

Since patients may have no neurological symptoms at admission [147], early radiological diagnosis is of great significance [148]. Coronal CT scanning is indispensable for diagnosing orbital roof fractures; the axial CT scans show the optic canal and the superior orbital fissure: foreign bodies are most likely to penetrate into these cranial areas [142]. MRI visualizes direct traumas of the brain parenchyma, hematomas, internal carotid artery, and cavernous sinus lesions.

Early diagnosis and timely and adequate surgical and medical treatment often allow a surgeon not only to save the patient's life but also to prevent persistent neurological deficits, as well as vision and ocular motility disorders [109, 149].

References

1. Raveh, J., & Vuillemin, T. (1988). The surgical one-stage management of combined craniomaxillo-facial and frontobasal fractures. Advantages of the subcranial approach in 374 cases. *Journal of Cranio-Maxillo-Facial Surgery, 16*(4), 160–172.
2. Burstein, F., Cohen, S., Hudgins, R., & Boydston, W. (1997). Frontal basilar trauma: Classification and treatment. *Plastic and Reconstructive Surgery, 99*(5), 1314–1321.
3. Holt, G. R., & Holt, J. E. (1983). Incidence of eye injuries in facial fractures: An analysis of 727 cases. *Otolaryngology – Head and Neck Surgery, 91*(3), 276–279.
4. Manolidis, S., Weeks, B. H., Kirby, M., et al. (2002). Classification and surgical management of orbital fractures: Experience with 111 orbital reconstructions. *The Journal of Craniofacial Surgery, 13*(6), 726–737.

5. Bell, R. B., Dierks, E. J., Brar, P., et al. (2007). A protocol for the management of frontal sinus fractures emphasizing sinus preservation. *Journal of Oral and Maxillofacial Surgery, 65*(5), 825–839.
6. Piccolino, P., Vetrano, S., Mundula, P., et al. (2007). Frontal bone fractures: New technique of closed reduction. *The Journal of Craniofacial Surgery, 18*(3), 695–698.
7. Montovani, J. C., Nogueira, E. A., Ferreira, F. D., et al. (2006). Surgery of frontal sinus fractures: Epidemiologic study and evaluation of techniques. *Brazilian Journal of Otorhinolaryngology, 72*(2), 204–209.
8. Manolidis, S., & Hollier, L. H. (2007). Management of frontal sinus fractures. *Plastic and Reconstructive Surgery, 120*(7 Suppl 2), 32S–48S.
9. Freihofer, H. P. (1995). Effectiveness of secondary post-traumatic periorbital reconstruction. *Journal of Cranio-Maxillo-Facial Surgery, 23*(3), 143–150.
10. Amrith, S., Saw, S. M., Lim, T. C., & Lee, T. K. (2000). Ophthalmic involvement in cranio-facial trauma. *Journal of Cranio-Maxillo-Facial Surgery, 28*(3), 140–147.
11. Chen, K.-T., Chen, C.-T., Mardini, S., et al. (2006). Frontal sinus fractures: A treatment algorithm and assessment of outcomes based on 78 clinical cases. *Plastic and Reconstructive Surgery, 118*(2), 457–468.
12. Cole, P., Kaufman, Y., Momoh, A., et al. (2009). Techniques in frontal sinus fracture repair. *Plastic and Reconstructive Surgery, 123*(5), 1578–1579.
13. Sivori, L. A., de Leeuw, R., Morgan, I., & Cunningham, L. L. (2010). Complications of frontal sinus fractures with emphasis on chronic craniofacial pain and its treatment: A review of 43 cases. *Journal of Oral and Maxillofacial Surgery, 68*(9), 2041–2046.
14. Whatley, W. S., Allison, D. W., Chandra, R. K., et al. (2005). Frontal sinus fractures in children. *Laryngoscope, 115*(10), 1741–1745.
15. Clauser, L., Dallera, V., Sarti, E., & Tieghi, R. (2004). Frontobasilar fractures in children. *Childs Nervous System, 20*(3), 168–175.
16. Hewitt, D. K., Scheidt, T. D., & Calhoun, K. H. (2009). Depressed anterior table fracture: A minimally invasive method of reduction. *Ear, Nose, and Throat Journal, 88*(1), 734–735.
17. Potter, J. A., Siddoway, J. R., & Mathog, R. H. (1987). Injury to the orbital plate of the frontal bone. *Head & Neck Surgery, 10*(2), 78–84.
18. Madhusudan, G., Sharma, R. K., Khandelwal, N., & Tewari, M. K. (2006). Nomenclature of frontobasal trauma: A new clinicoradiographic classification. *Plastic and Reconstructive Surgery, 117*(7), 2382–2388.
19. Dryden, R. M., & Wulc, A. E. (1986). Pseudoepiphora from cerebrospinal fluid leak: Case report. *British Journal of Ophthalmology, 70*(8), 570–574.
20. Piotrowski, W. P., & Beck-Mannagetta, J. (1995). Surgical techniques in orbital roof fractures: Early treatment and results. *Journal of Cranio-Maxillo-Facial Surgery, 23*(1), 6–11.
21. Solomon, K. D., Pearson, P. A., Tetz, M. R., & Baker, R. S. (1993). Cranial injury from unsuspected penetrating orbital trauma: A review of five cases. *Journal of Trauma, 34*(2), 285–289.
22. Koc, R. K., Kurtsoy, A., Oktem, I. S., & Akdemir, H. (1999). Growing skull fracture of the orbital roof. Case report. *Pediatric Neurosurgery, 30*(1), 35–38.
23. Gill, H. S., & van As, A. B. (2008). Tension pneumocranium in childhood trauma. *World Journal of Pediatrics, 4*(3), 231–233.
24. Waring, G. O., & Flanagan, J. C. (1975). Pneumocephalus. A sign of intracranial involvement in orbital fracture. *Archives of Ophthalmology, 93*(9), 847–850.
25. Jain, S. A., Manchio, J. V., & Weinzweig, J. (2010). Role of the sagittal view of computed tomography in evaluation of the nasofrontal ducts in frontal sinus fractures. *The Journal of Craniofacial Surgery, 21*(6), 1670–1673.
26. Chirico, P. A., Mirvis, S. E., Kelman, S. E., & Karesh, J. W. (1989). Orbital "blow-in" fractures: Clinical and CT features. *Journal of Computer Assisted Tomography, 13*(6), 1017–1022.
27. Piotrowski, W. P. (1992). The primary treatment of frontobasal and midfacial fractures in patients with head injuries. *Journal of Oral and Maxillofacial Surgery, 50*(12), 1264–1268.
28. Piotrowski, W. P. (1995). The primary treatment of traumatic lesions of the orbital roof. *Japanese Journal of Ophthalmology, 39*(3), 295–301.

29. Alvi, A., Doherty, T., & Lewen, G. (2003). Facial fractures and concomitant injuries in trauma patients. *Laryngoscope, 113*(1), 102–106.
30. Mandrioli, S., Tieghi, R., Galiè, M., et al. (2008). Anterior skull base fractures: Guidelines for treatment. *The Journal of Craniofacial Surgery, 19*(3), 713–717.
31. Sollmann, W. P., Seifert, V., Haubitz, B., & Dietz, H. (1989). Combined orbito-frontal injuries. *Neurosurgical Review, 12*(2), 115–121.
32. Cascone, P., Gennaro, P., Ramieri, V., & Esposito, V. (2009). Forehead trauma outcomes: Restoration of brain, soft tissues, and bone defects: A 3-step treatment. *The Journal of Craniofacial Surgery, 20*(2), 498–501.
33. Robotti, E., Forcht Dagi, T., Ravegnani, M., & Bocchiotti, G. (1992). A new prospect on the approach to open, complex, craniofacial trauma. *Journal of Neurosurgical Sciences, 36*(2), 89–99.
34. Lee, T. T., Ratzker, P. A., Galarza, M., & Villanueva, P. A. (1998). Early combined management of frontal sinus and orbital and facial fractures. *Journal of Trauma, 44*(4), 665–669.
35. Wang, M. C., Temkin, N. R., Deyo, R. A., et al. (2007). Timing of surgery after multisystem injury with traumatic brain injury: Effect on neuropsychological and functional outcome. *Journal of Trauma, 62*(5), 1250–1258.
36. Bell, R. B., & Chen, J. (2010). Frontobasilar fractures: Contemporary management. *Atlas of the Oral and Maxillofacial Surgery Clinics of North America, 18*(2), 181–196.
37. Ohjimi, H., Taniguchi, Y., Tanahashi, S., et al. (2000). Accessing the orbital roof via an eyelid incision: The transpalpebral approach. *Skull Base Surgery, 10*(4), 211–216.
38. Szabo, K. A., Cheshier, S. H., Kalani, M. Y., et al. (2008). Supraorbital approach for repair of open anterior skull base fracture. *Journal of Neurosurgery Pediatrics, 2*(6), 420–423.
39. Deschamps-Braly, J. C., Sawan, K., Iliff, N., & Manson, P. N. (2010). Decision making in isolated orbital roof fractures with a case report of the upper eyelid approach to treatment. *Plastic and Reconstructive Surgery, 126*(6), 308e–309e.
40. Tedaldi, M., Ramieri, V., Foresta, E., et al. (2010). Experience in the management of frontal sinus fractures. *The Journal of Craniofacial Surgery, 21*(1), 208–210.
41. Park, D. H., Lee, J. W., Song, C. H., et al. (1998). Endoscopic application in aesthetic and reconstructive facial bone surgery. *Plastic and Reconstructive Surgery, 102*(4), 1199–1209.
42. Malhotra, R., Saleh, G. M., de Sousa, J. L., et al. (2007). The transcaruncular approach to orbital fracture repair: Ophthalmic sequelae. *The Journal of Craniofacial Surgery, 18*(2), 420–426.
43. Mueller, R. (2008). Endoscopic treatment of facial fractures. *Facial Plastic Surgery, 24*(1), 78–91.
44. Hinohira, Y., & Hyodo, M. (2009). Endoscopic endonasal reduction surgery for diplopia caused by orbital roof fractures. *Journal of Plastic, Reconstructive & Aesthetic Surgery, 62*(10), 345–348.
45. Moe, K. S., Kim, L. J., & Bergeron, C. M. (2011). Transorbital endoscopic repair of cerebrospinal fluid leaks. *Laryngoscope, 121*(1), 13–30.
46. Eppley, B. L., Custer, P. L., & Sadove, A. M. (1990). Cutaneous approaches to the orbital skeleton and periorbital structures. *Journal of Oral and Maxillofacial Surgery, 48*(8), 842–854.
47. Kim, K. S., Kim, E. S., Hwang, J. H., & Lee, S. Y. (2010). Transcutaneous transfrontal approach through a small peri-eyebrow incision for the reduction of closed anterior table frontal sinus fractures. *Journal of Plastic, Reconstructive & Aesthetic Surgery, 63*(5), 763–768.
48. Hopper, R. A., Salemy, S., & Sze, R. W. (2006). Diagnosis of midface fractures with CT: What the surgeon needs to know. *Radiographics, 26*(3), 783–793.
49. Murphy, J., & Jones, N. S. (2004). Frontal sinus obliteration. *The Journal of Laryngology and Otology, 118*(8), 637–639.
50. Fattahi, T., & Dipasquale, J. (2009). Utility of the pericranial flap in frontal sinus and anterior cranial fossa trauma. *International Journal of Oral and Maxillofacial Surgery, 38*(12), 1263–1267.
51. Kim, Y. H., Youn, S. K., Kim, J. T., et al. (2011). Treatment of the severely infected frontal sinus with latissimus dorsi myocutaneous free flaps. *The Journal of Craniofacial Surgery, 22*(3), 962–966.

52. Rontal, M. L. (2008). State of the art in craniomaxillofacial trauma: Frontal sinus. *Current Opinion in Otolaryngology & Head and Neck Surgery, 16*(4), 381–386.
53. Frodel, J. L. (2008). Computer-designed implants for fronto-orbital defect reconstruction. *Facial Plastic Surgery, 24*(1), 22–34.
54. Messinger, A., Radkowski, M. A., Greenwald, M. J., & Pensler, J. M. (1989). Orbital roof fractures in the pediatric population. *Plastic and Reconstructive Surgery, 84*(2), 213–216.
55. Martello, J. Y., & Vasconez, H. C. (1997). Supraorbital roof fractures: A formidable entity with which to contend. *Annals of Plastic Surgery, 38*(3), 223–227.
56. Kinnunen, I., & Aitasalo, K. (2006). A review of 59 consecutive patients with lesions of the anterior cranial base operated on using the subcranial approach. *Journal of Cranio-Maxillo-Facial Surgery, 34*(7), 405–411.
57. Hwang, K., & Kim, E. Y. (2008). Delayed development of mucocele in the fractured frontal sinus. *The Journal of Craniofacial Surgery, 19*(5), 1419–1422.
58. Jo, A., Rizen, V., Nikolic, V., & Banovic, B. (1989). The role of orbital wall morphological properties and their supporting structures in the etiology of "blow-out" fractures. *Surgical and Radiologic Anatomy, 11*(3), 241–248.
59. Takizawa, H., Sugiura, K., Baba, M., et al. (1988). Structural mechanics of the blowout fracture: Numerical computer simulation of orbital deformation by the finite element method. *Neurosurgery, 22*(6 pt 1), 1053–1055.
60. Lee, H. J., Jilani, M., Frohman, L., & Baker, S. (2004). CT of orbital trauma. *Emergency Radiology, 10*(4), 168–172.
61. Haug, R. H., Van Sickels, J. E., & Jenkins, W. S. (2002). Demographics and treatment options for orbital roof fractures. *Oral Surgery, Oral Medicine, Oral Pathology, Oral Radiology, and Endodontics, 93*(3), 238–246.
62. Kummoona, R. (2009). Management of injuries of the orbital skeleton. *The Journal of Craniofacial Surgery, 20*(3), 762–767.
63. Fulcher, T. P., & Sullivan, T. J. (2003). Orbital roof fractures: Management of ophthalmic complications. *Ophthalmic Plastic and Reconstructive Surgery, 19*(5), 359–363.
64. Rinna, C., Rocchi, G., Ventucci, E., et al. (2009). Bilateral orbital roof fracture. *The Journal of Craniofacial Surgery, 20*(3), 737–742.
65. Chapman, V. M., Fenton, L. Z., Gao, D., & Strain, J. D. (2009). Facial fractures in children: Unique patterns of injury observed by computed tomography. *Journal of Computer Assisted Tomography, 33*(1), 70–72.
66. Das, U. M., Nagarathna, C., Viswanath, D., et al. (2006). Management of facial trauma in children: A case report. *Journal of the Indian Society of Pedodontics and Preventive Dentistry, 24*(3), 161–163.
67. Guly, C. M., Guly, H. R., Bouamra, O., et al. (2006). Ocular injuries in patients with major trauma. *Emergency Medicine Journal, 23*(12), 915–917.
68. Koltai, P. J., Amjad, I., Meyer, D., & Feustel, P. J. (1995). Orbital fractures in children. *Archives of Otolaryngology – Head and Neck Surgery, 121*(12), 1375–1379.
69. Donahue, D. J., Smith, K., Church, E., & Chadduck, W. M. (1997). Intracranial neurological injuries associated with orbital fracture. *Pediatric Neurosurgery, 26*(5), 261–268.
70. Rothman, M. I., Simon, E. M., Zoarski, G. H., & Zagardo, M. T. (1998). Superior blowout fracture of the orbit: The blowup fracture. *American Journal of Neuroradiology, 19*(8), 1448–1449.
71. Antonelli, V., Cremonini, A. M., Campobassi, A., et al. (2002). Traumatic encephalocele related to orbital roof fractures: Report of six cases and literature review. *Surgical Neurology, 57*(2), 117–125.
72. Patel, P. N., & Kenney, I. J. (2009). A rare case of 'blow-up' fracture of the orbit in a child. *Pediatric Radiology, 39*(8), 869–871.
73. Curtin, H. D., Wolfe, P., & Schramm, V. (1982). Orbital roof blow-out fractures. *American Journal of Roentgenology, 139*(5), 969–972.
74. Ma, C., & Nerad, J. A. (1988). Orbital roof fracture with ocular herniation. *American Journal of Ophthalmology, 105*(6), 700–701.

75. Kulvin, D. R., & Leadbetter, M. G. (1989). Orbital rim trauma causing a blowout fracture. *Plastic and Reconstructive Surgery, 84*(6), 969–970.
76. Brucoli, M., Giarda, M., & Benech, A. (2011). A peculiar orbital roof blow-in fracture. *The Journal of Craniofacial Surgery, 22*(1), 358–360.
77. Sullivan, W. G. (1991). Displaced orbital roof fractures: Presentation and treatment. *Plastic and Reconstructive Surgery, 87*(4), 657–661.
78. Tuncbilek, G., Vargel, I., & Erk, Y. (2004). Isolated supraorbital rim fracture displaced out of scalp: A case report. *The Journal of Craniofacial Surgery, 15*(3), 451–453.
79. Ohtsuka, H., & Nakaoka, H. (1987). Impaired upward gaze due to subperiosteal hemorrhage of the orbital roof. *Annals of Plastic Surgery, 18*(6), 547–549.
80. Landa, M. S., Landa, E. H., & Levine, M. R. (1998). Subperiosteal hematoma of the orbit: Case presentation. *Ophthalmic Plastic and Reconstructive Surgery, 14*(3), 189–192.
81. Saiful, M. N., Azmi, A., & Saffari, M. H. (2007). Proptosis presenting as a delayed sign of frontal extradural haematoma. *The Medical Journal of Malaysia, 62*(2), 156–157.
82. Keane, J. R. (1993). Ptosis and levator paralysis caused by orbital roof fractures. Three cases with subfrontal epidural hematomas. *Journal of Clinical Neuro-Ophthalmology, 13*(4), 225–228.
83. Hwang, K., Kim, S. G., Lee, S. I., & Ha, Y. (2004). Blepharoptosis caused from compression of levator muscle by fractured orbital roof fragment. *The Journal of Craniofacial Surgery, 15*(6), 942–945.
84. Waller, P. Y., Chossegros, C., Semeria, E., & Gola, R. (1991). Posttraumatic ptosis. *Revue de Stomatologie et de Chirurgie Maxillo-Faciale, 92*(4), 237–246.
85. Lauer, S. A., Sauer, H., & Pak, S. M. (1998). Brown's syndrome diagnosed following repair of an orbital roof fracture: A case report. *The Journal of Cranio-Maxillofacial Trauma, 4*(4), 20–22.
86. Al-Qurainy, I. A., Dutton, G. N., Moos, K. F., et al. (1988). Orbital injury complicated by entrapment of the superior oblique tendon: A case report. *British Journal of Oral and Maxillofacial Surgery, 26*(4), 336–340.
87. Bahloul, K., & Xhumari, A. (2009). Epidural hematoma revealed by exophthalmia, two cases reports. *Clinical Neurology and Neurosurgery, 111*(10), 893–895.
88. Sibony, P. A., Anand, A. K., Keuskamp, P. A., & Zippen, A. G. (1985). Posttraumatic cerebrospinal fluid cyst of the orbit. Case report. *Journal of Neurosurgery, 62*(6), 922–924.
89. Karesh, J. W., Kelman, S. E., Chirico, P. A., & Mirvis, S. E. (1991). Orbital roof "blow-in" fractures. *Ophthalmic Plastic and Reconstructive Surgery, 7*(2), 77–83.
90. Penfold, C. N., Lang, D., & Evans, B. T. (1992). The management of orbital roof fractures. *British Journal of Oral and Maxillofacial Surgery, 30*(2), 97–103.
91. McLachlan, D. L., Flanagan, J. C., & Shannon, G. M. (1982). Complications of orbital roof fractures. *Ophthalmology, 89*(11), 1274–1278.
92. Neigel, J. M., & Ruzicka, P. O. (1996). Use of demineralized bone implants in orbital and craniofacial reconstruction and a review of the literature. *Ophthalmic Plastic and Reconstructive Surgery, 12*(2), 108–120.
93. Piotrowski, W. P., & Mayer-Zuchi, U. (1999). The use of polyglactin 910-polydioxanon in the treatment of defects of the orbital roof. *Journal of Oral and Maxillofacial Surgery, 57*(11), 1301–1305.
94. Jacono, A. A., & Moskowitz, B. (2000). Alloplastic implants for orbital wall reconstruction. *Facial Plastic Surgery, 16*(1), 63–68.
95. Gazioğlu, N., Ulu, M. O., Ozlen, F., et al. (2008). Acute traumatic orbital encephalocele related to orbital roof fracture: Reconstruction by using porous polyethylene. *Ulusal Travma ve Acil Cerrahi Dergisi, 14*(3), 247–252.
96. Cayli, S. R., Kocak, A., Alkan, A., et al. (2003). Intraorbital encephalocele: An important complication of orbital roof fractures in pediatric patients. *Pediatric Neurosurgery, 39*(5), 240–245.
97. Koehler, P. J., & Blaauw, G. (1992). Late posttraumatic nonvascular pulsating eye. *Acta Neurochirurgica (Wien), 116*(1), 62–64.

98. Mohindra, S., Mukherjee, K. K., Chhabra, R., & Gupta, R. (2006). Orbital roof growing fractures: A report of four cases and literature review. *British Journal of Neurosurgery, 20*(6), 420–423.
99. Greenwald, M. J., Lissner, G. S., Tomita, T., & Naidich, T. P. (1987). Isolated orbital roof fracture with traumatic encephalocele. *Journal of Pediatric Ophthalmology and Strabismus, 24*(3), 141–144.
100. Bayar, M. A., Iplikcioglu, A. C., Kokes, F., & Gokcek, C. (1994). Growing skull fracture of the orbital roof. *Surgical Neurology, 41*(1), 80–82.
101. Amirjamshidi, A., Abbassioun, K., & Tary, A. S. (2000). Growing traumatic leptomeningeal cyst of the roof of the orbit presenting with unilateral exophthalmos. *Surgical Neurology, 54*(2), 178–182.
102. Suri, A., & Mahapatra, A. K. (2002). Growing fractures of the orbital roof. A report of two cases and a review. *Pediatric Neurosurgery, 36*(2), 96–100.
103. Menku, A., Koc, R. K., Tucer, B., et al. (2004). Growing skull fracture of the orbital roof: Report of two cases and review of the literature. *Neurosurgical Review, 27*(2), 133–136.
104. Arslantas, A., Vural, M., Atasoy, M. A., et al. (2003). Posttraumatic cerebrospinal fluid accumulation within the eyelid: A case report and review of the literature. *Childs Nervous System, 19*(1), 54–56.
105. Caffo, M., Germano, A., Caruso, G., et al. (2003). Growing skull fracture of the posterior cranial fossa and of the orbital roof. *Acta Neurochirurgica (Wien), 145*(3), 201–208.
106. Unger, J. M. (1984). Orbital apex fractures: The contribution of computed tomography. *Radiology, 150*(3), 713–717.
107. Linnau, K. F., Hallam, D. K., Lomoschitz, F. M., & Mann, F. A. (2003). Orbital apex injury: Trauma at the junction between the face and the cranium. *European Journal of Radiology, 48*(1), 5–16.
108. Bater, M. C., Ramchandani, P. L., Ramchandani, M., & Flood, T. R. (2008). An orbital apex fracture resulting in multiple cranial neuropathies. *British Journal of Oral and Maxillofacial Surgery, 46*(2), 163–164.
109. Dunn, I. F., Kim, D. H., Rubin, P. A., et al. (2009). Orbitocranial wooden foreign body: A pre-, intra-, and postoperative chronicle: Case report. *Neurosurgery, 65*(2), 383–384.
110. Taylor, K. H., Mizen, K. D., & Spencer, N. (2010). Isolated fracture of the superior orbital fissure. *British Journal of Oral and Maxillofacial Surgery, 48*(3), 178–179.
111. Li, Y., Wu, W., Xiao, Z., & Peng, A. (2011). Study on the treatment of traumatic orbital apex syndrome by nasal endoscopic surgery. *European Archives of Oto-Rhino-Laryngology, 268*(3), 341–349.
112. Cook, M. W., Levin, L. A., Joseph, M. P., & Pinczower, E. F. (1996). Traumatic optic neuropathy. A meta-analysis. *Archives of Otolaryngology – Head and Neck Surgery, 122*(4), 389–392.
113. Chang, E. L., & Bernardino, C. R. (2004). Update on orbital trauma. *Current Opinion in Ophthalmology, 15*(5), 411–415.
114. Lee, V., Ford, R. L., Xing, W., et al. (2010). Surveillance of traumatic optic neuropathy in the UK. *Eye, 24*(2), 240–250.
115. Soparkar, C. N. S., & Patrinely, J. R. (2007). The eye examination in facial trauma for the plastic surgeon. *Plastic and Reconstructive Surgery, 120*(7 Suppl 2), 49S–56S.
116. Warner, J. E. A., & Lessel, S. (1995). Traumatic optic neuropathy. *International Ophthalmology Clinics, 35*(1), 57–62.
117. Anderson, R. L., Panje, W. R., & Gross, C. E. (1982). Optic nerve blindness following blunt forehead trauma. *Ophthalmology, 89*(5), 445–455.
118. Papageorgiou, K. I., Mathew, R. G., Ghazi-Nouri, S. M., et al. (2007). Optochiasmal avulsion secondary to minor occipital trauma. *Orbit, 26*(1), 71–74.
119. Gossman, M. D., Roberts, D. M., & Barr, C. C. (1992). Ophthalmic aspects of orbital injury. A comprehensive diagnostic and management approach. *Clinics in Plastic Surgery, 19*(1), 71–85.
120. Wang, B. H., Robertson, B. C., Girotto, J. A., et al. (2001). Traumatic optic neuropathy: A review of 61 patients. *Plastic and Reconstructive Surgery, 107*(7), 1655–1664.

121. Tsai, H. H., Jeng, S. F., Lin, T. S., et al. (2005). Predictive value of computed tomography in visual outcome in indirect traumatic optic neuropathy complicated with periorbital facial bone fracture. *Clinical Neurology and Neurosurgery, 107*(3), 200–206.
122. Chen, C. T., Huang, F., Tsay, P. K., et al. (2007). Endoscopically assisted transconjunctival decompression of traumatic optic neuropathy. *The Journal of Craniofacial Surgery, 18*(1), 19–26.
123. Mine, S., Yamakami, I., Yamaura, A., et al. (1999). Outcome of traumatic optic neuropathy. Comparison between surgical and nonsurgical treatment. *Acta Neurochirurgica (Wien), 141*(1), 27–30.
124. Stanley, R. B., Sires, B. S., Funk, G. F., & Nerad, J. A. (1998). Management of displaced lateral orbital wall fractures associated with visual and ocular motility disturbances. *Plastic and Reconstructive Surgery, 102*(4), 972–979.
125. Linberg, J. V. (1987). Orbital compartment syndromes following trauma. *Advances in Ophthalmic, Plastic, and Reconstructive Surgery, 6*, 51–62.
126. Song, A., & Carter, K. D. (2006). Bilateral traumatic globe subluxation. *Ophthalmic Plastic and Reconstructive Surgery, 22*(2), 136–137.
127. Tsopelas, N. V., & Arvanitis, P. G. (1998). Avulsion of the optic nerve head after orbital trauma. *Archives of Ophthalmology, 116*(3), 394.
128. Kiratli, H., Tumer, B., & Bilgic, S. (1999). Management of traumatic luxation of the globe. A case report. *Acta Ophthalmologica Scandinavica, 77*(3), 340–342.
129. Wohlrab, T. M., Maas, S., & de Carpentier, J. P. (2002). Surgical decompression in traumatic optic neuropathy. *Acta Ophthalmologica Scandinavica, 80*(3), 287–293.
130. Almousa, R., Amrith, S., Mani, A. H., et al. (2010). Radiological signs of periorbital trauma – The Singapore experience. *Orbit, 29*(6), 307–312.
131. Soudant, J., Lamas, G., Senechal, G., & Girard, B. (1989). Decompression of the optic nerve through the trans-ethmoid-sphenoidal approach in orbital injuries. Technic and results apropos of a new series. *Annales De Chirurgie Plastique Esthetique, 34*(5), 417–420.
132. Moe, K. S., Bergeron, C. M., & Ellenbogen, R. G. (2010). Transorbital neuroendoscopic surgery. *Neurosurgery, 67*(3 Suppl Operative), 16–28.
133. Villarreal, P. M., de Vicente, J. C., & Junquera, L. M. (2000). Traumatic optic neuropathy. A case report. *International Journal of Oral & Maxillofacial Surgery, 29*(1), 29–31.
134. Metzger, M. C., Schön, R., Weyer, N., et al. (2006). Computer-assisted extracorporeal orbital reconstruction after optic nerve decompression by removal of sphenoid bone. *Annals of Plastic Surgery, 57*(2), 223–227.
135. Kallela, I., Hyrkäs, T., Paukku, P., et al. (1994). Blindness after maxillofacial trauma: Evaluation of candidates for optic nerve decompression surgery. *Journal of Cranio-Maxillo-Facial Surgery, 22*(4), 220–225.
136. Amrith, S., Pham, T., Chee, C., & Chan, T. K. (1993). Visual recovery following transethmoidal optic nerve decompression in traumatic optic neuropathy. *Ophthalmic Surgery, 24*(1), 49–52.
137. Goldberg, R. A., & Steinsapir, K. D. (1996). Extracranial optic canal decompression: Indications and technique. *Ophthalmic Plastic and Reconstructive Surgery, 12*(3), 163–170.
138. Maurer, J., Hinni, M., Mann, W., & Pfeiffer, N. (1999). Optic nerve decompression in trauma and tumor patients. *European Archives of Oto-Rhino-Laryngology, 256*(7), 341–345.
139. Kampshoff, J. L., Cogbill, T. H., Mathiason, M. A., et al. (2010). Cranial nerve injuries are associated with specific craniofacial fractures after blunt trauma. *The American Journal of Surgery, 76*(11), 1223–1227.
140. Gasco, J., Hooten, K., Ridley, R. W., et al. (2009). Neuronavigation-guided endoscopic decompression of superior orbital fissure fracture: Case report and literature review. *Skull Base, 19*(3), 241–246.
141. McNab, A. A. (2001). Orbital and optic nerve trauma. *World Journal of Surgery, 25*(8), 1084–1088.
142. Mono, J., Hollenberg, R. D., & Harvey, J. T. (1986). Occult transorbital intracranial penetrating injuries. *Annals of Emergency Medicine, 15*(5), 589–591.

143. Mandat, T. S., Honey, C. R., Peters, D. A., & Sharma, B. R. (2005). Artistic assault: An unusual penetrating head injury reported as a trivial facial trauma. *Acta Neurochirurgica (Wien), 147*(3), 331–333.
144. Chattopadhyay, S., Sukul, B., & Das, S. K. (2009). Fatal transorbital head injury by bicycle brake handle. *Neurosurgery, 65*(2), 383–384.
145. Mitilian, D., Charon, B., Brunelle, F., & Di Rocco, F. (2009). Removal of a chopstick out of the cavernous sinus, pons, and cerebellar vermis through the superior orbital fissure. *Acta Neurochirurgica (Wien), 151*(10), 1295–1297.
146. Hegde, V., Appaswamy, S., & Ahluwalia, H. (2005). Cranio-orbital injury with internal carotid artery laceration and a missing eyelid. *Ophthalmic Plastic and Reconstructive Surgery, 21*(6), 467–469.
147. Siegel, E. B., Bastek, J. V., Mehringer, C. M., & Yee, R. D. (1983). Fatal intracranial extension of an orbital umbrella stab injury. *Annals of Ophthalmology, 15*(1), 99–102.
148. Chibbaro, S., & Tacconi, L. (2006). Orbito-cranial injuries caused by penetrating non-missile foreign bodies. Experience with eighteen patients. *Acta Neurochirurgica (Wien), 148*(9), 937–941.
149. Agrillo, A., Sassano, P., Mustazza, M. C., & Filiaci, F. (2006). Complex-type penetrating injuries of craniomaxillofacial region. *The Journal of Craniofacial Surgery, 17*(3), 442–446.
150. Nahum, A. M. (1975). The biomechanics of facial bone fracture. *Laryngoscope, 85*(1), 140–156.
151. King, A. B. (1951). Traumatic encephaloceles of the orbit. *AMA Arch Ophthalmol.* 46(1), 49–56.
152. Miabi, Z., Nezami, N., & Midia, R. (2009). Intracranial displacement of the eye after blunt trauma. *J Neuroophthalmol.* 29(4), 311.